SRPSKO HEMIJSKO DRUŠTVO (BEOGRAD)

BULLETIN OF THE CHEMICAL SOCIETY Belgrade

(Glasnik Hemijskog društva — Beograd)
Vol. 32, No. 1, 1967

Published by
SRPSKO HEMIJSKO DRUŠTVO (BEOGRAD)
1967

Translated and published for U.S. Department of Commerce and
the National Science Foundation, Washington, D.C., by
the NOLIT Publishing House, Terazije 27/II, Belgrade, Yugoslavia
1969

Edited by
PAUL PIGNON

Printed in "Prosveta", Belgrade

12th MEETING OF THE CHEMISTS OF THE SOCIALIST REPUBLIC OF SERBIA

and

ANNUAL CONVENTION OF THE SERBIAN CHEMICAL SOCIETY

January 23—25, 1967

HELD AT THE SCHOOL OF TECHNOLOGY
UNIVERSITY OF BEOGRAD

CONTENTS

SYMPOSIUM ON BIOCHEMISTRY

INORGANIC AND ORGANIC CHEMISTRY

PHYSICAL CHEMISTRY

ANALYTICAL CHEMISTRY

RADIOCHEMISTRY AND RADIATION CHEMISTRY

CHEMISTRY AND TECHNOLOGY OF SILICATES

METALLURGY

CHEMICAL ENGINEERING

TEXTILE CHEMISTRY AND TECHNOLOGY

ABSTRACTS

SYMPOSIUM ON BIOCHEMISTRY

POLYMERIZATION PROPERTIES OF THETIN-HOMOCYSTEINE-METHYL-FERASE

P. BERKEŠ-TOMAŠEVIĆ, M. SLAVIĆ and V. TERZIĆ

School of Veterinary Medecine, Beograd

Thetin–homocysteine-methyl-ferase was isolated from pig liver and purified by adsorption on calcium phosphate gel. One mg of the purified enzyme protein catalyzed the methylation of 4.92 μM of homocysteine into methionine, whereas the crude enzyme catalyzed the methylation of only 0.10 μM of homocysteine under the same experimental conditions.

The phenomenon of enzyme polymerization and depolymerization was studied by means of starch-gel electrophoresis. It was established that a decrease of the enzyme concentration in the solution and dialysis favorably affected the polymerization.

Reducing agents (sodium sulphite and sodium bisulphite) and thiols (glutathione and homocysteine) depolymerized the enzyme molecule.

The polymerization in the course of the dialysis was assumed to be due to increased autooxidation of sulphydryl into disulphide groups.

Depolymerization is effected by splitting disulphide bonds with reducing agents and thiols.

Free radicals and X-rays inactivated the enzyme but had no influence on the degree of polymerization. Therefore it may be concluded that the polymerization centers are not identical with the active centers of the enzyme.

THE INFLUENCE OF GLUCOSOXIME CONFIGURATION ON THE ACTIVITY OF TRANSOXIMASE

I. PEJKOVIĆ-TADIĆ, M. HRANISAVLJEVIĆ-JAKOVLJEVIĆ and M. MARIĆ

School of Sciences and Institute of Chemistry, Technology and Metallurgy, Beograd

The enzymatic specificity of transoximase was investigated. Transoximase was obtained from hen liver homogenate. The two theoretically predicted, but not previously isolated glucosoximes were used as donors of oximino groups, and pyruvic acid as acceptor.

It was established that transoximation takes place only in the presence of one isomer, which proves that the enzymatic specificity of transoximase is highly dependent on the configuration of the donor substance.

PROPERTIES OF INVERTASE FROM A THERMOTOLERANT STRAIN OF SACCHAROMYCES CEREVISIAE

V. M. GALOGAŽA

School of Technology, Beograd

I. Activation energies and the transition energy of invertase isolated from a strain of *Saccharomyces carlsbergensis* (breweris yeast) and from a thermotolerant strain of *Saccharomyces cerevisiae* (cultivated in our laboratory) were compared with those of a commercial invertase sample in order to establish whether the adaptation of *Saccharomyces cerevisiae* to higher temperature affects the thermodynamic properties of the invertase. It was established that the activation energies and the transition temperature remained almost unchanged.

The course of the inversion at temperatures from 0 to 50°C and the transition temperature are shown in three graphs.

II. The release of invertase in the course of autolysis at 30°C in the presence of toluene from a suspension of a strain of *Saccharomyces cerevisiae* cultivated at 40°C and from a suspension of the same strain cultivated at 30°C was compared with that from a suspension of a strain of *Saccharomyces carlsbergensis* under the same experimental conditions. Cell suspensions were buffered to pH 5.8.

The invertase release from the *Saccharomyces cerevisiae* strain cultivated at 40°C was similar to that from *Saccharomyces carlsbergensis*. The release from *Saccharomyces cerevisiae* cultivated at 30°C was much slower. The highest percentage of invertase was obtained from the *Saccharomyces carlsbergensis* autolyzate and the lowest from the thermotolerant strain of *Saccharomyces cerevisiae*. The invertase activity calculated per gram of dried cells was lowest in case of the thermotolerant strain of *Saccharomyces cerevisiae*.

The release of invertase from the thermotolerant strain was studied at 30, 36 and 40°C. It was found that at higher temperature the liberation of invertase was faster. However, the invertase was inactivated in autolysis at 36 and 40°C.

NUCLEOTIDE COMPOSITION OF RIBONUCLEIC ACID FROM SUBCELLULAR FRACTIONS OF CORN SEEDLINGS

S. GRUJIĆ and B. BELIA

School of Sciences and School of Agriculture, Novi Sad

Four subcellular fractions were isolated from three-days-old seedlings of some hybrid corns. The ribonucleic acid was extracted from each fraction and its nucleotide composition was determined.

It was found that the RNA from nuclei, mitochondria and microsomes had very similar nucleotide compositions in all the corns. The nucleotide compositions of RNA from soluble fractions were also similar. However, the nucleotide composition of RNA from the soluble fraction differed from that of RNA from the other subcellular fractions. These findings indicate that two types of RNA, which differ in nucleotide composition, are distributed in corn seedling cells.

According to the characteristic ratios (purine/pyrimidine and Gp+Cp/Ap +Up) all the RNA obey Chargaff's rule and belong to the GC-type.

THIN-LAYER CHROMATOGRAPHY OF BETA-SITOSTEROLS FROM *HELLEBORUS ODORUS* OIL

D. ŽIVANOV and M. MLADENOVIĆ

School of Pharmacy, Beograd

Beta-sitosterols in the oil isolated from the roots and rhizomes of *Helleborus odorus* were identified by thin-layer chromatography on silica gel G containing 40 mg% of fluorescein. Mixtures of chloroform and carbon tetrachloride (4 : 1 and 9 : 1) were used as solvents. Without application of detecting reagent, red spots on a yellow background were obtained.

TRANSFORMATIONS OF STEROIDAL 3-KETO-4 BETA, 5 BETA-EPOXIDES

M. STEFANOVIĆ, M. LJ. MIHAILOVIĆ, J. FORŠEK and LJ. LORENC

School of Sciences and Institute of Chemistry, Technology and Metallurgy, Beograd

By lead tetraacetate oxidation of steroidal 3-keto-4 beta, 5 beta-epoxides of the androstane and cholestane series, followed by column chromatography on aluminum oxide (or silica gel), the corresponding 2-hydroxy- $\Delta^{1,4}$ -diene-3-ones were obtained:

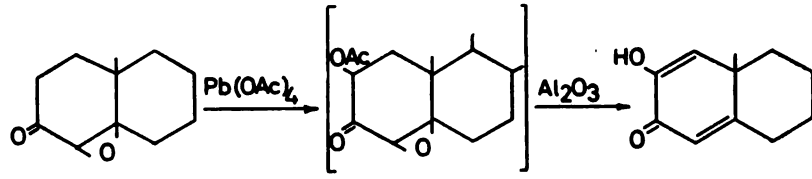

The dienonols were identified by means of analytical data and by condensation with *o*-phenylenediamine, whereby they were converted to the corresponding quinoxaline derivatives. By the action of mineral acids in anhydrous media, the $\Delta^{1,4}$ -dienonols underwent dienone-phenolic rearrangement and the A ring of the steroid molecule became aromatic. The primary products of this reaction, i.e. the corresponding 2 alpha-acetoxy-3-keto-4 beta, 5 beta-epoxides, were identified by independent syntheses according to the following scheme:

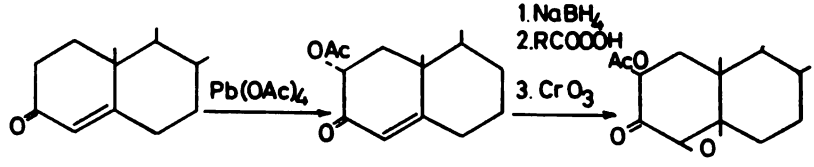

Other steroidal epoxy-ketones are under investigation.

STUDY OF RAW SUGAR BEET SAPONIN

Đ. STEFANOVIĆ, M. STEFANOVIĆ and O. GAŠIĆ

School of Sciences, Beograd, and School of Agriculture, Novi Sad

Raw saponin was isolated by various methods from ripe sugar beet, unripe sugar beet, sugar beet tails and saturated mush. It was identified by the reaction with chloroformic antimony pentachloride solution and cholesterol, and by its ability to make foam; it caused hemolysis and was toxic to fish.

A new method for the determination of saponin by thin-layer-chromatography was developed.

It was found that the raw saponin consisted of six components but their separation on a column of neutral aluminium oxide was not quite successful.

Raw saponin from sugar beet did not exhibit insecticidal properties but was shown to be valuable as a fungicide.

SEPARATION OF GLUCOSIDES AND CARBOHYDRATES OF THE *SALICACEAE* FAMILY ON SEPHADEX GEL AND A COLORIMETRIC DETERMINATION OF SALICIN

A. REPAŠ and B. NIKOLIN

School of Sciences, Sarajevo

Salicin glucosides isolated from the bark and leaves of *Populus Tremula* and *Salix Alba* were successfully separated from carbohydrates by means of gel filtration on sephadex G-15 and G-25. The glucosides and carbohydrates were examined by thin-layer chromatography on cellulose and silica gel.

New colorimetric methods for the determination of salicin by means of sulphuric and barbituric acid were developed; they can be used for rapid determination of salicin in amounts from 10 to 100 μg.

THIN-LAYER CHROMATOGRAPHY OF AMINO ACID ESTERS ON CELLULOSE AND SILICA GEL

A. REPAŠ and K. DURSUN GROM

School of Sciences, Sarajevo

Methyl and ethyl esters of some amino acids were separated and identified by thin-layer chromatography on cellulose and silica gel. Separations were carried out in various solvents. Spots were detected by means of hydroxylamine hydrochloride.

It was established that this method can be used for the simple and rapid separation and identification of amino acid esters.

Some *N*-derivatives of amino acids were examined as well.

BIOGENESIS OF TANNIN IN LEAVES OF NATIVE *RHUS COTINUS L.*

D. MURKO

School Engineering, Sarajevo

Variations of tannin content in leaves of native *Rhus cotinus L.* during the growth period were investigated from 1961 to 1966. The individual components were followed by means of paper choromatography, colorimetry and UV-spectrophotometry. Simultaneously, some accompanying substances were determined.

EXTRACTABLE MATERIALS IN *GERANIUM MACRORRHIZUM* L.

S. RAMIĆ, D. MURKO, Z. DEVETAK and M. HADŽIMUSIĆ

Institute of Chemistry, Sarajevo

Essential oils in leaves and tannins and carbohydrates in rhizomes of *Geranium macrorrhizum* L. from the surroundings of Svrljig and Maglić were investigated. It was found that young leaves from Svrljig contained about 0.113% and older about 0.06% of essential oils. Tannin contents ranged from 16.9% (Svrljig) to 11.5% (Maglić), total carbohydrates from 6.91% (Svrljig) to 6.3% (Maglić).

The tannins exhibited reactions characteristic for pyrogallol tannins; spectrophotometric determinations of aqueous 0.002% tannin solution showed a maximum in the UV-region at 270—274 mμ and minimum absorption at 252—256 mμ.

ANALYTICS OF NATURAL COUMARINS

J. GRUJIĆ-VASIĆ and M. DEŽELIĆ

School of Medecine and School of Sciences, Sarajevo

The present communication represents a continuation of our earlier investigations in the field of coumarins; it deals with the analytics of aesculin (6-beta-glucosido-7-hydroxycoumarin), fraxin (8-beta-glucosido-7-hydroxy-6--methoxy coumarin), aesculetin (6,7-dihydroxycoumarin) and fraxetin (7,8--dihydroxy-6-methoxycoumarin), and also of some of their derivatives which we have synthetized. Various reactions of these compounds and methods for their identification and quantitative determination are described. The results contribute to the understanding of the structure and reactivity of coumarins. The investigations were carried out by means of polarography, UV- and IR-spectroscopy and thin-layer chromatography.

Application to the examination of aesculin, fraxin, easculetin and fraxetin in plant materials is also reported.

FRACTIONAL DETERMINATION OF NEUTRAL 17-KETOSTEROIDS IN URINE

VERA BOŽIĆ-STAMATOVIĆ

Military Medical Academy, Beograd

Fractional determination of neutral 17-ketosteroids is of great importance for the diagnosis of adrenal gland diseases. Good separation of neutral 17-ketosteroids was achieved by adsorption chromatography. We applied a modification of Keler's method which though simplified gives good separat'on of alpha- and beta- steroids and can be satisfactorily used in routine work.

HEMICELLULOSE FROM BEECH SULPHATE COOKING LIQUOR

S. SMILJANSKI

Institute of Chemistry, Technology and Metallurgy, Beograd

A new procedure for the isolation of hemicellulose from alkaline cooking liquor was developed and applied to beech wood sulphate under different cooking conditions. Considerable concentrations of relatively undegraded polymeric hemicellulose were found to be present in the beech black liquor.

The effect of the alkalinity on the hemicellulose concentration in the cooking liquor was investigated. Increasing alkalinity resulted in an increase of the hemicellulose concentration. In the investigated range of alkalinity the dissolving effect of the increased alkalinity dominated over its degrading effect.

The effect of the prehydrolysis conditions (with water) on the concentration of the hemicellulose in the sulphate cooking liquor were investigated. When the prehydrolysis involved only heating up to the maximum temperature, the concentration of hemicellulose in the cooking liquor was almost equal to that in a parallel sulphate cooking liquor which was not subjected to prehydrolysis. Prolonged heating at the maximum temperature of the prehydrolysis resulted in a sharp decrease of the hemicellulose concentration in the liquor at all investigated alkalinities.

Conclusions concerning the dissolution and degradation of the hemicellulose component of beech wood in the course of cooking under different prehydrolysis conditions are derived.

INORGANIC AND ORGANIC CHEMISTRY

STUDY ON THE REACTION OF ERDMANN'S SALT WITH AMINO ACIDS. I. THE SYNTHESIS OF TRINITROGLYCINATOAMMINECOBALTATES (III), TRINITROALANINATOAMMINECOBALTATES (III) AND TRINITRO (ALPHA-AMINOBUTYRATO)-AMMINECOBALTATES (III)

M. B. ĆELAP, M. J. MALINAR and T. J. JANJIĆ

School of Sciences and Institute of Chemistry, Technology and Metallurgy, Beograd

The reaction of Erdmann's salt with glycine, DL-alanine and DL-alpha-aminobutyric acid was investigated. In all cases one nitro group and one ammonia molecule of the complex ion were substituted by an aminoacid ligand yielding three new classes of coordination compounds:

1. trinitroglycinatoamminecobaltates (III)
2. trinitroalaninatoamminecobaltates (III)
3. trinitro (alpha-aminobutyrato) amminecobaltates (III).

In this way complex sodium and potassium salts were obtained, whereas the corresponding silver salts were prepared by the double decomposition of the alkali salts with silver nitrate.

Experimental conditions for the direct synthesis of the above coordination compounds were found to involve the oxidation of divalent cobalt salt in the presence of ammonia, alkali nitrite, and alkali salt of the corresponding amino acid.

The structure of the compounds obtained was also investigated. The failure to resolve them into optical antipodes indicated that they were peripheral isomers, which is consistent with the *trans* configuration of Erdmann's salt determined by X-ray analysis.

The electronic and infrared spectra of the compounds are discussed.

STUDY ON THE REACTION OF HEXANITROCOBALTATES (III) WITH AMINO ACIDS. IV. THE REACTION WITH DL-NORVALINE, L-LEUCINE AND DL-ISOLEUCINE

M. B. ĆELAP, F. A. ČOHA and T. J. JANJIĆ

School of Sciences, Beograd, Institute for the Application of Nuclear Energy in Ayriculture, Veterinary, and Forestry, Zemun, and Institute of Chemistry, Technology and Metallurgy, Beograd

The reaction of potassium and sodium hexanitrocobaltates (III) with DL-norvaline, L-leucine and DL-isoleucine was investigated. It was established that in these reactions four nitro groups of the complex ion are substituted by two amino acid ligands, whereby the following three new classes of complex compounds are obtained:

1. dinitrodinorvalinatocobaltates (III)
2. dinitrobis (L-leucinato) cobaltates (III)
3. dinitrodiisoleucinatocobaltates (III).

The corresponding silver and mercurous salts were obtained by the double decomposition of the alkali salts with silver and mercurous nitrate, respectively.

It was also found that these compounds could be prepared from components in approximately the same yields by air oxidation of divalent into trivalent cobalt (by bubbling air through a solution of cobaltous acetate), in the presence of alkali nitrite and alkali salt of the corresponding amino acid.

The electronic and infrared absorption spectra of dinitrobis (aminoacido) cobaltates (III) are discussed.

STUDY ON THE REACTION OF HEXANITROCOBALTATES (III) WITH AMINO ACIDS. V. DETERMINATION OF THE CONFIGURATION OF DINITRODIALANINATOCOBALTATES (III), DINITROBIS (BETA-ALANINATO) COBALTATES (III), DINITROBIS (ALPHA-AMINOBUTYRATO) COBALTATES (III), AND DINITROBIS (L-LEUCINATO) COBALTATES (III).

M. B. ĆELAP, D. J. RADANOVIĆ, T. J. JANJIĆ and P. RADIVOJŠA

School of Sciences and Institute of Chemistry, Technology and Metallurgy, Beograd

The configuration of previously synthesized dinitrodialaninatocobaltates (III), dinitrobis (beta-alaninato) cobaltates (III), dinitrobis (alpha-aminobutyrato) cobaltates (III), and dinitrobis (L-leucinato) cobaltates (III) was investigated.

From the electronic absorption spectra and the resolution of the dinitrodialaninatocobaltates (III) into optical antipodes it was established that the nitro groups are in the *cis* position. Since the action of D- and L-alaninate on alkali hexanitrocobaltates (III) afforded in each case two inner diastereoisomers, which in fact represent two pairs of optical antipodes, it was concluded that these compounds represent only one of three possible *cis* isomers. The same pairs of optical antipodes were obtained in the mixture by the action of DL-alanine on alkali hexanitrocobaltates (III). By the action of potassium alaninate on these compounds the facial isomers of trialaninatocobalt (III) were obtained, and it was deduced that the dinitrodialaninatocobaltates probably have the *cis, cis, cis* configuration.

The *cis* configuration of dinitrobis (beta-alaninato) cobaltates (III) was established by their resolution into optical antipodes.

All attempts to resolve dinitrobis (alpha-aminobutyrato) cobaltates (III) into optical antipodes have so far been unsuccessful, although resolution was tried by means of three different alkaloids. It might therefore be deduced that in this compound the nitro groups are in the *trans* position, this being an exeption among the investigated compounds of this type.

In case of dinitrobis (L-leucinato) cobaltates (III) it was also concluded that the two nitro groups are in the *cis* position since the reaction products were optically active and exhibited absorptions characteristic of a *cis*-dinitrocobalt (III) compound.

The kinetics of racemisation and the circular dichroism spectra of the dinitrobis (aminoacido) cobaltates (III) were also investigated.

INVESTIGATION OF ALUMINUM (III) FLUORIDE SOLUTION

S. RADOSAVLJEVIĆ, V. ŠĆEPANOVIĆ and M. JOVANOVIĆ

School of Technology, Beograd

In our recent communication we assumed that so-called alpha-$AlF_3 . 3H_2O$, which is obtained from the reaction of HF (or H_2SiF_6), with Al_2O_3, is a soluble autocomplex salt $Al(AlF_6)$.

In the present investigation we attempted to prove this assumption by investiging complex compounds in solutions. Two methods were used: ion-exchange and spectrophotometry. Both confirmed our assumption; it was proved that one half of the total aluminum in the solution is present in the form of Al^{3+} ion, whereas the other half is bonded in the complex ion $(AlF_6)^{3-}$.

SYNTHESIS OF STEROIDAL SAPOGENINS AND ALKALOIDS

M. STEFANOVIĆ, A. JOKIĆ and I. MIĆOVIĆ

School of Sciences and Institute of Chemistry, Technology and Metallurgy, Beograd

The condensation of dehydroepiandrosterone with aromatic aldehydes (benzaldehyde, anisaldehyde and piperonalaldehyde) afforded the corresponding 16-arylidene derivatives in quantitative yield. Acetylation of these products was followed by reduction with metal hydrides and hydrogenation at atmospheric pressure in the presence of PtO_2, or of Raney nickel at 100 atm pressure and a temperature of 80°—100°C in ethylacetate or dioxane solution. Substituted derivatives of 16-cyclohexylmethyl steroids were obtained. By means of metal alkoxides they were cyclized into steroidal sapogenins, whereby the *F* ring contained no heteroatom.

However, when the condensation product of dehydroepiandrosterone with 2-pyridinealdehyde was reduced with metal hydrides and hydrogenated in the presence of PtO_2 catalyst, the cyclization occurred and compounds of the steroidal alkaloid type were obtained.

CONDENSATION REACTIONS OF POLYHYDROXYCOUMARINS WITH ALDEHYDES AND FATTY ACIDS

M. DEŽELIĆ, M. TRKOVNIK, M. HADŽIMUSIĆ and M. JANKOVIĆ-ZOVKO

School of Sciences, Sarajevo

4,7-dihydroxycoumarin and some other derivatives of polyhydroxycoumarins were synthesized by the reaction of resorcinol or phloroglucinol or some other polyphenol with ethyl cyanoacetate in the presence of zinc chloride and anhydrous hydrochloride. Cyclization took place and the ketimides of the corresponding polyhydroxycoumarins were obtained. Acid hydrolysis afforded polyhydroxycoumarins.

All the coumarin derivatives posses active hydrogen atoms in positions which easily react with aldehydes and monocarboxylic acids giving the corresponding 3,3'-alkylidene-, 3,3'-arylidene- and 3-acyl-polyhydroxycoumarins.

Some of these derivatives might be of interest as potential anticoagulants and substances with bactericidal activity.

HYDRAZONES OF SOME SUBSTITUTED PYRROLEALDEHYDES

M. DEŽELIĆ and K. DURSUN GROM

School of Sciences, Sarajevo

Condensation products of substituted pyrrolealdehydes with aliphatic, aromatic and heterocyclic hydrazides were prepared. The stability of these compounds towards hydrolytic decomposition in basic and acid media was investigated. It would be also of interest to examine the pharmacological properties of the acid hydrazones of pyrrolealdehydes, since some of the hydrazides and hydrazones synthetized so far have been found to be active in the therapy of many diseases.

DEMONSTRATION OF THE STRUCTURE OF THE 1,2-DITHIACYCLOHEXADIENE SYSTEM

F. BOBERG and J. JOVANOVIĆ

Petroleum Institute, Hanover and School of Technology, Beograd

By alkaline hydrolysis of 4-chloro-dithiacyclopentene-3-ones which contained the following groups in the 5-position

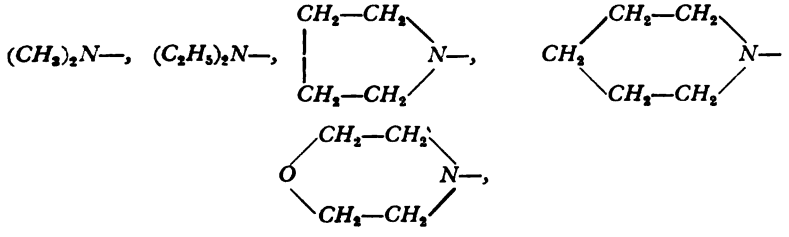

the corresponding substituted 1,2-dithiacyclohexadienes were obtained.

We determined the position of the substituents and established the structure of the 1,2-dithiacyclohexadiene system by the reaction with Grignard's reagent. The reaction of the reagent with the disulphide bond was "abnormal". Via several well characterized products we obtained dithiasuccinic acid diamide, whose structure was verified by synthesis starting from succinic acid.

CONCENTRATION RATIO OF *cis*- AND *trans-2*- BUTENE IN THE REACTION PRODUCT OBTAINED BY CATALYTIC DEHYDROGENATION OF *n*-BUTANE

DJ. DIMITRIJEVIĆ, O. STOJANOVIĆ, and A. TOT

Institute of Chemistry, Technology and Metallurgy and School of Technology, Beograd

The process of *n*-butane dehydrogenation over chromium-aluminum catalyst in the temperature interval 535—595°C at volume rates from 200 to 1000 h^{-1} was investigated. According to data reported in the literature, the concentrations of isomeric n-butenes in the reaction mixture obtained under analogous conditions should be approximately as follows: 33% of 1- butene, 30% of *cis*-2-butene and 37% of *trans*-2-butene. However, at all rates studied we found that at lower temperatures in the given temperature interval the concentration of *trans*-2-butene in the reaction product was higher than that of the *cis*-isomer, whereas at higher temperatures the ratio was inverted, i.e. less *trans*-2-butene than *cis*-isomer. The point of intersection of the two curves of isomeric 2-butene against temperature, was found to lie in the temperature interval 565—575°C. In all cases the concentration of 1-butene was higher than that of the isomeric 2-butenes.

ALKYLATION OF BENZENE WITH OLEFINS

A. TOT and DJ. M. DIMITRIJEVIĆ

School of Technology, Beograd

In a previous study on the alkylation of benzene with propylene and cyclohexene it was established that the reaction product consists of a mixture of monoalkyl and dialkyl derivatives in which there is a linear dependence between the monoalkyl: dialkyl molar ratio and the initial benzene: olefin molar ratio.

However, in the alkylation of benzene with isobutylene in the presence of nitromethane- aluminum trichloride as complex catalyst it was established that the monoalkyldialkyl molar ratio is practically independent of the initial benzene: isobutylene molar ratio.

It is of interest that in addition to the expected tert-butylbenzene, the presence of isobutylbenzene — another monoalkyl derivative — was observed.

REACTION OF POLYDIMETHYLSILOXANES WITH ALUMINUM ALKOXIDE

S. RADOSAVLJEVIĆ, D. VASOVIĆ and S. M. RADOSAVLJEVIĆ

Institute of Chemistry, Technology and Metallurgy and School of Technology, Beograd

The reaction between linear polydimethylsiloxanes containing hydroxyl groups at the end of the chain and aluminum alkoxide was investigated. Molecular weights of the polymers obtained, the change of the hydroxyl group content due to the reaction, and the effect of adding some substances on polymer formation were determined.

GRAFTING POLYACRYLATES ON CELLULOSE ACETATE IN ACETIC ACID SOLUTION

V. DRAGOVIĆ-BOŽOVIĆ

Institute of Chemistry, Technology and Metallurgy, Beograd

Conditions for the synthesis of graft copolymers of polymethyl- and polyethylacrylates on cellulose acetate were investigated, using ceric ammonium sulphate as initiator, and acetic acid solution as solvent. The results indicate that the dilution of the acetic acid solution with water increases the grafting in most cases. Graft copolymers of polyacrylates on cellulose acetate were shown to be more hydrophobic than the starting cellulose acetate. The expected increase of the thermostability of the graft copolymers was not found in all cases, but with some samples a slight increase was observed.

DEPOLYMERIZATION OF COTTON CELLULOSE IN THE COURSE OF TREATMENT WITH SODIUM HYDROXIDE SOLUTION

S. JOVANOVIĆ

School of Technology, Beograd

The degree of polymerization of cotton cellulose was determined by viscosimetry before and after dipping the samples into a 20% sodium hydroxide solution. It was found that this operation decreased the polymerization by $15 \pm 3\%$.

By varying the duration of the treatment from 0.5 to 6 hours it was shown that in the time interval examined depolymerization was not dependent on the treatment duration.

Curves of the molecular weight distribution of the cotton cellulose before and after treatment were determined, and it was found that the depolymerization was not statistical.

PHYSICAL CHEMISTRY

DETERMINATION OF THE CONSTANT IN THE EQUATION OF STATE OF INERT GASES

J. M. ŽIVOJINOV

University of Belgrade, Physics Institute of the School of Technology

The equation of state of the saturated vapor of monoatomic elements given previously by the author was compared with the equation of a saturated vapor given by D. Milosavljević. It was found that the constant in the above equation is given as the quotient of the sublimation energy of the monoatomic element at 0°K and the product of the universal gas constant and the critical temperature of the element. The value of this constant is given only for the inert gases for which experimental data were available. It was established that it was the same for all the inert gases studied. D. Milosavljević has determined it graphically and found a value of 6.55, which is only slightly different from the value found by the author. It was concluded that the value of this constant is equal to the change of the logarithm of the probability of state of the inert gase at the critical temperature with respect to the atoms of an ideal gas at the same temperature. This refers both to the constant in the author's equation and to that in D. Milosavljević's equation since their numerical values are approximately the same.

EQUILIBRIUM BETWEEN A SOLID AND ITS VAPOR

J. M. ŽIVOJINOV

University of Belgrade, Physics Institute of the School of Technology

This work is based on some relations from statistical mechanics which refer to the equilibrium state between a solid and its vapor at any temperature ranging from absolute zero to the triple point temperature of the element. It had been found that in the equilibrium state the ratio of the functions of particle energy distribution in the vapor and the solid is always the same regardless of the number of particles (atoms) passing reversibly from the same energy quantum states in one phase to the other. The total energy of the solid-vapor system is therefore always constant.

ADSORPTION PROPERTIES OF COBALT (II) FERROCYANIDE

T. ĆERANIĆ and M. ŠUŠIĆ

School of Sciences, Beograd

The mechanism of the adsorption and desorption of Cs^+ on cobalt (II) ferrocyanide complex from aqueous solutions was examined. The ion-exchange character of the adsorption and the validity of the law of mass action for that process was confirmed. The thermodynamic constant of $Cs^+ - K^+$ exchange, the enthalpy of the process and the change of the free energy were calculated. The kinetics of this heterogeneous process was considered and the activation energy was calculated. From data on the desorption of Cs^+ *by* NH_4^+, K^+ *and* H^+, conclusions on the affinities of these cations for the complex cobalt salt were drawn.

The radioactive marker ^{137}Cs was used and the process was followed by radiometry.

SORPTION ON A-ZEOLITE FROM NONAQUEOUS MEDIA

V. RADAK, M. ŠUŠIĆ and Z. MAKSIMOVIĆ

School of Sciences, Beograd
Boris Kidrič Institute of Nuclear Sciences, Vinča

The sorption of some metallic salts on A-zeolite from nonaqueous media was studied. Attempts were made to obtain data on the nature of the process by comparing the results obtained in nonaqueous media with those obtained in aqueous medium. The results of several preliminary experiments concerning the influence of parameters such as dieletric constant, nature of the solvent etc., are presented and discussed.

KINETICES OF FORMATION OF Ni_2Al_3-AND $NiAl_3$-*PHASES*

M. JANČIĆ, Ć. PETROVIĆ and D. TRIFUNOVIĆ

School of Technology, Beograd

The formation of intermetallic Ni_2Al_3 and $NiAl_3$ compounds at temperatures lower than the melting point of aluminum was studied. The reaction between nickel and aluminum in the solid state gave two sharply distinct

phases: Ni_2Al_3 and $NiAl_3$, unlike the pyrometallurgical process in which mixtures of β- and γ-phase were obtained. The γ-phase thickness against temperature and reaction time was determined and the penetration coefficient k, the temperature coefficient k_θ and the activation energy of γ-phase formation were calculated.

STUDY OF KINETICS OF THE REACTION Sn^{2+}/Sn^{4+} AT MERCURY ELECTRODE BY ANALOGUE COMPUTER

A. R. DESPIĆ and D. JOVANOVIĆ

School of Technology, Beograd

The change of potential during cathodic and anodic polarization of a mercury electrode in concentrated acid solution of 0.05 *N* Sn^{2+} and 0.05 *N* Sn^{4+} was followed by a galvanostatic method.

A mathematical model of a possible reaction mechanism was worked out and examined on a PACE-231 R analogue computer.

Experimental galvanostatic curves and computer output curves for the same values of cathodic and anodic current were compared. The reaction mechanism is discussed. Kinetic parameters of the process have been determined.

ELECTROCHEMICAL DEPOSITION OF MONOLAYERS OF METAL ON AN INERT METAL ELECTRODE

K. I. POPOV-SINĐELIĆ and M. V. VOJNOVIĆ

School of Technology, Beograd

The potential change of an inert metal electrode with time in the course of the electrochemical deposition of one or several monolayers of another metal was examined. It was established that in the systems *Ag-Pb* and *Pt-Cu* the curves of potential against time at various current densities and different concentrations of electrolyte could be approximately described by an equation derived by a simple theoretical analysis.

POLAROGRAPHIC BEHAVIOR OF SILVER IN SULPHITE SOLUTIONS

D. S. OVCIN, K. I. POPOV-SINĐELIĆ and M. V. VOJNOVIĆ

School of Technology, Beograd

The nature of the polarographic wave obtained in sulphite solutions containing silver was examined. It was found that the cathodic part of the wave could be explained by a rapid chemical reaction between mercury and complex silver-sulphite ions whereby complex mercury-sulphite ions are formed; the latter are reduced at the dropping mercury electrode.

ANODIC DISSOLUTION OF MERCURY IN SULPHITE SOLUTIONS AT DIFFERENT *pH*-VALUES

D. S. OVCIN, M. V. VOJNOVIĆ and K. I. POPOV-SINĐELIĆ

School of Technology, Beograd

The process of anodic dissolution of mercury in sulphite solutions at different *pH's* was examined. It was established that in the investigated *pH* range anodic dissolution takes place by a two-electron transfer and the formation of $Hg(SO_3)_2$. The dependence of the half-wave potential on *pH* is shown.

REDUCTION OF ARSENIC (III) AT DROPPING MERCURY ELECTRODE

M. PJEŠČIĆ and M. ŠUŠIĆ

School of Mining and Metallurgy, Bor and School of Sciences, Beograd

The reduction of arsenic(III) at the dropping mercury electrode in some organic acids as supporting electrolytes was investigated in dependence on the nature of the supporting electrolyte and the pH of the reaction medium.

The investigations were carried out in the pH range from 2.5 to 4 by studying two well-defined waves. The formation of complex compounds between arsenic and the supporting electrolytes was not observed. With change of the pH the half-wave potentials of both waves changed, that of the first more rapidly than that of the second, so that at *pH* 4 only one wave was obtained. Hence the number of hydrogen ions taking part in the first

and second electrode reaction process was determined, while the number of electrons in the total and individual processes was obtained coulometrically.

The first process involves one electron and two hydrogen ions, and the second two electrons and two hydrogen ions. Hence the total electrode reaction involves three electrons and four hydrogen ions, whereby arsenic(III) is reduced to the elementary state. The electrode reaction is estimated as irreversible.

STUDY OF THE EFFECT OF Cl^- -IONS ON THE PASSIVITY OF PR 11 STEEL

Z. PAVLOVIĆ and D. POPOVIĆ

School of Technology, Tuzla

The behavior of PR11 (18/8 steel) was studied by means of the J-V and V-t, curves in 0.005 *N*, 0.01 *N* and 0.1 *N* sodium chloride solutions, at temperatures of 20°, 40° and 60°C.

The J-V measurements were carried out in a modified Flade apparatus. From values obtained for the passivity range and the shapes of curves in the transpassive range the following was concluded:

With increasing temperature and Cl^- concentration the current density also increased, whereas the passivity range decreased. From the shape of curves in the transpassive range it was concluded that with increasing Cl^- concentration the slope of the curves also increased, i.e. the alloy dissolved more rapidly, which is consistent with the thermodynamic interpretation of the effect of Cl^- -ions on PR 11 in nonoxidizing medium, decreasing passivity.

V-t measurements were performed at 20°, 40° and 60°C with 0.005 N and 0.1 *N NaCl* solutions since it was found that PR 11 behaved in the same way in solutions of different concentrations. In order to explain the results the V-t plots were interpreted in terms of the electrochemical thermodynamics of chloride complexes of iron-chromium-nickel.

BEHAVIOR OF Ni^{2+}-IONS IN SULFATE SOLUTIONS

Z. PAVLOVIĆ and R. POPOVIĆ

School of Technology, Tuzla

The behavior of Ni^{2+} -ions in sulfate solutions was examined by adding known amounts of a base to a series of $Ni\ SO_4 + H_2SO_4$ samples. The results are presented graphically (plots of *pH* against *ml* of base added), the characteristic ranges have been determined by $a = [OH^-] / [Ni^{2+}]$. Characteristic ranges for $NiOH^+$, $Ni(OH)_2$, $Ni(OH)_3^-$ and $Ni(OH)_4^{=}$ were thus obtained. Characteristic changes in the position of the curves in these ranges were observed. The thermodynamic interpretation of the results is shown in π (volt.-kcal-) —*pH* plots. The stability ranges of individual ionic species of nickel are thus given.

Hydroxocomplexes of *Ni* were defined by means of the calculated or graphically predicted values of $\triangle G^\circ$.

By using $\triangle G^\circ$-values in the π—*pH* diagrams it was possible to show the mechanism of $Ni(OH)_2$ formation under exactly defined conditions, and the behavior of $Ni(OH)_2$ in acid and alkaline media.

The equilibrium potential in a series of samples was measured with an *Ni*-electrode against an S.C.E. The values were reduced to normal hydrogen electrode, and the results shown on an E—pH graph for the Ni-aqueous solution system.

THE EFFECT OF VARIOUS CATIONS AS AGGRESSORS ON CEMENTED MORTAR

S. STOJADINOVIĆ

School of Engineering, Sarajevo

The effect of calcium, sodium and magnesium cations on the rate of aggression of cemented mortar samples made in ratios of 1 : 2, 1 : 3, and 1 : 4 under the action of weak SO_4''-ion solution was examined.

The stability of the mortar was measured after one to two years by determining its mechanical strength and by X-ray analysis.

APPLICATION OF ROTATING DISK IN STUDY OF KINETICS OF HETEROGENOUS CATALYTIC REACTIONS

D. DELIĆ and S. JOKSIMOVIĆ-TJAPKIN

School of Technology, Beograd

A new method has been developed for the study of the kinetics of rapid heterogenous catalytic reactions under nonisothermal conditions when the reaction rate is affected by mass and heat transfer. The catalyst was in the form of a rotating disk and therefore the theory developed by Levich could be applied for the calculation of heat and mass fluxes. The method was developed by investigating the heterogenous catalytic decomposition of H_2O_2 solutions. The reaction in the kinetic and diffusional regions was studied by changing the concentration of the H_2O_2 solution and the rate of rotation of the disk. Hence the kinetic parameters of the H_2O_2 decomposition were determined.

DETERMINATION OF SULPHIDES, POLYSULPHIDES, SULPHITES AND THIOSULPHATES IN WASTE WATER

Lj. BOGUNOVIĆ, S. RADOSAVLJEVIĆ, V. REKALIĆ

Institute of Chemistry, Technology and Metallurgy, Beograd and School of Technology, Beograd

Waste water from polysulphide polymer production contains the following sulphur compounds: sulphides, polysulphides, sulphites and thiosulphates. In addition, they may contain sodium chloride, a small amount of polysulphide polymers of low molecular weight and traces of chlorinated hydrocarbons.

For the determination of these compounds we have developed a procedure which consists of four iodometric titrations. In the first titration all four compounds are determined. In the second, after the addition of zinc carbonate, sulphite and thiosulphate are determined. The third, after the addition of zinc carbonate and formaldehyde, gives the content of thiosulphate. After the treatment of the waste water with sodium sulphite and zinc carbonate, the fourth titration in the presence of formaldehyde allows determination of polysulphides and thiosulphates.

ARGENTOMETRIC DETERMINATION OF $K_4[Fe(CN)_6]$ USING THE DEPOLARIZATION END POINT

M. JOVANOVIĆ and M. DRAGOJEVIĆ (Mrs)

School of Technology, Beograd

Not long ago we suggested a new method for end point detection. Applying the potentiometric system of pre-balanced circuits and titrating irreversal systems by means of reversal titrants, the beginning of the electrode response, due to the beginning of depolarization, could be observed as a sudden off-balance current. It was shown that platinum could be used as the indicator electrode for these argentometric determinations. In the present work we studied potassium ferrocyanide solution, which had been succesfully used as the titrant for determinatoins of zinc, cadmium and some other metals.

DETERMINATION OF COPPER IN THE PRESENCE OF IRON BY CORROSIMETRIC TITRATION WITH EDTA

O. VITOROVIĆ and A. R. DESPIĆ

School of Technology, Beograd

The titration curve equation was derived for the titration of cupric ions with EDTA in the presence of large amounts of ferric ions, with dropping bismuth amalgam as indicator electrode. It was shown that a *pH* range could be found which was high enough to precipitate all iron in the form of hydroxide but not too high to prevent complexing of copper with EDTA. It was also shown that iron was redissolved with EDTA only after the titration of copper was practically completed. Hence, the dependence of the potential of the indicator electrode on the amount of EDTA added exhibited a pronounced minimum at the end point of copper titration. The conclusions were confirmed experimentally and it was shown that there exists an optimum *pH* value at which the titration can be accomplished with sufficient accuracy.

DETERMINATION OF Pd^{2+} WITH EDTA BY DIRECT POTENTIOMETRIC TITRATION

V. VAJGAND and O. KNEŽEVIĆ

School of Sciences, Beograd and "Galenika", Beograd

Large amounts of Pd^{2+} by means of EDTA have so far only been determined by indirect titration methods, whereas micro amounts of Pd^{2+} are determined by spectrophotometric titration. The present paper describes a successful direct potentiometric titration of large amounts of Pd^{2+} with EDTA, using an *Hg*-indicator electrode in solutions containing an acetate buffer of *pH* 4—4,7 and *Hg(II)EDTA*. In determining quantities of about 25 *mg* of palladium, in 26 successive titrations, $99.9 \pm 0.3\%$ of *Pd* was found.

DETERMINATION OF SULPHURIC AND TARTARIC ACID IN MIXTURES, AND THE APPLICATION OF THIS METHOD TO THE STUDY OF ION-EXCHANGE SEPARATION EFFICIENCY

D. J. STOJKOVIĆ and J. L. ĐURIĆ

Institute of Chemistry, Technology and Metallurgy, Beograd

The investigation of the efficiency of the separation of sulphate and tartrate ions by ion-exchange chromatography required the appropriate analytical methods. Therefore preliminary potentiometric and conductometric determinations of sulphuric and tartaric acid in mixtures were performed.

Comparative potentiometric determinations with glass, quinhydrone and antimony electrodes gave satisfactory results for the total acidity, while the conductometric method was used for the determination of the individual acids in a mixture.

The application of these two methods to the analysis of the eluate from an ion-exchange column made it possible to study the process of sulphate and tartrate ion separation.

DETERMINATION OF NOVALGIN IN AQUEOUS SOLUTIONS

V. VAJGAND and V. NIKOLIĆ

School of Sciences, Beograd

The gravimetric methods for the determination of novalgin as Na_2SO_4 or $BaSO_4$ were reexamined and since the sources of errors were found, they were modified to give satisfactory results. In addition, a new gravimetric method for the determination of novalgin in the form of sodium-zincacetate was developed.

The iodometric methods for the determination of novalgin were thoroughly reinvestigated and were proved to give unsatisfactory results, although they were recommended by most pharmacopoeias. The authors established that the most precise volumetric method consists in titrating, by means of sodium hydroxide solution, the sulphonic acid liberated on passing novalgin solution through a cation-exchanger.

POLAROGRAPHIC AND COULOMETRIC DETERMINATION OF NOVALGIN

V. VAJGAND, D. POCKOVA and R. MIHAJLOVIĆ

School of Sciences, Beograd, School of Sciences, Skoplje and School of Philosophy, Priština

Small amounts of novalgin were determined polarographically by determining SO_2 liberated upon addition of acid to the solution. Novalgin showed a different polarographic behavior to other sulphonic acids. The determinations were carried out in 1 *N HCl*, and the Ilkovič equation was proved to be correct for novalgin solutions up to $8.10^{-3}M$. By using methanol or ethanol instead of water, a higher diffusion current was obtained.

Attempts to determine novalgin coulometrically by the method of Feczko, which consists in iodometric determination of SO_2 liberated in acidified solutions, were unsuccessful. Satisfactory results were obtained by a new method in which novalgin is determined coulometrically by means of the excess of $HClO_4$ in a mixture of acetic acid, acetic anhydride and $NaClO_4$ as catolyte solution.

DETERMINATION OF INDIUM IN YUGOSLAV MATERIALS

V. GOLUBOVIĆ and V. REKALIĆ

School of Technology, Beograd and Institute of Chemistry, Technology and Metallurgy, Beograd

Determination of indium in materials which contain a number of interfering elements *(Cu, Pb, Zn, Bi, Fe, Mn, Al, Ca, Mg)* was carried out by polarography after quantitative separation of interfering components by precipitation or by passing through an ion- exchanger. The results, depending on the quantity of indium present, were compared with those obtained by complexometry or by extractive titration with dithizone.

POLAROGRAPHIC BEHAVIOR OF NIOBIUM IN THE PRESENCE OF COMPLEXON

A. GHONAIM and M. ŠUŠIĆ

School of Sciences, Beograd

The behavior of *Nb* in the presence of complexon as a function of the concentrations of *Nb* and complexon and the *pH* of the supporting electrolyte was studied.

It was found that *Nb* can be determined polarographically in the presence of complexon III as described in the literature, but that good results could be obtained in acetic acid or acetate solutions containing diethylenetriaminopentaacetic acid as complexing reagent.

Complexon I had no effect on the polarographic behavior of *Nb*.

The *pH* of the supporting electrolyte had a great effect on the formation of the polarographic wave, the half-wave potential and the diffusion current.

SPECTROPHOTOMETRIC DETERMINATION OF MICROGRAM QUANTITIES OF COPPER IN SOME MINERAL WATERS OF SERBIA

V. B. GOLUBOVIĆ and M. M. JOVANOVIĆ

School of Technology, Beograd

A fast spectrophotometric method for the determination of copper in mineral waters was examined. Investigations were carried out using oxalyldihydrazide acetaldehyde. The method was proved to be very convenient, and a number of different samples of mineral waters from Serbia were examined. By this method copper quantities ranging from 5 to 50 μg/25 *ml* could be determined.

METHODS FOR THE DETERMINATION OF GASES OF FISSION

F. SIGULINSKI and M. STEVANOVIĆ

Boris Kidrič Institute of Nuclear Sciences, Vinča

Procedures for the determination of gases of fission by measuring the amounts of gas liberated from and retained in the fuel after irradiation are described. They are based on the application of gamma scintillation spectrometry, mass spectroscopy and gas chromatography.

Experiments are described in which the pressure of gases in the jacket of the combustible element and the amounts of gas liberated from the fuel in the course of irradiation in the pile were determined.

EXTRACTION OF GOLD AND ITS DETERMINATION IN ORES BY RADIOACTIVATION ANALYSIS

D. B. STEVANČEVIĆ and G. T. HAJDUKOVIĆ

School of Technology, Beograd and Boris Kidrič Institute of Nuclear Sciences, Vinča

A method for the separation and determination of gold in ores is described. Gold was extracted from 5N hydrochloric acid solutions with a chloroform solution of 1-phenyltetrazol-5-thiol. It was shown that by a single extraction radiochemically pure gold could be obtained from irradiated samples and thus separated from a number of other elements. Radioactivity of the separated ^{199}Au was measured with a Geiger-Müller counter, and the gold content was determined by a comparative method.

DETERMINATION OF TRITIUM IN HUMAN URINE BY LIQUID SCINTILLATION METHOD

Ž. UBOVIĆ and D. PALIGORIĆ

Boris Kidrič Institute of Nuclear Sciences, Vinča

The determination of tritium in human urine by a liquid scintillation method is described. The maximum sensitivity of the method for distilled urine is 6.7×10^{-4} $\mu Ci/ml$.

Optimum conditions for achieving this sensitivity were investigated and the conditions for the application of the method in routine monitoring and emergency cases are presented.

RADIOCHEMICAL METHOD FOR THE DETERMINATION OF ^{239}Pu IN HUMAN URINE

D. JANKOVIĆ and LJ. DOBRILOVIĆ

Boris Kidrič Institute of Nuclear Sciences, Vinča

A radiochemical method for the quantitative determination of ^{239}Pu in human urine has been developed. It uses the coprecipitation of ^{239}Pu with calcium- and magnesium- ammonium phosphate, extraction with cupferron in chloroform, followed by ion-exchange on "Deacidite" FFSRA 67 resin of 100—200 mesh, and electrodeposition from slightly acid solution of aluminum oxalate.

The ^{239}Pu samples obtained were measured on a 2-pi methane-flow proportional counter at atmospheric pressure.

The relative chemical yields of ^{239}Pu from samples of human urine contaminated with it at a level of 1.40—14.05 pCi averaged $94.4 \pm 2.2\%$.

RADIOCHEMISTRY AND RADIATION CHEMISTRY

MEASUREMENTS OF THE RADIOACTIVITY OF ELECTRON-CAPTURED NUCLIDES BY THE 4-π X-METHOD

DJ. BEK-UZAROV and LJ. DOBRILOVIĆ

Boris Kidrič Institute of Nuclear Sciences, Vinča

A 4-π counter operating in the pressure region of 1 to 3 atmospheres was constructed, and was used for measuring the characteristic X-radiation of electron-captured nuclides.

The efficiency of the counter was determined from the counts of k-x radiation as a function of the inverse pressure. In the case of a 90% Ar + 10% CH_4 gas mixture at atmospheric pressures it was 93.8%, 77.6% and 51.1% for ^{51}Cr, ^{55}Fe, and ^{65}Zn, respectively.

The absolute activity of the ^{51}Cr, ^{55}Fe and ^{65}Zn sources was measured with an accuracy of ± 2.0%, ± 3.8% and ± 3.5%.

SOME DATA OBTAINED IN A STUDY ON ENERGY EFFICIENCY OF A PROPORTIONAL COUNTER

K. BURAJ and DJ. BEK-UZAROV

Boris Kidrič Institute of Nuclear Sciences, Vinča

The counter used was a cylindrical 4-π β-proportional counter consisting of two symmetrical parts each having the following dimensions:

depth — 2.8 ± 0.05.

effective length of the collecting wire — 4.0 ± 0.05 *cm*

diameter of the collecting wire — 18 microns.

The filling gas was commercial methane.

The results were obtained at room temperature and atmospheric pressure.

The energy efficiency of the counter was determined as a function of the internal amplification factor (gas multiplication factor) under normal working conditions. At the same time, the efficiency was found to be

a function of the energy dissipated in the counter and the end point energy of the beta-emitter (E_{max}).

Under normal conditions, the minimum detectable energy was found to be 500 ± 5% *eV*.

AN APPROACH TO G-VALUE EVALUATION IN MIXED PILE RADIATION

B. RADAK

Boris Kidrič Institute of Nuclear Sciences, Vinča

Radiation chemical yield (G) in a mixed radiation field (various LET) using an aqueous solution as the model system was studied. In the case of pile radiation, the neutron (i.e. proton) yield is a problem of basic interest and it was considered in more detail. A theoretical approach for the evaluation of proton yield from the known initial neutron spectrum, neutron scattering cross sections, and the G-value dependence on LET is presented. Theoretically calculated proton G-values are compared with the experimental ones so far available and the results of the comparison are discussed.

CHEMICAL DOSIMETRY OF IN-PILE RADIATION. A NEW METHOD FOR ROUTINE MEASUREMENTS

V. MARKOVIĆ

Boris Kidrič Institute of Nuclear Sciences, Vinča

The main problems encountered in using chemical dosimeters for in-pile experiments are discussed. The properties of several systems which can be used for such purposes are given. The application of the aqueous oxalic acid dosimeter for routine measurements of in-pile absorbed doses is discussed in detail.

USE OF THE AQUEOUS OXALIC ACID DOSIMETER FOR ROUTINE MEASUREMENTS IN MULTI-MEGARAD REGION OF GAMMA ABSORBED DOSES

V. MARKOVIĆ

Boris Kidrič Institute of Nuclear Sciences, Vinča

In spite of numerous attempts the problem of chemical dosimetry in the multi-megarad region has not been solved satisfactorily. Although there the oxalic dosimeter has promising properties it is still not accepted for routine use. This can be attributed to some disadvantages of the previously given procedure for its application. These disadvantages are analyzed and a new procedure in which most of them are avoided is described. The results of the determination of factors for ^{60}Co gamma radiation required for routine measurements of absorbed doses in the region of 1.6 to 110 *Mrad* is given.

RADIOLYSIS OF OXYGENATED OXALATE SOLUTIONS IN HEAVY WATER. THE INFLUENCE OF *pD* ON PRIMARY YIELDS OF HEAVY WATER RADIOLYSIS

M. NENADOVIĆ and Z. DRAGANIĆ

Boris Kidrič Institute of Nuclear Sciences, Vinča

Data on the influence of *pD* on primary yields of heavy water radiolysis are rather scarce and contradictory. By measuring the stable products of radiolysis of oxygenated oxalate heavy water solutions in the *pD* region 1.6 to 14, we obtained data on primary yields and on their variation with increasing *pD*. The radiolysis mechanism of these solutions is known from similar systems in light water. Therefore it was possible to make a direct comparison of the corresponding results. For determining carbon dioxide and molecular deuterium gas chromatography was used, and deuterium peroxide was determined by spectrophotometry. We also studied the competition between oxygen and oxalate ions for O^- -ion radicals and calculated the rate constant ratio of these two reactions. The calculated primary radical yields in hevay water are slightly higher and the yields of molecular products lower than in light water.

RADIOLYSIS OF WATER: SOME COMPARATIVE MEASUREMENTS OF PRIMARY RADIOLYSIS PRODUCTS IN D_2O AND H_2O

O. MIĆIĆ and Z. DRAGANIĆ

Boris Kidrič Institute of Nuclear Sciences, Vinča

The numerous studies of water radiolysis have mainly been concerned with light water. Data on products of heavy water radiolysis are scarce and contradictory. There is practically no information concerning the rate constants of the *D* and *OD* radical reactions or the rate constants of solvated electrons in heavy water. By measuring the stable products of radiolysis and applying steady state and competition kinetics we obtained various data which allow the comparison of primary radiolysis products and some reaction rate constants, and allow some conclusions on heavy water. The systems studied were degassed heavy water solutions of copper sulfate and heavy water solutions of ethanol and oxygenated *KBr* and ethanol. Experimental techniques involved gas chromatography for the determination of molecular deuterium and spectrophotometry for deuterium peroxide. The radical yields obtained were slightly higher than for light water, the yield of molecular deuterium was lower, and the deuterium peroxide yield was the same. Special attention was paid to the determination of relative rate constants in reactions involving *D*, e_{aq}^- and *OD* radicals, and to the evaluation of the isotopic effect in these reaction rates. The results show that the greater distribution of reducing radicals in heavy water is due to the different physico-chemical properties of heavy water relative to light water.

BEHAVIOR OF RECOIL ^{51}Cr IN IRRADIATED ANIONIC DOPED POTASSIUM CHROMATE

S. M. MILENKOVIĆ and S. R. VELJKOVIĆ

Boris Kidrič Institute of Nuclear Sciences, Vinča, and School of Sciences, Beograd

The hot atom reactions of recoil ^{51}Cr in neutron irradiated anionic doped potassium chromate were studied. Experiments with *KCl*, *KBr*, *KI* and *MgO* doped potassium chromate showed some reduction of initial retention, and increased susceptibility to thermal annealing of the irradiated material. Incorporation of ^{51}Cr into the parent chemical form during thermal annealing in doped crystals was much faster than in undoped potassium chromate, especially around 180°C. The results are discussed in the light of the chemistry of imperfect crystals.

EFFECT OF RADIATION DAMAGE OF Al_2O_3 ON ITS ADSORPTION CAPACITY

LJ. JAĆIMOVIĆ and S. VELJKOVIĆ

Boris Kidrič Institute of Nuclear Sciences, Vinča

Changes in the adsorption of phosphate ions from aqueous solutions onto Al_2O_3 in dependence on the radiation damage of the adsorbent were investigated. A 50% increase of the adsorption capacity was found after irradiation in an integral fast neutron flux of 10^{18} n/cm^2 and a gamma radiation dose of 2.4×10^{19} *rad*, when the target was in the open system. Subsequent thermal annealing of the target at above 350°C decreased the adsorption capacity to approximately the pre-irradiation value.

Irradiation in a closed system, such as a sealed quartz ampoule, did not increase the adsorption capacity, irrespective of whether there was air, nitrogen, oxygen or vacuum over the target.

These results indicate a complex behavior of the defects caused by irradiation in which the interaction with gases present during irradiation must be taken into account. On this basis it was possible to discuss the selective character of individual adsorption centers of Al_2O_3.

AUTORADIOGRAPHIC STUDIES ON THE ADSORPTION OF *I*-131, *S*-35 AND *Co*-60 ON VARIOUS MATERIALS

D. S. RISTIĆ and J. D. DIMITRIJEVIĆ

School of Sciences, Beograd

Adsorption of *I*-131, *S*-35 and *Co*-60 on two groups of materials was studied: metals (copper, brass, stainless steel, etc.) and nonmetallic systems (concrete, brick, ceramic, textiles, etc.).

The aim of this study was to determine the conditions under which contamination and decontamination of these materials occurs in aqueous and nonaqueous solutions.

Special attention was paid to the determination of active centers and active sites on adsorbing surfaces. An autoradiographic method was developed for this and gave satisfactory results.

A technique for obtaining surfaces with controlled activity was developed in order to find the conditions for minimum adsorption capacity.

The results indicate that contamination processes mainly depend on adsorption laws are valid for chemical systems in general.

STATE OF RADIOACTIVE COBALT (^{60}Co) IN THE EFFLUENTS PRODUCED BY DECONTAMINATING PARTS OF THE PRIMARY SYSTEM OF THE RA REACTOR AT VINČA

Ž. VUKOVIĆ and O. JANKOVIĆ-GAĆINOVIĆ

Boris Kidrič Institute of Nuclear Sciences, Vinča

Decontamination with a solution of 7% H_3PO_4 and 2% CrO_3 gave radioactive effluents containing a micro component of ^{60}Co.

By ion exchange and electrodialysis ^{60}Co was found to be in a negatively charged form.

By investigating the effects of some electrolytes we made deductions on the possible states of ^{60}Co in these effluents.

ENTRAINMENT OF RADIOACTIVE STRONTIUM BY RAPID PRECIPITATION OF $SrCO_3$ AND $CaCO_3$

O. JANKOVIĆ-GAĆINOVIĆ and Ž. VUKOVIĆ

Boris Kidrič Institute of Nuclear Sciences, Vinča

Radioactive strontium was removed from solution by precipitating $SrCO_3$ (strontium was added as an isotope carrier) and $CaCO_3$. Precipitation in two steps was shown to give a much higher decontamination factor F_d than if $SrCO_3$ and $CaCO_3$ were precipitated simultaneously. The two-step procedure consisted in precipitating first $SrCO_3$ and after a while $CaCO_3$. The present study deals with the dependence of F_d on the following parameters: the *pH* of carbonate, precipitation, the concentration of Ca^{++}, Sr^{++} and Na_2CO_3 used for the formation of the precipitate, the time of mixing the carbonate suspension, the order of addition of the reacting components, the $NaNO_3$ concentration, etc.

INVESTIGATION OF THE EFFECT OF CHROMATE AND PHOSPHATE ANIONS ON THE CATION EXCHANGE OF ^{60}Co IN THE PRESENCE OF *Ni*, *Al* AND *Fe* IONS

A. ŠVABIĆ, P. RADOVANOV and LJ. JANKOVIĆ

Boris Kidrič Institute of Nuclear Sciences, Vinča

In a study to develop a method for the removal of radioactive cobalt from effluents produced by decontamination of parts of reactor systems with chromium-phosphoric acid, we examined the effect of chromate and phosphate anions of a given concentration on the cation exchange of ^{60}Co in the presence of *Ni*, *Al* and *Fe* cations. The aim of this investigation was to examine under what conditions and to what extent these effects occur, and to contribute to their explanation, in order to establish the most favourable conditions for removal of ^{60}Co from effluents of given compositions.

BEHAVIOR OF ^{60}Co RELEASED INTO A STREAM

T. TASOVAC and R. RADOSAVLJEVIĆ

Boris Kidrič Institute of Nuclear Sciences, Vinča

The behavior of ^{60}Co in surface water was studied by releasing effluents into the Mlaka stream under various conditions. The dispersion and transport of effluents were examined. Samples were collected from the bed in selected regions of deposition. From the results it was possible to determine the amount of radioactive effluent which may be released into the stream without causing too high a concentration od ^{60}Co in the surroundings.

THE USE OF RADIOISOTOPES IN THE PRODUCTION OF SELF-LUMINOUS MATERIALS

Ž. TODOROVIĆ and Ž. RADOSAVLJEVIĆ

Boris Kidrič Institute of Nuclear Sciences, Vinča

The dependence of the light output and the radiation damage upon the radioluminous layer thickness, the specific activity, the granulation and the activator type was studied using a *ZnS*-luminator with *Pm*-147 and *Tl*-204.

From the experimental results we wanted to determine the optimum specific activity, the luminofor layer thikness and the granulation required to see the sample clearly from a definite distance after a given time-period, i.e. to find a self-luminofor which would last long enough and emit the required light intensity.

For the preparation of self-luminous material, we used *ZnS* activated with *Cu, Al, Ag* and *Mn*. Radioisotopes *Pm*-147 and *Tl*-204 were adsorbed onto the luminous material of given granulation. The radioluminous material was placed in polystyrene vessels and the light output intensity was measured by means of the current induced by the sample at the output of a photomultiplier.

The choice and chemical state of the isotopes and the choice of luminous material are discussed. The effect of water glass (as binder) and of the polystyrene vessel on the light output were investigated. By placing the samples on a metal plate (*Al*, about 3 *mm* thick) the light output was intensified by about 30%.

The self-luminous material can be widely applied for luminous signs in mining, navigation, instrument scales and in all cases where no external power supply is available.

CHEMISTRY AND TECHNOLOGY OF SILICATES

THE TEMPERATURE COEFFICIENT OF THE EQUILIBRIUM CONSTANT OF THE CATION EXCHANGE REACTION OF MONTMORILLONITE

D. DELIĆ and M. TECILAZIĆ-STEVANOVIĆ

School of Technology, Beograd

Cation exchange reactions in systems consisting of *K*-montmorillonite and isonormal solutions of potassium and calcium chloride were investigated. Equilibrium ratios were determined at 4 different temperatures, 0°, 18°, 50° and 70°C. At each temperature, equilibrium constants for four solutions of different starting compositions were determined. A fraction of Wyoming bentonite whose grain size was less than 2 microns was used for the preparation of *K*-montmorillonite samples by standard methods. The experimental data were analyzed thermodynamically and the following parameters were determined: the exchange reaction heat output, the temperature coefficient of the equilibrium constant, and the change of the standard free energy.

KINETIC AND STRUCTURAL CHANGES OF TALC DURING HEATING

S. BOŠKOVIĆ, M. GAŠIĆ, V. NIKOLIĆ, B. ŽIVANOVIĆ and M. M. RISTIĆ

Boris Kidrič Institute of Nuclear Sciences, Vinča

In the course of heating talc, a two-stage dehydration occurs, which represents a typical example of a solid state reaction, giving gaseous and solid reaction products. By analyzing the kinetic parameters in the light of modern theories, we established that the dehydration is a two-stage process. The activation energy of the first stage is 15.1 *kcal/mol* and that of the second 50.2 *kcal/mol*.

At the temperatures corresponding to the different stages of dehydration structural changes occur, as was confirmed by X-ray analysis. During heating talc loses its layer structure, and a qualitative transformation of the original structure at 950°C was established from the (001) lines.

PRODUCTION OF ZIRCON-CORDIERITE CERAMICS FOR METAL-LAYER RESISTORS

V. NIKOLIĆ, S. BOŠKOVIĆ, M. GAŠIĆ, F. SIGULINSKI and S. MALČIC

Boris Kidrič Institute of Nuclear Sciences, Vinča

The use of natural kaoline, bentonite and talc for obtaining a ceramic structure suitable for making metal-layer resistors was investigated. In the temperature range from 1100 to 1250°C, which is the most suitable for the synthesis of cordierite, the formation of cordierite structure was followed, and the structure observed was compared with that of commercial samples. It was shown that materials of satisfactory properties were obtained. X-ray, dilatometric and thermal analysis showed that the best results were obtained when the components were heated in the narrow temperature range 1150—1200°C. The duration of heating was of secondary importance.

KINETICS OF GRAPHITE OXIDATION WITH CHROMIC ACID AND ITS APPLICATION FOR THE DETERMINATION OF STRUCTURAL DEFECTS

Č. SUŽNJEVIĆ and S. MARINKOVIĆ

Boris Kidrič Institute of Nuclear Sciences, Vinča

The rate of oxidation of graphite in an H_2SO_4—$Ag_2Cr_2O_7$ mixture depends mainly on its structure. The apparatus described allows the measurement of graphite oxidation kinetics (by manometric determination of liberated CO_2) and qualitative and quantitative determination of individual structural constituents.

Various commercial polycrystalline graphites and pyrocarbons prepared in the laboratory, were examined. Polycrystalline graphites with neutron-induced defects were investigated as well.

Polycrystalline graphites oxidized rapidly, showing the presence of only one "graphitic" constituent. The oxidation of pyrolytic carbon showed: a) that it contained a low percentage of the "graphitic" constituent and a high percentage of a "nongraphitic" constituent which oxidized much more slowly; b) that the content of "graphitic" constituent increased with increasing pyrolysis temperature. Polycrystalline graphites with radiation defects behaved very similarly to pyrocarbon.

PYROLYTIC DEPOSITION OF CARBON UNDER DIFFERENT EXPERIMENTAL CONDITIONS

S. MARINKOVIĆ, Č. SUŽNJEVIĆ, V. PETROVIĆ, S. MALČIĆ and I. DEŽAROV

Boris Kidrič Institute of Nuclear Sciences, Vinča

Pyrolytic carbon deposition on supports of polycrystalline graphite and molybdenum foil is described. Depending on the experimental conditions (temperature, flow-rate, gas-mixture composition) different products were obtained. Products were examined by optical and electron microscopy, X-ray diffraction and other methods.

The carbon coatings were compact and practically impermeable to gases, with excellent mechanical properties and adhesion to the support. Therefore they are suitable for various practical applications some of which are pointed out.

KINETICS OF SINTERING OF *Ni-Zn*-FERRITES

J. MOMČILOVIĆ, Š. KIŠ and D. CEROVIĆ

Boris Kidrič Institute of Nuclear Sciences, Vinča

The sintering kinetics of *Ni-Zn*-ferrites was studied with the aim of getting information about the sintering process.

Ni-Zn-ferrite samples of various compositions were sintered in the temperature range srom 1150° to 1300°C cor 1, 3, 5 and 8 hours.

The characteristic parameters of sintering, i.e. time exponent, rate constant and experimental activation energy, were determined by means of relative volume and density changes during sintering.

Equations of sintering for ferrites at different temperatures are given.

STRUCTURAL INVESTIGATIONS IN THE NiO-ZnO-Fe_2O_3 SYSTEM

M. TOMIĆ, S. MALČIĆ and Š. KIŠ

Boris Kidrič Institute of Nuclear Sciences, Vinča

X-ray analysis of the reaction products of the NiO-ZnO-Fe_2O_3 system was performed in order to identify the phases and to follow the lattice constant of individual phases by varying the composition of the starting mixture.

The investigations were carried out with stoichiometric mixtures (definite ferrite phase) and with nonstoichiometric mixtures containing individual components in excess.

A certain regularity was found in the phase composition of the reaction products in dependence on the starting ratio of oxides, and the change of the lattice constant of the ferrite phase in dependence on ZnO content was determined.

Investigations were carried out on a Siemens diffractometer with $CrK\alpha$ radiation.

REACTIONS IN THE NiO-Fe_2O_3 SYSTEM CONTAINING Fe_2O_3 IN EXCESS

LJ. PETROVIĆ, M. TOMIĆ, S. MALČIĆ and Š. KIŠ

Boris Kidrič Institute of Nuclear Sciences, Vinča

The reactions taking place in the NiO-Fe_2O_3 system in the course of the formation of the ferrite phase and solid solutions were studied. Changes occuring at a given cooling regime were also examined.

Investigations were carried out in the temperature range 800° to 1000°C with polydispersed NiO-Fe_2O_3 mixtures of molar ratio 30/70 and 40/60, at time intervals ranging from 5 minutes to 4 hours.

From data obtained for the degree of reaction in dependence on time and temperature, the experimental activation energy was calculated; values of 22.1 *kcal/mole* and 19.7 *kcal/mole* were obtained.

Using the results in the Ginstling-Brounshtein equation gave the changes of kinetic reaction parameters.

The separation out of excess Fe_2O_3 in the course of cooling was studied by microstructural and electromagnetic investigations. It was established that the lower the cooling rate the greater the amount of Fe_2O_3 which separated.

DETERMINATION OF MICROSTRUCTURAL CHARACTERISTICS OF FERRITES

M. RADULOVIĆ, V. PETROVIĆ and Š. KIŠ

Boris Kidrič Institute of Nuclear Sciences, Vinča

A detailed study of microstructural characteristics of ferrites was made, since their effect on the electromagnetic properties is of great importance in the technology of ferrites.

Methods for the preparation of samples for microscopic investigation are described, especially for the study of porosity, for the detection of phases and for the determination of grain size and shape. Methods for microscopic investigation of powdered samples are also described; they permit the study of the homogeneity of mixtures of different oxides and of different grain size and shape, and the investigation of agglomerates of mixtures and ferritized powders.

The results obtained by studying the microstructural characteristics of sintered samples of NiO-ZnO-Fe_2O_3 and MnO-Fe_2O_3 systems in dependence on technological parameters of their preparation are presented.

STUDY OF FERRITISATION OF THE MnO-Fe_2O_3 SYSTEM

J. PAVLOVIĆ and Š. KIŠ

Boris Kidrič Institute of Nuclear Sciences, Vinča

The sensitivity of manganese towards oxygen raised new problems in the ferritisation of the MnO-Fe_2O_3 system, due to the undefined composition of the reaction products.

Some results obtained in the study of ferritisation in the temperature range from 950 to 1100°C are presented.

The change of the specific surface area with temperature was investigated, and X-ray and thermogravimetric analysis of the reaction products were performed. It was shown that with regard to the composition of the reaction products the optimum temperature for ferritisation in the MnO-Fe_2O_3 system is 1050°C.

PREPARATION OF FERRITE POWDER FOR PRESSING

V. BAČIĆ and Š. KIŠ

Boris Kidrič Institute of Nuclear Sciences, Vinča

Problems involved in the preparation of ferrite powder for pressing were considered. The effect of adhesives and lubricants on the mechanical stability of the pressed samples were investigated and the value of preliminary granulation was examined. It was found that a suitable granulation considerably increased the fluidity of the powder, which is very important for automatic pressing. It was established that by choosing suitable adhesives and lubricants and using a suitable granulation pressed and sintered samples of reproducible density could be obtained.

THERMAL CONDUCTIVITY OF UO_2

J. KATANIĆ-POPOVIĆ and M. STEVANOVIĆ

Boris Kidrič Institute of Nuclear Sciences, Vinča

The factors influencing the thermal conductivity of sintered UO_2 are analyzed, mainly from the point of view of its application as fuel. The effect of temperature, density, porosity, additives and irradiation in the pile are described. Data reported so far on the measurement of the thermal conductivity of sintered UO_2 in the pile and out of it are critically considered.

VIBRATORY COMPACTION OF CERAMIC NUCLEAR FUEL

J. VOGT and B. ŽIVANOVIĆ

AB Atomenergi, Stockholm, Sweden and

Boris Kidrič Institute of Nuclear Sciences, Vinča

In comparison with sintering, vibratory compaction is simpler and cheaper for the production of nuclear ceramic fuel elements. Earlier experiments in this field were carried out with uranium dioxide samples obtained either by fusing and crushing or by sintering and crushing uranium dioxide. The aim of the present work was to compare the properties of irregularly shaped ceramic fuel with those of geometrically well-defined spherical UO_2 particles, obtained by a new method.

The relation between fuel density and production parameters (particle size distribution, frequency, and time of compacting) is presented graphically.

RECOVERY OF IRRADIATED SINTERED *MgO*

M. STEVANOVIĆ

Boris Kidrič Institute of Nuclear Sciences, Vinča

The recovery of sintered *MgO* irradiated with an integral fast neutron flux of 10^{20} n/cm^2 was studied by following the variations of crystal lattice parameters, the dimensions and the elasticity modulus of irradiated sintered samples in the temperature range from 400 to 1200°C. The lattice parameter recovery in the course of isothermal reheating was approximated by an analytical expression. The experimental activation energy of the process was determined from the lattice recovery data.

FORMATION OF PROTOENSTATITE AND CORDIERITE IN CERAMIC MASSES OF THE MgO-Al_2O_3-SiO_2 SYSTEM

S. BOŠKOVIĆ, M. GAŠIĆ, V. NIKOLIĆ and M. M. RISTIĆ

Boris Kidrič Institute of Nuclear Sciences, Vinča

By heating natural clays, bentonites and talc in the temperature range 1100—1300°C, ceramics of cordierite structure were obtained. Selected combinations which in an MgO-Al_2O_3-SiO_2 three-component diagram lie on the straight line enstatite (MgO-SiO_2)-cordierite ($2MgO\ 2Al_2O_3\ 5SiO_2$) were found to give predominantly cordierite and protoenstatite when heated at the above temperatures. The increase of the cordierite content in dependence on temperature and composition was determined by X-ray diffraction.

METALLURGY

TRANSFORMATION KINETICS AND STRUCTURAL CHANGES OF THE ZIRCALLOY-2 DURING CONTINUOUS COOLING

B. DROBNJAK

Boris Kidrič Institute of Nuclear Sciences, Vinča

The *KH*-diagram of the alloy was determined by thermal analysis. It was established that at cooling rates slower than 500°C/sec, the beta →alpha transformation started with a proeutectoid reaction and was followed by a eutectiod or martensite reaction at lower temperatures, depending on the cooling rate. Two discontinuities which appeared on the *KH*-diagram indicated that the eutectoid reaction was not followed immediately by a martensite reaction, but that in the intermediate temperature region the transformation involved a beinitic reaction as well.

The structure formed at low cooling rates consisted of Widmanstätten α-plates and an intermetallic precipitate which was located mainly along the plate boundaries. At cooling rates about 230°C/sec the structure contained groups of martensite plates as well as Widmanstätten plates. Boundary α-allotrimorphies were always present, regardless of the cooling rate.

TRANSMISSIONS ELECTRON MICROSCOPY INVESTIGATION OF EFFECT OF ANNEALING ON SECONDARY PHASES IN *U-1%Mo* ALLOY

O. NEŠIĆ and DJ. LAZAREVIĆ

Boris Kidrič Institute of Nuclear Sciences, Vinča

The effect of annealing on the secondary eutectoidal gamma phase in *U-1%Mo* alloy was investigated by transmission electron microscopy. With short annealing at 530°C coarsening of the precipitate took place, whereas at 450°C there were no changes even on prolonged annealing.

The observed effects are discussed with respect to the radiation stability of this alloy.

EFFECT OF CURVATURE OF THE SOLID-LIQUID INTERFACE ON RADIAL MICROSEGREGATION DURING DIRECTIONAL SOLIDIFICATION

DJ. MILOSAVLJEVIĆ

Boris Kidrič Institute of Nuclear Sciences, Vinča

Radial microsegregation in crystals grown from the melt and the efficiency of zone refining are discussed on the basis of the experimental data obtained in a study of the effect of the curvature of the solid-liquid interface.

The proposed hypothesis of "two-directional solidification" explains the effect of thermal factors on radial microsegregation indirectly, via the cellular substructure.

Some suggestions for the improvement of the homogeneity of crystals grown from the melt and for increasing the zone refining efficiency are presented.

THE INFLUENCE OF THERMAL TREATMENT ON THE SIZE AND THE DISTRIBUTION OF SECOND PHASE PARTICLES IN DILUTE URANIUM

M. JOVANOVIĆ

Boris Kidrič Institute of Nuclear Sciences, Vinča

In this work we studied the effect of different thermal treatments on the size and distribution of precipitated phases in unalloyed uranium of Yugoslav origin and in uranium alloyed with 1000 *ppm* of aluminum. The precipitated phases were studied by transmission electron microscopy. In specimens of uranium alloyed with 1000 *ppm* of aluminum which were furnace-cooled from the gamma phase the formation of rod-shaped precipitate at beta grain boundaries was observed, whereas considerably smaller particles were formed at alpha grain and sub-grain boundaries. Upon ageing at 550°C and after quenching from the gamma region the precipitate was deposited mostly at alpha grain and sub-grain boundaries. The particles were the larger the longer the time of ageing. On cooling from the gamma phase in vacuum a dispersion of very fine particles, smaller than 0.01 micron in diameter, was formed. These particles were smaller than the particles of furnace-cooled or alpha-aged samples. In furnace-cooled specimens of alloyed and unalloyed uranium the dispersed phases were similar in size and shape, but in specimens of unalloyed uranium no particles characteristic of the beta phase were observed.

DECOMPOSITION OF AUSTENITE OF HADFIELD STEEL WITH A HIGH MANGANESE CONTENT

B. BOŽIĆ and N. VIDOJEVIĆ
School of Technology, Beograd

Isothermal decomposition of Hadfield steel austenite, either in direct or indirect decomposition after cooling, was found to begin at 450—700°C by the separation of carbide. At temperatures from 450 to 650°C the separation of carbide was followed by the separation of perlite. The transformation of austenite was not completed at any temperature studied. However, the transformation of austenite was accompanied with an increase of steel hardness. The effect of perlite on the hardness was much greater than that of carbide. By comparing the decomposition kinetics of the two different thermal treatments it was established that the transformation of austenite during isothermal decomposition after cooling started earlier than the direct isothermal decomposition. It was evident that a sudden cooling in water from the austenitization temperature yields a great number of cavities in the crystalline structure of the austenite which accelerate the formation of centers for the crystallization of the carbide phase.

GROWTH RATE OF PROEUTECTOID BETA PHASE IN A URANIUM-NIOBIUM ALLOY

B. DJURIĆ
Boris Kidrič Institute of Nuclear Sciences, Vinča

The rate of one-dimensional growth of proeutectoid beta phase in a uranium-2 wt.% niobium alloy at 680°C and 690°C was determined experimentally. It was found that the rate was proportional to time to the power ($-^1/_2$). Theoretical considerations assuming a diffusion controlled growth rate lead to the same relationship. It was concluded that the rate of the process is determined by the rate of diffusion of niobium in uranium.

DIRECTION OF CELLULAR GROWTH AS A FUNCTION OF THE CURVATURE OF THE SOLID-LIQUID INTERFACE

DJ. MILOSAVLJEVIĆ

Boris Kidrič Institute of Nuclear Sciences, Vinča

According to the literature, the direction of cellular growth depends on the crystallographic orientation of the specimen and the rate of growth. However, the experimental data presented in this work do not support this conclusion.

In a study on the direction of cellular growth, polycrystal tin specimens (99.98% *Sn*) having a different curvature of the solid-liquid interface were grown from the melt. It was found that the grain orientation had no effect on the cellular substructure continuity, and that the cells were always oriented normal to the solid-liquid interface. A hypothesis has been set up that the direction of the cellular growth is a function of the curvature of the solid-liquid interface.

ELECTROMETRIC DETERMINATION OF SULFUR IN IRON AND STEEL BY A COMBUSTION METHOD

LJ. NEDELJKOVIĆ, M. JOVANOVIĆ and R. OBRADOVIĆ

School of Technology, Beograd

The disadvantage of Holthaus's combustion method for the determination of sulfur is that the titration end-point is detected visually. We succeeded in determining the titration end-point of the sulfuric acid generated either *pH*-metrically or by biamperometric titration with bismuth electrodes.

CONDITIONS FOR THE PRODUCTION OF CHARCOAL PIG IRON

V. G. LOGOMERAC

School of Technology—University of Zagreb, Department of Metallurgy, Sisak

The possibilities of obtaining high grade concentrates from relatively poor iron ores offer good perspectives for the production of high quality pig iron using charcoal as reducing agent. This is particularly of interest in areas whose climate is suitable for plants used for charcoal production.

Yugoslavia is one of the countries which export most of their charcoal. This charcoal is of metallurgical quality.

Data on blast furnaces suitable for charcoal are presented and operating details, results and indicators are given. A comparison of operating and other data for the production of high quality pig iron using charcoal and metallurgical coke is given.

SHRINKING OF GREY CAST IRON

M. BRANKOVIĆ

School of Technology, Beograd

Factors affecting the shrinking of grey cast iron and influencing its behavior during transition from liquid to solid state are presented. Big volume change occuring during the transition lead to the formation of pores, on account of which the castings are of poor quality. In addition, abnormal shrinking causes strain which sometimes results in the appearance of fissures inside castings. The investigations indicate that by adjusting various factors undesirable consequences could be avoided, and the number of sub-standard castings could be reduced.

THE EFFECT OF THE FINAL ROLLING TEMPERATURE ON THE DEFORMATION CAPACITY OF *FeSi 3,2* ALLOY

B. MIŠKOVIĆ and N. MIŠKOVIĆ

School of Technology, Beograd

The results of a study on the effect of the final rolling temperature (750—850°C) on the deformation capacity are presented and an interpretation of the data is given. The deformation capacity was determined by measuring the pressure of the metals on the rollers. A study was also made of the effect of the final temperature of hot rolling on the deformation capacity in cold rolling at room temperature. Analysis of the curves obtained showed a dependence of the resistence to deformation on the degree of deformation.

HYDROMETALLURGICAL TREATMENT OF COPPER TAILINGS OBTAINED IN THE FLOTATION OF BOR COPPER ORES

M. SPASIĆ, D. VUČUROVIĆ, I. ILIĆ and R. VRAČAR

School of Technology, Beograd

Leaching of the copper tailings was investigated. In order to extract copper, they were treated with dilute aqueous solutions of sulphuric acid with or without additives. The methods of percolation, aeration and agitation were applied. The results indicate that further investigations on a semi--industrial scale might be of interest for working out a process for better utilization of copper.

INVESTIGATIONS OF THE POSSIBILITY OF OBTAINING MANGANESE FROM POOR MANGANESE ORES AT NOVO BRDO, KOPAONIK

M. SPASIĆ, D. VUČUROVIĆ, R. VRAČAR and I. ILIĆ

School of Technology, Beograd

A short review of the results of hydrometallurgical treatment of the ores is presented. The investigations covered many different methods whose aim was the sulphatization of manganese and its dissolution. The authors studied the procedure and give conditions for a 95—96.5% extraction of manganese.

THE INFLUENCE OF ZINC CONTENT IN MANGANESE CONCENTRATE ON THE UTILIZATION OF MANGANESE IN THE REDUCTION PROCESS, AND ON THE QUALITY OF FERROMANGANESE

J. KRIŠTO

Trepča Institute for Lead and Zinc, Zvečan

The production of ferromanganese with a high carbon content from manganese concentrate obtained by hydrometallurgical treatment of poor manganese ores of the psilomelane type was investigated. The concentrate

contained 1—12% of zinc, 52—56% of manganese, 2—8% of iron, 0.3—1% of sulphur, 0.07—0.15% of phosphorus, etc.

It was established that the utilization of manganese was only slightly reduced by the presence of different amounts of zinc.

The ferromanganese produced was of the following quality: 76—78% of manganese, 0.17% of phosphorus, 0.05% of sulphur, and 6.2% of carbon. The dust had a high zinc content and could be used as a raw material for zinc production.

THERMOMECHANICAL TREATMENT OF *Cu* 58 *Zn Pb* BRASS IN THE PLASTIC STATE

S. BLEČIĆ

School of Mining and Metallurgy, Bor

Diagrams of plasticity, resistence to deformation, recrystalization and state for *Cu* 58 *Zn Pb* brass are presented. They are interpreted, and conclusions on the optimum thermomechanical parameters for the treatment of this brass in the plastic state are given.

METALLURGICAL CONCENTRATION AND PRODUCTION OF INDIUM FROM INTERMEDIATES OF ZINC PRODUCTION

B. DJURKOVIĆ and D. SINADINOVIĆ

School of Technology, Beograd

The results of laboratory investigation of the metallurgical concentration of indium from intermediates of zinc production (Zorka chemical works, Šabac) are described. The following intermediates were used as raw materials: the residue left after leaching of zinc, the residue left after leaching of cadmium sponge, and oxide sublimate obtained by the Wälz-process from the residue left after leaching of zinc. In order to concentrate indium the above materials were treated pyrometallurgically and hydrometallurgically. Ion exchange was used to concentrate indium in the solution.

THE BEHAVIOR OF WALLS AND INDIVIDUAL BRICKS OF REFRACTORY LININGS OF VARIOUS METALLURGICAL FURNACES

D. CVETKOVIĆ

School of Mining and Metallurgy, Bor

This work continues our study on the behavior of walls and bricks of furnace linings. The walls and bricks were of various kinds of refractory material (fire-clay, silica, magnesite and chromite) and the investigations were carried out on Siemens-Martin, electric-arc, and open-hearth furnaces, blast furnaces for copper, reverberatory and rotating furnaces, etc. From the data obtained a regularity in the behavior of different materials under various conditions was observed. Detailed interpretations of the behavior of bricks are discussed, giving an answer to the question of primary and secondary causes of the present behavior of refractory materials. Conclusions were also drawn and verified in practice.

HEAT TRANSFER FROM A FLAT HORIZONTAL VIBRATING DISK DURING BOILING

M. MITROVIĆ, M. BILIĆ and B. DJORDJEVIĆ

School of Technology, Beograd

Heat transfer from a thin flat horizontal copper disk to water was measured during boiling of the water on the surface of the disk at atmospheric pressure, under conditions of natural convection and with harmonic vibrations of the plate normal to its plane. The diameter of the plate was ¢50 *mm*. The amplitude of vibrations was 0—3 *mm* at a frequency of 20—50 c/s. The heat flux from the plate during boiling was varied from 1.10^4 to 7.10^4 $Kcal/m^2h$.

The results show that heat transfer increased with increasing amplitude and frequency of the vibration, the rate of increase decreasing with increasing of the frequency. The higher the heat flux the less the effect of the vibration on heat transfer. In these experiments the maximum increase of heat transfer with respect to natural convection was 450%.

CONTRIBUTION TO THE THEORY AND PRACTICE OF SCALING BY MODELING

A. DEDIJER

School of Technology, Beograd

Scaling of technological processes is considered as one among the most difficult tasks connected with the design and industrial realization of processes in the chemical industry. Empirical experiments and mathematical analysis of phenomena occurring during scale-up give only *approximate* solutions and are extensive and expensive.

The similarity principle and physico-mathematical methods allow more effective guidance of experimental and theoretical study. Process modeling represents a further advance in this technique in which, by generalization of conclusions based on the similarity principle and obtained experimen-

tally it is possible to scale up or down from one system (the original one) to another.

This work presents a new concept in modeling some phenomena identified on a small, laboratory or pilot scale, which have to be scaled up to industrial. It is concerned with statics, dynamics, heat and mass transfer, thermodynamics and chemical kinetics.

IMPROVEMENT OF UNIT OPERATIONS IN THE PRODUCTION OF ANTIBIOTICS

V. ALIĆ

Prva Iskra, Barič, Beograd

Secondary vapors of low condensation temperatures are of importance in unit operations of antibiotics production where low operating temperatures are required. The condensation temperatures of secondary vapors and at the same time the operating temperatures are limited by the temperature of the cooling water. Small temperature differences mean a high water consumption.

In the distillation, rectification, extraction and drying of thermolabile material in vacuum secondary vapors can be condensed either with cold water provided by refrigerating equipment or by an expanded cooling agent. However, the disadvantage of both systems is the necessity of water for the condenser of the refrigerating equipment.

The author's suggestion avoids the use of water in the following way. Secondary vapors are condensed by a combination of equipment for vacuum distillation, rectification, extraction and drying and parts of a refrigerating system such that heating is effected by the compressed cooling agent while the secondary vapors are condensed by the expanded cooling agent. In this system, two separate fluids for heating and cooling are not required, but only an electrically controlled compressor. The problem of pressure in the heating space of the equipment can be solved by a well chosen design.

OPTIMIZATION OF PROCESS DESIGN BY MEANS OF A MECHANICAL MATHEMATICAL MODEL

A. DEDIJER

School of Technology, Beograd

There have been various attempts to automate process design optimization, but none — without regard to author's authority — have given any real results. The essential cause of this failure is that in spite of all the progress of technology and systematization, man has remained the basic creative force — he is still the only one who can analyze and evaluate new situations, coordinate and schedule them, improve them, and above all, create them.

The aim of this work is to consider the combination of a man as creator and technology in design. A "mechanical mathematical model" helps liberate man's creative potential from tedious and cumbersome calculations, and allows it to take up more essential creative functions which lead to the choice of an optimum solution.

In addition to the identification of basic requirements and characterization of the construction and manipulation of a "mechanical mathematical model" on a chemical industrial process as an example, a method of choosing a practical optimum solution is described as well.

DYEING OF "MALON" FIBER IN THE PRESENCE OF ALCOHOL

D. DŽOKIĆ

School of Technology, Beograd

The adsorption properites of polyacrylonitrile fiber, "Malon", in dyeing with basic dyes were investigated. The fiber was a product of Organic Chemical Industry of Skoplje.

Dyeing was carried out in the absence of alcohol, and in the presence of methyl, ethyl, *n*-propyl, *n*-butyl, *n*-amyl, *n*-hexyl and benzyl alcohol.

It was found that the rate of dyeing, the establishment of the equilibrium, and the time of half-dyeing were affected by the nature and the concentration of the alcohol. In all cases studied, a higher degree of dyestuff utilization was achieved in the presence of alcohol.

THE EFFECT OF THERMAL TREATMENT OF "MALON" FIBER ON THE ADSORPTION OF DYES

D. DŽOKIĆ and R. TRAJKOVIĆ

School of Technology, Beograd

The adsorption of dyes on "Malon" fiber treated at temperature from 100 to 180°C in different media (hot air, hot water, water vapor) or heated by an infra-red lamp was studied.

It was established that the rate of dye fixation, the half-dyeing time and the maximum degree of dyestuff utilization depended on the treatment, i.e. on the temperature, the medium and the time.

STABILIZATION OF POLYAMIDE TEXTILE FABRICS

D. DŽOKIĆ and S. KOVAČ

School of Technology, Beograd

The effect of stabilization — thermofixation — on the properties of polyamide textile fabrics was examined. Washed and dyed raw fabrics were used.

The stabilization was carried out in different media (hot air, hot water, water vapor) by heating with an infra-red lamp and in aqueous solutions of various organic and inorganic materials.

The effect of the temperature and time on stabilization was examined, and the optimum conditions of treatment were determined.

DECOMPOSITION KINETICS OF SOME FLUORESCENT DYES FOR THE "OPTICAL BLEACHING" OF CELLULOSE TEXTILE FABRICS UNDER *UV* IRRADIATION

R. RUNAC, LJ. POPOVIĆ and V. MIJOVIĆ

Institute of Chemistry, Technology and Metallurgy, Beograd

Decomposition kinetics of fluorescent dyes synthesized from stilbene derivatives, and of corresponding dyes of foreign production (Blankophor, Tinopal) was investigated. The dependence of decomposition upon the irradiation time was expressed in terms of the fluorescence intensity of the textile.

The decomposition rates were expressed in the form of rate constants of a first-order reaction, as the percentage of the fluorescent dye decomposed in the course of one hour. The analysis of log-linear curves showed that the decomposition of fluorescent dyes under the influence of *UV* irradiation was accompanied by two parallel first-order reactions with different rate constants (K_1 and K_2).

THE APPLICATION OF DIMETHYLOL DERIVATIVES OF ETHYLENECARBAMIDE AND DIHYDROXYETHYLENECARBAMIDE FOR THE MODIFICATION OF PROPERTIES OF CELLULOSE TEXTILES

LJ. POPOVIĆ, V. MIJOVIĆ and R. RUNAC

Institute of Chemistry, Technology and Metallurgy, Beograd

Ethylenecarbamide and dihydroxyethylenecarbamide were obtained by the condensation of carbamide with ethylenediamine and glyoxal, respectively, by addition of formaldehyde these products were converted into the corresponding dimethylol derivatives. The effect of experimental conditions on the course of the syntheses was investigated.

The conditions for the application of the products synthesized for the improvement of cellulose textiles was studied with a view to obtaining optimum crease-resistance and non-ironing property.

CHANGE OF THE CONSISTENCY OF SODIUM DODECYLSULPHONATE PASTE

V. MIJOVIĆ, R. RUNAC and LJ. POPOVIĆ

Institute of Chemistry, Technology and Metallurgy, Beograd

Viscosity and density changes of sodium dodecylsulphonate paste (produced by Prva Iskra-Barič) in the temperature range from 35 to 90°C were investigated.

The change in percentage composition across a vertical section through a sample obtained under definite cooling conditions was also studied.

DETERMINATION OF THE STABILITY OF SODIUM HYDROSULPHITE AS REDUCING AGENT FOR VAT DYES

D. DŽOKIĆ and B. TIRNANIĆ

School of Technology, Beograd

In dyeing of cotton fabrics with vat dyes, sodium hydrosulphite is decomposed by air oxygen.

The stability of aqueous sodium hydrosulphite solution at temperatures ranging from 20° to 100°C was examined and compared with the stability of sodium hydrosulphite on cotton fabric worked up on foulard and then exposed to air and water vapor.

The stability of sodium hydrosulphite in the presence of various salts and the stability of its alkaline solutions were also studied.

Izdavač:

IZDAVAČKO PREDUZEĆE "NOLIT", BEOGRAD, TERAZIJE 27/II

•

Štampa:

GRAFIČKO PREDUZEĆE "PROSVETA", BEOGRAD,
ĐURE ĐAKOVIĆA 21

SRPSKO HEMIJSKO DRUŠTVO (BEOGRAD)

BULLETIN OF THE CHEMICAL SOCIETY Belgrade

(Glasnik Hemijskog društva — Beograd)
Vol. 32, No. 2-3-4 1967

Published by
SRPSKO HEMIJSKO DRUŠTVO (BEOGRAD)
1967

Translated and published for U. S. Department of Commerce and the National Science Foundation, Washington, D.C., by the NOLIT Publishing House, Terazije 27/II, Belgrade, Yugoslavia

Translated by
IVAN STOJANOVIĆ

Edited by
PAUL PIGNON

Printed in "Prosveta", Belgrade

CONTENTS

GLASNIK HEMIJSKOG DRUŠTVA, Vol. 32, No. 2-3-4, 1967, pp. 125—136

METHODOLOGICAL ASPECTS OF THE STUDY OF COMPLEX CHEMICAL REACTIONS. III.

ESTIMATION OF PLAUSIBILITY OF DIFFERENT INTERMEDIATE STATES AND UNIT STEPS

by

ALEKSANDAR R. DESPIĆ and PETAR M. RAKIN

I. INTRODUCTION

In the first paper of this series[1] an attempt was made to formulate a discriminatory criterion which would permit analysis of all forseeable intermediate states, with respect to the plausibility of their participation in the reaction path of a complex chemical reaction. This was found as a combination of thermodynamic and kinetic considerations, essentially based on the model used in transition state theory. Experience in subsequent attempts to apply this criterion indicated that more precise definitions of certain terms were needed, and also some revision of the formulation of the criterion itself. It is the purpose of this communication to clear up some of these problems.

II. ENERGETICS OF COMPLEX REACTIONS AND THE DISCRIMINATION CRITERION

In the first formulation of the discrimination rule the basic condition was that no intermediate species should have a potential energy higher than that of the activated state, and hence the enthalpies of different intermediates relative to that of the initial state had to be compared with the activation energy (i.e. enthalpy difference between the transition state and the initial one). However, the essential idea of the discrimination rule was to compare the concentration of the activated complex of the RDS, i e. of the reaction as a whole, with the concentration of the activated complex of any given potential unit step, it being maintained that (in case of equal stoichiometric numbers of the two steps) the latter cannot be lower than the former since otherwise it would control the overall reaction rate and itself be the rate determining step. This being the case it appears that the standard free enthalpies of activated complexes of the potential intermediate unit steps relative to the initial state should be compared with the free ent-

halpy of activation, since it is these thermodynamic quantities that directly govern the maximum (i.e. equilibrium) concentrations of the species involved for a given set of concentrations of the species constituting the initial state.

The free enthalpy of activation can be assessed directly from the rate constant if transition state theory is assumed to be applicable. Hence, no temperature dependence of the rate constant or assumptions concerning the entropy of the activated state are needed. However, it should be noted that $\Delta \overset{+}{G}{}^{0+}$ calculated from the equation

$$K = \frac{kT}{h} \exp\left(-\frac{\Delta \overset{+}{G}{}^{0+}}{RT}\right) \tag{1}$$

is a deficient free enthalpy change and cannot be directly used for calculating the concentration of the activated complex. The full value of the standard free enthalpy of the activated state referred to the initial state should be larger by a term equal to the logarithm of one translation partition function multiplied by RT. This can be accounted for if the energy equipartition principle is used and the experimental value corrected by adding a fraction of it corresponding to the reciprocal of the total number of degrees of freedom of the activated state. Although this requires making assumptions concerning the structure of the activated state, in most cases of complex systems this number must in any case be so large that the correction can be neglected for all practical purpose.

The concentration of the activated complex of the potential intermediate unit step cannot be known since no data exists about the rate of this step. However, it can be taken as certain that this concentration cannot be larger than the concentration product of the intermediate state from which the unit step process develops, since the absolute rate theory equilibrium constant cannot be larger than 1, i.e. the standard free enthalpy of activation cannot be negative. Hence the potential unit step can be considered plausible only if the concentration product of the species taking part in it is larger than the concentration of the activated complex of the RDS. The former is again defined by a quantity which may be termed the free enthalpy of formation of the intermediate state from the initial state and a concentration term accounting for departure of the concentrations of the corresponding species in the initial state from unity.

III. INITIAL STATE IN THE ENERGETICS OF COMPLEX REACTION PATHS

In the above considerations the "initial" state is chosen as a reference state to which the free enthalpies of the intermediate states are referred. Some points in the definition of that state which may otherwise be a cause of considerable misunderstanding must be cleared up. It could seem logical to take as the initial state the thermodynamic initial state as indicated by the left-hand side of the stoichiometric equation of the overall reaction. However, it was concluded by Eyring, Laidler and Glasstone[2] that as

far as the transition state is concerned, irrespective of how complex a reaction may be, the initial state is always defined by the rate equation, in the sense that the concentration factors in a rate equation of the type

$$\text{rate} = \frac{dc_i}{dt} = KC_A^a C_B^b \cdots C_I^i \cdots C_X^x \qquad (2)$$

indicate the equilibrium between the initial state P and the transition state T described by the stoichiometric equation

$$P = aA + bB + \cdots iI + \cdots xX \rightleftarrows M^+ = T \qquad (3)$$

Needless to say, in most cases this is different from the thermodynamic initial state. The stoichiometric factors in such an initial state indicate how much (in moles) of the corresponding stable species — reactants — is consumed before the energy barrier, and the difference between these amounts and the amounts pertaining to the overall process indicate the consumption of the reactants after the RDS. Thus they are some indication of the position of the barrier along the reaction coordinate.

One should note, also, that the concentrations of species in the reference state are all equal to unity, since the free enthalpy of activation is calculated from the rate constant, i.e. the specific rate at unit concentration of the reactants.

If it is assumed that an intermediate state can be built from those elements alone and from the numbers of moles contained in the activated complex, then the potential intermediate states must be related to the same initial state as defined above in estimating the standard free enthalpy change. However, this need not be the case. First of all, an intermediate state may require the formation of a different number of moles of the same species, and second, other species present can also contribute to its formation. Obviously these would have to drop out somewhere further along the reaction path before the energy barrier and hence act as a kind of catalyst for unit steps preceeding the *RDS*. To illustrate this let us consider the following example. Suppose that in the electrooxidation of ammonia in aqueous solution the reaction of activated-complex formation is

$$a\,NH_3 \rightleftarrows (NH_3)_a^*$$

Obviously, an intermediate state

$$a\,NH_3 \rightleftarrows a(NH + H) \rightleftarrows (NH_3)_a^*$$

could be interpolated but it would be highly improbable because of the high free enthalpy changes involved in the formation of atomic hydrogen. Molecular nitrogen is present in the system but it is outside even the thermodynamic initial state (since it is a reaction product). If this is taken into account the set of reactions can be written

$$a\,NH_3 + a\,N_2 \rightleftarrows 3\,a\,NH \rightleftarrows (NH_3)_a^* + a\,N_2$$

The intermediate state *NH* is certainly much more probable than the one above. Hence, any intermediate state as a basis for a unit step should be investigated by the plausibility criterion if it can be formed from any of the stable species present in the system. The definition of the initial state should then be extended to encompass all the species needed for the formation of the intermediate state concerned as well. Correspondingly, the transition state should encompass not only the activated complex but also the other stable species, not taking part in the formation of the complex but forming the initial state, and also the intermediate state should contain the rest of the stable species in their original state as well as those forming a basis for the unit step. The situation is illustrated in Fig. 1.

On the grounds of the qualitative arguments given above it is possible to derive the plausibility criterion as follows:

$$(\pi C_i^{\prime})_I > C_A^{\ddagger} \quad \text{or} \quad \ln \pi (C_i^{\prime})_I > \ln C_A^{\ddagger} \tag{4}$$

where $(\pi C_i^{\prime})_I$ is the concentration product for the participants in the unit step, and $C_A^{\ddagger}$ is the concentration of the activated complex of the RDS.

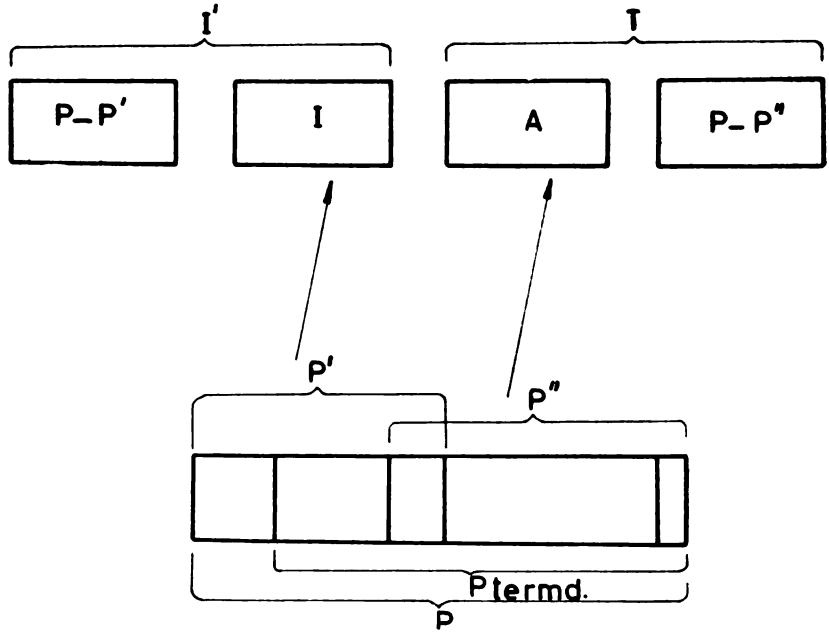

Figure 1

Schematic representation of the formation of an intermediate state and the transition state from an initial state.

It is seen from Fig. 1 that

$$\Delta G^0_{I'-P} = G^0_I + G^0_{P-P'} - G^0_{P'} - G^0_{P-P'} \tag{5}$$

and

$$\Delta G^0_{T-P} = G^0_A + G^0_{P-P''} - G^0_{P''} - G^0_{P-P''} \tag{6}$$

Hence

$$\Delta G^0_{I'-P} = G^0_I - G^0_{P'} = \Delta G^0_{I-P'} \tag{7}$$

is the standard free enthalpy of formation of one set of species forming the intermediate state from the initial state, and

$$\Delta G^0_{T-P} = G^0_A - G^0_{P''} = \Delta G^0_{A-P''} \tag{8}$$

is the same entity corresponding to the formation of the activated complex.

Since these participants forming the intermediate state I are in equilibrium with the part of the initial state P', we can write

$$\ln (\pi C_i^i)_I = \ln K_c + \ln (\pi C_j^j)_{P'} \tag{9}$$

where $(\pi C_j^j)_{P'}$ is the concentration product of the species which are outside the kinetic initial state P''.

From the known relation between K_c and the standard free enthalpy change of the process underlying the equilibrium it follows that

$$\ln (\pi C_i^i)_I = -\frac{\Delta G^0_{I-P'}}{RT} - \Delta n_{I-P'} \cdot \ln (V)_{P'} + \ln (\pi C_j^j)_{P'} \tag{10}$$

where Δn is the change in the number of moles in the formation of the states from the corresponding initial state and V is the molar volume of the system in equilibrium expressed in the same units as the concentration.

Similarly, for the activated state of the *RDS*

$$\ln C_A^{+} = -\frac{\Delta G^0_{A-P''}}{RT} - \Delta n_{A-P''} \ln (V)_{P''} \tag{11}$$

Hence

$$\Delta (\Delta G^0) = -\Delta G^0_{I-P'} - \Delta n_{I-P'} RT \ln (V)_{P'} - RT \ln (\pi C_j^j)_{P'} + \Delta G^0_{A-P''} + \Delta n_{A-P''} RT \ln (V)_{P''} > 0 \tag{12}$$

is the quantitative expression of the criterion. The concentration term takes account of the fact that the concentrations of species in the initial state *other than those* participating in the formation of the activated complex of the *RDS* need not be unity.

The last two terms in equation (12) represent the experimentally determined free enthalpy of activation ΔG^{0+}.

Since one should compare the free enthalpy of formation of *one* set of intermediate species rendering the activated complex of the unit step

with the standard free enthalpy of formation of one activated complex of the *RDS*, *the initial state must be the sum of as many moles of the different species as are necessary for the formation of the set and the activated complex of the RDS*. To form the concentration term those elements which the former and the latter have in common should be taken to be at unit concentration, while the rest should be taken at the concentrations actually present.

Obviously, the standard free enthalpy change between the intermediate and the initial state $\Delta G^0_{I-P'}$ can be calculated from the thermodynamic data for the standard free enthalpies of formation of the corresponding compounds.

It should be noted that in deciding that a unit step may be discarded on the grounds of the criterion it is assumed that in the mechanism it might take part in it could only participate with a stoichiometric number equal to that of the *RDS*. Naturally this need not be so. The chance for a unit step to take part increases the lower the stoichiometric number since then a lower concentration product can still give the rate necessary for maintaining the observed production of the activated state. However, stoichiometric numbers five to ten times smaller than that of the RDS are highly improbable. Even a that much smaller concentration product involves only a very small reduction in the $\Delta G^0_{I-P'}$ because of the exponential dependence. Hence, this factor can be neglected in using the plausibility criterion.

An extension of the discrimination rule has been suggested by Dragojević* based on the idea that no state more stable than the thermodynamic final state of the reaction can be an intermediate state, since otherwise the reaction would terminate at it. The standard free enthalpy of the final state relative to the thermodynamic initial state is obviously given by the ΔG° of the reaction.

Hence, this represents the lower limit of $\Delta G^0_{I-P'}$ and the criterion is extended to

$$\Delta G^0_{I-P'} > \Delta G^0_{total}$$

IV. APPLICATION OF THE CRITERION TO THE EXAMPLE OF THE ELECTROOXIDATION OF AMMONIA

To test the method the example of the electrooxidation of ammonia was worked out since some kinetic data were at hand[3]. One should note, though, that difficulties had to be overcome which would not have been met had a system been selected and specially worked out experimentally for this purpose. They were: (a) the available experimental data did not allow determination of the reaction order with respect to one of the reactants, viz. OH^- ions, since their concentration was maintained constant throughout the experiments; (b) the treatment of the heterogeneous reaction required assumptions about the free energies of hemisorption which are known with much less certainty than the homogeneous phase free energy

* Departmental discussion of the subject held December 1966.

changes; (c) an additional uncertainty, inherent in electrochemical reactions, is the need to estimate either the absolute value of the potential difference across the interface or the free enthalpy change of the electron exchange reaction of the reference electrode.

Still, the results were considered to be ilustrative enough to warrant this presentation.

To obtain an approximate value of the free enthalpy of activation the following equation was assumed to hold:

$$\frac{i}{zF} = \frac{kT}{h} \exp\left(-\frac{G^{0+}}{RT}\right) \exp(BV) \exp(BE)(C_{NH_3})^a(C_{OH^-})^b(1-\theta)^c \quad (13)$$

where i is the measured current density at a potential difference V between the reference electrode and the electrode under investigation, E is the absolute value of the reference electrode potential (for the reference electrode employed it was assumed to be approximately equal to the zero charge potential, i.e. $+0.19\ V$), z is the number of electrons exchanged in the overall reaction and B is a factor of the type F/RT, depending on the number of electrochemical steps occurring before the rate determining step.

The concentration factors (C_{HN_3}) and (C_{OH^-}) are bulk concentrations.

In calculating ΔG^{0+} from equation (13), a reaction order of 1 is taken for NH_3 (on the basis of (3,4)), while the reaction order with respect to OH^- was considered irrelevant since $C_{OH^-} \sim 1$.

Also it was assumed that all the species at the surface are mobile and hence the concentration of metal sites for adsorption does not enter into equation (5) but only a geometrical factor $(1 - \theta)$. High values of surface coverage by the different species were assumed and a reaction order of 1 was also assumed for the participation of free surface sites in the formation of the activated complex.

Experimental values of the quantities i (at constant V) and E, based on galvanostatic investigation of the electrooxidation of ammonia in alkaline electrolytes described earlier[3] are listed in Table 1.

TABLE 1

Standard free enthalpies of activation for the anodic oxidation of ammonia at different ammonia concentrations

$T = 300°K$; $V = 0.450\ V$; $E = 0.190\ V$; $\theta = 0.9$

C_{NH_3} (g mol/l)	i (A/cm^2) · 10^5	B	ΔG^{0+} (Kcal/mol)
5.00	25.00	47	10.1
3.20	14.5	42	11.1
0.48	1.15	42	12.3
0.36	3.8	48	9.6
0.07	3.8	47	8.8
		average	10.4

Calculated values of ΔG^{0+} are also listed in Table 1.

For rates (i) at a constant potential (—0.450 *V Hg/HgO*) electrode it is seen that an approximately constant free enthalpy of activation is obtained for varying bulk concentration of ammonia.

To calculate standard free enthalpies of intermediate states relative to corresponding initial states, the standard free enthalpy of formation ΔG_f^0 for each species involved was estimated.

The species that are potential participants of the initial states are $NH_3(aq)$, $OH^-(aq)$, $N_2(aq)$, $H_2O(aq)$, $H^+(aq)$ and e(metal). ΔG_f^0 for $NH_3(aq)$, $H_2O(aq)$ is found in thermodynamic tables (6), while that of N_2 is zero by definition. That of $H^+(aq)$ was first calculated by accounting for the formation of H atoms from H_2 (ΔG_f^0 from tables (6)) and then for the heat and entropy of ionization of H in the gaseous phase and its dissolution into the electrolyte. ΔG_f^0 for $OH^-(aq)$ was calculated as the difference between that for ionized water and that for the formation of $H^+(aq)$. ΔG_f^0 for the ionized water was obtained from that of $H_2O(aq)$ by adding the energy of ionization and taking into account the entropy change. The standard free enthalpy of formation of an electron in the metal was taken as equal to the work function of platinum.

All species participating in intermediate states are considered to be absorbed at the surface, except OH^- ions and molecular nitrogen since the former is unlikely to be adsorbed at negative potentials (used), while the latter is known to undergo only dissociative adsorption[7, 8].

To obtain the ΔG_f^0 for $NH_3(ads)$, the ΔG_f^0 of adsorption is added to the value for $NH_3(aq)$ obtained earlier. ΔG_0 can be estimated in two ways. The heat of adsorption is first obtained by using an estimated value (—40 *kcal/mol*) for gaseous phase adsorption on platinum in a process analogous to that used by Gileadi[9] for adsorption of ethylene from aqueous solution, it being taken that this adsorption is in effect also an exchange process in which two molecules of ammonia from solution replace three water molecules fixed to the surface. A value of —13 *kcal/mol* was thus obtained. This was checked against the value obtained by the second method which consists of taking the heats of adsorption of NH_2 and H radicals and the energy of NH_2—H bond formation, which is the same as the dissociation energy for the ammonia molecule[10]. Values in the range —7 to —17 *kcal/mol* were obtained. In both cases a term for the standard entropy of adsorption was added. The latter was considered not to be outside the range of ± 10 *kcal/mol* °*K*, but a closer estimate could not be made.

The heat of adsorption of water from the aqueous phase was estimated to be —12.4 *kcal/mol* by taking the data for the gas phase adsorption and for dissolution of water in water cited in the literature[11]. A considerable entropy change occurs in this process, and —10 to —20 *cal/mol* °*K* was taken as the probable value. The ΔG° of adsorption from the Gibbs-Helmholtz equation was added to the value for the H_2O molecule in the bulk, giving ΔG_f^0 for $H_2O(ads)$.

A similar procedure was used for obtaining ΔG_f^0 for all the other intermediate species adsorbed at the surface. Thus for NH_2 and NH radicals

the heat of adsorption was taken as equal to and double that for adsorption of atomic hydrogen, respectively, since there are indications[10] that a single M—N bond in an amine is of the same strength as the M—N bond. That heat of adsorption was taken to be —61 *kcal/mol*, as estimated by Breiter[12]. The heats of formation of these radicals in the gas phase were taken from Altschuler[13] and hence ΔH_f^0 for all three species obtained. The standard entropy of formation of $H(ads)$ is also given by Breiter [12], while for $NH_2(ads)$ and $NH(ads)$ radicals it was taken to be the standard entropy of formation in the gas phase ± 10 *cal/mol* °K[6] — since the entropies of adsorption for these species were unknown.

The standard enthalpy of formation of $(NH)_2(gas)$ was not available and was hence calculated using the approximate formula of Pauling[14]. Since the standard entropy of formation was not known, this term was neglected and it was taken that $\Delta G_f^0 = \Delta H_f^0$. The heat of adsorption of this species was calculated, assuming dissociative chemisorption, from the known heat of adsorption of NH and dissociation energy of $(NH)_2$. The entropy of adsorption was taken to be within the limits of ± 10 *cal/mol*.

ΔG_f^0 for $(NH_2)_2(gas)$ was calculated from the tabulated values of H_f^0 and S^0. The adsorption was treated as in the previous case and thus ΔG_f^0 for $(NH_2)_2$ calculated.

For $NH_2OH(gas)$ only ΔH_f^0 was available. This was taken to be ΔG_f^0. The adsorption was treated as in the previous case and ΔG_f^0 for $NH_2OH(ads)$ calculated.

ΔG_f^0 for $OH(gas)$ was taken from tables (6). The heat of adsorption from the gas phase was obtained using Eley's formula[15], and that from the aqueous phase using Gileadi's procedure mentioned earlier, since other quantities were available from tables. The standard entropy of adsorption was assumed to be within ± 10 *cal/mol*.

TABLE 2

Standard free enthalpies of formation of the species in the initial and intermediate states

Species	ΔG^0 (*Kcal mol*)	Species	ΔG^0 (*Kcal mol*)
$NH_3(aq)$	-6	$(NH)_2$	65 — 77
$N_2(aq)$	0	$(NH_2)_2$	3 — 27
$H_2O(aq)$	-57	NH_2OH	-54 — -28
$OH^-(aq)$	-100	H	-9
$H^+(aq)$	99	H^+	30 — 46
NH_3	-26 — -10	H_2	- 6
NH_2	0 — 16	OH^-	-100
NH	-7 — -19	OH	-34 — -18
N	-33 — -17	H_2O	-66 — -63
N_2	0		

All the values of ΔG_f^0 are presented in Table 2. From it, the standard free enthalpies of different intermediate states relative to corresponding initial states were calculated, using

$$\Delta G^0_{I-P'} = \Sigma i G_i^{0(I)} - \Sigma j G_j^{0(P')}$$

where $G_i^{0(I)}$ is the standard free enthalpy of formation of the species i pertaining to the intermediate state I with a stoichiometric factor i, and $G_j^{0(P')}$ and j are the corresponding quantities for the initial state. A range of possible values is obtained for each unit step because of uncertainties in the calculation of ΔG_f^0. The result is shown in Fig. 2, in which each step is given an ordinal number on the abscissa and its $\Delta G^0_{I-P'}$ is presented as the ordinate. The horizontal line represents the ΔG^{0+}. Hence, only those unit steps whose $\Delta G^0_{I-P'}$ values are below the ΔG^{0+} line should be taken into account for speculations concerning the mechanism of the reaction.

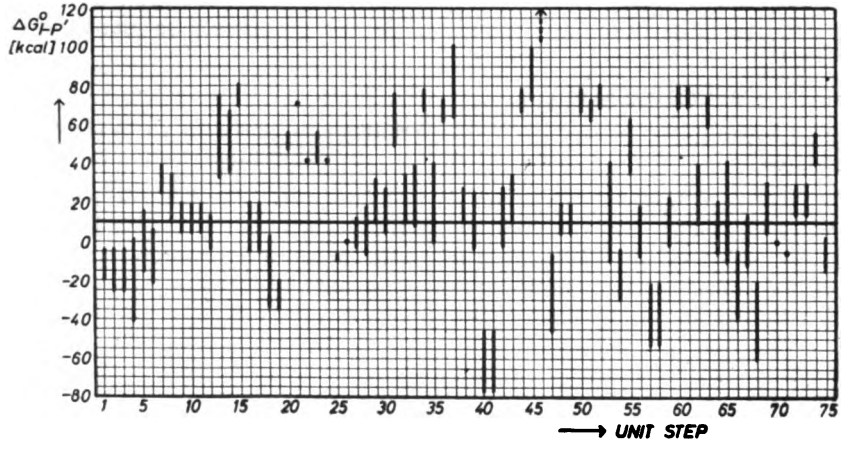

Figure 2

Free enthalpies of intermediate states relative to corresponding initial state for possible unit steps in anodic oxidation of amonia.

The extension of the plausibility criterion for stable intermediate states cannot be applied to heterogeneous reactions, since because of adsorption many intermediate states at the surface will be of more negative G° than the final state of the reaction, merely as a result of the increased concentration of the species at the surface relative to the bulk phase, which has little bearing on the yield of the reaction as a whole.

Hence the list of plausible unit steps obtained by applying the derived discrimination criterion is shown to be shorter than the list of all possible unit steps by 34. It also proves that no intermediate *species* could be a priori excluded from consideration and hence justifies the objection raised against the

conclusion of Spahrbier and Wolf[4] who discarded some intermediates solely on the grounds of standard electrode potential considerations, and further, that contrary to the conclusion of Oswin and Salomon[16], the formation of atomic hydrogen by chemical decomposition of ammonia is a plausible unit step.

School of Technology,
University of Beograd
and Institute of Chemistry, Technology
and Metallurgy, Beograd

Received December 27, 1966.

REFERENCES

1. Despić, A. — *Glasnik hemijskog društva* (Beograd) 30*: 293—903, 1965.
2. Laidler, K., S. Glasstone and H. Eyring. — *Journal of Chemical Physics* 8: 667—676, 1940.
3. Despić, A., D. Dražić and P. Rakin. — *Electrochimica Acta* 11: 997—1005, 1966.
4. Spahrbier, D. and G. Wolf. — *Zeitschrift für Naturforschung* 19a: 614—619, 1964.
5. Salomon, M. — *Journal of the Electrochemical Society* 113: 940—943, 1966.
6. Rossini, F. — *Selected Values of Chemical Thermodynamic Properties* — Washington: United States Government Printing Office, 1952.
7. Hayward, D. and B. Trapnell. *Chemisorption* — London: Butterworths, 1964.
8. Bond, G. *Catalysis by Metals* — New York: Academic Press, 1962.
9. Gileadi, E. — *Journal of Electroanalytical Chemistry* 11: 137—151, 1966.
10. Wahba, M. and C. Kemball. — *Transactions of the Faraday Society* 49: 1351—1360, 1953.
11. Breiter, J. and S. Gilman — *Journal of the Electrochemical Society* 109: 622—627, 1962.
12. Altschuler, A. — *Journal of Physical Chemistry* 22: 1947—1948, 1954.
13. Pauling, L. *The Nature of the Chemical Bond* — New York: Cornell University Press, 1960.
14. Eley, D. — *Discussions of the Faraday Society* 8: 34—38, 1950.
15. Oswin, H. and M. Salomon. — *Canadian Journal of Chemistry* 41: 1686—1694, 1963.

* Available in English translation from Clearinghouse for Federal Scientific and Technical Information, Springfield, Virginia 22151.

GLASNIK HEMIJSKOG DRUŠTVA, Vol. 32, No. 2-3-4, 1967, pp. 137—152

ON THE SPECTROCHEMICAL DETERMINATION OF THE ANTHOCYANOSIDES OF HYBRID ORIGIN

Fluorescence of the 3,5-diglucoside of 3,5,7-trihydroxy-2-(3',5'-dimethoxy--4'-oxy-phenyl) benzopyranol

by

SLOBODAN M. RISTIĆ and JELISAVETA M. BARANAC

1. INTRODUCTION

In his doctoral thesis P. Ribereau-Gayon (1959)[1] studied the anthocyanosides from grapes and wine. He noted that crossing leads to the formation of special diglucosidic anthocyanosides with characteristic properties. According to him, the presence of these anthocyanosides in hybrid grapes, juice and wine can be established by the brick-red fluorescence due to the most abundantly represented anthocyanoside, 3,5-diglucoside of malvidol. This characteristic fluorescence (which in some countries is now legally recommended as for the presence of hybrid diglucosides)[2], will be called the Ribereau-Gayon, or RG-test. This paper deals both with the verification of this test and spectrochemical study of the nature and mechanism of the characteristic fluorescence for which no exact data have been given so far, only some qualitative statements. Such data could have general importance for the 3,5-substitution of all anthocyanols, as has been pointed out by R. Robinson (1936)[3] and J. Harborne (1958)[4].

2. EXPERIMENTAL, MATERIAL, APPARATUS, METHODS

Chemicals were of p.a. purity unless otherwise stated. We had several samples of chromatographically pure anthocyanidols by Fluka A. G. (Switzerland), and a specially purified preparation of malvinoside (3,5-diglucoside 3,5,7-trihydroxy-2(3',5'-dimethoxy-4'-oxyphenyl)-benzopyranol) standardized for the RG-test. The absorption spectra were recorded on a UNICAM SP 500 spectrophotometer. Spectrophotofluorimetry was done on an *AMINCO-BOWMAN* spectrophotofluorimeter (USA). For spectrographic determination of the fluorescent spectrum an ISP-51 spectrograph (with $F = 120\ mm$ and $F = 270\ mm$ cameras) was used.

A well-defined sample of wine made from hybrid vine (with all specifications) was gotten from the Viticulture Institute, Sremski Karlovci,

for which we want to express our gratitude. Some samples of the best known domestic wines were submitted to the RG-test, after being taken from the sealed cases supplied directly from the wholesaler.

Spectrophotometry. Spectrophotometric determinations were carried out in order to define more accurately the absorption spectra obtained on the Aminco-Bowman spectrophotofluorimeter and to check certain deformations of excitation spectra inherent in this instrument[5]. In these determinations special care was paid to checking the wavelength calibration scale by means of standard calibration solutions[6].

Spectrophotofluorimetry measurements on the Aminco-Bowman, in spite of its sensitivity and easy operation nevertheless introduce a certain looseness in the definition of the excitation spectra. The two monochromators of this apparatus do not have a big dispersion, and the excitation spectrum of the sample differs considerably from the absorption spectrum, except under especially favorable conditions. Extensive and critical discussion about the characteristics of this apparatus has already appeared in various publications[7].

Spectrography. The spectrographic method permits precise determination of the especially important wavelength of the fluorescent emission maximum, thereby also checking the accuracy of the calibration scale of the spectrophotometer and spectrophotofluorimeter monochromators. Ilford R-20 emulsion was used. The spectrograms were qualitatively and quantitatively evaluated with a registering microphotometer (Higler).

3. RESULTS AND DISCUSSION

The main anthocyanoside in red wine is 3,5-diglucoside of malvidole whose structure is represented by the formula (I) and whose gross composition can be written $C_{29}H_{35}O\ Cl$. This compound shows a characteristic

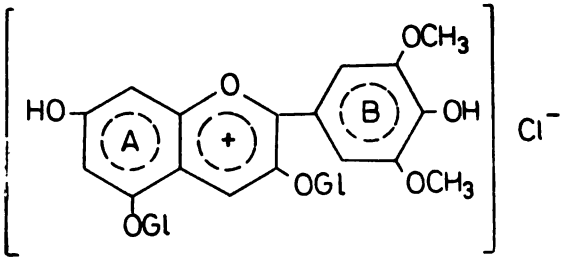

absorption spectrum which greatly depends on medium *pH* and the nature of the solvent. Figure 1 shows the spectral absorption of the three main forms of malvinoside: red cationic form $(Ms)^+$, blue anionic form $(Ms)^-$ and neutral form $(Ms)^{\pm}$.

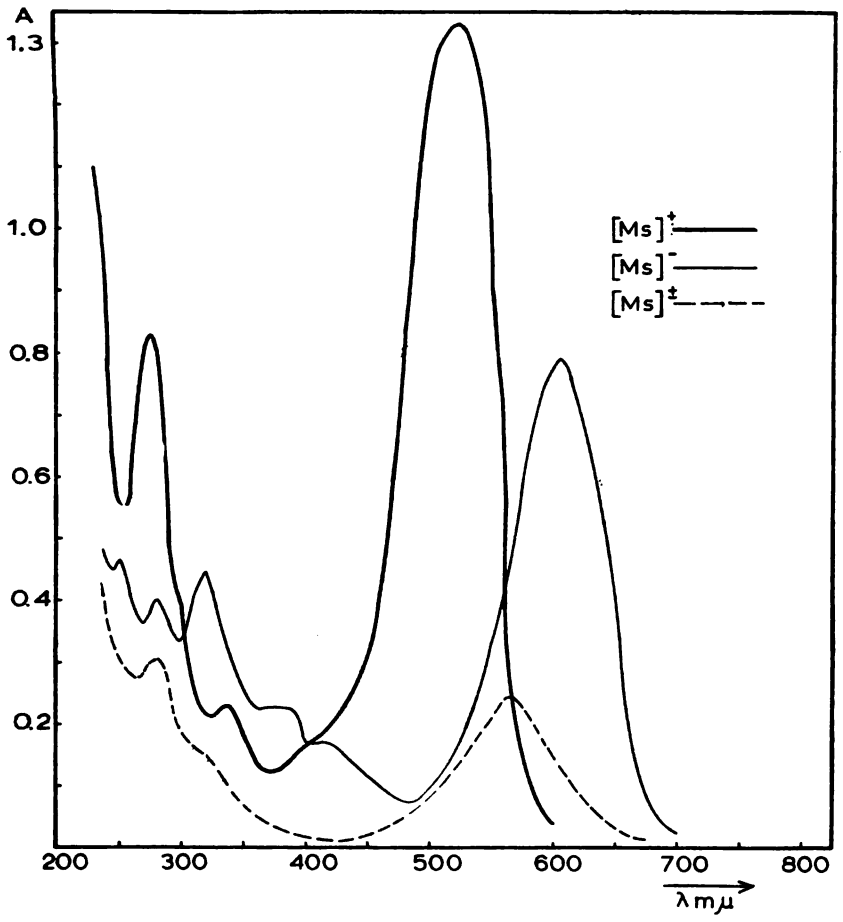

Figure 1

Absorption spectra of malvinoside chloride, conc. 2.10^{-4} *M* in buffer solution of different *pH*: $(Ms)^+$ *pH* = 0.75; $(Ms)^-$ *pH* = 11.75; $(Ms)^{\pm}$ *pH* = 7.10.

Fluorescence of the red cationic form was observed by R. Robinson (1936)[3] and J. H. Harborne (1958/62)[4] and directly associated with the substitution of hydroxyl-5 in the A-ring of the anthocyanide framework with a glucoside residue (further substitution of hydrocyl-3 decreases the fluorescence a little). This fluorescence was first defined by spectrofluorograms measured on the pure standard in methanol (Fig. 2), ethanol (Fig. 3) and isobutanol (Fig. 4), with 0.01% *HCl* added to ensure acidity. As can be seen, without regard to variations of the excitation spectrum, the maximum of the fluorescent emission of the cationic form of malvinoside comes at the beginning of the red spectral region ($\lambda^{F}_{[Ms]^+} = 595\ m\mu$) which was corrected to 600 $m\mu$ after more precise spectrographic determination.

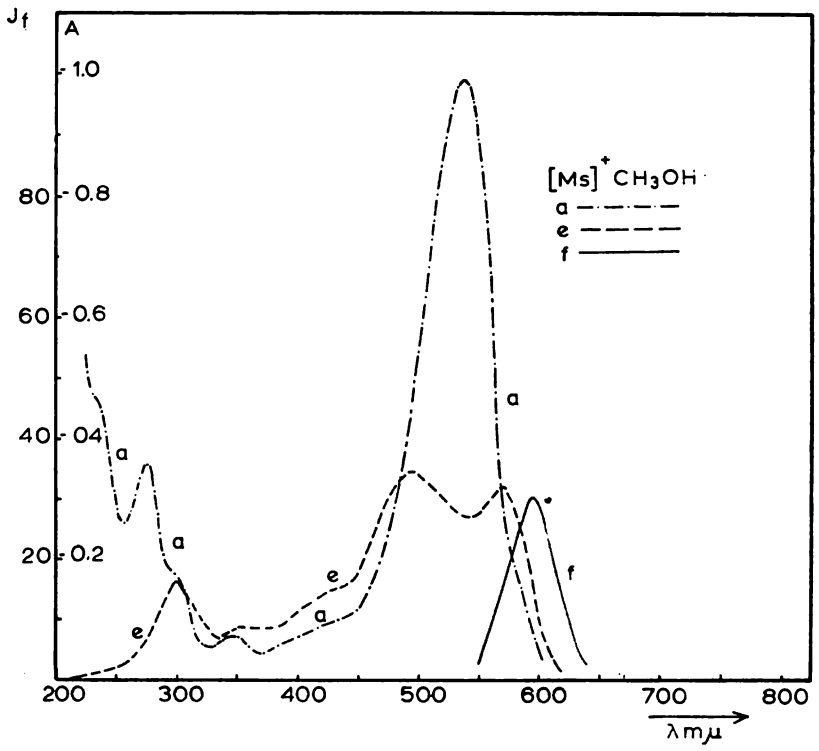

Figure 2

Absorption, excitation and fluorescent spectra of malvinoside chloride, conc. $5 \cdot 10^{-5}$ *M* in methanol with 0.01% *HCl*

Having in mind from our previous investigations of anthocyanidols and anthocyanosides[8, 9] that the cationic forms become more stable with decreasing *pH* of the medium, the fluorescent spectra of $(Ms)^+$ were determined in hyperacidic media. Figures 5 and 6 show absorption, excitation and fluorescent spectra of malvinoside in concentrated sulphuric acid (37 *N*) and concentrated phosphoric acid (85%). It may be seen that here to the fluorescence is most probably due to the cationic form because the wavelength of the fluorescence maximum remains more or less the same (taking into account the considerable change of dielectric constant of the medium).

Fluorescence of the blue anionic form of malvinoside $(Ms)^-$ is not reported in the available literature, although according to our investigations it is even considerably more intense than that of the cationic form. Spectrophotofluorograms of this fluorescence are given for methanol (Fig. 7) and ethanol alkaline solutions (Fig. 8). It can be seen that the maximum of the fluorescent emission is greatly shifted to the shorter wave end, lying in the blue green spectral region ($\lambda^F_{[Ms]} = 505\ m\mu$). The neutral form of malvinoside $(Ms)^{\pm}$ does not fluoresce.

The spectrographic spectra of the different forms of malvinoside are given in the following figures. Fluorescence of the red form in methanol, ethanol and isobutanol is shown in Fig. 9. The solutions were acidified with *HCl* (0.01%). The reference spectrum is *He*, whose orange and red lines lie on either side of the maximum of the fluorescence band of the red

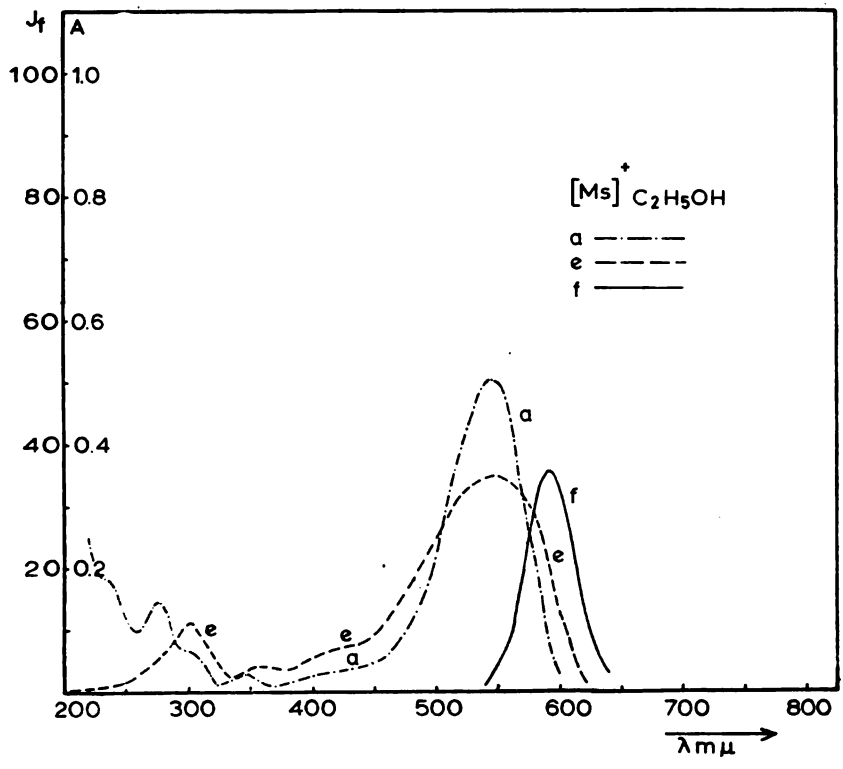

Figure 3

Absorption, excitation and fluorescent spectra of malvinoside chloride, conc. 3.10^{-5} *M*, in ethanol with 0.01% *HCl*

form ($\lambda^{F}_{[Ms]^+} \approx 600\ m\mu$), thereby allowing it to be determined more accurately. Figure 10 shows spectrograms of the fluorescence of the blue form together with that of the red form (in buffer solutions), with *He* and *Hg* lines as the reference spectrum. The fluorescence maximum of this form lies in the blue region ($\lambda^{F}_{[Ms]^-} = 505\ m\mu$).

The fluorescent behavior of closely related anthocyanidols can be compared on the spectrograms in Fig. 11 of malvinoside, pelargonidol, dephinidol and apigenine. The fluorescence of cyanidol was so weak that even after long exposure it could not be registered. It can be seen that there

is a considerable difference in wavelength between different fluorescence maxima besides great differences in the intensity of emission, which allows differentiation of these compounds, at least in pure samples as used here.

Having obtained data about the more important compounds which could influence the RG-test, we examined a well-defined wine sample obtained from hybrid grapes and some domestic wines, in order to verify the test. Figure 12 shows the absorption spectra of the marketed wines (Nos. 1, 2, 3, 4, 5) and the hybrid wine[6]. By suitable dilution the main malvinoside

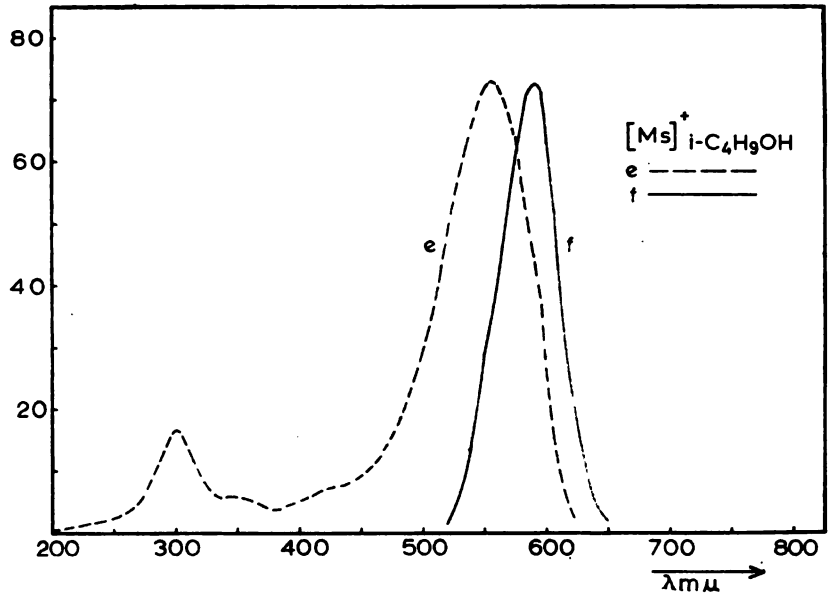

Figure 4

Excitation and fluorescent spectra of malvinoside chloride, conc. $1.3.10^{-4}$ *M*, in isobutanol with 0.01% *HCl*

absorption maximum in all samples ($\lambda^{A}_{[Ms]^+} = 515\ m\mu$) has been emphasized. The absorption of all samples in the visible region, has, as can be seen, a very similar character, so that excitation conditions for fluorescence are comparable for all the samples.

The fluorescent spectrum of the hybrid wine, given together with that of malvinoside $(Ms)^+$ (Fig. 13), confirms well enough the correctness of the RG-test, although the latter is in principle differently checked. While in all his investigations[10, 11] Ribereau-Gayon has always suggested qualitative examination of the fluorescence on paper, here the fluorescent spec-

trum is examined quantitatively and its characteristic maximum is spectrophotofluorimetrically measured directly, in the solution. Similarly, the author of the test suggests chromatographic separation of pigments in the wine, and subsequent fluorescent investigation of the spots, while here,

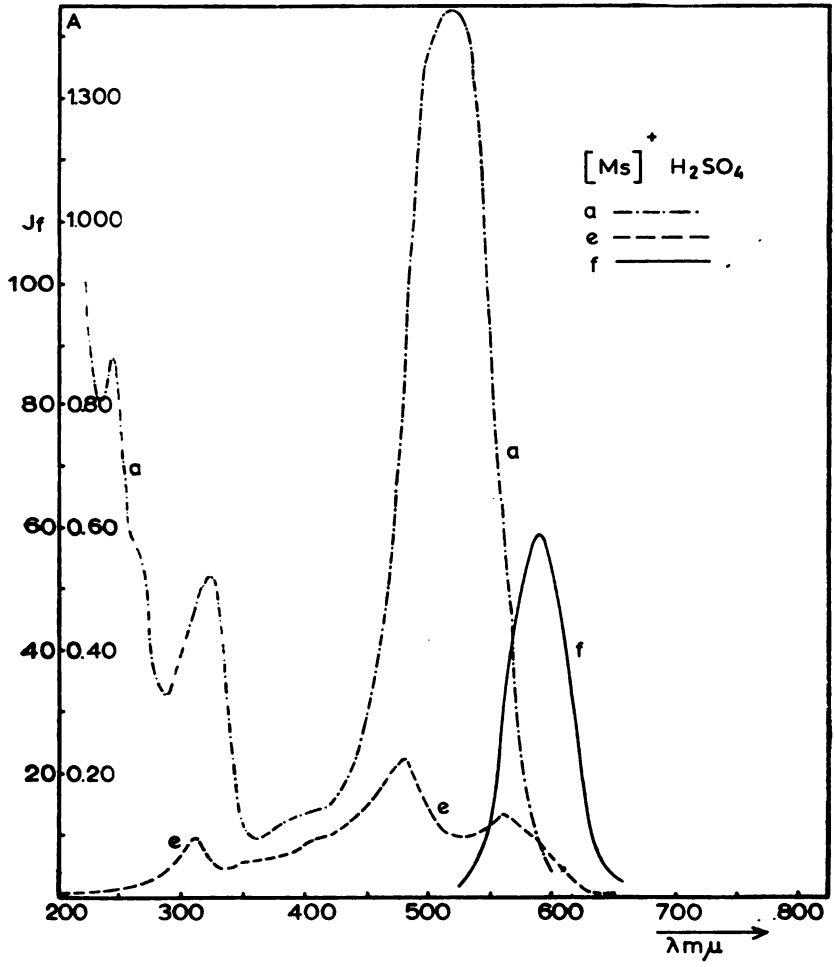

Figure 5

Absorption, excitation and fluorescent spectra of malvinoside chloride, conc. 8.10^{-5} *M*, in concentrated sulphuric acid.

at the chosen optimum concentration, it was possible to indentify the specific fluorescence maximum in the solution, which is certainly an improvement in time and procedure.

The fluorescent spectrum of the blue anionic form of malvinoside can also be employed for the RG-test, even with a certain increase of sensitivity. This can be seen in Figure 14 where spectrophotofluorograms of the anionic form of standard malvinoside ($/Ms/^-$ at $pH = 11.75$) and of the hybrid wine with addition of 0.1 *N NaOH* are shown together in

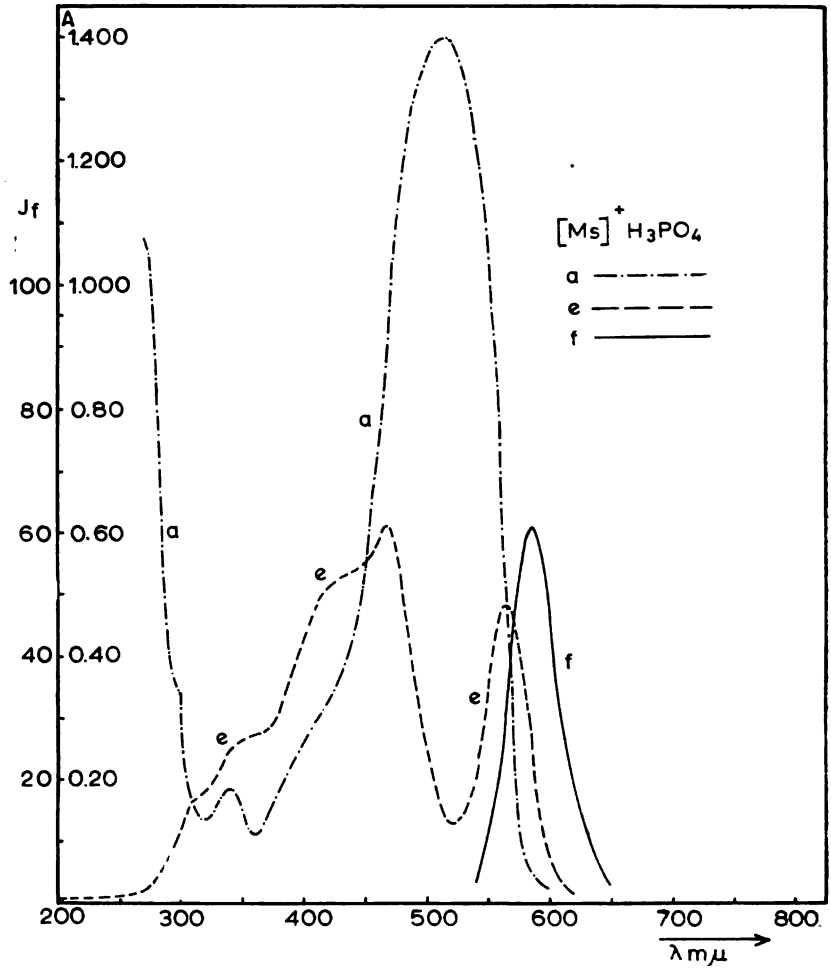

Figure 6

Absorption, excitation and fluorescent spectra of malvinoside chloride, conc. 2.10^{-4} *M*, in 85% H_3PO_4

a 1 : 15 ratio. The fluorescence maximum of the anionic form retains its characteristic value ($\lambda^F_{[Ms]^-} = 505\ m\mu$), i.e. with a considerable hypsochromic shift compared to the cationic form ($\lambda^F_{[Ms]^+} = 600\ m\mu$).

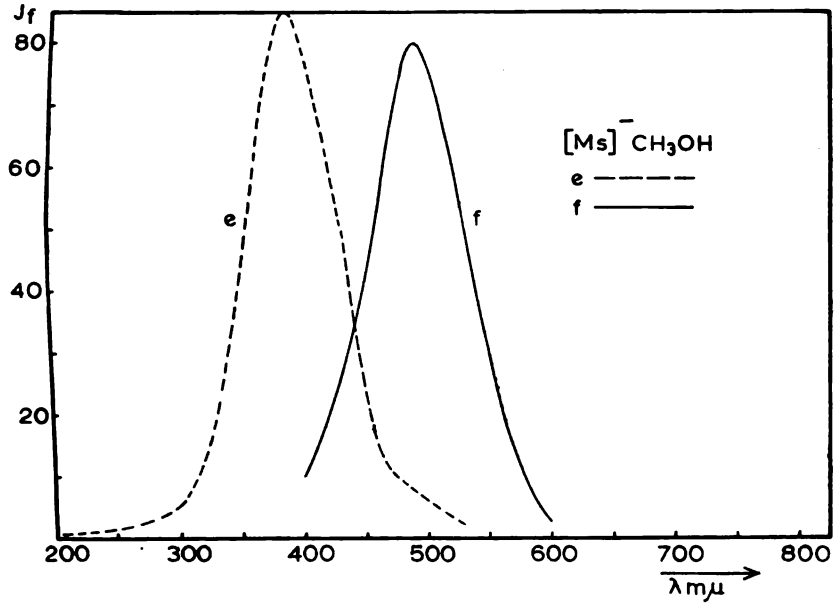

Figure 7

Excitation and fluorescent spectra of malvinoside chloride (anionic form), conc. $1.3.10^{-4}$ *M*, in methanol with 0.1 *N NaOH*

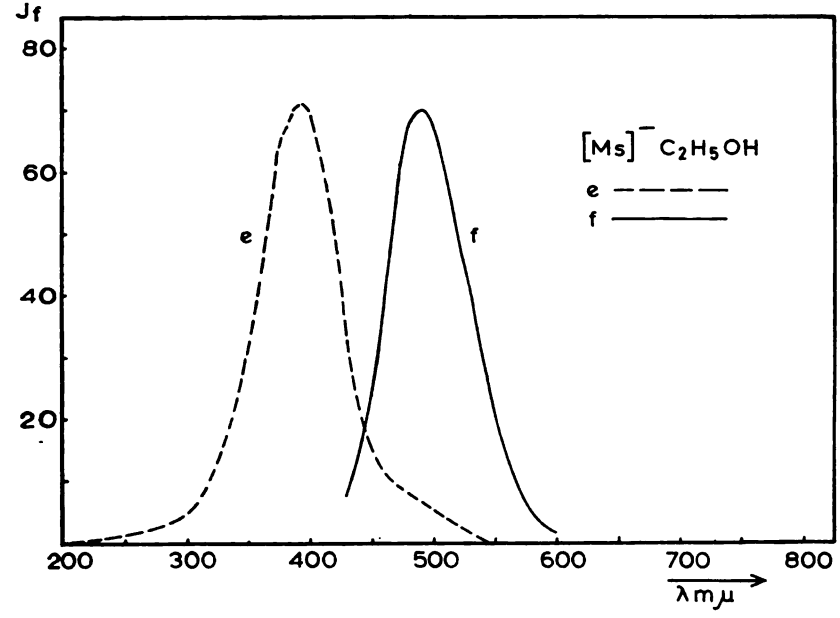

Figure 8

Excitation and fluorescent spectra of malvinoside chloride (anionic form), conc. $1.3 \cdot 10^{-4}$ M in ethanol with 0.1 *N NaOH.*

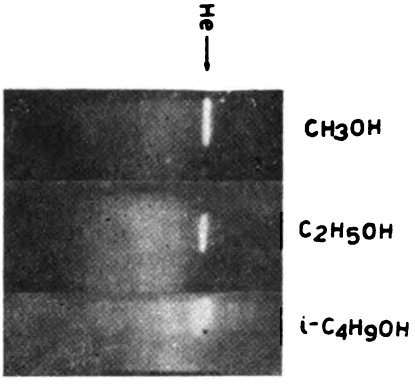

Figure 9

Spectrograms of the cationic form of malvinoside chloride in methanol, ethanol, and isobutanol (exposure time 10 min.)

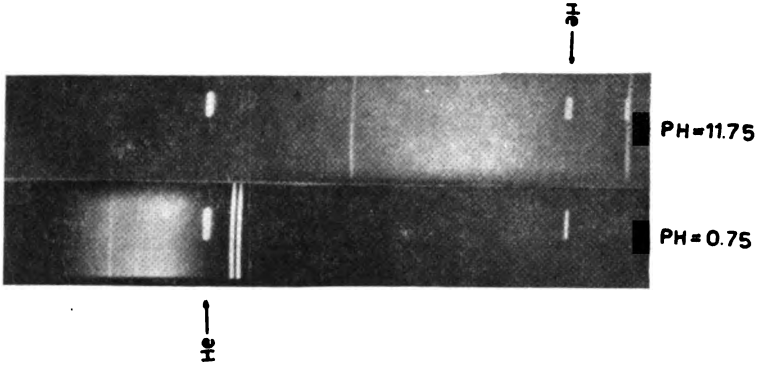

Figure 10

Spectrograms of cationic $(Ms)^+$ (30 min) and anionic $(Ms)^-$ (5 min) form of malvinoside chloride in buffer solutions, $pH = 0.75$ and $pH = 11.75$

Figure 11

Spectrograms of fluorescent bands of pelargonidol $(P)^+$, delphinidol $(D)^+$, and apigenine $(Ap)^+$ compared to spectrograms of malvinoside chloride $(Ms)^+$

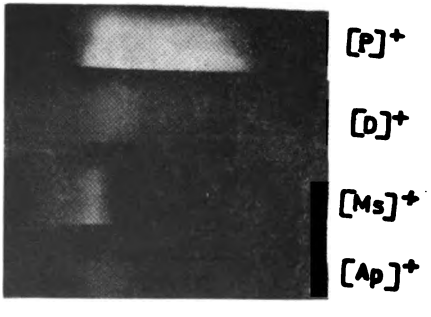

Practical possibilities of applying these results are briefly illustrated in Fig. 15, where spectrophotofluorograms for a mixture of the clearly non-hybrid wine Merlot with the hybrid wine in different ratios are shown. The presence of hybrid can be clearly noticed down to a ratio of 1 : 0.1 *ml*, i.e. 10% of hybrid, and even less when all the available sensitivity of the spectrophotofluorimeter is used. None of the domestic wines tested showed any hybrid down to the limit of our test.

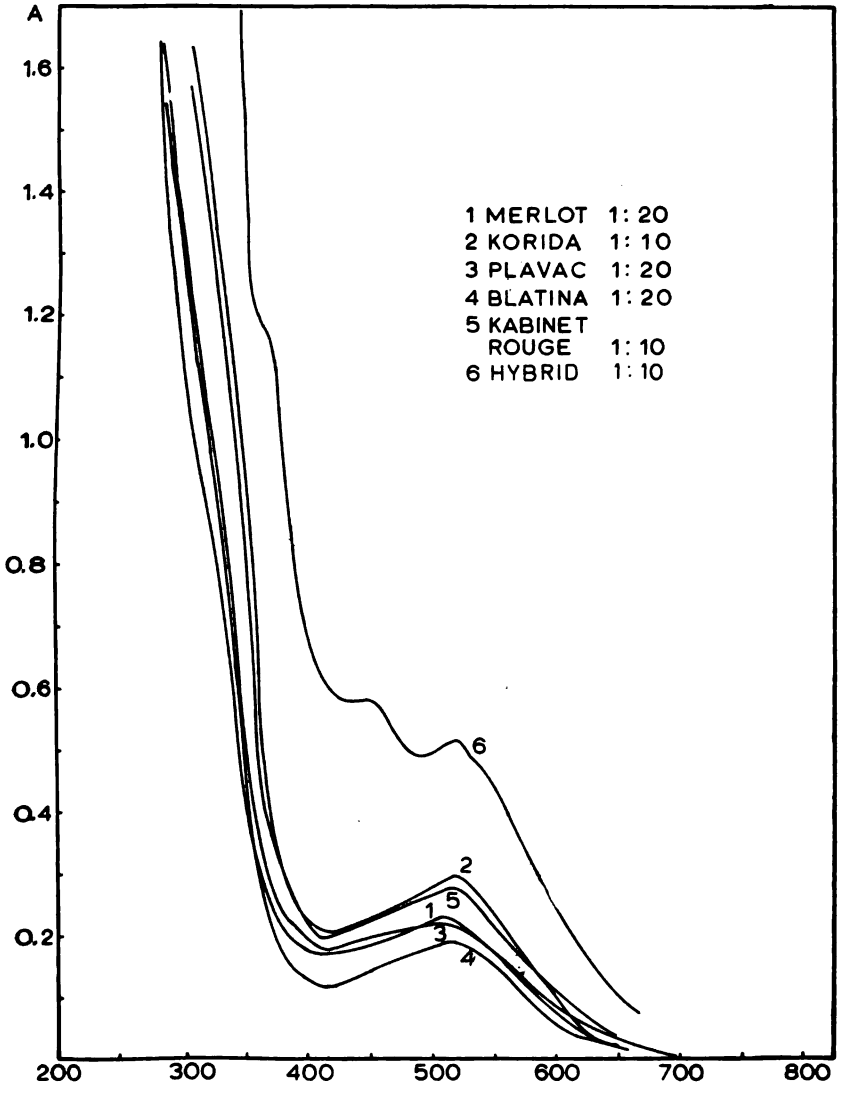

Figure 12

Absorption spectra of the wines, including the hybrid wine

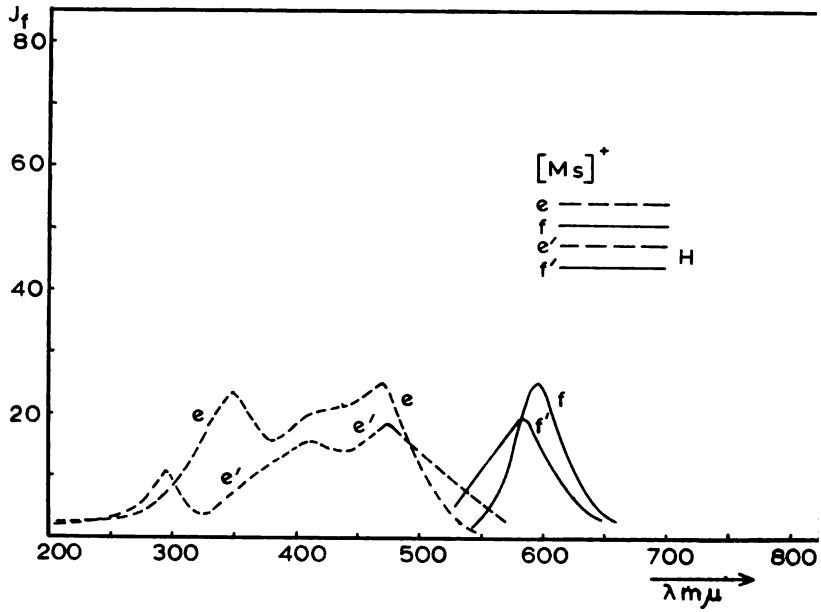

Figure 13

Excitation and fluorescent spectra of malvinoside chloride $(Ms)^-$ in buffer pH — (and in acidified hybrid wine $pH = 1.50$

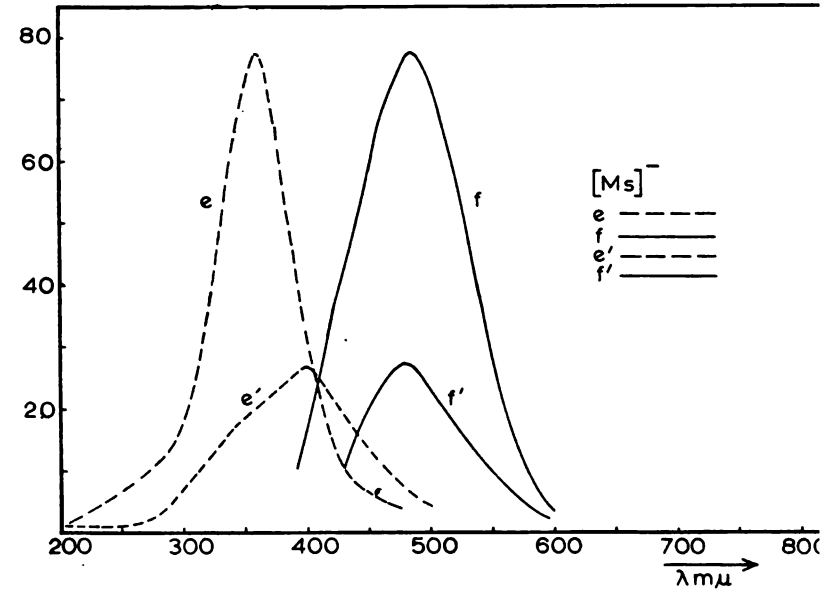

Figure 14

Excitation and fluorescent spectra of malvinoside chloride $(Ms)^-$ in buffer $pH = 1$ and hybrid wine alkalized with 0.1 *N NaOH*

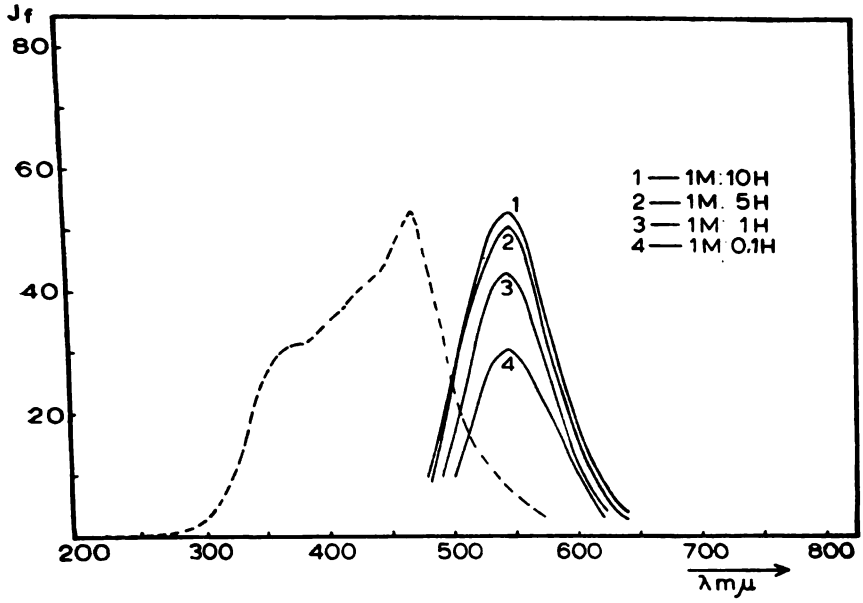

Figure 15

Spectrophotofluorograms of mixtures (volume ratios) of the non-hybrid wine Merlot and the hybrid wine (*H*)

4. CONCLUSION

The fluorescent spectrum of standard (chromatographically pure) malvinoside, measured both spectrophotofluorimetrically and spectrographically in acidic medium, has its maximum in the red spectral region between the red line of helium — *He* 6560.13 Å and its orange line *He* 5875.618 Å (6560.13 Å $> \lambda^{F}_{[Ms]^+} >$ 5875.618 Å). This fluorescence is due to the malvinoside cations (cf. Figs. 2, 3, 4, 9, 10, 11), which remains stable in hyperacidic medium too (conc. H_2SO_4, conc. H_3PO_4; cf. Figs. 5, 6).

The anionic form of malvinoside $(Ms)^-$ also shows fluorescence, with its maximum in the blue green region, between the lines *Hg* 5460.74 $>$ $> \lambda^{F}_{[Ms]^-} >$ *He* 5875.618 Å, well characterised both spectrophotofluorimetrically and spectrographically (cf. Figs. 7, 8, 10, 14).

Hence the RG-test has sound and reliable basis in the variation of the fluorescent spectra of the anthocyanoside and anthocyanol components of the main pigments in wine (and grape-juice). The fluorescent maximum of malvinoside cation $(Ms)^+$ shows the biggest shift towards the long wave end compared to other possible components (cf. Fig. 11).

It is interesting and important to note that the characteristic fluorescence of $(Ms)^+$ persists in hyperacidic media. However, it is of special interest that in alkaline medium malvinoside anion $(Ms)^-$, with the opposite charge, shows the capacity even for more intense fluorescence.

The fluorescence of malvinoside cation $(Ms)^+$ in hyperacidic medium can, according to our study of it[12], help to explain the reaction properties of such structures in the anthocyanole compounds.

Received 28 December, 1966.

REFERENCES

1. Ribereau-Gayon, P. *Recherches sur les anthocyannes des végétaux. Application au genre Vitis* — Paris, 1959.
2. Tanner, H., H. Rentschler, and M. Brunner. "Zur Identifizierung der für rote Hybridentraubensäfte und Weine charakteristischen Anthocyanfarbstoffe" (1 to 3) — *Mitteilungen aus dem Gebiete der Lebensmitteluntersuchung und Hygiene veröffentlicht vom Eidgenossischen Gesundheitsamt* (Bern) 50: 533, 1959; 51: 130, 1960; 52: 312, 1961.
3. Robinson, R. "Synthesis of a Natural Colouring Matter" — *Nature* (London) 137: 94—95, 1936.
4. Harborne, J. B. — *Forschritte der Chemie organischer Naturstoffe* (Wien) 20: 170, 1962
5. Willard, H. H., L. L. Merritt, and J. A. Dean. *Instrumental Methods of Analysis* — New York-Toronto-London: D. Van Nostrand, 1958.
6. Mellon, M. J. *Analytical Absorption Spectroscopy* — New York, 1957.
7. Price, M. J., M. Kaihara, and H. K. Howerton. "Influence of Scattering on Fluorescence Spectra of Dilute Solutions Obtained with the Aminco-Bowman Spectrophotofluorimeter" — *Applied Optics* (Easton) 1: 521, 1962.
8. Ristić, S. and J. Baranac. "Uticaj pH-vrednosti rastvora na apsorpcione spektre pelargonidola, delfinidola i malvinozida" (Effect of pH on the Absorption Spectra of Pelargonidol, Delphinidol and Malvinoside) — *Glasnik hemijskog društva Beograd* (Beograd) 29 (7): 283—299, 1964.
9. Ristić, S. and J. Baranac. "Etudes sur le Comportement Spectrochimique et photochimique des Anthocyanols et des Anthocyanosides", in: *Proceedings of* XII *Colloquium Spectroscopicum Internationale, London*, 1965, — pp. 230—241.
10. Ribereau-Gayon, P. and P. Sudraud. "Les anthocyannes des espèces differentes du genre Vitis" — *Comptes Rendus de l'Academie des Sciences* (Paris) 244: 233—236, 1957.
11. Ribereau-Gayon, P. "Nouvelles observation sur la differenciation des vins de Vitis Vinifera et d'hybrides" — *Comptes Rendus de l'Academie d'Agriculture de France* (Paris) 135—140, 1965.
12. Ristić, S. and J. Baranac. "La fluorescence des anthocyanols dans les milieux hyperacides" — *Journal de Chimie Physique* (Paris) 64 (1): 191—195, 1967.

GLASNIK HEMIJSKOG DRUŠTVA, Vol. 32, No. 2-3-4, 1967, pp. 153—165

STUDY OF BEHAVIOR OF CATIONIC FORM OF PELARGONIDOL IN HYPERACIDIC MEDIA

by

SLOBODAN M. RISTIĆ, JELISAVETA M. BARANAC, and AURORA A. MUK

1. INTRODUCTION

In our previous investigations[1] it was shown that the stability of cationic forms of 2-phenylbenzopyrone (flavanol) salts increases with decreasing medium *pH*. It was of interest to find out to what extent increasing acidity favors the stabilization of the chromophore group in this class of chemical compounds, and to establish what chemical processes are involved in reversible or irreversible decomposition of this group. Since the absorption spectra of these compounds in different solvents have been studied well enough[2], and are especially suitable for indentifying new chemical individuals in photochemical transformations[3], it appeared recommendable to apply a spectrophotometric method.

2. EXPERIMENTAL, MATERIALS, APPARATUS, METHODS

All chemicals were of p.a. purity unless otherwise stated. The pelargonidol sample was a commercial product (Fluka A. G., Switzerland), chromatographically purified. For spectrophotometry we mainly used a Unicam SP 500 quartz spectrophotometer, as well as a Beckman DK-1A for some control determinations.

Solutions of known concentrations were made by measuring solid substance on a microbalance and dissolving it in concentrated H_2SO_4, 37 *N* (Chemapol, Czechoslovakia), and subsequent dilution of the starting solution except in cases when fresh solution were required.

3. RESULTS AND DISCUSSION

General features of spectrophotograms of pelargonidol in the 37 *N* sulphuric acid for several different concentrations are shown in Fig. 1. It can be seen that the absorption spectrum has five characteristic maxima

($\lambda_I - \lambda_V$) in the examined region, the long wave maximum being the most intense ($\lambda_I = 490.0$ $m\mu$); it is characteristic for the cationic form of all anthocyanidols. Although this maximum, compared to its position in other less polar media, undergoes a very strong hypsochromic shift, it still remains in the blue green region, which gives the cations of the whole class of antho-

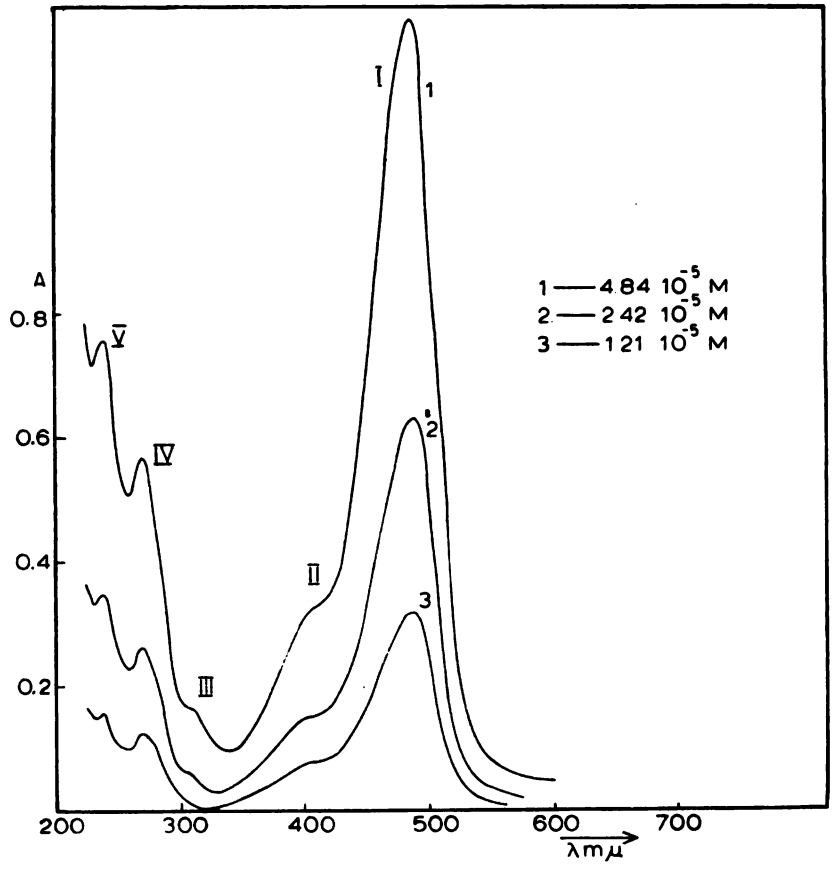

Figure 1

Absorption spectra of pelargonidol in concentrated sulphuric acid (37 N H_2SO_4) for several different concentration

cyanidols a characteristic red color. The great attenuation almost to total disappearance, of the second maximum, λ_{II} (at 410 $m\mu$), which is according to Harborne[4] characteristic for the substitution of hydroxyl-5 in the A-ring of anthocyanidols, is striking. It is probable that direct dissolution of pelargonidol in conc. sulphuric acid caused the reaction in this position which can be compared to the process of glucosidification for which Harborne's

TABLE I

Some characteristics of the absorption spectra of pelargonidol chloride in hyperacidic medium (37 N H_2SO_4)

Concentr. c x 10^{-5} mol/l	Absorption maxima, mμ					Absorptivity (x 10^4)					Relative intensities of absorption maxima, %(A_I = 100)			
	λ_V	λ_{IV}	λ_{III}	λ_{II}	λ_I	a_V	a_{IV}	a_{III}	a_{II}	a_I	A_V/A_I	A_{IV}/A_I	A_{III}/A_I	A_{II}/A_I
4.84	240	270	310	410	490	1.6	1.2	0.3	0.7	2.6	59.2	43.9	12.6	25.8
3.30	240	270	310	410	490	1.4	0.9	0.3	0.7	2.5	56.1	36.6	11.6	24.4
2.42	240	270	310	410	490	1.4	1.1	0.2	0.7	2.6	56.5	42.1	8.7	25.4
1.21	240	270	310	410	490	1.3	1.0	0.1	0.6	2.6	48.7	39.1	3.8	24.4

observation is valid. More precise data about the characteristic positions of pelargonidol cation absorptions are given in Table I, where, beside the values of the absorption maxima wavelengths ($\lambda_I - \lambda_V$) and corresponding absorptivities ($a_I - a_V$), relative absorption of some absorption bands is also given, taking that of the main maximum ($\lambda_I^{[P]+}$) as unity (i.e. 100). This allows closer comparison and consideration of the changes observed, to be discussed later.

The Lambert-Beer law could be tested for all the five maxima in a wide enough range of concentrations (10^{-3}—10^{-7} M), because the solutions, if protected from moisture, showed quite good stability. Linear analytical absorption characteristics for all the maxima are given in Fig. 2. It can be seen that from λ_I to λ_V, the L—B law is undoubtedly obeyed by all maxima within the range examined. This clearly shows that the cationic chromophoric group remains well preserved under hyperacidic conditions too (up to the hyperacidity characterised by Hammett's number $H^0 = -8.96$), though some changes (as the one in position 5) do occur.

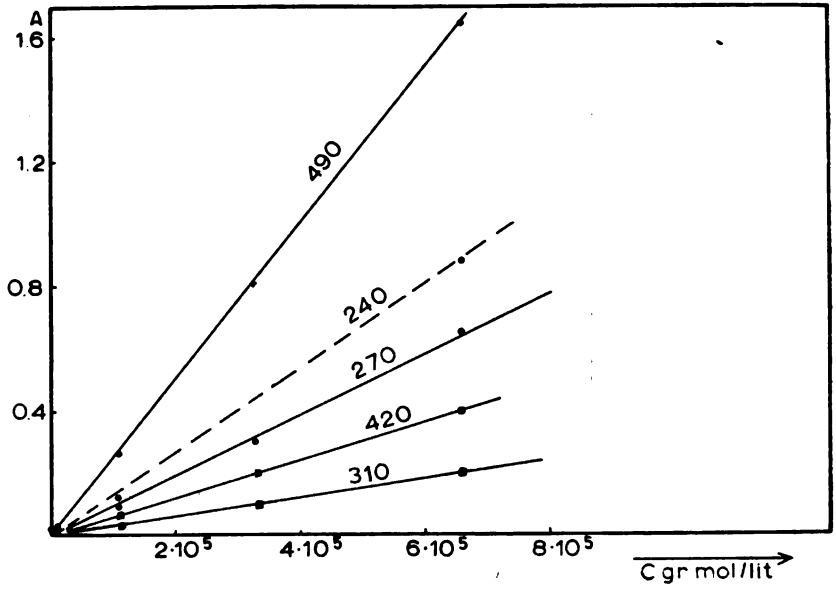

Figure 2

Linear analytical absorption characteristics of the maxima at different pelargonidol chloride concentrations in conc. sulphuric acid

The effect of diluting the hyperacidic solution is of special interest because from the physical standpoint it involves a considerable change of dielectric constant of the medium ($\varepsilon^{25}_{H_2SO_4} = 100$ to $\varepsilon^{25}_{H_2O} = 80$) while from the chemical standpoint it should signify changed chemical reacti-

vity of the cationic form $[P]^+$ through the transition from hyperacidic (Hamett's) to normally acidic (Sörensen's) medium. From a large number of spectrograms those characteristic for the above changes are shown in Fig. 3. Restitution of the λ_{II} maximum indicates probable occupation of position 3 while different intensities of selective absorption of λ_{IV} and λ_V, in this case only partialy in keeping with Harborne's observations, presumably indicate acylation of the basic cationic structure. The bathochro-

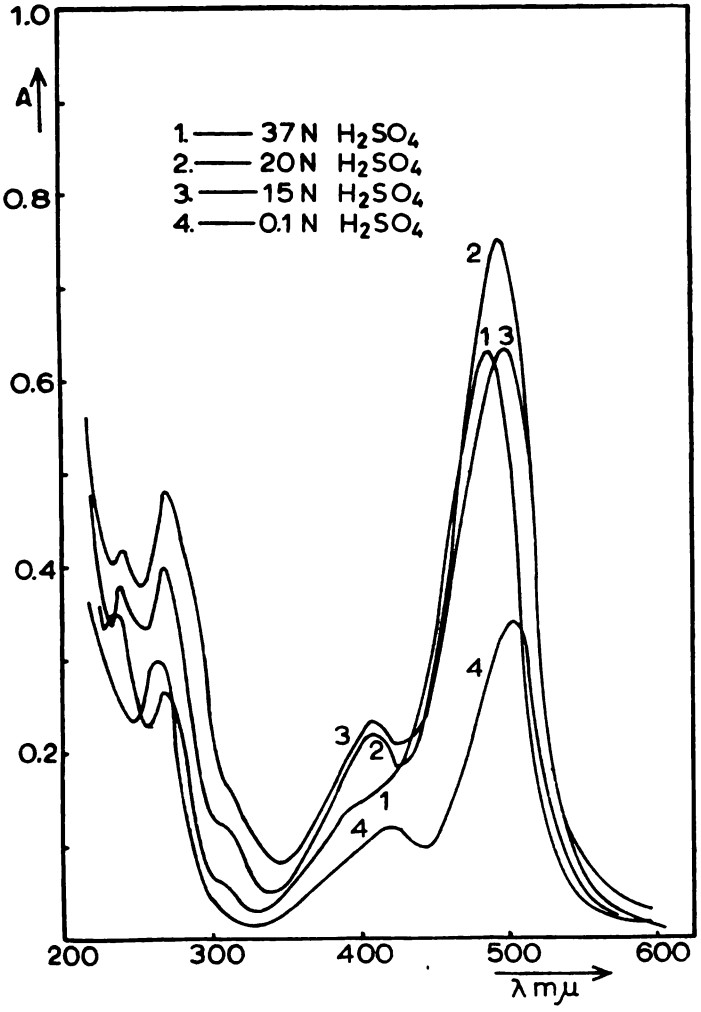

Figure 3

Absorption spectra of pelargonidol chloride at 2.42.10 ^{5} *M* concentration as a function of sulphuric acid dilution

mic shift of the main maximum (λ_I) with dilution is in accordance with the previously observed shift of the longwave maximum of anthocyanidols (λ_I) with decreasing polarity of the solvent. Detailed explanation and possible interpretations of the process will be given later.

Time-dependent changes of hyperacidic pelargonidol solution must be taken into account not only because they could directly affect the results of spectrophotometry but also because they can give additional data about the physico-chemical changes of the chromophore. Figure 4 shows several spectrograms of pelargonidol samples which stood long enough to show measurable changes. The evolution of the λ_{II} maximum shows that immediately after almost instantaneous substitution of hydroxyl-5 slower substitution of the enol hydroxyl from position 3 probably occurs.

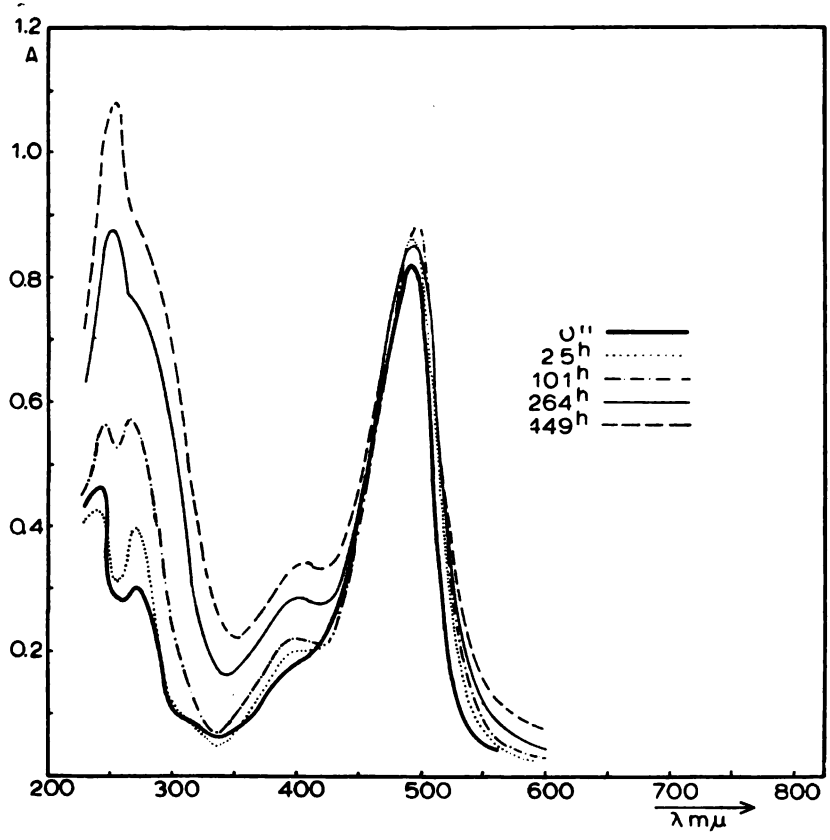

Figure 4

Absorption spectra of $3.3.10^{-5}$ *M* pelargonidol chloride solution as a function of time (in completely isolated system)

These changes are evidently slow, because after more than 300 hours of observation, the general characteristics of an anthocyanol chromophore remain well preserved.

The changes in the absorption spectrum of pelargonidol in hyperacidic media must be discussed starting from Harborne's observation, but taking into account the resonant hybrid structures of anthocyanols, especially pelargonidol, and the specific characteristics of concentrated sulphuric acid as the solvent, a strongly reactive electrophilic medium.

In general appearance the absorption spectrum does not differ much from that in the normal acidity region, for example at $pH = 1.0$ (cf. Fig. 3): the main longwave maximum is shifted up about 15 $m\mu$ (as would be expected considering the increased polarity of the medium), while the intensities of the λ_{I}, λ_{III}, and λ_{IV} maxima vary considerably with the nature of the medium (cf. Fig. 3). This variability becomes more apparent on careful study of the relative absorption at dilution of the solution (cf. Table II). It can be seen that the absorbance ratio A_{410}/A_{490} doubles by an H_2SO_4 concentration of 30 N, as Harborne observed for complete occupation of position 5. The fact that in spite of these variations the Lambert-Beer law is obeyed in hyperacidic medium too, shows the existence of an absorptiometrically perfectly defined chemical compound, which does not differ much in composition and structure from a 2-phenyl-benzopyrone cation. The effect of dilution shows existence of a causal connection between "purely" physical changes (change of dielectric constant of the medium) and "purely" chemical changes (substitution, i.e. acylation in positions 5 and 3), these latter being accompanied by the fluorescence characteristic for such processes in this class of compounds (this fluorescence was disscused

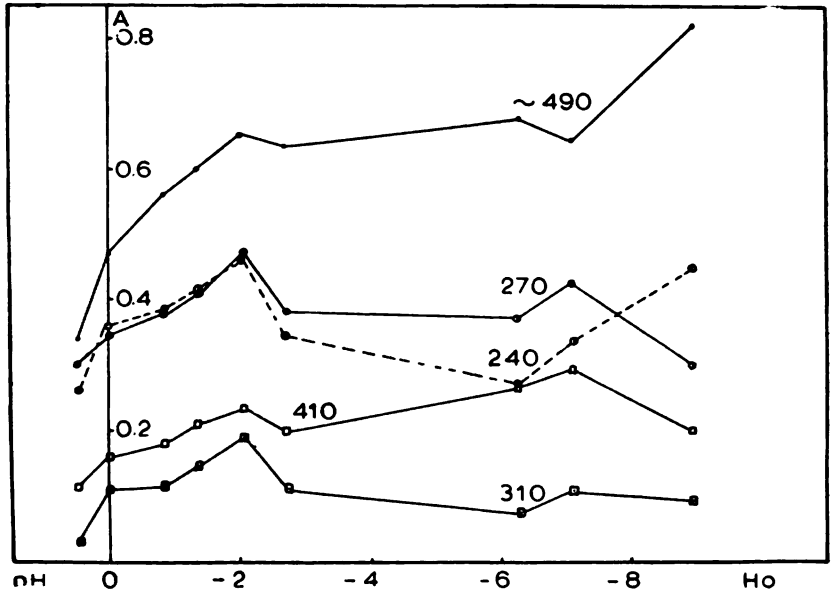

Figure 5

Absorption intensities of characteristic maxima as a function of H-value (Hammett's function)

TABLE II

Effect of dilution of initial pelargonidol chloride solution in conc. sulphuric acid ($C = 2.42 \times \times 10^{-5} M$) *with water on the absorption spectra*

Normality H_2SO_4	Hammett's function $-H_0$	Absorption maxima, mμ					Absorptivity (x 10^4)					Relative intensities of absorption maxima, % (A_I = 100)			
		λ_V	λ_{IV}	λ_{III}	λ_{II}	λ_I	a_V	a_{IV}	a_{III}	a_{II}	a_I	A_V/A_I	A_{IV}/A_I	A_{III}/A_I	A_{II}/A_I
37.0	8.96	240	270	310	410	490	1.4	0.9	0.3	0.6	2.5	55.1	36.6	11.6	24.2
30.0	7.10	240	270	310	410	495	1.0	1.3	0.3	0.9	2.0	52.7	65.9	17.1	45.7
27.0	6.27	240	270	310	410	495	0.8	1.1	0.2	0.9	2.0	39.8	54.6	10.9	39.5
13.0	2.70	240	270	310	410	500	1.0	1.1	0.3	0.6	1.9	54.2	60.0	17.4	31.6
11.0	2.02	240	270	310	410	500	1.4	1.4	0.6	0.7	2.0	70.2	72.5	29.0	35.9
8.5	1.37	240	270	310	410	500	1.3	1.2	0.4	0.6	1.8	69.7	68.9	24.4	34.8
5.9	0.85	240	270	310	410	500	1.2	1.1	0.3	0.6	1.7	68.8	67.7	20.7	32.1
1.1	0.0	240	270	310	410	500	1.1	1.0	0.3	0.5	1.4	76.7	73.4	23.6	34.0
pH = 0.50		240	270	310	410	505	0.9	1.0	0.1	0.4	1.1	76.5	88.2	8.8	33.8

TABLE III

Time — dependent changes of the absorption spectra of pelargonidol chloride sulphuric acid solution ($C = 3.3 \times 10^{-5}$ *M*)

Time (hours)	Absorption maximum, mμ					Absorptivity (x 10^4)					Relative intensities of absorption maxima, % ($A_I = 100$)			
	λ_V	λ_{IV}	λ_{III}	λ_{II}	λ_I	a_V	a_{IV}	a_{III}	a_{II}	a_I	A_V/A_I	A_{IV}/A_I	A_{III}/A_I	A_{II}/A_I
0	240	270	310	410	490	1.4	0.9	0.3	0.6	2.5	56.1	36.6	11.6	24.4
25	240	270	310	410	490	1.3	1.2	0.3	0.6	2.6	49.4	46.3	10.5	23.8
101	240	270	—	410	490	1.7	1.7	—	0.7	2.7	63.6	64.2	19.9	25.0
264	240	270	—	410	495	2.6	2.3	—	0.8	2.6	102.9	89.4	47.7	32.9
449	240	270	—	410	495	3.3	2.7	—	1.0	2.6	127.4	105.5	64.6	40.2

in a previous work[5]). The dependence of absorbance changes at dilution on the acidity of the medium (Fig. 5) indicates the existence of some discontinuities at values $H_0 \approx -7$; -2 and $pH \approx 0$ although they are not so great considering a wide range of acidity.

Time-dependent changes of the absorption spectrum of pelargonidol in 37 N H_2SO_4, are also predominately manifested through changes in λ_{IV} and λ_V and to a less extent in λ_{II} and λ_{III} (cf. Fig. 4 and Table III). These changes can be further discussed with respect to the initial statements of this discussion. The complex possibilities existing in the hyperacidic medium cannot be precisely defined on the basis of these investigations, but we consider that the formulation of some hypotheses which can be of interest for further research is justified.

Immediately after dissolving in concentrated sulphuric acid (37 N) process (1) occurs, forming an acidic ester of sulphuric acid ("pelargonidil-sulphuric acid"), i.e. 5-bisulphate-pelargonidol cation:

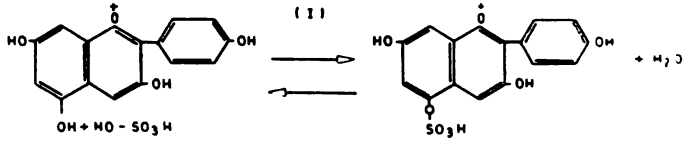

This explains the near disappearance of λ_{II} (cf. Fig. 1) which according to Harborne[4] exhibits a very pronounced hypsochromic effect which on bonding of glucosidyl residue in position 5. It also explains the appearance of the special fluorescence, which R. Robinson and other authors associate with the substitution if hydrogen in the phenol hydroxyl-5 glucosidyl residue, and which we have observed and studied[5]. Process (I) is relatively fast, establishing an equilibrium with the gradually stable acidic ester which in 100 hours at room temperature (in a closed system) retained well preserved the essential absorptiometric properties of the original pelargonidol chromophore (cf. Tables I, II, and Figs. 1 and 2).

However after a longer period under hyperacidic conditions (excluding the influence of air) esterification of phenol hydroxyls, first in position-3 and then probably in positions -7 and 4', proceeds analogous to process (I). This can be concluded on the basis of the λ_I[2] restitution, which after some hundred hours (cf. Table III), and by means of the hyperchromic effect, almost doubles its intensity (cf. Fig. 4). The hyperchromic changes of λ_{IV} and λ_V lead at a given time ($\tau \approx 100$ hours) near to equality of these two maxima, and continue to evolve so that eventually ($\tau \geqslant 400$ hours) they strongly favor hyperchromimum of λ_V, with lagging and attenuation of λ_{IV} (cf. Fig. 4, Table III). Analogous hyperchromic effects of the ultraviolet maxima of anthocyanidols have been reported by Harborne (*l.c.*), studying acylation of these compounds in positions 7 and 4'.

Changes resulting from dilution of the system with water only partially correspond with the previous observations. Restitution of the λ_{II} maximum (at about 20 N H_2SO_4 concentration) also has hyperchromic effects on λ_{IV} and λ_V with approximate equalization of the absorbances at this concentration (cf. Fig. 3; Table II), but probably from some other reasons,

because this here with further dilution and entering Sörensen's acidity region λ_{IV} is hyperchromically favored with lagging and disappearance of λ_{V}. It is very probable that process (I) is occurring in the opposite direction (hydrolysis of acidic ester into pelargonidol cation). Disappearance of the fluorescence immediately on dilution is in good agreement with this.

More detailed interpretation of the mechanisms of esterification cannot be given on the basis of the available experimental data.

CONCLUSION

Absorption study of pelargonidol, one of the main representatives of the anthocyanols, in hyperacidic medium (37 N H_2SO_4) confirms the increasing flavanol cationic stability expected from our previous investigations, since the Lambert-Beer law is obeyed by all the important maxima of the anthocyanidol chromatophore.

The behavior of hyperacidic pelargonidol solution during dilution down to the Sörensen's region and the timedependent processes in the solution in a closed vessel show that after relatively rapid initial esterification of the $[P]^+$ cation (process (I)) further relatively slow changes proceed leading to further stages of multiple esterified ionic products. Possible processes are tentatively formulated, in which multiply esterified pelargonidol cations as a new species, responsible for somewhat altered absorption spectra.

Received 21 February, 1967.

REFERENCES

1. Ristić, S. and J. Baranac. "Uticaj pH-vrednosti rastvora na apsorpcione spektre pelargonidola, delfinidola i malvinozida" (Effect of pH on the Absorption Spectra of Pelargonidol, Delphinidol and Malvinoside) — *Glasnik hemijskog društva Beograd* (Beograd) 29 (7): 283—299, 1964.
2. Ristić, S. and J. Baranac. "Spectres d'absorption des anthocyanols et des anthocyanosides et leur caractéristiques particulières dans les différents solvants" in: XI. *Colloquium Spectroscopicum Internationale, Beograd*, 1963, — p. B-88.
3. Ristić, S. and J. Baranac. "Etudes sur le Comportement Spectrochimique et photochimique des Anthocyanols et des Anthocyanosides", in: *Proceedings of the* XII*th Colloquium Spectroscopicum Internationale, London*, 1965 — pp. 230—241.
4. Harborne, J. B. — *Forschritte der Chemie organischer Naturstoffe* (Wien) 20: 170, 1962.
5. Ristić, S. and J. Baranac. "La fluorescence des anthocyanols dans les milieux hyperacides" — *Journal de chimie Physique* (Paris) 64 (1): 191—195, 1967.

GLASNIK HEMIJSKOG DRUŠTVA, Vol. 32, No. 2-3-4, 1967, pp. 167—180

ANODIC DISSOLUTION OF MERCURY IN SULPHITE SOLUTIONS AT DIFFERENT *pH* VALUES*

by

DRAGICA S. OVCIN, MILAN V. VOJNOVIĆ and
KONSTANTIN I. POPOV

INTRODUCTION

Anions which form complexes with mercury, such as CN^-, SO_3^{2-}, $S_2O_3^{2}$ and CNS^-, produce anodic waves during polarographic determinations of their solutions at the dropping mercury electrode[1, 2]. The nature and possible application of anodic waves of this type have hitherto been insufficiently studied. Revenda[3], Kolthoff and Miller[4] and Tanaka and Murayama[5] studied the anodic waves in solutions of cyanide, sulphite, thiosulphite and rodanide. Matyska and co-workers[6, 7] and Goffart and co-workers[8] studied them in the presence of ethylenediaminetetraacetic acid and 1,2-diaminecyclohexanetetraacetic acid. Anodic waves in solutions containing ethylenediamine were studied by Watters and Mason[9].

While investigating the problem of polarographic determination of certain components of non-cyanide electrolytes for silver plating[10], which we were systematically studying[11, 12], it was observed that there is little information concerning sulphite electrolyte in the literature[4], and it does not permit unique determination of the character of the anodic process at the dropping mercury electrode, particularly at different *pH* values. The aim of this study was to obtain information, by more detailed investigation of anodic polarographic waves of the dissolution of mercury in the presence of sulphite, which would make possible a complete definition of this process. Considering that in polarography sulphite is often used for removing disolved oxygen in the basic fundamental electrolytes, such information could be of general interest.

THEORETICAL CONSIDERATIONS

In the case when the solution does not contain a complexing agent, the process of anodic dissolution of mercury can be represented with the equation

* Communicated at the 12th Conference of Chemists of the SR of Serbia, Beograd, January 1967.

$$nHg \longrightarrow nHg^{2+} + 2n\,e \tag{1}$$

where the electrode potential is given by

$$E = E^0 + \frac{RT}{2F} \ln [Hg^{2+}]_0 \tag{2}$$

in which E^0 is the standard electrode potential, $[Hg^{2+}]^0$ the concentration of Hg^{2+} ions on the surface of the mercury drop, and the other symbols have their usual electrochemical meanings.

However, in the presence of a sufficient concentration of sulphite several complex ions can be formed, such as $Hg(SO_3)_2^{2-}$, $Hg(SO_3)_3^{4-}$, $Hg(SO_3)_4^{6-}$ (whose general instability constants are 2.19×10^{-23}, $1.70 \times \times 10^{-23}$ and 1.45×10^{-23} respectively)[13]. In view of this and of the fact that sulphite ion is an anion of a weak divalent acid (with first and second dissociation constants $K_{a,I} = 1.58 \times 10^{-2}$ and $K_{a,II} = 6.31 \times 10^{-8}$)[13], the anodic dissolution of mercury can be represented, depending on the pH of the solution, in the following three ways:

a) basic medium (with pH above the values corresponding to the second dissociation constant of sulphurous acid, $pK_{a,II} = 7.2$),

$$nHg + mSO_3^{2-} \longrightarrow Hg_n(SO_3)_m^{2(m-n)-} + 2ne \tag{3}$$

The electrode potential in this process is given by the equation

$$E = E^f_{a,1} + \frac{RT}{2nF} \ln \frac{[Hg_n(SO_3)_m^{2(m-n)-}]_0}{[SO_2^{3-}]_0^m} \tag{4}$$

in which $E^f_{a,1}$ is the formal potential defined as by

$$E^f_{a,1} = E^0 + \frac{RT}{2nF} \ln K \tag{5}$$

where K is the general instability constant of the complex ion $Hg_n(SO_3)_m^{2(m-n)-}$.

It is easy to demonstrate that in polarographic determinations

$$[SO_3^{2-}]_0 = \frac{i_d - i}{k_{1,a}} \tag{6}$$

and

$$[Hg_n(SO_3)_m^{2(m-n)-}]_0 = \frac{i}{k_{2,a}} \tag{7}$$

where i_d is the diffusion and i the working current, and $k_{1,a}$ and $k_{2,a}$ are the proportionality constants of Ilkovich's equation. Substituting these expressions in equation (4) gives the equation of the polarographic wave of anodic dissolution of mercury in basic sulphite solutions:

$$E = E^f_{a,1} + \frac{RT}{2nF} \ln \frac{k^m_{1,a}}{k_{2,a}} + \frac{RT}{2nF} \ln \frac{i}{(i_d - i)^m} \tag{8}$$

or

$$E = E^f_{a,2} + \frac{RT}{2nF} \ln \frac{i}{(i_d - i)^m} \tag{9}$$

which shows that potential is a linear function of log $i/(i_d - i)^m$ with a slope 2.3 $RT/2nF$.

The half-wave potential is obtained from equation (9):

$$E_{1/2} = E^f_{a,2} + \frac{RT}{2nF}(m-1)\ln 2 - \frac{RT}{2nF}(m-1)\ln i_d \tag{10}$$

or

$$E_{1/2} = E^f_{a,3} - \frac{RT}{2nF}(m-1)\ln i_d \tag{11}$$

from which it follows that $E_{1/2}$ is a linear function of log i_d with slope $-2.3\ RT(m-1)/2nF$.

b) Weakly acid medium (pH between the values corresponding to the first, and the second dissociation constants of sulphurous acid, $pK_{a,I} = 1.8$ and $pK_{a,II} = 7.2$.

In this case the process is described by

$$nHg + mHSO_3^- \longrightarrow Hg_n(SO_3)_m^{2(m-n)-} + mH^+ + 2ne \tag{12}$$

or in the presence of the buffer system HR/R^-

$$nHg + mHSO_3^- + mR^- \longrightarrow Hg_n(SO_3)_m^{2(m-n)-} + mHR + 2ne \tag{13}$$

The electrode potential for process (12) is given by the equation

$$E = E^f_{b,1} + \frac{RT}{2nF} \ln \frac{[Hg_n(SO_3)_m^{2(m-n)-}]_0 [H^+]_0^m}{[HSO_3^-]_0^m} \tag{14}$$

and for process (13) by

$$E = E^f_{b,2} + \frac{RT}{2nF} \ln \frac{[Hg_n(SO_3)_m^{2(m-n)-}]_0 [H^+]_0^m}{[HSO_3^-]_0^m} \tag{15}$$

It is easy to demonstrate that

$$E^f_{b,l} = E^0 + \frac{RT}{2nF} \ln \frac{K}{K^m_{a,II}} \tag{16}$$

and

$$E^f_{b,2} = E^f_{b,1} - \frac{mRT}{2nF} \ln K_A \tag{17}$$

where K_A is the dissociation constant of HR.

Similar considerations as under (a) give the equation of the polarographic wave of anodic dissolution of mercury in weakly acid sulphite solution:

$$E = E^f_{b,3} + \frac{RT}{2nF} \ln \frac{k^m_{1,b}}{k_{2,b}} + \frac{mRT}{2nF} \ln [H^+] + \frac{RT}{2nF} \ln \frac{i}{(i_d - i)^m} \tag{18}$$

where the constant $E^f_{b,3}$ has the value of $E^f_{b,2}$ in the presence of the HR/R^- system, and the value of $E^f_{b,1}$ if it is absent, while the other symbols have the same meanings as before.

Equation (18) written in the form

$$E = E^f_{b,4} + \frac{mRT}{2nF} \ln [H^+] + \frac{RT}{2nF} \ln \frac{i}{(i_d - i)^m} \tag{19}$$

shows that in this case the potential is a function of pH and $\log i/(i_d - i)^m$.

For the half-wave potential we get

$$E_{1/2} = E^f_{b,4} + \frac{RT}{2nF} (m-1) \ln 2 + \frac{mRT}{2nF} \ln [H^+] - \frac{RT}{2nF} (m-1) \ln i_d \tag{20}$$

or

$$E_{1/2} = E^f_{b,5} + \frac{mRT}{2nF} \ln [H^+] - \frac{RT}{2nF} (m-1) \ln i_d \tag{21}$$

showing that $E_{1/2}$ is a function of pH and of the limiting diffusion current.

(c) Strongly acid medium (up to the pH corresponding to the first dissociation constant of sulphurous acid, $pK_{a,1} = 1.8$), when the reaction is

$$nHg + mH_2SO_3 \longrightarrow Hg_n(SO_3)^{2(m-n)-}_m + 2mH^+ + 2ne \tag{22}$$

or in the presence of the buffer system HR/R^-

$$nHg + mH_2SO_3 + 2mR^- \longrightarrow Hg_n(SO_3)^{2(m-n)-}_m + 2mHR + 2ne \tag{23}$$

By analogy with the previous considerations, the equation for the polarographic wave of anodic dissolution of mercury is here

$$E = E^f_{c,3} + \frac{RT}{2nF} \ln \frac{k^m_{1,c}}{k_{2,c}} + \frac{mRT}{nF} \ln [H^+] + \frac{RT}{2nF} \ln \frac{i}{(i_d - i)^m} \tag{24}$$

where the formal potential $E^f_{c,3}$ has the value of $E^f_{c,2}$ in the presence of the system HR/R^-, and the value of $E^f_{c,1}$ in it's absence, it being easily demonstrated that

$$E^f_{c,1} = E^0 + \frac{RT}{2nF} \ln \frac{K}{K^m_{a,\,I}\, K^m_{a,\,II}} \tag{25}$$

and

$$E^f_{c,2} = E^f_{c,1} - \frac{mRT}{nF} \ln K_A \tag{26}$$

Equation (24) written in the form

$$E = E^f_{c,4} + \frac{mRT}{nF} \ln [H^+] + \frac{RT}{2nF} \ln \frac{i}{(i_d - i)^m} \tag{27}$$

shows that in this case too the potential is a function of pH and $\log i/(i_d - i)^m$.

The expression for the half-wave potential is

$$E_{1/2} = E^f_{c,4} + \frac{RT}{2nF}(m-1) \ln 2 + \frac{mRT}{nF} \ln [H^+] - \frac{RT}{2nF}(m-1) \ln i_d \tag{28}$$

or

$$E_{1/2} = E^f_{c,5} + \frac{mRT}{nF} \ln [H^+] - \frac{RT}{2nF} \ln i_d \tag{29}$$

showing that $E_{1/2}$ is a function of pH and of the limiting diffusion current.

EXPERIMENTAL TECHNIQUE

The initial solution for the polarographic determinations was prepared just before measurement by dissolving a measured amount of sodium sulphite, p.a., in freshly boiled double-distilled water through which purified hydrogen had been bubbled. Strictly measured volumes of the initial solution diluted to the desired concentration of sulphite with a basic electrolyte (0.1 N KNO_3 or the corresponding buffer solution with 0.003% gelatine) through which purified hydrogen had been bubbled too. Polarograms were recorded in a closed cell of conventional shape after brief passage of purified hydrogen. During preparation of the solution measures were taken to prevent contact with the air.

For the determinations at different solution pH values standard biphathalate, borate and phosphate buffer solutions[13] prepared from p.a. chemicals, were used as basic electrolytes.

All the basic electrolytes contained 0.003% gelatine to supress the maximum.

All the polarographic determinations were done on a Radiometer *PO* 3′ polarograph, and pH measurements on a Radiometer M 22 pH-meter.

Currents were corrected for the precurrents of the basic electrolytes, and half-wave potentials for ohmic drops within the cell, determined in the usual way[1].

Polarography was done with a 7 *mm* long capillary at a dropping rate of 4.57 *mg* sec^{-1} and a mercury column of 28 *cm*.

RESULTS AND DISCUSSION

Results of a number of tests showed that the best anodic waves of sulphite were obtained in 0.1 *N* KNO_3, which can be accounted for by the fact that nitrate ions do not depolarize on the dropping mercury electrode.

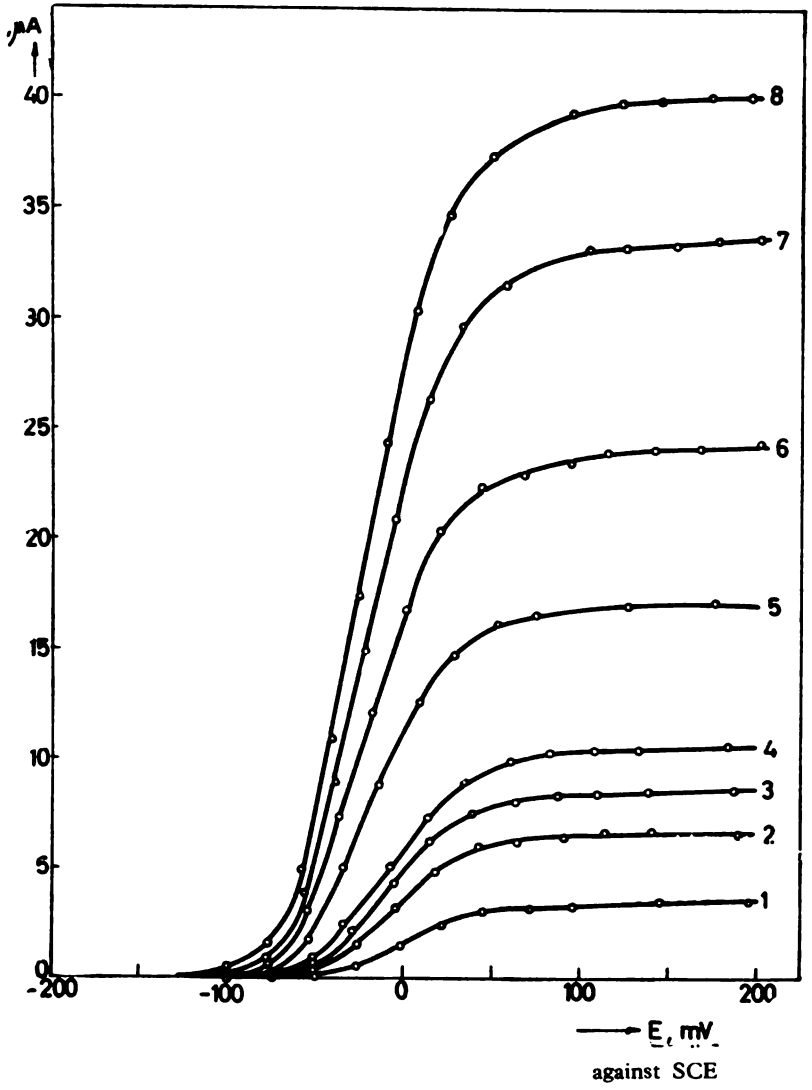

Figure 1

Anodic polarographic waves of sulphite in 0.1 *N* KNO_3 + 0.003% gelatine. Na_2SO_3 concentration (*mmol.lit*$^{-1}$): 1—0.66; 2— 1.32; 3— 1.60; 4— 1.95; 5— 315; 6— 4.60; 7—6.03; 8—7.47

It may be seen in Fig. 1, which shows a series of typical polarograms at different sulphite concentrations, that waves appeared at about —100 *mV* (against SCE) and had a well defined limiting difusion current.

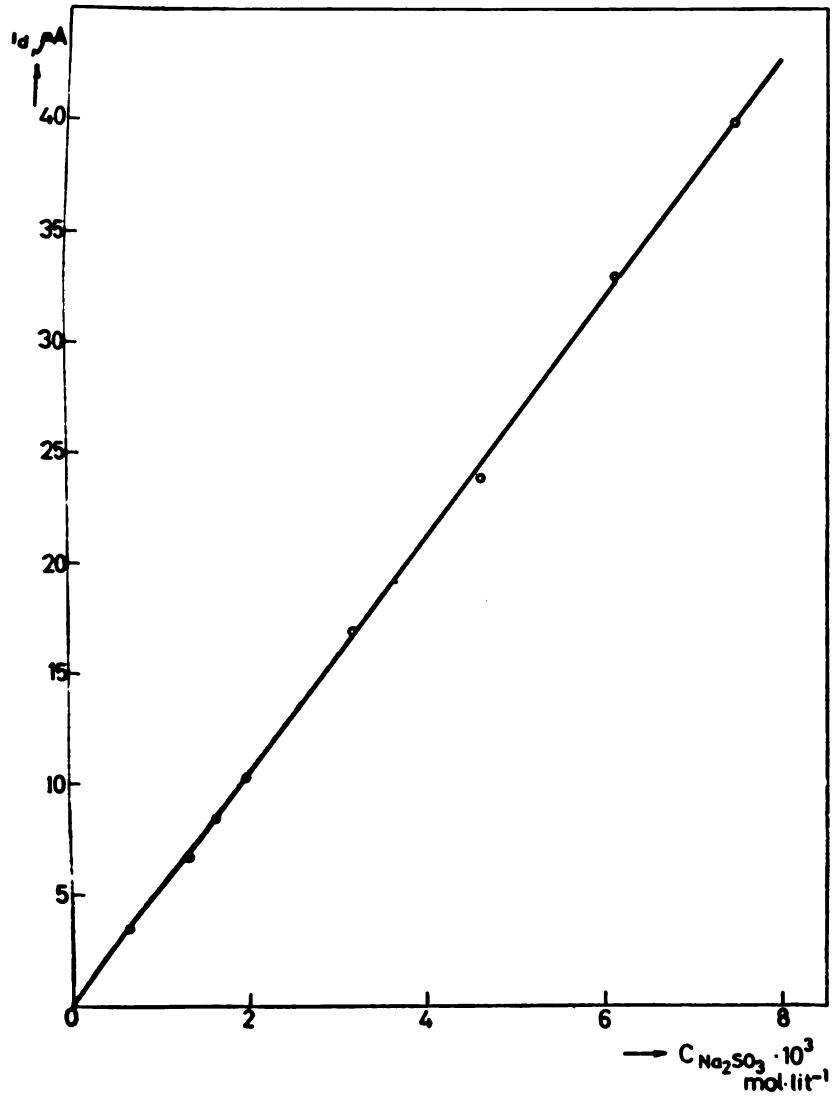

Figure 2

Dependence of the limiting diffusion current of sulphite in 0.1 *N* KNO_3 + 0.003% gelatine on concentration

The dependence of the limiting diffusion current on the sulphite concentration is represented, as seen in Fig. 2, by a straight line with slope $k = 53.\ \mu A \cdot lit \cdot mmol^{-1}$.

Considering that sulphite solutions in 0.1 $N\ KNO_3$ are basic (pH at the lowest concentration of sulphite was ~ 8), the theoretical considerations formulated in equations (3) — (11) can be applied here. A typical analysis of the sulphite anodic wave using equation (9) is shown in Fig. 3.

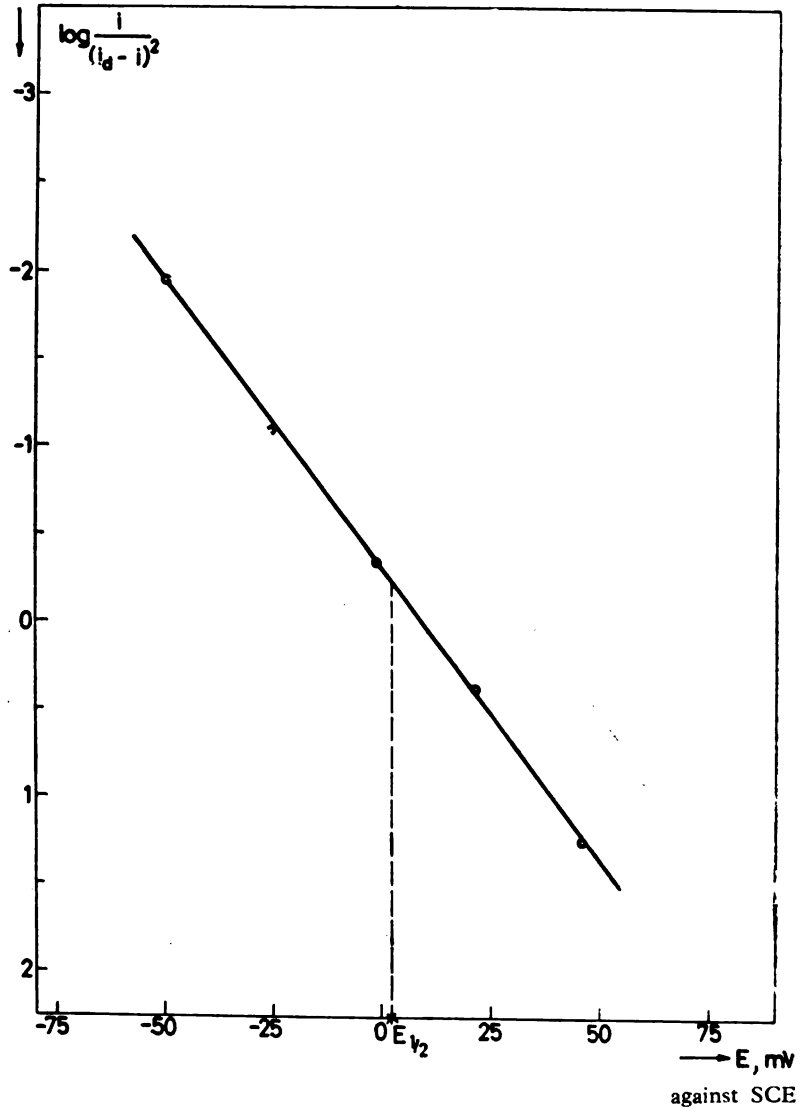

Figure 3

Logarithmic analysis of the anodic wave of sulphite in 0.1 $N\ KNO_3$ + 0.003% gelatine
Na_2SO_3 concentration (*mmol. lit.*$^{-1}$): 0.66

It may be seen that the dependence of E on $\log i/(i_d - i)^2$ is given by a straight line with slope 30 mV per decade, so that from equation (9) it follows that $n = 1$ and $m = 2$, meaning that the anodic process is a two-electron exchange with formation of $Hg(SO_3)_2^{2-}$ ions. These results agree with those of Kolthoff and Miller[2].

Figure 4 shows the dependence of the half-wave potential on $\log i_d$ for the given waves. In accordance with equation (11) with $n = 1$ and $m = 2$ a straight line was obtained with slope 27 mV per decade.

With change of the sulphite concentration in 0.1 N KNO_3 the pH of the solution showed a slight change, the lowest value in the investigated concentration range having been ~ 8. This however did not influence the half-wave potential, which was also in accordance with equation (11).

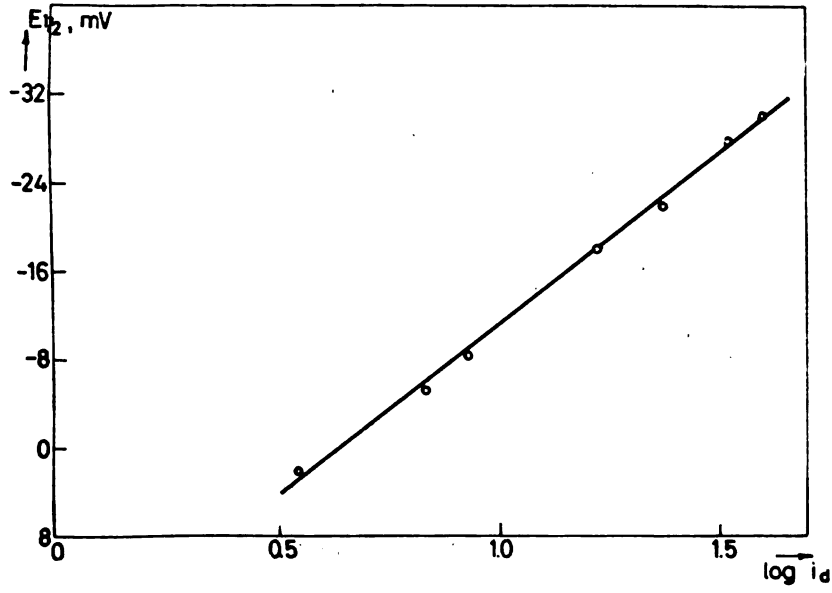

Figure 4

Dependence of the half-wave potential on $\log i_d$ for anodic waves of sulphite in 0.1N KNO_3 + 0.003% gelatine

When investigating anodic waves in solutions of different pH, certain difficulties arose because in some buffer solutions the waves were not well developed, as seen in Fig. 5 which shows a series of typical polarograms for a constant sulphite concentration and different solution pH. The unfavorable wave shape was probably due to depolarization of anions from the buffer itself[14]. However, a number of experiments showed that despite this disadvantage within the pH range 4.0 to 9.2 with some practice reproducible i_d and $E_{1/2}$ values could be obtained from the polarograms. With pH values above about 9.5 superposition of the sulphite wave with the wave of hydroxy ion depolarization became marked[4]. On the other hand because

of a very low $pK_{a,I}$ value, non-reproducibility of the results and other experimental difficulties polarography in highly acid solution was not practical.

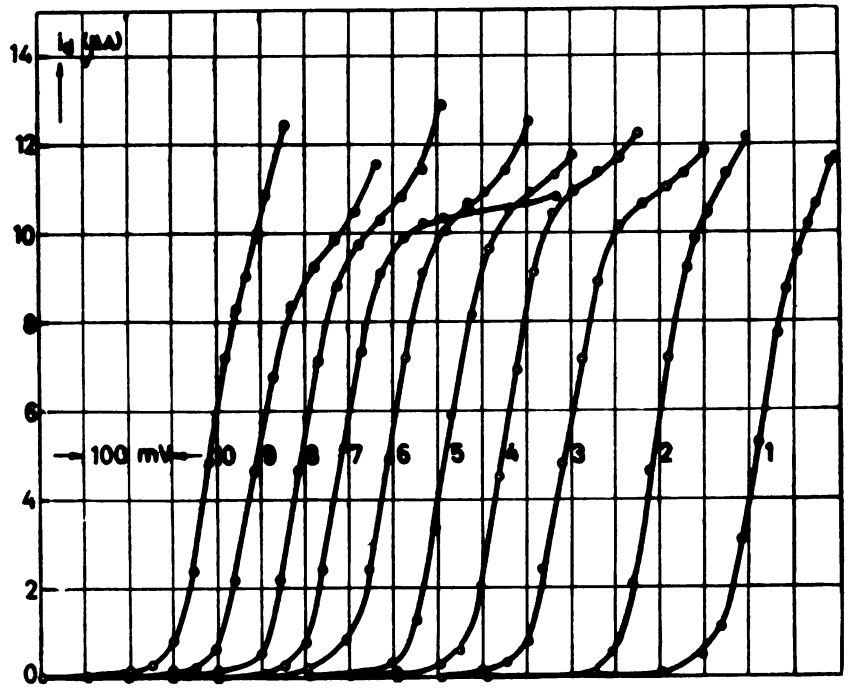

Figure 5

Anodic polarographic waves of sulphite at different *pH* values
Na_2SO_3 concentration (*mmol.lit*$^{-1}$): 1.90

pH values of the solutions: 1—4.0; 2—5.0; 3—6.0; 4—6.4; 5—6.8; 6—7.2; 7—0.1 *N* KNO_3; 8—7.6; 9—8.0; 10—9.2

1, 2 — biphthalate buffer
3—6, 8, 9 — phosphate buffer
10 — borate buffer

All polarographic waves start at 200 *mV* vs *SCE*, but for clarity they are shifted apart 50 *mV*

Figure 6 shows the dependence of E on $\log i/(i_d - i)^2$ for the polarographic waves in Fig. 5. In accordance with equations (9) and (19) for $n = 1$ and $m = 2$ straight lines were obtained with slope of 32 *mV* per decade, shifted with rising *pH* towards more negative potential values, up to $pH \sim 7$ (corresponding approximately to $pK_{a,II}$)[2] after which it did not shift. The results show that throughout the *pH* range studied the process had the character of a two-electron exchange with the formation of $Hg(SO_3)_2^{2-}$ ions.

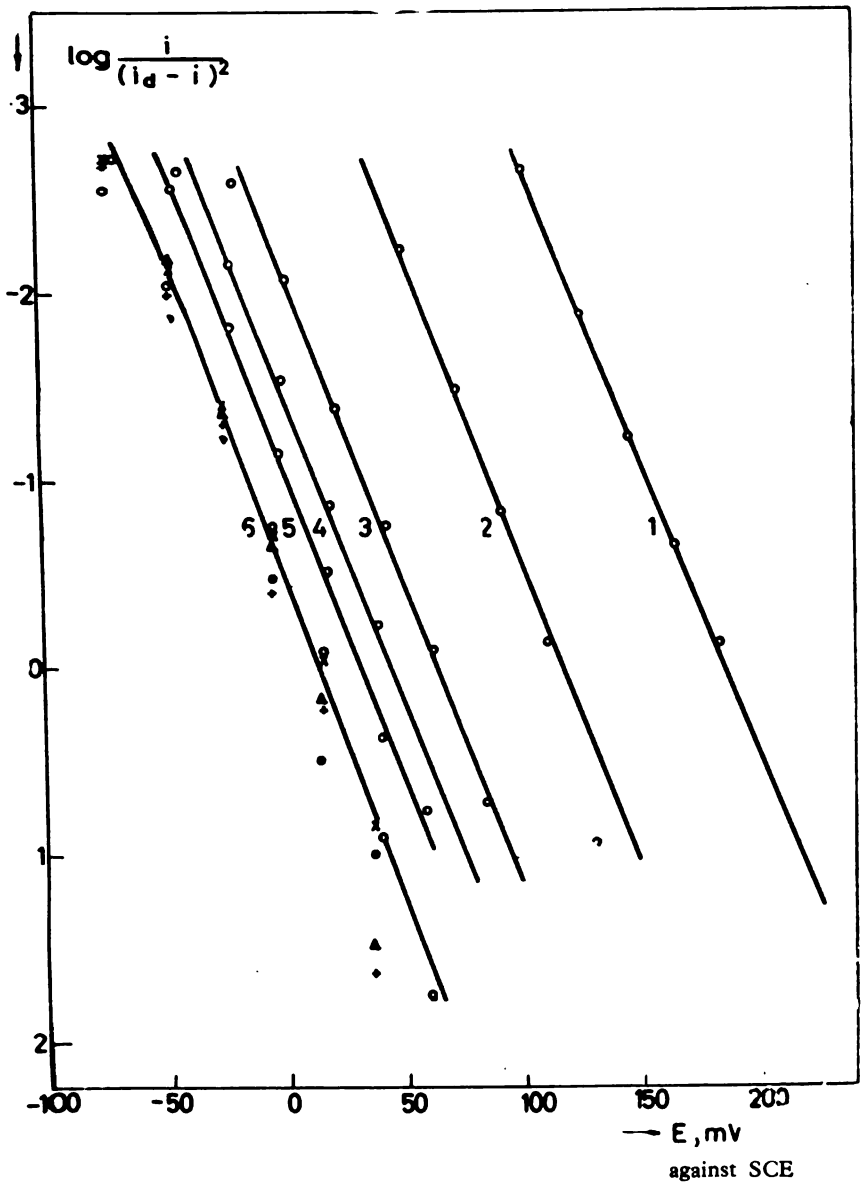

Figure 6

Logarithmic analysis of anodic waves of sulphite at different *pH* values
Na_2SO_3 concentration (*mmol.lit*$^{-1}$): 1.90

pH values of the solutions: 1—4.0; 2—5.0; 3—6.0; 4—6.4; 5—6.8; 6—7.2; —x— 0.1 *N* KNO_3; —Δ— 7.6; — + — 8.0; —·— 9.2

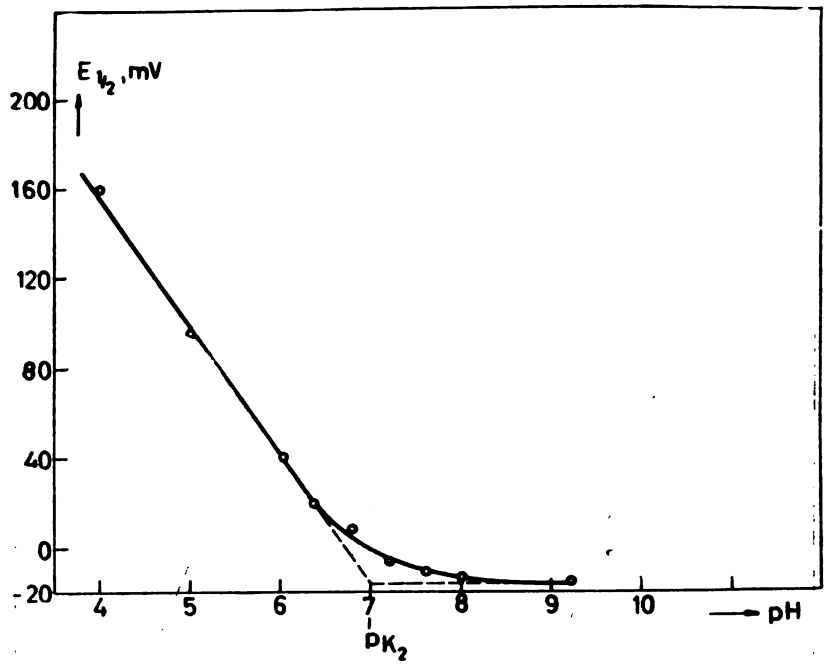

Figure 7

Dependence of the half-wave potential on *pH*. Na_2SO_3 concentration (*mmol.lit*$^{-1}$): 1.90

Figure 7 shows the dependence of the half-wave potential on *pH*; when $E_{1/2}$ values are read from Fig. 6. In accordance with equation (21) with constant i_d, $n = 1$ and $m = 2$, the change of $E_{1/2}$ with *pH* up to the value $pH \sim 7$ (corresponding to $pK_{a,\,II}$) is represent by a straight line with slope of 57 *mV* per *pH* unit. At $pH \geqslant 7$, $E_{1/2}$ in accordance with equation (11) becomes practically independent of *pH*.

Institute of Physical Chemistry and
Electrochemistry, School of Technology,
Beograd

REFERENCES

1. Geirovskii, Ia. and Ia. Kuta. *Osnovy polarografii* (Fundamentals of Polarography) — Moskva: Mir, 1965, pp. 158—160, 54.
2. Charlot, G., J. Badoz-Lambling and B. Trémillon. *Electrochemical Reactions* — Amsterdam—New York: Elsevier, 1962, pp. 84—89.
3. Revenda, J. "Polarographic Studies with the Dropping Hg Electrode. (I) Anodic Polarization and the Influence of Anions" — *Collection of Czechoslovak Chemical Communications* (Praha) 6: 453—460, 1934.
4. Kolthoff, I. and C. Miller. "Anodic Waves Involving Electrooxidation of Mercury at the Dropping Mercury Electrode" — *Journal of the American Chemical Society* (Easton, Pa.) 63: 1405—1411, 1941.
5. Tanaka, N. and T. Murayama. "Anodic Waves of the Cyanide at the Dropping Mercury Electrode and the Dissociation Constants of Cyanomercurate (II) Complexes" — *Zeitschrift für Physikalische Chemie* (Frankfurt) 11: 366—378, 1957.
6. Matyska, B. and I. Kösler. "Polarographic Study of Complex Formation between Mercury (II) and Ethylenediaminetetraacetic Acid" — *Collection of Czechoslovak Chemical Communications* (Praha) 16: 221—229, 1951.
7. Matyska, B., J. Doležal and D. Roubalová. "Note on the Polarographic Behaviour of Ethylenediaminetetraacetic Acid and 1,3-Diaminocyclohexane-N,N,N′,N′-tetraacetic Acid" — *Collection of Czechoslovak Chemical Communications* (Praha) 21: 107—112, 1956.
8. Goffart, J., G. Michel and G. Duyckaerts. "Etude polarographique du mercure (Hg^{2+}) en présence d'acide éthylenediaminotétraacétique. I. Influence du pH sur le potentiel de demi-vague-constante de stabilité du complexe" — *Analytica Chimica Acta* (Amsterdam) 9: 184—193, 1953.
9. Waters, J. and J. Mason. "Investigation of the Complexes of Mercury Electrode" — *Journal of the American Chemical Society* (Easton, Pa.) 78: 285—289, 1956.
10. Ovcin, D., M. Vojnović and K. Popov. "Polarografske osobine srebra u rastvorima sulfita" (Polarographic Behavior of Silver in Sulphite Solutions) — *Glasnik Hemijskog društva* (Beograd) (in press).
11. Rikovski, G., M. Vojnović, M. and K. Popov. "Non-cyanide Electrolytes for Silver Plating" — *Zaštita materijala* (Beograd) 14: 111—116, 1966.
12. Popov, K., M. Vojnović and G. Rikovski. "Stationary Polarization Curves in Non-cyanide Electrolytes for Silver Plating" — *Hemijska industrija* (Beograd) (in press).
13. *Spravochnik Khimika* (Handbook for Chemists) — Moskva: Khimiia, 1964, pp. 79, 136, 168—176.
14. Lingane, J. "Peculiarities of Polarography in Phosphate Medium" — *Journal of Electroanalytical Chemistry* (Amsterdam) 12: 173—182, 1966.

GLASNIK HEMIJSKOG DRUŠTVA, Vol. 32, No. 2-3-4, 1967, pp. 181—191

POLAROGRAPHIC BEHAVIOR OF SILVER IN SULPHITE SOLUTIONS*

by

DRAGICA S. OVCIN, MILAN V. VOJNOVIĆ and KONSTANTIN I. POPOV

INTRODUCTION

Relatively few authors have studied the problem of polarographic determination of silver ion[1-4]. They observed that under standard conditions cathodic waves formed at the dropping mercury electrode are not well defined as they overlap with the anodic waves of dissolution of mercury as a result of the fact that silver ions undergo reduction at a more positive potential than the potential at which mercury is dissolved. Because of this polarography does not allow selective measurement of the silver ion content of a solution.

Formation of complexes, as a means of separating the polarographic wave of silver from the anodic wave of mercury dissolution, did not yield satisfactory results. In this case the solution usually contains an excess of a complexing agent, the majority of which give more stable complexes with mercury than with silver. Because of this the relative position of the polarographic wave of the silver complex with respect to the anodic wave of mercury dissolution cannot be changed.

However, Bowers and Kolthoff[5], in their study of induced reduction of colloidal silver bromide with argento-cyanide ion, observed a welldefined compound cathodo-anodic wave of argento-cyanide ion in solutions without excess cyanide. They explain the cathodic part of the wave by reduction of argento-cyanide ion, while according to them the anodic part is a composite process due to summation of argento-cyanide reduction and oxidation of mercury in the presence of cyanide ions formed during reduction of argento-cyanide ion.

Large and Przybylowicz[6] made more detailed investigations of this compound wave. They concluded that it is the result of anodic dissolution of mercury in the presence of cyanide ion and mercuro-cyanide reduction, where mercuro-cyanide and cyanide ions (as well as elementary silver) are formed in a fast chemical reaction between mercury and argento-cyanide

* Communicated at the 12th Conference of Chemists of the SR of Serbia, Beograd, January 1967.

ion. One of the direct proofs of this reaction path is, according to these authors, the fact that in the electrolysis of a solution of argento-cyanide ion labeled with Ag^{110} the same radioactivity of the mercury drop was recorded on the potential plateau of the anodic part of the wave as in open circuit electrolysis of the same solution.

While examining the possibility of polarographic determination of silver in non-cyanide electrolytes for silver plating, which we were systematically studying [7-9], we found that compound cathodo-anodic waves whose height depended on the concentration of silver were obtained in sulphite solutions containing silver too.

PRELIMINARY CONSIDERATIONS

It is known[10] that in sulphite solutions of sufficient concentration silver forms the complex ions $Ag(SO_3)^-$ and $Ag(SO_3)_2^{3-}$ with general instability constants $5.0 \cdot 10^{-6}$ and $4.5 \cdot 10^{-8}$, respectively. From the consideration presented in the introduction it follows that there are two possible ways in which one of these ions can react at the dropping mercury electrode: electrochemical and chemical. Let us consider these two possibilities on the example of $Ag(SO_3)_2^{3-}$.

If we assume that $Ag(SO_3)_2^{3-}$ reacts electrochemically at the dropping mercury electrode, then the cathodic process will be:

$$Ag(SO_3)_2^{3-} + Hg + e \longrightarrow Ag(Hg) + 2\,SO_3^{2-} \qquad (1)$$

The sulphite ions bring about an anodic current:

$$Hg + 2\,SO_3^{2-} \longrightarrow Hg(SO_3)_2^{2-} + 2\,e \qquad (2)$$

As the processes (1) and (2) occur simultaneously, the total anodic process obtained by adding (1) and (2) is

$$Ag\,(SO_3)_2^{3-} + 2\,Hg \longrightarrow Ag\,(Hg) + Hg(SO_3)_2^{2-} + e \qquad (3)$$

According to this picture of the electrode processes, the cathodic part of the compound wave would be the result of reaction (1) and the anodic reaction (3). Comparing equations (1) and (3) shows that the heights of the two parts should be equal and that their characteristics should correspond to single-electron exchange. The polarographic wave would be of a specific type as the cathodic and anodic parts correspond to the entirely different processes. The role of the half-wave potential in such a wave would be played by the zero current potential which would represent a typical mixed potential.

Let us now consider the other possibility, a previous chemical reaction of argento-sulphite ion and mercury:

$$3\,Hg + 2\,Ag\,(SO_3)_2^{3-} \longrightarrow Hg(SO_3)_2^{2-} + 2\,SO_3^{2-} + 2\,Ag(Hg) \qquad (4)$$

where it is assumed that the reaction rate is determined exclusively by $Ag(SO_3)_2^{3-}$ ion diffusion towards the surface of the drop.

The mercury-sulphite ions can undergo reduction by a cathodic current

$$Hg(SO_3)_2^{2-} + 2e \longrightarrow Hg + 2SO_3^{2-} \tag{5}$$

and the sulphite ions formed in reaction (4) can bring about an anodic current:

$$Hg + 2SO_3^{2-} \longrightarrow Hg(SO_3)_2^{2-} + 2e \tag{6}$$

Thus if this interpretation is correct, one would expect a compound wave whose cathodic part is due to reaction (5) and anodic to reaction (6). By comparing the equations (4), (5) and (6) it is readily concluded that the heights of the two waves, in the absence of excess sulphite, should be proportional only to the concentration of argento-sulphite ion and aproximately equal. As equations (5) and (6) represent a reversible electron exchange process, the cathodic part of the compound wave should obey the equation[7, 11, 12]:

$$E = E' + \frac{RT}{2F} \ln \frac{i_{d,k} - i}{i^2} \tag{7}$$

and the anodic part the equation

$$E = E' + \frac{RT}{2F} \ln \frac{i}{(i_{d,a} - i)^2} \tag{8}$$

while the equation for the compound wave should be

$$E = E' + \frac{RT}{2F} \ln \frac{i_{d,k} - i}{(i - i_{d,a})^2} \tag{9}$$

E' is the formal potential defined by

$$E' = E^0 + \frac{RT}{2F} \ln K + \frac{RT}{2F} \ln \frac{k_1^2}{k_2} \tag{10}$$

In equations (7) — (10) E is the potential, E° the standard potential of the Hg/Hg^{2+} system, i the working current, $i_{d,a}$ and $i_{d,k}$ the anode and cathode limiting diffusion currents, K the general constant of instability of the complex ion $Hg(SO_3)_2^{2-}$, k_1 and k_2 the proportionality coefficients of Ilkovich's equation; the other symbols have the usual electrochemical meaning.

EXPERIMENTAL

Solution for polarographic determination were prepared by mixing accurately measured volumes of initial solutions of $AgNO_3$ and $NaSO_3$ of known concentrations and diluting the mixture with a solution of 0.1

$N\ KNO_3 + 0.003\%$ gelatine as the supporting electrolyte up to the required volume. The initial solutions were prepared immediately before measuring from p.a. quality chemicals in freshly boiled double-distilled water freed of dissolved oxygen by bubbling through hydrogen. In the preparation of solutions measures were taken to prevent prolonged contact with air. Before each run purified hydrogen was briefly passed through the solution.

In the experiments in which polarograms were recorded at constant excess of sulphite and different concentrations of silver, the solution was prepared by adding a sulphite solution from a micro-burette to a strictly measured volume of the silver nitrate solution until a just visible opalescence was obtained. The opalescent solution approximately represents a solution of argento-sulphite ion. To this solution always the same volume of sulphite solution was added.

All the polarographic determinations were done on a Radiometer PO3'' polarograph.

The currents given on the graphs in Figs. 1—5 have been corrected for the precurrents of the supporting electrolyte, and the anodic limiting diffusion currents on the graphs in Figs. 2 and 4 for the dilution of the sulphite solution by the addition of silver solution.

In the polarography a 7 *cm* long capillary was used; the dropping rate was 4.57 *mg* sec^{-1} with a mercury column of 28 *cm*.

RESULTS AND DISCUSSION

Figure 1 shows the compound cathodic and anodic polarographic waves observed in solution of argento-sulphite ion with constant excess of sulphite.

It may be seen that the waves are well-defined with pronounced plateaus of the limiting diffusion currents. The heights of the cathodic and anodic parts increase with increasing silver concentration.

Figure 2 shows the dependence of the limiting diffusion currents of the anodic and cathodic parts on the concentration of silver. It is clearly seen from the graph that both limiting diffusion currents are proportional to the concentration of silver. The coefficients of the straight-line relationships between $i_{d,k}$ and c_{Ag} (5.3 μA lit $mmol^{-1}$) and $i_{d,a}$ and c_{Ag} are approximately equal, and also equal to the slope of the corresponding line for the anodic wave of pure sulphite (5.3 μA *lit* $mmol^{-1}$) given in our previous paper[7]. If the anodic limiting current for the constant excess of sulphite (5.0 μA, from Fig. 2) is subtracted from the values of the limiting diffusion current of the anodic part of the wave, then the limiting diffusion currents of the cathodic and anodic parts become approximately equal.

Figure 3 shows typical cathodic and anodic waves obtained when starting from a constant initial concentration of sulphite the concentration of silver was progressively increased. The cathodic part gets higher and the anodic lower.

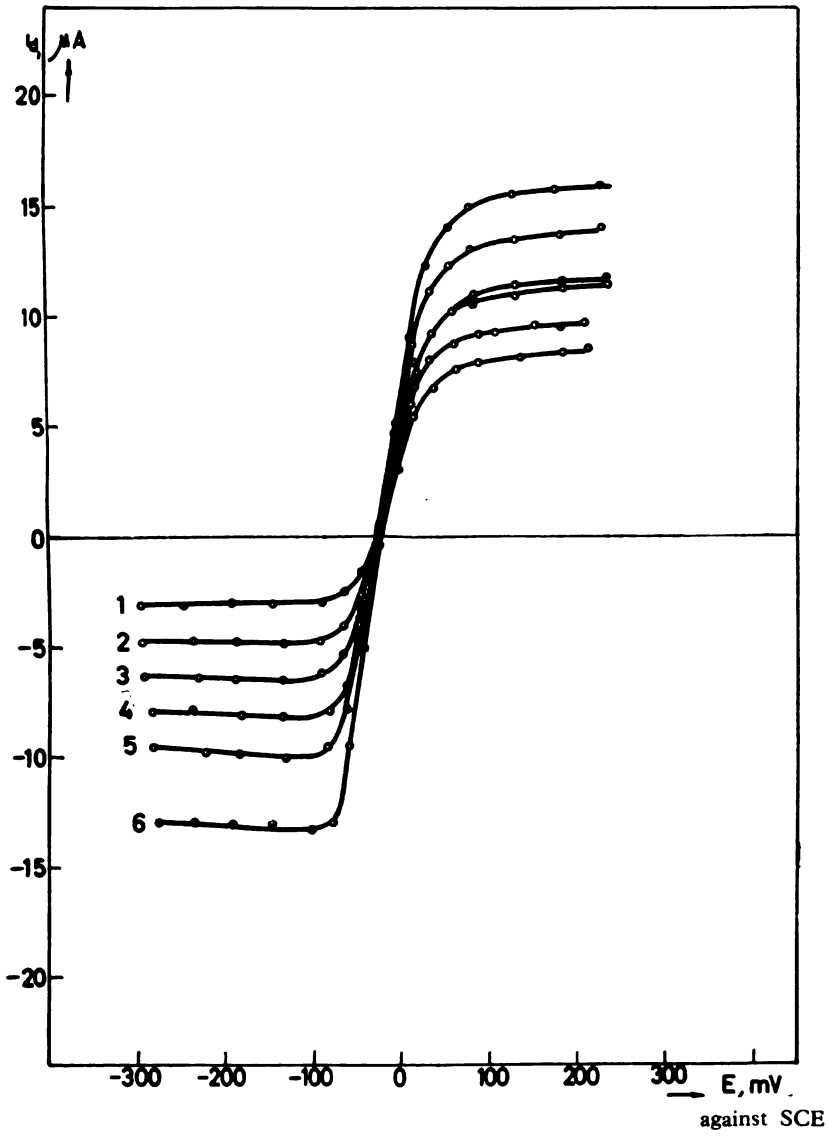

Figure 1

Polarographic waves in solutions containing argento-sulphite ion and a constant excess of sulphite

Ag concentration (*mmol.lit*$^{-1}$): 1—0.64; 2—0.95; 3—1.26; 4—1.56; 5—1.85; 6—2.43
Supporting electrolyte: 0.1 *N* KNO_3 + 0.003% gelatine

Figure 4 shows the dependence of the limiting diffusion currents of the cathodic and anodic parts and their sum on the concentration of silver. It may be concluded that the dependence is approximately linear with approximately equal coefficients, while the sum of the limiting diffusion currents is approximately constant.

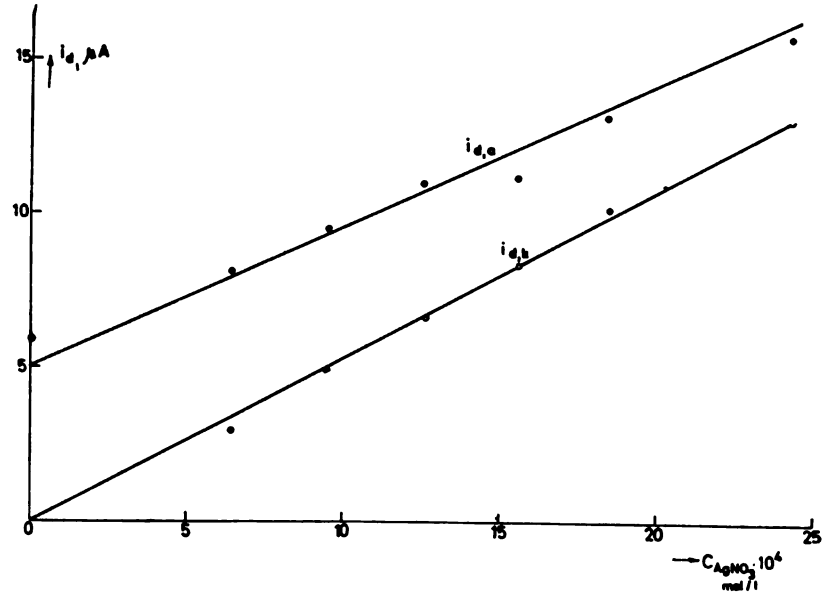

Figure 2

Dependence of cathodic ($i_{d,k}$) and anodic ($i_{d,a}$) limiting diffusion current on the concentration of silver

The results of a typical logarithmic analysis of a compound wave are shown in Fig. 5. The analysis is based on the dependence of E on $\log \frac{i}{(i_d - i)^2}$ where the limiting diffusion current of the cathodic part of the wave is taken to be zero, so that the diffusion current used in the calculation represents the sum of the cathodic and anodic limiting diffusion current. It is easy to show that the procedure is equivalent to the application of equation (9), i.e. to the logarithmic analysis of a compound wave formed in the presence of both forms of the reversible redox system.

It is seen from the graph that the dependence of E on $\log \frac{i}{(i_d - i)^2}$ for the compound wave (line 1) is a straight line with a slope of 32 *mV*. The dependence of E on $\log \frac{i}{(i_d - i)^2}$ (i_d being here the anodic limiting diffusion current) for the anodic wave of pure sulphite is also given.

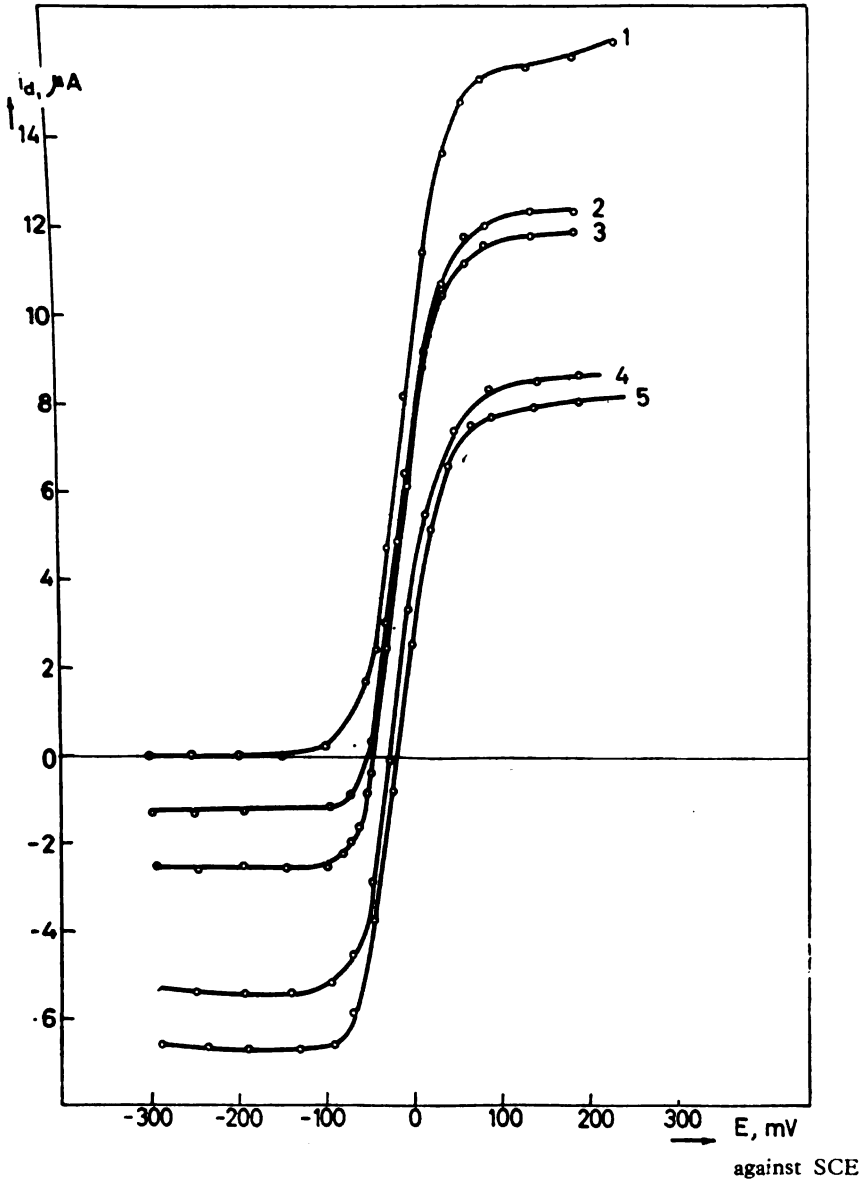

Figure 3

Polarographic waves in solutions containing argento-sulphite ions and a variable excess of sulphite

Ag concentration (*mmol.lit*$^{-1}$): 1— 0; 2— 0.25; 3— 0.50; 4— 0.98; 5— 1.21
Initial Na_2SO_3 concentration (*mmol.lit*$^{-1}$): 2.80
Supporting electrolyte: 0.1 *N* KNO_3 + 0.003% gelatine

The following conclusions can be drawn from these results.

(1) From the logarithmic analysis it follows that the compound wave is the result of two-electron exchange in the presence of both forms of the reversible redox system.

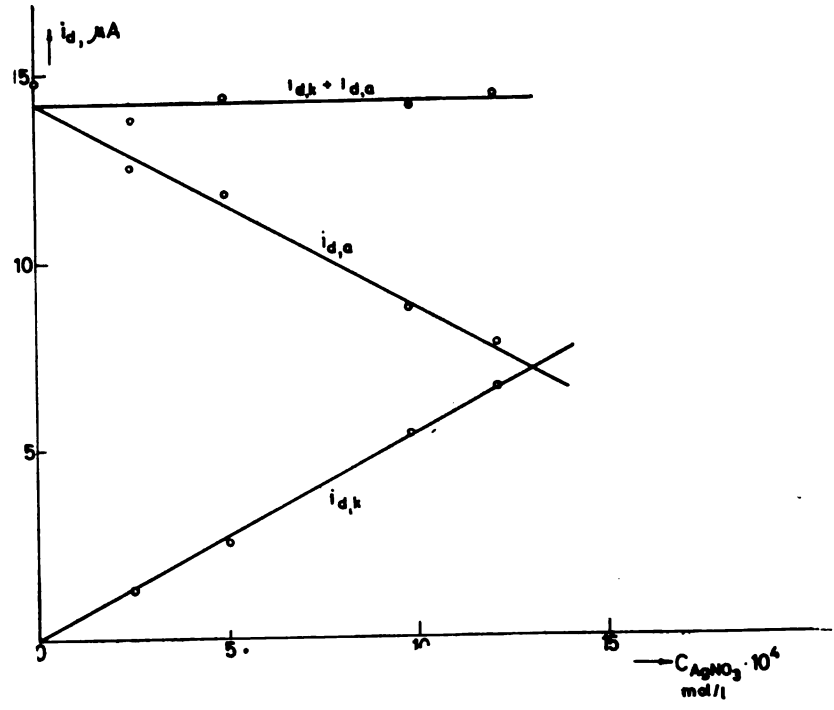

Figure 4

Dependence of limiting diffusion currents on the concentration of silver

(2) From the magnitudes and ratio of the limiting diffusion currents and their dependence on concentration it follows that the cathodic and anodic waves are the result of exchange of the same number of electrons and that the anodic process probably consists of oxidation of mercury in the presence of sulphite to mercury-sulphite ion.

The above properties of the wave can only be in accordance with the chemical reaction of the argento-sulphite ion:

$$3\,Hg + 2\,Ag(SO_3)_2^{3-} \longrightarrow 2\,Ag(Hg) + Hg(SO_3)_2^{2-} + 2\,SO_3^{2-}$$

where the $Hg(SO_3)_2^{2-}$ and SO_3^{2-} ions formed at the dropping mercury electrode give the compound cathodo-anodic wave of the reversible double-electron exchange

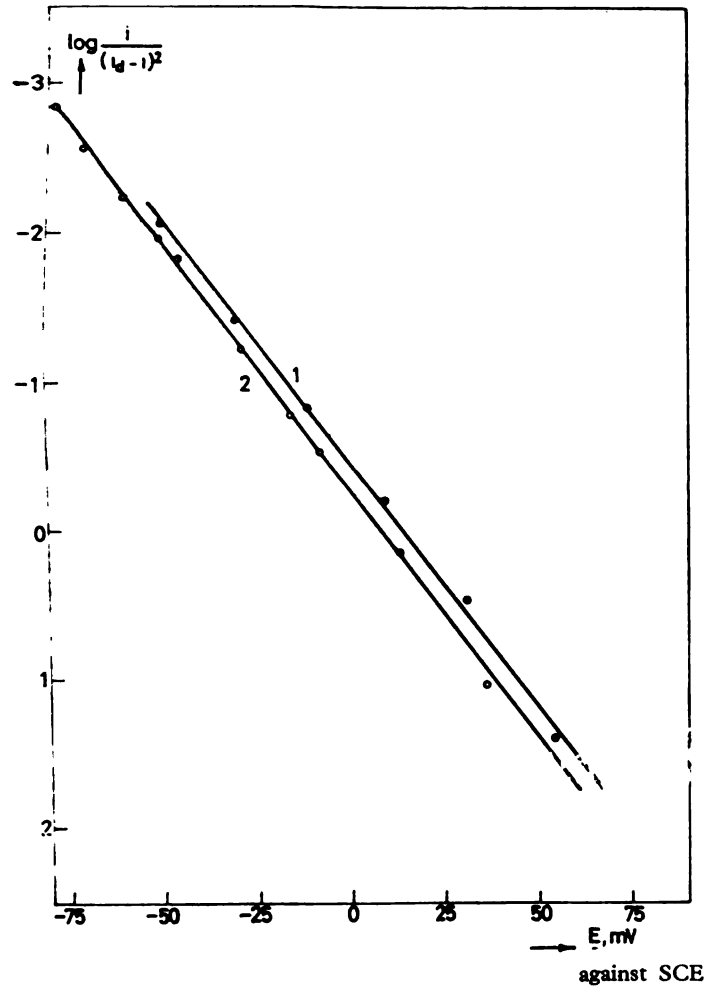

Figure 5

Logarithmic analysis of polarographic waves

1 — compound wave 3 from Fig. 3; 2 — anodic wave of sulphite 1 from Fig 3.

$$Hg(SO_3)_2^{2-} + 2e \longrightarrow Hg + 2SO_3^{2-}$$

$$Hg + 2SO_3^{2-} \longrightarrow Hg(SO_3)_2^{2-} + 2e$$

If the reaction rate of the argento-sulphite ion is determined only by its diffusion towards the mercury drop, the limiting diffusion currents of the cathodic and anodic parts of the wave will be proportional to the concentration of silver in the solution and approximately equal (if the dif-

ference between the coefficients diffusion of SO_3^{2-} and $Ag(SO_3)_2^{3-}$ ions is neglected) in the absence of excess sulphite. In the presence of excess sulphite the limiting diffusion current of the anodic part of the wave will be greater than that of the cathodic part.

The compound cathodic and anodic wave can be used for the determination of the concentration of silver and excess sulphite, as the dependence of the limiting diffusion currents on concentration allows analysis with sufficient accuracy.

Instityte of Physical Chemistry and
Electrochemistry, School of Technology,
Beograd

REFERENCES

1. Cave, G. and D. Hume. "Polarographic Determination of Low Concentrations of Silver" — *Analytical Chemistry* (Washington) 24: 588, 1952.
2. Israel, Y. and A. Vroman. "Rapid Polarographic Determinations of Silver in the Presence of Interfering Elements" — *Analytical Chemistry* (Washington) 31: 1470—1473, 1959.
3. Meites, L. and T. Meites. "Studies in the Theory of the Polarographic Diffusion Current. III. Diffusion Current Constants of Some Ions in Solutions Containing Gelatine. A Critique of the Strehlow-von Stackelberg Equation" — *Journal of American Chemical Society* (Easton, Pa.) 73: 395—398, 1951.
4. West, P., J. Dean and E. Breda. "Polarographic Behaviour of Ions Using Sodium Fluoride as Supporting Salt" — *Collection of Czechoslovak Chemical Communications* (Praha) 13: 1—10, 1948.
5. Bowers, R. and I. Kolthoff. "The Induced Reduction at the Dropping Mercury Electrode of Colloidal Silver Bromide by Dicyanide Argentate (I) Ion" — *Journal of American Chemical Society* (Easton, Pa.) 81: 1836—1840. 1959.
6. Large, R. and E. Przybylowicz. "Polarographic Behaviour of Silver in Cyanide Solutions" — *Analytical Chemistry* (Washington) 36: 1648—1652, 1964.
7. Ovcin, D., M. Vojnović and K. Popov. "Anodno rastvaranje žive u rastvorima sulfita pri različitim pH-vrednostima" (Anodic Dissolution of Mercury in Sulphite Solution at Different pH Values) — *Glasnik Hemijskog društva* (Beograd) (in press).
8. Rikovski, G., M. Vojnović and K. Popov. "Non-cyanide Electrolytes for Silver Plating" — *Zaštita materijala* (Beograd) 14: 111—116, 1966.
9. Popov, K., M. Vojnović and G. Rikovski. "Stationary Polarization Curves in Non-cyanide Electrolytes for Silver Plating" — *Hemijska Industrija* (Beograd) (in press).
10. *Spravochnik Khimika* (Handbook for Chemists) — Moskva: Khimia, 1964, p. 136.
11. Geirovskii, I. and I. Kuta. *Osnovy polarografii* (Fundamentals of Polarography) — — Moskva: Mir, 1965, pp. 112—118.
12. Charlot, G., J. Bavoz-Lambling, and B. Trémillon. *Electrochemical Reactions* — Amsterdam-New York: Elsevier, 1962, pp. 84—89.

GLASNIK HEMIJSKOG DRUŠTVA, Vol. 32, No. 2-3-4, 1967, pp. 193—197

SPECTROPHOTOMETRIC DETERMINATION OF PLATINUM AND RHODIUM IN GLASS WOOL

by

SRBOBRAN R. RAJIĆ

1. INTRODUCTION

The use of platinum-rhodium alloy as a catalyst in industry has made it necessary to analyze glass wool for these two metals. As both metals are expensive, their separation and purification is worthwhile. As far as we know, spectrochemical methods have not so far been used for analysis of glass wool for platinum and rhodium. Other materials used for container linings are analysed for these elements by means of X-ray fluorescence; the sensitivity of this procedure is 1% for platinum and 0.1% for rhodium[1, 2].

Spectrochemical analysis is the most convenient method for the determination of low concentrations of platinum and rhodium in glass wool and other materials. Our aim was to determine them at much lower concentrations than the above, which is of importance considering the high prices of both metals.

2. ANALYTICAL PROCEDURE

Preparation of the standard. An alloy of 90% platinum and 10% rhodium of high purity was used for the preparation of the standard. A measured quantity of the alloy was dissolved in *aqua regia*, then transferred to a volumetric flask which was filled up to the mark. Platinum-rhodium alloy dissolves in *aqua regia* if the amount of rhodium does not exceed 10%; if there is more it dissolves less or not at all if there is much more rhodium. The standard platinum and rhodium solution was put on a known quantity of finely ground Pyrex glass so that a standard glass sample with a known amount of platinum and rhodium was obtained. The solution was evaporated to dryness under an infra-red lamp and then the standard was heated at 500°C for half an hour to transform the chlorides of platinum and rhodium into the metals. After heating the standard was mixed in a mortar. This standard was the basic one from which others with alower content of platinum and rhodium were made by successive dilution with glass wool. Standards were made with a platinum concentration range of 0.0022—0.9% and rhodium 0.0002—0.1%.

Preparation of samples. Samples of glass wool containing platinum and rhodium were transferred to a mortar, care being taken that all was transferred, so that no powder remained at the bottom of the bag. After homogenization of the samples reproducible results were obtained. The mixing should be done long enough and with care as glass woll fibers grind slowly.

Palladium was chosen as the internal standard. It satisfies many criteria necessary for an internal standard in spectrochemical analysis: similarity of chemical properties with Pt and Rh, similar ionization potential, etc. Metallic palladium was dissolved in *aqua regia*, the solution evaporated to dryness, and then dissolved in water and transferred to a volumetric flask. The concentration of Pd in the measuring cylinder was 1 *mg/ml*. One *ml* of Pd solution was put on 1 gram of grafite powder, which was dried and heated at 500°C for 15 minutes to transform the palladium into metallic form. The sample was mixed in a mortar and then samples of grafite and the standards were again mixed in a mortar in the ratio 1 : 1. The samples were now ready for analysis.

Twenty milligrams of each standard was measured and transferred to a grafite electrode made from rods produced by the National Carbon Co. The electrodes were made in the form of small cups 3 *mm* in diameter and 3.5 *mm* deep. The electrode with the sample ignited with an 11 amp D.C. arc until completely burnt.

Spectra were recorded on a Jarrel Ash 3.4 *m* spectrograph with a plane grating and a reciprocal linear dispersion in the first-order spectrum of 5 Å/*mm*. Spectra were photographed on Illford Ordinary No. 30 plate and developed in Kodak D-19, processed for 4 minutes at 20°C. During photographing a rotating two-step sector was placed in front of the slit, with a step ratio of 1 : 2. The emulsion was calibrated with the iron lines by plotting tabular intensity on the apscissa and line density measured with a microphotometer on the ordinate. Correction for background was not made as it was unnecessary.

Analytical line pairs were:

Pt 2830 Å, first step,
Rh 3396 Å, second step
Pd 2763 Å, second step (internal standard).

Working curves were obtained by plotting the concentrations (u%) on the apscissa (log scale) against logarithm of the intensity line ratio on the ordinate.

Reproducibility was calculated from the formula

$$\% \, d = \frac{\Sigma | \bar{c} - c_i |}{n} \cdot \frac{100}{\bar{c}}$$

for a number of concentrations of both elements; it varied decreasing with increasing concentration. It ranged from ± 3.4 to $\pm 6.1\%$.

3. RESULTS AND DISCUSSION

In developing this method we had to take into account the chemical composition of the basic component — glass; the standards were made of the same components and in as close as possible the same ratio, in order to avoid the influence of the carrier which is frequent in spectrochemical analysis. Qualitative analysis of different kinds of glass showed differences in their chemical composition. For us it was important to use glas whose chemical composition corresponded to that which was to analysed for platinum, rhodium. The extent of the influence of different components on the intensity of the spectral lines of platinum, rhodium and palladium is shown in Table 1. Each component was added separately to quartz as the base. Measured amounts of platinum, palladium and rhodium were added to pure quartz powder and a standard was made with the following concentrations: *Pt* 0.09%, *Rh* 0.01% and *Pd* 0.005%. To this standard Fe_2O_3, *CaO* *CuO*, Al_2O_3, *MgO*, and Na_2CO_3 were added separately to give mixtures containing 10% of each of these salts.

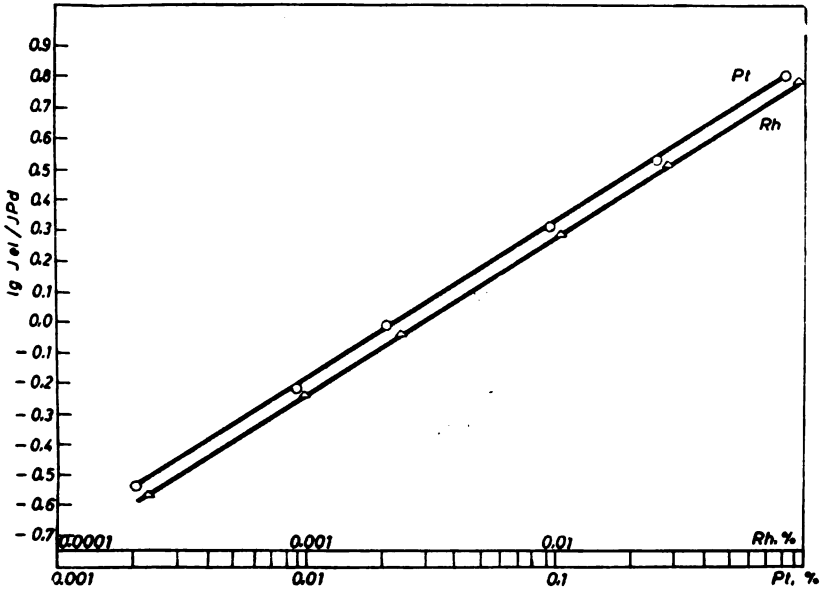

Figure 1

Curves for the determination of *Pt* and *Rh* in glass wool

Iron oxide had little influence in the spectral lines of platinum, rhodium and palladium. Sodium carbonate caused the most marked reduction in intensity, i.e. line density, followed by magnesium oxide, copper oxide, and aluminum trioxide with the least influence. By increasing the concentrations of the added compounds their influence became greater, but from 1% upwards there were no significant changes.

TABLE 1

The effect of some salts on density of spectral lines of Pt, Pd and Rh. Content of: Pt 0.09%, Rh 0.01%, Pd 0.005% in quartz

Wavelength, λ	*Pt* 2850	*Pd* 2763	*Rh* 3396
Quartz	1.06	1.03	1.23
Quartz with 10% Fe_2O_3	1.02	1.12	1.28
Quartz with 10% CaO	0.75	0.86	0.83
Quartz with 10% CuO	0.99	0.86	1.06
Quartz with 10% Al_2O_3	0.76	0.89	0.84
Quartz with 10% MgO	0.72	0.80	0.71
Quartz with 10% Na_2CO_3	0.69	0.74	0.66

TABLE 2

Determination of Pt and Rh in glass wool samples; results obtained by emission spectrography and X-ray fluorescence method

Sample	Found			
	Pt %		*Rh* %	
	Spectrogr.	X-Ray anal.	Spectrogr.	X-Ray anal.
1	20.5	21.2	0.86	1.0
2	1.63	1.55	0.04	0.1

The accuracy of the method was checked against analysis for platinum and rhodium by the X-ray fluorescence method used at the Institute. The results are shown in Table 2. The concentrations of platinum and rhodium above the range of our study were measured by diluting with glass. Thus the conditions of comparison are less favorable than in direct determination. Our procedure is for lower concentrations than can be measured by X-ray fluorescence analysis.

Institute of Nuclear Science,
Beograd

Received 10 February, 1966.

REFERENCES

1. Lincoln, A., and E. Davis. — *Analytical Chemistry* 31 (8): 1317—1320, 1959.
2. Van Nordstrand, R., A. Lincoln and A. Carnevale. — *Analytical Chemistry* 36 (4): 819—824, 1964.

GLASNIK HEMIJSKOG DRUŠTVA, Vol. 32, No. 2-3-4, 1967, pp. 199—211

CALCULATION OF TRUE CONCENTRATIONS OF THE MEASURED COMPONENTS IN THE SURFACE LAYER OF A SPECIMEN FOR QUANTITATIVE X-RAY DIFFRACTION ANALYSIS OF POWDER MIXTURES*

by

VERICA D. RAJKOVIĆ

In previous papers it was observed that in specimens for quantitative X-ray powder analysis prepared by the method of K. Kay there was selective sedimentation of the components[1-4]. A consequence of this is a new weight ratio of the components in the surface layer which is different from that in the specimen from which the sample was made.

From the results presented in this paper certain regularities were observed on the basis of which two hypotheses were set up, namely: (1) that the X-ray intensity diffracted from the crystals of a component of the mixture is proportional to the concentration of the component in the surface layer of the specimen; (2) that only that part of the radiation diffracted from the crystals in the surface layer is certainly recorded by the goniometer counter at the position corresponding to the line measured. Rays which penetrate to deeper layers of the specimen and get diffracted from crystals in these layers most probably later impinge on the corresponding crystal faces in layers closer to the surface, from which they are again diffracted, so that the counter records them as diffuse radiation.

In order to verify these hypotheses it is necessary to calculate the concentration of a component or the ratio of the concentrations of two components of the dispersed mixture in the surface layer of a specimen at a time t after the beginning of sedimentation. The calculated ratio C_A/C_B must then be compared with the measured ratio I_A/I_B for the same specimen.

Since in the available literature we did not find any formula for calculating the concentration of one component or the ratio of the concentrations of two components in the surface of a sample in which sedimentation has been stopped by drying, the aim of this study was to derive such a formula on the basis of:

a) experimental findings;

b) considerations of the phenomena which take place in the suspension from application to the slide until completion of drying;

* The paper is a part of a report communicated at the Symposium on Chemical Engineering held as part of the XIth Conference of Chemists of Serbia, Beograd, 1965.

c) conditions under which surface layer concentrations in the sample do not alter from the concentrations in the specimen from which the sample was obtained.

SEDIMENTATION IN SUSPENSIONS OF POLYDISPERSED MIXTURES

From the very beginning of sedimentation all the particles start to move and under conditions of constrained fall very soon reach a constant terminal velocity. Several zones are then formed in the suspension layer:

a) the zone of coarse particles at the bottom;

b) above zone *a* is a zone consisting of particles of different size and in which the concentration ratios of the components are uneven;

c) on top of this there is a zone of the finest particles of all the components in which the concentration ratios are uniform;

d) above the last zone of the suspension there is only pure dispersion medium[5].

If we let the volatile dispersion medium evaporate right from the start of sedimentation, which is the case in powder samples for X-ray diffraction analysis prepared by the method of K. Kay, the sedimentation will eventually be interrupted by drying. It may be assumed with considerable certainty that during the interval from the beginning of sedimentation to complete drying out of the specimen the coarse particles will have fallen to the bottom, and that the zones *b* and *c* will have been formed, and it is certain that in zone *c* the concentration ratios will not always be the same as in the initial suspension or in the specimen from which the suspension was prepared.

By detailed investigation of sedimentation in suspensions of polydispersed mixtures of different components, such as *CaO*, $CaCO_3$, *Mgo*, $MgCO_3$, PbO_2, *CuO* and *ZnO*, and particularly Sb_2O_3, *Sb* and SiO_2[6—8], it was found that the rate of sedimentation, the occurrence of selective sedimentation and the distribution of the components in the precipitated sediment depend on:

— the concentration of the dispersed mixture in suspension,

— the composition of the dispersing medium,

— the weight ratio of the components in the mixture,

— specific gravity of the mixture, which is a function of the specific gravity of the components,

— specific gravity of the suspension, which is a function of the specific gravities of the dispersed mixture and the dispersing medium,

— the mean grain size distribution of the dispersed mixture which is a function of the grain size distribution of the components.

Apart from this it was observed that for the weight ratio of components in zone *c* of a sample prepared by Kay's method two factors have decisive influence:

1. — the precipitation of coarse particles with dimensions $D - D_{max}$;

D denotes the dimension of the observed particles, D_{max} that of the largest particles, and D_{min} that of the smallest.

2. — selective sedimentation of finer particles with dimensions $D_{min} - D$ in the suspension above the layer with dimensions $D - D_{max}$.

To derive a formula for calculating the concentrations of concentration ratios in the surface layer the terms ideal, theoretical and real calibration curve were introduced.

IDEAL, THEORETICAL AND REAL CALIBRATION CURVE

It was previously assumed that the X-ray intensity ratio I_A/I_B is proportional to the ratio of concentrations of the components in the surface layer of the specimen C_A/C_B. The "ideal calibration curve" is the curve which would be obtained if the following conditions were fulfilled by the suspension from which samples for plotting this curve are prepared:

1. specific gravities of all components the same,
2. grain size distributions of all components the same,
3. a given concentration increase produces the same change of viscosity of the suspension for all components.

Under these conditions particles of same size of any component in suspensions of any of the mixtures from the same series move at the same speed, there is no selective sedimentation and the concentration ratios in all layers of the suspension remain constant from the beginning to the end of sedimentation.

In practice it is almost impossible to get a system which fulfills the above three conditions as well as the conditions required by X-ray analysis. Therefore the term "theoretical calibration curve" was introduced. In suspensions for the preparation of samples for the calibration curve difference in specific gravity and grain size distribution between some of the components and the occurrence of selective sedimentation are permitted. However, a change in the percentage concentration of a component in mixtures of a given series must not change the rate of selective sedimentation via a change in:

1. — the mean specific gravity of mixtures in a series,
2. — the mean grain size distribution of the mixtures in a series,
3. — viscosity of the suspensions prepared from the mixtures of a series,
4. — the duration of drying of samples of a given series.

The theoretical calibration curve is a straight line, like the ideal calibration curve.

The "real calibration curve" can differ from the theoretical curve due to a deviation from any of the above conditions. It may be a straight line or an exponential curve and can lie above or below the theoretical curve.

From now on all the values which refer to an ideal sample or an ideal calibration curve will be given the suffix i, those referring to the theoretical calibration curve t, and those to the real calibration curve without a suffix.

The methods for quantitative X-ray diffraction analysis of powder mixtures can be classified according to the number of measured compo-

nents, the number of components in the mixture and the manner of interpretation of the results:

1) methods which measure the X-radiation diffracted from a single component:

a) direct analysis

b) analysis of binary mixture systems

2) methods which measure the X-radiation diffracted from two components:

a) analysis of two-component mixture systems

b) internal standard method

Calibration curves for all four methods were considered under the condition that the change in the intensity diffracted from a given component was proportional to the change in the concentration of that component in the surface layer of the sample. The ideal, theoretical and real calibration curves for these methods were defined in the following way:

Direct analysis

The calibration curve shows the dependence of I (X-ray intensity diffracted from crystals of the component) or C (% concentration of the component in the surface layer) on the % concentration of the component in the sample from which the specimen was prepared. The ideal calibration curve is a straight line, e.g. line 1 in Fig. 1. Because of selective sedimentation in specimens prepared from pure component the theoretical calibration curve can differ from the ideal curve, as illustrated by curves 2 and 3,

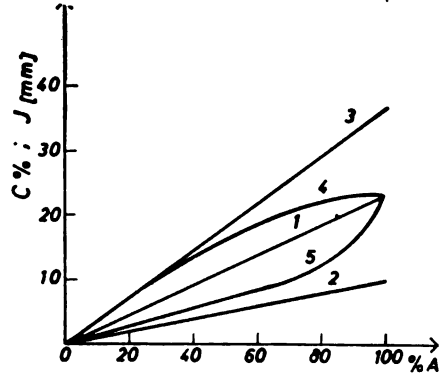

Figure 1

Calibration curves for direct analysis: (1) ideal, (2) (3) theoretical, (4) (5) real.

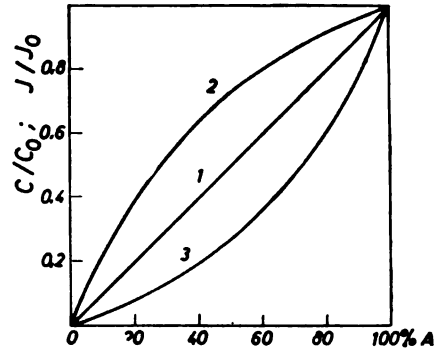

Figure 2

Calibration curves for analysis of binary systems with one component measured: (1) ideal and theoretical, (2) (3) real

exclusively due to the influence of powder particle size on the measured diffraction maximum. This influence was not investigated in the present study. In its absence the ideal and theoretical calibration curves coincide.

Because of selective sedimentation in samples prepared from mixtures with concentrations of components between 0% and 100%, the real calibration curve can lie either above or below the theoretical curve and have a shape like that of curves 4 and 5.

Analysis of binary mixture systems with one measured component. The calibration curves of some authors[9] represent the dependence of the ratio C/C_0 and of others[10] of the ratio $\frac{C}{C_0} \times 100$ on the % concentration of the measured component in the sample when:

I_0, the intensity diffracted from the measured component, is measured on a specimen prepared from the pure measured component, and

C_0, the concentration of the measured component in the surface layer of the specimen on which I_0 was determined.

I and C have the same meaning as in direct analysis.

The straight line connecting the values for 0% and 100% of measured component in Fig. 2 at the same time represents the ideal and theoretical calibration curve. The real calibration curve, because of selective sedimentation in specimens prepared from mixtures with concentrations of the measured component between 0% and 100%, can have a shape like that of curve 2 or 3 in Fig. 2.

Analysis of two-component mixture with two measured components. The calibration curves represent the dependence of the ratio I_A/I_B or the ratio C_A/C_B on the % concentration of component A in the sample from which the specimen was prepared. The symples have the following meaning:

I_A — intensity diffracted from component A, measured on a sample prepared from a mixture with a concentration A between 0% and 100%,

I_B — intensity diffracted from component B, measured on the same sample,

C_A — concentration of component A in the surface layer of the sample on which I_A was measured,

C_B — concentration of component B in the surface layer of the same sample.

The method can be considered as a special case of the internal standard method as it gives the ratio of the intensity of the measured components in mixtures for the case of 100% of the measured component in the internal standard method. The theoretical and real calibration curves, because of sedimentation in the specimens, can lie above or below the ideal curve, as shown by curves 2 and 3 in Fig. 3.

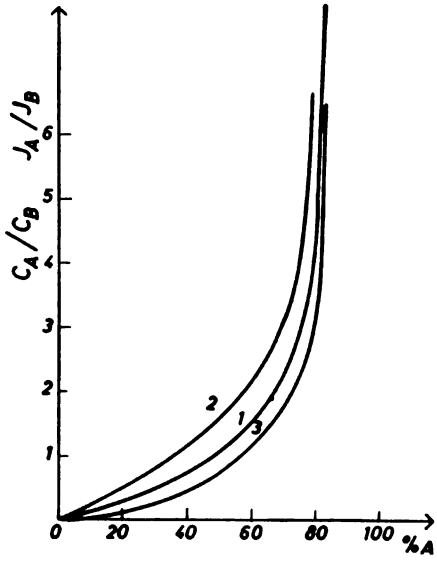

Figure 3

Calibration curves for analysis of two-component systems with two components measured: (1) ideal and theoretical, (2) (3) real

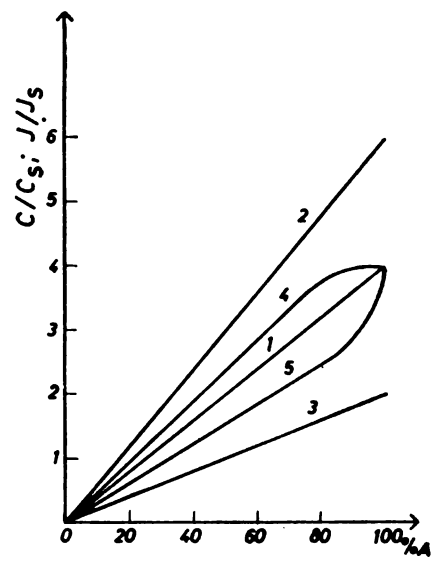

Figure 4

Calibration curves for the method internal standard: (1) ideal, (2) (3) theoretical, (4) (5) real

Internal standard method. The calibration curves for this method give I/I_s or C/C_s as a function of the % concentration of the measured component in the initial mixture. The symbols have following meaning:

I_s — intensity diffracted from the internal standard, measured on a specimen prepared from a mixture with a concentration of the measured component between 0% and 100%, and

C_s — concentration of the internal standard in the surface layer of the specimen on which I_s was determined.

I and C have the same meaning as in direct analysis.

The ideal calibration curve in this case is the line 1 in Fig. 4. It connects the zero point with the point denoting 100% of the measured component under study, which corresponds to a specimen in which there is no selective sedimentation. The theoretical calibration curve is also a straight line and often lies above or below the ideal curve, like curves 2 and 3. The difference of the theoretical 100% point from the corresponding ideal point is due to selective sedimentation in the specimen and its consideration is covered in the previous method.

The real calibration curve can have any of the shapes schematically represented by curves 4 and 5 in Fig. 4.

Equation for the calculation of the true concentration or concentration ratio in the surface layer

By means of the ideal, theoretical and real calibration curves a distinction is made between the sedimentation in real specimens and "theoretical" specimens in which sedimentation would take place under the same conditions as in specimens prepared from a mixture with 100% of the measured component. Formulas are derived for the true concentration of concentration ratios in the surface layer which differed from the corresponding theoretical values because of (1) the precipitation of particles with dimensions $D - D_{max}$ and (2) selective sedimentation of particles with dimensions $D_{min} - D$.

Sedimentation of particles with dimensions $D - D_{max}$

Immediately after applying the suspension to the slide particles of all the components larger than a certain dimension D fall to the bottom. Smaller particles, of dimensions $D_{min} - D$, remain in suspension. The number of these particles per 100 particles of the mixture is the minus fractional composition of the mixture and in this paper will be denoted as ψ_{sm}.

In a series of mixtures of two components A and B a change in the concentration of A causes a change in the concentration of B. In cases when $\gamma_A \neq \gamma_B$ and $\psi_A \neq \psi_B$, the values γ_{sm} and ψ_{sm} will change with a change in the concentrations of the components and *vice versa*.

Considerations of suspensions of two-component polydispersed mixtures show that the change in the concentration of the lighter component in the surface layer is directly proportional to the change of γ_{sm} and inversely proportional to the change of ψ_{sm}.

Applying this to real and theoretical samples for direct diffraction analysis, the following formula for C, the true concentration of the measured component in the surface layer, in terms of the corresponding theoretical value C_t is obtained:

$$C = C_t \left(\frac{\gamma_{sm} \cdot \psi_{sm_t}}{\gamma_{sm_t} \cdot \psi_{sm}} \right)^{\frac{\gamma - \gamma_{sm}}{\gamma_{sm_t} - \gamma_{sm}}}$$

The theoretical specimen is prepared from pure measured component. γ is the specific gravity of the measured component.

From the formula it may be seen that:

a) the concentration of the lighter component, that is of the component with the higher ψ value, is higher in the surface layer if $\gamma < \gamma_{sm}$ and $\psi > \psi_{sm}$, and *vice versa*.

b) the concentration of the measured component in the surface layer of a dried specimen decreases with increasing thickness of the layer of particles of the supporting components between the surface of the specimen and the particles of the measured component. This is due to the differences in the exponent.

c) the difference $(\gamma - \gamma_{sm})$ in the numerator of the exponent determines the thickness of the layer of particles of the supporting components between the particles of the measured component and the surface of the specimen and its influence on the concentration of the measured component in the surface layer.

d) the difference $(\gamma(\gamma_{sm_t} - \gamma_{sm})$ in the denominator of the exponent defines the influence of the thickness of the layer of particles of the supporting components located between the particles of the measured component and the surface of the specimen due to change of the mean specific gravity of the mixture.

In the analysis of binary mixture systems with a single measured component the true value of the ratio C/C_0 are calculated from the formula

$$\left(\frac{C}{C_0}\right) = \left(\frac{C}{C_0}\right)_t \left(\frac{\gamma_{sm} \cdot \psi_{sm_t}}{\gamma_{sm_t} \cdot \psi_{sm}}\right)^{\frac{\gamma - \gamma_{sm}}{\gamma_{sm_t} - \gamma_{sm}}}$$

which is arrived at by setting up the proceding formula for a specimen with a concentration of the measured component between 0% and 100% and for a specimen prepared from pure measured component, and dividing.

In two-component mixture systems with two measured components the true value of the ratio C_A/C_B is to be calculated. The formula is derived by setting up the basic formula for each of the measured components in the surface layer, taking into account the fact that A is the measured component and that the theoretical specimen has the properties of a pure measured component. By dividing these two formulas a formula is obtained for calculating the ratio

$$\frac{C_A}{C_B} = \left(\frac{C_A}{C_B}\right)_t \left(\frac{\gamma_{sm} \cdot \psi_{sm_t}}{\gamma_{sm_t} \cdot \psi_{sm}}\right)^{\frac{\gamma_A - \gamma_B}{\gamma_{sm_t} - \gamma_{sm}}}$$

To calculate the value of C/C_s in the surface layer prepared from a mixture with 100% of the measured component by the internal standard method, the formula has the following form:

$$\frac{C}{C_s} = \left(\frac{C}{C_s}\right)_t \left(\frac{\gamma_{sm} \cdot \psi_{sm_t}}{\gamma_{sm_t} \cdot \psi_{sm}}\right)^{\frac{\gamma - \gamma_s}{\gamma_{sm_t} - \gamma_{sm}}}$$

Considerations of suspensions of three-component polydispersed mixtures in the internal standard method showed that the change in the concentration ratio of a lighter and a heavier measured component in the surface layer is inversely proportional to the change of γ_{sm} and directly proportional to the change of ψ_{sm}. The resulting formula is:

$$\frac{C}{C_s} = \left(\frac{C}{C_s}\right)_t \left(\frac{\gamma_{sm_t} \cdot \psi_{sm}}{\gamma_{sm} \cdot \psi_{sm_t}}\right)^{\frac{\gamma - \gamma_s}{\gamma_{sm_t} - \gamma_{sm}}}$$

The theoretical specimen is prepared from a mixture with 100% of the measured component. γ_s is the specific gravity of the internal standard.

Analysis of the above formula shows the following:

a) The concentration ratio of the measured component and of the internal standard in the surface layer when $\gamma < \gamma_s$ and $\psi > \psi_s$ is increased if $\gamma_{sm_t} > \gamma_{sm}$ and $\psi_{sm_t} < \psi_{sm}$ and decreased if $\gamma > \gamma_s$ and $\psi < \psi_s$.

b) The concentration of each of the measured components in the surface layer of a dried specimen decreases with increasing thickness of the layer of particles of the supporting components between the surface of the specimen and the particles of the measured component. However, the distance between particles of the measured components of the same size (in the surface layer) increases with increasing thickness of the layer of particles of the supporting components. This change and its influence on the concentration ratio of the measured components in the surface layer are expressed by the difference in the exponent in the above formula.

c) The differences $(\gamma - \gamma_s)$ in the numerator of the exponent expresses the influence of the difference in specific gravities of the measured components on the thickness of the layer of particles of the supporting components between particles of same size of the measured components in the surface layer and on the value of C/C_s.

d) The difference $(\gamma_{sm_t} - \gamma_{sm})$ in the denominator of the exponent expresses the influence of a change in the thickness of the layer of particles of the supporting components located between the particles of same size of the measured components in the surface layer of the specimen, due to a change in the mean specific gravity of the mixture.

Sedimentation of the particles with dimensions $D_{min} - D$

After the precipitation of the particles with dimensions $D - D_{max}$, in the remaining suspension selective sedimentation of the particles with dimensions $D_{min} - D$ occurs. During some time t, depending on the conditions, i.e. the rate of sedimentation, these particles will be distributed in some volume V, equal to the product of the path length S traversed by particles of dimension D during time t and the area of the specimen P. S is equal to the product of the particle velocity v and the time t. If the particle speed is expressed by Stokes's equation, then

$$V = S \cdot P = v \cdot t \cdot P = \frac{(\gamma - \gamma_{susp})\, g\, D^2}{18\, \eta_{susp}} \cdot t \cdot P$$

In a series of mixtures of components A and B, a difference in the concentration of A caused a difference in the concentration of B. When $\gamma_A \neq \gamma_B$, a change in the concentration with one component of the mixture also means a change of γ_{sm}. Since a change of γ_{sm} causes a change of γ_{susp} and η_{susp}, it is clear that it also causes a change of the velocity of particles of the same size and a change of S.

Two facts should be noted here:

1. The concentration of each of the components in the surface layer, with respect to its concentration in the suspension before the beginning of sedimentation, shows a decrease with increasing volume V. Therefore the concentration of a component in the surface layer is inversely proportion to the volume V for that component, $C\ 1/V$.

2. The concentration of a component in the surface layer, with respect to its concentration in the mixture before the beginning of sedimentation can decrease or increase with increasing V of the mixture.

Considerations of suspensions of two-component polydispersed mixtures show that the change in the concentration of the lighter component in the surface layer of the specimen is directly, and the change in the concentration of the heavier component inversely proportional to the change of the volume in which they are distributed, that is to the path length which the particles of dimensions D traverse during the same time t from the beginning of sedimentation. However, a change in volume V, or path S due to a change in the duration of sedimentation can be caused by a change in the quantity of dispersing substance in the suspension layer or by a change in the drying temperature. The quantity of dispersing substance in the suspension layer of specimens of the same series changes with the specific gravity of the mixture.

For the method of direct analysis the change in the concentration of the measured component in the surface layer produced by a change of V, i.e. of S, or the true concentration of the measured component, can be calculated according to the formula:

$$C = C_t\left(\frac{S}{S_t}\right)^{\frac{\gamma-\gamma_{sm}}{\gamma_{sm_t}-\gamma_{sm}}} = C_t\left[\frac{\eta_t+(\gamma-\gamma_{susp})t}{\eta(\gamma-\gamma_{susp_t})t_t}\right]^{\frac{\gamma-\gamma_{sm}}{\gamma_{sm_t}-\gamma_{sm}}}$$

The ratio C/C_0 in the analysis of binary systems with one component measured is given by

$$\frac{C}{C_0} = \left(\frac{C}{C_0}\right)_t\left(\frac{S}{S_t}\right)^{\frac{\gamma-\gamma_{sm}}{\gamma_{sm_t}-\gamma_{sm}}} = \left(\frac{C}{C_0}\right)_t\left[\frac{\eta_t(\gamma-\gamma_{susp})t}{\eta(\gamma-\gamma_{susp_t})t_t}\right]^{\frac{\gamma-\gamma_{sm}}{\gamma_{sm_t}-\gamma_{sm}}}$$

and for analysis of two-component mixture systems with two components measured by

$$\frac{C_A}{C_B} = \left(\frac{C_A}{C_B}\right)_t\left(\frac{S}{S_t}\right)^{\frac{\gamma_A-\gamma_B}{\gamma_{sm_t}-\gamma_{sm}}} = \left(\frac{C_A}{C_B}\right)\left[\frac{\eta_t(\gamma_A-\gamma_{susp})t}{\eta(\gamma_A-\gamma_{susp_t})t_t}\right]^{\frac{\gamma_A-\gamma_B}{\gamma_{sm_t}-\gamma_{sm}}}$$

S and S_t are the thicknesses of the layer of pure dispersing substance. With decreasing specific gravity of the dispersed mixture there is an increase of its volume and a decrease of the volume of the dispersing substance in the same volume of suspension. For the evaporation of a smaller volume of the dispersing substance less time is necessary. Sedimentation takes less time in such a sample, and the layer of particles of the supporting components between the surface of the specimen and the particles of the measured

component is increased. This means a decrease in the concentration of the measured component in the surface layer relative to its concentration under theoretical conditions. If the specific gravity of the mixtures in a series increases with decreasing concentration of the measured component, the concentration of the measured component is higher in the surface layer.

The last formula is also used for calculating C/C_g in a sample prepared from a mixture with 100% of the measured component, under the condition that component A is the one to be determined.

When similar considerations are applied to specimens prepared from three-component mixtures for the internal standard method, with concentrations of the component measured between 0% and 100%, we arrive at the formula

$$\frac{C}{C_s}=\left(\frac{C}{C_s}\right)_t\left(\frac{S_t}{S}\right)^{\frac{\gamma-\gamma_s}{\gamma_{sm_t}-\gamma_{sm}}}=\left(\frac{C}{C_s}\right)_t\left(\frac{\eta\,(\gamma-\gamma_{susp_t})\,t_t}{\eta_t\,(\gamma-\gamma_{susp})\,t}\right)^{\frac{\gamma-\gamma_s}{\gamma_{sm_t}-\gamma_{sm}}}$$

As in the case of two-component mixtures, a reduction of the specific gravity of the mixture by reducing the concentration of the measured component decreases the quantity of dispersing medium and the duration of drying, and hence the selective sedimentation. This means a decrease in the thickness of the layer of particles of the supporting components between particles of the same size of the components measured, which changes the ratio C/C_s. When $\gamma < \gamma_s$ the ratio C/C_s decreases, and when $\gamma > \gamma_s$ it increases, relative to its value under theoretical conditions.

Analysis of the proposed formulae on schematically represented ideal, theoretical and real calibration curves in Figs. 1—4 indicates the possibility that selective sedimentation during preparation of specimens causes a change in the shape of the calibration curves. Experimental verification of these formulas will be given in future papers and will consist of a comparison of calibration curves from the literature determined by means of X-rays with the corresponding calibration curves calculated by using the formulas.

School of Technology,
Department of Food Technology,
Beograd.

Received 15 November, 1966

REFERENCES

1. Rajković, V. "Uticaj sedimentacije na oblik kalibracionih krivih za rentgensku difrakcionu analizu nekih jedinjenja antimona. I. Uticaj količine suspenzije po primerku na odnos I/I_s" (The Influence of Sedimentation on the Form of Calibration Curves for X-Ray Diffraction Analysis of Some Antimony Compounds. I. The Influence of the Quantity of Suspension per Specimen on the Ratio I/I_s) — *Glasnik Hemijskog društva* (Beograd) 29*: 23—28, 1964.
2. Rajković, V. "Uticaj sedimentacije na oblik kalibracionih krivih za rentgensku difrakcionu analizu nekih jedinjenja antimona. II. Uticaj koncentracije komponenata čiji se intenziteti ne mere na vrednost odnosa I/I_s" (The Influence of Sedimentation on the Form of Calibration Curves for X-Ray Diffraction Analysis of Some Antimony Compounds. II. The Influence of the Concentration of Components whose Intensity is not Measured on the Value of I/I_s) — *Glasnik Hemijskog društva* (Beograd) 29*: 29—34, 1964.
3. Rajković, V. "Uticaj sedimentacije na oblik kalibracionih krivih za rentgensku difrakcionu analizu nekih jedinjenja antimona. III. Direktna analiza" (The Influence of Sedimentation on the Form of Calibration Curves for X-Ray Diffraction Analysis of Some Antimony Compounds. III. Direct Analysis) — *Glasnik Hemijskog društva* (Beograd) 29*: 35—44, 1964.
4. Kay, K. "Rapid Quartz Analysis by X-Ray Spectrometry" — *American Industrial Hygiene Association Quarterly* 11 (12): 185—194, 1950.
5. Faust, A. and co-workers. *Principles of Unit Operations* — New York: John Wiley, 1960.
6. Petronić-Rajković, V. "Sedimentacija u suspenzijama smeša sprašenih Sb_2O_3, *Sb* i SiO_2 u amilacetatu" (Sedimentation in Suspensions of Powder Mixtures of Sb_2O_3, *Sb* and SiO_2 in Amylacetate) — *Hemijska industrija* (Beograd) 15 (11): 2032—2032c, 1961.
7. Petronić-Rajković, V. "Uticaj kolodijuma na sedimentaciju suspenzija Sb_2O_3, *Sb* i SiO_2 u amilacetatu" (The Influence of Collodium on Sedimentation of Sb_2O_3, *Sb* and SiO_2 in Amylacetate) — *Hemijska industrija* (Beograd) 16 (1): 121—124, 1962.
8. Rajković, V. "Uticaj čvrstog razblaživača na sedimentaciju smeša Sb_2O_3 i *Sb* suspendovanih u amilacetatu, etilalkoholu i njihovim smešama" (The Influence of Solid Dilutant on Sedimentation of Sb_2O_3 and *Sb* Mixtures Suspensed in Amylacetate, Ethyl Alcohol and Their Mixtures) — *Hemijska industrija* (Beograd) 19 (3): 548—550, 1965.
9. Alexander, L. and H. Klug. "Basic Aspects of X-Ray Absorption in Quantitative Diffraction Analysis of Powder Mixture" — *Analytical Chemistry* (Washington) 20: 886—889, 1948.
10. Stefanović, A. and V. Simić. "Determination of Quartz Content in the Mines of P. R. Serbia by Chemical and Rapid X-Ray Diffraction Methods", in: XII *International Congress on Occupation Health, Helsinki*, 1957, July 1—5.

GLASNIK HEMIJSKOG DRUŠTVA, Vol. 32, No. 2-3-4, 1967, pp. 213—224

THE INFLUENCE OF SPECIFIC GRAVITY AND GRAIN SIZE DISTRIBUTION ON THE SELECTIVE SEDIMENTATION IN POWDER SPECIMENS FOR QUANTITATIVE X-RAY DIFFRACTION ANALYSIS AND ON THE SHAPE OF THE CALIBRATION CURVE*

by

VERICA D. RAJKOVIĆ

From considerations of the phenomena which take place in powder specimens for quantitative diffraction analysis during preparation, and numerous experimental results, in our previous paper a formula was proposed for calculating the true concentration or concentration ratio of the measured components in the surface layer when the corresponding value in the mixture from which the suspension was prepared is known.[1]

In the present study we verified the justification of the assumption that selective sedimentation is a source of systematic discrepancy between the real and the theoretical calibration curve, and the validity of the proposed formulas for the case of a change in selective sedimentation due to a change of specific gravity (γ_{sm}) and of minus cumulative grain size composition (Ψ_{sm}). It should be borne in mind here that a change of γ_{sm} also means a change of γ_{susp}, of the apparent viscosity of the suspension (η_{susp}) and of the quantity of the dispersing substance in the same volume of suspension.

The verification consisted of the comparison of the calibration curves calculated by means of the proposed formulas with those determined by X-ray measurement on the same specimens.

The subject of study were chiefly the calibration curves for quantitative analysis of Sb_2O_3 and Sb by the internal standard method, but some verification was also made on some calibration curves for binary systems with one component measured and for two-component systems with two-components measured, although these will later be the subject of more detailed studies.

The calibration curve determined by diffraction were taken either from our previous studies or from the reports of other authors[2-4].

* This paper is a part of a communication presented at the Symposium on chemical engineering, held as part of the XIth Conference of the Chemists of Serbia, Beograd, 1965.

EXPERIMENTAL

The technique for the preparation of synthetic samples, mixtures, suspensions and specimens, and the conditions of the X-ray measurement are described in the papers from which the experimental calibration curves were taken[2, 3].

The grain size compositions of the Sb_2O_3, Sb and SiO_2 for quantitative analysis of Sb_2O_3 and Sb were determined microscopically. For the calculation of grain size composition and ψ the average values from five recordings were taken.

Preliminary determinations of changes of the apparent suspension viscosity (η_{susp}) with changing concentration of the dispersed mixture and of the concentrations of mixture components had already been made in separate studies on suspensions of pure components and their mixtures[5] by measuring the out-flow time of 10 *ml* of the suspension.

Considering that the ratio of the apparent viscosity (real and theoretical) was of particular interest in this study, this was calculated by means of the formula used by A.v. Buzagh and co-workers[6, 7]:

$$\frac{\eta}{\eta_t} = \frac{t \cdot \gamma_{susp}}{t_t \cdot \gamma_{susp_t}}$$

where t is the time of out-flow of a certain volume of suspension (in our study 10 *ml*).

Analysis of Binary Systems with One Component Measured

The difference between real values of the ratio C/C_0 and the corresponding theoretical values was analyzed on the calibration curves for the analysis of binary systems, for the mixtures

quartz — zinc
quarz — calcium carbonate

The real values of the ratio C/C_0 were calculated from the formula

$$\frac{C}{C_0} = \left(\frac{C}{C_0}\right)_t \left(\frac{\gamma_{sm} \cdot \psi_{sm_t}}{\gamma_{sm_t} \cdot \psi_{sm}}\right)^{\frac{\gamma-\gamma_{sm}}{\gamma_{sm_t}-\gamma_{sm}}} \left(\frac{\eta_t (\gamma-\gamma_{susp}) t}{\eta (\gamma-\gamma_{susp_t}) t_t}\right)^{\frac{\gamma-\gamma_{sm}}{\gamma_{sm_t}-\gamma_{sm}}}$$

The verification of this formula was only partial because without the original powders it was not possible to determine the corresponding values of γ_{sm} and ψ_{sm}. Since in the series of two-component mixtures $\gamma = \gamma_{sm_t}$, the value of the exponent in the above formula was unity.

Quartz-zinc

The specific gravities of the components showed considerable differences, $\gamma_{quartz} = 2.66$ g/cm³ and $\gamma_{Zn} = 7.14$ g/cm³, and hence $\gamma_{sm_t} < \gamma_{sm}$. According to the literature the grain size distributions of the components

were the same, which means that $\psi_{quartz} = \psi_{Zn}$ and $\psi_{sm_t} = \psi_{sm}$. Therefore the first factor of the above formula depended only on γ_{sm}. Because of this the real calibration curve should lie above the theoretical curve.

A preliminary study of the change of apparent viscosity of the suspension of powdered zinc and quartz with change of their concentrations in the suspension showed that the viscosity rise with increasing concentration was relatively small and about equal for the two components. Therefore the influence of changes in suspension viscosity on the position of the calibration curve was also small. In the present verification it was neglected.

Differences in the duration of drying of the specimens were a minimum, as all authors dried at 39°C. Thus the location of the real calibration curve relative to the theoretical curve (*a*) does not change as consequence of change in drying time.

In the majority of cases the ratio $(\gamma - \gamma_{susp})/(\gamma - \gamma_{susp_t})$ was very close to one.

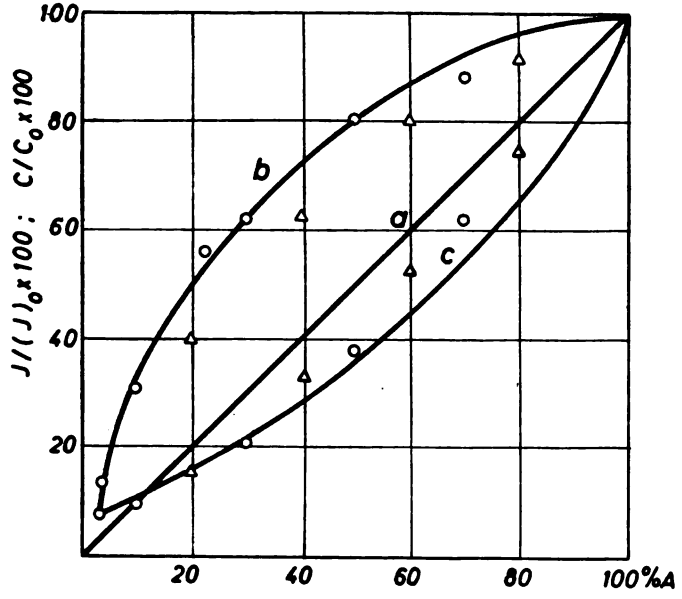

Figure 1

Calibration curves for the analysis of binary systems with one component measured: (*a*) theoretical, (*b*) real for the system quartz-*Zn*, (*c*) real for the system quartz-$CaCO_3$

It may be concluded from all the above that for the two-component mixtures of quartz and zinc the change in the position of the calibration curve due to changes in the second factor of the above formula was small.

The resulting real calibration curve for the quartz-zinc system should be above the theoretical curve. The experimentally determined curve (*b*) taken from the literature[2] is also above the theoretical curve.

The calculated values of γ_{sm} and C/C_0 and the experimental I/I_0 ($\times$ 100) values are shown in Table 1. The corresponding calibration curves are shown in Fig. 1. The experimental curve, as drawn by the original authors, is shown with a full line. Experimental I/I_0 values are shown with small full circles, and the calculated C/C_0 values with x's.

Quartz-calcium carbonate

The specific gravities of the components were very similar, $\gamma_{\text{quartz}} = 2.66\ g/cm^3$ and $\gamma_{CaCO_3} = 2.71\ g/cm^3$. Hence $\gamma_{\text{quartz}} < \gamma_{CaCO_3}$ and $\gamma_{sm_t} < \gamma_{sm}$. According to the data from literature the grain size distributions of the components were the same, i.e. $\psi_{\text{quartz}} = \psi_{CaCO_3}$ and $\psi_{sm_t} = \psi_{sm}$.

The first factor in the formula negligibly influences the position of the calibration curve for this system of mixtures.

A preliminary study of the viscosity of quartz and calcium carbonate suspensions showed that the viscosity increase with increasing concentration of the dispersed phase was much greater for $CaCO_3$ than for the corresponding quartz suspensions. Differences in drying time were here, too, reduced to a minimum as all the specimens were dried at 39°C. This means that the real calibration curve was considerably below the theoretical curve because of influences expressed in the second factor of the formula, i.e. because of change in the viscosity of the suspension.

The resulting real calibration curve for this system should be below the theoretical curve. The experimentally determined curve (*c*) taken from the literature[2] is also below the theoretical curve.

TABLE 1

Comparison of the calculated values of C/C_0 with the measured values of I/I_0 for the quartz-zinc and quartz-calcium carbonate systems, and the values necessary for calculating the ratio C/C_0

Quartz %	SiO_2* — Zn			SiO_2* — $CaCO_3$			
	γ_{sm} (g/cm^3)	C/C_0	I/I_0	γ_{sm} (g/cm^3)	t_{susp} (sec)	C/C_0	I/I_0
100	2.660	1.000	1.000	2.660	10.300	1.000	1.000
80	3.042	0.914	—	2.670	11.014	0.744	—
70	—	—	0.883	—	—	—	0.620
60	3.551	0.801	—	2.680	11.728	0.521	—
50	—	—	0.807	—	—	—	0.381
40	4.172	0.627	—	2.690	12.442	0.326	—
30	—	—	0.623	—	—	—	0.211
20	5.341	0.402	—	2.700	13.156	0.154	—
10	—	—	0.308	—	—	—	0.105
3	—	—	0.142	—	—	—	0.081

* The SiO_2 was quartz.

The values for the out-flow time of the suspensions (t_{susp}) and the calculated values of C/C_0, together with the experimentally determined

values of I/I_0 for some concentrations of quartz, are shown in Table 1. The corresponding calibration curves are shown in Fig. 1 in the same way as the curves for the quartz-zinc system. To calculate true values of C/C_0 the suspension out-flow time was used, as γ_{susp} was approximately constant for the entire series.

Analysis of two-component mixtures with two components measured

The determination of the ratio $C_A/_BC$ in the surface layer of specimens prepared from a two-component mixture has particular significance because in this way one can calculate the optimal ratio of the measured component and the internal standard in mixtures for the internal standard method. One can also calculate the ratio of the measured component and the standard in the surface layer of the specimen prepared from a mixture for 100% of the measured component. The corresponding formula is

$$\frac{C_A}{C_B} = \left(\frac{C_A}{C_B}\right)_t \left(\frac{\gamma_{sm} \cdot \psi_{sm_t}}{\gamma_{sm_t} \cdot \psi_{sm}}\right)^{\frac{\gamma_A - \gamma_B}{\gamma_{sm_t} - \gamma_{sm}}} \left(\frac{\eta_t (\gamma - \gamma_{susp}) t}{\eta (\gamma - \gamma_{susp_t}) t_t}\right)^{\frac{\gamma_A - \gamma_B}{\gamma_{sm_t} - \gamma_{sm}}}$$

was verified on two-component mixtures of Sb_2O_3-Sb and Sb-Sb_2O_3 which contained a filling medium of unkown composition, making this verification only partial.

The theoretical, (ideal) calibration curve in this case is marked *a* in Fig. 2. The experimental intensity ratios of the measured components for the system Sb_2O_3-Sb lie above the theoretical calibration curve, and for the system Sb-Sb_2O_3 below it.[3] An analysis by means of the above formula and using values of γ_{sm} and ψ_{sm} from Table 2 shows that the corresponding calculated concentration ratios of the components in the specimens would also lie above and below the theoretical calibration curve, respectively.

The calculated values of C/C_s for specimens prepared from mixtures for 100% antimony trioxide and antimony (internal standard method) whose γ_{sm} and ψ_{sm} values were known, are given later, on the calibration curves for quantitative analysis of Sb_2O_3 and Sb by the internal standard method.

TABLE 2

Mean specific gravities and mean cumulative grain size compositions of the Sb_2O_3—Sb and Sb—Sb_2O_3 mixtures

Sb_2O_3 — Sb			Sb — Sb_2O_3		
Sb_2O_3 %	γ_{sm} (g/cm^3)	ψ_{sm} %	Sb %	γ_{sm} (g/cm^3)	ψ_{sm} %
100	5.670	48.000	100	6.684	24.950
90	5.757	45.697	90	6.567	27.273
70	5.940	41.090	70	6.344	33.879
50	6.135	36.485	50	6.135	36.485
30	6.344	33.879	30	5.940	41.090
10	6.567	27.273	10	5.757	45.697

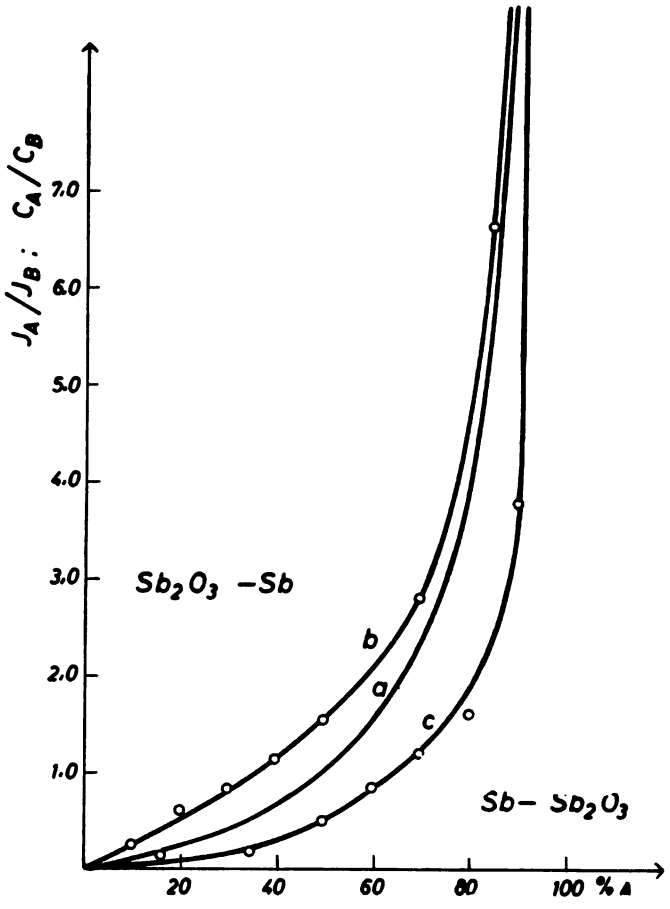

Figure 2

Calibration curves for two-component systems with two components measured: (*a*) ideal or theoretical, (*b*) real for the system Sb_2O_3-*Sb* (measured), (*c*) real for the system *Sb*—Sb_2O_3 (measured)

The internal standard method

The formula for calculation of the true values of C/C_s in the internal standard method

$$\frac{C}{C_s} = \left(\frac{C}{C_s}\right)_t \left(\frac{\gamma_{sm_t} \cdot \psi_{sm}}{\gamma_{sm} \cdot \psi_{sm_t}}\right)^{\frac{\gamma-\gamma_s}{\gamma_{sm_t}-\gamma_{sm}}} \left[\frac{\eta(\gamma-\gamma_{susp_t})t_t}{\eta_t(\gamma-\gamma_{susp})t}\right]^{\frac{\gamma-\gamma_s}{\gamma_{sm_t}-\gamma_{sm}}}$$

was verified on mixtures of the following composition:

$$(Sb_2O_3 + SiO_2) : Sb = 1 : 1$$
$$(Sb + SiO_2) : Sb_2O_3 = 8 : 1$$

by comparing the experimentally determined calibration curves with the calculated ones.[3, 4] The effect of the second factor in the above formula was verified for a change in the ratio S_t/S.*

Antimony trioxide

The verification was performed on the experimental calibration curve determined with specimens prepared with 0.08 *ml* of Sb_2O_3 suspension on slides. The dilution was 0.4*g* of mixture per 1.5 *ml* of the dispersing substance. The data necessary for calculating C/C_s are given in Tables 3 and 4.

TABLE 3

Specific gravities and cumulative grain size compositions of powdered Sb_2O_3, Sb and SiO_2

Values for pure powder	Sb_2O_3	Sb	SiO_2
γ (g/cm^3)	5.67	6.684	2.20
ψ %	48.00	24.95	24.28

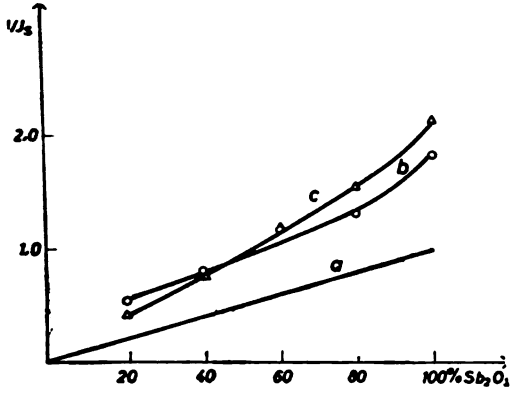

Figure 3

Calibration curves for analysis of Sb_2O_3 by the internal standard method: (a) ideal, (b) real (measured), (c) real (calculated)

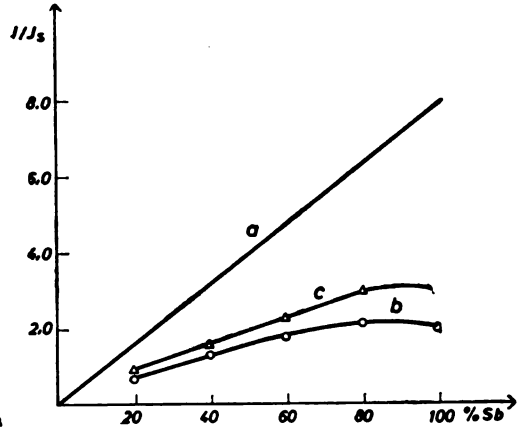

Fipure 4

Calibration curves for analysis of *Sb* by the internal standard method: (a) ideal, (b) real (measured) (c) real (calculated)

* S and S_t are the path lengths gone by particles of dimension D during the time of observation t (drying) in the real and theoretical specimen. In a previous study[1] this was equated to the thickness of the layer of pure dispersing substance.

For calculating C/C_s in the specimen for 100% of the measured component the weight ratio between the measured component and the internal standard was taken as the ideal value. The calculation was done by means of the formula for two-component mixtures with two components measured.

The ideal values (C/C_s), the experimental values I/I_s, the theoretical values (C/C_s) and the calculated C/C_s values for the same specimens are given together in Table 5. Some of these values are graphically presented in Fig. 3. The straight line (a) represents the ideal calibration curve. The experimental I/I_s values are marked with small full circles and the corresponding calculated C/C_s values with x's. The theoretical calibration curve is not drawn.

TABLE 4

Mean specific gravities and mean cumulative grain size compositions of the mixtures of Sb_2O_3 Sb and SiO_2, and free path lengths of particles in the specimens

% Sb_2O_3	100	80	60	40	20
γ_{sm} (g/cm^3)	6.1351	5.2410	4.5740	4.0580	3.6461
ψ_{sm} (%)	36.485	34.113	31.741	29.369	26.997
S cm	0.01278	0.01269	0.01260	0.01251	0.01242

TABLE 5

Comparison of the calculated values of $(C/C_s)_i$, $(C/C_s)_t$ and C/C_s with measured values of I/I_s for Sb_2O_3, Sb and SiO_2 mixtures

% Sb_2O_3	100	80	60	40	20
$(C/C_s)_i$	1.00	0.80	0.60	0.40	0.20
I/I_s	1.80	1.31	1.15	0.81	0.54
$(C/C_s)_t$	2.180	1.744	1.308	0.872	0.436
(C/C_s)	2.180	1.560	1.174	0.783	0.395

The values (C/C_s) are not included in the graph in Fig. 3.

Antimony

The verification was done on the experimental calibration curve obtained with specimens prepared with 0.08 *ml* of antimony suspension per slide. The dilution of the suspensions was 0.4 *g* of mixture per 1.5 *ml* of the dispersing substance. The data necessary for the calculation of C/C_0 is given in Table 6.

TABLE 6

Mean specific gravities and mean cumulative grain size compositions of the Sb, Sb_2O_3 and SiO_2 mixtures, and path lengths of particles in the specimens

% Sb	100	80	60	40	20
γ_{sm} (g/cm^3)	6.5537	4.8359	3.8314	3.1722	2.7059
ψ_{sm} (%)	27.53	27.41	27.28	27.16	27.04
S (cm^2)	0.01281	0.01263	0.01246	0.01229	0.01213

The ideal values, the experimental I/I_s values and the calculated values of C/C_s for the theoretical and the real calibration curve are given together in Table 7. Some of these values are presented graphically in Fig. 4. The straight line (a) represents the ideal calibration curve. The experimentally deterimed I/I_s values are shown with small full circles and the corresponding calculated values of C/C_s with x's.

TABLE 7

Comparison of the calculated values of $(C/C_s)_i$, $(C/C_s)_t$ and C/C_s with measured values of I/I for the Sb, Sb_2O_3 and SiO_2 mixtures

% Sb	100	80	60	40	20
$(C/C_s)_i$	8.00	6.40	4.80	3.20	1.60
I/I_s	2.00	2.15	1.80	1.31	0.71
$(C/C_s)_t$	3.078	2.4624	1.8468	1.2312	0.6156
C/C_s	3.078	2.963	2.271	1.543	0.785

The values of $(C/C_s)_t$ are not included in the graph in Fig. 4.

CONCLUSION

By comparing the ratio of the diffracted X-ray intensity with the corresponding concentration ratio of the measured components in the surface layer of the specimens it was concluded that in all the cases studied a change of conditions of sedimentation in the specimens was associated with corresponding very similar changes of the measured intensity ratio and of the calculated ratio of concentrations of the components measured. This indicates the correctness of the earlier hypothesis that the counter on the goniometer registers only some of the radiation diffracted from the crystals of the measured components in the surface layer.

This investigation was concerned with the changes in selective sedimentation due to changes of the mean specific gravity and of the grains size distribution of the dispresed mixture, i.e. of γ_{sm} and ψ_{sm}. The veri-

fication showed that the influence of these parameters on selective sedimentation and on the shape of the calibration curves was great.

Selective sedimentation and the concentration ratio in the surface layer were found to be influenced by other changes as well as changes of γ_{sm} and ψ_{sm}. This refers to change of the quantity of suspension per specimen, change of the dilution of the suspension from which the specimen is prepared, and change of the drying temperature.

Considering that in diffraction there is absorption of radiation which depends on the composition of the mixture from which the specimen was prepared, and that on sedimentation, in the precipitated sediment ordered orientation of the crystals of some components occurs, to an extent depending on the nature of the other components present, it follows that the measured intensity ratio is determined by these factors as well as by selective sedimentation. A study of their influence in future research will show whether the incomplete agreement between the experimentally determined and calculated calibration curves is due to them or the inaccuracy of the method used for the determination of the grain size distribution of the mixtures.

School of Technology,
Department of Food Technology,
Beograd.

Recived 16 December, 1966.

REFERENCES

1. Rajković, V. "Izračunavanje stvarnih koncentracija mernih komponenata u površinskom sloju primerka za kvantitativnu rentgensku difrakcionu analizu praha" (Calculation of True Concentrations of the Measured Components in the Surface Layer of a Specimen for Quantitative X-Ray Diffraction Analysis of Powder Mixtures) — *Glasnik Hemijskog društva* (Beograd) (this no.).
2. Stefanović, A. and V. Simić. "Determination of Quartz Content in the Mines of P. R. Serbia by Chemical and Rapid X-Ray Diffraction Methods", in: XII *International Congress on Occupational Health, Helsinki*, 1957, July 1—5.
3. Rajković, V. *Analiza uticaja sedimentacije u primercima za rentgensku difrakcionu analizu praha na vrednost odnosa difraktovanih intenziteta merenih komponenata i predlog nove računske metode za kvantitativnu obradu rezultata* (Analysis of the Influence of Sedimentation in Specimens for X-Ray Diffraction Powder Analysis on the Ratio of Diffracted Intensities of the Components Measured and a Proposed New Method of Calculation Method for the Quantitative Analysis of the Results) — Thesis, Beograd, 1964.
4. Rajković, V. "Uticaj sedimentacije na oblik kalibracionih krivih za rentgensku difrakcionu analizu nekih jedinjenja antimona. II. Uticaj koncentracije komponenata čiji se intenzitet ne meri na vrednost odnosa I/I_s" (Influence of Sedimentation on the Shape of Calibration Curves for X-Ray Diffraction Analysis of Some Antimony Compounds. II. Influence of the Concentration of Components Whose Intensity is not Measured on the Ratio I/I_s) — *Glasnik Hemijskog društva* (Beograd) 29*: 29—34, 1964.
5. Rajković, V. and M. Jovanović. Unpublished study.
6. Buzágh, A. v. and E. Erényi. "Über den Einflus der starken Elektrolyte auf die Viskosität der Quarzsuspensionen" — *Kolloid Zeitschrift* 91: 279—287, 1940.
7. Buzágh, A. v. "Über den Einflus der starken Elektrolyte auf die Viskosität der Stärke- und Bentonitsuspensionen" — *Kolloid Zeitschrift* 103: 119—121, 1943.

GLASNIK HEMIJSKOG DRUŠTVA, Vol. 32, No. 2-3-4, 1967, pp. 225—227

SYNTHESIS OF 4-HYDROXY-4′-IODOTHIOBENZANILIDE

by

MIROSLAVA M. JANČEVSKA

The amides of carbonic acids can easily be transformed into the corresponding thioamides by means of phosphorus pentasulphide in dry organic solvents (pyridine, dioxane, benzol, xylene, and others)[1, 2, 3, 4]. This simple and general method cannot be applied to amides which have a free phenol-hydroxyl group, unless the hydroxyl group is previously protected[5, 6]. Protection is only possible achieve with acyl protective groups which can be introduced in a simple way into the hydroxy-amide molecule and which, after interacting with phosphorus pentasulphide, can again be easily liberated, leaving the thioamide group unchanged.

Attemps at obtaining halogen-substituted hydroxythioamide by halogenation of the corresponding acetoxythio derivative under different reaction conditions have been unsuccessful. Substances without sulphur were always obtained.

It was therefore necessary to approach the synthesis of 4-hydroxy--4′-iodothiobenzanilide in another way. It is similar to the previously described synthesis of 4-hydroxy-4′-bromthiobenzanilide[7] and can be represented by the following schema:

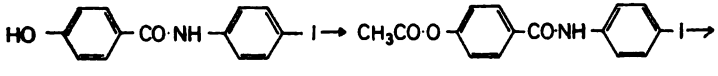

A I

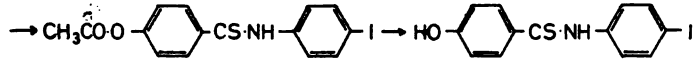

II III

Compound III reacting with the anhydride of acetic acid involves simultaneous acetylation of the hydroxyl group and of the thioamide group, and the corresponding *O*, *N*-diacetylthio derivative with the following structure is formed:

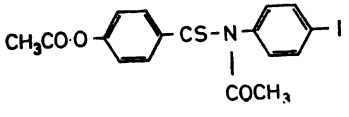

IV

EXPERIMENTAL

The melting points are not corrected.

4-acetoxy-4'-iodobenzanilide (*I*)

Into a solution of 2.19 *g* (0.01 *mol*) 4-iodoaniline[8] in 20 *ml* of pyridine, cooled to 0°, 1.98 *g* (0.01 *mol*) of 4-acetoxybenzoilchloride[9] (freshly prepared and dissolved in 10 *ml* of dry ether) was gradually added with continuous mixing through 15 minutes. The reaction mixture was mixed for another 30 minutes at room temperature and then poured into 250 *ml* of ice-cold water. 3.65 *g* (96%) of the raw product, m.p. 209—210°C, was obtained. By recrystallization from ethanol colorless flakes were obtained, m.p. 218—219°C.

Analysis: $C_1 H_{12} NO_3$ *I* (381.18)

Calculated: C 47.28, *H* 3.17, *N* 3.68%
Found: C 47.26, *H* 3.40, *N* 3.55%

4-acetoxy-4'-iodothiobenzanilide (*II*)

3.81 *g* (0.01 *mol*) of dried compound I was dissolved in 10 *ml* of dry pyridine with mild heating on an oil bath. 2.22 *g* (0.01 *mol*) of powdered phosphorus pentasulphide was added to the warm solution and the heating continued so that the solution boiled gently for 45 minutes. The dark red reaction mixture was poured into 300 *ml* of water, whereupon a dark crystalline substance separated out, which was filtered, washed with water and dried. 3.46 *g* (87%) of raw product was obtained, m.p. 169—172°C. By recrystallization from ethanol yellow needles were obtained, m.p. 178—179°C.

This synthesis was also done with dry xylene as the solvent, with a yield of 80% of dry product.

Analysis: $C_{15} H_{12} NO_2 SI$ (397.25)

Calculated: *C* 45.38, *H* 3.05, *N* 3.53%
Found: *C* 45.22, *H* 2.38, *N* 3.64%

4-hydroxy-4'-iodothiobenzanilide (*III*)

3.97 *g* (0.01 *mol*) of compound II was dissolved in 20 *ml NaOH* with heating on a water bath at 60—70°C for 10—15 min. The yellow alkaline solution (*pH* 8—9) was filtered and after cooling was acidified with 1 *N HCl* to *pH* 5—6. The yellow crystalline substance formed was filtered, washed with water and dried. 3.3 *g* (93%) of raw product was obtained, m.p. 190—193°C. By recrystallization from ethanol yellow prisms were obtained, m.p. 197—198°C.

Analysis: $C_{13}H_{10}NOSI$ (355.20)
Calculated: *C* 43.98, *H* 2.84, *N* 3.95%
Found: *C* 44.01, *H* 3.07, *N* 3.77%

O,N-diacetyl-4-hydroxy-4'-iodothiobenzanilide (IV)

3.55 *g* (0.01 *mol*) of substance III was dissolved in 15 *ml* of pyridine, and 5.12 *g* (0.05 *mol*) of acetic acid anydride added into the solution. After 2—3 hours at room temperature the red reaction mixture was poured into 300 *ml* of ice-cold water. The red crystalline product was filtered, washed and dried. The yield of raw product was 3.5 *g* (82%), m.p. 126—128°C. By recrystallization from ethanol red needles were obtained, m.p. 135—136°C.

Analysis: $C_{17}H_{14}NO_3SI$ (439.28)
Calculated: *C* 46.51, *H* 3.23, *N* 3.19%
Found: *C* 46.68, *H* 3.47, *N* 3.30%

School of Science,
Institute of Chemistry,
Skopje

Received 24 March 1967.

REFERENCES

1. Klingsberg, E. and D. Papa. — *Journal of American Chemical Society* 73: 4988, 1951.
2. Jakopčić, K. and V. Hahn. — *Naturwissenschaften* 51: 482, 1964.
3. Rivier, G. and J. Zeltner. — *Helvetica Chimica Acta* 20: 691, 1937.
4. Price, C. and B. Velzen. — *Journal of Organic Chemistry* 12: 386, 1947.
5. Jančevska, M. — Thesis, Universitet u Skopju, 1964.
6. Jančevska, M., K. Jakopčić and V. Hahn. — *Croatica Chemica Acta* 37: 67, 1965.
7. Jančevska, M. — *Glasnik Hemijskog društva* (Beograd) 31*: 255, 1966.
8. Militzer, Smith and Evans. — *Journal of American Chemical Society* 63: 436, 1941.
9. Robertson, A., and R. Robinson. — *Journal of the Chemical Society* 1716, 1926.

* Available in English translation from: Clearinghouse for Federal Scientific and Technical Information, Springfield, Virginia, 22151.

GLASNIK HEMIJSKOG DRUŠTVA, Vol. 32, No. 2-3-4, 1967, pp. 229—237

THERMOLYSIS OF SOME ACETYLACETONATES

by

MIRA J. GLAVAŠ and TIBOR J. RIBAR

INTRODUCTION

The compounds of metals with 1,3 diketones, because of their specific properties, are interesting both from a theoretical and from a practical point of view. The methods for obtaining them, their properties, structure and application have been the subject of numerous investigations. However, there is relatively little information on the thermal behavior of acetylacetonates. Charles[1, 2] compared the heat stability of some by analyzing the products formed on heating at certain temperatures. By mass spectrography he identified acetone, carbon dioxide and methane as the main products of decomposition and acetylacetone in some chelates which disintegrate at lower temperatures. Acetylacetone itself is more heat stable than its metal derivatives, although the main decomposition products of pyrolysis are the same.[3] Geiseler and Scherzer[4] in their studies of the kinetics and mechanism of thermal decomposition of acetylacetonates, found that apart from the above main decomposition products, involatile high-polymer substances were formed in significant quantity.

In the present study, by means of thermogravimetric (TGA) and differential thermal analysis (DTA), the thermal behavior of the following acetylacetonate was studied: BeA_2, AlA_3, $(TiA_3)_2TiCl_6$, ThA_4, WOA_2, CrA_3, MoO_2A_2, MnA_3, MnA_2, FeA_3, CoA_3, CoA_2, NiA_2, CuA_2, CdA_2, HgA_2, and the hydrates $MnA_2 \cdot 2H_2O$, $CoA_2 \cdot 2H_2O$, $NiA_2 \cdot 2H_2O$ and $ZnA_2 \cdot 2H_2O$ (where $A = C_5H_7O_2$).

EXPERIMENTAL

The formation of acetylacetonates. All the compounds for study were obtained by the procedures described in the literature.[1, 5, 6, 7, 8, 9] The composition of the chelates was checked by determining metals, whose deviations in all cases ranged within 0.5% of the theoretical value.

TGA was done on an Chévenard-type Amsler thermo-balance. A sample of 80—100 *mg* was heated in an open quartz beaker in air atmosphere, at a heating rate of 300°C/h.

DTA: An apparatus of the firm Linseis with optical registration was used. Layered "packing" was applied: 100 *mg* of sample was put between two equal layers of Al_2O_3 in a platinum cylindrical holder. Heated Al_2O_3 was used as the reference substance. The temperature and differential temperature were measured by means of *Pt-Pt/Rh* thermocouples. The heating rate was again 300°C/h.

RESULTS AND DISCUSSION

The TGA curves (Figs. 1, 2 and 3) show that all the chelates were relatively heat stable, and started to decompose at temperatures above 100°C.

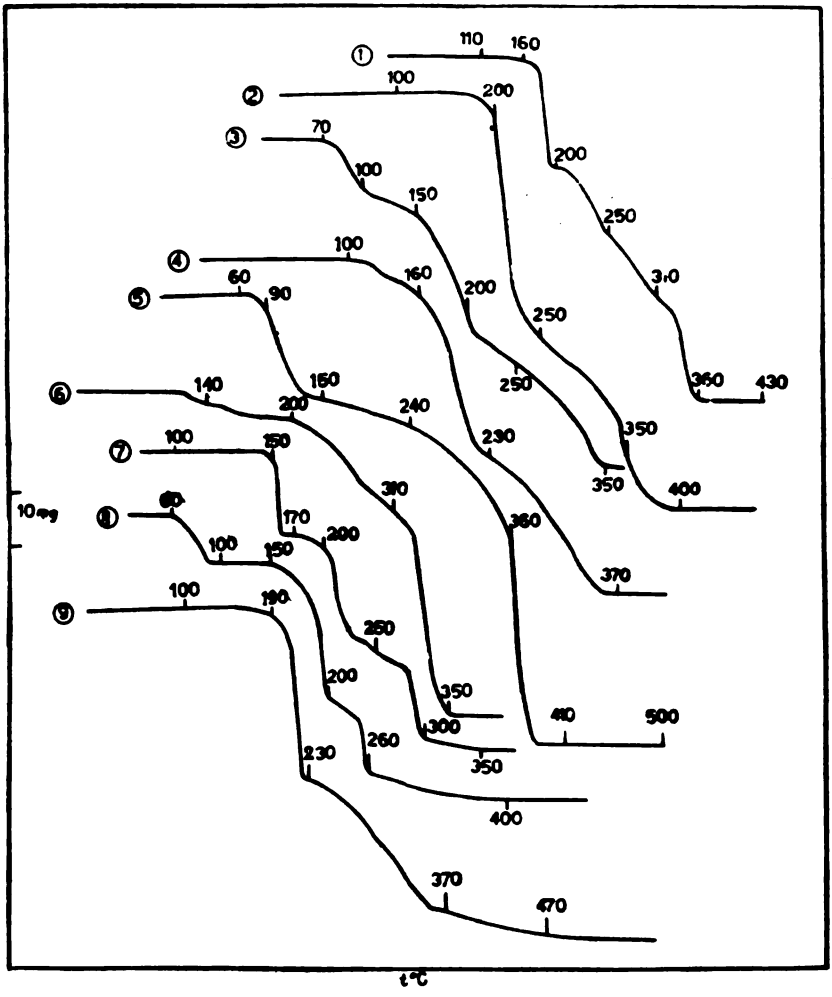

Figure 1

TGA curves: 1. — FeA_3, 2. — CoA_3, 3. — $CoA_2 \cdot 2H_2O$, 4. — CoA_2, 5. — $NiA_2 \cdot 2H_2O$ 6. — NiA_2, 7. — MnA_3, 8. — $MnA_2 \cdot H_2O$, 9. — MnA_2

The process of decomposition was associated with the formation of intermediate products which, in some cases, it was not possible to identify by this technique. The thermolysis curves of some chelates indicate a stepwise

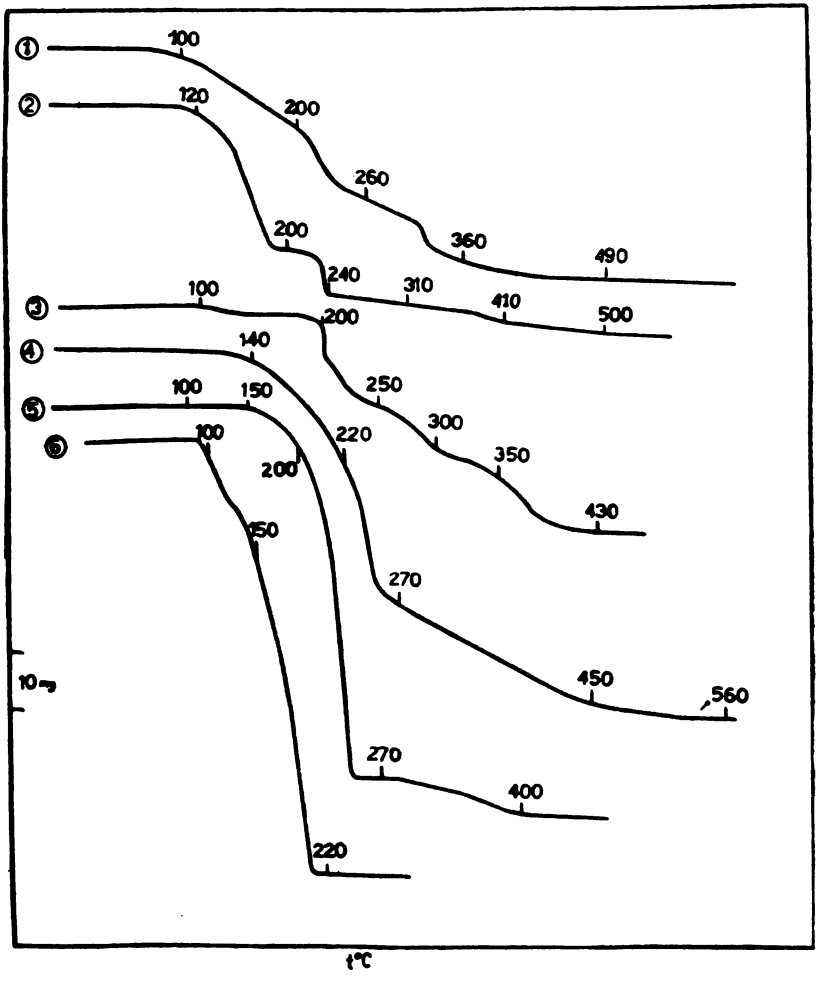

Figure 2

TGA curves: 1. — ThA_4, 2. — MoO_2A_2, 3. — CdA_2, 4. — $TiA_3/_2TiCl_6$, 5. — WOA_2, 6. — $ZnA_2 \cdot 2H_2O$

liberation of acetylacetone. A simple interpretation of the curves at higher temperatures is not possible because of the concomitant decomposition of acetylacetone itself and of oxidation. The final product of thermal decomposition was the oxide of the corresponding metal.

The liberation of water from the hydrated chelates occurred separately from the process of decomposition, in a single step, except with $NiA_2 \cdot 2H_2O$. The thermolysis curves in Fig. 1 show that the chelate of manganese, after giving off one molecule of acetylacetone, formed a stable intermediate compound, whose formation showed up on the curves as an almost

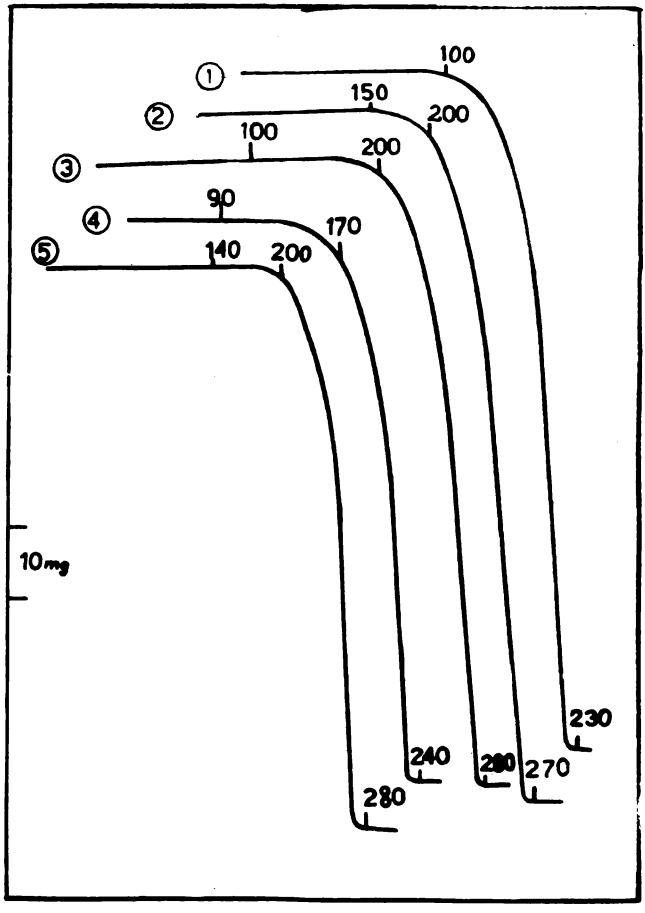

Figure 3

TGA curves: 1. — BeA_2, 2. — CuA_2, 3. — CrA_3, 4. — AlA_3, 5. — HgA_2

perfectly flat plateau, with the chelates of both *Mn* (III) and *Mn* (II). The intermediate products formed after the liberation of one molecule of acetylacetone by FeA_3 and CoA_2 appeared within a narrower temperature interval.

During dehydration of $NiA_2 \cdot 2H_2O$ there was simultaneous decomposition of the chelate. This was also confirmed by the curve for anhydrated NiA_2, where the change in weight in the interval 100° to 150°C precisely corresponded to the difference between the total weight change of $NiA_2 \cdot 2H_2O$ and its known water content.

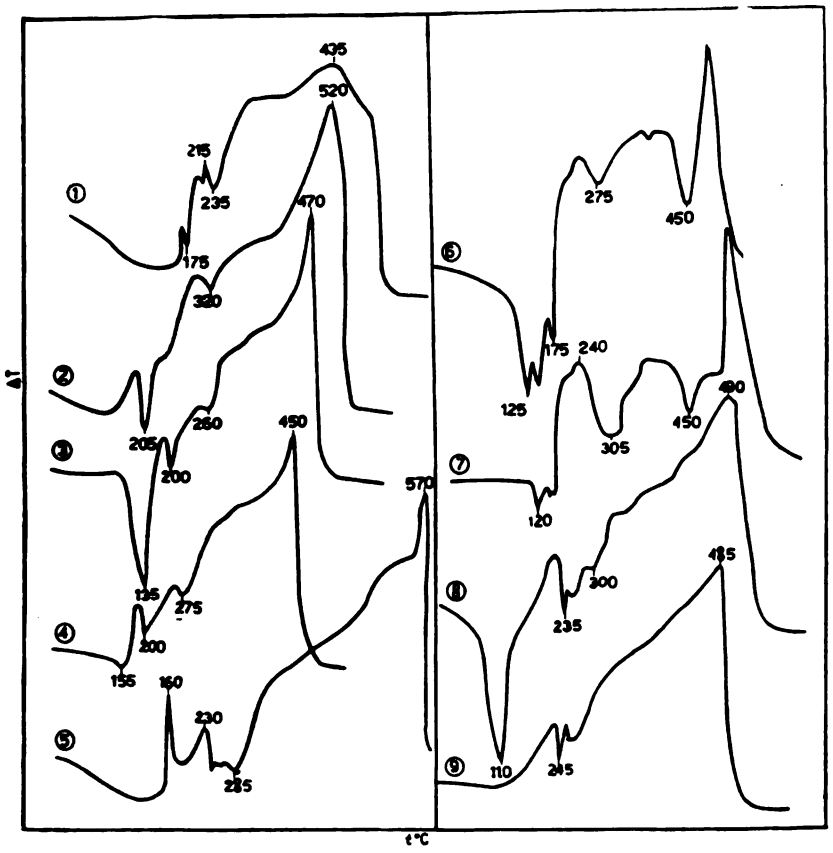

Figure 4

DTA curves: 1. — FeA_2, 2. — CoA_2, 3. — $CoA_2 \cdot 2H_2O$, 4. — CoA_2, 5. — MnA_2, 6. — $NiA_2 \cdot 2H_2O$, 7. — NiA_2, 8. — $MnA_2 \cdot 2H_2O$, 9. — MnA_2

In thermolysis of WOA_2 and $ZnA_2 \cdot 2H_2O$ the decomposition was continuous. The bend in the thermolysis curve of $(TiA_3)_2TiCl$ indicates separate evolution of HCl. It was not possible to identify the intermediate products of ThA_4, MoO_2A_2 and CdA_2.

Sublimation during TGA was characteristic of BeA_2, CuA_2, CrA_3, AlA_3 and HgA_2.

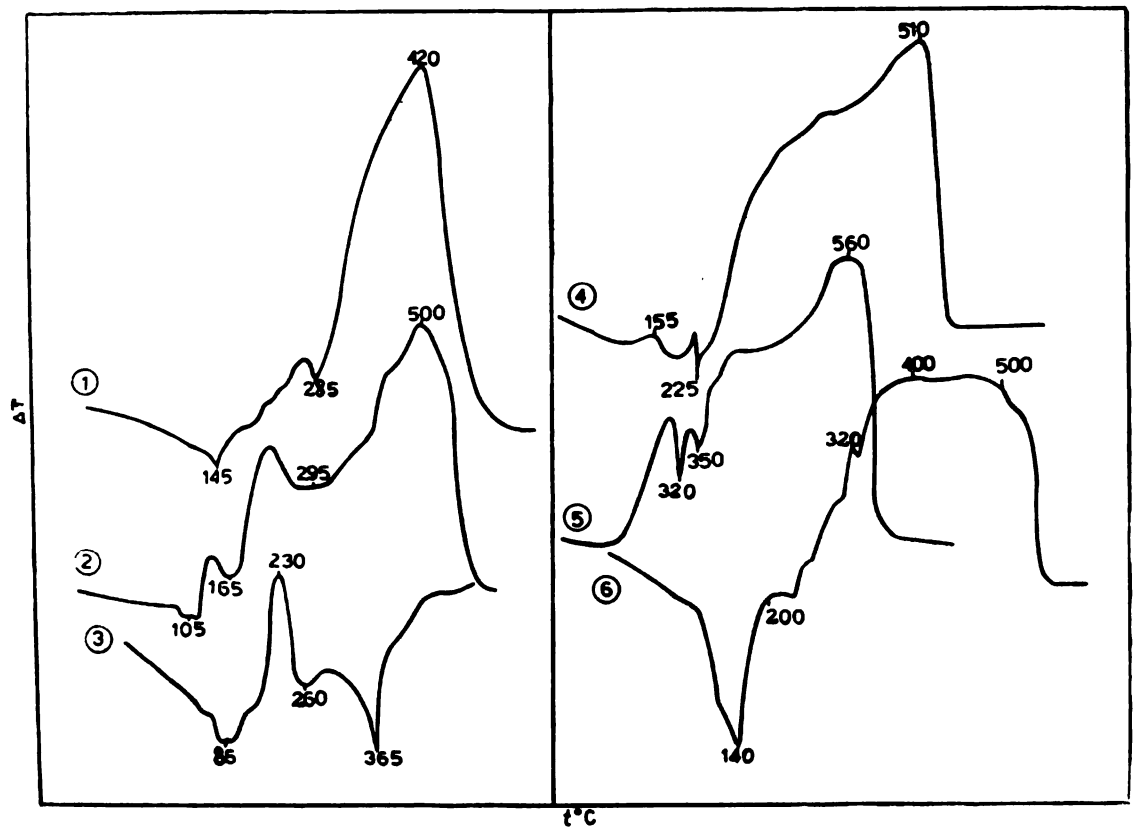

Figure 5

DTA curves: 1. — ThA_4, 2. — MoO_2A_2, — 3. CdA_2, 4. — TiA_3, 5. — WOA_2, 6. — $ZnA_2 \cdot 2H_2O$

Investigation of the energy changes during decomposition by means of DTA showed that the greatest energy change occurred in the liberation of water from the hydrated acetylacetones and that oxidation of the chelates was exothermic. This was recorded on all the curves (Figs. 4, 5, and 6), with markedly exothermic peaks in the temperature range 300° to 500°C. The endothermic peaks corresponding to melting, boiling and sublimation were mostly poorly expressed or not at all, because of superposition with strong exothermic oxidation.

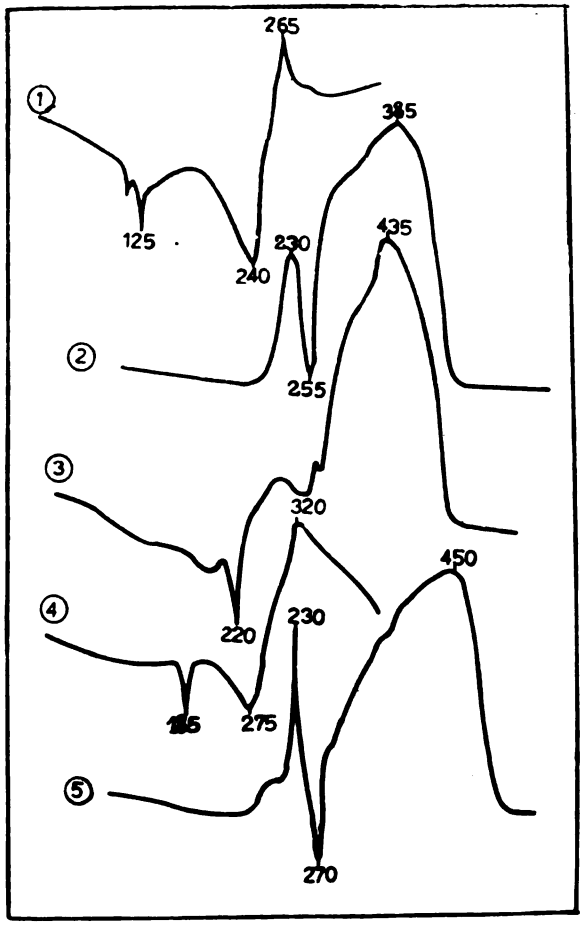

Figure 6

DTA curves: 1. — BeA_2, 2. — CuA_2, 3. — CrA_3, 4. — AlA_3, 5. — HgA_2

It is characteristic that on the DTA curve of $NiA_2 \cdot 2H_2O$ dehydration is not represented by a simple maximum (peak) as is the case with the other hydrated acetylacetones. This is in agreement with the earlier conclusion that dehydration causes decomposition of the chelate.

Although the TGA curves in Fig. 3 show that chelates underwent sublimation, the different packing of the samples in DTA (between two layers of Al_2O_3 in a container of smaller diameter than in TGA) allowed observation of effects which occurred above the sublimation point as well.

School of Science,
Institute of Chemistry,
Sarajevo.

Received 22 March, 1967.

REFERENCES

1. Charles, R. and M. Pawlikowski. "Comparative Heat Stabilities of Some Metal Acetylacetonate Chelates" — *The Journal of Physical Chemistry* (Washington) 62 (4): 440—444, 1958.
2. Hoene, J., R. Charles and W. Hickam. "Thermal Decomposition of Metal Acetylacetonates" — *The Journal of Physical Chemistry* (Washington) 62 (9): 1098—1101, 1958.
3. Charles, R., W. Hickam and J. Hoene. — *The Journal of Physical Chemistry* 63 (11): 2084—2085, 1959.
4. Geiseler, G. and K. Scherzer. "Kinetik und Mechanismus des thermischen Zerfalls von Acetylaceton" — *Zeitschrift für Physicalische Chemie, Neue Folge* (Frankfurt am Main) 44: 67—81, 1965.
5. Fernelius, C. *Inorganic Synthesis* — New York: Mc Graw Hill Book Co., 1946, Vol. I, pp. 17, 25, 123.
6. Moeller, T. *Inorganic Synthesis* — New York: Mc Graw Hill Book Co., 1957, Vol. V, pp. 115, 130, 188.
7. Rochow, E. *Inorganic Synthesis* — New York: Mc Graw Hill Book Co., 1960, Vol. VI, pp. 147, 164.
8. Kleinberg, J. *Inorganic Synthesis* — New York: Mc Graw Hill Book Co., 1963, Vol. VII, p. 183.

Holm, R. and F. Cotton. "X-Ray Powder Data and Structures of Some bis-(Acetylacetonate)-Metal (II) Compounds and Their Dihydrates" — *The Journal of Physical Chemistry* (Washington) 65 (2): 321—323, 1961.

GLASNIK HEMIJSKOG DRUŠTVA, Vol. 32, No. 2-3-4, 1967, pp. 239—246

VOLATILE ACIDS IN THE AROMA OF YOGHURT*

by

MIROSLAV N. TURČIĆ, DANICA B. BOTIĆ and
VELIMIR D. CANIĆ

INTRODUCTION

Yoghurt is made by sowing boiled milk with microorganisms which cause lactic acid fermentation of lactose. After a certain time a drink is obtained which has a mildly acid taste and an agreeable aroma.

The aroma of yoghurt is derived from the aroma of milk and from the products formed by fermentation.

Data on the microflora of yoghurt is rather scarce. Rašić and Milić[1] recently reviewed present knowledge and presented results of a study of yoghurt microflora on samples collected from different parts of Yugoslavia. In all the samples these authors confirmed the presence of *Streptococcus thermophilus*. Members of the suborder *Thermobacterium* found were *Lactobacillus bulgaricus*, *Lactobacillus joghurti*, and in one sample *Lactobacillus helveticus*. *Lactobacillus bulgaricus* was found in 2/3 of the samples and these authors therefore concluded that it was the dominant species of yoghurt *Lactobacilli* in Yugoslavia.

Data about the aroma of yoghurt is still insufficient, and its mode of formation has also not been adequately studied. Information in the literature on the influence of different yoghurt microorganisms on the formation of aroma is contradictory. According to some authors[2] *Streptococcus thermophilus* plays the main part in producing the aroma, while others[3] are of the opinion that the characteristic aroma is due to the action of *Lactobacillus bulgaricus*, and that *Streptococcus thermophilus* only decreases the viscosity, i.e. improves the consistency of the yoghurt. Pette and Lolkema[3] are of the opinion that acetaldehyde is one of the main factors responsible for the aroma of yoghurt.

In order to study its composition and origin we isolated the yoghurt aroma and quantitatively and qualitatively determined the volatile acids which, because of their smell, make important contributions to it.

---

* Communicated at the IInd Yugoslav Congress for Pure and Applied Chemistry, Beograd, June 1966.

This study was financially supported by the Research Fund of the AP of Vojvodina.

EXPERIMENTAL

1. *Yoghurt samples*

Two samples from the Novi Sad City Dairy were examined. Sample No. 1 was fresh while sample No. 2 was kept at room temperature 24 hours before isolating aroma from it. Because of this the organoleptic properties of sample No. 2 were poorer.

2. *Isolation of aroma*

One liter of yoghurt was put into 3-liter round-bottomed flask with a Liebig condenser and steam distilled. Air was previously removed from the apparatus with a stream of nitrogen. Steam distillation was continued until about 1 liter of distillate had been collected in the condenser. During distillation the condenser was cooled with a mixture of ice and salt.

The distillate containing yoghurt aroma was saturated with *NaCl* and extracted three times with 150 *ml* of ether each time. The ether extract was dried over waterfree Na_2SO_4 overnight and ether removed by distillation by means of a 30 *cm* long column with Raschig's rings. The distillation was continued until 1 *ml* of concentrated aroma was left in the flask. Chromatography was done with 10 mm^3 samples of aroma.

3. *Isolation of acids*

Acids were isolated from the ether extract of the distillate by steam, the extract being shaken in a separation funnel with 100 *ml* of 3% Na_2CO_3 solution. The acids, being sodium salts, move into the water layer, while the remaining components of the aroma remain in the ether layer. After separation of the layers, the water layer was acidified with H_2SO_4 and the liberated acids again extracted with ether. They were then concentrated in the same way as the total aroma.

4. *Chromatography of the aroma*

Chromatography was done on a Beckman GC-2*A* gas chromatograph with a thermal conductivity detector at a temperature of 125°C. A 180 *cm* long column was used, internal diameter 0.6 *cm*, packed with 20% poly-(diethyleneglycolsuccinate) on Chromosorb W 42/60 mesh (Thyler), washed with acids for deactivation. The gas carrier was hydrogen under a pressure of 25 psi at the column inlet and flow-rate a of 130 *ml/min*. The detector current was 250 *mA*; full sensitivity of the apparatus was used. The Recorder — Bristol 1 *mV*, paper speed — 0.5 inch/*min*, sample quantity 10 mm^3.

RESULTS AND DISCUSSION

The chromatograms of the total aroma are shown in Figs. 1 and 2. It may be seen that they were not quite identical, as the peaks Nos. 4, 17, 26 and 27 in the chromatogram of yoghurt No. 2 which was kept longer

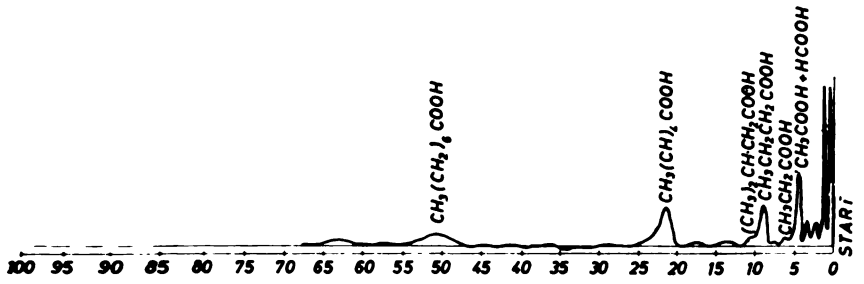

Figure 1
Aroma of yoghurt No. 1

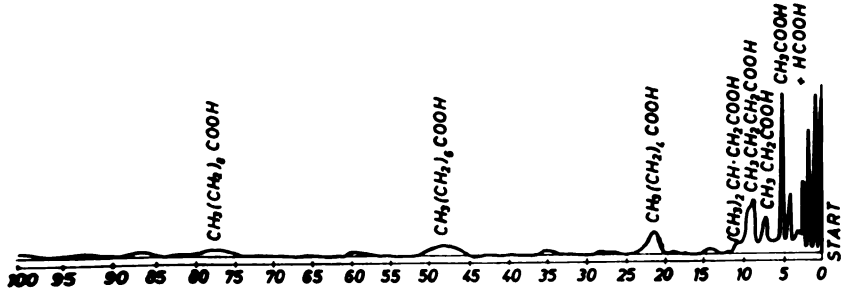

Figure 2
Aroma of yoghurt No. 2

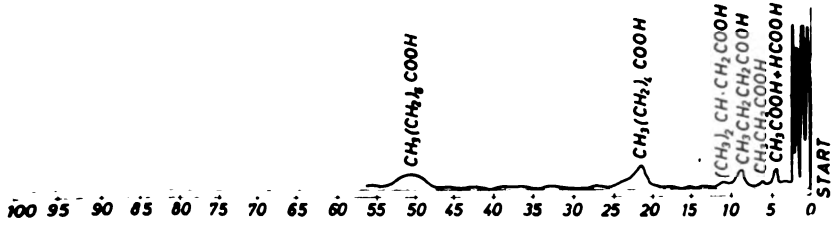

Figure 3
Free acids of aroma of yoghurt No. 2

are missing in the chromatogram of No. 1. There are also differences in the area under the peaks which indicates differences in the quantity of aroma components of the two yoghurts.

TABLE 1

Retention time of some volatile components in the aroma of yoghurt

Number of peak	Yoghurt No. 1 t_{dr} (min)	Yoghurt No. 2 t_{dr} (min)	Identification
1	0.13	0.11	
2	0.19	0.19	
3	0.25	0.28	
4	—	0.43	
5	0.58	0.53	
6	0.82	0.74	
7	1.01	0.93	
8	1.57	1.59	
9	1.79	1.74	
10	2.50	2.48	
11	3.66	3.66	
12	4.64	4.62	Acetic + Formic Acid
13	6.01	6.01	
14	6.47	6.47	Propionic Acid
15	8.20	7.44	
16	9.00	9.13	Butyric Acid
17	—	9.71	
18	10.15	10.77	Isovaleric Acid
19	14.85	15.23	
20	18.72	18.80	
21	21.45	21.60	Caproic Acid
22	26.80	27.10	
23	36.70	37.05	
24	50.00	50.06	Caprylic Acid
25	63.20	60.03	
26	—	80.00	Capric Acid
27	—	109.20	

The retention times of different peaks are shown in Table 1. It may be seen that they are pretty well the same for the aromas of both samples, considering that samples No. 2 was chromatographed later.

It is seen from the chromatograms and the table that in the aroma of yoghurt No. 1 there were 23 components, of which the first two peaks represent air and the solvent (ether), so that there were 21 components making up the aroma. In yoghurt No. 2 there were 4 more components, that is altogether 25 (excluding peaks for air and ether).

The differences in the number of the components and in their relative amounts represented by the peak areas are explained by the fact that the sample No. 2 was kept at room temperature for 24 hours before isolating the aroma, and because of that the microbiological process had gone further. During that time some new aroma components formed were, while the relative quantity of the others increased. This was also confirmed by the organoleptic assessment which was, as already stated, poorer.

Figure 3 shows the chromatogram of the free acids from the aroma of yoghurt No. 2, isolated by the described procedure. By comparing the chromatograms of the total aroma and the volatile acids the peaks on the total aroma chromatogram which belong to the acids can be identified. Acids were identified by comparing their retention times with the values for pure acids chromatographed under identical conditions separately and in a mixture. In this way we were able to identify in both samples propionic, butyric, isovaleric, caproic and caprylic acid, while formic and acetic acid gave a single peak, i.e. the column did not separate them. In the aroma of yoghurt No. 2 capric acid was found as well. It is considered that it was formed during the prolonged microbiological process.

The retention times of the volatile acids in the aroma and of pure acids chromatographed separately and in a mixture are shown in Table 2. It is interesting that formic and acetic acids chromatographed separately showed different retention times but when chromatographed in a mixture gave a single peak.

The ratios between different volatile acids in the aroma is of significance, considering that these acids, particularly butyric and isovaleric, have a strong smell and constitute important smell components. Since this is a homologous series of lower fatty acids, in quantitative calculations one can assume that the areas under the peaks are proportional to the weight proportions of the acids. The values obtained are also shown in Table 2. It is seen from the table that the quantities of different acids differed in the two samples studied. The differences are marked for acetic (+ formic) and isovaleric acids, of which both the relative and absolute ratio was higher in the aroma yoghurt No. 2. The relative quantity of butyric acid was the same, but those of caproic and caprylic acid were in sample No. 2, in which capric acid also appeared.

If we compare the ratios of the different volatile acids with caproic acid, which was the acid with the highest proportion in the aroma of yoghurt No. 1 (this ratio is obtained by dividing the relative percentage of a given acid by the percentage of caproic acid), it is seen that in yoghurt No. 2 the greatest increase relative to caproic acid occurred with isovaleric acid, followed by acetic and butyric acid. As isovaleric and butyric acids have a very unpleasant smell, this may explain why sample No. 2 had poorer organoleptic properties, that is a less agreeable taste.

The increase in acetic acid in the aroma of yoghurt No. 2 can be explained by further microbiological breakdown of lactose. This is in accord with the findings in cheese[4] in which the quantity of acetic acid increased until all the lactose was consumed. The increased content of butyric and isovaleric acid is explained by breakdown of lactic fats or of free amino acids by the microorganisms.

TABLE 2

Retention-times and ratios of volatile acids in the aroma of yoghurt

Acid	Alone (min)	Mix-ture (min)	Yoghurt No. 1 (min)	Yoghurt No. 2 (min)	Relative percentage ratio		Ratio to caproic acid	
					Yogh. No. 1	Yogh. No. 2	Yogh. No. 1	Yogh. No. 2
Formic	4.98	4.52	4.64	4.62				
Acetic	4.51	4.52	4.64	4.62	8.04	25.20	0.20	1.32
Propionic	6.40	6.40	6.47	6.47	1.64	0.65	0.029	0.034
Isobutyric	5.31	5.53	—	—	—	—	—	—
Butyric	8.55	8.55	9.00	9.13	14.37	14.97	0.35	0.78
Isovaleric	10.07	10.13	10.15	10.77	2.10	10.78	0.052	0.57
Caproic	21.40	21.40	21.45	21.60	40.02	19.16	1.000	1.000
Caprylic	52.60	52.60	50.00	50.06	34.41	15.12	0.85	0.79
Capric	87.70	87.70	—	80.00	—	14.40	—	0.75

Hence if we take the ratio of volatile acids in yoghurt No. 1 as favorable for a good aroma, we can conclude that a low ratio of isovaleric and butyric acid to the other acids which have a less unpleasant smell is characteristic.

Institute for Food Technology, Novi Sad
Department of Chemistry, University of Novi Sad

Received 12 August, 1966.

REFERENCES

1. Rašić, J. and S. Mitić. "Prilog ispitivanju mikroflore jogurta" (On Yoghurt Microflora) — *Prehrambena industrija* (Beograd) 16: 158—159, 1962.
2. Foster, E., E. Nelson, M. Speck, H. Doetsch and J. Olson. *Dairy Microbiology* — Englewood Cliffs (New Jersey, USA): Prentice-Hall Inc., 1957, p. 328.
3. Pette, J. and H. Lolkema. "Yoghurt. III. Acid Production and Aroma Formation in Yoghurt" — *Netherlands Milk and Dairly Journal* 4: 261—263, 1950.
4. Golovna, P., G. Mironov and S. Sokolov. "Khimiia zapakha pishchevykh produktov" (Chemistry of Food Aromas) — *Uspekhi khimii* 33: 816—854, 1964.

GLASNIK HEMIJSKOG DRUŠTVA, Vol. 32, No. 2-3-4, 1967, pp. 247—251

SEPARATION OF PYRIDINE-CARBOXYLIC AND PYRIDINE-DICARBOXYLIC ACIDS BY THIN-LAYER CHROMATOGRAPHY

by

VELIMIR D. CANIĆ, SUZANA E. PETROVIĆ and
SLOBODAN M. PETROVIĆ

The separation of isomers of pyridine- and quinoline-carboxylic acids has been performed by paper chromatography with different solvents and different methods of detection.[1, 2, 3, 4, 5] Thin-layer chromatography, to our knowledge, has not been used, although it has been used for the separation of a number of heterocyclic nitrogen compounds.[6, 7, 8, 9] In the present study we separated pyridine-monocarboxylic acids, pyridine-dicarboxylic acids and three isomers of quinoline-monocarboxylic acids by thin-layer chromatography on silica-gel as the adsorbent.

EXPERIMENTAL

Stahl silica-gel *G* was used as the adsorbent in the usual chromatographic technique. One to five microliters of 1% aqueous solution of the ammonium salts of the acids was put on the thin layer (see Table). The mixtures were made from 1% solutions of each acid. The chromatogram was twice developed by the entry method, without preceding activation of the thin layer and without saturation of the chromatographic chamber. The following solvents were used:

I. Methanol-water-25% amonia (100 : 12 : 16)
II. Ethanol-water-25% ammonia (100 : 12 : 16)
III. n-Propanol-water-25% ammonia (100 : 12 : 16)
IV. n-Butanol-water-25% ammonia (100 : 12 : 16)

We were thus able to study the influence of the change in the number of *C* atoms in the alcohol on the separation.

Chromatograms were developed with the following reagents:

1. 1% fluorescein solution in 96% ethanol. Immediatley after spraying, illumination with filtered UV-light (250 $m\mu$) revealed dark spots against the yellow fluorescent background. After several minutes of exposure to daylight, yelow spots of pyridine-mono- and -dicarboxylic acids appeared

against the yellow-brownish background. After several days the yelow-brownish background disappeared and only yellow, clearly visible spots remained. The quinoline-monocarboxylic acids could only be seen in UV-light.

2. 0.04% solution of bromo-cresol-green in 96% ethanol. After spraying with the solution, which was adjusted to the transitional color with 0.1 *N NaOH*, yellow spots appeared against a blue background. Before developing it was necessary to remove ammonia from the chromatogram by warming it in a drying chamber.

3. 1% aqueous solution of $FeSO_4$. This reagent was used for the identification of pyridine-dicarboxylic acid. The color of the spots disappeared soon after spraying.

The color of the spots of different acids is shown in the table.

DISCUSSION

The solvent with methanol was not suitable for the separation of pyridine- and quinoline-monocarboxylic acids because the *R* values obtained were to high and the spots were distorted and overlapped. The solvents with ethanol and propanol were also found unsuitable as it was not possible to separate nicotinic from isonicotinic acid and 3-quinoline-carboxylic

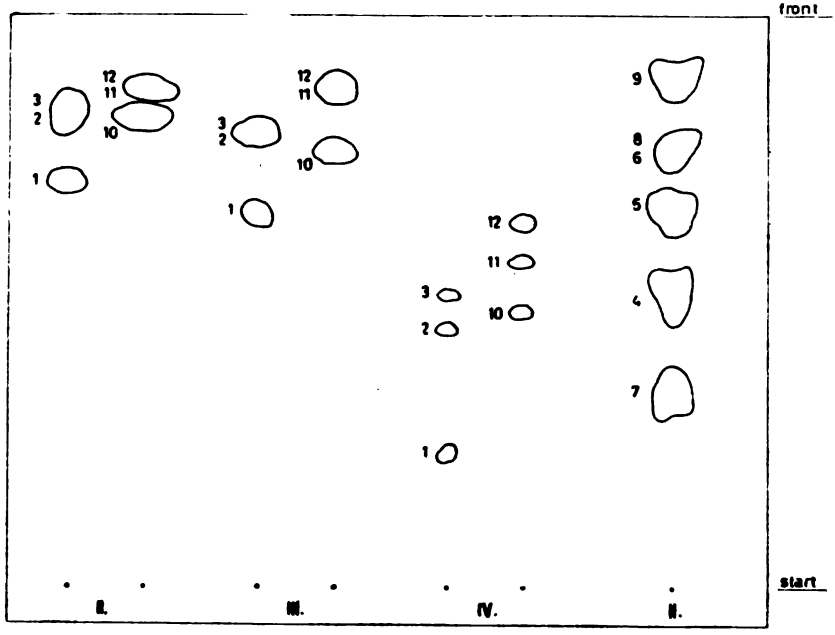

Figure 1

Chromatograms of pyridine-carboxylic and quinoline-carboxylic acids developed in solvents II, III and IV, and chromatogram of pyridine dicarboxylic acids developed in solvent II. The acids are numbered as in Table I.

TABLE 1

Acid	R_f x 100 Solvent			Colour of spot with $FeSO_4$
	II	III	IV	
1. Picolinic	66(71)	51(65)	10(23)	—
2. Nicotinic	82(83)	67(79)	24(45)	—
3. Isonicotinic	82(83)	67(79)	29(51)	—
4. Quinolinic (2,3)	25(50)	24(23)	0	light orange
5. Lutidinic (2,4)	39(66)	67(75)	0	orange
6. Isocinchomeronic (2,5)	62(77)	44(49)	0	light orange
7. Dipicolinic (2,6)	17(34)	10(11)	0	reddish
8. Cinchomeronic (3,4)	62(77)	44(49)	0	—
9. Dinicotinic (3,5)	69(89)	68(75)	0	yellow
10. Quinaldinic	79(82)	62(76)	24(48)	—
11. 3-Quinolinecarboxylic	82(87)	70(87)	30(57)	—
12. Cinchoninic	82(87)	70(87)	37(64)	—

R_f-values in parentheses refer to twice developed chromatograms

from cinchoninic acid. The solvent containing butanol appeared to be the most suitable. Thus the efficiency of separation of pyridine- and quinoline-monocarboxylic acids increased with increasing number of *C* atoms in the alcohol.

The best results in separating pyridine-dicarboxylic acids were obtained with the solvents containing ethanol, with double-development. The solvent with propanol was somewhat less good. The solvent containing butanol was not suitable as the acids remained at the starting point. Thus the efficiency of separation of pyridine-dicarboxylic acids decreased with increasing number of C atoms in the alcohol.

Figure 1 shows the separation of mixtures of the acids in the solvents with ethanol, propanol and butanol, while the R_f values are shown in Table 1. It may be seen from the figure and from the table that the R_f values of all the acids decreased with increasing number of *C* atoms in the alcohol.

It should be noted that the R_f values of pyridine-dicarboxylic acids changed with the number of acids in the mixture, although the order of separation remained unchanged. The change was great if there were two or three acids in the mixture. When there were four or more acids the R_f did not change and corresponded to the values shown in the Table, regardless of the combination of acids. The R_f values of the acids applied separately also did not correspond to those for the mixture. The cause of this was the phenomenon known in chromatography as the matrix effect, which depends on the concentration and nature of the substance. During development some substance leave a "tail" behind them, and a substance which travels slower in fact gets chromatographed on the remnants of the substance in front of it. By reducing the concentration of the substance this effect can be avoided or reduced to a minimum. In some cases, like ours, the reduction of the concentration is limited by the sensitivity of the developer. The most sensitive reagent, in our study it was fluorescein, does not detect amounts of acid less than 10 micrograms.

The behavior of quinolinic acid was interesting. When alone (on non-activated silica-gel), it remained at the starting point in all the solvents except the one with methanol. However, when it was in a mixture with other acids, even with only one, it occupied a place in front of dipicolinic acid, which had the lowest R_f value. When the silicagel was activated it remained at the start even if in a mixture. It is obvious that the adsorptive forces of silica-gel had the strongest effect on this acid and that this effect grew weaker if it was in a mixture with other acids. The weakening of the adsorptive forces is probably due to the influence of the intermolecular forces of the different acids, which were not capable of overpowering these forces on activated silica-gel. The explanation for this behavior of quinolinic acid should probably be sought in the position of its carboxyl groups.

We were not able to separate cinchomeronic from isocinchomeronic acid with any of the solvents used.

Institute of Chemistry,
University of Novi Sad.

Received 11 October, 1966.

REFERENCES

1. Jerchel, D. and W. Jacobs. "Paper Chromatography Analysis of Alkylpyridines" — *Angewandte Chemie* (Weinheim) 65 (2): 342, 1953.
2. Kuffner, F. and N. Faderl. "Paper Chromatography of Pyridinemono- and -Dicarboxylic Acids and Some Alkylpyridines" — *Monatshefte für Chemie* (Wien) 86 (3): 995, 1965.
3. Morimoto, I., K. Furuta and H. Oida. "Paper Chromatography of Pyridine-Carboxylic Acids" — *Bunseki Kagaku* (Japan) 10: 664—666, 1961; *C. A.*, 57, 4041h, 1962.
4. Morimoto, I. and K. Furuta. "A New Method for Detection of Pyridine-Carboxylic Acids no Paper Chromatograms" — *Analytical Chemistry* (Washington) 34 (8): 1033, 1962.
5. Schindler, F. and F. Kuffner. "Paper Chromatography of Pyridine-polycarboxylic Acids and Some Other Heterocyclic Carboxylic Acids" *Monatshefte für Chemie* (Wien) 94 (1): 252—257, 1963.
6. Petrowitz, H. "Thin-Layer Chromatography of Heterocyclic Nitrogen Compounds" — *Chimia* (Aarau) 19 (7): 426, 1965.
7. Petrowitz, H., G. Pastuska and S. Wagner. "Thin-layer Chromatography of Some Pyridines and Quinolines" — *Chemiker-Zeitung* (Heidelberg) 89 (1): 7—12, 1965.
8. Grandberg, I., G. Faizova and A. Kost. (Chromatography of Pyridine Derivatives on a Thin Unfixed Layer of Aluminum Oxide) — *Zhurnal analiticheskoi khimii* (Moskva) 20 (2): 268—271, 1965.

Grimmett, M. and E. Richards. "Separation of Imidazoles by Cellulose Thin-layer Chromatography" — *Journal of Chromatography* (Amsterdam) 20 (1): 171—173, 1965.

Izdavač:

IZDAVAČKO PREDUZEĆE "NOLIT", BEOGRAD TERAZIJE 27/II

•

Štampa:

GRAFIČKO PREDUZEĆE "PROSVETA", BEOGRAD,
ĐURE ĐAKOVIĆA 21

SRPSKO HEMIJSKO DRUŠTVO (BEOGRAD)

BULLETIN OF THE CHEMICAL SOCIETY Belgrade

(Glasnik Hemijskog društva — Beograd)
Vol. 32, No. 5-6-7, 1967

Published by
SRPSKO HEMIJSKO DRUŠTVO (BEOGRAD)
1967

Translated and published for U.S. Department of Commerce and
the National Science Foundation, Washington, D.C., by
the NOLIT Publishing House, Terazije 27/II, Belgrade, Yugoslavia
1969

Translated by
IVAN STOJANOVIĆ

Edited by
DIRK MOELLER

Printed in "Prosveta", Belgrade

CONTENTS

GLASNIK HEMIJSKOG DRUŠTVA, Vol. 32, No. 5-6-7, 1967, pp. 253—259

X-RAY CRYSTAL STRUCTURE ANALYSIS OF 2 AMINO-4'--BROMO BENZOPHENONE AND 2 AMINO-4'-CHLORO BENZOPHENONE*

by

JELICA D. MIŠOVIĆ and S. M. RAMASESHAN

1. INTRODUCTION

This investigation was undertaken to determine the accurate crystal structures of the substituted benzophenones, with a view to determining how substitution of groups in various positions and the formation of inter and intra molecular hydrogen bonds affect the angle between the planes of the two benzene rings. It has become increasingly clear that the steric hinderance between the hydrogens in the 6,6' positions would prevent the molecule from being coplanar.

Study of the stereochemistry of benzophenone derivatives by physical methods (magnetic susceptibility, dipole moment and ultraviolet spectra) started as early as 1935. Earlier workers were primarily interested in the angle between the 1.4 axes of the two benzene rings, and from these studies values varying from 122° to 133° have been suggested. Perhaps the most satisfactory determination from dipole moment studies has been that of Coomber and Partington[1], who have given a value of $125° \pm 3°$ for the case of benzophenone.

Recently, changes of the frequencies and intensities of ultraviolet absorption bands were used successfully to get an idea of the non-coplanarity of molecules. Special mention may be made of the work of Braude[2], O'Shaughnessy and Rodebush[3], Jones[4], Rekker and Nauta[5]. The last mentioned authors have made an attempt to investigate how the various symmetrically substituted benzophenones differ in this respect from the unsubstituted benzophenone. For this the investigators had to assume the tilt of the benzene rings from the common plane

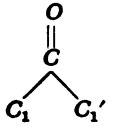

* This work represents a part of the thesis submitted to the Indian Institute of Science, Bangalore, India, 1958.

To compute the order of this angle one has to make a series of assumptions as to bond lengths, bond angles, the minimum disctance of approach of the hydrogen atoms, etc. Hence there is quite a large discrepancy between the calculated angles used by different investigators. For example, while Coates[6] and Sutton find this angle to be 28°, Jones[4] gives a value of 15°.

On the experimental side there are only two investigations which give fairly precise value for this angle. Ramaseshan and Venkatesan[7] report an angle of 22°4′ in the case of 3.3′ dibromo benzophenone from x-ray studies and Karle *et al.*[8] report an angle of 30° for this angle in the case of 4,4′ dimethoxy benzophenone. This difference is quite understandable because the methoxy groups at the 4.4′ positions are of the electron realizing types and would therefore have the effect of shortening the bond connecting the phenyl group to the carbonyl group. The shortening of the bond would have a tendency to make the molecule more skewed, so as to maintain the two hydrogens at 6.6′ positions at a distance of at least 2.2 *Å*.

2. EXPERIMENTAL PROCEDURE

The two compounds chosen were 2 amino-4′-bromo benzophenone and 2 amino-4′-chloro benzophenone. The substances under study have not been previously investigated. The morphological investigations showed that the crystals were isomorphous and that they belong to the orthorombic class-point group mm^2. The unit cell dimensions and the space group were determined by x-ray method[9]. The crystals belong to the non-centro symmetric space group $Pna2_1$ with cell dimensions:

$a = 7.48$, $b = 25.54$ and $c = 5.86$ *Å*

for the bromo-compound and

$a = 7.896$, J $= 25.21$ and $c = 5.74$ *Å*

for the chloro-compound.

The unit cell contains four molecules.

Three-dimensional Weissenberg data were obtained with CuK_α radiation and the intensities were estimated visually. The structures were solved by various methods.

The centro-symmetric *hk*0 projection was first taken up. Using the *hk*0 data of the bromine compound, a Patterson projection was made and the heavy atom position was determined. The other features of the Patterson could not be easily interpreted. Hence, a different Patterson projection was made using the data of the bromo and the chloro-compounds. The latter showed practically the same features as the Patterson and the heavy atom position was confirmed. From knowledge of the position of the *Br* atom, on computing its contribution to the structure factors, the signs of 27 reflection having $h + k = 2n$ could be assigned with a fair degree of certainty. Unfortunately, the *Br* atom practically did not contribute to the structures amplitude of the reflections having $h + k = 2n + 1$, and hence the signs of these reflections could not be determined. To discover the signs of some of these reflections the method of inequalities was used. The Okaya-Nitta linear inequalities were used and the signs of 38 reflections could be assigned. Of these, 11 belong to the group with $h + k = 2n + 1$. Using these signs (27 from the heavy atom method and 17 from

inequalities) a Fourier projection was made from which the molecule could be approximately identified. By the iterative process of Fourier synthesis, the R factor was brought down to about 0.19.

At this stage the non-centro symmetric projection was taken up. Since accurate data were available for the two isomorphous compounds, the method Bijvoet[10] used in solving the non-centro symmetric projection of strychnine sulphate pentahydrate was used. There was a slight difference in the present case, as the heavy atom was not at the center of symmetry. The data for the crystals were accurately scaled and the temperature factor determined. Using these, the phases of the various reflections were computed by a slight modification of Bijvoet's method[11]. Since in this method there is an inherent ambiguity of the phase angle, a projection was made using both the phase angles simultaneously, and it was possible to pick out the structure and its inverse replica. A calculation of the structure factors using the atomic positions from this projection gave $R = 0.23$. It was shown later that the simple heavy atom method as applied to the non-centro symmetric case could also be used to unravel the structure of the molecule in this projection.

Having obtained the approximate structure in two projections, the refinement of the structure was a comparatively simple task. The refinement was effected by judiciously combining the method of difference projections with the trial and error method. In the difference projection (*hk*0) it was possible to identify the approximate positions of hydrogen atoms.

The atomic parameters obtained were used to calculate the structure factors of the *hk*1 and *hk*2 reflections. After a series of nine difference projections, the *R* factor was brought down to about 0.11.

The bond angles and bond distances were calculated. The two benzene rings are not coplanar (Fig. 1); the angle they make with each other is about 61° (Table I).

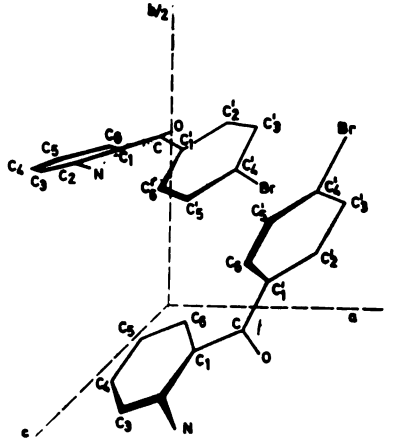

Figure 1

Structure of 2-amino-4′-bromo-benzophenone

TABLE I

Angles between benzene rings in both compounds

	Angles
I Benzene ring and C'_4—CO—C_4	41°31′*
II Benzene ring and C'_4—CO—C_4	30°30′
I and II Benzene rings	61°13′

* The angles represented in Fig. 2.

The final atomic coordinates are given in Tables II and III. The intramolecular distances and angles are indicated in Figs. 2 and 3. The standard deviation in the bond lengths estimated by Cruickshank's[12] method is of the order of 0.02 Å for C—C, 0.019 Å for C—Br and 0.02 Å for $C{=}O$ bonds.

TABLE II

Atomic co-ordinates of 2 amino-4′-bromo benzophenone

Atom	x/a	y/b	z/c	Co-ordinates in Å.U.		
				a	b	c
Br	0.98	0.292	0.00	7.68	7.46	0.00
O	0.954	0.057	0.583	7.48	1.45	3.42
N	0.790	0.024	1.00	6.19	0.62	5.86
C_1	0.675	0.081	0.687	5.29	2.07	4.03
C_2	0.646	0.052	0.898	5.06	1.32	5.26
C_3	0.486	0.044	0.986	3.81	1.13	5.78
C_4	0.352	0.071	0.883	2.76	1.81	5.18
C_5	0.383	0.102	0.692	3.00	2.60	4.06
C_6	0.541	0.107	0.583	4.24	2.73	3.42
C	0.839	0.088	0.546	6.58	2.26	3.20
C'_1	0.875	0.140	0.408	6.86	3.58	2.39
C'_2	0.960	0.140	0.193	7.53	3.58	1.13
C'_3	0.990	0.186	0.067	7.76	4.75	0.39
C'_4	0.940	0.234	0.158	7.37	5.96	0.93
C'_5	0.859	0.234	0.375	6.73	5.96	2.20
C'_6	0.822	0.187	0.500	6.44	4.77	2.93

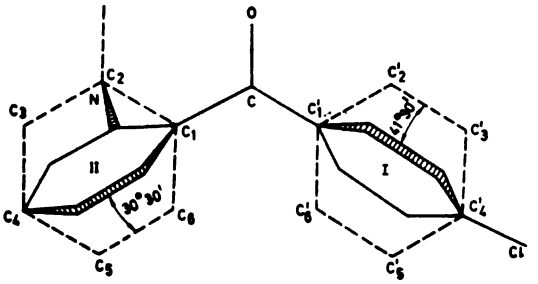

Figure 2

Angle between benzene rings and C_4'-CO-C_4 plane

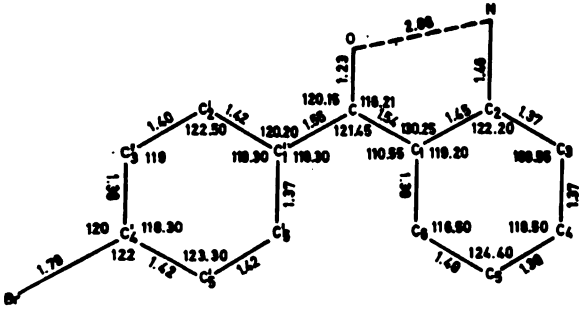

Figure 3

Intramolecular distances in 2-amino-4'bromobenzophenone

TABLE III

Atomic co-ordinates of 2 amino-4'-chloro benzophenone

Atom	x/a	y/b	z/c	Co-ordinates in Å.U.		
				a	b	c
Cl	0.982	0.290	0.008	7.75	7.31	0.05
O	0.954	0.057	0.583	7.53	1.43	3.35
N	0.790	0.024	1.00	6.24	0.61	5.74
C_1	0.675	0.081	0.687	5.33	2.04	3.95
C_2	0.646	0.052	0.898	5.10	1.30	5.16
C_3	0.486	0.044	0.986	3.84	1.11	5.66
C_4	0.352	0.071	0.883	2.78	1.79	5.07
C_5	0.383	0.102	0.692	3.02	2.56	3.97
C_6	0.541	0.107	0.583	4.27	2.69	3.55
C	0.839	0.088	0.546	6.63	2.23	3.13
C_1'	0.875	0.140	0.408	6.91	3.53	2.34
C_2'	0.960	0.140	0.193	7.58	3.53	1.11
C_3'	0.990	0.186	0.067	7.82	4.68	0.39
C_4'	0.940	0.234	0.158	7.42	5.88	0.91
C_5'	0.859	0.234	0.375	6.78	5.88	2.15
C_6'	0.822	0.187	0.500	6.49	4.71	2.87

3. CONCLUDING REMARKS

1. The angle between the 1.4 axes of the two phenyl rings is 121°45;

2. Since the molecule is not symmetrically substituted, the angles which the two phenyl rings make with the commom plane are different. They are 41°31′ for the ring containing the *Br* atom and 30°30′ for the ring containing the NH_2 group. The angle between the planes of the benzene rings is 61°13′;

3. The atoms of each phenyl ring are on the same plane;

4. The angles are practically the same in the case of both the Bromo and the Chloro-compounds;

5. The distance between the nitrogen atom and the oxygen atom is about 2.8 *Å*, suggesting the possibility of a hydrogen bond being formed as follows:

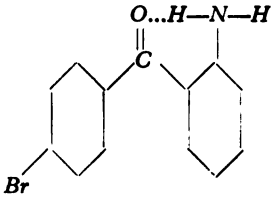

This is consistent with concepts of the hydrogen bond. Indeed Pauling[13] has suggested from purely chemical considerations that the structure of 2,2′ dihydroxy-benzophenone is:

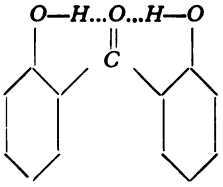

Unfortunately the X-ray crystal structure of this compound has not been studied.

6. The distance of minimum approach of the hydrogen atoms at the 6 and 6′ positions is approximately 2.8 *Å*.

7. The minimum distance between the atom of the neighboring molecules is 3.2 *Å*.

8. It is perhaps worth noting that because of its skew nature each single molecule in the solid state would be optically active, but because the crystal belongs to the group with two glide planes, the molecules in the unit cell would consist of equal numbers of optical enantiomers. It would be of interest to study these molecules in the state of solution. Of particular interest would be the problem of separating the two optical isomers.

Indian Institute of Science
Department of Physics
India, Bangalore

Received 10 April, 1967

REFERENCES

1. Coomber, D. and J. Partington. "The Dipole Moments of Some Aliphatic and Aromatic Aldehydes and of Anthrone" — *Glasnik Hemijskog društva* (Beograd) 1444—1452, 1938.
2. Braude, E., F. Sondheimer and W. Forbes. "Steric Effects in the Electronic Spectra of Organic Compounds" — *Nature* 173: 117—119, 1954.
3. O'Shaughnessy, M. and W. Rodebush. "Ultraviolet Absorption Spectra of Organic Molecules: the Dependence upon Restricted Rotation and Resonance" — *Journal of the American Chemical Society* 62: 2906—2911, 1940.
4. Norman Jones, R. "Some Factors Influencing the Ultraviolet Absorption Spectra of Polynuclear Aromatic Compounds. I. A General Survey" — *Journal of the American Chemical Society* 67: 2127—2150, 1945.
5. Rekker, R. and Th. Nauta. "Steric Effects in the Electronic Spectra of Substituted Benzophenones. I. Symmetrically Substituted Methyl Benzophenones" — *Recueil des travaux chimiques des Pays-Bas* 73: 969—979, 1954.
6. Coates, G. and L. Sutton. "The Determination of the Angle Between the Phenyl Groups in α,α-diphenylethylene, from Electric Dipole Moment Measurements" — *Journal of the Chemical Society* 567—570, 1942.
7. Ramaseshan, S. and K. Venkatesan. "Crystal and Molecular Structure of 3,3'-dibromobenzophenone" — *Experientia* 14: 237—238, 1958.
8. Karle, I., H. Hauptman, J. Karle and A. Wing. "Crystal and Molecular Structure of p,p'-dimethoxybenzophenone by the Direct Probability Method" — *Acta Crystallographica* 10: 481—483, 1957.
9. Mišović, D. and S. Ramaseshan. "The Space Group Determination of 2 amino 4' bromo benzophenone and 2 amino 4'chloro benzophenone" — *Glasnik Hemijskog društva* (Beograd) 28 (5—6): 191—197, 1964.
10. Bokhoven, C., J. Schoone and J. Bijvoet. "Fourier Synthesis of the Crystal Structure of Strychnine Sulfate Pentahydrate" — *Acta Crystallographica* 4: 275—280, 1951.
11. Mišović, D. "A Modification of the Bijvoet's Method for Solving Structures of Noncentro Symmetric Crystals" — *Glasnik Hemijskog društva* (Beograd) 27 (4): 185—189, 1962.
12. Cruickshank, D. "Accuracy of Electron-Density Maps in X-Ray Analysis with Special Reference to Bibenzyl" — *Acta Crystallographica* 2: 65—82, 1949.
13. Pauling, L. *The Nature of the Chemical Bond* — Ithaca, New York: Cornell University Press, 1948 and London: Humphrey Milford, 1948.

GLASNIK HEMIJSKOG DRUŠTVA, Vol. 32, No. 5-6-7, 1967, pp. 261—265

CHRISTIANSEN'S EFFECT IN INFRARED SPECTRA OF ORGANIC AND INORGANIC SUBSTANCES

by

DRAGAN A. MIOČ and UBAVKA B. MIOČ

In studies of absorption spectra of suspensions in the visible part of the spectrum, it may be seen that at one wavelength the suspension suddenly becomes much more transparent than in other parts of the spectrum. The appearance of this transparent peak was noticed by Christiansen in 1884[1, 2].

The effect of "anomalous transparency"[3], or as it was later named "Christiansen's effect", occurs at wavelengths at which the dispersion curves of the suspension components, that is, of the dispersed particles and medium, intersect at the moment when their diffraction indexes become equal. This phenomenon has been used for obtaining monochromatic filters in the visible[4] and ultraviolet part of spectrum[5, 6]. In the infrared part, Christiansen's effect has been used for making monochromatic filters up to the region of 90 μ[7a], as well as being of considerable aid in the determination of diffraction indexes of solid substances in this region[7b].

In all these studies substances were used whose dispersion curves cross at a single point, and hence a pair of substances gives Christiansen's effect only at one wavelength.

Our experiments have shown that in the infrared spectra of some substances, in the suspension form, there is simultaneous appearance of a number of transparent peaks for one pair of substances. The site of these peaks is closely related to the different absorption bands of the material under study. The peaks are most marked on the short-wave side of isolated absorption bands.

Under the conditions under which the effect appears, the transparency of a substance at shorter wave-lengths is small, until it gets near one of the characteristic bands. At this point the transparency of the test sample shows an abrupt rise and a steep drop at the frequency of resonant absorption. Further on, the transparency shows a gradual rise and the curve acquires an asymmetrical form (curve *a* in Fig. 1).

The effect completely disappears in the spectrum of the solution of the same substance, where the band acquires a fully symmetrical form (curve *b* in Fig. 1). A slight displacement of the wave-length of the absorption peak can be explained on the basis of a change in the state of aggregation.

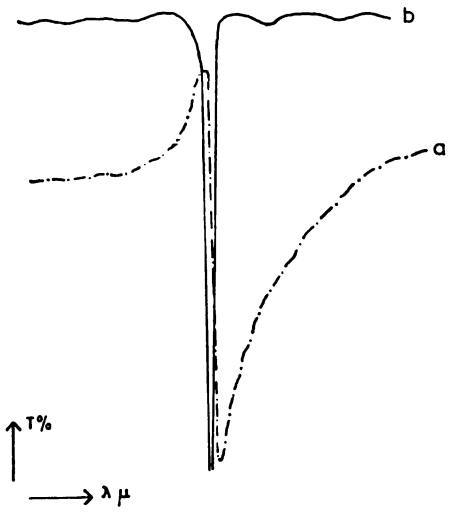

Figure 1

Characteristic form of the absorption bands of test samples: a. in solid state, b. in solution

EXPERIMENTAL

We studied the infrared spectra of a series of nitrate compounds ($CsNO_3$, $RbNO_3$, and $Ca(NO_3)_2$), a group of halogenous derivates of diphenyl-diselenide ($(BrC_6H_4Se)_2$ and $(ClC_6H_4Se)_2$), a group of halogenous derivates of diphenyl-disulfide ($(BrC_6H_4S)_2$ and $(ClC_6H_4S)_2$), and a series of thiocyanates: $NaSCN$, $KSCN$ and NH_4SCN.

The substances in the group of nitrates and thiocyanates were commercial products, purity p.a., while the diphenyl compounds were synthesized in the laboratory of M. F. Taboury of the Faculté des Sciences in Poitiers (France).

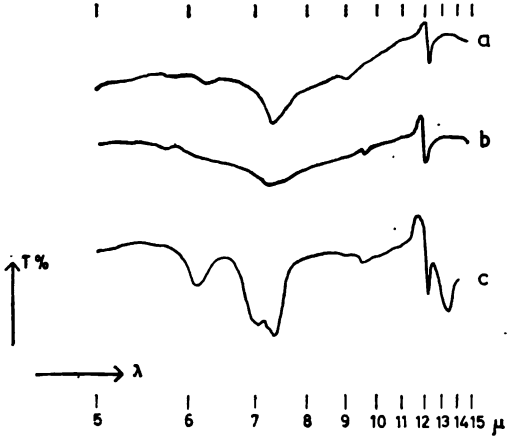

Figure 2

Infrared spectra:

a. $CsNO_3$,
b. $RbNO_3$,
c. $Ca(NO_3)_2$

Samples for obtaining the spectra were prepared in two ways: in the form of *KBr* pastilles with 1% of the substance under study, and in the form of suspension in paraffin oil: 2 *mg* of powder of the substance in 0.1 *ml* of paraffin oil.

The infrared spectra were obtained on two spectrophotometers: Perkin Elmer M 21 in the range of 2.5 to 15 μ and Zeiss UR-10 in the range from 2.5 to 25 μ.

The spectra of the nitrate compounds are shown in Fig. 2. The form typical of Christiansen's effect is present in the bands at $\lambda = 12\ \mu$, while in the bands at $\lambda = 7.3\ \mu$, which are more intensive than the first, it did not appear.

In the spectra of halogenous derivates of diphenyl-diselenide shown in Fig. 3 it may also be seen that Christiansen's effect appeared only in some bands, while in the others it was absent. The effect was marked in the bands at $\lambda = 10\ \mu$, while in the bands at the same or higher intensity at about $\lambda = 12\ \mu$ and $\lambda = 21\ \mu$ it was hardly perceptible or absent. When comparing the bands at $\lambda = 7\ \mu$ and $\lambda = 9\ \mu$, on spectrum *a* in Fig. 3, it may be seen that in this case the effect was more marked in the weaker band, while in spectrum *b* in Fig. 3 it may be seen that in the bands at $\lambda = 9\ \mu$ and $\lambda = 10\ \mu$ the effect can differ greatly in bands of approximately the same intensity.

Analogous behavior of Christiansen's effect was noted also in the spectra of diphenyl-disulfide and its halogenous derivates, which gave spectra similar to those in Fig. 3. The case was similar with the spectra of the group of alkaline thiocyanates under study.

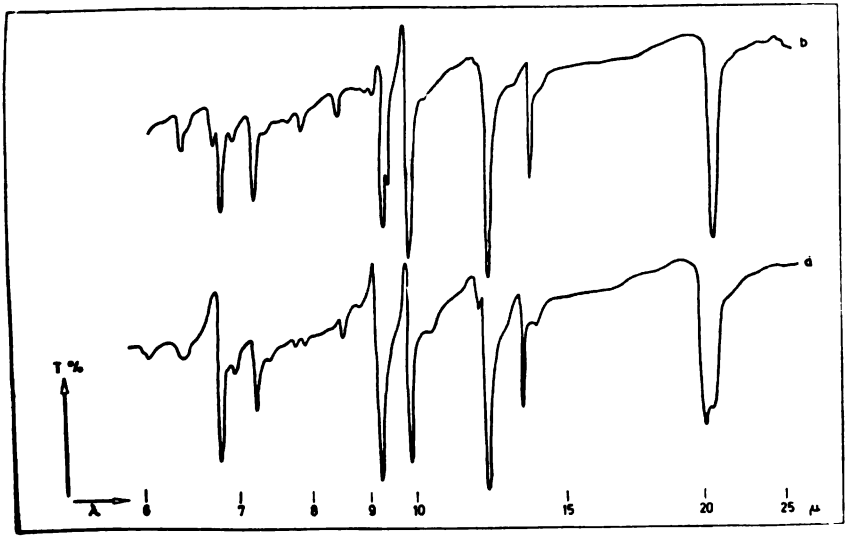

Figure 3

Infrared spectra: *a.* $(ClC_6H_4Se)_2$, *b.* $(BrC_6H_4Se)_2$

From these findings we can draw the following conclusions, which have not been described in the literature up until now, concerning Christiansen's effect in the infrared range:

a. the effect does not appear in all strongly isolated absorption bands of a single substance,

b. for a given substance, in which Christiansen's effect appears in several basic bands, the intensity of the effect is not a function of the intensity of absorption.

DISCUSSION

If we consider the basic explanation for the effect itself, the absence of Christiansen's effect in some bands shows that in the range of these bands there is no intersection of the dispersion curves of the substance and the dispersion medium under study. As in these ranges the dispersion curves on the materials used as the medium (*KBr* and paraffin oil) are continuous and monotone functions[8], the diffraction index of the substance under study in the range of this band therefore does not reach an adequate value to intersect the first curve — as is the case for some other band in the same spectrum, in which the effect appears.

On the other hand, it may be stated for the bands in which the effect is present that there was an abrupt and marked change in the diffraction index in its immediate vicinity, which led to the intersection of the two dispersion curves. According to Lecomte [7b], such a change of the diffraction index is due to the appearance of anomalous dispersion in the vicinity of the resonant frequency, which is in our case the absorption band.

In accordance with the quantum mechanic considerations of dispersion[9], for description of the appearance of anomalous dispersion in the vicinity of the basic oscillatory frequencies (ν_k) we can adopt the following equation given by Lecomte[7]:

$$n_k^2 = 1 + \frac{[N_o e^2 f_k/\pi m'][\nu_k^2 - \nu^2]}{[\nu_k^2 - \nu^2]^2 + [\nu\, b_k/2\pi m']^2} + F[\nu^2]$$

in which f_k is the oscillatory intensity of the k-band, m' = the reduced mass of the oscillator, b_k = the constant characteristic for the k-band and $F(\nu^2)$ = = the contribution of all the other frequencies involved.

According to this equation, in the vicinity of all the resonant oscillatory frequencies of the molecules, the effect of anomalous dispersion would be approximately equal. Our experiments, however, indicate a particularly selective nature of Christiansen's effect. We also found that its appearance did not depend on the intensity of the band in which it occurred, nor on the spectral region, since of two near bands, of approximately the same intensity, one is associated with the effect and the other is not. We consider that the form of molecule oscillations from which the bands ensue is decisive for the appearance of Christiansen's effect. On the basis of the identification of several bands in which the effect was either present or ab-

sent[10, 11], we came to the conclusion that a change in the ability of molecules to polarize with a given oscillation is necessary for appearance of the effect.

Therefore, the equation for anomalous dispersion, which would include and explain this selective property in the field of basic oscillatory frequencies, should have an additional member $G(\Delta\mu_k)$, representing the influence of the change in the ability of molecules to polarize with a given oscillation, on the dispersion curve.

More detailed experimental and theoretical studies will be necessary to establish the explicit expression for this additional member and for its correlation with the other molecular factors.

School of Science, Belgrade,
Institute of Physical Chemistry

Received 4 October, 1966.

REFERENCES

1. Christiansen, C. "Untersuchungen über die optischen Eigenschaften von fein vertheilten Körpern" — *Annalen der Physik und Chemie* (Leipzig) 23: 298—306, 1884.
2. Christiansen. C. "Untersuchungen über die optischen Eigenschaften von fein vertheilten Körpern II" — *Annalen der Physik und Chemie* (Leipzig) 24: 439—446, 1885.
3. Ostwald, W. *Licht und Farbe in Kolloiden* — Dresden, 1924, p. 393.
4. Weigert, F. and H. Staude. "Über monochromatische Frabfilter" — *Zeitschrift für Physicalische Chemie* 130: 607—615, 1927.
5. Gaydon, A. and G. Minkoff. "A Christiansen Filter for the Ultraviolet" — *Nature* 158: 788, 1946.
6. Sinsheirner, R. and R. Leofbourow. "Christiansen Filters for the Ultraviolet" — *Nature* 160: 674, 1947.

7a. Flugge, S. *Encyclopedia of Physics* — Berlin, 1958, Vol. 26, pp. 307 and 920.

7b. Flugge, S. *Encyclopedia of Physics* — Berlin, 1958, Vol. 26, p. 914.

8. Voronkova, E., B. Grechushnikov, G. Distler and I. Petrov. *Opticheskie materiiali dlia infrakrasnoi tekhniki* — Moskva: Nauka, 1965.
9. Korolev, F. *Teoreticheskaia optika* — Moskva: Vysshaia shkola, 1966.
10. Herzberg, G. *Molecular Spectra and Molecular Structure II* — New York: D. Van Nostrand Co., 1954.
11. Bellamy, L. *The Infrared Spectra of Complex Molecules* — London: Methuen and Co. Ltd., 1954.

GLASNIK HEMIJSKOG DRUŠTVA, Vol. 32, No. 5-6-7, 1967, pp. 267—272

APPLICATION OF CHRISTIANSEN'S EFFECT IN THE INFRARED SPECTRA OF SOLID SUBSTANCES IN THE IDENTIFICATION OF BANDS*

by

DRAGAN A. MIOČ and UBAVKA B. MIOČ

In the infrared spectra of solid substances, when the technique of test-sample suspension is used, some absorption bands have a characteristic asymmetrical form. The asymmetry is manifested by a sudden increase in transparency of the sample in respect to the fon, near the absorption band, followed by a rapid decrease at a characteristic frequency and a gradual increase in transparency on the other side of the band (Fig. 1).

This effect, which appears both in the visible and UV range of the spectrum, is known as Christiansen's effect[1, 2]. The appearance and influence of this effect in infrared spectra has been the subject of several studies[3, 4, 5].

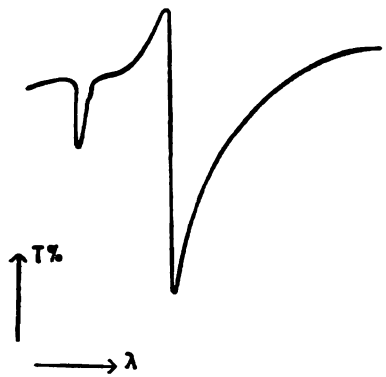

Figure 1

Appearance of a band with Christiansen's effect

The bands whose shape is deformed by Christiansen's effect present great difficulties in quantitative studies with infrared spectra. As the effect depends on the size of suspended particles of the substance under study, it can be partly suppressed by decreasing the dimensions of the particles in the sample.

* This study was reported at the IInd Yugoslav Congress of Pure and Applied Chemistry in Belgrade, 1966.

Our studies were done on spectrophotometers Perkin Elmer M-21 and Zeiss UR-10. We used the technique of *KBr* pastilles containing 1% of the substance under study and the technique of suspensions in paraffin oil, with the particle size giving the greatest Christiansen's effect.

The substances studied, listed in Table 1, were of p.a. purity and commercially produced, while the compounds of the diphenyl-diselenide group (Table 2) were synthesized in the laboratory.

We studied a series of substances in whose spectra Christiansen's effect appears. It was noted that it did not appear in all absorption bands, but behaved selectively. While studying the causes of the appearance of the effect only in some isolated bands, we came to the conclusion that the selectivity is not related to the intensity of absorption. We hypothesized that the form of the oscillations from which the given bands ensue is decisive for the appearance of Christiansen's effect in these bands[5]. To check this hypothesis, we identified the bands in which the effect appeared in the spectra of several known solid substances, with the aid of data from standard tables[6, 7].

In the group of thiocyanate compounds, in the spectral range from 2 to 15 μ, the effect appeared in the band at about $\lambda = 4.9\ \mu$ (Table 1, 1—4), which can be ascribed to the valent oscillations of $-C\equiv N$ bonds (Fig. 2a). In the studied group of nitrate compounds, the effect was marked in the band at $\lambda = 12\ \mu$ (Table 1, 5—7), which comes from the curving (ν_2) oscillation of the group $-NO_2$ (Fig. 2b).

TABLE 1

Identified bands with Christiansen's effect

No.	Substance	$\nu\,cm^{-1}$	$\lambda\mu$	Form of oscillations
1	*NaSCN*	2020	4.95	
2	*KCNS*	2040	4.90	of $-C\equiv N$ valence
3	NH_4SCN	2050	4.88	
4	$Hg(SCN)_2$	2090	4.78	of $-C\equiv N$ valence
5	$RbNO_3$	836	11.96	
6	$CsNO_3$	825	12.12	of groupe $-NO_2$
7	$Ca(NO_3)_2$	820	12.20	

The identified oscillation forms are shown schematically in Fig. 2.

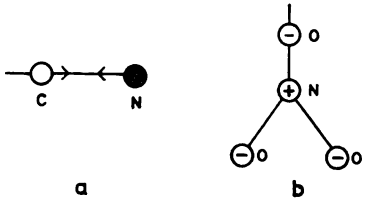

Figure 2
Identified oscillation forms
a. oscillations of $-C\equiv N$ valence
b. oscillations v_2 of $-NO_2$ group

It is readily noted that in the oscillation forms under observation there was considerable change of the polarizing capacity of the oscillating molecules. Therefore, such movement should produce a sudded and great change in the molecule diffraction, which is, in the end, the condition for the appearance of Christiansen's effect in the vicinity of the frequencies resonant for that form of oscillation.

These considerations enable us to ascribe the bands which manifest Christiansen's effect with more certainty to certain forms of oscillation of the molecules studied. This greatly facilitates the identification of such bands. This procedure would be of particular significance for the identification of bands in the spectra of composite molecules.

The procedure suggested consists of achieving the conditions for the appearance of the most marked Christiansen's effect by choice of the corresponding particle size of the substance studied. By considering all the possible forms of oscillation for the molecule studied, one can ascribe the bands with the effect to the oscillations which are followed by the greatest changes in the polarizing capacity.

We have successfully applied this procedure in the identification of bands of diphenyl-diselenide and its halogenous derivates. The results of this identification are shown in Table 2, while the forms of oscillation are schematically presented in Fig. 3, a, b, c, d.

TABLE 2

Identified bands in the spectra: $(SeC_6H_5)_2$, $(SeC_6H_4Cl)_2$ *and* $(SeC_6H_4Br)_2$

Compound	$\nu\ cm^{-1}$	$\lambda\mu$	Form oscillation
$(SeC_6H_5)_2$	1480	6.75	analogous to ν_{13} of benzene
„	1020	9.80	analogous to ν_{14} of benzene
„	740	13.51	analogous to ν_4 of benzene
$(SeC_6H_4Cl)_2$	1480	6.75	analogous to ν_{13} of benzene
„	1090	9.17	analogous to ν_{10} of benzene
„	1010	9.90	analogous to ν_{14} of benzene
„	730	13.70	analogous to ν_4 of benzene
$(SeC_6H_4Br)_2$	1485	6.73	analogous to ν_{13} of benzene
„	1070	9.35	analogous to ν_{10} of benzene
„	1010	9.90	analogous to ν_{14} of benzene
„	710	14.08	analogous to ν_4 of benzene

It may be seen that in the spectra of these substances (Table 2) Christiansen's effect appeared in four bands out of fifteen present in the investigated range, that is, at: $\lambda = 6.7\ \mu$, $\lambda = 9.2\ \mu$ (except for the compound $(SeC_6H_5)_2$ which had no H atoms substituted by halogens), $\lambda = 9.9\ \mu$ and $\lambda = 13.7\ \mu$. These bands can be ascribed, on the basis of the above considerations, to the molecule oscillation forms associated with the greatest polarization. These are the oscillation forms analogous to the oscillations of benzene molecule ν_{13}, ν_{10}, ν_{14} and ν_4, which are shown in Fig. 3.

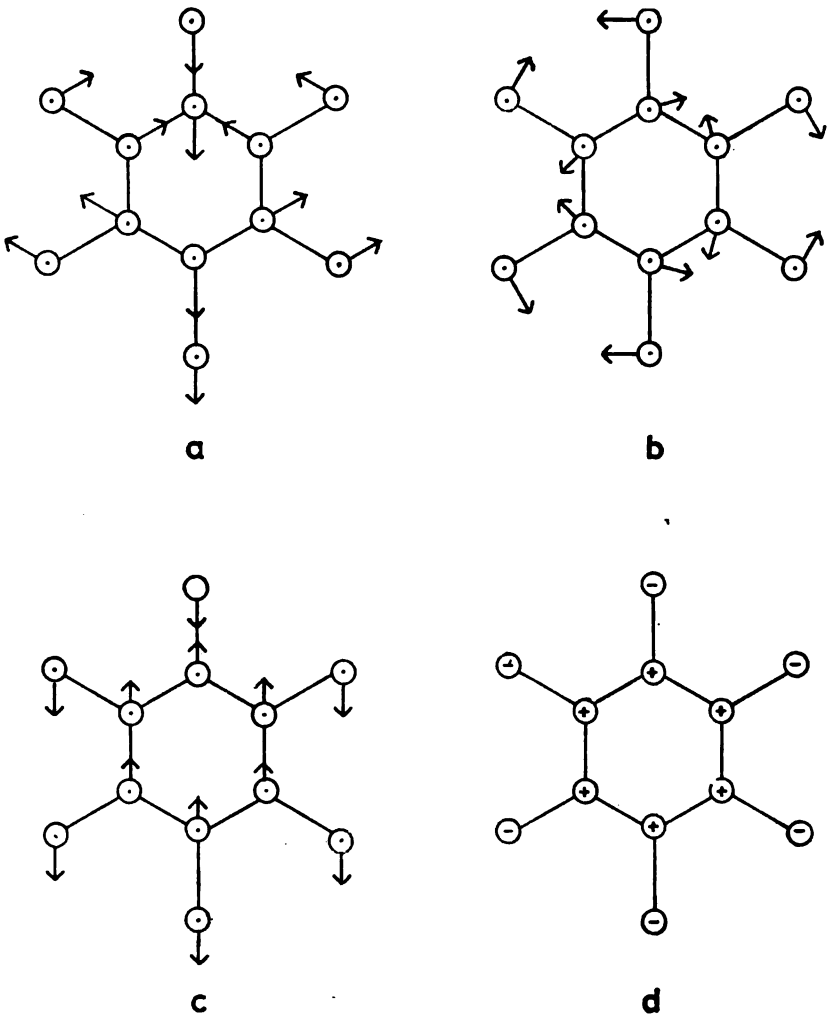

Figure 3

Identified molecule oscillation forms of *Se* compounds

a. oscillations ν_{13} of benzene
b. oscillations ν_{10} of benzene
c. oscillations ν_{14} of benzene
d. oscillations ν_{4} of benzene

It may be seen that Christiansen's effect, which, on the one hand, represents an obstacle in quantitative studies with solid samples, can, on the other hand, considering its selectivity, be used as an important aid in the identification of spectra.

School of Science, Belgrade,
Institute of Physical Chemistry

Received 4 October 1966

REFERENCES

1. Christiansen, C. "Untersuchungen über die optischen Eigenschaften von fein vertheilten Körpern" — *Annalen der Physik und Chemie* (Leipzig) 23: 298—306, 1884.
2. Christiansen, C. "Untersuchungen über die optischen Eigenschaften von fein vertheilten Körpern II" — *Annalen der Physik und Chemie* (Leipzig) 24: 439—446,1885
3. Flugge, S. *Encyclopedia of Physics* — Berlin, 1958, Vol. 26.
4. Rao, C. *Chemical Applications of Infrared Spectroscopy* — New York: Academic Press, 1963.
5. Mioč, D. and U. Mioč. "Prilog proučavanju Kristiansenovog efekta u infracrvenim spektrima organskih i neorganskih supstanci" (Christiansen's Effect in Infrared Spectra of Organic and Inorganic Substances) — *Glasnik Hemijskog društva* (Beograd) (5—6—7), 1967.
6. Herzberg, G. *Molecular Spectra and Molecular Structure II* — New York: D. Van Nostrand Co., 1954.
7. Bellamy, L. *The Infrared Spectra of Complex Molecules* — London: Methuen and Co., Ltd., 1954.

GLASNIK HEMIJSKOG DRUŠTVA, Vol. 32, No. 5-6-7, 1967, pp. 273—284

INFLUENCE OF FOREIGN INCORPORATIONS ON THE SPECTROCHEMICAL AND CRYSTALLOCHEMICAL PROPERTIES OF BERYL

by

SLOBODAN M. RISTIĆ, DRAGAN A. MIOČ, ANKICA M. JOVANOVIĆ and MILORAD G. JEREMIĆ

The mineral beryl with the ideal chemical composition $Be_3Al_2Si_6O_{18}$ represents, with its hexagonal crystal lattice, a very interesting case of so-called open crystal structures in which the inclusion or incorporation of foreign particles is particularly favored. The great number of studies on this problem, of which those appearing up to 1955 are rather completely covered and discussed in a thesis of one of the present authors[1], is continuing to grow with new investigations, a good review of which has been given in a recent publication by F. Kamenskiĭ[2].

The aim of the present study was to investigate, continuing in part the previous studies[3], particularly the influence of water, alkali and metal of the "transitional series" on the spectrochemical and crystallochemical properties of natural and synthetic beryls.

EXPERIMENTAL WORK AND RESULTS

In order to determine the water content, we made *thermogravimetric studies* of a large number of domestic and foreign beryls, using partly the standard thermogravimetric technique and partly apparatus improvized in the laboratory. The obtained thermogravimetric curves are shown together in Figs. 1 and 2 (*a* and *b*).

The course of thermogravimetry, which has been explained in a previous study[1], is illustrated in Fig. 1. Curves 3 and 4 in Fig. 1 show the usual way of representing thermogravimetric curves, while curves 1 and 2 show the relative weight losses at a given temperature in respect to the total loss. It may be seen that this way of presentation has considerable advantage, because the thermogravimetric discontinualities stand out more clearly as the *characteristic maximums* for the observed process of escape of the volatile constituents from the beryl lattice during heating. The presence of two different types of water, almost simultaneously and independently established by Ginzburg in 1955[4] and Ristić in 1955/56[1, 5], is well confirmed in Fig. 2 on five Yugoslav (*P*, *K*, *C*, *B*, *M*) and five foreign beryls (from the Rayleigh-Paneth collection, marks PB 1, 4, 7, 16, 40).

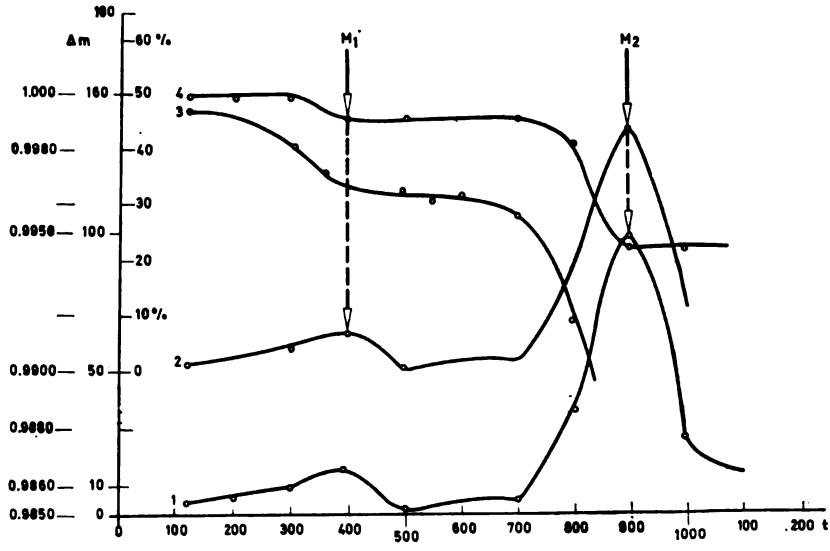

Figure 1

Two different ways of presenting thermogravimetric results, illustrated on two natural beryls

The interpretation of the presence and origin of this water in natural beryls is somewhat clearer, although not absolutely clear yet, after a series of rather important studies by Soviet authors (Belov, Ginzburg, Feklichev, Beus, Kameneckiĭ and others). At present it is clear that this water content cannot be regarded separately from the content of alkali and perhaps of other "inner impurities" in the beryl lattice. Hence there is a necessity for the use of other methods in explaining this situation.

Our investigations by means of the IR-spectrum on several commercial spectrophotometers (Infracord Perkin-Elmer Model 137-B, Carl Zeiss-Jena UR-10, and Leitz Wetzlar IR Model III) gave, first of all, somewhat more detailed information on the main absorption bands of the beryl crystal lattice and their relative intensities, although a definite identification of all the observed bands was not yet possible. By studying the absorption IR-spectrophotograms of more than twenty synthetic beryls (with p.a. pure chemicals) and more than ten natural beryls, Yugoslav and foreign, we arranged in a clear fashion all the known characteristic spots of IR-absorption. Besides the absorption maximums (in μ and cm^{-1}), Table 1 also shows the relative intensities of the registered bands, the band with the greatest intensity being taken as the unit for comparison (at 10.37 μ). This, we believe, so far most complete empirical register of IR-absorption bands of beryl is given for the entire here investigated range from 1 to 25 μ, or from 10,000 to 400 cm^{-1}, the bands being arranged both according to their relative intensities and their wavelengths.

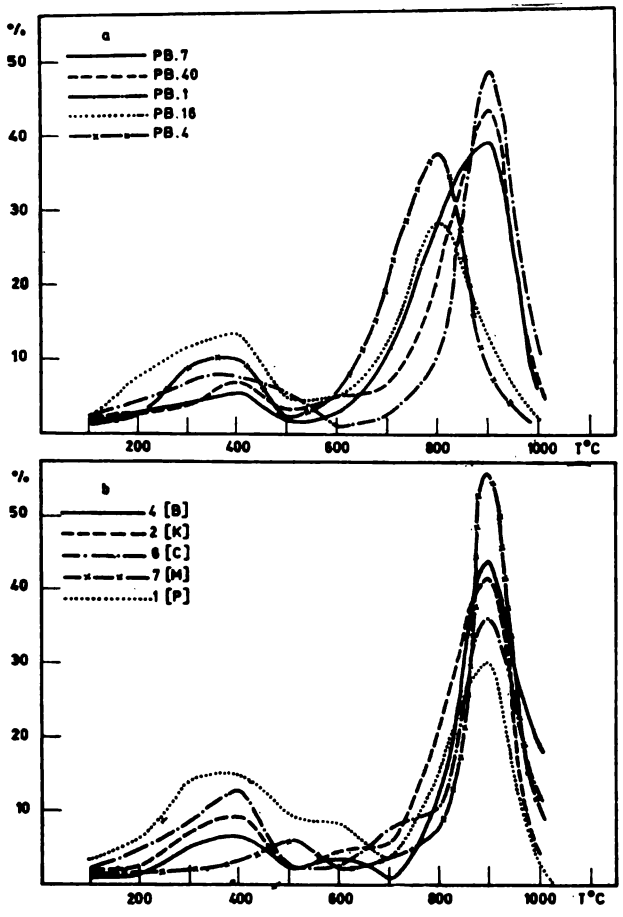

Figure 2

Thermogravimetric curves for *a*) five Yugoslav and *b*) five foreign beryls, presented by the procedure here recommended

It may be seen that the most intensive IR absorption range of the beryl lattice spreads from about 8.5 μ to slightly above 18.5 μ, where four more important bands are localized (T_1, T_2, T_3, T_4) whose identification, after a series of studies and according to Pliusnina[6], can now be considered as certain. Figure 3 shows parallelly the IR-spectrum of a synthetic (SB-4) and two natural beryls (PB 72 and PB 56) recorded by means of the Leitz IR-spectrophotometer in the range from 1 to 15 μ. It may be seen that the relative intensities of the more important bands of synthetic beryl quite reproducibly and closely follow those of the natural samples, which makes possible a very reliable differentiation of beryls from very closely related crystalline structures (cordiarite, dioptase, etc.) on the basis of IR- absorption spectra, while the determination of foreign incorporations in beryl, on the basis of the less intensive bands, is a separate problem.

TABLE 1

Characteristic IR absorption bands of the beryl lattice with their relative intensities

λ, μ	$\tilde{\nu}$, cm^{-1}	$I_{rel.}$	Ident. of bands	Band	$I_{rel.}$	λ, μ	$\tilde{\nu}$, cm^{-1}	Ident. of bands
1.19	8403	37		T_1	100	10.37	964	(SiO_4)
3.10	3226	11		T_2	93	8.28	1208	(BeO_4)
4.34	2304	11		T_3	90	14.67	681	(BeO_4)
5.17	1934	15		T_4	90	18.93	528	(AlO_6)
6.17	1621	29		T_5	88	23.26	430	
7.28	1374	38		T_6	87	22.73	440	
8.28	1208	93	(BeO_4)	T_7	85	20.15	496	
8.65	1156	63		T_8	84	16.88	592	(BeO_4)
9.78	1022	81		T_9	83	11.00	909	
10.37	964	100	(SiO_4)	T_{10}	81	9.78	1022	
11.00	909	83		T_{11}	81	12.35	810	(Si_6O_{18})
12.35	810	81	(Si_6O_{18})	T_{12}	79	21.87	457	
12.85	778	79		T_{13}	79	12.85	778	
13.47	742	78	(BeO_4)	T_{14}	78	13.47	742	(BeO_4)
14.67	681	90	(BeO_4)	T_{15}	72	15.34	652	
15.34	652	72		T_{16}	63	8.65	1156	
16.88	592	84	(BeO_4)	T_{17}	38	7.28	1374	
18.93	528	90	(AlO_6)	T_{18}	37	1.19	8403	
20.15	496	85		T_{19}	29	6.17	1621	
21.87	457	79		T_{20}	15	5.17	1934	
22.73	440	87		T_{21}	11	4.34	2304	
23.26	430	88		T_{22}	11	3.10	3226	

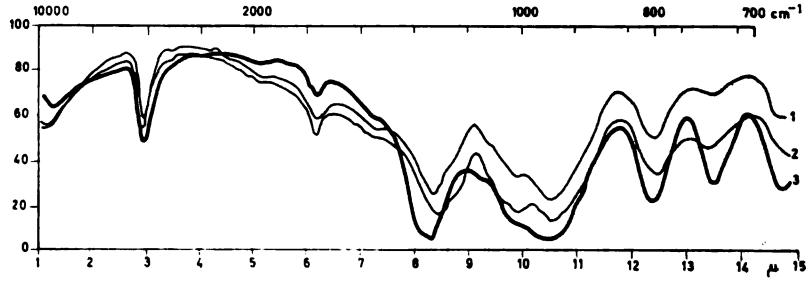

Figure 3

IR spectra of two natural (curves 1 and 2) and one synthetic beryl (curve 3)

The IR absorption spectra of Yugoslav beryls, both non-heated (N) and heated ($\check{Z}$) are shown in Fig. 4 on samples which were also studied thermogravimetrically (see Fig. 2).

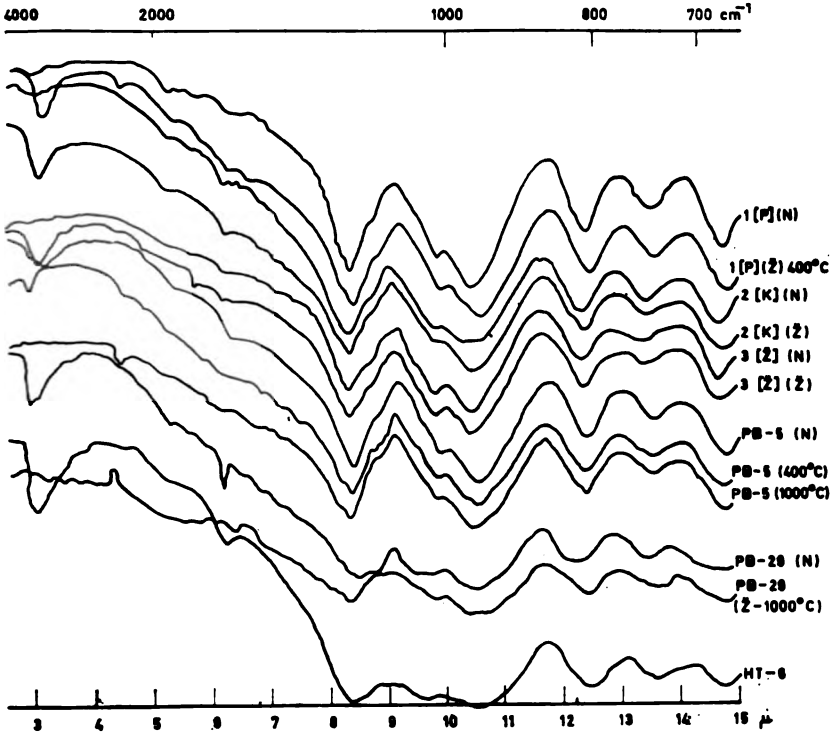

Figure 4

IR spectra of heated ($\check{Z}$) and non-heated (N) natural beryls

It may be seen from this figure, despite some inadequately marked changes in the less intensive bands, that the ratio of relative intensities in more intensive bands remains the same both in heated and non-heated samples, thus preserving the general character of the IR-spectrum as in synthetic beryl, which already by the character of the synthesis method here used contained no water at all as an "inner impurity". However, in the band at 3.10 μ, which originates from the water content, the effect of heating is evident. It may be seen from spectra numbers 4, 5 and 6 (Fig. 4) which correspond to non-heated natural beryl (PB-5), and to that heated to 400°C and 1000°C successively, that the relative intensity of the band was considerably decreased with heating to 400°C, but did not disappear completely, while with heating to 1000°C it completely disappeared. In the spectra of synthetic beryls the corresponding band did not appear.

The content of alkaline metals in the beryl lattice represents an important "inner impurity" which is regularly found in natural beryls. We have emphasized in some previous studies[1, 2] that in emission-spectroche-

mical studies done on a series of over seventy natural beryls no case was found in which any of the five alkalies was absent. Obviously it may be stated that these metals are, together with water, regular constituents of all natural beryls. A close relationship of the presence of these metals with the presence of water has been recently discussed in a paper by Bakakin and Belov in 1962[7] and by Feklichev in 1963[8]. In view of the possibility, demonstrated in our study, of controlling the variations within certain limits during the preparation of synthetic beryls of the content of alkali incorporated into the beryl lattice, for the case of lithium and cesium, which represent two extremes in their very different ionic radii ($r_{Li}+ = 0.68$ Å; $r_{Cs}+ = 1.67$ Å), we prepared a large number of such samples of synthetic beryls. The case of lithium is interesting, as its incorporation into the beryl lattice is supposed to cause a widespread disturbance of the lattice structure because of the "acid" function which lithium is capable of manifesting in it (by substitution of *Al* or *Be*). For the series of synthetic beryls, whose IR-spectra will be presented later on, the content of lithium was determined by means of a flame photometer after finely-ground samples were completely dissolved by means of evaporation with hydrofluoric acid (with the addition of H_2SO_4). Table 2 shows the lithium content (% metal and % Li_2O) in those samples of our synthetic beryls which were subsequently also studied by means of IR- spectrophotometry.

TABLE 2

Percentage of lithium (as Li and Li_2O) incorporated into the crystal lattice of synthetic beryls

No.	Synthetic beryl samples	% *Li*	% Li_2O	Remark
1	*SB* 4	0.028	0.060	(*V*)
2	*SB* 47	0.044	0.095	(*Cs*)
3	*SB* 55	0.049	0.105	(*Co*)
4	*SB* 39	0.055	0.118	(*Co*)
5	*SB* 45	0.058	0.125	(*Cs*)
6	*SB* 21	0.075	0.161	(*Fe*)
7	*SB* 26	0.125	0.269	(*Cs*)
8	*SB* 49	0.145	0.312	(*Cs*)
9	*SB* 15	0.390	0.838	(*Sc*)

It may be seen from the table that in our samples of synthetic beryl we succeeded in inducing variations of the percentage of incorporated lithium from 0.028 to about 0.40% (that is from about 0.060 to 0.80% Li_2O), therefore slightly more than a whole power, while at the same time the crystal lattice maintained all its essential radiographic and IR-characteristics.

The IR-absorption spectra of synthetic beryls with different contents of lithium are shown in Fig. 5.

It may be seen that the water bands at 3.10 μ were absent, while the relative intensities of the main absorption bands remained quite well preserved, as in none of the cases (even among all the other synthetic beryls

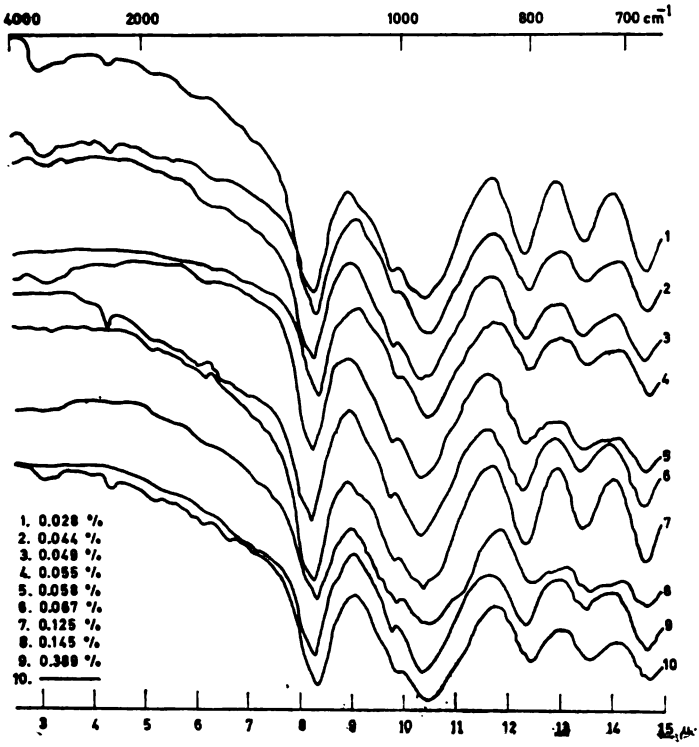

Figure 5

IR spectra of synthetic beryls with different contents of incorporated lithium

which we studied with other foreign incorporations) was there any inversion of the intensities, as seen in Table 1. However, the bands of lower intensity which remained for deciphering in order to detect the presence of foreign material, including lithium, did not seem to justify optimism in respect to the detection and determination, as the reproducibility of the registration of these lower intensities is markedly poorer than with higher intensities. The relatively small dispersion of the IR-spectrophotometers used did not allow us, as may be seen, to obtain the absorption band of the LiO_4-tetraedric group (1053 cm^{-1}), which Pliusnina in a recent study[9] believed to have established (together with some other bands) for Li_2O concentrations from 0.257 to 0.428%. It must be taken into account here too that the preparation of samples in the two cases was different. While we always used the usual technique of *KBr*-pastilles (with relatively small amounts of the substance under study — about 0.5%), Pliusnina used a special method. However, showing full respect for the critical objections concerning older attempts at interpreting the IR-oscillations in the Si_6O_{18}-group in the crystal lattices containing Be^{2+} ions, more recently pointed out particularly by A. N. Lazarev[11], some empirical observations can nevertheless be made regarding the clearly visible changes of intensity in some of the main ab-

sorption bands (T_3, T_4, . . .). Exact identification and precise determination of the effects depends on the greater dispersing capacity of the apparatus and on the more strict definition of the preparation of samples.

The intentional incorporation of cesium and cobalt into the crystal lattice of beryl, these two elements having been chosen for being particular examples of heterovalent and homovalent incorporation into this lattice, by the method of IR- absorption again, was hardly if at all noticeable. Figures 6 and 7 show a series of IR-spectra of synthetic beryls with incorporated cesium and cobalt, registration of the spectra this time being done with a Zeiss UR-10 spectrophotometer.

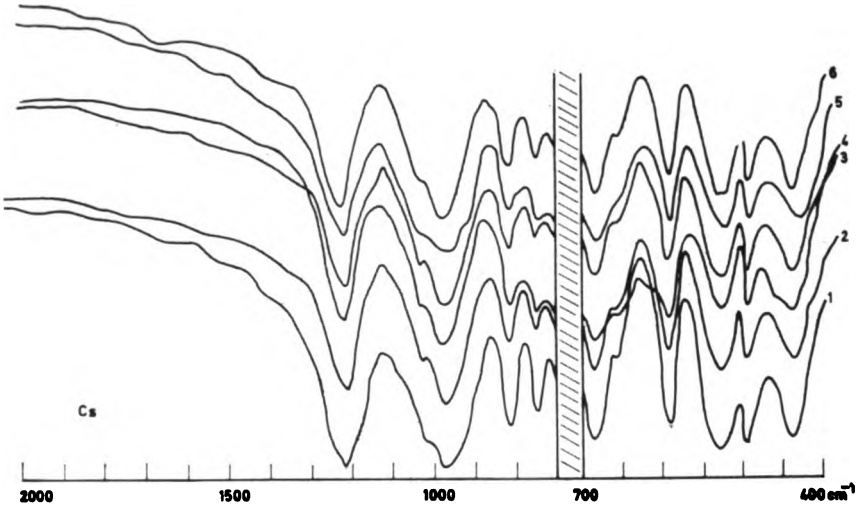

Figure 6
IR spectra of synthetic beryls with incorporated cesium

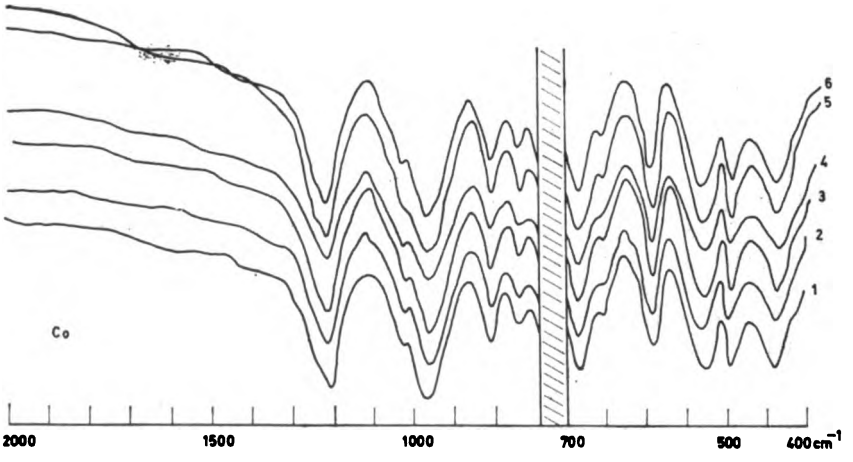

Figure 7
IR spectra of synthetic beryls with incorporated cobalt

Neither the presence of such large Cs^+ ions (which doubtlessly enter the "open" structural tunnels of this lattice), nor the incorporation of cobalt as a typical representative of metals of the transitional series (which certainly substitute homovalently *Al* in the beryl lattice), as seen in Figs. 6 and 7, caused sufficiently great disturbances of the structure to be noticed in the IR-spectra under the conditions of our study. One could notice only, as in the above described case of the influence of lithium, a marked disturbance in the relative intensities of the bands at 13.5 μ which nevertheless did not show a strict correlation with the content of incorporated cesium or cobalt.

The reflexion spectra of synthetic beryls in which metals from the transitional series (primarily *Fe*, *Co*, *Ni* and *Cr*) were present, incorporated as foreign additions, were however, sufficiently sensitive to exactly define their presence in the crystal lattice of beryl. Figure 8 shows two such reflexion spectra, recorded by means of a Unicam SP 500 spectrophotometer, for the case of incorporation of cobalt into the beryl lattice, which causes a pink coloration of the crystals. This characteristic coloration, which has been produced only in synthetic beryls (in natural beryls it has never been demonstrated with certainty), has been reproduced and studied recently also in hydrothermally synthesized beryls by a group of scientists in the Soviet Union (Emelianova, Grum-Grzhimailo and others) [12].

CONCLUSION

The described experimental results indicate that the beryl crystal lattice can be well characterized by its IR-spectra from 1 to 25 μ, as both the absorption bands and their relative intensities were sufficiently specific for differentiation from all the other related crystal structures (see Table 1). However, the problem of detecting and determining the main "inner im-

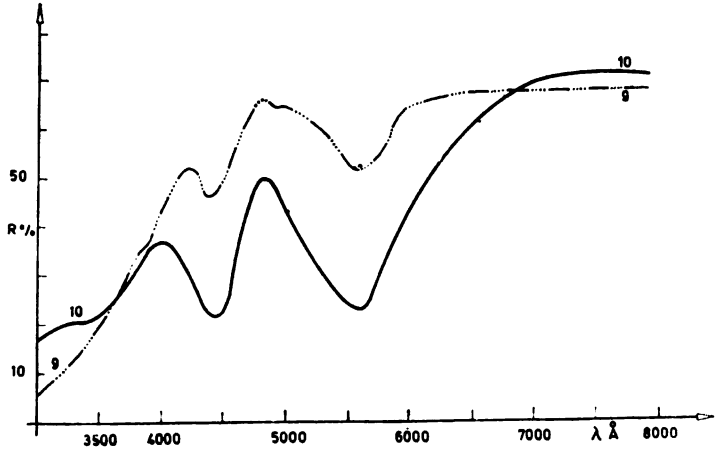

Figure 8

Reflexion spectra of a synthetic beryl with varying amounts of incorporated cobalt

purities" in the crystal lattices of natural beryls, that is, water, alkali and transitional metals, is not yet easy to solve only by using the usual *KBr*-technique and IR-spectrophotometers of smaller dispersion. The application of complementary methods — above all of spectrochemical character, but other as well — can greatly simplify and accelerate the solution of certain problems.

On a number of Yugoslav and foreign natural beryls, the presence of two kinds of water in the beryl lattice (Figs. 1 and 2) was once again confirmed thermogravimetrically, while by means of flame photometry the amount of lithium incorporated into the lattice of a number of samples of synthetic beryls was determined, which it was not possible to do reliably by means of IR-spectra.

Finally, the method of reflexion spectra was used for exact definition of the presence of transitional elements in the beryl lattice (see Fig. 8).

School of Science,
Institute of Physical Chemistry,
Belgrade
Institute of Chemistry, Technology
and Metallurgy, Belgrade

Received 10 March, 1967

REFERENCES

1. Ristić, S. *Physikalisch-Chemische Untersuchungen an Beryllen in Zusammenhang mit ihrem Heliumgehalt* — Mainz, (Thesis), 1956.
2. Frank-Kameneckĭ, V. *Priroda strukturnih primesei v mineralakh* (Nature of Structural Incorporations in Minerals) — Leningrad: Izdatel. Leningr. Univerziteta, 1964.
3. Ristić, S., A. Antić-Jovanović, and M. Jeremić. "Sadržaj alkalnih metala u nekim našim berilima uz opšti osvrt na spektrohemiju i geohemiju ovog berila" (Content of Alkaline Metals in Some Yugoslav Beryls with a Review of the Spectrochemistry and Geochemistry of This Beryl), in: *I Geohemijski Simpozijum, Beograd*, 1965, pp. 409—431.
4. Ginzburg, A. "K voprosu o khimicheskom sostave berilla" (The Problem of Chemical Composition of Beryl) — *Trudi Minerologicheskogo muzeia* 7: 56—69, 1955.
5. Baier, E. and J. Pense. "Die verschiedene Kanalsysteme des Berylls" — *Chemie der Erde* 22: 18—30, 1962.
6. Pliusnina, I. "Infrakrasnie spektry pogloshcheniia berillievykh mineralov" (Infrared Absorption Spectra of Beryl Minerals) — *Geokhimiia* 2: 158—173, 1963.
7. Bakakin, V. and N. Belov. "Kristallokhimiia berilla" (Crystallochemistry of Beryl) — *Geokhimiia* 5: 420—433, 1962.
8. Feklichev, V. "O khimicheskom sostave mineralov gruppy berilla, kharaktere izomorfizma i polozheniĭ v kristallicheskoĭ strukture glavneĭshykh primeseĭ" (Chemical Composition of the Beryl Group of Minerals, Isomorphic Character and Distribution of the Main Incorporations in the Crystalline Structure) — *Geokhimiia* 4: 391—401, 1963.
9. Pliusnina, I. "Infrakrasnie spektri pogloshcheniia berillov" (Infrared Absorption Spectra of Beryl) — *Geokhimiia* 1: 31—41, 1964.
10. Bokiĭ, G. and I. Pliusnina. "Infrakrasnie spektri pogloshcheniia ciklicheskykh silikatov v oblasti spektra dlini volny ot 7—21 *nm*" (Infrared Absorption Spectra of Cyclic Silicates in the Spectral Region of Wave-Lengths from 7—21) — *Nauchnie dokladi Vysshei shkoly geologichesko-geograficheskykh nauk* 3: 116, 1958.
11. Lazarev, A. "Kolebatel'nye spektri silikatov (IV)" (Oscillation Spectra of Silicates — IV) — *Optika i spektroskopiia* 12: 60—65, 1962.
12. Emelianova, E., S. Grum-Grzhimailo, O. Boksha and T. Varina. "Ob iskusstvenykh berillakh, soderzhashchykh V, Mn, Co i Ni" (On Synthetic Beryls, Containing V, Mn, Co and Ni) — *Kristallografiia* 10: 59—62, 1965.

GLASNIK HEMIJSKOG DRUŠTVA, Vol. 32, No. 5-6-7, 1967, pp. 285—293

OXIME HYDROLYSIS IN HYDROCHLORIC ACID SOLUTIONS

by

NATALIJA N. IKONOMOV

Oximes and amides in the presence of acids show similar behavior. The hydrolysis velocity constant increases with the concentration of acid to a maximum value, which depends on the nature of the oxime, or amide, as well as on the acid used. With further increase of the concentration of acid, the velocity constant falls rapidly. Edward and Meacock[1] have studied the hydrolysis of some benzamides in the presence of strong acids. The hydrolysis of amides in the presence of strong acids is, according to these authors, a bimolecular reaction between a molecule of water and a positive amide ion. The hydrolysis velocity constant, obtained experimentally, is given by the following formula: $k_{ex} = k_2 K c_{H_2O} + (K + h_0)$, where k_2 is the hydrolysis velocity constant, K the constant of equilibrium, and h_0 Hammett's[2] non-logarithmic function of acidity ($h_0 = -$ antilog H_0). With higher concentrations of acid there is a decrease of k_{ex} because in that range h_0 increases much more rapidly with the concentration of acid than does the concentration of H_3O^+ ion. However, it is a fact that k_{ex} decreases more rapidly than is given by the formula of Edward and Meacock. Rosenthal and Taylor[3] also considered that the slowest reaction in acid hydrolysis of amides is an interaction of a molecule of water and a positive amide ion, and obtained a final formula for the hydrolysis velocity constant of the following form: $k_{ex} = k_2 K \frac{c_{H_2O^+}}{1 + K h_0} B c_{acid}$, where B is the constant. On the basis of this formula it is difficult to explain the maximum of the hydrolysis velocity constant as the function of acid concentration. Vinnik and Zarahani[4] were the first to make a detailed study on the kinetics of hydrolysis of cyclohexanoneoximes in the presence of hydrochloric and sulfuric acid. Their theory starts from the fact that oxime solutions in the presence of acids contain, besides the non-ionized oxime molecule *RNOH* (R radical bound to the oxime group), also a positive $RNOH_2^+$ ion. In the case of hydrolysis in the presence of hydrochloric acid, a hypothesis about the existence of the ionic pair $RNOH_2^+Cl^-$ was introduced and proved. According to these authors, in the presence of hydrochloric acid the following equilibriums exist:

$$RNOH + H^+ \overset{K_B}{\rightleftarrows} RNOH_2^+ \underset{k}{\overset{\text{slow}}{\longrightarrow}} RNOH_2^+ + H_2O \xrightarrow{\text{fast}} ROH + NH_2OH \quad (1)$$

$$RNOH_2^+ + Cl^- \overset{K_C}{\rightleftarrows} RNOH_2^+ Cl^- \quad (2)$$

The slowest reaction is monomolecular. From a system of three equations it is possible to calculate the equilibrium constants K_B and K_C and the constant k:

$$k_{ex} = \frac{k}{1 + \frac{K_B}{h_o} + \frac{a_{HCl}}{K_C' h_o}}, \quad (3)$$

$$K_B K_C' = h_{o\,max}^2, \quad (4)$$

$$k_{ex\,max} = \frac{k}{1 + \frac{2\,h_{o\,max}}{K_C'}}, \quad (5)$$

where $K_C' = K_C \frac{f_{RNOH_2^+ Cl^-}}{f_{RNOH}}$, $k_{ex\,max}$ = the maximal value of the experimental velocity constant of hydrolysis, $h_{0\,max}$ = the value of h_0 in $k_{ex\,max}$. Vinnik and Zarahani have checked their equations in that range of concentrations of hydrochloric acid in which k_{ex} decreases.

On the basis of the study of hydrolysis of cyclohexanoneoxime, cyclopentanoneoxime and acetoxime in solutions of hydrochloric acid, a new procedure for the analysis of experimental results of the kinetics of oxime hydrolysis was given.

EXPERIMENTAL RESULTS

Synthesis of oximes was done in the usual way, by adding the corresponding ketone to an alkaline solution of hydroxylaminechloride.

The reaction of oxime hydrolysis in acid medium is a reversible process which, on the example of acetoxime, can be presented in a summed-up form in the following way:

$$CH_3{-}\underset{\underset{NOH}{\|}}{C}{-}CH_3 + H_2O \underset{k_2}{\overset{k_{ex}}{\rightleftarrows}} CH_3{-}\underset{\underset{O}{\|}}{C}{-}CH_3 + NH_2OH \quad (6)$$

The course of hydrolysis was followed spectrophotometrically at the wavelength of 2220 Å.

By using the equation $D = \varepsilon c_{RNOH}$, in which D is the absorbancy, c_{RNOH} the concentration of the corresponding oxime and ε the absorptivity, the following formula is obtained for the velocity constants:

$$k_{ex} = 2.3 \operatorname{tg} \alpha \frac{D_0 - D_\infty}{D_0 + D_\infty} \tag{7}$$

$$k_2 = 2.3 \operatorname{tg} \alpha \frac{D_\infty}{D^2 - D_\infty} \tag{8}$$

where D_0 is the absorbancy in time $t=0$, D is the absorbancy in time t, and $D\infty$ is the absorbancy at the end of the reaction. The expression $\operatorname{tg} \alpha$ which appears in the equation represents the slope of the line which is obtained if the values of $\log \frac{(D_0^2/D_\infty) - D}{D - D_\infty}$ as a function of time t are plotted on the ordinate.

The appearance of the maximum on the curves, which indicate a change of the experimental velocity constant of hydrolysis of oximes as a function of time, is shown on the example of acetoxime (Fig. 1). This maximum is, as already pointed out, typical of the hydrolysis of oximes.

The value of the maximal velocity constant, $k_{ex\ max}$, depends on the concentration of acid, temperature and nature of oxime (Table 1).

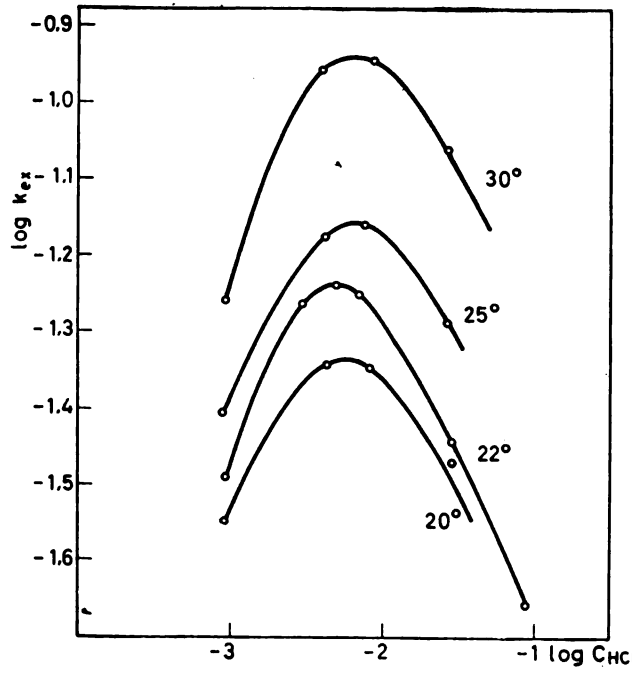

Figure 1

Hydrolysis of acetoxime. Dependence of log k_{ex} on log c_{HCl}

The part of the curve $k_{ex} = f(c_{HCl})$, which corresponds to higher concentrations of acid, is attributed to the dominant role of the poorly dissociated ionic pair $RNOH_2^+Cl^-$. If we assume that the concentration of the ionic pair increases with the concentration of acid, then we can hypo-

TABLE 1

Dependence of hydrolysis rate constants of cyclohexanone oxime, cyclopentanone oxime and acetoxime on the temperature and acid concentration

c_{HCl}	Temp. °C	Cyclohexanone Oxime		Acetoxime		Cyclopentanone Oxime	
		k_{ex} min^{-1}	k_2 $\frac{lit}{mol\ min}$	k_{ex} min^{-1}	k_2 $\frac{lit}{mol\ min}$	k_{ex} min^{-1}	k_2 $\frac{lit}{mol\ min}$
$5.\ 10^{-4}$	20.0	0.103				0.005	
$1.\ 10^{-3}$	16.0	0.105	433				
	20.0	0.156	578	0.028	89	0.009	
	22.0			0.033			
	25.0	0.202	654	0.040	128		
	24.0					0.011	26
	30.0			0.056		0.016	45
	35.0					0.024	48
$3.\ 10^{-3}$	20.0					0.014	
	22.0			0.054			
$5.\ 10^{-3}$	16.0	0.140	119				
	20.0	0.232	124	0.047	30	0.016	
	24.1					0.025	
	25.0	0.335	236	0.067	42		
	30.0			0.115	75		
$7.\ 10^{-3}$	20.0					0.016	
	22.0			0.058			
$9.\ 10^{-3}$	16.0	0.132					
	20.0	0.228	75	0.046		0.020	
	22.0			0.054			
	24.0					0.028	
	25.0	0.321	101	0.069			
	30.0			0.119			
$1.\ 10^{-2}$	22.0			0.050			
$3.\ 10^{-2}$	16.0	0.095					
	20.0	0.159		0.033		0.021	
	22.0			0.037			
	24.1					0.024	
	25.0	0.196		0.054			
	30.0			0.089			
$5.\ 10^{-2}$	22.0			0.033			
	20.0					0.014	
$6.\ 10^{-2}$	25.1	0.156					
$7.\ 10^{-2}$	20.0					0.011	
	22.0			0.026			
$9.\ 10^{-2}$	20.0					0.004	
	22.0			0.023			

thesize that the speed of reaction of oxime hydrolysis, in the range of concentrations 1×10^{-4} to 1×10^{-3} *M HCl*, is dependent only on the concentration of the positive ion $RNOH_2^+$, and the total concentration of oxime c_0 in time t is equal to: $c_0=c_{RNOH}+c_{RNOH_2^+}$. In aqueous solution in the presence of acid there exists the following equlibrium:

$$RNOH+H^+ \underset{}{\overset{K_B}{\rightleftharpoons}} RNOH_2^+. \tag{9}$$

The constant of equilibrium K_B is given by the following formula:

$$K_B=\frac{a_{RNOH}\,a_{H^+}}{a_{RNOH_2^+}} \tag{10}$$

where a is the activity. Hence the concentration of oxime molecules c_{RNOH} is given by the formula:

$$c_{RNOH}=\frac{K_B\cdot c_{RNOH_2^+}}{c_{H^+}}\,\frac{f_{RNOH_2^+}}{f_H+f_{RNOH}}. \tag{11}$$

If this expression is substituted in the formula for c_0 then:

$$c_0=c_{RNOH_2^+}\left[1+\frac{K_B}{c_{H^+}}\cdot\frac{f_{RNOH_2^+}}{f_H+f_{RNOH}}\right]=c_{RNOH_2^+}\left[1+\frac{K_B}{h_0}\right], \tag{12}$$

from which is obtained the expression for the concentration of the reactive ion $RNOH_2^+$

$$c_{RNOH_2^+}=\frac{c_o}{1+\frac{K_B}{h_0}} \tag{13}$$

Since

$$v=c_o\cdot k_{ex}=k\cdot c_{RNOH_2^+}, \tag{14}$$

the following formula is obtained for the velocity constant:

$$k_{ex}=\frac{k}{1+\frac{K_B}{h_0}} \tag{15}$$

The reciprocal value of formula 15 has the form:

$$\frac{1}{k_{ex}}=\frac{1}{k}+\frac{1}{h_0}\cdot\frac{K_B}{k} \tag{16}$$

If $\frac{1}{k_{ex}}$ is plotted on the ordinate and $\frac{1}{h_0}$ on the abscissa, then the section on the ordinate is equal to $\frac{1}{k}$ and $\operatorname{tg}\alpha=\frac{K_B}{k}$.

We have used equation 16 for the calculation of k and K_B on the assumption of the existence only of ion $RNOH_2^+$. The linear correlation of $\frac{1}{k_{ex}}$ and $\frac{1}{h_0}$, which stops at a concentration 5×10^{-3} *M HCl*, confirms our hypothesis of the existence of only this ionic type (Fig. 2) at low concentrations of acid.

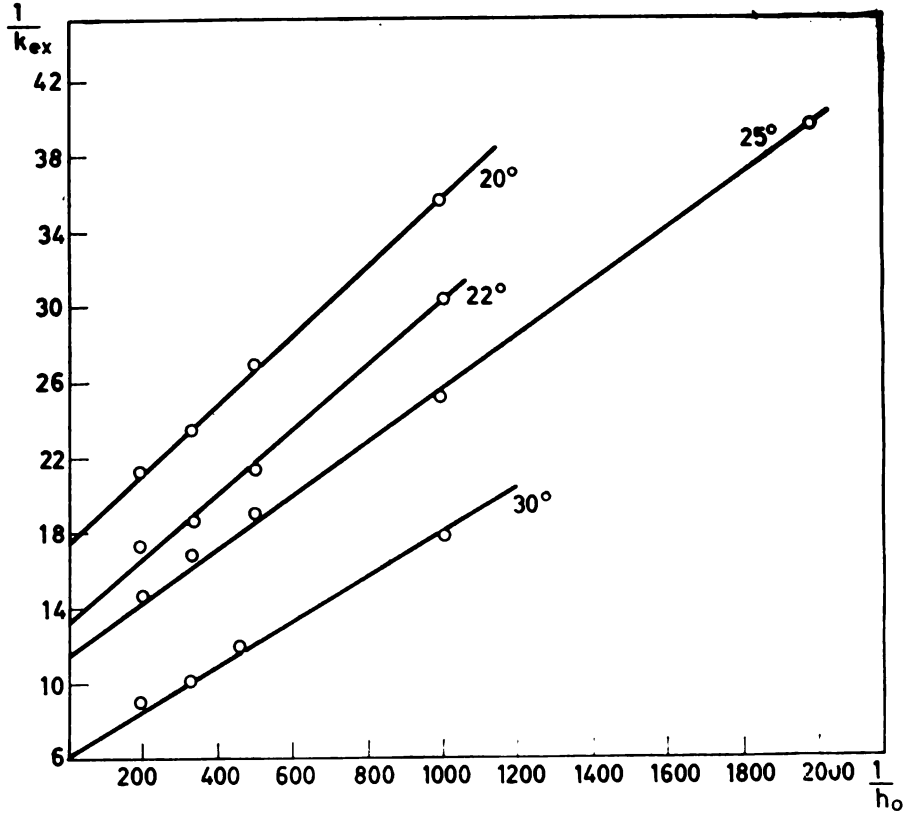

Figure 2

Application of equation 16 to acetoxime hydrolysis

From a comparison of the values for k and K_B obtained by means of our graphical method and by the method of Vinnik and Zarahani (Table 2), it may be seen that there is agreement between the two methods. On the basis of the work of Vinnik and co-workers[5], in the investigated range of concentrations of hydrochloric acid the ratio $h_0 = c_{acid}$ is valid.

TABLE 2

Values of hydrolysis constants calculated using the Vinnik-Zarahani equation and by means of our graphical method

Compound	temp. °C	Vinnik-Zarahani equation			Graphical method	
		k min^{-1}	$K_B\ 10^{-3}$	$K'_C\ 10^{-3}$	k min^{-1}	$K_B\ 10^{-3}$
Cyclohexanone Oxime	16.0	0.199	0.84	1.9	0.180	0.6$_3$
	20.0	0.344	1.1	2.2	0.322	1.2
	25.0	0.536	1.7	1.8	0.540	1.8
Acetoxime	20.0	0.073	1.5	2.2	0.062	1.1
	22.0	0.086	1.7	2.0	0.079	1.4
	25.0	0.117	1.8	1.9	0.106	1.6
	30.0	0.200	2.3	2.1	0.180	2.0
Cyclopentanone Oxime	20.0	0.030	2.3	3.5	0.031	2.8
	24.0	0.044	2.9	3.0	0.045	2.9

The graphical method is based on measurements at low concentrations of acid, far from the maximum of the curve $k_{ex}=f(c_{HCL})$, (Fig. 1), while the method of Vinnik and Zarahani requires a precise knowledge of the maximum of the curve, which is experimentally far more difficult to achieve.

DISCUSSION

The breaking of the double bond $>C=N-$ in oxime hydrolysis can occur because of a monomolecular or bimolecular reaction between a positive oxime ion and a water molecule. On the basis of this study it is possible to confirm the theory of Vinnik and Zarahani on the monomolecular nature of the reaction of oxime hydrolysis. The velocity constant of oxime hydrolysis in the investigated compounds decreases from cyclohexanoneoxime to acetoxime and cyclopentanoneoxime. If we compare the values of the equilibrium constant K_B of the reaction $RNOH+H^+ \overset{K_B}{\rightleftarrows} RNOH_2^+$, the order is the reverse. Therefore, it may be concluded that the concentration of $RNOH_2^+$ in the state of equilibrium is greater with cyclohexanoneoxime than with cyclopentanoneoxime.

By means of equations 3, 4, 5 and 16 it is possible to calculate the change of concentration of $RNOH_2^+Cl^-$ and $RNOH_2^+$ as the function of acid concentration. At low concentrations of acid there is only $RNOH_2^+$ ion, the concentration of which increases with the concentration of acid up to a certain maximum. At a concentration of 1 *M HCl*, almost the entire oxime is to be found in the form of the poorly reactive ionic pair $RNOH_2^+Cl^-$, because of which the speed of the reaction is very slow.

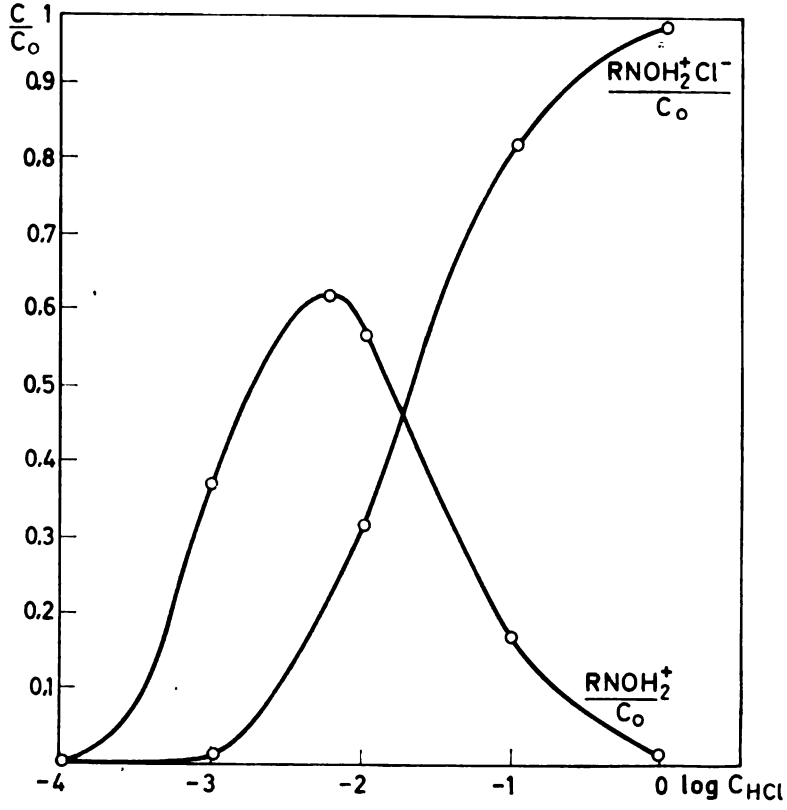

Figure 3

Relative concentrations of the positive oxime ion $RNOH_2^+$ and the ionic pair $RNOH_2^+Cl^-$ in dependence on *pH*

It may be seen from Table 2 that the equilibrium constant K_B shows a marked temperature dependency, which, within the limits of error, is not the case with K_C'. Because of this variability, depending on the temperature, of the ratio K_B/K_C', the position of the maximum on the curves $k_{ef}=f(c_{HCL})$ changes also (Fig. 1).

School of Science, Belgrade
Institute of Physical Chemistry

Received 10 February, 1967

REFERENCES

1. Edward, J. and S. Meacock. "Hydrolysis of Amides and Related Compounds. Part I. Some Benzamides in Strong Aqueous Acid" — *Journal of the Chemical Society* 2000—2007, 1957.
2. Hammett, L. and A. Deyrup. "A Series of Simple Basic Indicators. I. The Acidity Functions of Mixtures of Sulfuric and Perchloric Acids with Water" — *The Journal of the American Chemical Society* 54: 2721—2739, 1932.
3. Rosenthal, D. and T. Taylor. "A Study of the Mechanism and Kinetics of the Thioacetamide Hydrolysis Reaction" — *The Journal of the American Chemical Society* 79: 2684—2690, 1957.
4. Vinnik, M., N. Zarakhani, I. Medvedstaĭa and N. Chirkov. "O roli solobrazovaniĭa v kislotno-kataliticheskikh protsesakh. Kinetika gidroliza tsiklogeksanonoksima" (Role of solobrazovanie in Acid-Catalytic Processes. Kinetics of Cyclohexanonoxime Hydrolysis) — *Doklady Akademiĭ Nauk SSSR* 126: 1300—1303, 1959.
5. Vinnik, M. and N. Zarakhani. "Kinetika i mekhanizm reaktsiĭ v sredakh kontsentrirovanykh silnykh kislot. III. Kinetika gidroliza oksima tsiklogeksanona v sredakh solĭanoĭ i sernoĭ kislot" (Kinetics and Mechanism of Reaction in Medium with High Concentrations of Strong Acids. III. Kinetics of Cyclohexanonoxime Hydrolysis in the Presence of Hydrochloric and Sulfuric Acid) — *Zhurnal Fizicheskoĭ Khimiĭ* 34: 2671—2681, 1960.
6. Vinnik, M., R. Kruglov and N. Chirkov. "Funktsiĭ kislotnosti vodnykh rastvorov bromistovodorodnoĭ i solianoĭ kislot" (Acid Functions of Aqueous Solutions of Hydrobromic and Hydrochloric Acid) — *Zhurnal Fizicheskoĭ Khimiĭ* 30: 827—836, 1956.

GLASNIK HEMIJSKOG DRUŠTVA, Vol. 32, No. 5-6-7, 1967, pp. 295—301

EFFECT OF HEAVY WATER AS THE SOLVENT ON OXIME HYDROLYSIS IN THE PRESENCE OF HYDROCHLORIC ACID

by

NATALIJA N. IKONOMOV

It is known that the ratio of dissociation constants of ordinary and heavy water is $K_{H_2O}/K_{D_2O}=6.5$[1]. Because of this difference of the dissociation constants, there is a difference in the behavior of intermediary products, conjugated acids and bases, in both these solvents. Rule and La Mer[2] have found that the dissociation constant of weak acids is greater in ordinary water than in heavy water and that the isotopic effect shows an inversely proportional increase as the acid becomes weaker.

The numerical value of the *D*-isotopic effect of the solvent depends on the mechanism of chemical reaction[3]. In reactions in which the catalyst is an acid, of great importance is the determination of time and mode of proton transfer, that is, whether the proton is transferred reversibly, at the formation or breaking of the bond, as is the case in specific hydrogen catalysis:

$$H_3O^+ + X \rightleftarrows HX^+ + H_2O \qquad \text{(fast)}$$

$$HX^+ \xrightarrow{k} \text{products} \qquad \text{(slow)} \quad (1)$$

or whether the proton transfer from the acid to the reactant takes place in the slowest phase of the chemical reaction, as is the case in general acid catalysis:

$$H_3O^+ + X \xrightarrow{k} \text{products} \qquad \text{(slow)} \quad (2)$$

or

$$HA + X \xrightarrow{k} \text{products} \qquad \text{(slow)} \quad (3)$$

The speed of reaction v in specific catalysis is proportional to the concentration of conjugated acid $v=k[HX^+]$, and as the concentration of conjugated acid in heavy water is greater than in ordinary water, the speed of reaction is greater in heavy water. In cases 2 and 3, the speed of reaction is proportional to the concentration of acid $v=k[H^3O^+][X]$. As the proton transfer is slower in heavy water than in ordinary water, here $k_{H_2O}/k_{D_2O} > 1$.

Reitz[4] measured the speed of acetamide hydrolysis in ordinary and heavy water and found that, at low acid concentrations, the reaction was faster in heavy than in ordinary water, while in solution of amides and concentrated acids, the reaction was faster in ordinary water. This is a unique example in the literature in which the numerical value for the ratio of the reaction speed constants in ordinary and heavy water, k_{H_2O}/k_{D_2O}, changes its sign depending on the concentration of acid.

Our study of the reaction kinetics in heavy water is aimed at further clarifying the mechanism of acid oxime hydrolysis.

EXPERIMENTAL RESULTS

The course of hydrolysis was studied in the same way as in the previous study on cyclohexanonoxime, cyclopentanonoxime and acetoxime[6].

DCl was obtained by dissolving concentrated hydrochloric acid in heavy water with 99.6% *D*.

Oxime hydrolysis was studied spectrophotometrically at a wavelength of 2220 *Å*.

In the previous study[6] the methods for the calculation of the kinetic values were described: experimental speed constant k_{ex}, direction of the speed constant k, equilibrium constant K_B, which during oxime hydro-

TABLE 1

Dependence of hydrolysis rate constants of cyclohexanone oxime, cyclopentanone oxime and acetoxime on temperature and acid concentrations

c_{DCl}	Temp. °C	Cyclohexanone Oxime		Acetoxime		Cyclopentanone Oxime	
		k_{ex}	k_2	k_{ex}	k_2	k_{ex}	k_2
$5 \cdot 10^{-4}$	20.0	0.152					
$1 \cdot 10^{-3}$	16.0	0.162	178				
	20.0	0.222	273	0.046	48		
	22.0			0.048		0 018	
	23.9					0.019	16
	25.0	0.278		0.067	69		
	30.0			0.094	89	0.027	43
$5 \cdot 10^{-3}$	16.0	0.180	36				
	20.0	0.284		0.066			
	22.0					0.029	
	24.1					0.034	
	25.0	0.408		0.107			
	30.0			0.158			
$9 \cdot 10^{-3}$	20.0	0.230					
	30.0			0.144			
$3 \cdot 10^{-2}$	20.1	0.112		0.034			
	25.1	0.160		0.058			
	30.0			0.078			
$6 \cdot 10^{-2}$	25.1	0.103					

k_{ex}, min^{-1}; k_2, *lit.* $mol^{-1}min^{-1}$

lysis in D_2O refers to the reaction $RNOD+D^+ \rightleftarrows RNOD_2^+$, and equilibrium constant K_C', which with the equlibrium constant K_C in the case of reaction $RNOD_2^+ + Cl^- \rightleftarrows RNOD_2^+\ Cl^-$ is in the correlation $K_C' = \frac{f_{RNOD_2^+ Cl^-}}{f_{RNOD}} K_C$, where f is the coefficient of activity.

Experimental values for the reaction speed constants given in condensed form by the equilibrium $RNOD+D_2O \underset{k_2}{\overset{k_{ex}}{\rightleftarrows}} RCO+NH_2OD$, where *RNOD* denotes an oxime molecule and *RCO* a molecule of ketone, showed a maximum at a certain concentration of acid (Table 1).

If the experimental values for k_{ex} in H_2O and D_2O are shown as a function of acid concentration (Fig. 1), a shift of the maximum for the reaction in ordinary water is noted.

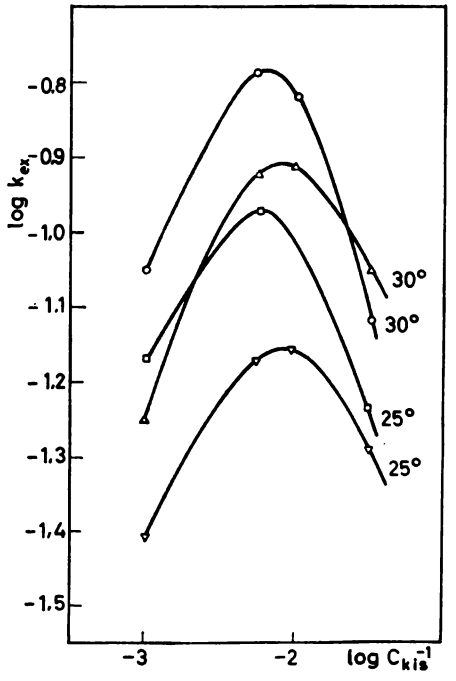

Figure 1

Dependence of hydrolysis rate constant k_{ex} of acetoxime on acid concentration at 25° and 30°C. ○ denotes the reaction in H_2O and Δ the reaction in D_2O

Because of non-conformity of the curves (Fig. 1), the ratio of experimental speed constants in ordinary and heavy water changes with the concentration of acid (Table 2).

Högfeldt and Bigeleisen[7] found that in aqueous *DCl* solutions the following relationship is valid: $H_0=D_0=-\log c_{acid}$ for concentrations from 1×10^{-4} to 1 *M HCl*. As our measurements were in the range of acid concentrations from 5×10^{-4} to 9×10^{-2} *M DCl*, the ratio was

$$h_0=d_0=c_{acid} \qquad (4)$$

TABLE 2

Ratio of hydrolysis rate constants k_{ex} of oximes in H_2O and D_2O at different hydrochloric acid concentrations

c_{DCl}	Temp. °C	Cyclohexanone Oxime k_{exD_2O}/k_{exH_2O}	Acetoxime k_{exD_2O}/k_{exH_2O}	Cyclopentanone Oxime k_{exD_2O}/k_{exH_2O}
$5 \cdot 10^{-4}$	20.0	1.48		
$1 \cdot 10^{-3}$	16.0	1.54		
	20.0	1.42	1.64	
	24.0			1.70
	25.0	1.38	1.67	
	30.0		1.67	1.66
$5 \cdot 10^{-3}$	16.0	1.29		
	20.0	1.21	1.40	
	24.1			1.33
	25.0	1.21	1.39	
	30.0		1.37	
$9 \cdot 10^{-3}$	20.0	1.01		
	30.0		1.28	
$3 \cdot 10^{-2}$	20.1	0.70	1.04	
	25.0	0.81	1.08	
	30.0		0.87	
$6 \cdot 10^{-2}$	25.1	0.66		

TABLE 3

Hydrolysis constants for the reaction in D_2O calculated by the Vinnik-Zarakhani equation and by our graphical method[6]

Compound	t°C	Vinnik-Zarakhani equation				Graphical method	
		k, min^{-1}	$K_C 10^{-2}$	$K_B 10^{-3}$	$c_{omax} 10^{-3}$	k, min^{-1}	$K_B 10^{-3}$
Cyclohexanone Oxime	16.0	0.294	0.88	0.7	2.5	0.264	0.5_3
	20.0	0.474	0.98	1.0	3.2	0.465	1.0
	25.0	0.802	0.80	1.5	3.6	0.800	1.6
Acetoxime	20.0	0.107	1.2	1.2	4.0	0.091	1.0
	25.0	0.176	1.4	1.5	4.7	0.164	1.4
	30.0	0.282	1.25	1.9	4.9	0.264	1.8_4
Cyclopentanone Oxime	22.0					0.043	1.5
	24.0					0.062	2.5

In calculating k, K_B and K_C' we used the study of Halpern[8] and Rule and La Mer[2] who found that there was not much difference between the coefficients of activity of *HCl* and *DCl* ions.

The values for k, K_B and K_C' were obtained by means of the Vinnik-Zarakhani equations. The constants k and K_B were calculated also by our graphical method[6]. The values of the constants are shown in Table 3.

The value for $c_{0\,max}$ corresponded to the numerical value of *DCl* concentration at the maximal value of the speed constant.

We were unable to calculate the constants of hydrolysis for cyclopentanonoxime by means of the Vinnik-Zarakhani equations as the available data were inadequate for this method, and therefore Table 3 contains only the values obtained by means of the graphical method.

On the basis of the data in Table 3 and data obtained in a previous study[6], the ratio of the reaction speed constants in D_2O and H_2O acquires a constant value (Table 4).

TABLE 4

Ratio of the rate constants and equilibrium constants of oxime hydrolysis in D_2O and H_2O

Compound	t°C	Equation Vinnik-Zarakhani		Graphical method	
		k_{D_2O}/k_{H_2O}	K_{BD_2O}/K_{BH_2O}	k_{D_2O}/k_{H_2O}	K_{BD_2O}/K_{BH_2O}
Cyclohexanone Oxime	16	1.4_7	0.8_3	1.4_6	0.8_4
	20	1.4_1	0.9_0	1.4_4	0.8_2
	25	1.4_9	0.8_8	1.4_8	0.8_8
Acetoxime	20	1.4_7	0.8_0	1.4_9	0.9_0
	25	1.5_0	0.8_3	1.5_4	0.8_7
	30	1.4_1	0.8_2	1.4_6	0.9_2
Cyclopentanone Oxime	24			1.4_0	0.8_6

DISCUSSION

The ratio $k_{ex}D_2O/k_{ex}H_2O$ which changed depending on the concentration of acid did not indicate the mechanism of reaction. The shift of the curves (Fig. 1), which indicates the dependence of the experimental values for the constants of the speed of hydrolysis on the concentration of acid, is due to the difference in the values of K_B and K_C' in heavy and ordinary water. The relationship of equilibrium constants $K_{BD_2O} = \frac{a_{RNOD}\, a_{D^+}}{a_{RNOD_2^+}}$ and $K_{BH_2O} = \frac{a_{RNOH}\, a_{H^+}}{a_{RNOH_2^+}}$ shows that in comparison with ordinary water the equilibrium of hydrolysis in heavy water was more shifted towards the formation of $RNOD_2^+$ ions (Table 4).

The mere fact that the speed of hydrolysis in heavy water was greater than in ordinary water shows that conjugated acid was the carrier of the reaction, here $RNOH_2^+$ and $RNOD_2^+$, and that the speed of the reaction depended on its concentration. This would at the same time indicate that during oxime hydrolysis the transfer of protons takes place in a rapid and intermediary equilibrated reaction which precedes the slowest phase of the reaction. This would be in accordance with the mechanism of reaction described in the previous study[6].

Bearing in mind the expression for K_C', which is $K_C' = \frac{a_{RNOH_2^+} a_{Cl^-}}{a_{RNOH_2^+} c_{l^-}}$ and that the factor relating K_C and K_C' in the case of the reaction in H_2O and D_2O can be taken as a constant, then the fact that the ratio $K'_{CH_2O}/K'_{CD_2O} > 1$ indicates the existence of a higher concentration of $RNOD_2^+Cl^-$. Because of this there is a more rapid decrease of the concentration of $RNOD_2^+$ at higher concentrations of the acid, which is also associated with a more rapid change of the experimental constant of the speed of hydrolysis in heavy water.

School of Science, Belgrade
Institute of Physical Chemistry

Received 10 February, 1967

REFERENCES

1. Kingerley, R. and V. La Mer. "Exchange and Transfer Equilibria of Acids, Bases and Salts in Deuterium-Protium Oxide Mixtures. The Ion Product Constant of Deuterium Oxide" — *The Journal of the American Chemical Society* 63: 3256—3263, 1941.
2. Rule, C. and V. La Mer. "Dissociation Constants of Deutero Acids by E.m.f. Measurements" — *The Journal of the American Chemical Society* 60: 1974—1981, 1938.
3. Bunton, C. and V. Shiner. "Isotope Effects in Deuterium Oxide Solution. Part II. Reaction Rates in Acid, Alkaline and Neutral Solution, Involving only Secondary Solvent Effects" — *The Journal of the American Chemical Society* 83: 3207—3214, 1961.
4. Reitz, O. "Zur Säure- und Basenkatalyse in leichtem und schwerem Wasser. II. Hydrolyse und Deuteriumaustausch von Acetamid und Acetonitril" — *Zeitschrift für Physicalische Chemie* 183: 371—391, 1939.
5. Reitz, O. "Säure und alkalische Hydrolyse von Acetamid und Acetonitril in schwerem Wasser" — *Zeitschrift für Elektrochemie und Angewandte Physikalische Chemie* 44: 693—695, 1938.
6. Ikonomov, N. "Ispitivanje hidrolize oksima u rastvorima hlorovodonične kiseline" (Oxime Hydrolysis in Hydrochloric Acid Solutions) — *Glasnik Hemijskog društva* (Beograd) 32, (5—6—7), 1967.
7. Högfeldt, E. and J. Bigeleisen. "Acidity Constants of Some Hammett Indicators in Heavy Water. The Hammett Acidity Function, D_0, for DCl and D_2SO_4 Solutions" — *The Journal of the American Chemical Society* 82: 15—20, 1960.
8. Halpern, O. "On the Dissociation Constants of Acids in Light and Heavy Water" — *The Journal of Chemical Physics* 3: 456—457, 1935.

GLASNIK HEMIJSKOG DRUŠTVA, Vol. 32, No. 5-6-7, 1967, pp. 303–307

PHOTOCHEMICAL REACTIONS. II.

ADDITION OF THIOACETIC ACID TO BISURETHANES AND BISAMIDES OF UNSATURATED AROMATIC ALDEHYDES

by

KSENIJA SIROTANOVIĆ and ZORICA NIKIĆ

According to the literature[1], thioacetic acid is readily added to cimthaldehyde in the presence of benzoilperoxide or ascaridole, forming β-acetylthiohydrocimthaldehyde in an almost quantitative yield:

$$C_6H_5\cdot CH=CH\cdot \overset{H}{C}=O+HS\cdot COCH_3\rightarrow C_6H_5\cdot \underset{S\cdot COCH_3}{CH}-\!\!-CH_2\cdot \overset{H}{C}=O \qquad \text{(I)}$$

We were interested in the behavior of the double bond in unsaturated aromatic aldehydes under the influence of thioacetic acid if the aldehyde group is blocked by the formation of di-derivates. Therefore one of us, in a previous study[2], attempted the addition of thioacetic acid to bisurethane and bisamide of cimthaldehyde by using benzoilperoxide as the catalyst. However, there was no addition and the initial products were isolated.

Yet, when we stared from unsaturated aldehyde itself, thioacetic acid and urethane or acetamide[2, 3], in the presence of hydrochloric acid we succeeded in obtaining a considerable number of bisurethanes and bisamides of β-acetylthioaldehyde in good yields:

$$Ar-CH=CH\cdot \overset{H}{C}=O+HS\cdot COCH_3+2\,NH_2\cdot CO\cdot R\rightarrow Ar-\underset{S\cdot COCH_3}{CH}-\!\!-CH_2\cdot CH\begin{matrix}\diagup NH\cdot CO\cdot R\\ \diagdown NH\cdot CO\cdot R\end{matrix} \qquad \text{(II)}$$

(where Ar is the aromatic residue, and $R=CH_3$— or —OC_2H_5)

In the present study, both reactions were carried out with ultraviolet irradiation, on the basis of positive results obtained in a similar study with thiophenole[4].

Bisurethanes and bisamides of the following unsaturated aromatic aldehydes were used:

1) cimthaldehyde
2) *o*-chlorcimthaldehyde
3) *m*-chlorcimthaldehyde
4) *p*-chlorcimthaldehyde
5) *o*-nitrocimthaldehyde
6) *m*-nitrocimthaldehyde
7) *p*-nitrocimthaldehyde

The reaction was done so that the mixture of bisurethanes (or bisamides) and thioacetic acid in dioxane, in the presence of benzoilperoxide or bortrifluoride, was irradiated by means of a mercury low-pressure lamp (Hanau NK 6/20). Irradiation was done either from the side, using quartz containers, or by introducing the lamp into an ordinary glass container. These mixtures were subjected to irradiation for from 10 minutes to 3 hours, the time necessary for the reaction having been determined at the same time.

In this way the addition of thioacetic acid to bisurethanes of cimthaldehyde, *o*-nitrocimthaldehyde and *m*-nitrocimthaldehyde was successful. The other bisurethanes disintegrated, while bisamides remained unchanged.

When starting from unsaturated aromatic aldehydes (cimthaldehyde, *o*-, *m*- and *p*-chlorcimthaldehyde, *o*- and *p*-nitrocimthaldehyde) thioacetic acid and urethane, in the presence of the same solvent and catalyst and using the mercury lamp for irradiation of the mixture, we obtained the bisurethanes of β-acetylthiohydrocimthaldehyde, *o*-chlorhydrocimthaldehyde and *p*-chlorhydrocimthaldehyde. The other aldehydes gave bisurethanes of the unsaturated aldehydes themselves, while there was no addition of thioacetic acid. The number of obtained products as well as the yields were better if the reaction was done without irradiation[3].

When using acetamide instead of urethane, only bisamides of unsaturated aldehydes were obtained. None of the used aldehydes gave an addition product.

The analyses of the obtained bisurethanes of β-acetylthioaldehyde corresponded to the calculated values, and the mixed melting points with these compounds synthesized during earlier studies[2, 3] did not show depression.

All the obtained bisurethanes of β-acetylthioaldehyde were hydrolyzed in the presence of 2,4-dinitrophenylhydrazine, during which reaction the corresponding 2,4-dinitrophenylhydrazones of β-acetylthioaldehyde were obtained, except in the case of the bisurethane of β-acetylthio-*p*-chlorhydrocimthaldehyde, from which 2,4-dinitrophenylhydrazone of *p*-chlorcimthaldehyde itself was obtained.

EXPERIMENTAL

I. **Bisurethanes of β-acetylthioaldehyde**

A. *Obtained from bisurethanes of unsaturated aromatic aldehydes and thioacetic acid.*

1/400 mols of bisurethane, 1/400 mols of thioacetic acid, 5 *ml* of dioxane and a drop of bortrifluoride-etherate (or several *mg* of benzoilperoxide)

TABLE 1

Bisurethanes of β-acetylthioaldehydes

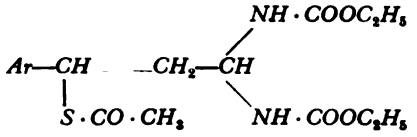

Obtained by method *A*			Obtained by method *B*		
Ar =	Yield	M. p.	*Ar* =	Yield	M. p.
C_6H_5-	43%	148°	C_6H_5-	30%	148°
o-NO_2-C_6H_4-	25%	169°	*o*-Cl-C_6H_4-	21%	142°
m-NO_2-C_6H_4-	27%	174°	*m*-Cl-C_6H_4-	17%	174°

2,4—Dinitrophenylhydrazones of β-acetylthioaldehydes

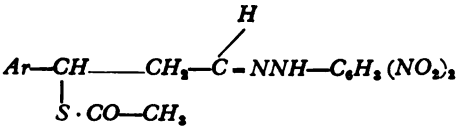

Ar =	M. p.	Formula	Calculated *N*%	Found *N*%
C_6H_5-*	145°	$C_{17}H_{16}O_5N_4S$	14.43	14.17
o-Cl-C_6H_4-	120°	$C_{71}H_{15}O_5N_4SCl$	13.25	13.64
m-Cl-C_6H_4-	136°	$C_{17}H_{15}O_5N_4SCl$	13.25	13.48
o-NO_2-C_6H_4-	134.5°	$C_{17}H_{15}O_7N_5S$	16.17	16.45
m-NO_2-C_6H_4-	126°	$C_{17}H_{15}O_7N_5S$	16.17	16.04
p-NO_2-C_6H_4-	141°	$C_{17}H_{15}O_7N_5S$	16.17	16.13

* This compound was earlier obtained from β-acetylthiohydrocimthaldehyde[1].

was irradiated by means of a low-pressure mercury lamp (Hanau NK 6/20) from 10 minutes to 3 hours.

B. *Obtained from unsaturated aldehyde, thioacetic acid and urethane.*

1/200 mols of aldehyde, 1/200 mols of thioacetic acid, $2 \times 1/200$ mols of urethane, 5 *ml* of dioxane and a drop of bortrifluoride-etherate (or benzoilperoxide) was irradiated from 10 minutes to 3 hours.

II. **2, 4-Dinitrophenylhydrazones of β-acetilthioaldehyde**

These were obtained by hydrolysis of β-acetylthioaldehyde in the presence of 2,4-dinitrophenylhydrazine.

The yields, melting points and results of analysis of the obtained products are shown in the table.

The microanalysis in this study were done by Radmila Dimitrijević, assistant at the Institute of Chemistry of the School of Science, to whom we express our gratitude.

School of Science,
Institute of Chemistry,
Belgrade
Institute of Chemistry, Technology
and Metallurgy, Belgrade.

Received 17 April, 1967

REFERENCES

1. Brown, R., W. Jones and A. Pinder. "The Addition of Thioacetic Acid to Unsaturated Compounds" — *Journal of the Chemical Society* (London) 2123—2125, 1951.
2. Sirotanović, K. and M. Bajlon. "Adicija tiosirćetne kiseline na nezasićene aldehide" (Addition of Thioacetic Acid to Unsaturated Aldehydes) — *Glasnik Hemijskog društva* (Beograd) 23—24: 157—161, 1958—1959.
3. Sirotanović, K. and M. Bajlon-Pastor. "Adicija tiosirćetne kiseline na nezasićene aldehide. II. Bisamidi i bisuretani β-acetiltioaldehida" (Addition of Thioacetic Acid to Unsaturated Aldehydes. II. Bisamides and Bisurethanes of β-acetylthioaldehyde) — *Glasnik Hemijskog društva* (Beograd) 31, 1966.
4. Sirotanović, K. and Z. Nikić. "Photochemical Reactions — I. Addition of Thiophenol to Bisamides and Bisurethanes of Unsaturated Aromatic and Heterocyclic Aldehydes" — *Tetrahedron* 22: 1561—1564, 1966.

GLASNIK HEMIJSKOG DRUŠTVA, Vol. 32, No. 5-6-7, 1967, pp. 309—314

SULFONATION OF HIGHER ALKYLBENZENES. I.
SULFONATION OF TECHNICAL DODECYLBENZENE*

by

JOVAN S. MIĆIĆ, ZOLTAN L. ROMODA, NEVENKA M. VUČKOVIĆ
and ĐORĐE M. DIMITRIJEVIĆ

The reaction of sulfonation of technical dodecylbenzene, which is obtained by alkylation of benzene with the tetramere of propylene and represents a fraction of the obtained alkylate with an average length of the alkyle row of 12 C-atoms, has been amply studied[1]. Nevertheless, considering that sulfonates of technical dodecylbenzene, by the size of their production, today represent the most important materials with surface activity, we concluded that it would be of interest to study this reaction in more detail, particularly as regards the influence of certain factors on which there is not adequate information in the literature.

Our aim was to study in more detail the influence of temperature, concentration of sulfuric acid, the weight ratio of acid and hydrocarbon and the duration of the reaction on sulfonation of different alkylate fractions.

Of similar studies, we shall mention the investigations by J. E. Kircher and co-workers[2], who studied the influence of temperature on the degree of alkylate conversion at the end of the reaction of sulfonation of technical dodecylbenzene 100 with 5% sulfuric acid for 1 hour within the temperature interval 40—60° and at a weight ratio of acid/hydrocarbon of 1.5. The same authors have also studied the influence of the duration of the terminal phase of the reaction at 40°C on the degree of alkylate conversion within the interval 0—3 hours after sulfonation with oleum (104, 5% sulfuric acid) at an acid/hydrocarbon weight ratio of 1.25.

A. Metzger and co-workers[3] have determined the degree of alkylate conversion in sulfonation of samples of technical dodecylbenzene of different origin with the monohydrate of sulfuric acid at 55°C and at an acid/hydrocarbon weight ratio of 1.5 and a duration of 3 hours, as well as with 20% oleum at 25° and 50°C at a ratio of oleum/hydrocarbon of 1.1 and a duration of 3 1/4 hours.

In the present study, our investigations of the effect of temperature, concentration of sulfuric acid and acid/hydrocarbon weight ratio on the yield of dodecylbenzene-sulfonic acid involved the temperature interval 30—70°C, the interval of sulfuric acid concentration 93—99.5%, as well as 23% oleum and an acid/hydrocarbon weight ratio interval from 1 : 1 to 2.5 : 1.

* Reported at the IXth Symposium of Chemists of Serbia, Belgrade, January 1961.

EXPERIMENTAL METHOD

All the experiments were done with technical dodecylbenzene which had the following characteristics: distillation interval (Engler) 280—296°, specific gravity (15°) 0.871, bromin number (ASTM) 1.4. The sulfuric acid was of p.a. quality and the concentration was determined by using the standard method with 0.1 *N NaOH*.

Sulfonation was done in a glass laboratory apparatus with 100 *g* of dodecylbenzene to which during 1 hour a certain quantity of acid was added before continuing the mixing in order to terminate the reaction. The desired temperature was maintained within the limits of $\pm 2°$.

Determination of the sulfonate content in the reaction mixture was done by the standard method with *p*-toluidinechlorhydrate.

RESULTS

93.4% *sulfuric acid*

Sulfonation was done under the following conditions:

— temperature 50°, 60° and 70°

— weight ratios: acid/hydrocarbon 2.0, 2.25 and 2.50; and total SO_3/hydrocarbon 1.53, 1.80 and 1.93.

— duration of the terminal phase of the reaction was 7 hours.

The results showed that it is necessary to use acid in great excess of hydrocarbon (2.5 : 1), a high temperature and a long duration of the terminal phase of the reaction in order to obtain a satisfactory yield. The increase

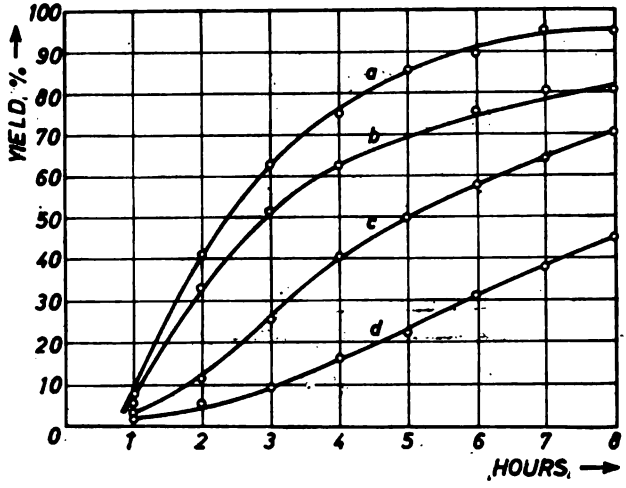

Figure 1

Sulfonation of dodecylbenzene with 93.4% sulfuric acid

a. 70°C, total SO_3/hydrocarbon 1.93

b. 70°C, total SO_3/hydrocarbon 1.53

c. 60°C, total SO_3/hydrocarbon 1.93

d. 50°C, total SO_3/hydrocarbon 1.93

of the amount of acid did not significantly affect the yield, while with an increase of temperature of 10°C the yield was increased by about 25%.

Typical curves representing the course of sulfonation are shown in Fig. 1.

95.4% *and* 97.1% *sulfuric acid*

Sulfonation with 95.4% acid was done under the same conditions as in the previous case, except that, because of the increased concentration of acid, the weight ratio of total SO_3/hydrocarbon was 1.56, 1.76 and 1.95.

Sulfonation with 97.1% acid was done only at the acid/hydrocarbon ratio of 2.0 and total SO_3/hydrocarbon ratio of 1.58 at temperatures of 50°C and 60°C.

The results showed that the course of sulfonation with these acids was similar. Satisfactory yields were also obtained by using acid in great excess and at higher temperatures with a corresponding duration of the reaction. Thus, at a temperature of 50°C a satisfactory yield could be obtained with an acid/hydrocarbon ratio of 2.5, while this was possible at 60° and 70°C with the ratio of 2.25. Increase of the acid/hydrocarbon ratio was associated with an increase in yield, while increased temperature also caused an increase in yield and affected particularly the speed of the reaction.

A comparison of the results for these two acids showed that the course of the curves changed with regularity following a change of the ratio of total SO_3/hydrocarbon regardless of the concentration of the agent used for sulfonation (Fig. 2).

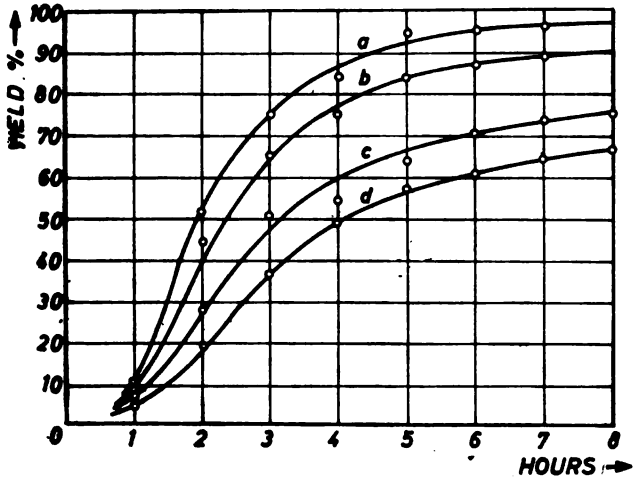

Figure 2

Sulfonation of dodecylbenzene with sulfuric acid at 50°C

a. 95.4% sulfuric acid; total SO_3/hydrocarbon 1.95
b. 95.4% sulfuric acid; total SO_3/hydrocarbon 1.76
c. 97.1% sulfuric acid; total SO_3/hydrocarbon 1.58
d. 95.4% sulfuric acid; total SO_3/hydrocarbon 1.56

99.5% sulfuric acid

Sulfonation was done under the following conditions:

— temperature 40°, 50° and 60°

— acid/hydrocarbon weight ratios 1.0, 1.25, 1.50, 1.75 and 2.0 and total SO_3/hydrocarbon 0.81, 1.01, 1.22, 1.42 and 1.62.

— duration of the terminal phase of the reaction was 3 hours.

The results showed that unsatisfactory yields were obtained only with the acid/hydrocarbon ratio of 1.0. Increase of this ratio to 1.50 was associated with satisfactory results at all temperatures above 40°C. Further increase of the amount of acid and of temperature had relatively little effect on the yield and speed of the reaction.

23% oleum

Sulfonation with 23% oleum was done under the following conditions:

— temperature 20°, 30° and 40°C

— weight ratios: oleum/hydrocarbon 1.0, 1.25 and 1.50; total SO_3/hydrocarbon 0.86, 1.07 and 1.29.

— duration of the terminal phase of the reaction was 3 hours.

The results showed that an unsatisfactory yield was obtained only with the acid/hydrocarbon ratio of 1.0. An increase of this ratio to 1.25

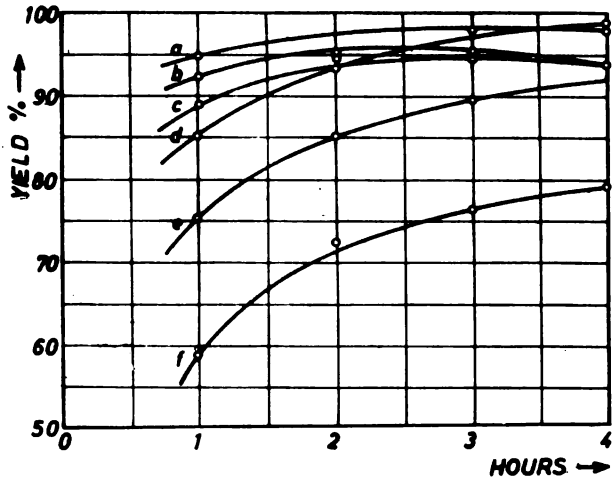

Figure 3

Sulfonation of dodecylbenzene with 99% sulfuric acid and 23% oleum at 40°C

a. acid, total SO_3/hydrocarbon 1.62

b. oleum, total SO_3/hydrocarbon 1.29

c. oleum, total SO_3/hydrocarbon 1.07

d. acid, total SO_3/hydrocarbon 1.22

e. oleum, total SO_3/hydrocarbon 0.86

f. acid, total SO_3/hydrocarbon 0.81

rapidly led to satisfactory yields, while further heating produced a slight decrease of the yield.

A comparison of the results of sulfonation with 99.5% acid and with oleum showed that the course of the curves was also similar and that in the majority of cases it changed with regularity with the ratio of total SO_3/hydrocarbon regardless of concentration, as shown in Fig. 3. However, with further duration of the reaction there was divergence from this regularity.

CONCLUSIONS

The following observations were made for the intervals of working conditions used in this study:

Satisfactory yields of dodecylbenzene-sulfonic acid can be obtained by sulfonation of dodecylbenzene with concentrations of sulfuric acid above 95% with a corresponding excess of acid in relation to hydrocarbon, and the corresponding temperature and duration of the reaction. In certain intervals the course of the reaction did not depend on the concentration of acid, but depended only on the ratio of active agent to hydrocarbon.

Temperature increases had a relatively great effect on the yield when low concentrations of the acids were used, while with concentrations above 99% this effect was relatively small. When higher concentrations of acids were used the speed of the reaction was much greater, and under other corresponding conditions (ratio of acid/hydrocarbon and temperature) a maximum was quickly reached so that further duration of the reaction did not significantly affect the yield.

Institute of Organic Chemistry,
School of Technology, Belgrade

Received 10 March, 1967

REFERENCES

1. Gilbert, E. *Sulfonation and Related Reactions* — New York: Interscience Publishers, Inc., 1965.
2. Kircher, J., E. Miller and P. Geiser. — *Industrial and Engineering Chemistry* 46: 1925—1930, 1954.
3. Metzger, A., G. Kelchner and M. Gennert. — *Fette, Seifen, Anstrichnittel* 61:1131—1138, 1959.

GLASNIK HEMIJSKOG DRUŠTVA, Vol. 32, No. 5-6-7, 1967, pp. 315—325

POLYMERIZATION PROPERTIES OF THETIN-HOMOCYSTEIN-METHYLTRANSFERASE FROM SWINE LIVER

by

PERSIDA BERKEŠ-TOMAŠEVIĆ, MIRJANA SLAVIĆ
and VERA TERZIĆ

Durrel *at al.* showed that purified Thetin-Homocystein-Methyltransferase (THMenz) from horse liver is a mixture of various polymers, and that under the influence of glutathione of *D,L*-homocystein the enzyme is changed into a monomeric form[3,4,5]. The same authors also established that various other thioles, such as, mercaptoethylamine, cystein and thioglycolic acid, as well as certain other reducing agents (sodium sulphate and potassium sulphate) also have a depolymerizing effect.

On the basis of results obtained it can be concluded that the monomer units are kept together in the polymers by disulphide compounds. Since many compounds which depolymerize enzymes are known to split disulphide thanks to its replacing reaction, it may be assumed that depolymerization of enzymes occurs by the breakage of these intramolecular disulphide compounds.

The present work intended to establish whether the THMenz from swine liver has the same depolymerizing properties as the THMenz from horse liver.

The occurrence of enzyme depolymerization was observed in starch gel electrophoretically.

The influence of Roentgen rays and free radicals on the enzyme activity and polymerization readiness was also investigated in order to establish whether the enzyme active centers are identical with the polymerization centers.

SUBSTANCES AND METHOD

The enzyme was isolated from swine liver by the Durrel *at al.* method and purified with calcium phosphate gel. By purifying, the enzyme specific activity was increased 50—60 times. One *mg* protein of the purified enzyme catalized the formation of 4.92 μM methionine after one hour incubation at 37°.

Substrate: 0.06 *M D,L*-homocystein and 0.01 *M* dimethylacetothetin (*DMAT*)* were dissolved in a 0.0128 *M* phosphate buffer *p*H=7.4 with 0.123 *M NaCl*, 0.0005 *M KCl* and 0.003 *M* $MgSO_4$.

Determination of enzyme activity: 0.1 *ml* enzyme solution in 0.0128 *M* phosphate buffer *pH*=7.4 with 2 *ml* homocystein and 2 *ml* DMAT solution was incubated. After incubation the unchanged homocystein was determined according to a method described by us[6]. The control sample contained 2 *ml* phosphate buffer instead of DMAT solution.

The starch gel electrophoresis was in principle carried out according to Smithies[7]. Due to a modification in the process carried out in a thin starch slice, the cutting of gel was made unnecessary[2]. Electrophoresis with a 0.5 *mA/cm* wide gel strip lasted 18 hours.

Free radicals were obtained by influencing the $FeSO_4$ solution with H_2O_2. 0.2 *ml* enzyme solution was filled with this reaction mixture to 2 *ml*. The final concentration of $FeSO_4$ was 2×10^{-4} *M*, and of H_2O_2 2×10^{-2}. The reaction with free radicals was stopped with the addition of 0.5 *ml* 1% complex III after 5, 10, 20 and 25 minutes, and the enzyme activity determined and compared with the activity of untreated enzyme. In order to prevent the Fe^{++}, Fe^{+++}, H_2O_2 or the complex from hampering the enzyme activity, the action of each of these substances was tested beforehand. No inactivation was observed in any of the concentrations used.

The exposure of the THMenz to Roentgen rays was performed in a polythene 16 *mm* Ø test tube which contained 1 *ml* of enzyme solution, the thickness of the liquid layer being 0.5 *cm*. The distance of the X-ray source from the liquid upper surface was 20 *cm*. The X-ray characteristics were: 120 *kW*, 20 *mA* and 2 *mm Al*-filter thickness. Under these conditions, the X-ray energy on the upper surface of the solution was 420 *R*/minute.

With both irradiated and nonirradiated enzyme solutions the transmethylation evaluation was carried out in a similar way.

The irradiated and nonirradiated enzyme solutions of the same concentration were exposed to a starch gel electrophoresis in order to establish the effect of free radials and X-rays upon the polymerization properties of THMenz.

RESULTS

The investigations consisted of:

1. Electrophoretic investigation of the purified enzyme from various preparations.

2. Investigation of the influence of various substances (thiols and reducing agents) on the behavior of the enzyme in an electric field.

3. Investigation of the influence of free radicals and Roentgen irradiation on enzyme activity and its behavior in an electric field.

Our aim was to establish whether the enzyme preparation was homogenous, and if so, whether it polymerized. We worked with various enzyme concentrations, with different *pH* values before and after dialysis. The purified enzyme preparations contained different protein concentrations.

* We are indebted to the firm Koch-Light Laboratories, Colnbrook, Bucks, England, for the dimethylacetothetin supplied.

From the purified enzyme preparations we obtained two to four fractions corresponding to the respective solutions. In order to establish the number of fractions which depended on the enzyme concentration, a preparation composed of two fractions was diluted, and the diluted solution investigated.

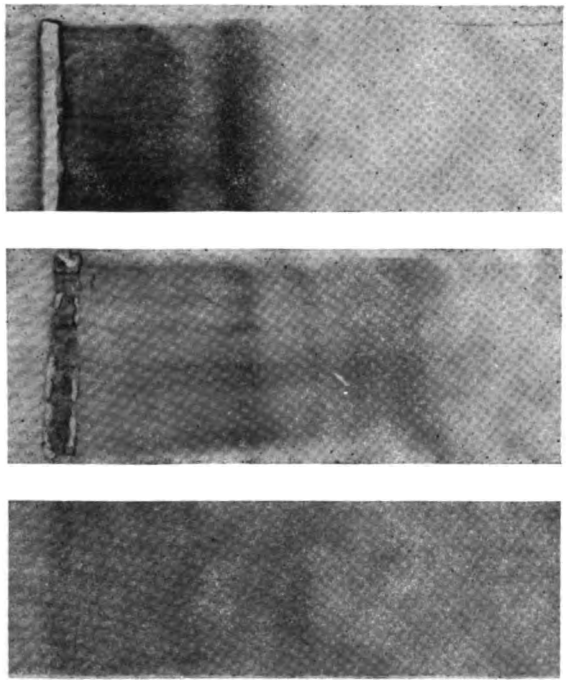

Figure 1

Electropherogram of a purified enzyme preparation containing: 1.58 *g* % protein (*A*); 0.79 *g* % protein (*B*). and 0.40 *g* % protein (*C*)

As can be seen in Fig. 1, after diluting we obtained four fractions. Further diluting did not increase the number of fractions, but they were less visible because of a lower protein content.

These investigations showed that the enzyme preparations were homogenous, and that they polymerized through dilution.

The electrophoresis of purified enzyme was carried out at the following pH values: 6.3, 6.6, 6.9, 7.5 and 8.6. In this pH range the number of fractions did not change, only in the acid zone one fraction migrated to the cathode.

The influence of dialysis on the enzyme polymerization was also investigated. Nondialysed enzyme of various concentrations and enzyme of corresponding concentrations dialysed by a phosphate buffer of pH 7.6 were compared.

The results obtained showed that regardless of the concentration (i.e., the number of fractions in the preparation) the dialysis favored poly-

merization. The fractions of dialyzed enzymes moved faster in the electric field. The number of fractions was at least four, and sometimes more (Figs. 2 and 3).

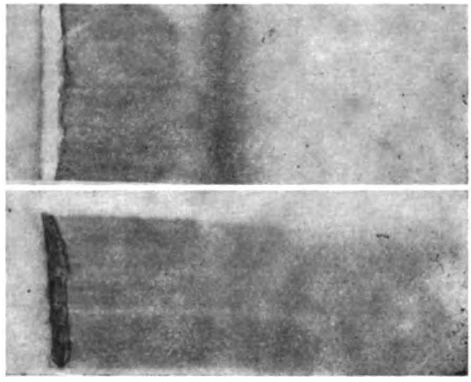

Figure 2
Electropherogram of an enzyme preparation with two fractions (above) and after dialysis (below)

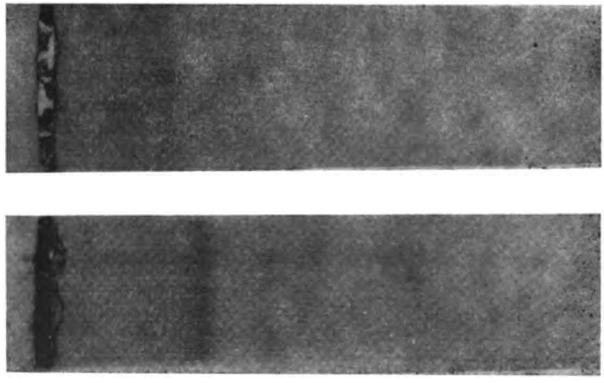

Figure 3
Electropherogram of an enzyme preparation with four fractions before (above) and after dialysis (below)

Having established that purified enzyme polymerized under definite conditions, we approached the study of the influence of some thioles (glutathione and *D,L*-homocystein) and reducing agents (sodium sulphate and sodium bisulphite).

A test was carried out in the following way: 0.1 *ml* enzyme preparation was replaced with 0.1 *ml* glutathione or *D,L*-homocystein, each time of a different concentration, kept for 15 minutes at 37°C, and the reaction mixture placed on the starch gel. Depolymerization was obtained with a 0.11 M thiole solution (Fig. 4).

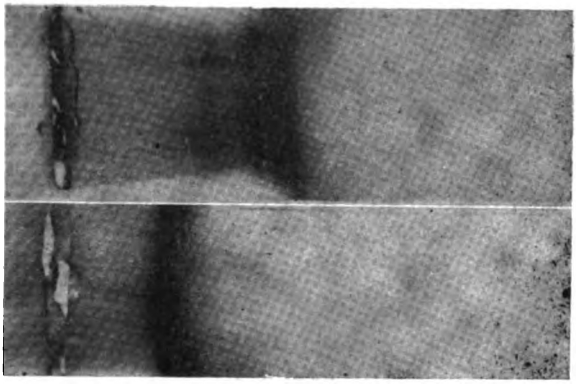

Figure 4

Scheme of enzyme depolymerization under the action of 0.11 *M D,L*-homocystein

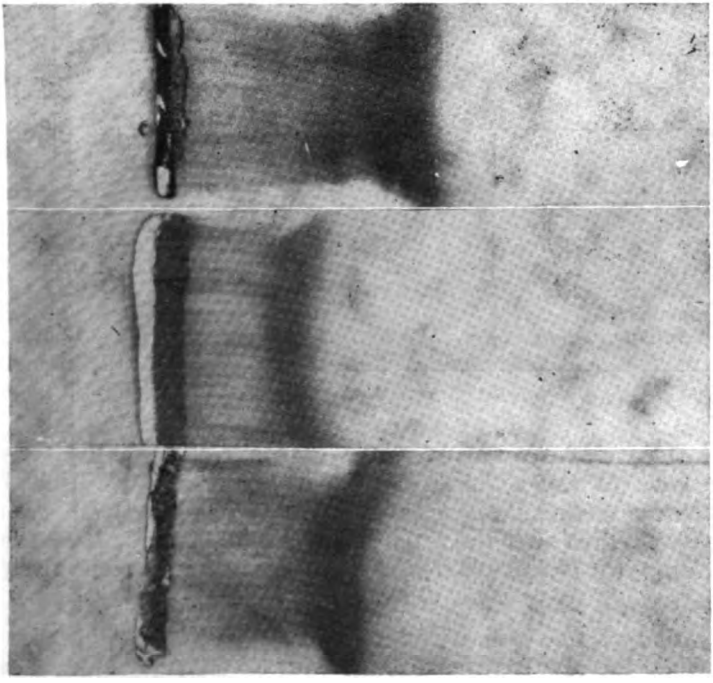

Figure 5

Scheme of enzyme depolymerization after the action of (*A*) 1-M sodium sulphite and (*B*) sodium bisulphite

Figure 4 shows that after the enzyme preparation was exposed to the influence of the 0.11 *M D,L*-homosystein only one fraction of a smaller movement velocity occurred in the electric field. Klee also showed that THMenz was homogenous, i.e., composed of one fraction,[6] only in the presence of thioles.

The influence of sodium sulphite and sodium bisulphite was also tested in the same way. The results are shown in Fig. 5. By the action of the above mentioned substances the enzyme was depolymerized. In addition to this, a slowed migration was observed in the electric field.

TABLE 1

Decrease in THMenz activity after the action of free radicals

Sample no. 1: 0.2 *ml* enzyme solution, 1.8 *ml* H_2O, 0.5 *ml* Complex III, 2 *ml* 0.006 *M D,L*-homocystein and 2 *ml* 0.01 *M* dimethylacetothetine

Sample no. 2: 0.2 *ml* enzyme solution, 0.9 *ml* 4×10^{-2} *M* H_2O_2 and 0.9 *ml* 4×10^{-2} *M* $FeSO_4$; Complex III was added after the time intervals given in the table. Afterwards, 2 *ml* 0.006 *M D,L*-homocystein and 2 *ml* dimethylacetotheine were added and the transmethylazation measured.

μM originating methionine in

Sample I		Sample 2 after the action of free radicals for			
		5	10	20	25 Minutes
	2.78	2.34	1.82	1.04	0.52
	2.86	2.08	1.82	0.91	0.26
	2.72	1.82	1.69	0.78	0.26
Average	*2.75*	*2.08*	*1.78*	*0.91*	*0.35*
Value of the remaining activity	100%	74.8%	64.0%	32.7%	12.6%

The influence of free radials on the THMenz of swine liver was manifested in a decrease of activity. The results are shown in Table 1 and Fig. 6. When the methionine formation of the untreated enzyme was assumed to be 100%, then after the action of free radicals for 5, 10, 20 and 25 minutes a drop to 74,8%, 64.0%, 32.7% and 12.6 % respectively was observed.

The action of free radicals on the enzyme polymerization was thus examined, while the raw enzyme together with an enzyme solution beforehand incubated for 30 minutes at 37° with 2×10^{-4} *M* $FeSO_4$ and 2×10^{-2} *M* H_2O_2, was exposed to the starch gel electrophoresis (Fig. 7). Free radicals showed no effect on the polymerization grade of the enzyme, so the number of fractions remained the same as before.

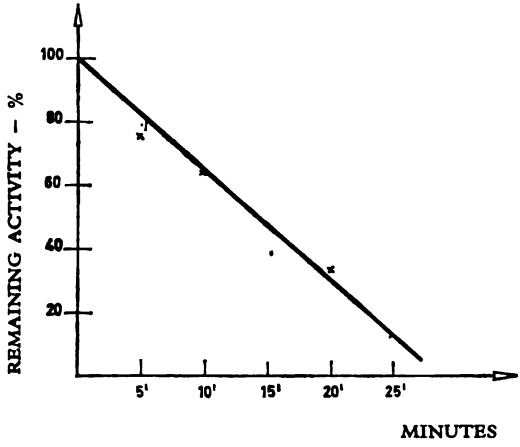

Figure 6

Action of free radicals on the activity of thetin-homocystein-metylpherase.

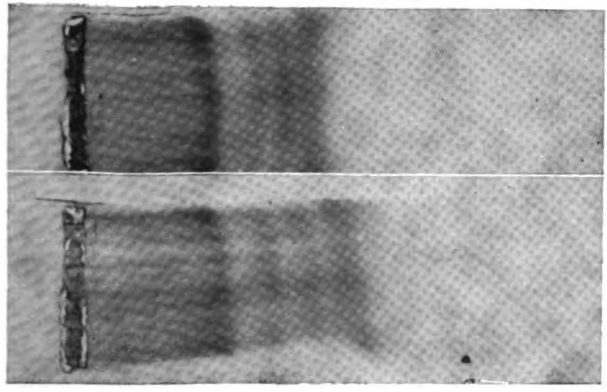

Figure 7

Schematically represented electropherogram of an enzyme before (above) and after the reaction of free radicals (below)

The results of Roentgen irradiation of THMenz are shown in Table 2 and Fig. 8. Table 2 shows that the enzyme activity decreased with the duration of Roentgen radiation: 80.6% after 5 minutes, 61.1% after 10 minutes, 25.0% after 20 and 8.3% after 25 minutes.

The electrophoretic test of an unirradiated enzyme solution and a solution irradiated with 18,900 R showed that Roentgen radiation did not affect the number of fractions, and therefore not the polymerization either.

TABLE 2

Activity of the thetin-homocystein-methyl-pherase after Roentgen irradiation

Sample 1.: 0.2 *ml* raw enzyme, 2 *ml* 0.006 *M D,L*-homocystein, 2 *ml* 0.01 *M* dimetyl-acetothetin and 1.8 *ml* PO_4 buffer.

Sample 2.: 0.2 *ml* irradiated enzyme solution, 2 *ml* 0.006 *M D,L*-homocystein, 2 *ml* 0.01 *M* dimethylacetothetin and 1,8 *ml* PO_4 buffer.

	µM originating methionine in				
Sample I		Sample 2 after Roentgen radiation for			
		5	10	20	25 Minutes
	2.68	2.16	1.68	0.60	0.24
	2.74	2.40	1.68	0.72	0.48
	2.92	2.40	1.92	0.84	0.00
Average	*2.75*	*2.32*	*1.76*	*0.72*	*0.24*
Value of the remaining activity	100%	80.6%	61.1%	25.0%	8.3%

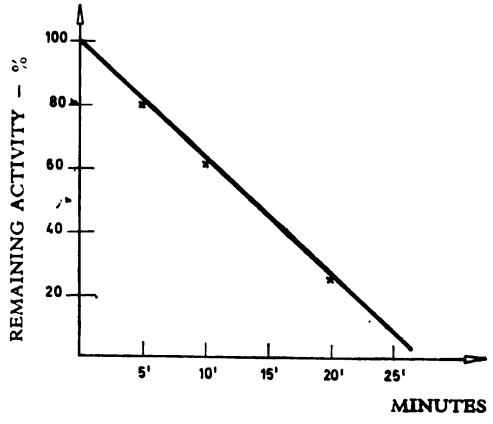

Figure 8

Influence of Roentgen irradiation on the activity of thetin-homocystein-methylepherase

DISCUSSION

Tests with purified enzymes showed that the THMenz from swine liver polymerized in a similar way as was established by Durrel *et al.* for the THMenz from horse liver. The decrease in enzyme concentration and dialysis favored the polymerization. Thiole and reducing agents depolymerized the THMenz from swine liver. It is of interest to note that the substrate homocystein, with its thiole function, also acted as a depolymerizer.

From the foregoing facts it can be concluded that during enzyme polymerization the oxidation of —*SH* groups into —*S*—*S* compounds takes place. During dialysis an acceleration of their autoxydation probably occurs due to the loss of the protective lower molecules of —*SH* compounds.

It is of interest whether the polymerization centers of enzyme molecules influence the enzyme activity. We tried to elucidate this problem by completely inactivating the enzyme with free radicals and comparing its electrophoretic picture with the picture of an active enzyme (Fig. 7). We found no difference in the electrophoretic pictures between the active and inactivated enzymes.

From the above it can be concluded that the polymerization centres and even the process of polymerization have no effect on enzyme activity.

The biological meaning of this occurrence cannot be easily explained, seeing that polymerization is not linked with the enzyme activity. According to the facts known so far, it is not possible to establish whether the enzymes occur in the cell in monomer or polymer form.

REFERENCES

1. Berkeš-Tomašević, P., M. Slavić and I. Berkeš — *Jugoslavica Physiologica et Pharmacologica Acta* 1: 29—37, 1965.
2. Berkeš-Tomašević, P. J. Rosić and M. Ignjatović — *Arhiv za farmaciju* (Beograd) 1: 9—17, 1963.
3. Durrel J., D. G. Anderson and G. L. Cantoni — *Biochemica et Biophysica Acta* 26: 270—282, 1957.
4. Durrel, J. and G. L. Cantoni — *Biochemica et Biophysica Acta* 35: 515—528, 1959.
5. Durrel, J. and G. L. Cantoni — *Biochemica et Biophysica Acta* 39: 248—256, 1960.
6. Klee, W. A. — *Biochemica et Biophysica Acta* 45: 537—540, 1960.
7. Smithies, O. — *Biochemical Journal* 61: 629—641, 1955.

GLASNIK HEMIJSKOG DRUŠTVA, Vol. 32, No. 5-6-7, 1967, pp. 327—334

METABOLIC RELATIONS OF PROTEINS, LIPIDS AND GLUCIDES. XI.

EFFECT OF INTRAVENOUS INJECTION OF GLUCOSE ON THE DISTRIBUTION OF SERUM LIPOPROTEIN FRACTIONS IN FASTING DOGS

by

JELENA J. BOJANOVIĆ, MILANKA O. ČORBIĆ
and PREDRAG P. MILOŠEVIĆ

Studies on the effect of glucose on the state of lipids in the circulation during fasting have been mainly concerned with the fatty acid[3, 4] and neutral fat composition[1, 6], while the state of lipoproteins has been little studied and the existing information on this effect of glucose is contradictory[5, 8]. In order to determine if any and what changes are caused by glucose in the serum lipoprotein spectrum during fasting, and whether these changes are analogous to those observed in hyperlipemia[2], we have studied the effect of intravenous injections of glucose on serum lipoproteins in dogs fasting for 48 hours. Besides, we considered that recognition of the changes produced under the effect of glucose in the organism in which carbohydrate stores were exhausted and in the organism in which alimentary hyperlipemie was induced in this state[2], as well as in the *in vitro* system, can yield information necessary for a better understanding of the metabolic relationships of proteins, lipids and carbohydrates, and also answer the question concerning the type of changes induced by glucose.

EXPERIMENTAL

The study was done on 8 dogs weighing from 12 to 15 *kg*. After 48 hours of fasting, blood was drawn for examination and then a 50% glucose solution (1.5 *g* glucose per *kg* of bodyweight) was injected intravenously, the blood being again taken 15, 30, 45 and 60 minutes after the injection of glucose. The blood was obtained from the veins of the front and hind extremities, and the serum was obtained in the usual way.

For the *in vitro* studies a 50% glucose solution (0.03 *ml*) was added to the obtained serum (2.5 *ml*) and incubated at 37.5°C for 15, 30, 45 and 60 minutes.

The determination of the lipoprotein fractions was done after the method of Swahn[9] by paper electrophoresis. Schleicher-Schüll 2043 bM paper was used. 0.03 *ml* of serum was put on paper tapes the dimensions

of which were 4 × 40 *cm*, and the separation of fractions done in veronal-sodium veronal buffer, pH = 8.6, ionic strength $\mu = 0.1$, with a voltage of 200 *V* for 5 hours.

Serum transparency was determined nephelometrically[7].

RESULTS AND DISCUSSION

Investigation of the state of serum lipoproteins in dogs in which the carbohydrate stores were exhausted (48 hours of fasting) showed that 15 minutes after the injection of glucose there was a decrease of the relative

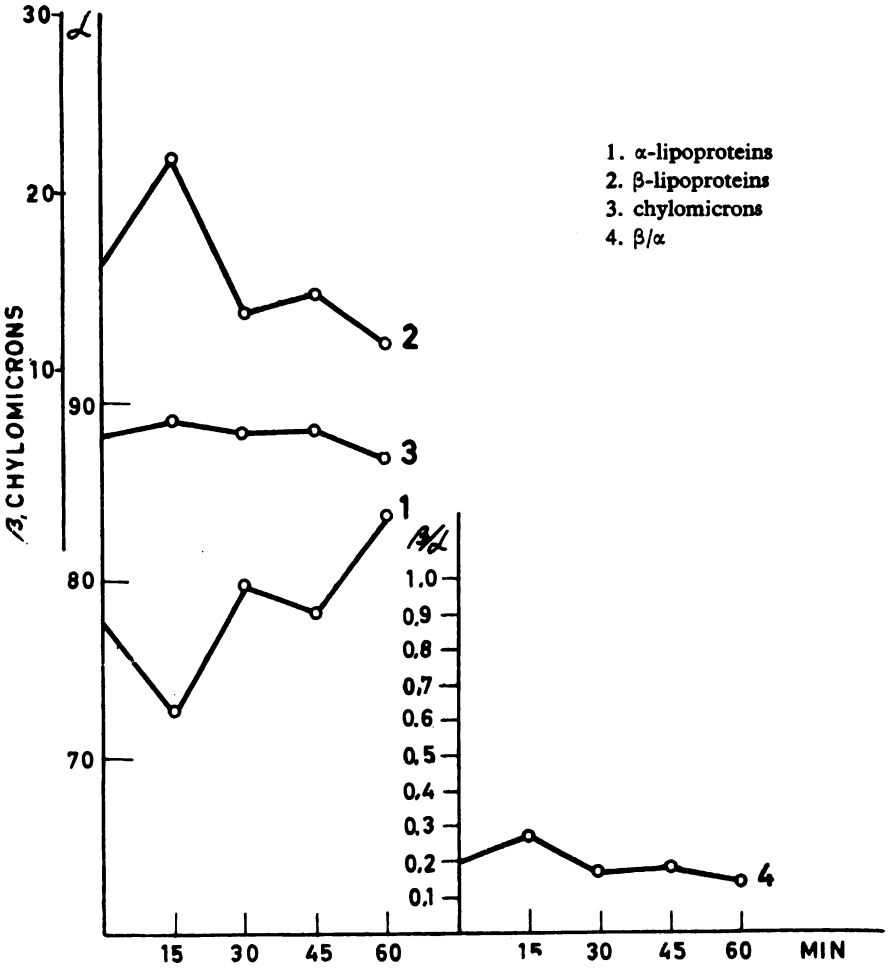

Figure 1

Relative values of lipoprotein fractions in the blood serum of dogs in fasting 15, 30, 45 and 60 minutes after the injection of glucose

content of α-lipoprotein and an increase of β-lipoprotein in the serum, which was observed in all cases under observation (the change was statistically significant, $p < 0.05$) (Table 1 and Figs. 1 and 2). It is significant

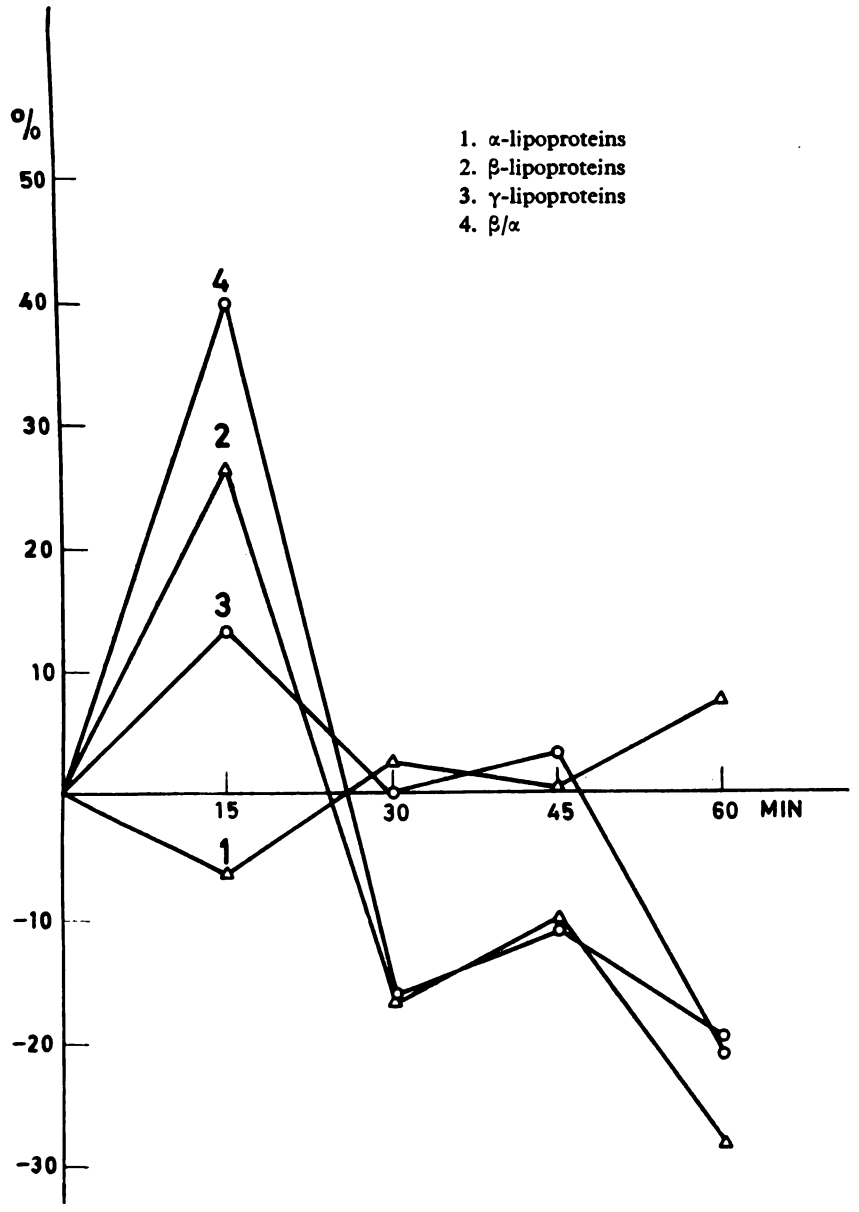

Figure 2

Changes in the relative values of lipoprotein fractions in dog blood serum with the injection of glucose given in percent decrease or increase

TABLE 1

Statistical analysis of the relative values of lipoprotein fractions in the blood serum of dogs in fasting after the injection of glucose

	α-lipoproteins					β-lipoproteins				
	N	15	30	45	60	*N*	15	30	45	60
No	8	6	6	6	6	8	6	6	6	6
R	73.9—83.6	67.6—76.5	72.1—86.6	70.7—86.3	77.1—88.3	12.1—21.1	14.8—24.5	9.4—19.2	8.7—19.0	7.9—15.7
M	77.8	72.7	79.8	78.2	83.7	15.19	20.2	13.2	14.3	11.4
SD	3.16	3.46	5.88	8.15	45.9	2.47	3.87	4.14	4.25	3.26
SE	1.12	1.41	2.40	3.33	1.87	0.87	1.58	1.69	1.73	1.33
CV%	4.06	4.76	7.37	10.42	5.48	15.55	19.20	31.34	29.78	28.70
a		—6.58	+2.50	+0.49	+ 7.54		+26.95	—16.81	—10.14	—28.46
b			+9.72	+7.56	+15.12			—30.47	—29.22	—43.65
c				+1.09	+ 4.91				+ 8.02	—14.00
d					+ 7.07					—20.39
a		$p<0.05$	$p>0.05$	$p>0.05$	$p<0.05$		$p<0.05$	$p>0.05$	$p>0.05$	$p<0.05$
b			$p<0.05$	$p>0.05$	$p<0.001$			$p<0.05$	$p>0.05$	$p<0.01$
c				$p>0.05$	$p>0.05$				$p>0.05$	$p>0.05$
d					$p>0.05$					$p>0.05$

	Chylomicrons					β|α				
	N	15	30	45	60	*N*	15	30	45	60
No	8	6	6	6	6	8	6	6	6	6
R	4.3—9.7	5.3—8.8	3.4—8.9	4.2—9.2	3.4—7.2	0.14—0.26	0.19—0.36	0.12—0.27	0.11—0.26	0.09—0.20
M	6.3	7.1	6.3	6.5	4.9	0.20	0.28	0.17	0.18	0.14
SD	2.12	1.30	2.77	1.97	1.47	0.03	0.07	0.06	0.07	0.04
SE	0.75	0.53	1.13	0.80	0.60	0.01	0.02	0.02	0.03	0.02
CV %	33.70	18.23	44.18	30.35	29.70	15.00	25.00	35.29	36.67	28.57
a		+13.35	0.00	+3.18	−21.30		+40.00	−15.00	−11.11	−20.00
b			−12.06	−8.98	−30.57			−39.28	−35.72	−50.00
c				+3.51	−21.05				+ 5.88	−17.64
d					−23.73					−22.22
a		$p>0.05$	—	$p>0.05$	$p>0.05$		$p<0.05$	$p>0.05$	$p>0.05$	$p<0.05$
b			$p>0.05$	$p>0.05$	$p<0.05$			$p<0.05$	$p<0.05$	$p<0.01$
c				$p>0.05$	$p>0.05$				$p>0.05$	$p>0.05$
d					$p>0.05$					$p>0.05$

No. — number of cases
R — range of values
M — mean values
SD — standard deviation
SE — standard error
CV% — coefficient of variation in %
a, b, c, d — % of decrease or increase and levels of significance in relation to values in fasting and 15, 30 and 45 minutes after the injection of glucose

that the observed increase of β-lipoproteins during this time interval was not only greater than the increase induced by glucose in hyperlipemia[2], but that it also reached a higher level. Considering that with such a high fasting β-lipoprotein content there were no changes in serum transparency, it is not possible to accept the opinion of certain authors that the slightest increase of the β-lipoprotein content causes serum turbidity. The low level of the neutral fat fraction during fasting increased after the administration of glucose at the stated time intervals, but although the increase was rather great in comparison with the values in untreated animals, the level of this fraction remained quite low and did not cause a change in the serum transparency. Only as late as 30 minutes after the injection of glucese did the content of α-lipoprotein increase and the level of β-lipoprotein as well as the level of the neutral fat fraction decrease in all the cases under observation. The observed changes in β-lipoproteins in chylomicrons were in correlation with the changes of glycemia, while with α-lipoproteins the correlation was reciprocal within the entire period of observation. The observed changes were estimated to be statistically significant in comparison with the changes observed after 15 minutes (except in the neutral fat fraction). The values of the lipoprotein fractions remained at the same level even 45 minutes after the injection of glucose. Sixty minutes after injection of glucose the relative content of α-lipoproteins increased and in the majority of cases (83%) reached values higher than the initial ones, while the level of β-lipoproteins and chylomicrons decreased. The changes of α and β-lipoproteins within this time interval were significant at the 5% level in comparison with the values in fasting, and at the 1% level of significance in comparison with the concentration of these fractions 15 minutes after the administration of glucose. The decrease of the neutral fat fraction was statistically significant only in respect to the value observed 15 minutes after the injection of glucose, while in comparison with the initial value it was not significant.

The ratio β/α-lipoproteins showed a great increase during the first 15 minutes after the injection of glucose ($p < 0.05$), then a decrease so that at 30 minutes it was even lower than the initial value. Considering that at 45 minutes there were no significant changes in the relative content of α and β-lipoproteins, the ratio β/α at that time showed almost no change. Only as late as 60 minutes after the injection their ratio suddenly decreased, the drop being great both as regards the initial value ($p = 0.05$) and the value at 15 minutes after the injection of glucose ($p < 0.01$).

The observed changes of the lipoprotein fractions under the influence of glucose are in contradiction with the findings of Rubin and co-workers[8], who found that the administration of carbohydrates in fasting did not change the concentration of blood serum lipoproteins during the first three hours after oral ingestion. However, Havel[5] considered that these authors obtained such results because inadequate amounts of carbohydrate were administered, and in his studies with large amounts of orally ingested glucose he found changes in the lipoprotein spectrum after three hours. The results of our studies are in agreement with those of Havel, but only in respect to the state of lipoproteins 60 minutes after the administration of glucose, when there was a rise in the level of α-lipoprotein and a drop of β-lipoprotein. It is obvious that in Havel's experiments it was impossible to observe

the changes caused by the direct influence of glucose, which we observed a short time after its administration and which represented the intermediary phase in the reduction of the large molecule lipoprotein levels. The increase of the large molecule lipoprotein fraction and of chylomicrons a short time after the injection of glucose was obviously associated with the activation of the process in the liver, as the experiment *in vitro* showed that a direct effect of glucose on the state of the serum lipoproteins was out of question.

The increase of the β-lipoprotein fraction and of chylomicron induced by glucose and observed 15 minutes after its administration, and the lipid content of these fractions, are the subject of our present investigations.

Institute of Chemistry,
School of Medicine, Belgrade
Institute of Biochemistry,
School of Medicine, Belgrade

Received 10 April, 1967

REFERENCES

1. Albrink, M., J. Fitzgerald and E. Man. "Reduction of Alimentary Lipemia by Glucose" — *Metabolism* 7: 162—170, 1958.
2. Bojanović, J., M. Čorbić and Dj. Panjević. "Odnos metabolizma belančevina, lipida i glicida. XII. Dejstvo intravenski date glukoze na raspodelu lipoproteinskih frakcija seruma pasa u alimentarnoj hiperlipemiji" (Metabolic Relations of Proteins, Lipids and Glucides. XII. Effect of Intravenous Glucose on the Distribution of Serum Lipoprotein Fractions in Dogs in Alimentary Hyperlipemia) — (in press).
3. Dole, V. "A Relation between Non-Esterified Fatty Acids in Plasma and the Metabolism of Glucose" — *Journal of Clinical Investigations* 35: 150—154, 1956.
4. Gordon, R. and A. Cherkes. "Unesterified Fatty Acid in Human Blood Plasma" — *Journal of Clinical Investigation* 35: 206—212, 1956.
5. Havel. R. "Early Effects of Fasting and of Carbohydrate Ingestion on Lipids and Lipoproteins of Serum in Man" — *Journal of Clinical Investigation* 36: 855—859, 1957.
6. Lossow, W. and J. Chaikoff. "Carbohydrate Sparing of Fatty Acid Oxidation. I. The Relation of Fatty Acid Chain Length to the Degree of Sparing. II. The Mechanism by Which Carbohydrate Spares the Oxidation of Palmitic Acid" — *Archives of Biochemistry and Biophysics* 57: 23—40, 1955.
7. Nešković, M., J. Bojanović, M. Čorbić, Lj. Stefanović, Z. Mladenović-Stojimirović, I. Kulić-Japundžić and D. Kostić. "Effect of Insulin on Metabolism of Proteins, Lipids and Clucides. VI. Action of Glucose on the Insulin Clearing Effect" — *Zbornik radova Medicinskog fakulteta Beograd* 1: 37—45, 1962.
8. Rubin, L. and F. Aladjem. "Serum Lipoprotein Changes during Fasting in Man" — *American Journal of Physiology* 178: 263—266, 1954.
9. Swahn, B. "Localization and Determination of Serum Lipids after Electrophoretic Separation on Filter Paper" — *Scandinavian Journal of Clinical and Laboratory Investigation* 4: 98—103, 1952.
10. Swahn, B. "Blood Lipids" — *Scandinavian Journal of Clinical and Laboratory Investigation* 5, Suppl. 9: 5—114, 1953.

GLASNIK HEMIJSKOG DRUŠTVA, Vol. 32, No. 5-6-7, 1967, pp. 335—341

METABOLIC RELATIONS OF PROTEINS, LIPIDS AND GLUCIDES. XII.

EFFECT OF INTRAVENOUS GLUCOSE ON THE DISTRIBUTION OF THE SERUM LIPOPROTEIN FRACTIONS IN DOGS IN ALIMENTARY HYPERLIPEMIA

by

JELENA J. BOJANOVIĆ, MILANKA O. ČORBIĆ
and ĐORĐE J. PANJEVIĆ

The effect of glucose on alimentary hyperlipemia has been investigated almost concomitantly with the studies of its effect on proteins. Bang[4] has shown that postprandial hyperlipemia in dogs decreases if the meal, besides fats, contains carbohydrates as well. Similar results were later also obtained by Rony and co-workers[16], but the mechanism of this effect was not explained. In 1956 Dole[8], and at the same time also Gordon and co-workers[12], observed that orally ingested glucose caused a decrease in non-esterified fatty acids (NEFA) in the plasma. These authors were of the opinion that glucose inhibits the mobilization of NEFA from depots, but they disagreed in explaining the cause of this phenomenon. While Gordon assumed that endogenous insulin is the cause of low NEFA level, Dole produced results which spoke against increased insulin activity induced by glucose. Albrink and co-workers[2] emphasized the process of decomposition of triglycerides in the circulation after oral ingestion of glucose, while Lossow and Chaikoff[14] showed that the administration of glucose lowered the decomposition of triglycerides and reduced the oxidation of fatty acids.

The different and even contradictory explanations of the phenomena which follow the ingestion of glucose are due to inadequate knowledge of the changes and complexity of metabolic relationships of proteins, lipids and carbohydrates in hyperlipemia, as well as to many unsolved questions regarding the metabolism of fats. Knowledge of the changes occurring under the influence of glucose in the organism in which carbohydrate reserves have been exhausted[6] and in the organism in which in this state hyperlipemia was induced by means of a meal rich in fats and proteins can yield information useful for a better understanding of metabolic relations ships as well as information on the type of changes induced by glucose. A particularly interesting question is whether glucose has a direct effect on lipids in the circulation or whether the effect is of a secondary nature, as well as what is the effect of glucose on the regulation of lipid levels in the circulation

and what is the probable mechanism of this action. In order to answer some of these questions, we have studied first the effect of glucose on the lipoproteins in the circulation after 48 hours of fasting[6] and in the maximum of alimentary hyperlipemia, the results of which study are presented in this paper. Glucose was administered intravenously in order to avoid the possible influence of other factors which accompany absorption.

EXPERIMENTAL

Investigations were done in the blood serum of six dogs, weighing from 12 to 15 kilograms. After 48 hours of fasting, a meal was given which contained 10 *g* pork fat per kilo of bodyweight mixed with 500 *g* of finely cut horse meat. Blood was drawn at the maximum of alimentary hyperlipemia (five hours after the intake of the fatty meal), and after that a 50% glucose solution (1.5 *g* of glucose per kilo of bodyweight) was injected and the blood again drawn after 15, 30, 45 and 60 minutes. The methods of glucose administration and of drawing blood for examination, as well as the conduction of *in vitro* experiments, were the same as described in a previous communication[6].

The determination of lipoprotein fractions and of serum transparency was done in the same way as described in previous communications[6, 15].

RESULTS AND DISCUSSION

Shortly after the intravenous introduction of glucose (15 minutes), increased lactascence of the serum was noticed, which was in contradiction to the generally accepted view about the effect of glucose on lipemia. The clearing effect in the hyperlimepic serum appeared not sonner than 30 minutes after the injection of glucose. In order to explain such an effect of exogenous glucose one could hypothesize that in the state of hyperlipemia there was either an increase in the amount of triglyceride chylomicrons, perhaps of large molecule lipoproteins, or that there was a direct effect of glucose on macromolecules in the circulation, which could cause a change in the size and charge and even in the colloidal state of these particles. The results of the studies on lipoprotein distribution in hyperlipemia showed that there was an analogy between the changes caused by the introduction of glucose and the changes caused by the introduction of glucose in fasting[6], the difference being in the extent of these changes. The α-lipoprotein fraction, whose level in hyperlipemia was lower than in fasting, showed a greater decrease under the effect of glucose after the first 15 minutes. At this time the β-lipoprotein fraction, whose level was about the same in fasting and in hyperlipemia, showed a higher value. Under the influence of glucose the high level of the chylomicron zone in alimentary hyperlipemia showed a marked increase during the first 15 minutes, which was in accordance with increased serum turbidity during this time interval. The observed increase of the chylomicron zone was in contradiction to the results of Albrink and co-workers[2] and of Dole and co-workers[5, 8, 9], and to their concept of the removal of triglycerides from the circulation under the in-

TABLE 1

Statistical analysis of the relative values of lipoprotein fractions in the serum of dogs in hyperlipemia after the injection of glucose

	α-lipoproteins					β-lipoproteins				
	N	15	30	45	60	*N*	15	30	45	60
No.	6	5	6	6	5	6	5	6	6	5
R	6.12—73.5	47.4—63.1	53.7—72.2	57.2—73.8	66.5—72.1	9.9—21.7	11.2—24.6	12.4—25.8	9.9—22.7	10.0—19.8
M	65.9	55.9	62.5	65.7	68.2	15.8	19.1	19.4	18.0	15.6
SD	4.40	6.05	7.54	6.75	2.43	4.39	6.19	4.70	4.94	3.64
SE	1.80	2.71	3.08	2.75	1.09	1.79	2.77	1.92	2.21	1.63
CV%	6.67	10.81	12.07	10.27	3.51	27.77	32.36	24.19	27.40	23.32
a		−15.14	−5.22	−0.30	+4.99		+21.00	+22.90	+14.04	−1.26
b			+11.69	+17.48	+23.72			+1.57	−5.75	−18.40
c				−10.12	−16.09				−12.50	−28.12
d					−6.65					−17.86
a		*p*>0.05	*p*>0.05	*p*>0.05	*p*>0.05		*p*>0.05	*p*>0.05	*p*>0.05	*p*>0.05
b			*p*>0.05	*p*=0.05	*p*<0.05			*p*>0.05	*p*>0.05	*p*>0.05
c				*p*>0.05	*p*>0.05				*p*>0.05	*p*>0.05
d					*p*>0.05					*p*>0.05

No — number of cases
R — range of values
M — mean values
SD — standard deviation
SE — standard error
CV% — coefficient of variation in %
a, b, c, d — % of decrease or increase and levels of significance in relation to values in hyperlipemia and 15, 30 and 45 minutes after the injection of glucose

fluence of glucose, as well as to the results of Ghata and co-workers[11] on the disappearance of chylomicrons under the influence of glucose. The difference in the results, and therefore in the explanation of the process itself, was probably due to the fact that these authors, while observing the changes which occurred at about 3 hours after the oral ingestion of glucose, were unable to note changes which took place at shorter time intervals after its intake. We observed the disappearance of chylomicrons only after 30 minutes, which was associated with clearing of the serum, and therefore there was no question of a direct effect of glucose on chylomicrons in the circulation. It was clear from the distribution of lipoprotein fractions that glucose in fasting also caused an increase of the chylomicron fraction, whose level was not as high as in hyperlipemia. In the chylomicron zone in alimentary hyperlipemia there appeared also a clearly separated electrophoretic fraction, which was marked with x, which was not present in fasting. It is important that the changes in the fractions of the chylomicron zone under the influence of glucose depended on the mode of its administration. Thus, after the injection of glucose there was an increase in the chylomicron

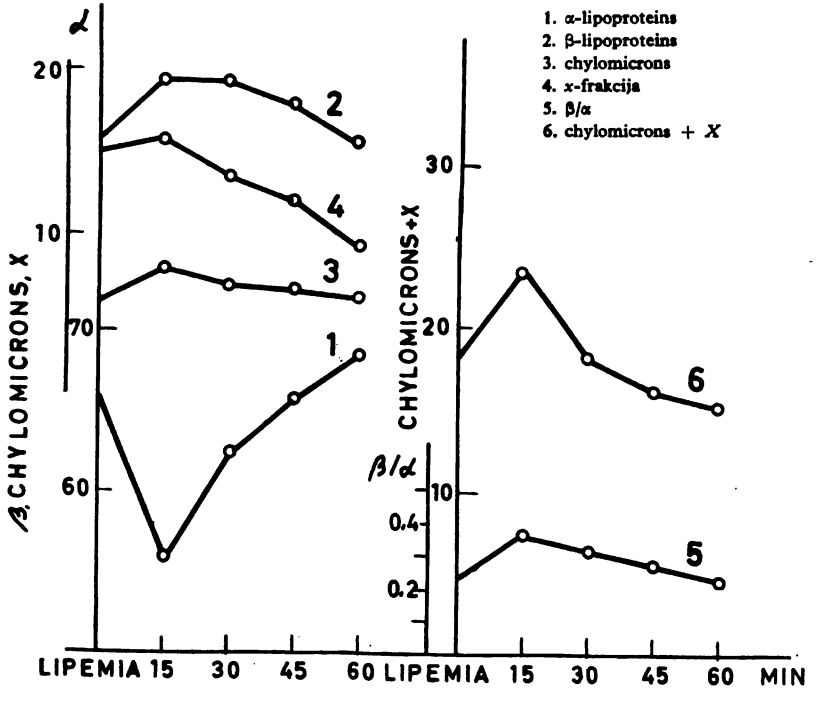

Figure 1

Relative values of lipoprotein fractions in the serum of dogs in alimentary hyperlipemia 15, 30, 45 and 60 minutes after the injection of glucose

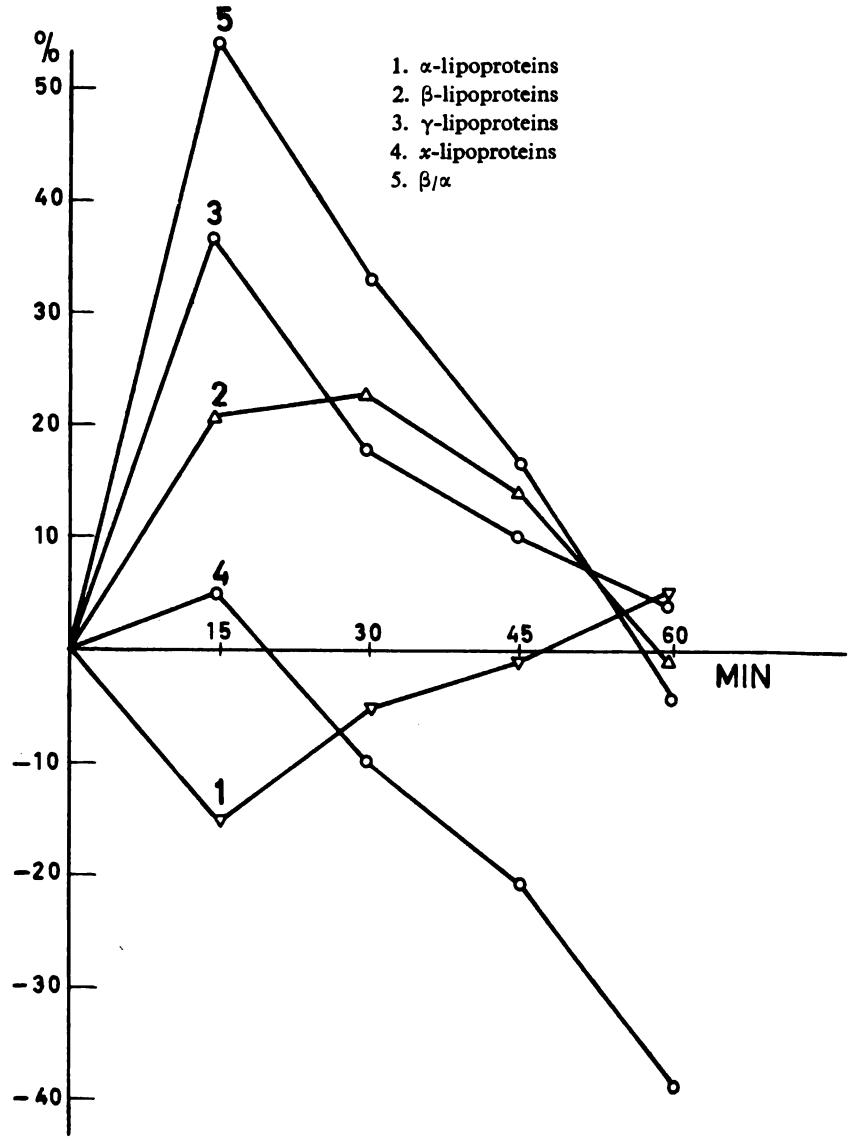

Figure 2

Changes in the relative values of lipoprotein fractions in dog serum induced by the injection of glucose in alimentary hyperlipemia (given in percent of decrease or increase)

content, which, however, was practically unchanged in the less mobile x-fraction. Contrary to this, slow introduction of glucose by infusion caused opposite changes*, as there was a great increase in the content of the x-

* Unpublished data.

fraction. However, during the clearing of the serum, regardless of the mode of introduction of glucose, there was a much more marked decrease in the content of the x-fraction, which in the majority of cases completely disappeared. As the increase in chylomicrons and in turbidity occurred at the time of highest glycemia, the elimination of alimentary hyperlipemia cannot be considered to be a direct effect of glucose, but rather evidently occurs as a consequence of certain reactions in its metabolism. This is supported by the results of *in vitro* experiments, in which during incubation of the lipemic serum with glucose changes analogous to those found *in vivo* were not observed. That the elimination of alimentary hyperlipemia depended on the metabolic activity of carbohydrates, and not only on the increased level of blood sugar, was supported by the fact that glucagon[3], which causes increased blood sugar levels and increases the utilization of glucose, decreases postprandial hyperlipemia, while epinephrine[1], which also increases the blood sugar level but prevents the utilization of glucose, does not show the same effect.

The changes of β-lipoproteins and chylomicrons obtained by rapid introduction of glucose with a single injection during the state of maximal hyperlipemia showed a positive correlation with the changes of glycemia, except for a slight deviation of the β-fraction, whose level increased until 30 minutes after the administration of glucose, when the blood sugar decreased. Between α-lipoproteins and glycemia there was, however, a negative correlation.

The differences in the lipoprotein spectrum caused by glucose during fasting and in alimentary hyperlipemia were probably due to the presence of different kinds of lipids. This was, above all, supported by the fact that during fasting the subfraction of chylomicrons, marked with an x, was absent, while in lipemia it was very marked. Different kinds of lipids could appear because of different pathways in glucose metabolism. According to Siperstein and Fagan[17] the kind of lipid formed depends on the pathway of glucose. The question as to the nature of the quantitative ratio between the two possible pathways in the metabolism of glucose in fasting and in hyperlipemia has not yet been answered.

The mechanism of removal of chylomicrons from the circulation is still little understood. Havel and Fredrickson[13] were of the opinion that there is close association between the process of chylomicron removal and hydrolysis of triglycerides, which occurs under the influence of lipolytic enzymes. Contrary to this view, Bragdon and Gordon[7] consider that chylomicrons are removed from the tissue without previous decomposition, the manner of removal being dependent on the state of nutrition of the organism. According to these authors, during fasting triglycerides go into the liver where they decompose, and the fatty acids formed by hydrolysis are then transported through the circulation to the organs in which they are oxidized and the energy is liberated, while in hyperlipemia the triglycerides are stored in fat tissues. There is, however, data in the literature suggesting direct oxidation of triglyceride chylomicrons without previous hydrolysis[10].

The finding in our experiments that intravenous injection of glucose markedly increased the fraction of chylomicrons, already very marked in hyperlipemia, could be explained either by increased fat absorption or by

prevented hydrolysis of triglyceride oxidation. The possible influence of glucose on the absorption of fat was considered only from the point of view of oral ingestion of glucose, and although a definite correlation was not found, it was accepted as likely that glucose inhibits absorption[2]. On the basis of the finding of Lossow and Chaikoff[15] that glucose in fasting reduced the hydrolysis of triglycerides, and of Fredrickson and co-workers[10] that in hyperlipemia it reduced the oxidation of triglycerides, one can assume that the observed increase of chylomicrons in our experiments was caused by the influence of glucose on the speed of these triglyceride degradation processes. However, it is still possible that glucose acts on the mobilization of fat from depots.

Sixty minutes after the administration of glucose all the lipoprotein fractions returned to approximately the level found in hyperlipemia, except for the x-fraction, in which a great decrease in value continued even after 60 minutes.

Institute of Chemistry,
School of Medicine, Belgrade
Veterinary School, Belgrade

Received 10 April, 1967

REFERENCES

1. Albrinck, M. and E. Man. "Effect of Carbohydrate Ingestion on Postprandial Lipemia" — *Clinical Research Proceedings* 4: 121—126, 1956.
2. Albrinck, M., J. Fitzgerald and E. Man. "Reduction of Alimentary Lipemia by Glucose" — *Metabolism, clinical and experimental* 7: 162—171, 1958.
3. Albrinck, M. and R. Neuwirth. "Effect of Previous Starvation on the Response of Plasma Lipids and Free Fatty Acids to a Fat Meal" — *Journal of Clinical Investigation* 39: 441—446, 1960.
4. Bang, I. "Uber Lipämie. III." — *Biochemische Zeitschrift* 91: 111—121, 1918.
5. *Bierman*, E., I. Schwartz and V. Dole. "Action of Insulin on Release of Fatty Acids from Tissue Stores" — *American Journal of Physiology* 191: 359—362, 1957.
6. Bojanović, J., M. Čorbić, and P. Milošević. "Odnos metabolisma belančevina, lipida i glicida. XI. Dejstvo intravenski date glukoze na raspodelu lipoproteinskih frakcija seruma pasa u gladovanju" (Metabolic Relations of Proteins, Lipids and Glucides. XI. Effect of Intravenous Glucose on the Distribution of Serum Lipoprotein Fractions in Dogs during Fasting) — *Glasnik Hemijskog društva* (in press).
7. Bragdon, J. and R. Gordon. "Tissue Distribution of C^{14} after the Intravenous Injection of Labeled Chylomicrons and Unesterified Fatty Acids in the Rat" — *Journal of Clinical Investigation* 37: 574—578, 1958.
8. Dole, V. "A Relation between Non-Esterified Fatty Acids in Plasma and the Metabolism of Glucose" — *Journal of Clinical Investigation* 35: 150—154, 1956.
9. Dole, V., E. Bierman and T. Roberts. "Plasma NEFA as an Index of Carbohydrate Utilization" — *Journal of Clinical Investigation* 36: 884, 1957.
10. *Fredrickson*, D., D. McCollester and K. Ono. "The Role of Unesterified Fatty-Acid Transport in Chylomicron Metabolism" — *Journal of Clinical Investigation* 37: 1333—1341, 1958.
11. Ghata, J., L. Salamin, J. Lewin and E. Azérad. "Action du glucose sur l'hyperlipémie alimantaire chez le sujet normal et la diabetique" — *Nutritio et Dieta* 3: 264—280, 1961.
12. Gordon, R. and A. Cherkes. "Unesterified Fatty Acid in Human Blood Plasma" — *Journal of Clinical Investigation* 35: 206—212, 1956.

13. Havel, R. and D. Fredrickson. "The Metabolism of Chylomicra. I. The Removal of Palmitic Acid-1-C^{14} Labeled Chylomicra from Dog Plasma" — *Journal of Clinical Investigation* 35: 1025—1032, 1956.
14. Lossow, W. and J. Chaikoff. "Carbohydrate Sparing of Fatty Acid Oxidation. I. The Relation of Fatty Acid Chain Length to the Degree of Sparing. II. The Mechanism by which Carbohydrate Spares the Oxidation of Palimitic Acid" — *Archives of Biochemistry and Biophysics* 57: 23—40, 1955.
15. Nešković, M., J. Bojanović, I. Kulić-Japundžić, Ž. Dželatović and M. Čorbić. "Uticaj insulina na metabolizam belančevina, lipida i glicida. I. Brzo razbistravanje plazme pasa s postprandijalnom hiperlipemijom pod dejstvom insulina" (Effect of Insulin on the Metabolism of Proteins, Lipids and Glucides. I. Rapid Clearing of Plasma in Dogs with Postprandial Hyperlipemia under the Influence of Insulin) — *Zbornik radova Medicinskog fakulteta* (Beograd) 1: 25—36, 1962.
16. Rony, H. and T. Ching. "Fat Metabolism. II. The Effect of Certain Hormones on Fat Transport" — *Endocrinology* 14: 355—363, 1930.
17. Siperstein, M. and V. Fagan. "Studies on the Relation between Glucose Oxidation and Intermediary Metabolism. I. The Influence of Glycolysis on the Synthesis of Cholesterol and Fatty Acids in Normal Liver" — *Journal of Clinical Investigation* 37: 1185—1195, 1958.

GLASNIK HEMIJSKOG DRUŠTVA, Vol. 32, No. 5-6-7, 1967, pp. 343—356

EFFECT OF INSULIN ON THE METABOLISM OF PROTEINS, LIPIDS AND GLUCIDES. X.

EFFECT OF SUCCESSIVE HYPERINSULINEMIA ON THE DISTRIBUTION OF ELECTROPHORETIC PROTEIN FRACTIONS IN THE BLOOD SERUM OF SCHIZOPHRENICS

by

JELENA J. BOJANOVIĆ, ANKA D. JEVTOVIĆ, MILANKA O. ČORBIĆ and OLGA M. BUGARSKI

The theory that the immediate effect of insulin upon blood proteins is expressed in their increased metabolism has recently acquired a more profound meaning, since experimental data suggest that insulin has an important role in the regulation of protein biosynthesis. However, the mechanism by which insulin changes the speed and perhaps the direction of protein synthesis from intracellular aminoacids in the corresponding cells is not yet completely understood.

The fact that after prolonged successive administration of large quantities of insulin it loses its marked anabolic effect on blood proteins[2, 3] has induced us to study this problem with the aim of explaining this phenomenon and the consequences of the created state.

In the present paper we shall describe the results of study on the distribution of electrophoretic fractions of blood serum proteins in persons suffering from schizophrenia, in whom hyperinsulinemia had been induced daily. Through these studies we hope to contribute towards a better understanding of the immediate and delayed insulin effect on proteins, as well as of the conditions of insulin shock treatment.

MATERIAL AND METHODS

The study of the distribution of electrophoretic protein fractions was done in the blood serum of nine schizophrenics (females) who were admitted for treatment at the University Hospital for Neurology and Psychiatry of the Belgrade Medical School. Other diseases were excluded by preliminary clinical examinations. The age of the persons under study was between 20 and 30 years. The blood was drawn on an empty stomach, just before injecting insulin, and then during the first, tenth and twentieth shock, always two and a half hours after the injection of insulin (about 20 minutes after the onset of coma). Insulin was given intramuscularly. The number of insulin units was determined on an individual basis and ranged from 100

to 150 units. The dose of insulin throughout the entire treatment remained the same for each patient. Before the start of insulin shock treatment the patients were prepared by means of administration of small doses of insulin.

Electrophoretic studies of serum proteins were done after the method of Grassmann and Hannig with platinum electrodes[7].

Total proteins were determined by the micro Kjeldahl method[4].

RESULTS

Distribution of Different Electrophoretic Protein Fractions during Successive Insulin Shocks

Absolute values

The different blood serum protein fractions in absolute values are statistically analyzed in Table 1 and Fig. 1.

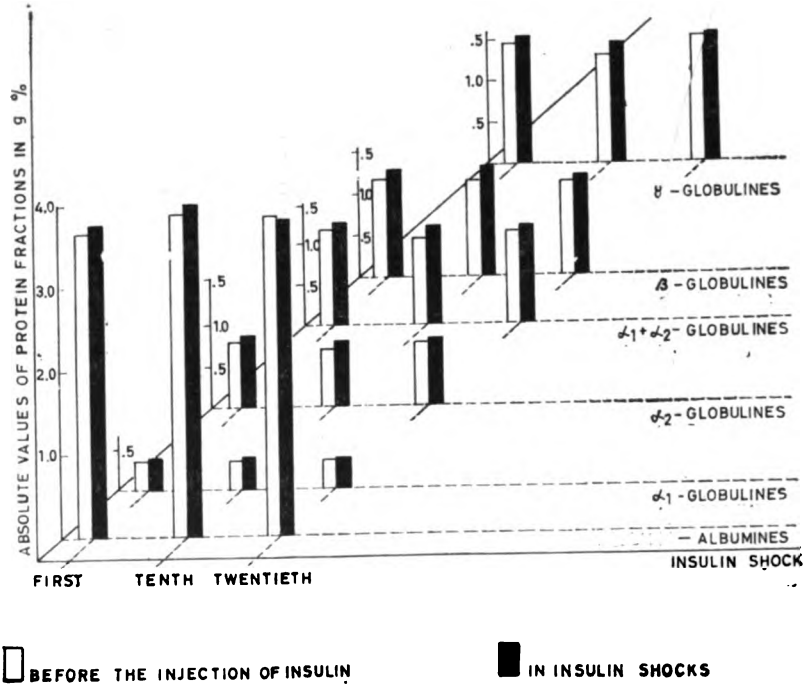

Figure 1

Absolute values of protein fractions in the blood serum of schizophrenics before the injection of insulin and in insulin shock

It was found that during the first and tenth shock the absolute values for albumins increased, although the increase was small (3% increase in comparison with the state before shock) and not statistically significant ($p > 0.05$). During the twentieth shock the mean albumin value remained practically unchanged. Nevertheless, despite such small changes, the level

of albumin during the tenth and twentieth shock was higher than before the first shock, i.e. by 10% and 4%, respectively (changes statistically significant, $p < 0.05$).

The changes of different globulin fractions during the successively induced insulin shocks mainly showed a tendency towards increase in absolute value, which was always particularly marked during the tenth and least marked during the twenteith shock.

The α_1-globulins during the observed shocks showed an increase: 6% in the first, 9% in the tenth and 6% in the twentieth shock (changes not statistically significant, $p > 0.05$). Because of the low level of α_1-globulin before shock, during the twentieth chock despite the increase of its concentration the observed values were approximately at the level found before the first shock.

The concentration of α_2-globulin during the successive shocks increased, perticularly during the tenth shock. The increase during the first shock was 9%, during the tenth 16% and during the twentieth 8%. However, despite the increase in concentration, during the tenth and twentieth shock the values were approximately at the level observed before the first shock. The changes were not statistically significant ($p > 0.05$).

The β-globulin fraction during the first and tenth shock increased by 10% and 14%, respectively, while during the twentieth shock the increase was only 6%. The change was statistically significant during the first shock ($p = 0.05$) and nonsignificant during the tenth and twentieth shock ($p > 0.05$). In all the shocks studied the level of this fraction was high despite the fact that just prior to each successive shock it was always reduced to a level approximately equal to that found before the first shock.

The level of the γ-globulin fraction increased by 8% during the first shock and 12% during the second, while during the twentieth the change was much smaller, being only 2.6%. Despite a marked increase of the γ-globuline concentration during the tenth shock, its values were at the level observed before the first insulin shock, and despite a much smaller increase during the twentieth shock the content of this fraction was high, which was determined from the changes of its level in the circulation during the successive treatment with large doses of insulin.

Relative values

The relative values of different protein fractions in the blood serum of nine persons (females) during the successive induction of insulin shocks are shown statistically analyzed in Table 2 and Fig. 2.

The percent composition of the albumin fraction decreased during all the shocks which were studied by about 3%. The changes were statistically significant ($p < 0.05$). The albumin level was lower during the first and twentieth shock and higher during the tenth compared with the values found before the first insulin shock.

The relative globulin values during the shocks showed a small increase during the observed treatment period. During the first and tenth shock there was practically no change in α_1-globuline, while during the twentieth shock their mean increased by 4%. The levels of this globulin fraction

TABLE I

Statistically analyzed absolute values of different protein fractions in the serum of schizophrenics before the injection of insulin and during insulin shocks

	Albumins						α_1-globulins					
	before I	in I	before X	in X	before XX	in XX	before I	in I	before X	in X	before XX	in XX
No.	9	9	6	6	8	8	9	9	6	6	8	8
R	46.3—52.5	43.4—54.2	46.1—58.8	48.3—54.5	47.3—54.1	44.5—52.5	3.6—6.1	3.7—6.2	3.5—7.0	3.7—5.8	3.3—6.3	3.7—5.5
M	49.4	48.1	52.6	51.2	50.3	48.9	4.8	4.8	4.7	4.7	4.5	4.7
SD	2.00	3.56	4.25	2.68	1.97	2.79	0.93	0.90	1.20	0.76	0.99	0.70
SE	0.67	1.19	1.73	1.10	0.70	0.99	0.31	0.30	0.49	0.31	0.35	0.25
CV%	4.05	7.40	8.03	5.22	3.92	5.71	19.17	18.56	25.53	16.10	22.00	14.89
a		−2.59		−2.73		−2.73		0.00		0.00		+4.44
b			+6.64		+1.80				−3.09		−7.22	
c					−4.54						−4.25	
a		$p>0.05$		$p>0.05$		$p>0.05$		—		—		$p>0.05$
b			$p>0.05$		$p>0.05$				$p>0.05$		$p>0.05$	
c					$p>0.05$						$p>0.05$	
	α_2-globulins						$\alpha_1+\alpha_2$-globulins					
No.	9	9	6	6	8	8	9	9	6	6	8	8
R	9.0—14.3	9.1—13.9	7.7—11.1	8.4—12.3	8.9—11.1	8.8—12.8	13.6—18.1	14.1—18.5	11.1—17.6	12.2—17.6	13.0—17.0	13.7—17.8
M	10.8	11.1	9.2	9.7	10.0	10.5	15.7	15.9	13.9	14.5	14.5	15.2
SD	1.54	1.40	1.35	1.53	0.78	1.18	1.39	1.46	2.34	1.96	1.19	1.38
SE	0.51	0.47	0.55	0.62	0.27	0.42	0.46	0.49	0.95	0.80	0.42	0.49
CV%	14.21	12.61	14.59	15.71	7.79	11.18	8.86	9.16	16.77	13.55	8.21	9.05
a		+2.40		+5.30		+5.39		+1.66		+3.66		+5.17
b			−14.67		−7.66				−11.03		−7.53	
c					8.22						+3.94	
a		$p>0.05$		$p>0.05$		$p>0.05$		$p>0.05$		$p>0.05$		$p>0.05$
b			$p>0.05$		$p>0.05$				$p>0.05$		$p>0.05$	
c					$p>0.05$						$p>0.05$	

β-globulins						
No.	9	9	6	6	8	8
R	13.2—19.1	14.1—18.4	13.4—17.6	13.4—19.0	13.1—16.7	14.0—17.2
M	15.8	16.4	15.2	15.8	15.1	15.7
SD	2.02	1.36	1.60	1.98	1.33	1.04
SE	0.67	0.45	0.65	0.81	0.47	0.37
CV%	12.79	8.27	10.55	12.55	8.80	6.61
a		+4.18		+3.95		+4.17
b			−3.93		−4.31	
c					−0.40	
a		*p*>0.05		*p*>0.05		*p*>0.05
b			*p*>0.05		*p*>0.05	
c					*p*>0.05	

A/G						
No.	9	9	6	6	8	8
R	0.86—1.11	0.77—1.18	0.86—1.43	0.93—1.20	0.90—1.17	0.80—1.10
M	0.98	0 93	1.13	1.05	1.01	0.96
SD	0.08	0.13	0.19	0.11	0.08	0.10
SE	0.03	0.04	0.08	0.05	0.03	0.04
CV%	8.16	13.98	16.81	10.48	7.92	10.42
a		−5.10		−7.08		−4.95
b			+15.31		+3.06	
c					−10.62	
a		*p*>0.05		*p*>0.05		*p*>0.05
b			*p*>0.05		*p*>0.05	
c					*p*>0.05	

γ-globulins						
9	9	6	6	8	8
16.9—23.4	15.3—24.2	14.2—20.9	16.5—21.1	17.9—21.9	17.0—23.7
19.?	19.5	18.2	18.5	20.1	20.1
2.06	3.35	2.42	1.52	1.54	2.42
0.69	1.12	0.99	0.62	0.54	0.85
10.71	17.17	13.28	8.19	7.65	12.01
	+ 1.40		+ 1.81		0.00
		−5.30		+4.57	
				+ 10.43	
	p>0.05		*p*>0.05		—
		p>0.05		*p*>0.05	
				p>0.05	

No. — number of cases
R — range
M — mean
SD — standard deviation
SE — standard error
CV% — coefficient of variation

% of decrease or increase and level of significance are given relative to values before the same shock (a), relative to values before the first shock (b) and relative to values 24 hours after the ninth shock

TABLE 2

Statistically analyzed relative values of different protein fractions in the serum of schizophrenics before the injection of insulin and during insulin shocks

	Albumins						α_1 — globulins					
	before I	in I	before X	in X	before XX	in XX	before I	in I	before X	in X	before XX	in XX
No	9	9	6	6	8	8	9	9	6	6	8	8
R	3.42—3.89	3.44—4.06	3.55—4.29	3.69—4.45	3.56—4.15	3.51—4.11	0.28—0.46	0.28—0.51	0.26—0.54	0.33—0.46	0.25—0.48	0.28—0.43
M	3.65	3.76	3.87	4.00	3.85	3.81	0.36	0.38	0.35	0.38	0.34	0.36
SD	0.14	0.17	0.26	0.27	0.20	0.19	0.07	0.08	0.10	0.05	0.07	0.06
SE	0.05	0.06	0.11	0.11	0.07	0.07	0.02	0.03	0.04	0.02	0.02	0.02
CV %	3.83	4.52	6.72	6.75	5.19	4.99	19.44	21.05	28.57	13.16	20.59	16.67
a		+3.01		+3.36				+5.55		+8.57		+5.88
b			+6.03		+5.19	—1.04			—2.78		—5.55	
c					—0.52						—2.86	
a		$p>0.05$		$p>0.05$		$p>0.05$		$p>0.05$		$p>0.05$		$p>0.05$
b			$p=0.05$		$p<0.05$				$p>0.05$		$p>0.05$	
c					$p>0.05$						$p>0.05$	

α_2-globulins

No	9	9	6	6	8	8
R	0.62—1.12	0.72—1.14	0.56—0.90	0.70—1.00	0.67—0.92	0.69—1.07
M	0.80	0.87	0.69	0.80	0.76	0.82
SD	0.14	0.13	0.13	0.11	0.08	0.11
SE	0.05	0.04	0.05	0.05	0.03	0.04
CV %	17.50	14.94	18.84	13.75	10.53	13.41
a		+8.75		+15.94		+7.89
b			—13.75		— 5.00	
c					+10.14	
a		$p>0.05$		$p>0.05$		$p>0.05$
b			$p>0.05$		$p>0.05$	
c					$p>0.05$	

$\alpha_1+\alpha_2^-$-globulins

9	9	6	6	8	8
0.94—1.41	1.06—1.51	0.81—1.36	1.07—1.43	1.01—1.28	1.06—1.49
1.16	1.25	1.03	1.19	1.11	1.19
0.14	0.14	0.21	0.13	0.10	0.14
0.05	0.05	0.09	0.05	0.03	0.05
12.07	11.20	20.39	10.92	9.01	11.76
	+7.76		+15.53		+7.21
		—11.21		—4.31	
				+7.77	
	$p>0.05$		$p>0.05$		$p>0.05$
		$p>0.05$		$p>0.05$	
				$p>0.05$	

β-globulins

No	9	9	6	6	8	8
R	1.01—1.45	1.14—1.44	0.99—1.26	1.04—1.51	1.06—1.33	1.10—1.34
M	1.17	1.29	1.16	1.32	1.15	1.22
SD	0.15	0.11	0.10	0.17	0.09	0.07
SE	0.05	0.04	0.04	0.07	0.03	0.02
CV %	12.82	8.53	8.62	12.88	7.83	5.74
a		+10.26		+13.79		+6.09
b			—0.85		—1.71	
c					—0.86	
a		$p=0.05$		$p>0.05$		$p>0.05$
b			$p>0.05$		$p>0.5$	
c					$p>0.5$	

γ-globulins

9	9	6	6	8	8
1.18—1.76	1.13—1.96	1.04—1.56	1.35—1.64	1.28—1.78	1.31—1.92
1.43	1.54	1.30	1.46	1.53	1.57
0.20	0.32	0.19	0.11	0.16	0.22
0.07	0.10	0.08	0.04	0.06	0.07
13.99	20.78	14.61	7.53	10.46	14.01
	+7.69		+12.31		+2.61
		—9.09		+6.99	
				+17.69	
	$p>0.05$		$p>0.05$		$p>0.05$
		$p>0.05$		$p>0.05$	
				$p<0.05$	

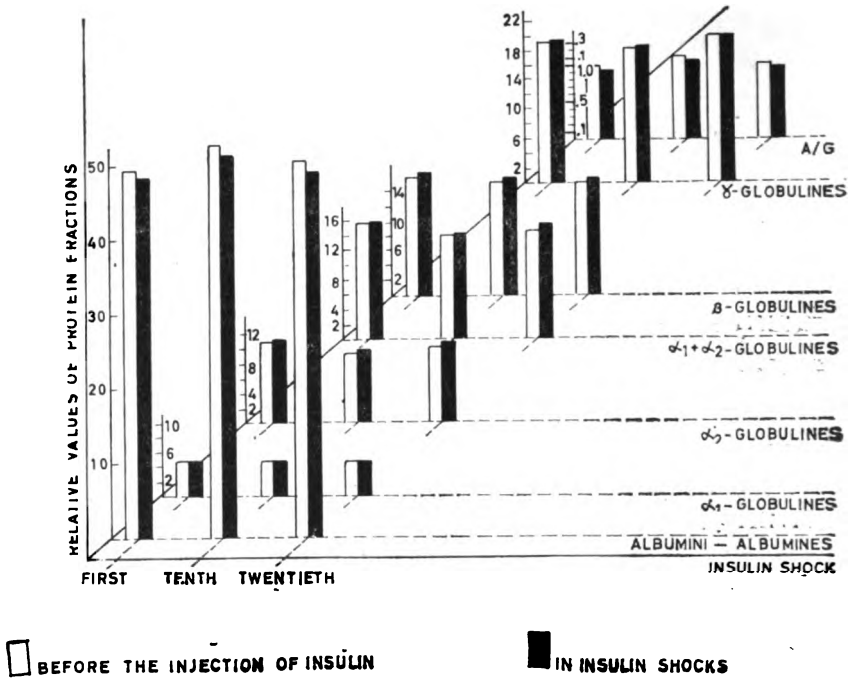

Figure 2

Relative values of protein fractions in the blood serum of schizophrenics before the injection of insulin and in insulin shock

during the shocks did not differ from the levels found before the first insulin shock.

The relative values of α_2-globulins during the shocks increased. During the first shock the level was increased by 2%, and during the tenth and twentieth shock by 5% (changes statistically nonsignificant, $p > 0.05$). The levels of α_2-globulins during the tenth and twentieth shock were lower than just before the first insulin shock.

The β-globulins were increased during all the shocks studied by about 4%, and their level fell so that during the twentieth shock it reached the level found before the first insulin shock.

The changes in the percent composition of γ-globulins during the shocks were small. During the first shock the increase was 1.4%, during the tenth 1.8%, while during the twentieth shock there was no change. However, although these changes were negligibly small, the level of γ-globulins during the shocks was different during the observed treatment period. During the first shock the level of γ-globulins was slightly higher than before the injection of insulin, during the tenth it was below this level, and during the twentieth there was again an increase of the level so that it was much higher than before the first insulin shock.

The albumin/globulin ratio changed during the period of observation, so that during the insulin shocks there was a decrease, most marked during the tenth shock (7%), although at that time the level was higher than before the first shock. The change of this ratio during the first and tenth shock was even smaller and statistically insignificant ($p > 0.05$).

Distribution of Different Electrophoretic Protein Fractions 24 Hours after the Successively Induced Insulin Shocks

Absolute values

The protein fractions several hours after the administration of insulin are statistically analyzed in Table 1 and presented graphically in Fig. 3.

During the successive administration of insulin the level of albumin in the circulation increased. Twenty-four hours after the ninth shock the increase was 6%, and after the nineteenth it was 5% in comparison with the level before the first shock (the changes were significant at the 5% level).

Globulins showed lower values than before the induction of insulin shocks and during the shocks.

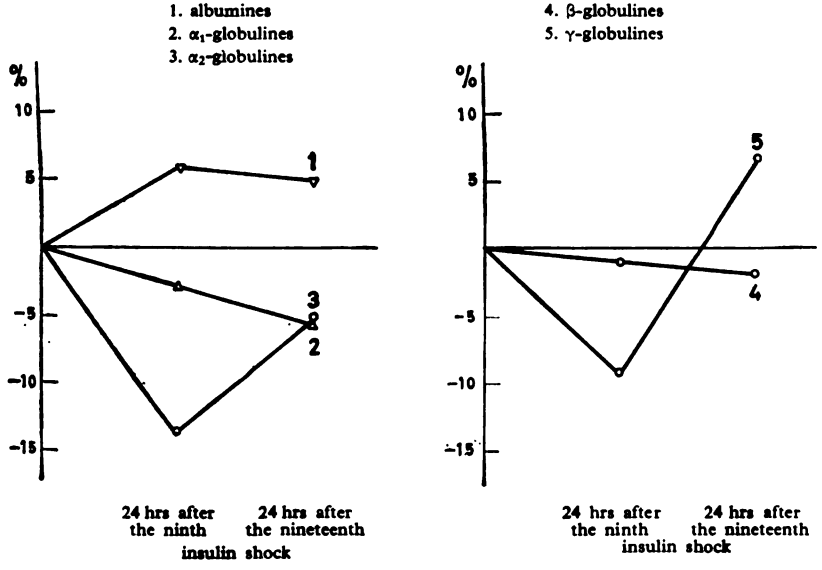

Figure 3

Changes in the absolute values of protein fractions in the blood serum of schizophrenics 24 hours after insulin shock (given in percent decrease or increase)

α_1-globulins 24 hours after the ninth shock were lower by 3% and after the nineteenth shock by 6% in comparison with the level before the first shock, but these changes were statistically nonsignificant ($p > 0.05$).

With α_2-globulins there was a decrease of 14% after the ninth and of 5% after the nineteenth shock in comparison with the state before the administration of insulin. These changes were also statistically nonsignificant ($p > 0.05$).

The concentration of β-globulins, expressed in absolute values, changed little several hours after the administration of glucose. Twenty-four hours after the ninth insulin shock the values of β-globulins were lower by 1% and after the nineteenth shock by 2% than before the first insulin shock. The changes were statistically nonsignificant ($p > 0.05$).

The values of the γ-globulin fraction also changed after the administration of insulin during the observed treatment period, but the changes of this fraction were somewhat more marked. 24 hours after nine successive insulin shocks there was a decrease of 9% (change statistically nonsignificant, $p > 0.05$). However, after nineteen shocks the values of γ-globulins were 7% higher than before the first insulin shock (change statistically nonsignificant, $p > 0.05$), and 18% higher than 24 hours after the ninth successive insulin shock (change statistically significant, $p < 0.05$).

Relative values

The relative values of different protein fractions several hours after the administration of insulin are statistically analyzed in Table 2 and presented graphically in Fig. 4.

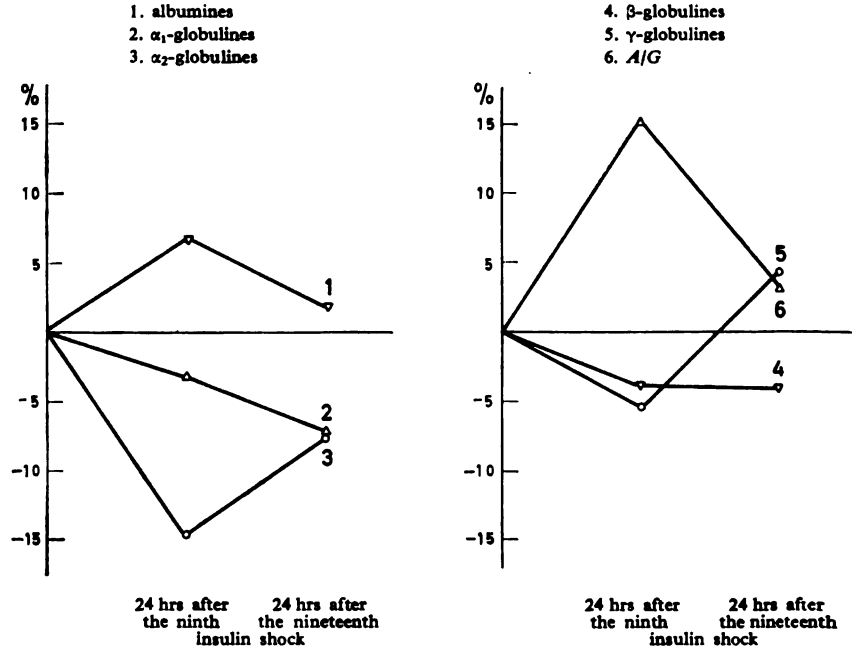

Figure 4

Changes in the relative values of protein fractions in the blood serum of schizophrenics 24 hours after insulin shock (given in percent decrease or increase)

The initial composition of the serum albumin fraction increased 24 hours after the administration of insulin during insulin shock treatment. After nine successive shocks the percent composition of albumin was 7% higher than before the first insulin shock, and after the nineteenth shock the increase was much less, being about 2%. These changes were statistically nonsignificant ($p > 0.05$).

The percent composition of globulins in the majority of cases decreased. The values for α_1-globulins 24 hours after the ninth shock were about 3% lower, and after the nineteenth shock about 7% lower than before the first shock. These changes were statistically nonsignificant ($p > 0.05$).

Twenty-four hours after the ninth successive shock the values of α_2-globulins were 15% lower, and after nineteen shocks 8% lower than before the first shock. These changes were statistically nonsignificant ($p > 0.05$).

The percent composition of β-globulins also decreased after nine and nineteen insulin shock — by 4% (the change not statistically significant, $p > 0.05$).

The concentration of γ-globulin, in comparison with its value before the first shock, after nine successive shocks was 5% lower, and after ninetteen shocks 5% higher. The difference in the γ-globulin level after nine and after nineteen shocks was 10%. These changes were statistically nonsignificant ($p > 0.05$).

The value of the A/G ratio was the highest 24 hours after the ninth shock (increase of 15%), but this change was not statistically significant ($p > 0.05$), while after nineteen shocks this ratio was 11% lower than after nine shocks, i.e. the increase in comparison with its value before the shocks was only 3%. The change was statistically nonsignificant ($p > 0.05$).

DISCUSSION

The fact that the state of total proteins changed during successive hyperinsulinemias[2, 3] has posed a question about the quality of these proteins. The question seems even more justified in the light of the results on the distribution of electrophoretic protein fractions during hypoglycemic shock induced by a single insulin injection. Gottfried[6] found that in insulin coma the ratio of albumin and globulin concentrations was not changed (except for a slight increase of pseudoglobulins), and Kaudritzer and Berrera[8] found that euglobulin values at this time were somewhat lower. Contrary to these findings, Saito[13] observed that during insulin coma the relative content of globulins was increased, which was confirmed by Noguchi[12], who studied the effect of insulin on the proteins of dog plasma and lymph.

In schizophrenics, although the concentration of total proteins is within the limits of normal values*, there are differences in the distribution of different electrophoretic fractions. Scoppa and Ventra[14] reported lower albumin values in these patients, while the globulin values were higher than in the serum of healthy persons, and he stated that these differences

* The values used for comparison were obtained from healthy persons of the same age and sex[9, 11, 1].

were caused by deficient protein synthesis and the state created by this disease. Kel'mishkeit and co-workers[9, 10] found that in these cases α-globulins had higher values and γ-globulins lower, while Chumburidze[5] reported that besides the increase of α-globulin levels, in catatonic schizophrenia there was also an increase of β-globulins. Our results on the distribution of electrophoretic protein fractions in the serum of schizophrenics before the first insulin shock were in partial agreement with the results of Scoppa and Ventra[14], as we found that in these patients the relative albumin values were 18% lower, and the γ-globulins 24% higher than in normal persons[1]. Besides, according to our electrophoregrams there was a difference in the β-globulin fraction, which was 40% higher than normal. However, for α_1-globulins we found that the level was unchanged, and α_2-globulins also had the same maximal values as in healthy persons of the same sex and age. With such a pattern of electrophoretic protein mobility in the persons under study, the observed changes during the successive insulin shocks and 24 hours after the administration of insulin suggested the existence of a difference in the quality of serum proteins and in the intensity of the insulin effect, particularly with a prolonged insulin effect.

Although the changes of the relative albumin values during the successive hyperinsulinemias were small and statistically nonsignificant, their ratio with globulins was changed. Somewhat lower initial albumin content was found in all the cases under study, but its level during the tenth and twentieth shock was higher than during the first. In the globulin fractions there was a small increase, except with α_1-globulins, the content of which did not change, and with γ-globulins, in which the changes were negligibly small. During the tenth and twentieth shock the level of globulin fractions was usually lower than during the first shock, which was particularly marked during the tenth. However, the changes in absolute values of all protein fractions were greater than with the relative values. The absolute values of the different fractions during all the shocks studied increased, which was particularly marked during the tenth shock. This change was, however, much greater in the globulin fractions than in albumin, in which during the first and the tenth shock the increase was negligibly small, and during the twentieth shock failed to occur. The changes in the globulin fractions were in positive correlation with the changes of total proteins.

On the basis of these results and of the A/G ratio it may be concluded that successive administration of large doses of insulin affects the composition of the blood proteins. The reason for this might lie in different conditions under which the anabolic processes take place, or in the fact that under these conditions proteins undergo certain changes, which causes different electrophoretic mobility of the proteins.

Our studies of the prolonged insulin effect have so far produced a very complex pattern of relationships, particularly in repeated hyperinsulinemias. It was found that the content of total proteins, polypeptides and free amino acids in the serum of persons undergoing successive insulin shocks (schizophrenia) was changed 24 hours after the injection of insulin, and that the changes reflecting prolonged insulin effect were not of the same type and intensity during the period of observation[3]. In the distribution of electrophoretic protein fractions 24 hours after the administration of insulin there were changes in the ratio of different fractions. Albumin levels were increased

(change statistically nonsignificant) both in the relative and in the aboslute sense, and the globulins were decreased, with the exception of γ-globulin after nineteen shocks, in which at that time there was a small increase. The greatest decrease in globulin fractions was noted with α_2-globulins. A great difference in the A/G ratio was particularly marked after nine insulin shocks. That is, the level of albumin which in persons suffering from schizophrenia had low values in comparison with the normal values, during the phase of prolonged insulin effect, 24 hours after the administration of insulin, showed a tendency towards increase. Globulins, which had higher values in persons suffering from schizophrenia, their level being further increased during insulin shock, were decreased during the phase of prolonged insulin effect (with the exception of γ-globulins after nineteen shocks). These results suggest a reparative effect of insulin on serum proteins in schizophrenics during insulin shock treatment, this effect being most marked after nine shocks and reduced after nineteen shocks.

Further studies in this field are aimed at investigating the nature of the changes which take place in the protein complex during successive hyperinsulinemias and at the significance of these changes for the state of the organism.

CONCLUSION

1. The distribution of electrophoretic proteins fractions in the blood serum of persons suffering from schizophrenia (females) suggest that the ratio of albumins and globulins, which is established during the insulin shock, changes during successive hyperinsulinemias.

2. During successively induced insulin shocks, in the phase of prolonged insulin effect, 24 hours after the administration of insulin, the level of albumins and globulins changes, approaching the normal values for the different fractions. This reparative effect of insulin was most marked after nine insuline shocks and reduced after nineteen shocks.

Institute of Chemistry,
Belgrade Medical School

Received 10 April, 1967

REFERENCES

1. Böhle, E., K. Böttcher, H. Piekarski and R. Biegler. "Die Serumlipoproteide und ihre Beziehungen zu den Protein und Lipidfraktionen des Blutes unter Berücksichtigung von Alter und Geschlecht" — *Deutsches Archiv für klinische Medizin* 203: 29—51, 1956.
2. Bojanović, J., A. Jevtović and P. Milošević. — (unpublished results).
3. Bojanović, J., A. Jevtović, M. Čorbić and K. Nikolić. "Uticaj insulina na metabolizam belančevina, lipida i glicida. V. Dejstvo uzastopnih hiperinsulinemija na belančevine krvnog seruma" (Effect of Insulin on the Metabolism of Proteins, Lipids and Glycids. V. Effect of Successive Hyperinsulinemias on Blood Serum Proteins) — *Glasnik Hemijskog društva* (Beograd) 28: 465—477, 1963.
4. Bojanović, J., M. Čorbić, A. Jevtović and S. Šibalić. "Prilog metodama odredivanja azotnih materija u biološkom materijalu. I. Mikro metoda za odredivanje azotnih sastojaka krvnog seruma ili plazme" (Methods for the Determination of Nitrogen Substances in Biologic Material. I. A Micro Method for the Determination of Nitrogen Constituents of Blood Serum or Plasma) — *Glasnik Hemijskog društva* (Beograd) 25—26: 361—366, 1961.
5. Chumburidze, R. "The Dynamics of the Composition of Blood in Schizophrenic Patients during Treatment" — *Obmen Veshchestv pri Psikhicheskih Zabolevaniiakh* (Institut Psikhiatrii Akademii Meditsinkikh Nauk) 99—106, 1959, in: *Chemical Abstracts* 55: 17861, 1961.
6. Gottfried, S. "Serum Protein-Fractionation Studies on Schizophrenics" — *Psychosomatic Medicine* 11: 334—337, 1949, in: *Chemical Abstracts* 44: 6008, 1950.
7. Grassmann, W. and K. Hannig. "Ein quantitatives Verfahren zur Analyse der Serumproteine durch Papierelektrophorese" — *Hoppe-Seyler's Zeitschrift für Physiologische Chemie* 290: 1—27, 1952.
8. Kondritzer, A. and S. Barrera. "A Study of Serum Proteins in Mental Disease" — *The Psychiatric Quarterly* 15: 336—342, 1941, in: *Chemical Abstracts* 35: 4091, 1941.
9. Kel'mishkeit, E. "Comparative Biochemical Study in Patients with Involutionary Psychosis and with Progressive Schizophrenia" — *Obmen Veshchestv pri Psikhicheskikh Zabolevaniiakh* (Institut Psikhiatrii Akademii Meditsinskikh Nauk) 94—98, in: *Chemical Abstracts* 55: 17860, 1961.
10. Kel'mishkeit, E. and A. Sigrist. "The Protein and Protein Fractions in Blood Serum of the Normal and Schizophrenic Individuals in Correlation to Age" — *Obmen Veshchestv pri Psikhicheskikh Zabolevaniiakh* (Institut Psikhiatrii Akademii Meditsinskikh Nauk) 85—93, 1959, in: *Chemical Abstracts* 55: 17860, 1961.
11. Nešković, M., J. Bojanović, A. A. Jevtović and M. Čorbić. — (unpublished results).
12. Noguchi, H. "Changes in the Distribution of Protein in Plasma and Thoracic Lymph, Induced by Insulin Shock. I. Changes in the Distribution of Plasma Proteins Induced by Insulin Shock" — *Nisshin Igaku* 39: 35—42, 1952, in: *Chemical Abstracts* 48: 8418, 1954.
13. Saito, G. "The Condition of Insulin Shock" — *Japanese Journal of Medical Sciences VII. Social Medicine and Hygiene* 3: 163—164, 1940, in: *Chemical Abstracts* 37: 4465, 1943.
14. Scoppa, A. and F. Ventra. "Serum Protein Picture in Patients with Schizophrenia by the Electrophoretic Technique" — *Acta Neurologica* (Napoli) 11: 816—831, 1956, in: *Chemical Abstracts* 52: 15723, 1958.

GLASNIK HEMIJSKOG DRUŠTVA, Vol. 32, No, 5-6-7, 1967, pp. 357—363

METALLOGRAPHIC STUDY OF THE INITIAL STAGE OF TRANSFORMATION OF THE GAMMA-PHASE IN URANIUM-NIOBIUM ALLOY

by

BRANKO LJ. ĐURIĆ and ALEKSANDAR Z. MIHAJLOVIĆ

INTRODUCTION

Morphological characteristics of the products of proeutectoid decomposition of austenite in iron alloys have been studied in great detail and classified. It has been shown that these investigations have a more general meaning and can be applied to a series of other phenomena, such as, precipitation from oversaturated solid solutions, aging, arranging, etc., in different alloys.

In the present study we have investigated the early stage of decomposition of the gamma-phase in an alloy of uranium with 1.85 weight % niobium during isothermal treatment in the range of diffusion transformation, with the aim of finding out the characteristics common with the products of austenite decomposition. In doing this, using only metallographic techniques, we limited our interest to morphological similarities.

EXPERIMENTAL

The uranium alloy used contained 1.85 weight % niobium (Mihajlović, Drobnjak and Wilkinson)[1]. The total content of metal impurities was below 500 ppm.

Homogenized samples (Ø 5 × 5 *mm*) were heated for a short time in the gamma-range (about 850°C), then quickly cooled to the temperature of isothermal treatment and after a certain time hardened in water. The temperature range within which the samples were isothermally treated was between 640 and 685°C, where the transformation of the gamma-phase occurs through the mechanism of germ formation and their growth by diffusion[2].

The samples, after hardening in water, were studied under the microscope. The usual metallographic preparation was used[2].

NOMENCLATURE

As this was, in our knowledge, the first attempt in Yugoslavia to apply systematically the terms of morphological classification of the products of proeutectoid decomposition of austenite which were developed by Dubé

and Aaronson[3], we faced the problem of creating corresponding Serbo-Croat terms. In the further text we shall use the following terms for the different morphological forms which appear in the alloy under study and correspond to descriptions from the mentioned classification:

Grain boundary allotriomorphs. These are the crystals whose germs are formed at grain boundaries and which grow mainly along these boundaries.

Widmanstätten sideplates or needles are plate-like crystals which grow from the grain boundaries towards the interior of the grains. The primary Widmanstätten sideplates grow directly from the boundary, and the secondary ones develop on crystals of different form (but of the same phase), usually on grain boundary allotriomorphs.

Widmanstätten sawteeth have a triangular form in the metallographic section and develop in the same way as the plates, either on grain boundaries (primary sawteeth) or on other forms (secondary sawteeth).

Widmanstätten intragranular plates or needles are plate-like or needle-shaped crystals whose germs are formed in the interior of the grains.

Idiomorphs are polygonal crystals which appear both on grain boundaries and in the interior of the grains.

Massive structures are not a special form of crystals as they develop by fusion of crystals of other forms. Most often they have the form of polygonal masses in their microstructure.

The marking of the phases of the uranium-niobium alloy was done in accordance with the nomenclature for uranium alloys by Lehmann and Hills[4].

RESULTS

By means of hardening in water the form of the products of transformation at the elevated temperature was preserved, but the high-temperature phases underwent transformation. The gamma-phase, which did not disintegrate at the temperature of isothermal treatment, was martensitically transformed into the metastable α'_{α} — phase. It seems that the niobium content was not suitable for stabilization of the proeutectoid beta-phase, so that only the alfa-phase was observed at room temperature.

Grain boundary allotriomorphs

Typical grain boundary allotriomorphs appeared practically on all the boundaries of the gama-phase grains if the transformation occurred at a temperature above 670°C. They had the shape of elongated lamellas which become narrower towards the ends (Fig. 1). Their growth, which was much faster longitudinally than laterally, continued in most cases alongside the boundaries until fusion occurred with the next lamella, the same as in the case of proeutectoid ferrite and cementite. However, it often happened that groups of adjoining lamellas grew parallel to each other in some direction different from the direction of the boundary on which their germs were formed (Fig. 2). These were probably cases of lamellar growth along certain crystallographic plates of the maternal gamma-phase.

The absence of geometrically regular edges does not necessarily imply the absence of a certain cristallographic connection of the grain boundary allotriomorphs with the base. Such a connection was found in austenite decomposition[3]. It was not possible to determine directly the orientational

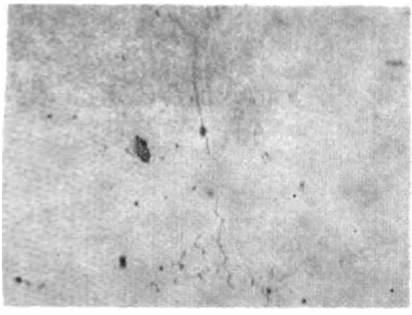

Figure 1

U-1.85% *Nb*. 25 min at 680°C. Ordinary light, 750 ×

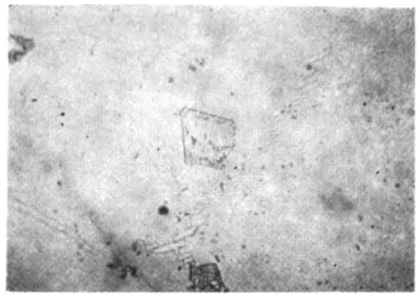

Figure 2

U-1.85% *Nb*. 25 min at 680°C. Ordinary light, 500 ×

dependency of the transformation products on the gamma-phase (for the alloy *U*-1.85% *Nb*) at room temperature, as it was transformed during hardening into the martensitic alfa-phase.

Further growth of grain boundary allotriomorphs, both longitudinally and sideways, led to their fusion and almost complete unification, so that it was very difficult to discover metallographically the boundary between two lamellas. Soon after this all the gamma-grain boundaries were continuously occupied by grain boundary allotriomorphs. Their development continued by slow spreading and separation of the secondary Widmanstätten sideplates.

Widmanstätten sideplates

In the alloy under study, Widmanstätten sideplates appeared abundantly in all three varieties: as primary and secondary sideplates and as intragranular sideplates.

Primary sideplates

The isothermal transformation of the gamma-phase in the temperature range between 640 and 670°C began by separation of primary Wid-

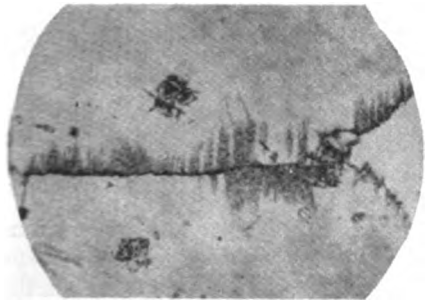

Figure 3

U-1.85% *Nb*. 30 sec at 645°C. Ordinary light, 650 ×

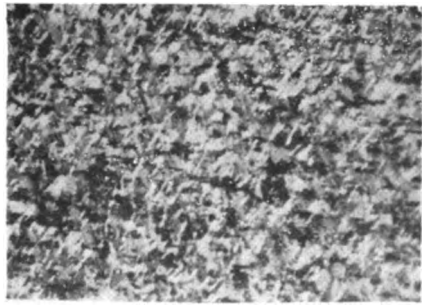

Figure 4

U-1.85% *Nb*. 2 min at 660°C. Polarized light, 150 ×

manstätten sideplates on almost all the boundaries of the maternal phase. In the metallographic section they had the form of thin needles which set apart from the grain boundaries in parallel sheaves (Fig. 3). The neighboring needles were very close to each other and grew almost exclusively lengthwise, leaving between themselves thin lamellas of the maternal phase.

The parallel distribution of the needles which developed within a single gamma-grain quite convincingly suggests that the growth took place along certain planes of the gamma-phase and, therefore, that there probably exists a certain degree of orientation dependency of the products on the maternal phase. All the needles within one sheaf had identical crystallographic orientation, which is seen from the fact that the whole sheaf reacted in the same way to polarized light, forming the so-called alfa-grain (Fig. 4).

Intragranular plates

It is often difficult to decide whether a plate which appears in the metallographic section unrelated to the grain boundary has in fact the germ in the grain or originates from some boundary not visible in the given section or which metallographically has not been discovered. This can be stated with certainty for the plates which have been formed at the connections, and with great probability for the plates which are in the middle of a grain in large-grain samples and which have around them plates which have developed along the second habital plane.

The metallographic appearance of intragranular plates was similar to the forms which developed on the boundaries of the maternal phase grains, i.e., at higher temperatures they had a form similar to grain boundary allotriomorphs, and at lower temperatures similar to primary Widmanstätten sideplates. The sites of connection seem to be as suitable for the development of new phase germs as the grain boundaries, so that it is impossible to state with certainty that the process of gamma-phase decomposition starts by separation on the boundaries.

With respect to the wealth of forms, the plates separated at higher temperatures — in the range where grain boundary allotriomorphs are formed — are doubtlessly more interesting. Quite frequently a plate seemingly changed habital plane and continued to grow along another plane which formed a very small angle with the original one. However, this was not a single plate, but a series of fused plates which grew independently along the other habital plane (Fig. 5). It is possible that we are dealing here with a case of the so-called "sympathetic nucleation", i.e., one plate serving as the center for the development of germs for another one[3].

Secondary sideplates

These were developed on almost all grain boundary allotriomorphs and intragranular plates at temperatures above 670°C, in the intermediary stages of transformation.

Secondary sideplates were formed in such a way that in a grain boundary allotriomorph (or in an intragranular plate) a growth of irregular shape developed which continued to grow in a direction which depended on the orientation of the grain (Fig. 6). The growths usually appeared in groups, the side plates formed from these groups continuing to grow parallel to one another.

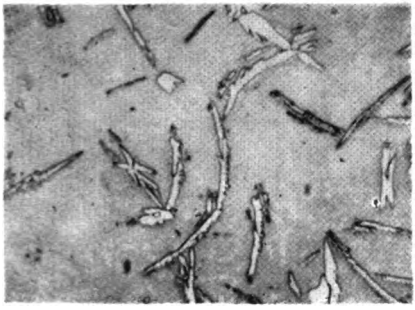

Figure 5

U-1.85% *Nb.* 8 min at 670°C. Ordinary light, 750 ×

Figure 6

U-1.85% *Nb.* 30 min at 680°C. Ordinary light, 750 ×

It was typical of the alloy under study that the secondary sideplates developed on allotriomorphs only up to a certain degree, and that the formation and growth of intragranular plates were much more marked in the intermediary stage of the reaction. Some of them seemed to have formed germs with allotriomorphs. There were also examples of further growth of sideplates into long plates.

Other Forms

The other morphological forms which appear less frequently in proeutectoid austenite decomposition were also noticed less frequently in the alloy under study.

An example of primary Widmanstätten sawteeth is shown in Fig. 7. This was a case of triangular precipitates which developed on the very boundary of gamma-grains. Similar forms are sometimes seen on the grain boundary allotriomorphs, but it is difficult to distinguish these from the secondary sideplates.

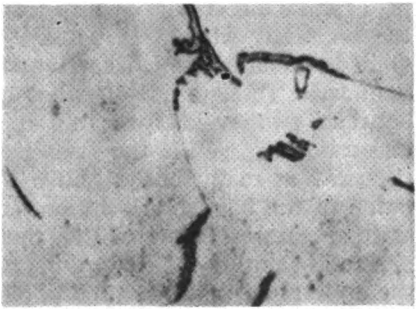

Figure 7

U-1.85% *Nb.* 6 min at 670°C. Ordinary light, 1000 ×

Idiomorphs are approximately polygonal crystals at the base, but in the special case of the alloy under study it was difficult to separate them metallographically from nonmetal inclusions.

Massive structures do not represent a separate type of structure. They develop through growth and fusion of various other forms.

DISCUSSION

The results show a great similarity between the products of proeutectoid austenite decomposition and the gamma-phase of the alloy *U*-1.85 weight % *Nb*. The classification of Dubé-Aaronson can be fully applied to the morphological forms which develop from decomposition of the gamma-phase of UNb alloy. However, by comparing the conditions of formation of different morphological forms, one can notice that there are certain differences between the alloy of iron and the alloy under study.

The association of the precipitate with the structure of the base was more clearly visible with the U-Nb system. While the formation of grain boundary allotriomorphs takes place on the boundaries, the growth often continues along certain planes of the maternal phase which do not run parallel to these boundaries.

From the structural point of view, the relationship between the gamma-phase and the precipitated alfa and beta phases is more similar to the relationship between austenite and cementite than between austenite and ferrite. Cementite has a complex orthorhombic structure and during the formation of cementite germs in the austenite base there are a number of habital planes over which the two phases can establish the relationship[5, 6], in contrast to structurally simple ferrite which has a limited number of possibilities for establishing relationships with austenite[5]. The alloy under study showed a great number of habital planes, particularly with intragranular plates. The composition of the alloy under study was not suitable for a precise determination of the orientation relations between the maternal and precipitated phase.

With the *U-Nb* alloy during the early stages of gamma-phase decomposition there was abundant separation of intragranular plates, so that secondary Widmanstätten plates on grain boundary allotriomorphs were less frequently formed.

The difference was particularly marked between the appearance of primary Widmanstätten sideplates in the case of austenite and the alloy under study. With austenite the formation of primary Widmanstätten sideplates was a direct consequence of the grain boundary structure: they appeared concomitantly with grain boundary allotriomorphs on about 2—3% of the grain boundaries, which corresponded to the percentage of the dislocation boundaries (boundaries on which a semicoherent connection is established between two grains over an approximately two-dimensional network of dislocations)[3]. With the U-Nb alloy the grain boundary allotriomorphs appeared at temperatures above 670°C, therefore in the range of precipitation of the beta solid solution, and the primary Widmanstätten sideplates at temperatures below 670°C, therefore in the range of separation of the alfa solid solution[2],. Here, thus, we are faced with a phenomenon in which the appearance of certain morphological forms is associated with the nature of the separated phase, in contrast to the case of austenite decomposition, in wich different morphological forms appear during the separation of the same phase.

Although a complete analysis of the common characteristics of the process of austenite decomposition and of the gamma-phase of uranium-niobium alloy requires complementary crystallographic and kinetic studies,

already on the basis of this metallographic study the conclusion may be drawn that there exists a marked similarity. Therefore, it can be reasonable expected that it will be possible to apply the relatively well developed apparatus of thermodynamic and kinetic analysis, which exists for cases of iron alloy, to uranium alloys, in which direction this study will be continued. The fact that in the iron-carbon alloy the alloy-forming component is interstitial, while in the uranium-niobium alloy it is supstitutional, seems to be of little significance, as identical morphological forms have been found in a series of other supstitutional alloys (*Al-Ag*, *Cu-Zn*, *Ti-Cr*, etc.).

Laboratory for Reactor Materials,
Institute for Nuclear Sciences "Boris Kidrič",
Vinča — Belgrade

Received 1 June, 1966

REFERENCES

1. Mihajlović, A., Đ. Drobnjak and W. Wilkinson. *Progress Report No. 1* — International Institute for Nuclear Sciences and Engineering, Argone National Laboratory, 1962.
2. Đurić, B. — *Bulletin of the Boris Kidrič Institute of Nuclear Sciences* (Beograd) 16 (3): 151, 1965.
3. Aaronson, H. in: Zackay, V. and H. Aaronson. *Decomposition of Austenite by Diffusional Processes* — New York: Interscience Publishers, 1962, p. 387.
4. Lehmann, J. and R. Hills. — *Journal of Nuclear Materials* 2 (3): 261, 1960.
5. Mehl, R., C. Barret and D. Smith. — *Transactions AIME* 105: 215, 1933, cited in: Zackay, V. and H. Aaronson. *Decomposition of Austenite by Diffusional Processes* — New York: Interscience Publishers, 1962.
6. Heckel, R., J. Smith and H. Paxton. — *Transactions AIME* 218 (3): 566, 1960.

Izdavač:

IZDAVAČKO PREDUZEĆE "NOLIT", BEOGRAD TERAZIJE 27/II

*

Štampa:

GRAFIČKO PREDUZEĆE "PROSVETA", BEOGRAD.
ĐURE ĐAKOVIĆA 21

SRPSKO HEMIJSKO DRUŠTVO (BEOGRAD)

BULLETIN OF THE CHEMICAL SOCIETY Belgrade

(Glasnik Hemijskog društva — Beograd)
Vol. 32, No. 8-9-10, 1967

Published by
SRPSKO HEMIJSKO DRUŠTVO (BEOGRAD)
1967

Translated and published for U.S. Department of Commerce and
the National Science Foundation, Washington, D.C., by
the NOLIT Publishing House, Terazije 27/II, Belgrade, Yugoslavia
1969

Translated by
ALEKSANDRA STOJILJKOVIĆ

Edited by
PAUL PIGNON

Printed in "Prosveta", Belgrade

CONTENTS

GLASNIK HEMIJSKOG DRUŠTVA, Vol. 32, No. 8-9-10, 1967, pp. 365—383

SOME BIOCHEMICAL ASPECTS OF CELLULASES AND HEMICELLULASES*

by

J. E. COURTOIS

INTRODUCTION

Cellulose is a widespread polysaccharide; it can be found in almost all vegetals and in some bacteria. It is also present in some lower animals like *Tunicates*. Enzymes which can break the β-glucoside bonds of cellulose are termed as cellulases. In the classification of enzymes made by the International Biochemical Union cellulases are defined as β-1,4 glucane-glucanohydrolase, with the index number 3.2.1.4.

In nature cellulose is always associated with other polysaccharides. Most often cellulose fibers are linked with substances called, rather vaguely, hemicelluloses. Very often lignin firmly binds these various polysaccharides, either by combining with some of their constituents or by a sort of encrustation.

The structure of cellulose has been studied in many works. Most frequently the subject of these studies was relatively pure cellulose, that of cotton in particular. Research on hemicelluloses, which until recently lagged behind somewhat, is also becoming intense.

Before describing cellulases something will be said about celluloses and hemicelluloses. Since this field is very wide we will limit ourselves to the properties most closely related to enzymatic hydrolysis. We have already mentioned that in nature cellulose and hemicelluloses are practically always associated. The same applies to enzymes depolymerizing these polysaccharides. The majority of organisms producing cellulases also produce hemicellulases. The limited scope of this study does not permit detailed consideration of all of these enzymes. We will therefore limit ourselves to some of their biochemical aspects, particularly to their distribution and the determination of their activity, which were studied in our laboratory.

---

* A lecture held at the general meeting of the Serbian Chemical Society, March 30, 1967.

GENERAL OBSERVATIONS ON CELLULOSE AND ITS REACTION TO CELLULASES

Cellulose makes up about one third of all carbon compounds resulting indirectly from photosynthesis. Consequently, all the vegetals on the Earth produce 1.10^{10} tons of cellulose a year. It logically follows that the carbon incorporated into cellulose must be returned to circulation. If this did not happen, the surface of the earth and even the bottom of the sea would be covered with a thick layer of cellulose. This would cause rarefaction of carbon dioxide in the air, which would limit photosynthesis and, consequently, the production of cellulose as well. Cellulose is none the less one of the polysaccharides from wich it is most difficult to return the carbon into cirulation. The dead leaves of forest litter show that the degradation of cellulose is slow. The relative stability of cellulose fibers (cotton, linen, hemp, jute, wood, paper) also confirms that cellulose depolymerization is a slow process. It is probable that the return of cellulose carbon into circulation is initiated by hydrolysis caused by cellulases.

After the works of Winogradsky it was considered that degradation by cellulolytic microorganisms started with an oxidative phase, with formation of an oxycellulose containing uronic acids. The works of Fahraeus and Charpentier[1] showed that the polysaccharide obtained was not oxidated cellulose but a substance synthesized by microorganisms from the products of cellulase hydrolysis of cellulose.

The structure of cellulose makes it very difficult for hydrolyzing enzymes to attack it. It consists of chains of glucose molecules linked by $1 \rightarrow 4$ bonds. The basic unit is cellobiose: 4-β-glucopyranosyl-glucose. It is in fact this disaccharide which results from the action of cellulases. X-ray spectra have shown that cellobiose is the basic element in the crystalline structre of cellulose. Cellulose can therefore be represented by the following diagram:

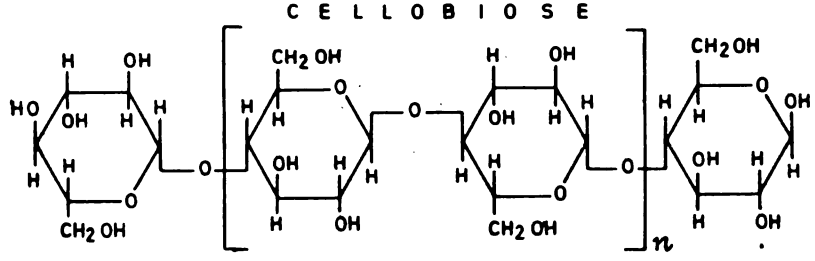

The number of cellobiose units *n* ranges from 1500 to over 5000 depending on the origin of the cellulose. In a β-glucopyranose molecule all the *OH* groups and the CH_2OH are equatorial, that is, in the same plane as the ring. This explains β-glucose polymers: β-glucanes tend to have a planar structure and to form aggregates in solution. In α-glucopyranose however, the anomeric group is axial, which interrupts the plane structure; α-glucanes can have a helical form.

These facts explain why amidone and glycogen consisting of (1 → 4) bonded α-glucopyranosyl units form colloidal dispersions in water while cellulose is insoluble.

Amidone and glycogen are the most widespread natural polysaccharides after cellulose. Unlike cellulose, which is composed exclusively of long linear (1 → 6) bonded chains, amidone and glycogen have branched structures consisting of shorter (1 → 4) bonded chains with (1 → 6) bonded branches.

Their glycosidic bonds are therefore easily accessible to many types of enzymes: various amylases break the (1 → 4) bonds and amylo-(1 → 6)-glycosidases cleave the chains at the points where they branch. The reserve of glucose in amidone and glycogen can therefore easily be returned to circulation. This fact dominates the intermediary glycidic metabolism in both vegetals with amidone and animals with glycogen.

Because cellulose is not easily accessible to enzymes it acts physiologically as a carrier. Its β anhydroglucose chains are parallel to an axis and the distances between the hydroxyl groups of the constituents of two chains allow the formation of hydrogen bonds. Van der Waals forces also take part, but their influence is less. As a result of this many crystalline forms appear in celluloses, mixed with its amorphous parts. From the practical point of view, in textiles for example, the crystalline zone gives tractive resistance while the amorphous zone makes the fibers less fragile.

The compact structure of cellulose offers great resistance to fixation of the active centers of hydrolyzing enzymes. This explains the stability of cellulose fibers and their manifold use, in the textile and paper industry, etc.

After treatment with acids which break some of hydrogen bonds, rinsing produces "swollen celluloses" which retain a large proportion of imbibition water. After having been macerated in hydrochloric or phosphoric acid, swollen celluloses, like cotton for example, are more accessible to cellulases. Swollen cotton is more easily hydrolyzed by cellulases than natural cotton. The hypothesis has even been made that the action of preparations with cellulolytic activity is started off by a "swelling factor" preceding the rupture of glycoside bonds by cellulases in the strict sense.

A substitution of some of the alcoholic functions of the glucose units causes rupture of the bonds binding alcoholic hydroxyls of adjacent glucose units in contiguous chains. The hydroxyls thus liberated are accessible to solvation. The substances obtained can be dispersed in water where they form viscous solutions. Some of the principal industrial products of this type are ether with methanol, ethylene-glycol and glycolic acid, known as methylcellulose, hydroxyethylcellulose (HEC) and carboxymethylcellulose (CMC), respectively.

There are many commercial kinds with a greater or lesser degree of substitution. The degree of substituion (D. S.) is usually expressed as the number of substituent units attached to an anhydroglucose molecule. Only the glucose hydroxyls 2, 3 and 6 can be substituted; 4 is involved in the glycosidic bond with the reducing group of the preceding glucose unit and 5 is included in the pyran ring. However, all glucose units are not always substituted so that the degree of substitution ranges from 0 to 3.

The dispersion in water and the viscosity of the resulting solution generally increase with the D. S. It seems that cellulases attack the non-substi-

tuted glucose units[2]. In the assay of cellulases it would therefore be convenient to use only slightly substituted derivatives. However, they give solutions with low concentration and viscosity so that it becomes difficult to saturate the enzymes with the substrate, which is a condition for measuring enzyme activity by the zero order reaction. In the study of cellulase hydrolysis by measuring, the depolymerisation of the substrate, which is accompanied by a reduction of viscosity, the starting point is already a medium of low viscosity and measuring its fluidification is a delicate task.

Substituted derivatives, a surce of trouble for enzymologysts, have many advantages in practical application. They are being used more and more in industry as thickeners, gellifiers and hardeners. Sodium carboxymethylcellulose is currently used in pharmaceutics as an excipient. Because of this the Pharmacopée française of 1965 authorizes the use of a number of sorts of carboxymethylcellulose with viscosities between 300 and 2200 centipoises.

In pharmaceutics carboxymethylcellulose is used exclusively as an excipient, so that a fairly large tolerance as to its use is justified. However, the Pharmacopée is not very liberal in this respect. Its strictness is only justified on one point: absence of toxins (arsenic and heavy metals) in the derivative.

It will be noted here — and should be born in mind in the last section on cellulase determination — that a carboxymethylcellulose with a precisely defined D. S. should be used as the substrate. Corresponding analytical criteria for the D. S. are indispensable.

HEMICELLULOSES

Until recently the definition of these compounds was rather ambiguous[3]. Old names ending in cellulose are still used, particularly in the wood and paper industry.

Payen*, was the first to show that wood consists of polysaccharides encrusted with lignin. This led him to differentiate celluloses analogous to those of cotton from other polysaccharides which he named hemicelluloses.

The following terminology is used in wood and paper industry:
The total of polysaccharides obtained after elimination of lignin is called holocellulose.

Lignin is usually degraded with chlorine or chlorinated oxidants like sodium chlorite.

Holocellulose is not homogenous although its name implies homogeneity: on the contrary, it is one of the most complex mixtures of various polysaccharides. Treatment of holocellulose with dilute alkalis extracts hemicelluloses, leaving a cellulose residue.

* All foreign authors are agreed in attributing the discovery of the cellulose of wood and of hemicelluloses to Anselme Payen (1795—1871). In 1963 the American Chemical Society inaugurated the Anselme Payen Prize for research in the chemistry of celluloses and hemicelluloses. The prize winner also receives a medal with Payen's effigy. It will be remembered that Payen and Persoz discovered and isolated the first enzyme: malt diastase. In Paris, where Payen was born and did his scientific research, a small street near the pont Mirabeau is named after him.

The composition of wood can therefore be represented by the following diagram:

Wood { Lignin 20 to 30%
Holocellulose 70 to 80% { cellulose 40 to 50%
hemicelluloses 25 to 35%
pectic substances 1 to 3% }

In gymnospermous and angiospermous wood the mean percentage of cellulose is 42 ± 2%[4]. Hemicelluloses are thus all the polysaccharides present in the cell walls of vegetals except cellulose and pectic substances.

In 1960 Roudier[3] proposed a division of hemicelluloses into three principal groups:

1. — Hemicelluloses whose main structure is composed of xylose units — xylans, glucuronoxylans and glucuronoaraboxylans.
2. — Hemicelluloses whose main structure is rich in mannose — glucomannans and galactoglucomannans.
3. — Hemicelluloses whose main structure is composed of galactose units — arabinogalactans and glucuronarabinogalactans.

The most abundant uronic acids are *D*-glucuronic acids (I) and their 4-methoxy derivative, mono-*O*-methyl-4-*D*-glucuronic acid (II):

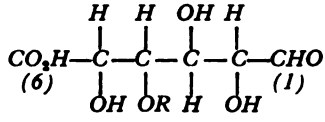

R = H (I)
R = CH_3 (II)

Although it was discovered only recently it has already been isolated from many hemicellulose fractions.

While neutral glycoses form the main yarn of the chain, uronic acids I and II branch off forming lateral ramifications and peripheries. The glycosidic bonds which bind the uronic acids through their reducing carbon at 1 either to another uronic acid molecule or to a neutral glycose (usally pentose or hexose), are resistant to acid hydrolysis. Partial hydrolysis of a hemicellulose gives oligosaccharides with a glucuronosyl group at their non-reducing end. An example is glucuronosylxylose.

To our knowledge no enzyme can cleave the bond between *O*-methyl-4-glycuronic acid and another glycose or uronic acid. This may explain the relative resistance of wood to ordinary moulds. So far in treatment of hemicelluloses with xylophagous insect preparations, a free *O*-methyl-4-glycuronic acid has not been detected. These preparations, however, contain a complete set of glucosidases wich act on the principal types of glycosidic bonds in hemicelluloses[5] [6].

The presence of a carboxyl at one end of the molecule, i.e. far from the reducing group which can take part in a glycosidic bond, gives an acidic character to hemicellulose fractions containg uronic acids. Some classifications of hemicelluloses use this property and distinguish between acid and neutral hemicellulose fractions.

The complexity of hemicelluloses is further augmented by the fact that they coexist with polysaccharides of similar characteristics. Galactomannans, abundant in the seeds of many *Leguminosae*, are a quite homogeneous group from the point of view of general structure. They consist of a central chain of $1 \rightarrow 4$ bonded β-mannopyranosyl units; the primary alcoholic function at 6 of some or all the mannose units is glycosidified by α-galactopyranose molecules. For a long time galactomannans were classified as hemicelluloses. Some authors still define enzymes able to hydrolize theme as hemicellulases. In these enzymes the successive actions of α-galactosidases followed by β-mannanases should be distinguished[7] [8] [9].

Pectic substances have always been differentiated from hemicelluloses. They can be found, in small quantities, in wood[10], in the middle lamella, and it is very difficult to separate them from other wood polysaccharides. Roudier and Gillet[11] have shown their great practical importance, especially in the production of paper pulp. Pectic substances are abundant in vegetals, particularly in some fruits.

In vegetal tissues various hemicellulose polysaccharides are associated with pectic and mucilaginous substances. Some authors differentiate between hemicelluloses and mucilage polysaccharides. It is often difficult to make a clear distinction between the two, but some mucilages characteristic of a species, such as *Linnaea* plantain and various *Malvaceae*, can be differentiated from hemicelluloses.

The percentage of hemicellulose constituents varies with the species. Hemicelluloses with a central xylan chain can be found in all lignified vegetal tissues. They make up 25 to 35 total weight % in ripe stalks of cereals and other *Graminae*, 15 to 25% in angiospermous trees and only 7 to 10% in gymnospermous trees.

These xylans are a transitional form between cellulose and other hemicelluloses. The central chain is made of $(1 \rightarrow 4)$ bonded β-*D*-xylopyranose units. *D*-xylose is a pentose (III) whose three secondary alcoholic functions have the same spatial configuration as alcoholic groups bound to carbon in positions 2, 3 and 4 of *D*-glucose (IV):

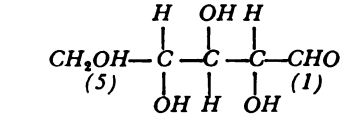

D-xylose (III)

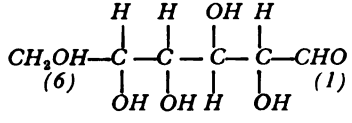

D-glucose (IV)

The central chain of xylans therefore corresponds to a cellulose which lacks the primary alcohol functions of the carbons at 6.

Some β-glycosidases, almond emulsin for instance, can hydrolize both β-*D*-glycosides and β-*D*-xylosides. There are enzymatic preparations which act on both the hylans and the celluloses, and it is possible that the depolymerizing enzyme is the same. However, there are purified xylanases which do not act on cellulose and cellulases which do not act on xylans. It seems that

the two types of polysaccharide are in general associated with two distinct groups of enzymes.

Our knowledge of the vast group constituted by the hemicelluloses has advanced considerably but there is still an immense field to be studied. It may be presumed, in view of the complex structure of various hemicelluloses, that numerous enzymes are necessary to cleave the many types of glycosidic bonds in these compounds. Recent studies have confirmed this.

THE DISTRIBUTION OF CELLULASE

The most important sources of cellulases are microorganisms. Cellulytic preparations with high activity can seldom be obtained from higher plants and animals.

I. Bacteria

Bacteria which produce cellulases are numerous[12]. There is an abundant cellulolytic microflora in the soil: aerobic and anaerobic bacteria, fungi, actinomycetes and myxobacteria. The most important representatives are aerobic bacteria, especially *Vibrio* and *Cytophaga*, which can be found in the soil in all temperature zones. *Cytophaga* utilize cellulose glucose to synthesize a mucopolysaccharide[1]. We may also note the anaerobic bacteria of marshes: *Cellulomonas* sp., and the bacteria of the rumen in ruminants.

II. Fungi

This group has the greatest variety of species producing active cellulases. Table I shows the main sources of fungal cellulases. *Saccharomycetaceae* are in general good sources of oligosaccharides. An example is β-fructosidase of brewer's and baker's yeast which hydrolizes saccharose. *Saccharomycetaceae* are less productive in polysaccharidases: it is well known that amidone has to be hydrolized by an amylase before it is subjected to alcoholic fermentation by yeast. This is why since ancient times a source of amylase (amylase of germinated barley or of *Aspergillus orizae*) has been used before fermenting with yeast. Yeasts rarely contain cellulases, and when they do they are mediocre as sources.

Together with Thuillier and Chararas[13] [14] we have isolated a yeast from *Hylobius abietis* L. (*Coleopterae*, *Curculionidae*). *Hylobius* is a xylophagous insect, a parasite of pines, where it causes major damage. Dissection of its larvae reveals the presence of mycetomes, mainly in the apex of the gastric sac between the epithelium and the musculature. Examination of fragments of mycetocytes in smears revealed an intracellular microorganism. Aseptic samples of fragments permitted isolation and culture of this yeast. After a determination of its cultural, morphological, fermentative and auxanographic characteristics, it was identified as the species *Candida brumptii*. The strain contains cellulases and hemicellulases. It does not attack swollen cellulose of cotton. Carboxymethylcellulose, lichenin, glucomannan and

TABLE I

Fungal Cellulases

Family	Main representatives	Remarks
Yeasts	*Candida brumptii*	In symbiosis with the xylophagous insect *Hylobius abietis (Coleoptera)*
Aspergillaceae	*Aspergillus niger, orizae,, aureus, flavus, luchuensis. Penicillium, funiculosum, parvum, pusillum, notatum*	Associated with many other glycosidases
Sordariaceae	*Neurospora crassa*	
Basidiomycetes over 200 species which attack wood	*Myrothecium verrucaria* *Stachybotrys atra* *Irpex lacteus* *Poria vaillantii* *Trichoderma viride* *Coniophora cerebella*	The most work has been done on the cellulase of *M. verrucaria;* *Coniophora cerebella* is the most widespread xylophagous fungus

galactomannan are moderately hydrolized. The secretion of these polysaccharides by the strain *Candida brumptii* seems necessary for its adaptation to parasitic existence in the mycetomes of the insect. In fact, these enzymes disappeared from cultures repeated on rich nutrient media. They were also absent in strains of *Candida brumptii* taken from various collections.

The *Aspergillaceae* include numerous species with a cellulolytic action. Some species are culltivated on mediums containing cellulose in production of the principal commercial cellulase preparations. They are usually obtained in a similar way as fungal amylases[15]. Selected species are usually cultivated on mediums with a cereal basis. Brans of wheat and rice are most frequently used. Sometimes the mycelium is just ground up with medium. Usually however, it is extracted either with water or a buffered solution. Enzymatic proteins are rendered insoluble either by means of ammonium sulphate or by adding miscible solvents (methanol, ethanol, acetone) to the water. The disadvantage of precipitation with these solvents is that saccharides and dextrins are also rendered insoluble.

The methods of selecting strains and cultivating them in fermentation tanks are analogous to those used in producing antibiotics. As a result, many industrial cellulase preparations are made by firms which produce antibiotics. In these preparations cellulase is usually associated with other enzymes: proteases, phosphatases and various polysaccharides (mainly amylase but some hemicellulases are also frequent). Assay of the activity of cellulase in commercial preparations therefore meets with certain problems.

In a determination of reducing saccharides by hydrolysis of cellulose the following points should be taken into account:

1. — Some preparations contain polysaccharides which can be hydrolyzed by the associated enzymes. Incubation of the preparation in the absence of any other associated substrate will liberate reducing saccharides and glucose. We have observed this with many commercial preparations[16] [17] [18]. The amylase of these preparations best hydrolizes the dextrins of the culture medium.

2. — In tests of long duration proteases of the preparation attack the cellulase, since it is also a protein. For a determination of cellulase activity it is therefore necessary to choose a method with a short duration of incubation of the enzyme with the substrate. We insisted on these two points in an earlier work[19]. We also pointed out that some producers dilute their preparations to a fixed titer. Sometimes the diluent is sodium chloride which may interfere in viscometric tests. Glucose sometimes gives the preparation a considerable reducing power, which should be substracted from the global reducing power determined from the action of the enzyme on a cellulose substrate. This correction factor is often very high and makes determination of reducing saccharides liberated by cellulase uncertain. Addition of lactose as a diluent results in even greater complications because it is a reducing disaccharide. Also, fermentative preparations almost always contain a β-galactosidase which during incubation hydrolizes the lactose into galactose and glucose. It is therefore almost impossible to deduce the reducing power for all three — non-hydrolized lactose and the liberated galactose and glucose.

We have made these observations here so as not to have to refer to them in the last section on the determination of cellulases.

For a long time preparations of *Aspergillaceae* were practically the only commerical sources of cellulases. In the last few years other fungal preparations, obtained from *Basidiomycetes*, have been made. More than 200 species of *Basidiomycetes* are known. They are xylophagous and their cellulase activity is usually associated with various hemicellulase and pectinase activities.

Myrothecium verrucaria is a lignicolous species whose cellulase has been the most thoroughly studied. The *Trichoderma*, particularly *T. viride*, *T. lignorum* and *T. Koji*, are rich in cellulase. The Japanese have put on the market commercial preparations obtained from cultures of *Trichoderma*. They are being used to make oranges and mandarines easier to peel, to increase the yield of the extraction of agar-agar from algae, to soften fibrous foods such as carrots and to digest the cell walls of alimentary yeasts[15].

Irpex lacteus (*Polyporus tulipiferae*) contains a cellulase purified by M. A. Jermyn, Australia. At Youy-en-Josas, France, Laboureur, the director of the Société d'Etudes et d'Applications Biologiques, recently obtained a very active cellulase preparation on an industrial scale. It was obtained with a strain of *Basidiomycetes* whose systematic position has not been determined but which probably belongs to the genus *Poria*. The research is continuing in collaboration with the Centre d'Etudes du Bouchet.

Numerous hemicellulases coexist with cellulases in these lignicol fungi. This is especially the case with *Coniophora cerebella* the most widespread xylophagous fungus in Great Britain[20].

III. Higher plants

To our knowledge no higher plant has a high cellulase activity. Moderate activities have been found in stalks, leaves and fruit. It is thought that a cellulase of endogenic origin may play a part in the plasticity of plants during their growth. Cellulases have been detected in grains in germination, including those of wheat and barley. The plantule probably uses this cellulase to pierce the cell walls. These cellulases enable the plantulae to pierce the sides of a cardboard box.

The cellulase activity of higher plants is less than that of the enzymes which are usually associated with the cellulase — hemicellulases and pectinases. It is in fact in the interest of the plant to protect itself from cellulases. Mandels and Reese[21] found natural inhibitors of cellulase in leaves, flowers and fruit of plants of many different botanical families. Natural inhibitors were also found in the wood of numerous trees.

IV. Animals

For a long time it was thought that higher animals were incapable of producing cellulase. Cellulase activity detected in pulverized organs, the digestive tract in particular, were attributed to protozoans, bacteria or fungi. It was even concluded that the production of cellulase by a vegetarian animal, secreting in in its digestive tract, would lead to giantism as a result of excessive nutrition. This giantism, conflicting with Nature, would sooner or later cause the disappearence of the species. The hypothesis was put forward that the huge reptiles of the Mesozoic era disappeared because they produced cellulase. Our lack of knowledge makes it equally difficult to defend or refute this hypothesis, made 15 years ago. However, recent studies have shown almost with certainty that animals can produce cellulases without developing into giants.

Table II shows the main species with a cellulolytic activity. The cilia of the rumen of polygastric animals contain numerous polysaccharidases. They attack cotton cellulose hardly or not at all, but cellodextrins are hydrolyzed by an extract of cells of *Epidinium ecaudatum*[22]. This extract contains various hemicellulases including arabonases and xylanases. Grasse and his school have shown that in termites cellulose is degraded either by symbiotic flagella or by the intestinal bacteria, depending on the species. Intestinal flagella have a cellulolytic action[23]. The slug *Arion ater* secretes β-(1 → 4)-glucosanases[24].

There are many types of enzymes which hydrolize cellulose substrates. This is why Anderson, Cunningham and Manners[25] proposed that the name "cellulases" should be reserved for enzymes which hydrolize natural insoluble celluloses, differentiating them thus from β-(1 → 4)-glucosanases which depolymerize (1 → 4) glucosanes whose molecular weight is less than that of cellulose. The β-(1 → 4)-glucosanases hydrolize both soluble derivatives of cellulose and carboxymethylcellulose. Animal cellulolytic enzymes are mainly β-(1 → 4)- glucosanases and have little or no action on cotton cellulose.

TABLE II

Animal Cellulases

Class	Principal representatives studied	Remarks
Protozoans	*Eremoplastron bovis* and various cilia including *Epidinium escaudatum; Polyplastron multivesiculatum;* various flagella	The cilia participate in digestion in the rumen
Molluscs	Slug *Arion ater* Snails: *Helix pomatia* and other *Helix* *Dolabella* Various *Teredo*	
Anellides	*Lumbricus terrestris* and various earthworms	
Crustaceans	*Oniscus asellus* *Procambarus clarkii* *Astacus — Homardus*	Localized in hepato-pancreas
Insects	*Ctenolepisma lineata* *Periplaneta americana* Numerous xylophages: *Pissodes notatus — Ips typographus — Capnodis miliaris*	In many species (termites for example) symbiotic presence of cellulolytic flagella
Echinoderms	*Paracentrotus lividus*	Intestinal

The cellulase of snails is the oldest known animal cellulase. It was discovered by Kukenberg in 1882 and studied by Billard in 1914. Billard was intrigued by the fact that some snails managed to get out of a paper bag, leaving circular holes in the paper, evidencing the regular action of an enzyme diffusing from a central point. In the digestive tract of the snail there are bacteria and protozoans producing cellulases, but an additional cellulase produced by the animal has also been found[26] [27]. Kooiman[28] identified numerous glycosidases, including cellulases and β-(1 → 4)-glucosanases, in the digestive juices of crustaceans (*Astacus*, *Homardus*). This explains why the extract of the hepatopancreas of crayfish hydrolyzes carboxymethylcellulose. The microsomes of the hepatopancreas of *Procambarus claridi* contain an enzyme which hydrolizes carboxymethylcellulose, and which seems to be synthetized by the hepatopancreas[29].

It is not likely that the production of cellulases would result in the giantism of the animal. On the other hand, it is certain that animals which use cellulases in their nutrition are appreciated from a gastronomic point of view. In fact, some of the most delicious dishes are made from lobsters and scampi, which produce digestive cellulases.

Some insect species also produce cellulases. In 1956 Lasker and Giese[30] showed that *Ctenolepisma lineata* uses the carbon from cellulose. After sterilization of the outer egg membrane by means of mercury chloride and aseptic rearing of the insect, a silverfish without bacteria was obtained. The sterile insect continued to metabolize cellulose and contained a cellulase in its middle intestine. Everything therefore seems to indicate that silverfish is capable of secreting a cellulase.

Wharton and Lola[31] [32] have shown that the cellulase of the American blatta *Periplenata americana* L. has two sources: an enzyme secreted by the salivary glands, and intestinal microorganisms. Administration of antibiotics did not inhibit the secretion of β-(1 → 4)-glucosanase acting on carboxymethylcellulose; on the contrary, the glucosanase activity was increased.

In 1961 Courtois, Chararas and Debris[5] found numerous glycosidases in the xylophagous insect *Ips typographus*. These enzymes can hydrolize the principal types of oligosaccharide bond. They detected α- and β-glucosidases, α- and β-galactosidases, and α- and β-mannosidases. The insect also contains a wide range of glycosidases which hydrolize polysaccharides of wood: amidone, pectic substances and hemicellulases. No action on cellulose or on a commerical highly substituted carboxymethylcellulose was detected. However, a carboxymethylcellulose with a degree of substitution close to 0.6 was hydrolized. This set of glycosidases was later found in all xylophagous insects that were studied [6, 33, 34, 35, 36, 37]. The sixteen species studied included parasites of conifers, poplar and oak. The swollen cellulose of cotton and cellophane were only attacked by two species: *Ips acuminatus* and *Pissodes notatus*. Carboxymethylcellulose on the other hand was hydrolized by all the species. The β-(1 → 4)-glucosanase which hydrolyzes this substrate seems therefore to differ distinctly from true cellulase which can attack insoluble cellulose substrates. At various stages of development this glucosanase was found in three insects: *Ips typographus* (larvae, adults after hibernation and adults during active nutrition); *Ips acuminatus* (larvae, nymphs and pigmented and non-pigmented adults)[36]; *Pissodes notatus* (larvae during nutrition, larvae before their transformation into nymphs, nymphs, adults before nutrition and adults at the beginning of nutrition)[33]. There is a correlation between the percentage of various glycosidases and the nutrition activity. At the time of intense nutrition the percentage is the highest. It is the lowest in nymphs.

In order to study whether these glycosidases had a bacterial or mycotic origin the insects were raised in the presence of antibiotics. The results obtained for β-(1 → 4)-glucosanase are similar to those for other oligosaccharidases and polysaccharidases studied at the same time. Table III gives only the results for a carboxymethylcellulose substrate. It shows that rearing in the presence of antibiotics or an antimycotic had no marked influence on the β-(1 → 4)-glucosanase activity of the various insects (or in *Capnodis*, of the different parts of the insect). In some specimens only the activity was slightly lower. A small part of the β-(1 → 4)-glucosanase may therefore come from bacteria or protozoans, but the rest is almost certainly produced by the insect. A similar conclusion was reached regarding the oligosaccharidases, amylase, pectinase and hemicellulases of the same insects.

TABLE III

Hydrolysis of carboxymethylcellulose by xylophagous insects raised in the presence and absence of antibiotics

Insect	Part studied	Antibiotic impregnated in the wood	Growth of control	Growth in the presence of antibiotics	Reference
Ips acuminatus pigmented adults	whole insect	chloramphenicol	(1) 64	(1) 64	36
Pissodes notatus adults	whole insect	chloramphenicol	75	72	36
	anterior part	sulfonamide	78	64	37
		mixture	78	69	id
	central part	sulfonamide	69	67	id
		mixture	69	68	id
	posterior part	sulfonamide	31	29	id
		mixture	31	24	id
Capnodis miliaris larvae	head with salivary glands	homycine	53.5	36	38
	caeca and esophagus	id	59	49	id
	diverticulum and middle intestine	id	65	49	id
	posterior intestine	id	46	42	id
	the rest of the larva after ablation of the digestive tract	id	52	56.5	id

The action of enzymes directly extracted with water from the ground whole insect or part of the insect (*Capnodis*) — 5 days of hydrolysis at 37° and pH 5.2. The antibiotics with which the wood was impregnated were: a) chloramphenicol; b) sulphamide and amidozol (sulphazomiosol Theraplix) with a wide antibacterial spectrum; c) the mixture consisted of chloramphenicol, transcycline, penicillin and cannamycin; d) homycin has extensive antimycotic properties.

(1) Given figures show the percentage of reducing saccharides (alkaline copper (II) reagent was used) liberated by the enzyme with respect to the reducing saccharides of the acid hydrolysate.

In comparative biochemistry, when antibiotics do not make the enzymatic activity of an animal considerably lower it is considered that the enzyme is not produced by microorganisms. In the case of xylophagous

insects the tests with antibiotics (as distinct from an antimycotics) confirm that most of the glycosidases are produced by the insects, and only a small amount by microorganisms. We believe therefore that xylophagous insects secrete β-(1 → 4)-glucosanase, hemicellulases and pectinases. These enzymes allow the insect to soften and pierce wood and also to hydrolyze polysaccharides to obtain glycoses which it can use. These glycoses are galactose, glucose, mannose and may be xylose.

The cellulases of metazoans which we have examined so far belong to families of the right branch of the classical phylogenetic tree. This branch ends with the arthropods, the insects being situated at its extreme end.

On the left branch, terminating with the mammals and having the primates at its extreme end, the presence of cellulases is exceptional. We know only one such case. Haltin and Wanntorp[39] have found a sea urchin, *Paracentrotus lividus*, in the bay of Naples, whose intestine contained a β-(1 → 4)-glucosanase which hydrolized carboxymethylcellulose and was stabilized by calcium salts. Mammals seem totaly incapable of producing a cellulase, and have to rely on the action of microorganisms. The ruminants are very well adapted: microorganisms of the rumen include numerous germs producing cellulases and hemicellulases. An example are the protozoans described at the beginning of the section on animal enzymes.

PROPERTIES OF CELLULASES

Many authors have purified cellulases and described their characteristics. However, even more works have been published on enzymes which act on glycogen and amidone, enough has been written on α-glucosanases to fill several shelves of a big university library. We shall give a summary of the results obtained with β-glucosanases.

There are several types of cellulase. Whitaker[40] has done a careful study of the enzyme of the basidiomycete *Myrothecium verrucaria*. He concludes that this cellulase causes total degradation beginning with the cellulose fibers. His argument in support of this interpretation is the homogeneity of the enzyme purified by electrophoresis and ultracentrifuging. During purification its activities with respect to different substrates increased in a similar way. The substrates were cotton fibers swollen with phosphoric acid, pulverized cotton fibers, carboxymethylcellulose and various oligosaccharides consisting of (1 → 4) bonded β-glucopyranosyl units.

Reese and Selby worked with preparations containing several enzymes acting successively. The first enzyme, C_1, transforms crystalline cellulose into linear chains. This rather delicate enzyme is sometimes called the swelling factor, abreviated *S*-factor. It attacks cellulose fibers, reducing the resistence to traction by over 15—20. This enzyme is inductible and highly adsorbed onto the insoluble cellulose of a culture medium.

The second is a group of enzymes, called C_x, believed to consist of β-(1 → 4)-glucosanases. It acts on both the cellulose swollen by the first enzyme or acids and on substituted celluloses such as carboxymethylcellulose. There seem to be several types of β-(1→4)-glucosanases which either attack the ends of the chains or get permanently attached, at random, to cellobiosyl bonds. There is a vast range of amylases whlich differ according

to the way in which they attack the bonds building the maltose units. It can also be presumed that there are β-(1→4)-glucosanases whoch differ by the way in which they attack the complex polysaccharide molecule. A great deal of research therefore remains to be done if we want to precisely define the enzymatic mechanism of cellulolysis. It should also be pointed out that, to our knowledge, no definite selective inhibitor or selective activator of cellulases has as yet been described.

DETERMINATION OF CELLULASE ACTIVITY

Many procedures have been suggested: the weight reduction of an insoluble substrate — the time required to produce lysis in a thread of cotton on which a heavy object is suspended; the lysis breaks the thread and the object falls. The method to be used must allow precise determination of a minimum cellulase activity.

We will deal here only with the determination of preparations used in pharmaceutics. In 1960 the Comission for Standardization of Enzymes of the International Pharmaceutic Federation assigned us the task of research on cellulase and hemicellulase determination. These enzymes are usually associated in pharmaceutic preparations, which often contain pectinases and amylases as well.

In 1931 Grassman and Rubenhauer[41] proposed that enzymatic preparations containing cellulases and hemicellulases could be used in therapeutics. These preparations, taken orally, should facilitate the digestion of polysaccharides present in vegetables. Silberschmidt[42] showed that a therapeutic dose did not cause complete hydrolysis of all glycosidic bonds, but that it dissociated cell walls. Slices of raw vegetables (cucumber, carrot, tomato, beet, radish) were put into Petri dishes together with the enzymatic preparation and a few drops of toluene. After 2—4 hours at 37° a dislocation of cell walls, sometimes even a complete fluidification of parenchymatous tissue, could be observed.

Since these first findings numerous therapeutic preparations containing cellulases and hemicellulases have appeared on the market. They are prescribed to be taken orally, and help the digestion of raw vegetables or vegetables which are hard to cook. They dissociate the components of cell walls by depolymerizing polysaccharides. This attenuate the irritation of the intestines caused by insoluble polysaccharides. On the other hand, cleavage of saccharides restrains intestinal fermentation, which is why these enzymes are indicated in cases of meteorism. Their effect is due not only to the action of cellulases but also of hemicellulases and often of pectinases. Thus the vegetal membranes are attacked by different types of enzymes in association. As we have already suggested, together with Bui Khac Diep[19], assey of these preparations should be done on definite substrates.

1. Carboxymethylcellulose (CMC)

We recently reported a laboratory technique for preparing CMC[43]. Carded cotton is delipidized with chloroform and then with ethanol. Heating in a solution of sodium carbonate under a nitrogen atmosphere eliminates

pectins and hemicelluloses. Treatment with a solution of sodium carbonate in the presence of isopropanol transforms the purified cotton into alkali-cellulose. Monochloracetic acid reacts with some alcoholic functions of the cellulose giving the corresponding cartomethoxy ethers according to the scheme

$$\text{Cell } (OH)^3 + n\ Cl CH_2\text{-}COOH \xrightarrow{Na\,OH} \text{Cell} \begin{matrix} (OH)^{(3-n)} \\ (O\text{—}CH_2\text{—}COO\,Na)^n \end{matrix} + n\,Na\,Cl$$

Sodium CMC is then washed with methanol. We have determined the proportions of the reactants so as to obtain a sodium CMC with a *DS* close to 0.6, i.e. in the above diagram $n = 0.6$.

We have worked out the following techniques for checking the substrate:

1. — Insolubilization of CMC in an acid medium and the titration of carboxylic functions by means of sodium carbonate.

2. — Determination of α-glycolic groups attached to carbons 2 and 3 of the glucose units. If neither of the alcoholic functions is substituted, a molecule of periodic acid cleaves the carbon chain between carbons 2 and 3.

$$R\text{—}CHOH\text{—}CHOH\text{—}R' + IO_4H \rightarrow R\text{—}CHO + OHC - R' + H_2O.$$

Standard oxidation by periodic acid is used to check for CMC.

3. — Nitrochrome oxidation on a boiling water-bath and iodometric determination of the excess of bichromate.

4. — Determination of the glycolic acid fraction by colorimetry. The glycolic acid bound in CMC reacts as a free glycolic acid if heated with chromotropic acid in a concentrated sulphuric medium. A violet color appears, whose maximum absorption is at about 580 nm.

CMC is not quite satisfactory as a substrate since:

a. — The amount of reducing saccharides liberated is not proportional to the amount of enzyme. We have already said that most commercial preparations of cellulases contain reducing saccharides and glucides which liberate reducing saccharides from the associated enzymes of the preparation. A correction made by means of a control run is important, but it is sometimes difficult to evaluate it with precision.

b. — Depolymerization by cellulases diminishes the viscosity of CMC solutions.

The measurement of a decrease of viscosity meets many obstacles. CMC is pseudo-plastic and thixotropic, its viscosity depends on the *pH* and ionic strength of the medium. The viscosity of solutions changes during keeping. On the other hand, CMC is a high polycarboxylic polymer which can combine with proteins. It can therefore be both a substrate and an inhibitor of cellulolytic enzymes[44]. Consequently, it is very difficult to obtain precise quantitative data on CMC, indispensable for a determination of enzymatic activity. On the other hand, CMC is a very useful substrate for qualitative and semi-quantitative determination of the activity of cellulase preparations.

2. *Hydroxyethylcellulose (HEC)*

Iwasaki, Tokuyasu and Funatsu[45] have also made objections to CMC as a substrate, while highly recommending hydroxyethylcellulose (HEC).

HEC is a non-polar derivative, the viscosity of solutions is not a function of pH and is only slightly influenced by the ionic strength of the medium. That the viscosity of solutions is not notably modified by keeping was confirmed in our laboratory where, with Bui Khac Diep[17], we studied a sample of HEC prepared in the laboratory.

We have described how HEC can be prepared in the laboratory using Whatman cellulose powder. The reaction of ethylene oxide in an alkaline medium proceeds according to the following scheme:

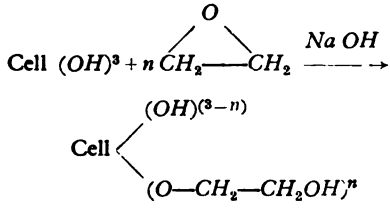

The procedure is delicate because several types of reactions may occur simultaneously.

a. — Attack on one of the hydroxyls at carbons 2,3 and 6 of the anhydroglycose units. The primary alcoholic function at 6 is preferentially but not exclusively attacked.

b. — Elongation of the substituted chain of the cellulose: a new ethylene-glycol molecule joins the hydroxyl function of the preceding molecule, and so on according to the scheme

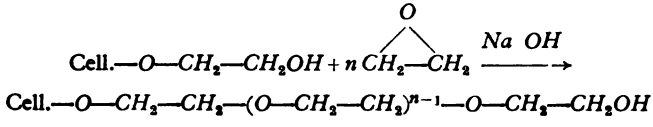

c. — Interreaction of the molecules of ethylene oxide forming polyethylene glycols.

If we want to utilize HEC as a soluble substrate two factors, with opposite effects, must be taken into account:

1. — The solubility of HEC in water increases with the proportion of substituant hydroxyethyl groups.

2. — Substitution inhibits the action of cellulases[2].

The method which we have adapted to the laboratory requires a detailed knowledge of the action of the ethylene oxide. In order to get this, the solution of ethylene oxide is put into isopropanol. The final product should be purified by prolonged repeated rinsing so as to eliminate polyethylene glycols. As a check on the final product we have proposed the following determinations:

a. — Viscosity of the aqueous solution.

b. — Determination of α-glycolic groups at carbons 2 and 3 of non-substituted glucose. We have found that this can always be done using periodic acid.

c. — Determination of aldoses in the acid hydrolysate by means of the hypoiodite method, and determination of glucose not substituted by hydroxyethyl groups using glucose-oxidase. We obtained a ratio (non-substituted glucose) (total adoses expressed as glucose) close to 0.36. Chromatography of the hydrolysate indicated the presence of at least five *O*-hydroxyethyl derivatives of glucose. HEC obtained in this way is an exellent substrate for the commercial cellulases used in pharmaceutics.

A. *Viscometric tests*

We have developed a procedure allowing observation of the decrease of viscosity at 25°. Figure 1 shows that depolymerization starts abruptly, slowing down when the decrease of viscosity (*Dec. visc.*) reaches about 60%. After 24 hours *Dec. visc.* reaches about 90%.

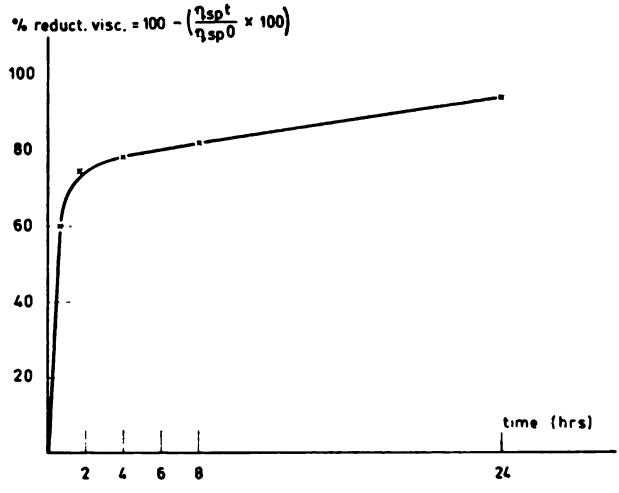

Figure 1

Viscosity of an HEC solution of concentration 6.4 *mg/ml* in the presence of cellulase VI in a concentration of 200 *μg/ml* as a function of contact time.

Under our experimental conditions it is possible to obtain in thirty minutes at 25° a rate of depolymerization of the substrate directly proportional to the amount of enzyme. Figure 2 gives the results obtained with three commercial preparations.

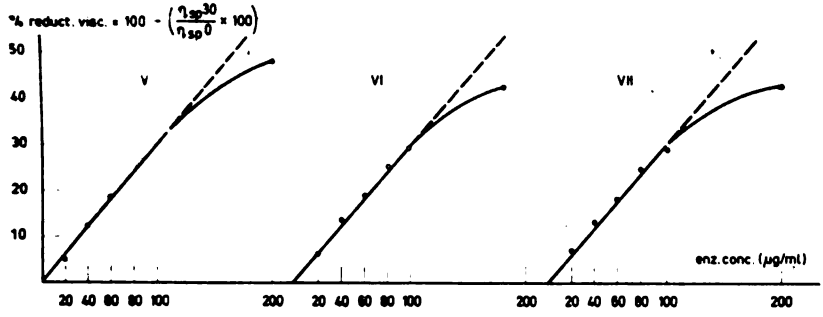

Figure 2

Curves of viscosity reduction of an HEC solution of concentration 16 *mg/ml* in the presence of increasing quantities of enzyme — cellulases V, VI and VII. Hydrolysis: 30 min. at 25°C.

Over a large interval *Dec. visc.* is directly proportional to the quantity of enzyme. Cellulase activity can be evaluated if *Dec. visc.* does not exceed 30%. The tests were reproduced to a satisfactory precision.

The results can be formulated by defining an Enzymatic Unit as the quantity which causes a decrease of viscosity of 1% per minute at 25°.

B. *Determination of liberated reducing saccharides*

The results were as poor as those obtained with CMC as a substrate. We were not able to find a zone in which the quantity either of total reducing saccharides liberated or liberated glucose was directly proportional to the quantity of enzyme. In some commercial preparations active cellobiase was found. Hydrolysis of one molecule of reducing cellobiose gives two glucose molecules.

Let us imagine the case of two preparations with the same cellulase activity of which one contains cellobiase. The preparation without this enzyme would liberate a much larger quantity of reducing saccharides and twice as much glucose.

In a determination of liberated reducing saccharides and glucose, CMC and HEC offer equal possibilities for a limited test verifying the minimum activity of a preparation. In the present state of our research an exact determination using the two substrates based on a determination of liberated reducing saccharides cannot be done.

Depolymerization of HEC, evaluated from the viscosity decrease, is the method recommended for determination of celullases in pharmaceutics.

CONCLUSION

Some points relative to cellulases and especially to hemicellulases have been deliberately omitted because of the limited scope of this work. Our intention was to point out the fact that cellulases are much more w-

despread than it was believed ten years ago. There are various cellulases with very different properties and mechanisms of various action. The same applies to the multiple enzymes classified, somewhat arbitrarily, as hemicellulases. Our aim was to show the importance of all these enzymes, by which most of the carbon of plants is returned into circulation.

School of Pharmacy
Paris University

Received 10 October, 1967

REFERENCES

1. Charpentier, M. *Etude de l'activité cellulolytique de Sporocytophaga myxococcoides* — Paris: 1965 (Doctoral thesis).
2. Klop, W., and P. Kooiman. — *Biochim. Biophys. Acta* 99: 102, 1965.
3. Roudier, A. "Les hémicelluloses et les oligosides provenant de leur hydrolyse" — *Bulletin de la Societé de Chimie Biologique* 42: 1493—1514, 1960 (hereafter to be called *Bull. Soc. Chim. Biol.*).
4. Timell, T. "Cellulose from Wood", in: Whistler, R., J. De Miller and M. Wolfrom. *Methods in Carbohydrate Chemistry* — Academic Press, 1965, pp. 100—103.
5. Courtois, J., C. Chararas and M. Debris — *Bull. Soc. Chim. Biol.* 43: 1173, 1961.
6. Courtois J., C. Chararas, M. Debris and H. Laurant-Hubé — *Bull. Soc. Chim. Biol.* 47: 2219, 1965.
7. Courtois, J., and P. Le Dizet — *Bull. Soc. Chim. Biol.* 45: 731, 1963.
8. Courtois, J., and P. Le Dizet — *Bull. Soc. Chim. Biol.* 45: 743, 1963.
9. Courtois, J., and P. Le Dizet — *Carbohydrate Research* 3: 141, 1966.
10. Roudier, A. — *Reveu de l'Association Technologique et Industrielle Papetière* 20: 135, 1966.
11. Roudier, A., and H. Gillet — *Bulletin de l'Association Technologique et Industrielle Papetière* 15: 432, 1961.
12. Gascoigne, J., and M. Gascoigne. *Biological Degradation of Cellulose* — London: Butterworths and Co., 1960.
13. Thuillier, A. *Doctoral Thesis.* — Paris: 1966.
14. Thuillier, A., J. Courtois and C. Chararas — *Biochimica applicata* 14: 1, 1967.
15. Toyama, N. "Degradation of Foodstuffs by Cellulase and Related Enzymes", in: Reese, E. *Advances in Enzymatic Hydrolysis of Cellulose and Related Materials* — Pergamon Press, 1963, pp. 235—253.
16. Courtois, J. and Bui Khac Diep — *Annuel de la Pharmacopée Francaise* 23: 705, 1965.
17. Courtois, J., and Bui Khac Diep — *Annuel de la Pharmacopée Francaise* 25: 177, 1967.
18. Bui Khac Diep. *Doctoral Thesis* — Paris: 1967.
19. Courtois, J., and Bui Khac Diep — *Annuel de la Pharmacopée Francaise* 23: 533, 1965.
20. King, N. — *Biochem. Journal* 100: 784, 1966.
21. Mandels, M., and E. Reese. "Inhibition of Cellulases and β-glucosidases", in: Reese, E. *Advances in Enzymatic Hydrolysis of Cellulose and Related Materials* — Pergamon Press, 1963, pp. 114—157.
22. Bailey, R. and B. Gaillard — *Biochemical Journal* 95: 758, 1965.
23. *Lavette*, A. — *Comptes Rendus de l'Academie des Sciences* 258: 2211, 1965.
24. Evans, W., and E. Jones — *Comparative Biochem. Physiol.* 5: 149, 1962.
25. Anderson, F., W. Cunningham, and D. Manners — *Biochemical Journal* 90: 30, 1964.
26. Thirlwell, M., G. Strasdine, and D. Whitaker — *Canadian Journal Biochem. Physiol.* 41: 1603, 1963.
27. Strasdine, G. and D. Whitaker — *Canadian Journal Biochem. Physiol.* 41: 1621, 1963.
28. Kooiman, P. — *J. Cell. Compar. Physiol.* 63: 197, 1964.

29. Yasumasu, I., and Y. Yokoe — *Science Paper of the College of General Education, Kyoto University* 15: 95, 1965.
30. Lasker, R., A. Giese — *Journal of Experimental Biology* 33: 542, 1956.
31. Wharton, D., M. Wharton, and J. Lola — *Journal of Insect Physilogy* 11: 947, 1965.
32. Wharton, D., and M. Wharton — *Journal of Insect Physiology* 11: 1401, 1965.
33. Chararas, C., J. Courtois, M. Debris, and H. Laurant-Hubé — *Bulletin de la Societé de Chimie Biologique* 45: 383, 1963.
34. Courtois, J., C. Chararas, and M. Debris — *C. R. Soc. Biol.* 158: 1038, 1964.
35. Debris, M., C. Chararas and J. Courtois — *C. R. Soc. Biol.* 158: 1241, 1964.
36. Courtois, J., C. Chararas, M. Debris, and H. Laurant-Hubé — *Annuel de la Pharmacopée Francaise* 22: 549, 1964.
37. Courtois, J., C. Chararas, and M. Debris — *Annuel de la Pharmacopée Francaise* 22: 629, 1964.
38. Chararas, C., J. Courtois, and H. Laurant-Hubé — *Annuel de la Pharmacopeé Francaise* 25: 257, 1967.
39. Haltin, E., and I. Wanntorp — *Acta Chemica Scandinavica* 20: 2667, 1966.
40. Whitaker, D. "Cellulases and β-Glucosidases. Aspects of Their Properties in the Hydrolysis of Cellulose and Its Derivatives" — *Bulletin de la Societé de Chimie Biologique* 42: 1701—1709, 1960.
41. Grassmann, W. and H. Rubenhauer — *Münchener mediz. Wschr.* 1817, 1931.
42. Silberschmidt, K. — *Münchener mediz. Wschr.* 1819, 1931.
43. Courtois, J., and Bui Khac Diep — *Annuel de la Pharmacopée Francaise* 23: 649, 1965.
44. Whitaker, D. "Criteria for Characterizing Cellulases", in: Reese, E. *Advances in Enzymatic Hydrolysis of Cellulose and Related Materials* — Pergamon Press, 1963, pp. 51—70.
45. Iwasaki, T., K. Tokuyasu, and M. Funatsu — *Journal of Biochemistry Japan* 55: 30, 1964.

GLASNIK HEMIJSKOG DRUŠTVA, Vol. 32, No. 8-9-10, 1967, pp. 389—399

INFLUENCE OF SOLVENTS ON THE ABSORPTION SPECTRA OF HYDROXYANTHRAQUINONES*

by

IVAN N. PETROV and BOJAN T. ŠOPTRAJANOV

INTRODUCTION

The absorption (ultraviolet and visible) spectra of hydroxyanthraquinones have been investigated by a number of authors[1—6], but the effects of solvents have not received much attention, except in the early work of Lauer and Horio[1] in which instrumental limitations affected the accuracy of the measurments. We therefore undertook this re-investigation of the absorption spectra of a group of hydroxyanthraquinones using a set of solvents which comprised: *n*-hexane, dioxane, carbon tetrachloride, benzene, diethyl ether, chloroform, pyridine, acetone, ethanol, methanol, acetonitrile and 0.1 *N* solution of *NaOH*. 1-hydroxyanthraquinone (1-HA)(I) and the following dihydroxyanthraquinones (DHA), were investigated: 1,2-DHA (II), 1,4-DHA (III), 1,5-DHA (IV), 1,8-DHA (V) and 2,6-DHA (VI).

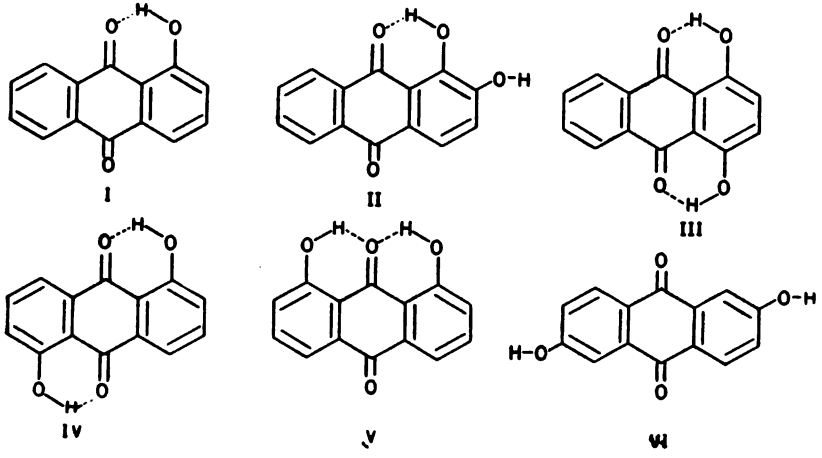

* Communicated at XI Colloquium Spectroscopicum Internationale, Beograd, 1963.

EXPERIMENTAL

The hydroxyanthraquinones were commercial products purified by repeated re-crystallization from suitable solvents (usually ethanol or acetic acid). The solvents were of spectroscopic purity or purified before use.

The spectra were obtained initially on a Jobin-Yvon Spectrophotomètre électronique and were later re-run on a Perkin-Elmer 137 UV recording instrument.

RESULTS AND DISCUSSION

Departing from the usual practice (to tabulate only the maxima of the absorption bands), we list the wavelengths (in mμ) of the absorption maxima and sub-maxima and of some of the shoulders in the absorption spectra of 1-HA, 1,2-DHA, 1,4-DHA, 1,4-DHA, 1,8-DHA and 2,6-DHA in Tables 1, 2, 3, 4, 5 and 6, respectively.

These results show that the absorption spectra are rather complex, although several common regions of absorption can be found. Three such regions are present for all hydroxyanthraquinones having α-hydroxyl groups: 210—230 *mμ* (this band is undetectable in most solvents, since they are not transparent that far), around 250 *mμ* (the most intense band of all the above-mentioned hydroxyanthraquinones), and between 400 and 500 *mμ*. One or two more bands (appearing sometimes as shoulders) are seen throughout the series of hydroxyanthraquinones in the region 275—285 *mμ*, and sometimes another one around 265 *mμ*. These latter bands have been characterized by Peters and Sumner[4] as "quinonoid", as distinct from the "benzenoid" bands around 250 and 320—330 *mμ*. In the spectra of 1,5-DHA and 1,8-DHA the band around 320—330 *mμ* could not be detected.

Five main bands (around 215, 240, 270, 300 and 350 *mμ*) were found in the spectrum of 2,6-DHA. The differences between the spectrum of this compound and those of the hydroxyanthraquinones having α-hydroxyl groups is not unexpected, since the conjugation is different, owing to the existence or non-existence of intramolecular hydrogen bonds. The spectra of the ionized forms (that is, in *NaOH* solution) are quite different from those of the nonionized forms for all the hydroxyanthraquinones studied. This is especially true for the longest-wavelength band which is considerably shifted towards longer wavelengths (lower frequencies).

In tihs work we attempted to classify the absorption bands according to their origin; it has been proposed[7] that changing from hexane to polar solvents shifts the bands originating from $\pi \rightarrow \pi^*$ transitions to longer wavelengths (red shift) and those originating from $n \rightarrow \pi^*$ transitions to shorter wavelengths (blue shift). For the so-called $n \rightarrow \pi^*$ blue shift phenomenon various explanations have been proposed. It has been considered that it is caused by the solvation[7], solvent polarization, various dipole--dipole interactions, hydrogen-bonding forces[8], etc. In the opinion of McRae[9] the dispersion forces between the solvent and solute molecules, dipole-dipole interactions and the quadratic Stark effect should be taken into consideration and he gives an expression which correlates band shift with the macroscopic properties of the solvent. Brealey and Kasha[10],

TABLE 1

*Absorption spectrum of 1-hydroxyanthraquinone**

n-Hexane	Dioxane	Carbon tetrachloride	Benzene	Diethyl ether	Chloroform
220				218	
224.5				221.5	
244.5				246 sh	
250	252.5			250	253
264.5	265.5 sh	264.5 sh		263.5 sh	269 sh
276	274.5 sh	278		274.5 sh	279.5
322.5	327	322.5	328.5	324.5	332.5
336		335		332	
362 sh					
390 sh		392 sh	397 sh	388 sh	
403	401	406	407	401	408
417 sh		416 sh	422 sh	425 sh	

Pyridine	Acetone	Ethanol	Methanol	Acetonitrile	*NaOH* 0.1 *N*
		218.5	217.5		
					233 sh
					246.5 sh
		251.5	251.5	252 ?	
		264.5 sh	264.5 sh	265 sh	270
		276	276.5 sh	278	312
333		329.5	330	330	
406.5	401	403	402	402	486

[1] The abbreviations used in this and in the following tables are: sh: shoulder; i.s.: insoluble; v.s.s.: very slightly soluble.

When more than one maximum or shoulder was observed in a complex band, the main maximum is underlined.

Pimentel[11] and other investigators[12–18] have pointed out that hydrogen bonding, when present, would be the most important effect to be considered. The observed shifts have also been correlated with some empirical quantities, such as Kosower's[19–21] Z-values or the F-values of Dubois and co-workers[22–23].

Although the blue shift of bands in polar solvents has been widely used to assign the absorption to $n \rightarrow \pi^*$ transitions, exceptions from such a behavior have also been reported[24, 25].

TABLE 2

Absorption Spectrum of 1,2-dihydroxyanthraquinone

n-Hexane	Dioxane	Carbon tetrachloride	Benzene	Diethyl ether	Chloroform
i.s.		i.s.	v.s.s.	226 ?	i.s.
	251			249	
	266 sh				
	279 sh				
				285 ?	
	322 sh			321	
	428		420	416	
			436	434	

Pyridine	Acetone	Ethanol	Methanol	Acetonitrile	*NaOH* 0.1 *N*
			235.5 sh		
		249	249.5	251	
		256 sh	256 sh	261 sh	265.5
		264 sh	263 sh	266 sh	
		279 sh	278 sh	278 sh	
		323 ? sh	326 ? sh	329? sh	
335					
439	431	427	423	425	
					555
					590 sh

An inspection of our results shows no drastic change in the positions of the maxima. The 250 $m\mu$ band of 1-HA shifts slightly up in wavelength going from hexane to ethanol and methanol, whereas the shift is difficult to observe in the case of dihydroxyanthraquinones because of the intensity redistribution which takes place within the band. Thus, although the maximum is shifted slightly to the blue, the whole band seems to be shifted in the opposite direction (red shift). The center of the band around 320—330 $m\mu$ in the spectra of 1-HA and 1,4-DHA also lies at longer wavelengths in ethanol than in hexane. Therefore these bands might be assigned to $\pi \rightarrow \pi^*$ transitions, as has been done[26] for the corresponding bands in the spectra of some hydroxynaphthaquinones.

On the other hand, the band found in the visible part of the spectrum (around 400—500 $m\mu$) seems to shift down in wavelength from hexane to alcohols. This may indicate an $n \rightarrow \pi^*$ transition (most probably of the $C{=}O$ group). Its relatively high intensity shows that this is an allowed transition, i.e. a $W \rightarrow A$ transition in Platt's[27, 28] notation.

The situation is less clear with 2,6-DHA, on account of its insolubility in inert solvents.

TABLE 3

Absorption Spectrum of 1,4-dihydroxyanthraquinone

n-Hexane	Dioxane	Carbon tetrachloride	Benzene	Diethyl ether	Chloroform
225				224	
229.5				227	
241.5					
249.5	249.5			248.5	250
256	255 sh			255.5	257
277	280	279.5	280.5	278	272
323					
334 sh	324	324.5	320 ? sh	323	327.5
458					
460	460 sh	460	460 sh	458	459
472	468 sh	473	474	469	472 sh
483	479	484	484	480	484
490 sh	494 sh				
504		505	500 sh	500	500 sh
516	510 sh	518	515	514	517
526 sh					

Pyridine	Acetone	Ethanol	Methanol	Acetonitrile	*NaOH* 0.1 *N*
		225.5	224.5		
		249	248	252 ?	249
		255.5	254.5	255	255 sh
		278.5	279	277	270 sh
325 sh		325	325.5	325	297 sh
	459 sh	459 sh			
475 sh	467 sh	469	467 sh	464 sh	
485	480	479	478	477	470
	494 sh	496 sh	493 sh		
514 sh	510 sh	513	510 sh		
				562	564
580					595

Correlations, difficult even when only hexane and alcohols are considered, become practically impossible with other solvents. Table 7 lists the quantities (refractive index n_D, dielectric constant D, dipole moment μ) usually employed to describe solvent polarity and some of combinations of them encountered in McRae's expression[9], as well as Kosower's[19] Z-values and the F-values of Dubois and co-workers[22, 23]. The values of these constants are taken from "Spravochnik Khimika"[29]. It can be

TABLE 4

Absorption spectrum of 1,5-dihydroxyanthraquinone

n-Hexane	Dioxane	Carbon tetrachloride	Benzene	Diethyl ether	Chloroform
226				225	
250 sh				250 sh	
254.5	254			253.5	255
261 sh					
274 sh	274.5 sh	274 sh		274 sh	278
286	284 sh	287	284 ? sh	285	288
		373 sh			401 sh
400 sh	400 sh	400 sh	402 sh	400 sh	420
415	415	418	422	415	435
433		435	437	433	

Pyridine	Acetone	Ethanol	Methanol	Acetonitrile	*NaOH* 0.1 *N*
		225	225		235
		250 sh	249 sh		
		253	253	254.5	
		275	275 sh	275 sh	276.5
		285.5	285.5	285	
405 sh	402 sh	400 sh	400 sh	400 sh	
423	418	416	415	416	
435	432	431	430	430	482

seen that the correlation of the observed shifts with any of these quantities is poor. No simple correlation could be established with the hydrogen-bonding ability of the solvents either. However, it should be borne in mind that when changing the solvent changes more than one parameter, whose effect might counteract or even cancel out. The dimensions and shape of the solvent molecules are also changed and this must have some consequences. In order to avoid complications of this type, mixtures of one polar and one non-polar solvent (or other suitable binary combinations) should be used. Such an investigation is presently under way.

Another known effect of polar solvents, especially those that can form hydrogen bonds, is the blurring of the fine-structure of the absorption bands, frequently present in hydrocarbon solvents. This fine-structure is due to transitions between the vibrational levels of two electronic states, and when a hydrogen-bonded complex is formed many more vibrational levels are

TABLE 5

Absorption spectrum of 1,8-dihydroxyanthraquinone

n-Hexane	Dioxane	Carbon tetrachloride	Benzene	Diethyl ether	Chloroform
224				224	
253	253.5			252	254.5
263					
273.5	272 sh	274.5		272.5	275.5
283.5	282.5	284.5		282.5	286
411		413	415 sh	411 sh	
422		424 sh			
430	427	431	432	428	431
440 sh		445 sh	445 sh	440 sh	445 sh
454		455 sh			

Pyridine	Acetone	Ethanol	Methanol	Acetonitrile	*NaOH* 0.1 *N*
		224	224		
		252.5	252.5	253	232
		273	273	273.5	
		283.5	283	283	280.5
420 sh	415 sh	413 sh			305 sh
433	428	429	427	427	
445 sh					
510					496

available, which could account for the blurring. Another factor which could lead to the disappearence of the vibrational fine-structure is the perturbing effect of dipolar electric fields. Such an effect was encountered in the spectra of the hydroxyanthraquinones studied, the most pronounced being probably in the case of the longest-wavelength band of 1,4-DHA: the well-defined peaks of the vibrational fine-structure in hexane solution were completely blurred in most of the polar solvents. The case was similar with the corresponding band of 1,8-DHA and, to a lesser extent, with most other bands. It should be noted that one of Peters and Sumner's "quinonoid" bands (the one having the longest wavelength) is always observed, regardless of the solvent, and this may support the hypothesis that it is a separate band.

One further fact which deserves attention is the structure of the 483 mμ band in 1,4-DHA (the case is similar with other bands and other compounds) is completely lost in dioxane, although this solvent can hardly be considered as polar, by any criterion. Dioxane can, however, act as a

TABLE 6

Absorption spectrum of 2,6-dihydroxyanthraquinone

n-Hexane	Dioxane	Carbon tetrachloride	Benzene	Diethyl ether	Chloroform
i.s.		i.s.	i.s.	216	
	243 sh			240	
	265 sh			262.5	
	273			270.5	275
	290 sh			288 sh	
	298			297	300.5
				335 sh	
	345.5			343	349

Pyridine	Acetone	Ethanol	Methanol	Acetonitrile	*NaOH* 0.1 *N*
		218	217		235
		241	240		
		268 sh	267 sh	265 sh	
		273	272	271	
				291 sh	294
		300	298	298	
346 sh	336 sh				
353	345.5	347	344	345.5	341
380 sh					414

proton acceptor, and a hydrogen-bonding mechanism for the blurring of the finestructure can be envisaged: intramolecular hydrogen bonds present in 1,4-DHA are partly ruptured and intermolecular hydrogen bonds are formed instead. Although dioxane is not considered a strong proton acceptor[30], such a mechanism could explanin some unexpected shifts in dioxane and other proton-accepting solvents. The very weak bands around 510 mμ in the spectrum of 1,8-DHA and around 580 mμ in the spectrum of 1,4-DHA in pyridine (their wavelengths both correspond to those of ionized forms) could possibly be attributed also to such a hydrogen-bonding mechanism, since pyridine is known as a strong proton acceptor.

From all the above it is clear that the study of solvent effects in the absorption spectra of hydroxyanthraquinones is far from being completed and should be continued.

TABLE 7

Some properties of the solvents

Solvent	n_D	D	μ	$\frac{n^2-1}{2n^2+1}$	Δ^*	Z	F
n-Hexane	1.375	1.90	0	0.186	0.002		0
Dioxane	1.422	2.21	0	0.203	0.033		0.10
Carbon tetrachloride	1.460	2.23	0	0.215	0.017		
Benzene	1.501	2.28	0	0.228	0.004		—0.05
Diethyl ether	1.353	4.22	1.17	0.178	0.301		0.07
Chloroform	1.446	4.72	1.06	0.210	0.287	63.2	0.08
Pyridine	1.510	12.3	2.20	0.230	0.491	64.0	
Acetone	1.359	20.74	2.85	0.180	0.648	65.7	
Ethanol	1.361	25.2	1.68	0.181	0.668	79.6	0.25
Methanol	1.329	32.65	1.71	0.169	0.710	83.6	0.34
Acetonitrile	1.344	37.4	3.94	0.175	0.712	71.3	0.16

* $\Delta = (D-1) \;/\; (D+2)-(n^2-1) \;/\; (n^2+2)$

Institute of Chemistry
School of Sciences — Skopje

Received 25 April, 1967

REFERENCES

1. Lauer, K. and Horio, M. — "Die Absorptionsspektren der Oxy-antrachinone in verschiedenen Lösungsmitteln" — *Journal für praktische Chemie* (Leipzig) 145: 273—80, 1936.

2. Spruit, C. J. P. — "Absorption Spectra of Quinones. I. Naphtoquinones and Naphthohydroquinones". — *Recueil des Travaux Chimiques des Pays-Bas* 68: 309—24, 1949.

3. Hartmann, H. and Lorenz, E. Über die Absorptionsspektren des Chinone" — *Zeitschrifr für Naturforschung* (Tübingen) 7a: 360—9, 1952.

4. Peters, R. H. and Sumner, H. A. — "Spectra of Antraquinone and Derivatives". *Journal of the Chemical Society* (London): 2101—10, 1953.

5. Sawicki, E., T. R. Hauser and T. W. Stanley; "Solvent Effects on the Photometric Determination of Weak Organic Acids in Alkaline Solution" — *Analytical Chemistry* (Washington, D. C.) 31: 2063—5, 1959.

6. Shcheglova, N. A., D. N. Shigorin and N. S. Dokumikhin. — "Spektry liuminist-sentsii i pogloshcheni'a α- i β-oksiantrakhinonov" (Emission and Absorption Spectra of α- and β-Oxyantraquinones" — *Zhurnal Fizicheskoi Khimii* (Moskva) 38: 1963—72, 1964.

7. McConnell, H. "Effect of Polar Solvents on the Absorption Frequency on n — Electronic States" — *The Journal of Chemical Physics* (New York) 20: 700—4, 1952.

8. Bayliss, N. S. and E. G. McRae. — "Solvent Effects in the Spectra of Acetone, Crotonaldehyde, Nitromethane and Nitrobenzene" — *The Journal of Physical Chemistry* (Washington, D. C.) 58: 1006—11, 1954.

9. McRae, E. G. "Theory of Solvent Effects on Molecular Electronic Spectra. Frequency Shifts" — *The Journal of Physical Chemistry* (Washington, D. C.) 61: 562—72, 1957.

10. Brealey, G. J. and M. Kasha. "The Role of Hydrogen Bonding in n — π*. Blue Shift Phenomenon" — *The Journal of the American Chemical Society* (Washington, D. C.) 77: 4462—8, 1955.

11. Pimentel, G. C. "Hydrogen Bonding and Electronic Transitions. The Role of Franck-Condon Principle" — *The Journal of American Chemical Society* (Washington, D. C. 4 79: 3323—5, 1957.

12. Balasubbramanian, A. and C. N. R. Rao. "n →π* (U →'A) Transitions in Aliphatic Nitrocompounds. Evidence for Hypercojugation in the Electronically Excited States of Molecules" *Chemistry and Industry* (London) 1025—6, 1960.

13. Rao, C. N. R., C. H. Goldman and A. Balasubramanian. "Structural and Solvent Effects on the n→π*(U→'A) Transitions in Aliphatic Carbonyl Compounds" — *Canadian Journal of Chemistry* (Ottawa) 38: 2508—13, 1960.

14. Krishna, V. G. and L. Goodman. "Solvent Effects on n→π* Transitions in Pyrazine" — *The Journal of Chemical Physics* (New York) 33: 381—6, 1960.

15. Ito, M., K. Inuzaka and S. Lmanishi. "Effect of Solvents on n→π* Absorption Spectra of Ketones" — The Journal of the *American Chemical Society* 82: 1317—22, 1960.

16. Chandra, A. K. and S. Basu — "Hydrogen Bonds. I." — *Transactions of Faraday Society* (Aberdeen) 56: 632—7, 1960.

17. Linnell, R. H. "Near Ultraviolet Solution Spectra of Pyrazine" — *The Journal of Chemical Physics* (New Yorks) 34: 698—9, 1961.

18. Balasubramanian, A. and C. N. R. Rao. "Evaluation of Solute-Solvent Interaction from Solvent Blue-Shifts of n→π* Transitions of C=O, C=S, NO_2 and N=N Groups. Hydrogen Bond Energies of Various Bonor-Acceptor Systems" — *Spectrochemica Acta* (Oxford) 18: 1337—52, 1962.

19. Kosower, E. M. "The Effect of Solvents on Change-Transfer Complex Spectra" — *The Journal of the American Chemical Society* 78: 5700—1, 1956.

20. Kosower, E. M. "The Effect of Solvents on Spectra. I. A New Empirical Measure of Solvent Polarity — z-Values" — *The Journal of the American Chemical Society* (Washington, D. C.) 80: 3253—60, 1958.

21. Kosower, E. M. "The Effect of Solvents on Spectra. II. Correlation of Spectral Absorption Data with z-Values" — The *Journal of the American Chemical Society* (Washington) 80: 3261—7, 1958.

22. Dubois, J. E. and E. Goetz. "Influences des solvents sur la transition n→π* des cetons saturées" — *Journal de Chimie Physique et de Physiologie Biologique* (Paris) 60: 1019, 1963.

23. Dubois, J. E., E. Goetz and A. Bienvenue. "Influence des solvents sur la transition n→π* des cetones saturées" — *Spectrochimica Acta* (Oxford) 20: 1815—28, 1964.

24. Ford, R. A. and F. Pary. "Electronic and Vibrational States of Carbonyl Compounds. I. Electronic States of Camphor Quinone" — *Spectrochemica Acta* (Oxford) 12: 78—87, 1958.

25. Hayes, W. P. and C. J. Timmons. "Solvent and Substituent Effect on the n→π* Absorption Bands of Some Ketones" — *Spectrochimica Acta* (Oxford) 21: 529—42, 1965.

26. Shcheglova, N. A. and D. N. Shigorin. "Osobenosti elektronnykh spektrov naftakhinona, 1,4 i nekotorykh ego proizvodnykh" (The Electronic Spectra of 1,4 Naphthaquinone and Some of Its Derivative) *Zhurnal Fizitseskoi Khimii* (Moskva) 38: 1261—7, 1958.

27. Platt, J. R. "Molecular Orbital Prediction of Organic Spectra" — *The Journal of Chemical Physics* (New York) 18: 1168—73, 1950.

28. Platt, J. R. "Classification of Assignments of Ultraviolet Spectra of Conjugated Organic Molecules" — *Journal of the Optical Society of America* (New York) 43: 252—7, 1953.

29. Nikol'skii, B. P. (Ed) Spevochnik Khimika Vol. 1. (The Chemist's Handbook, Vol. 1) (Leningrad—Moskva): Goskhimizdat, 1951.

30. Hadži, D., I. Petrov and M. Žitko. "The Influence of Hydrogen Bonding Upon the Frequency and Intensity of the OD In-Plane Deformation Vibration of Some Phenols and Alcohols" — in A. Mangini (Ed) *Advances in Molecular Spectroscopy* — Oxford: Pergamon Press, 1962.

GLASNIK HEMIJSKOG DRUŠTVA, Vol. 32, No. 8-9-10, 1967, pp. 401—408

ANODIC OXIDATION OF ETHANOL IN ALKALINE SOLUTION

by

VERA J. DRAŽIĆ and DRAGUTIN M. DRAŽIĆ

It has been shown that the potential of a platinized platinum electrode in an alkaline solution containing alcohol is controlled by adsorbed hydrogen formed at the electrode by dehydrogenation of the alcohol[1–6].

Both the presence of the adsorbed hydrogen and the occurence of the dehydrogenation reaction should affect the mechanism of the overall reaction of the electrochemical oxidation of alcohol. In this paper the effect of the dehydrogenation reaction is analyzed.

EXPERIMENTAL

Galvanostatic measurements were made in a cell already described[1]. The only difference from the previous arrangement of the cell was that the platinum electrode was now in the form of a plate (1.43 cm^2) with one side covered in polythene, and that during the experiment the electrode was not rotated. The electrolyte was 1*N KOH*, with ethanol in concentrations of 0.5*M*, 0.05*M* or 0.005*M*, deaerated by purified nitrogen. Before each run the eletrode was freshly platinized, always in the same way[1]. Potentials were measured by a vacuum-tube voltmeter with high input impedance. Galvanostatic transients were photographed on an oscilloscope (Tektronix 551). Potentials in this paper are referred to the normal hydrogen electrode.

In order to determine the overall reaction products and the coulombic efficiency of the oxidation reaction, long duration electrolysis experiments were made. They were carried out in a similar cell with separated anodic and cathodic compartments. The anodic compartment was much smaller than the cathodic (cca 50 ml of the solution). It contained a magnetic stirrer and a platinized nickel gauze anode (10 cm^2 projected area). The potential of the electrode at constant anodic current was recorded by a potential recorder. A rapid increase in the potential indicated that all the alcohol had been oxidized.

The concentration of acetic acid, a product of the electrolysis, was followed by taking samples from the cell at regular intervals. The acetic acid was distilled from the samples after addition of excess sulfuric acid, and then determined by titration with a hydroxide solution.

RESULTS AND DISCUSSION

The galvanostatic anodic transients showed two characteristic potential levels, the first at a value of a few millivolts, and the second in the range 50—200 *mV* (see Fig. 1). These levels depended on the current density. The rise time for the first level was of the order of milliseconds, and for the second of the order of seconds, and hence it was necessary, in order to detect both, to monitor the transients on two time scales. Typical transients on two scales are shown in Fig. 1. The first level is more pronounced when the potential-time curve is transferred to a log η-log t graph, as shown in

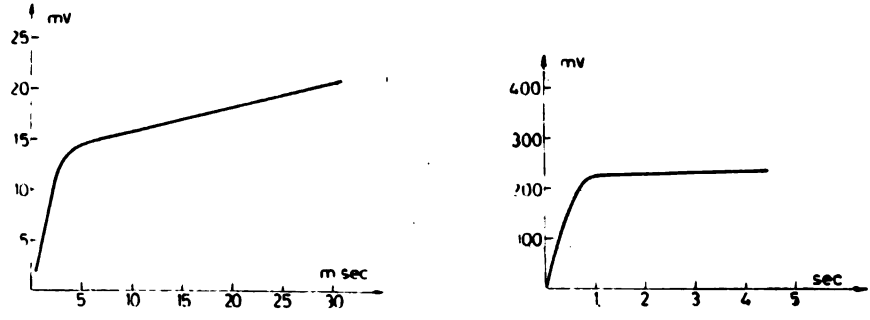

Figure 1

Galvanostatic transient at two different time scales for 0.5 *M* ethanol solution in 1 *N KOH*; $i = 0.45\ mA/cm^2$

Fig. 2. This transient indicates that the first level is due to some fast reaction which possibly soon reaches a limiting current after which the reaction changes and the potential of the second polarization level appears. It corresponds to an elctrochemical step, slower than the first.

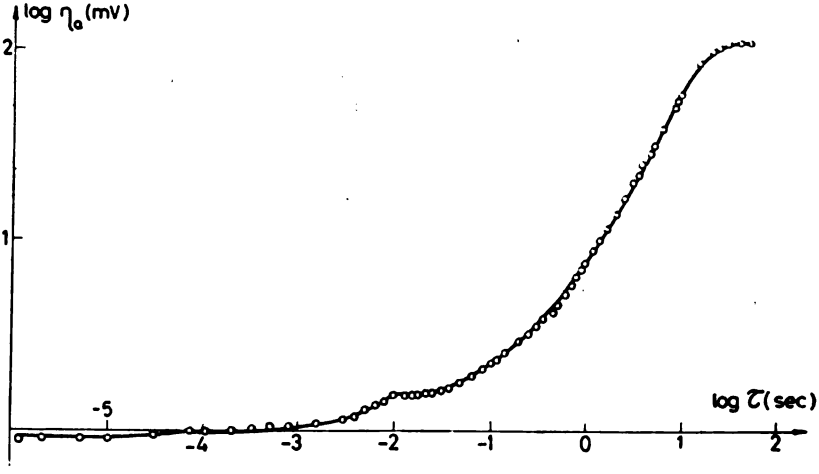

Figure 2

Galvanostatic transient plotted on a log η — log t scale

Similar experiments were carried out with freshly distilled acetaldehyde instead of ethanol. However, with the introduction of aldehyde into the alkaline solution in concentrations of 0.005*M* or higher, a resinous precipitate formed, so that the experiments comparable with those for alcohol could not be made. However, even with a few drops of aldehyde, the electrode reached a potential slightly more negative than that in alcohol solutions. Galvanostatic transients again showed two polarization levels, much the same as with alcohol.

When the potentials of the first level, corrected for the ohmic drop, are plotted against current density, linear dependence is obtained (Fig. 3). From the relation[7]

$$i = i_0 \frac{RT}{nF} \eta \qquad (1)$$

i_0 was calculated from Fig. 3. It appears that i_0 is independent of the alcohol concentration, lying in the range 15—22 mA/cm^2. However, in a few experiments it was smaller (4—5 mA/cm^2). This is ascribed to "poisoning" of the electrode in the process.

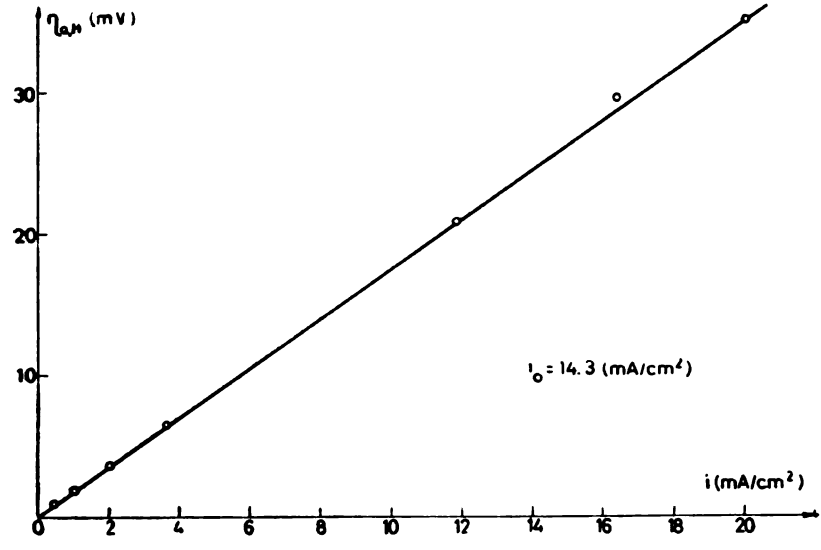

Figure 3

Relationship between first potential level and current density from galvanostatic transients in 0.5 *N* ethanol solutions

Experiments with the anodic oxidation of ammonia[8] showed the same behavior as this with alcohol. In the former case it has been suggested that the reaction of catalytic dehydrogenation of ammonia takes place and this process supplies the electrode surface with atomic hydrogen. The similarity

of the transients with alcohol and ammonia, and our earlier results concerning the nature of the rest potential in alcohol solutions[1], suggest that the first step in the overall reaction of alcohol oxidation is catalytic dehydrogenation.

Rise of the potential after the first polarization level is then due to the concentration polarization arrising from the decrease of hydrogen which is being used up by the anodic reaction. The second polarization is determined by the parallel electrochemical reaction of certain intermediate species formed by the dehydrogenation reaction.

This hypothesis was verified by modelling two parallel electrochemical reactions with a preceeding chemical reaction of the general type

$$AB \xrightarrow{k_1} A + B \tag{2}$$

$$A \xrightarrow{k_2} C + e \tag{3}$$

$$B \xrightarrow{k_3} D + e \tag{4}$$

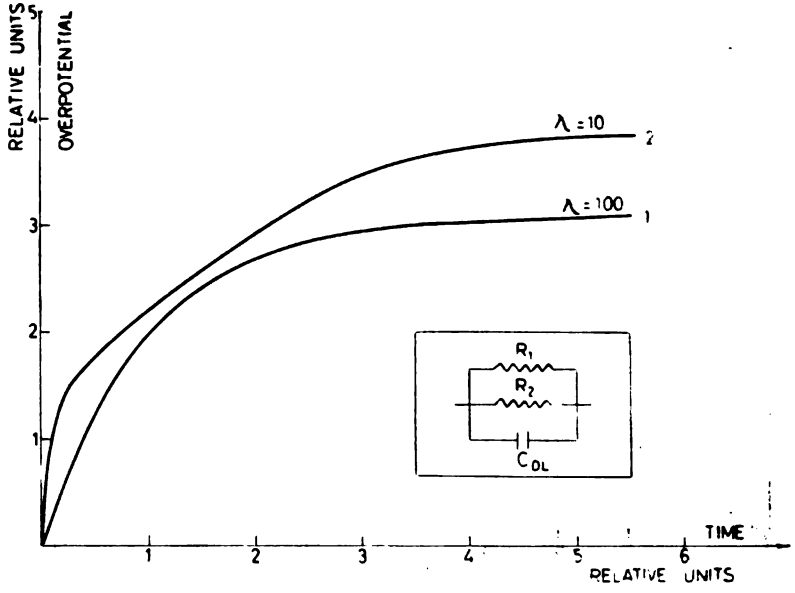

Figure 4

Analog computed transients for a mode of two parallel reactions: 1. ratio of rate constants $\lambda = 100$, 2. ratio of rate constants $\lambda = 10$.

on an analog computer and registering the potential against time under galvanostatic conditions for different ratios of k_2 and k_3 $\left(\lambda = \frac{k_2}{k_3}\right)$.

Two characteristic graphs of this type are shown in Fig. 4. Curve 1 is the most frequent case when the rates of the two parallel electrochemical reactions are very different (i.e. $\lambda \geqslant 100$). Curve 2 is the case when $\lambda = 10$, i.e. when the two rates are comparable. The qualitative behavior of the computed $\eta - t$ curve in the second case is similar to the experimental relationship, indicating that the first part of the overall mechanism is of the general type given by equations (2—4), or, more precisely, in view of the previously given arguments, that reaction (2) is the dehydrogenation reaction of alcohol followed by the electrochemical oxidation of intermediates formed, i.e. atomic hydrogen and alcohol radicals.

The fact that aldehyde shows a similar behaviour to alcohol indicates that the same general mechanism may be expected in the oxidation of aldehyde.

The second polarization level of the transient represents the steady state polarization, and an E-log i graph gives the linear Tafel relation for all three concentrations, with the same slope of about 120 mV (Fig. 5).

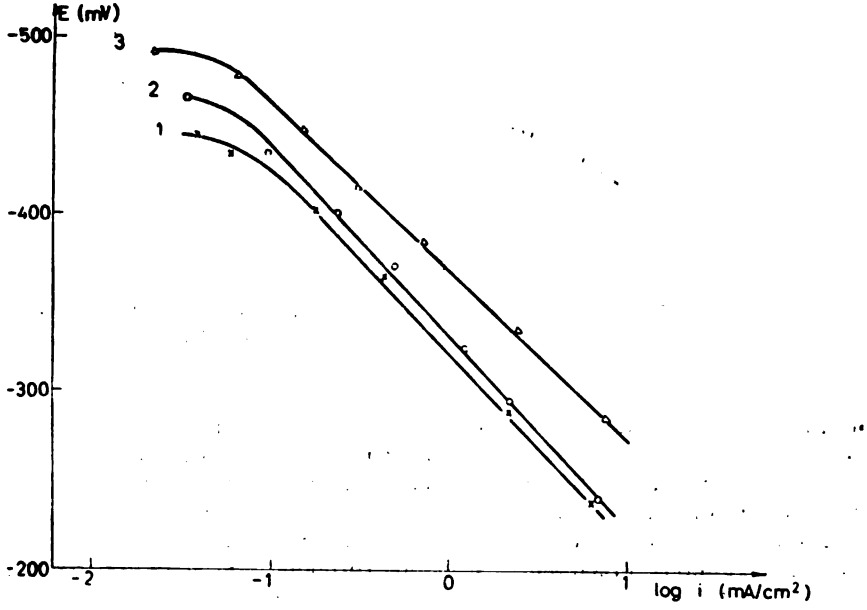

Figure 5

Steady state potential- *log i* curves for different ethanol concentrations in 1 *N KOH*. 1. 0.005 *M*; 2. 0.05 *M*; 3. 0,5 *M*

In the long duration electrolysis experiments the oxidation of the alcohol solution resulted in the formation of a yellow resinous precipitate. The solution started to smell of croton aldehyde. A positive qualitative test with the silver mirror reaction revealed the presence of unpolymerized aldehyde. The amount of acetic acid formed during the electrolysis is shown in Fig. 6. The straight line represents the relationship expected assuming that the oxidation of ethanol proceeds to acetic aicd. Under the given experimental conditions acetic acid does not oxidize further to carbon dioxide.

Simultaneous measurements showed that for a quantity of electricity equivalent to 4 electrons per molecule of alcohol was used up the electrode potential changed from about — 400 *mV* to a more positive value. This indicates that all the alcohol initially present in the solution was consumed. The initial overlap of the curves of concentration against number of coulombs

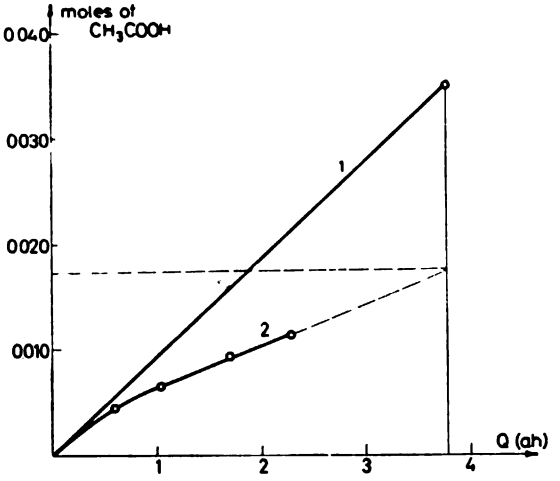

Figure 6

The yield of acetic acid at different amounts of current passed: 1. theoretical curve, calculated for quantitative oxidation of ethanol to acetic acid, 2. experimental curve.

in Fig. 6 shows that the oxidation of ethanol proceeded to the formation of acetic acid. The presence of aldehyde in the solution in the later stages of the electrolysis, and the precipitate, indicate that two parallel processes were going on, one the formation of acetic acid, and the other the chemical reaction of electrochemically formed aldehyde as an intermediate. This gave the resinous precipitate, probably through the aldol condensation reaction[9], known to proceed in alkaline solutions.

These secondary products of the oxidation obviously inhibit the overall oxidation reaction, decreasing the yield of acetic acid. The shape of the experimental curve *a* in Fig. 6 relative to the calculated curve *b* undoubtedly shows that at the begining of the electrolysis the yield of acetic acid was nearly 100%, while later when the electrode got poisoned it decreased to about 50%. A similar poisoning effect was observed by Podlovchenko *et al.*[2] in the case of ethanol.

It may be concluded that in alkaline media ethyl alcohol undergoes a dehydrogenation reaction at a platinum surface liberating atomic hydrogen which plays an important role in determining the steady state potential as well as in the mechanism of the overall oxidation reaction. The similar behaviour of aldehyde indicates its presence as an intermediate in the overall

process and its further oxidation through the dehydrogenation reaction. Additional experimental evidence is required for a more detailed discussion of the overall mechanism.

Acknowledgement: The authors are indebted to the Research Fund of the S. R. of Serbia for financial support.

Institute of Chemistry, Technology and Metallurgy, Beograd

Received 27 April, 1967

REFERENCES

1. Dražić, D. M. and V. J. Dražić. — *Electrochimica Acta* (Oxford) 11: 1235—41, 1966.
2. Podlovchenko, B. J., O. A. Petrii and A. N. Frumkin. — *Journal of Electroanalytical Chemistra* (Amsterdam) 11: 12—25, 1965.
3. Oxlea, J. E., G. K. Johnson and B. T. Buzalski. — *Electrochimica Acta* (Oxford) 9: 897—910, 1964.
4. Beskorovainaiy S. S., I. B. Vasiles and V. S. Bagotskii. — *Elektrokhimiia* (Moskva) 2: 44—49, 1966.
5. Beskorovainai S. S., I. B. Vasilev and V. S. Bagotskii. — *Elektrokhimiia* (Moskva) 2: 1676174, 1966.
6. Podlovchenko, B. I. — *Elektrokhimiia* (Moskva) 1: 101—106, 1965.
7. Bockris, J. O' M. *Modern Aspects of Electrochemistry:* London, Butterworths, 1954.
8. Despić, A. R., D. M. Dražić and P. M. Rakin — *Electrochimica Acta* (Oxford) 11: 997—1005, 1966.
9. Parrer, P. *Lehrbuch der Organischen Chemie.* — Stutgart: Thieme Verlag, 1959.

GLASNIK HEMIJSKOG DRUŠTVA, Vol. 32, No. 8-9-10, 1967, pp. 409—415

PHOTOLUMINESCENCE OF BORIC ACID PHOSPHOR ACTIVATED BY PAPAVERINE HYDROCHLORIDE

by

Ž. A. KUČER, B. J. DRAŠKOVIĆ and I. Đ. BURIĆ

Boric acid phosphor activated by papaverine hydrochloride and exposed to excitation radiation of 366 *nm* exhibits an intense luminescence[1]. The photoluminescent properties of this phosphor confirmed some general regularities of the photoluminescence of organophosphors: the influence of temperature on the luminescence spectra, the exponential decrease of phosphorescent intensity with time, and temperature quenching of the phosphorescence.

EXPERIMENTAL

Samples of boric acid phosphor containing different activator concentrations were prepared according to known methods[2, 3]. Luminescence spectra were recorded with a spectrophotometer adapted for fluorescence and phosphorescence spectra[4, 1]. The excitation source was a HANAU Q 81 high-pressure mercury lamp. The excitation was carried out with the 366 *nm* line which was isolated by means of a 2 *mm* BG 12 + 2 *mm* UG 2 (Schott) filter. The spectra were taken at the temperature of liquid air in a quartz Dewar of dimensions $160 \times 43 + 1.2$ *mm* (Heraeus Gmbh). The same equipment was used to study quenching of the phosphorescence. The phosphorescence mean life was measured by means of a device with synchronized automatic shutters for excitation and phosphorescence and a photomultiplier detector whose impulses were fed to a cathode ray oscillograph.[1]

EMISSION SPECTRA

The analysis of the luminescence spectrum and time parameters indicated the exsistence of two kinds of transition: a component with a very short mean life and a spectrum at a shorter wavelength corresponding to a transition between states of the same multiplicity (fluorescence), and a component with a long mean life and a spectrum at a longer wavelength corresponding to a transition between states of different multiplicity (beta phosphorescence).

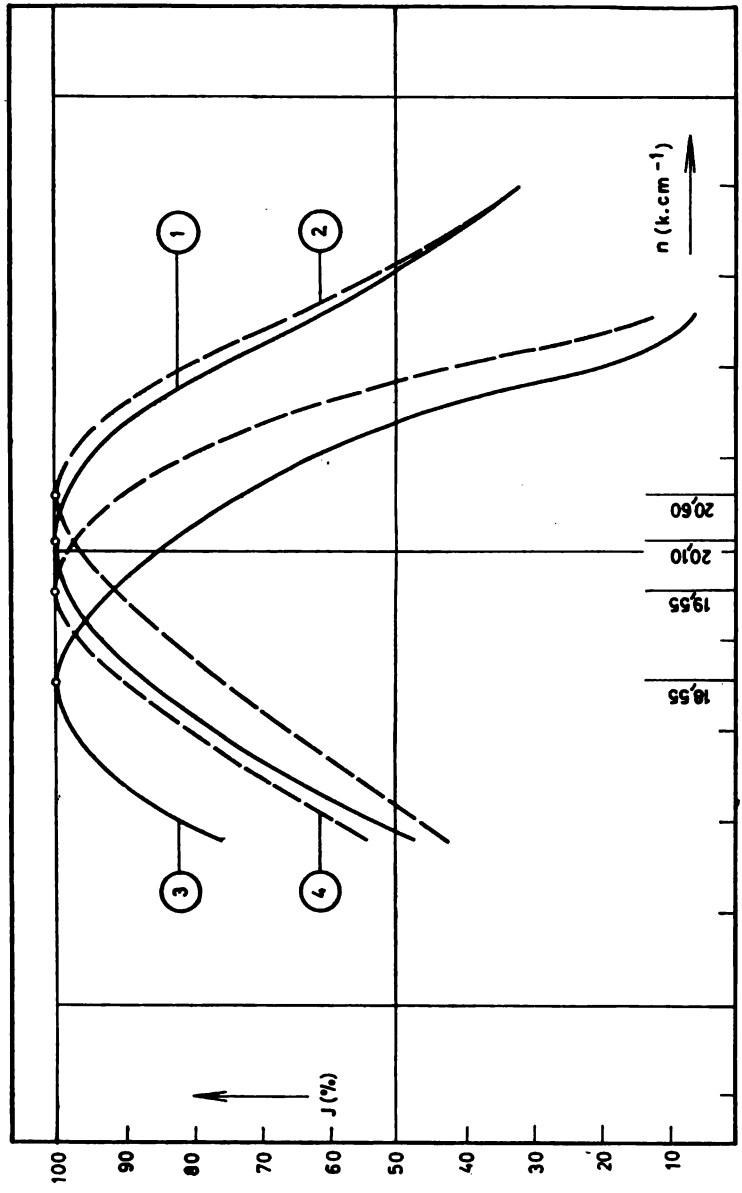

Figure 1

Spectra of integral luminescence and beta phosphorescence of boric acid phosphor activated by papaverine hydrochloride (activator concentrations: 10^{-2}, 10^{-3}, 10^{-4} and 10^{-5} *g/g*);
— integral luminescense: curve 1 (20°C), curve 2 (—183°C)
— beta phosphorescence: curve 3 (20°C), curve 4 (—183°C)

Figure 1 shows the relative energy distribution of the intergral* luminescence and beta phosphorescence of this phosphor. In both cases the curve of energy against wave number exhibits a broad band with one maximum.

Both spectra remained unchanged for a wide range of activator concentration (from 10^{-2} to 10^{-5} g/g).

At — 183°C (liquid air) both spectra were shifted towards shorter wavelengths (Table 1) and their emission bands narrower, which is due to a reduced density of oscillation levels between the ground and the excited state.

The maxima of the integral and phosphorescence spectra are very near, which was also observed visually. On the basis of the scheme given by Jablonovsky[5] it may be concluded that the metastable level M, which defines beta phosphorescence with respect to the ground level N, is very near to the level F from which the transition to the N is allowed, and that at temeratures of 20°C and — 183°C both transitions take place simultaneously: $M \rightarrow N$ and $F \rightarrow N$. On the other hand, if M is slightly below

TABLE 1

Maxima of the luminescent spectra

Conc. in (g/g)	Integral spectra		Phosphorescence spectra	
	Maximum ($k.\ cm^{-1}$)		Maximum ($k.\ cm^{-1}$)	
	20°C	—183 C	20°C	—183°C
10^{-2}, 10^{-3} 10^{-4}, 10^{-5}	20.10	20.60	18.55	19.55

F, a small increase of the temperature should be sufficient to raise the electrons from M to F, so that transitions of the type $F \rightarrow N$ with a long mean life should occur i.e., alpha phosphorescence. However, up to the temperature of phosphorescence quenching the phosphorescence spectra showed no change of this type.

CHANGE OF THE PHOSPHORESCENCE INTENSITY WITH TIME

The intensity decreases exponentially with time (Fig. 2).
The process of decay was not dependent on the activator concentration (concentrations from 10^{-2} to 10^{-5} g/g).

A considerable effect of the temperature on the mean life of the phosphorescence was observed. At low temperatures (— 183°C) the change of intensity with time was also exponential, but the mean life was considerably longer (Table 2), which is due to the effect of temperature on the density of oscillation levels of the ground and metastable states.

* Integral luminescence means the total intensity of fluorescence and beta phosphorescence.

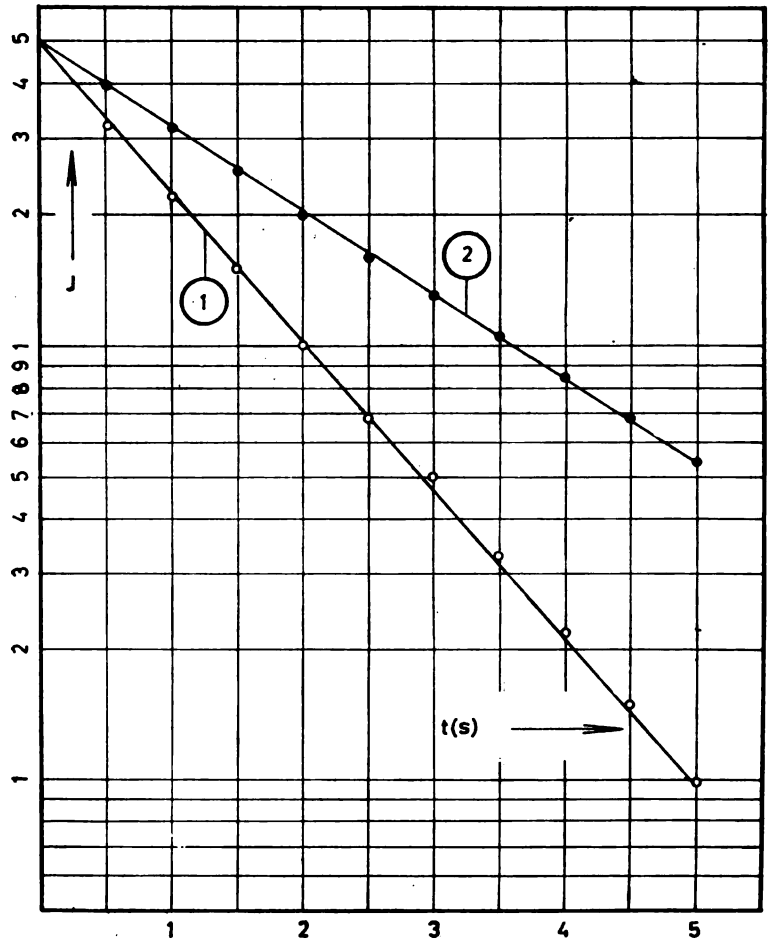

Figure 2

Curve of phosphorescence intensity against time (activator concentrations: 10^{-2}, 10^{-3}, 10^{-4} and 10^{-5} *g/g*):

curve 1. (20°C), curve 2. (—183°C)

TABLE 2

The mean-life of the phosphorescence

Conc. (*g/g*)	τ (sec.)	
	20°C	—183°C
10^{-2}, 10^{-3} 10^{-4}, 10^{-5}	1.25	2.25

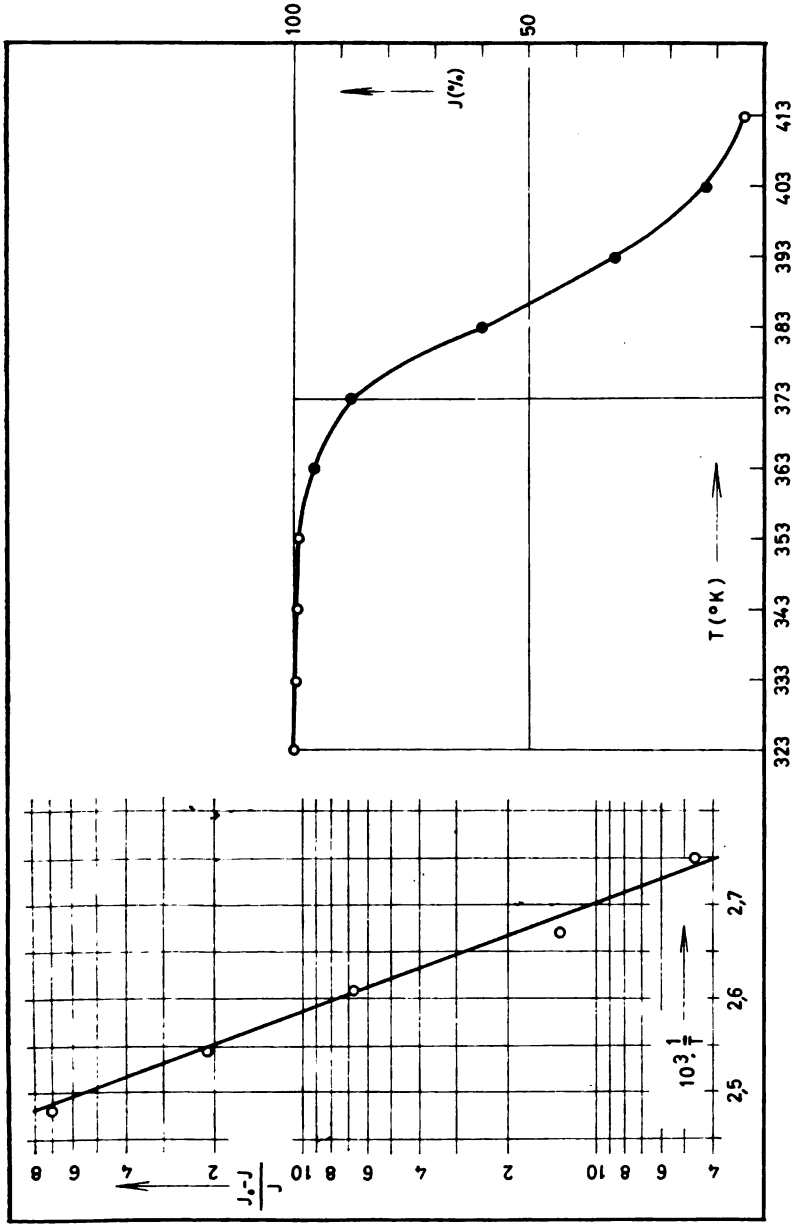

Figure 3

Curve of phosphorescence quenching with temperature (activator concentrations: 10^{-2}, 10^{-3}, 10^{-4} and 10^{-5} g/g); the auxiliary graph represents the verification of the Mott-Seitz formula (conc. from 10^{-2} to 10^{-5} g/g)

TEMPERATURE QUENCHING OF THE FLUORESCENCE

Quenching of the phosphorescence takes place with increasing temperature (Fig. 3). Up to 50°C the total intensity remains unchanged. Above 50°C, there is a gradual decrease, and between 90° and 130°C an abrupt decrease. Above 150°C the quenching is complete.

The change of phosphorescence intensity with temperature obeys the Mott-Seitz formula:

$$I = \frac{I_0}{1 + C_1 \exp\left(\frac{-C_2}{T}\right)},$$

I_0 — the initial intensity
I — the intensity for the given temperature
T — the absolute temperature
C_1, C_2 — constants.

The experimental data for five points of the $I = f(T)$ curve in the quenching range and the characteristic parameters of the Mott-Seitz formula are given in Table 3; a graphical verification of this formula is included in graph in Fig. 3.

TABLE 3

Temperature Quenching of the Phosphorescence

$T(°K)$	I	$\frac{1}{T} \cdot 10^3$ (^0K)	$\frac{I_0 - I}{I}$	C_1	$C_2(°K)$
323	100				
363	95	2.75	0.046		
373	88	2.68	0.132		
383	60	2.61	0.666	$2.29 \cdot 10^{22}$	$1.99 \cdot 10^4$
393	32	2.55	2.125		
403	12.5	2.48	7		

Institute of Physics
Beograd University

Received June 22, 1967

REFERENCES

1. **Kučer,** Z. *Luminiscencija bornog fosfora aktiviranog hinolinskim derivatima* (Luminescence of Boric Acid Phosphors Activated by Quinoline Derivatives) — Beograd, 1965 (Thesis).
2. **Tiede,** E. — *Chemische Berichte* 53: 2214, 1920.
3. **Filipovich,** B. A., and B. I. Sveshnikov. — *Optics and Spectroscopy* (USSR) 4: 541—543, 1958.
4. **Drašković,** B. J. *Fotoluminiscencija jedinjenja alkilpiridina i kuprohalogenida* (Photoluminiscence of Compounds of Alkylpyridines and Cuprous Halogenides) — Beograd, 1964 (Thesis).
5. **Jablonsky,** A. — *Zeitschrift für Physik* 94: 38, 1935.

GLASNIK HEMIJSKOG DRUŠTVA, Vol. 32, No. 8-9-10, 1967, pp. 417—428

STUDY OF THE REACTION OF HEXANITROCOBALTATES (III) WITH AMINO ACIDS. III.

PREPARATION OF POTASSIUM DINITRODIGLYCINATOCOBALTATE (III) FROM COMPLEX COBALTIC COMPOUNDS OF THE DIAMINE, TRIAMINE, TETRAMINE, PENTAMINE AND HEXAMINE TYPE*

by

MILENKO B. ĆELAP, DUŠAN J. RADANOVIĆ, TOMISLAV J. JANJIĆ, and MIJAT J. MALINAR

In a previous[1] paper we described the synthesis of a new class of complex compounds of cobalt (III) with amino acids: dinitrodiglycinatocobaltates, $M^I[Co\ gly_2(NO)_2]$. The synthesis involves the action of alkaline glycinates on alkaline hexanitrocobaltates (III) whereby four out of the six nitro groups present in the complex ion are substituted by glycine residue:

$$M^I_3[Co(NO_2)_6] + 2\,H_2N\cdot CH_2\cdot COOH = M^I\,[Co(H_2N\cdot CH_2\cdot COO)_2(NO_2)_2] + \\ + 4\,M^I NO_2$$

Continuing our investigations we have established that the above compounds can be obtained not only from the complex cobalt (III) compounds of the hexaacido type but also from these of the diamine, triamine, tetramine, pentamine and hexamine type.

By the action of potassium glycinate on Erdmann's salt, a complex cobaltic compound of the diamine type, we succeeded in synthesing potassium dinitrodiglycinatocobaltate (III) in a yield of 61%. In this reaction two out of four of the nitro groups present in the complex ion and two molecules of ammonia are substituted by two glycine residues:

$$NH_4[Co(NH_3)_2(NO_2)_4] + 2\,H_2N.CH_2.COOK = \\ = K[Co(H_2N.CH_2.COO)_2(NO_2)_2] + NH_4NO_2 + KNO_2 + 2NH_3.$$

We also established that dinitrodiglycinatocobaltate (III) could be obtained from cobaltic coordination compounds of the triamine type: in the reaction of the peripheral isomer of trinitrotriamminecobalt (III) with

* Preliminary communication: *Bulletin Scientifique, Conseil Acad. SFR of Yugoslavie* (Zagreb) 10 (Section A): 273, 1965.

Communicated at the XIth Conference of Chemists of the S.R. of Serbia, Beograd, 1965.

potassium glycinate three molecules of ammonia and one nitro group are substituted by two amino acid residues (yield 72%).

$$[Co(NH_3)_3(NO_2)_3]+2H_2N.CH_2.COOK=$$
$$=K[Co(H_2N.CH_2.COO)_2(NO_2)_2]+KNO_2+3NH_3.$$

Of the complex cobaltic compounds of the tetramine type we studied *cis*- and *trans*- isomers of dinitrotetramminecobalt (III) nitrate which were treated with potassium glycinate. Both isomers reacted in the same way: four ammonia molecules were substituted by two glycine residues whereas neither of the two nitro groups was substituted:

$$[Co(NH_3)_4(NO_2)_2]NO_3+2H_2N.CH_2.COOK=$$
$$K[Co(H_2N.CH_2.COO)_2(NO_2)_2]+KNO_3+4NH_3.$$

In these reactions potassium dinitrodiglycinatocobaltate (III) was obtained in a yield of 68% from the *cis* and of 63% from the *trans* isomer.

Nitropentamminecobalt (III) nitrate was chosen for study as a compound of the pentamine type. When one mole of this compound was allowed to react with a mixture containing one mole of potassium nitrite and two moles of potassium glycinate, four of its ammonia molecules were substituted by two glycine residues, whereas the fifth was substituted by a nitro group, so that dinitrodiglycinatocobaltate (III) was obtained in a yield of 74%:

$$[Co(NH_3)_5NO_2]\ (NO_3)_2+KNO_2+2\,H_2N.CH_2COOK=$$
$$=K[Co(H_2N.CH_2.COO)_2\ (NO_2)_2]\ +2KNO_2+5NH_3.$$

By the action of potassium glycinate and potassium nitrite on hexamminecobalt (III) chloride, four ammonia molecules in the complex ion were substituted by two glycine residues and the remaining two ammonia molecules by two nitro groups. In this way potassium dinitrodiglycinatocobaltate (III) was obtained in a yield of 71%:

$$[Co(NH_3)_6]Cl_3+2H_2N.CH_2.COOK+2KNO_2=$$
$$=K[Co(H_2N.CH_2.COO)_2\ (NO_2)_2]+6NH_3+3KCl.$$

Since the complex ion of potassium dinitrodiglycinatocobaltate contains two nitro groups and two glycine residues, this compound may be expected to exist in five geometrically isomeric forms: two isomers containing nitro groups in the *trans*-position and optically inactive, and the other three isomers with nitro groups in the *cis*-position. Each *cis*-isomer, due to its molecular assymetry, would be resolvable into optical antipodes (Fig. 1). Earlier[1] we studied the configuration of dinitrodiglycinatocobaltates (III) and established[2] that the configuration of these compounds is *cis*, i.e. that the nitro groups lie in the *cis*-position.

In order to establish whether the compounds prepared in this work also have the *cis*-configuration, we studied their ultraviolet, visible and infrared spectra. From the absorption curves obtained we established that all the above reaction products were identical and corresponded to the compound reported in our first paper[1]. The absorption curve in the visible and ultra-

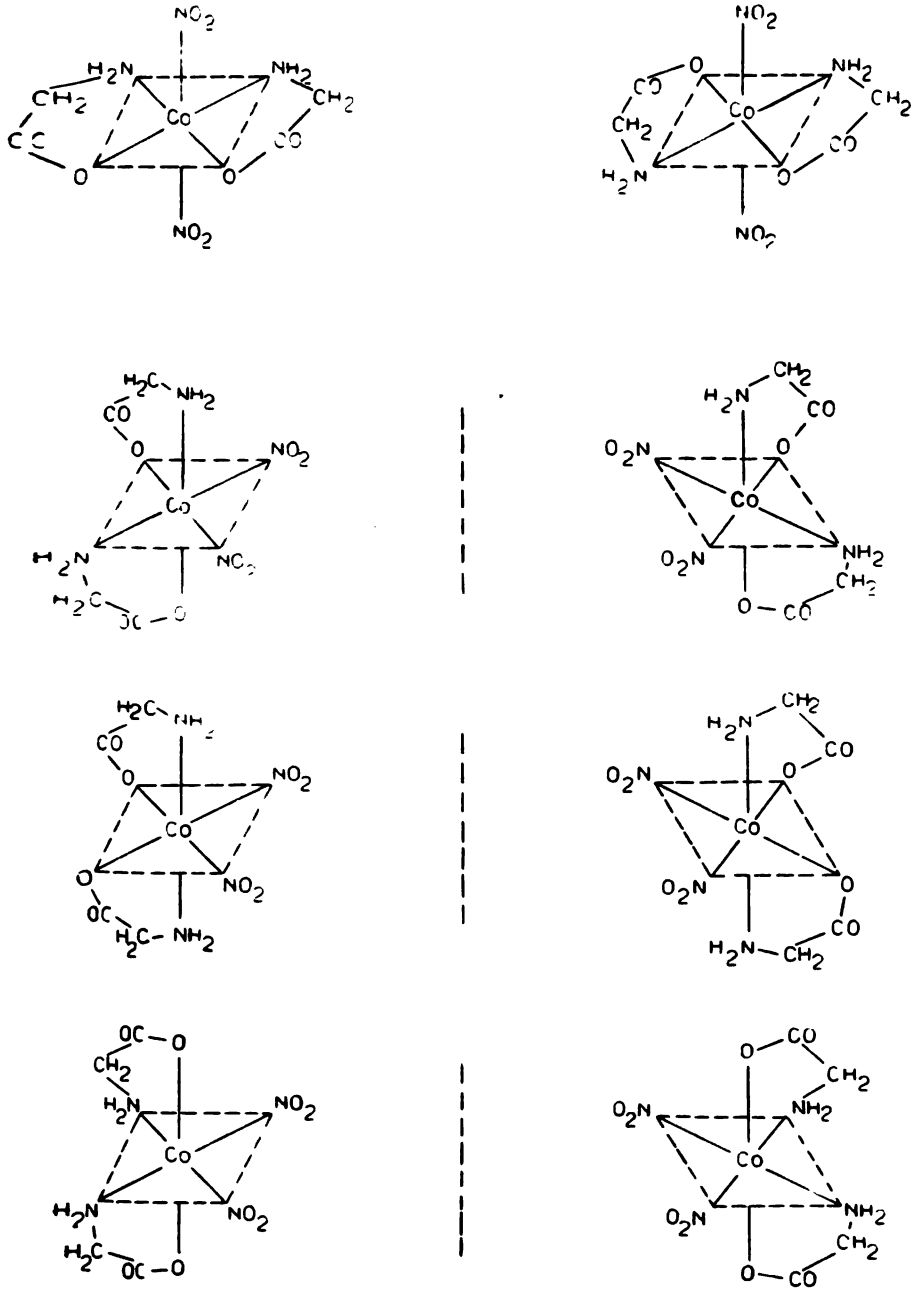

Figure 1

Isomeric forms of dinitrodiglycinatocobaltates(III)

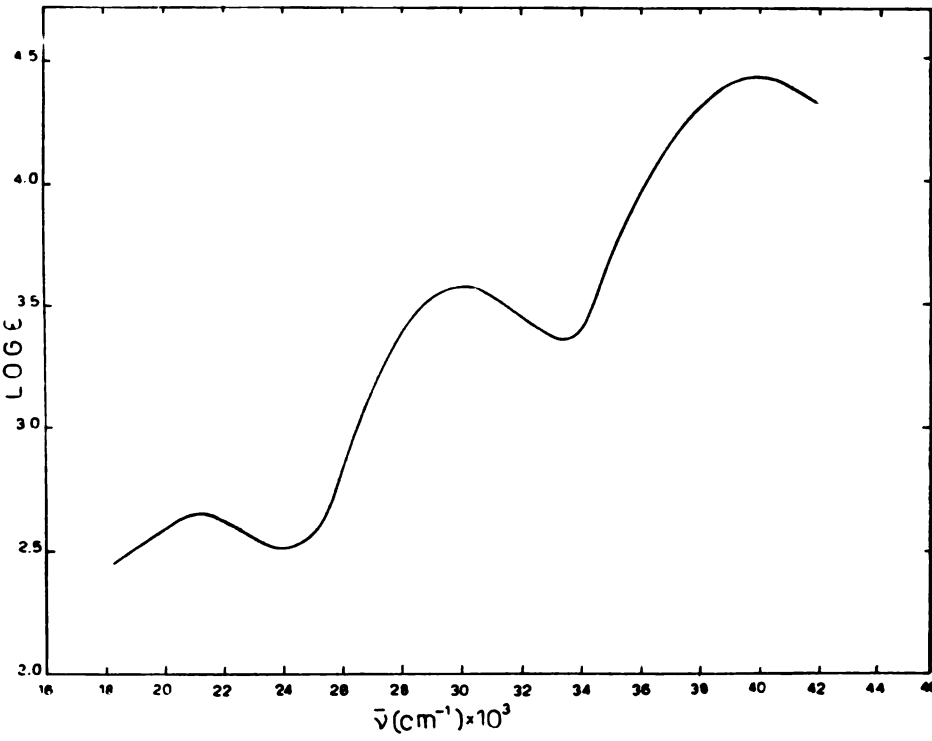

Figure 2

Absorption curve of potassium-dinitrodiglycinatocobaltate (III) in the visible and ultraviolet region

violet is shown in Fig. 2. Potassium dinitrodiglycinatocobaltate (III) has three absorption maxima: $\lambda_1 = 468$ $m\mu$ (log $\varepsilon_1 = 2.67 \pm 0.02$); $\lambda_2 = 334$ $m\mu$ (log $\varepsilon_2 = 3.59 \pm 0.01$); $\lambda_3 = 250$ $m\mu$ (log $\varepsilon_3 = 4.43 \pm 0.01$). Infra-red absorbtion maxima are given in Table 1 together with possible assignments of characteristic group frequencies.

Spectra were analyzed by comparing spectral data of deuterated and nondeuterated substance with those reported in the literature for similar compounds[3, 4, 5, 6, 7, 8]. From the values obtained it may be concluded that *NH*-stretching vibrations in potassium dinitrodiglycinatocobaltate (III) are shifted down in frequency (the corresponding bands of sodium glycinate are found at 3380—3340 cm^{-1} and 3290 cm^{-1})[7]. From Table 1 it may be seen that COO^--stretching vibrations are also shifted with respect to the corresponding vibrations of sodium glycinate which appear at 1600 and 1415 cm^{-1}[8]. The NO_2-stretching vibrations in potassium dinitrodiglycinatocobaltate (III) lie between the corresponding vibrations of NO_2 ion ($\nu_{as} = 1335$ cm^{-1}; $\nu_s = 1250$ cm^{-1}) and the covalently bonded nitro group ($\nu_{as} = 1582$ cm^{-1}; $\nu_s = 1384$ cm^{-1})[5], which it may be concluded that the cobalt-ligand bonds of potassium dinitrodiglycinatocobaltate (III) are to

some degree covalent, i.e. that hydrogen bonds are present in the solid crystal[3, 4, 5, 9].

TABLE 1

Vibrational Frequencies of Potassium Dinitrodiglycinatocobaltate (III)

Vibration Type	cm^{-1} *	Vibration Type	cm^{-1} *
$\nu(NH_2)$	3298 (*m*) 3230 (*m*)	$\delta\, t(CH_2)$	1045 (*vw*)?
		$\nu\, s(CCN)$	949 (*w*) 924 (*m*)
$\nu(CH_2)$	2996 (*w*) 2950 (*w*)		
		$\delta(NO_2)$	830 (*w*) 824 (*m*)
$\nu\, as(COO^-)$	1630 (*shld*) 1618 (*vs*)		
		$\rho\, r(NH_2)$	785 (*w*)
$\delta(NH_2)$	1580 (*m*)		
		$\rho\, r(CH_2)$	735 (*w*)
$\nu\, as(NO_2)$	1419 (*vs*)		615 (*m*)
$\delta(CH_2)$		$\rho\, w(NO_2)$	580 (*w*)
		$\rho r(COO^-)$	545 (*w*)
$\nu\, s(COO^-)$	1370 (*m*) 1342 (*vs*)?	$\nu(Co-N)$	508 (*w*) 490 (*w*) 433 (*w*) 408 (*m*) } ?
$\nu\, s(NO_2)$	1310 (*vs*)		
$\nu\, as(CCN)$	1180 (*m*)		
$\delta\, t(NH_2)$	1138 (*m*)		

* Band intensities

vs – very strong
s – strong
m – medium
w – weak
vw – very weak
shld – shoulder

A further proof that potassium dinitrodiglycinatocobaltate (III) obtained by procedures described has the *cis*-configuration is that all the products obtained, including the substance obtained previously[1], had the same R_f-values on paper chromatograms developed by means of three different solvents.

From all the aforesaid it may be concluded that the action of potassium glycinate on complex amines of cobalt (III), either in the presence or the absence of potassium nitrite, always yields the same product, i.e. *cis*

TABLE 2

R_f-values of Potassium Dinitrodiglycinatocobaltate (III) Prepared by Different Procedures

Obtained from	Solvent mixture*		
	I	II	III
$K_3[Co(NO_2)_6]$	0.62	0.70	0.56
$(NH_4)[Co(NH_3)_2(NO_2)_4]$	0.61	0.70	0.56
$[Co(NH_3)_3(NO_2)_3]$	0.61	0.68	0.55
$cis[Co(NH_3)_4(NO_2)_2]NO_3$	0.63	0.69	0.57
$trans[Co(NH_3)_4(NO_2)_2]NO_3$	0.63	0.70	0.56
$[Co(NH_3)_5NO_2](NO_3)_2$	0.63	0.68	0.56
$[Co(NH_3)_6]Cl_3$	0.61	0.70	0.55

* I *i*-Propanol (80) + HCl (1.19) (5) + H_2O (15)
II Acetone (80) + H_2O (20) + KI (1 *g*)
III Methanol (90 + HNO_3 (1.42) (5) + H_2O (5).

Time of development (hrs): I 20; II 6; III 4.

potassium dinitrodiglycinatocobaltate (III). This fact evidences great thermodynamic stability of the compound obtained in comparison with other compounds which could be formed in the reaction. Later on we attempt to explain its exclusive formation by the application of the Cherniaev rule.

In vew of the mentioned *trans*-effect it may be assumed that the action of potassium glycinate on alkaline hexanitrocobaltates leads first to the substitution of any two of six equivalent groups in the *cis*-position by one glycine residue*. Since such an intermediate compound** contains only two nitro groups in the *trans*-position it might be expected, on account of a stronger *trans*-effect of the nitro group*** than of amino or carboxylic groups that first one these two latter groups would be substituted. The substitution of the fourth nitro group by the other end of the bidentate would leave two nitro groups in the *cis*-position. The fact that the substitution of the remaining two nitro groups takes place with great difficulty even in the presence of a large excess of alkaline glycinate, in spite of the chelate effect, is also in accordance with the mentioned *trans*-effect: the *cis*-dinitrodiglycinatocobaltates (III) obtained contain no ligands in a *trans*-position with a sufficiently strong *trans*-efffect.

* Kinetic investigations of the substitution of nitro groups by glycine residue in sodium hexanitrocobaltates (III) have shown that this is a first-order reaction, i.e. its rate depends only on the concentration of the complex[12].

** After this paper had gone to press we succeeded isolating potassium tetranitroglycinatocobaltate (III), $Na_2[Cogly(NO_2)_4]$; this will be described in a subsequent paper.

*** The nitro group is first in the spectrochemical series of ligands and it shows a prounounced tendency to fill its p-orbital vacancies with electrons from low energy d-orbitals of the central ion; accordingly, it is a ligand with a very pronounced *trans*-effect.

The mechanism of the reaction with Erdmann salt, which according to X-ray analysis contains two ammonia molecules in the *trans*-position [13] might be assumed to involve first the substitution of one of the two equivalent ammonia molecules by one end of the chelate since ammonia molecules are less coordinated than the corresponding nitro groups, which form π-bonds with the central ion. The other end of the chelate would then substitute immediately one of the four equivalent nitro groups. In the second phase, as a result of the *trans*-effect, the second glycine residue might be assumed to substitute the second ammonia molecule and one of two nitro groups occuring in the *trans*-position, giving rise to *cis*-dinitrodiglycinatocobaltate (III) ion. The proposed mechanism is supported by the fact that we succeeded in isolating the intermediate peripheral isomer of potassium trinitroglycinatoamminecobaltate (III) which reacted further with glycine giving *cis*-isomer of dinitrodiglycinatocobaltate (III)[14].

The reaction of alkaline glycinate with trinitrotriamminecobalt (III), which was established by X-ray analysis to posses the peripheral configuration[15], may be assumed to start with the substitution of one ammonia molecule occurring in the *trans*-position with respect to the nitro group by one end of the chelate. The other end of the chelate would then substitute one of two ammonia molecules which are *trans* since they are less coordinated than nitro groups. This mechanism would lead to the formation of peripheral isomer of potassium trinitroglycinatoamminecobaltate (III) as an intermediate product, which has been proved by the isolation of this compound[14]. The mechanism of the subsequent reaction would be the same as already described for the reaction of alkaline glycinates with Erdmann salt.

The Cherniaev *trans*-rule does not explain the mechanism of other reactions* encountered in this work, for the following reasons: (a) according to the rule other reaction products (in case of *cis*-dinitrotetramminecobalt (III) nitrate) should be formed as well; (b) rearrangement of ligands in the course of the reaction (formation of the *cis*-isomer of potassium diglycinatodinitrocobaltate (III) from *trans*-dinitrotetramminecobalt (III) nitrate) are evident; (c) there is no simple substitution, the reaction is complex involving three components (the last two reactions).

ACKNOWLEDGEMENT

The authors express their thanks to D. Jeremić for useful discussions on infrared spectra, and to Lj. Galebović for aid in recording IR spectra.

EXPERIMENTAL

1. Preparation of Potassium Dinitrodiglycinatocobaltate (III) from Erdmann's Salt

In a 100 *ml* round-bottomed flask 5.9 *g* (0.02 mole) of Erdmann's salt[17] were suspended in 10 *ml* of water. To the suspension a solution of 3.0 *g* (0.04 mole) of glycine and 2.01 *g* (0.036 mole) of potassium hydroxide

* Similar examples of the nonapplicability of the Cherniaev rule to complex cobaltic compounds are also reported by some other authors[16].

in 10 *ml* of water was added. The flask was then heated on a water-bath with stirring for one hour (the required amount of water was added to keep the solution volume constant). The warm solution was filtered and left to stand in a refrigerator. The brown crystalline precipitate was filtered off and washed with water, ethanol and ether (2.3 *g*). The filtrate was concentrated by evaporation in vacuum at room temperature; on cooling an additional 1.8 *g* of substance was obtained. The total yield was 61%. The substance was recrystallized from warm water.

Analysis

The substance for analysis was dried at 105°C. Decomposition was carried out by heating the moistened substance with a small amount of conc. sulphuric acid. The sulphates obtained were weighed and dissolved in water. From the solution cobalt was determined electrogravimetrically and potassium content was calculated from the difference.

Calculated for $KCoC_4H_8O_8N_4$ (338.18): *K* 11.56 *Co* 17.43
Found : *K* 11.40 *Co* 17.60

2. Preparation of Potassium Dinitrodiglycinatocobaltate (III) from the Peripheral Isomer of Trinitrotriamminecobalt (III)

The reaction was carried out as described in 1. 4.96 *g* (0.02 mole) of the peripheral isomer of trinitrotriamminecobalt (III)[18], 3.0 *g* (0.04 mole) of glycine and 2.01 *g* (0.036 mole) of potassium hydroxide were used. The yield of potassium dinitrodiglycinatocobaltate (III) was 72.5% (4.9 *g*).

Analysis

Calculate for $KCoC_4H_8O_8N_4$ (338.18): *K* 11.56 *Co* 17.43
Found : *K* 11.54 *Co* 17.36

3. Preparation of Potassium Dinitrodiglycinatocobaltate (III) from Cis- and Trans-Dinitrotetramminecobalt (III) Nitrate

Both reactions were carried out in the same way as the reaction described under 1. 7.02 *g* (0.025 mole) of *cis-* or *trans* dinitrotetramminecobalt (III) nitfate[17], 5.62 *g* (0.075 mole) of glycine and 3.78 *g* (0.068 mole) of potassium hydroxide were used. In the first reaction 5.7 *g* (67.5%) of potassium dinitrodiglycinatocobaltate (III) were obtained, and in the second 5.3 *g* (62.7%).

Analysis

Calculated for $KCoC_4H_8O_8N_4$ (338.18): *K* 11.56 *Co* 17.43
Found for the product obtained from
the *cis*-isomer : *K* 11.50 *Co* 17.41
the *trans*-isomer : *K* 11.60 *Co* 17.38

4. Preparation of Potassium Dinitrodiglycinatocobaltate (III) from Nitropentaminecobalt (III) Nitrate

The procedure was the same as described under 1. 6.28 *g* (0.02 mole) of nitropentamminecobalt (III) nitrate[18] 3.0 *g* (0.04 mole) of glycine, 2.01 *g* (0.036 mole) of potassium hydroxide and 1.7 *g* (0.02 mole) of potassium nitrite were used. Crude potassium dinitrodiglycinatocobaltate (III) was obtained in a yield of 5 *g* (73.9%).

Analysis

Calculated for $KCoC_4H_8O_8N_4$ (338.18): *K* 11.56 *Co* 17.43
Found : *K* 11.48 *Co* 17.44

5. Preparation of Potassium Dinitrodiglycinatocobaltate (III) from Hexamminecobalt (III) Chloride

The reaction was carried out in the same way as described under 1, but the reaction time was 3 hours and the solution volume was kept at about 30 *ml.* 6.68 *g* (0.025 mole) of hexamminecobalt (III) chloride[30], 6.38 *g* (0.075 mole) of potassium nitrite, 5.62 *g* (0.075 mole) of glycine and 3.79 *g* (0.068 mole) of potassium hydroxide were used. The yield of crude potassium dinitrodiglycinatocobaltate (III) was 6 *g* (71%).

Analysis

Calculated for $KCoC_4H_8O_8N_4$ (338.18) *K* 11.56 *Co* 17.43
Found : *K* 11.53 *Co* 17.40

6. Preparation of Magnesium, Potassium and Copper (II) Dinitrodiglycinatocobaltate (III)

The above salts were obtained by passing a saturated solution of potassium dinitrodiglycinatocobaltate (III) through a column of very acid "Merck I" cationite previously converted to the corresponding form. The solution obtained was then evaporated to dryness under reduced pressure at room temperature.

Analysis

Magnesium was determined gravimetrically in the form of magnesium pyrophosphate; the substance for analysis was dried at 105°C for 2 hrs.

Calculated for $MgCo_2C_8H_{16}O_{16}N_8$ (622.46): *Mg* 3.91
Found : *Mg* 3.75

Calcium was determined gravimetrically in the form of calcium oxide; the substance for analysis was also dried at 105°C for 2 hrs.

Calculated for $CaCo_2C_8H_{16}O_{16}N_8$ (638.22): *Ca* 6.28
Found : *Ca* 6.20

Copper was determined electrogravimetrically; the substance for analysis was also dried at 105°C for 2 hrs, whereby it lost 12.20% of water (calculated for 5 H_2O: 11.98%)

Calculated for $CuCo_2C_8H_{16}O_{16}N_8$ (661.70): *Cu* 9.60
Found : *Cu* 9.57

Solubility

The solubility was determined by weighing the dry residue (after drying at 105°C) obtained on evaporation of 10 *ml* of saturated solution of the corresponding salt at room temperature. It was found that 100 *ml* of saturated solution at 20°C contained:

35.1 *g* (0.56 mole/lit) of the magnesium salt
10.6 *g* (0.17 mole/lit) of the calcium salt
9.6 *g* (0.15 mole/lit) of the copper salt

7. *Absorption Electronic and Molecular Spectra of Potassium Dinitrodiglycinatocobaltate (III)*

Absorption spectra in the visible and ultraviolet were taken with a Perkin Elmer 137-UV spectrophotometer. For spectra in the visible and near ultraviolet 3.5×10^{-4} M aqueous solution of the substance was used, and for spectra in the ultraviolet a ten times more dilute solution. The absorption curve is shown in Fig. 2.

Infra-red absorption spectra were run on a Perkin Elmer Model 137 Infracord spectrophotometer by the potassium bromide disk technique. Deuteration was performed in the usual way by dissolving the substance in heavy water and evaporating the solution to dryness at room temperature.

8. *Chromatographic Investigation of Potassium dinitrodiglycinatocobaltate (III)*

Chromatography was carried out in a 50 cm glass cylinder of 22 cm diameter, by the ascending method, on Whatman No. 1. paper strips (3×30 cm). The ambient temperature was 18 ± 1°C. The solution of the complex salt was put in the form of a thin line on one end of the strip, 2.5 cm from the edge. Before chromatography the solvent was left to stand in the cylinder for 1 hour in order to get the atmosphere in the cylinder saturated. The solvent travelled about 20 cm. Detection was performed by dipping the developed paper strips into ammonium sulphide solution. The R_f-values obtained are given in Table 2.

Institute of Chemistry, School of Sciences,
Beograd University
and
Institute of Chemistry, Technology
and Metallurgy, Beograd

Received 3 June, 1967

REFERENCES

1. Janić, T. J., M. B. Ćelap, and P. Spevak. "Proučavanje reakcija heksanitro-kobaltata (III) s amino-kiselinama. I. Dobivanje dinitrodiglicinato-kobaltata (III)" (Study of the Reactions of Hexanitro-cobaltates (III) with Amino Acids. I. Preparation of Dinitrodiglycinatocobaltates (III)) — *Glasnik hemijskog društva* (Beograd) 27 (2—3): 111—115, 1962.
2. Ćelap, M. B., D. J. Radanović and T. J. Janjić. "Study of the Reactions of Hexanitrocobaltates (III) with Amino Acids. II. Determination of the Configuration of Dinitrobis (glycinato) cobaltate (III) Ions" — *Inorganic Chemistry* 4: 1494—1495, 1965.
3. Saraceno, A. J., I. Nakagawa, S. Mizushima, C. Curran, and J. V. Quagliano. "Infrared Absorption Spectra of Inorganic Coordination Complexes. XVI. Infrared Studies of Glycino-Metal Complexes" — *Journal of the American Chemical Society* 80: 5018—5021, 1958.
4. Nakamoto, K., Y. Morimoto, and A. E. Martell. "Infra Red Spectra of Aqueous Solutions. I. Metal Chelate Compounds of Amino Acids" — *Ibid.*, 83: 4528—4532, 1961.
5. Nakamoto, K., J. Fujita, and H. Murata. "Infra Red Spectra of Metallic Complexes. V. Infra Red Spectra of Nitro and Nitrito Complexes" — *ibid.* 80: 4817—4823, 1958.
6. Puget, Y., and C. Duval. "Sur la structure de métallo-hexanitrites déterminée par absorption infrarouge" — *Comptes rendu* 250: 4141—4142, 1960.
7. Dupuy, B., and C. Garrigou-Lagrange. "Etude par spectroscopie infrarouge des sels, de sodium et d'argent du glycocolle de la DL-alanine et de la DL-β-phenylalanine" — *Journal de Chimie physique* 62: 1359—1365, 1965.
8. Tsuboi, M., T. Onishi, I. Nakagawa, T. Shimanouchi, and S. I. Mizushima. "Assignments of the Vibrational Frequencies of Glycine" — *Spectrochimica Acta* 12: 253—261, 1958.
9. Cotton, F. A. "The Infra-Red Spectra of Transitional Metal Complexes", in: J. Lewis and R. G. Wilkins, ed. *Modern Coordination Chemistry* — Interscience Publishers: New York, 1960, p. 388.
10. Cherniaev, I. I. "Mononitrity dvukvalentnoi platiny" (Mononitrites of Divalent Platinum) — *Izvestiia Instituta po izucheniiu planiny* 4: 213, 1926
11. *Gmelins Handbuch der anorganischen Chemie*, VIII auflg., Kobalt Teil B — Erganzungsband, Lieferung 2 — Weinheim Bergstr.: Verlag Chemie 1964, pp. 316—317.
12. Ćelap, M. B., T. J. Janjić, and P. Radivojša, unpublished paper.
13. Wells, A. F. — *Z. Krist.* 95: 74—82, 1936; (*Gmelins Handbuch der anorganischen Chemie*, VIII Auflg., Kobalt, Teil B — Ergänzungsband, Lieferung 2, Weinheim/ Bergstr: Verlag Chemie, 1964, p. 600).
14. Ćelap, M. B., M. J. Malinar and T. J. Janjić. Unpublished paper.
15. Tanito, Y., Y. Saito, and H. Kuroya. "Crystal Structure of Trinitrotriammineco-balt (III)" — *Null. Chem. Soc., Japan* 25: 188, 1952. (D. H. Busch. "Coordination Compounds of Cobalt", in: R. S. Young, ed. *Cobalt, Its Chemistry, Metallurgy, and Uses*, ACS Monograph, No 149, New York: Reinhold, 1960, p. 92).
16. Ablov, A. V., N. M. Samus, M. S. Popov. "Izorodanonitro- i izorodano-galogeno-bis-dimetilglioksimokobalti kisloti" (Hydrogen Nitrothiocyanatobis (dimethylglyoximato) cobaltate (III) and Hydrogen Halogenothiocynatobis (dimethylglyoximato)

cobaltate (III)) — *Doklady Akademii nauk SSSR* 106: 665—668, 1956, Ablov, A. V., and Samus, N. M. "O silnom trans-vliianii gidrokso gruppy u doksiminov treknvalentnogo kobalta" (The Trans-Effect of the Hydroxo Group in Co (III) Dyoximes) — *ibid.* 113: 1265—1268, 1957.

17. Jörgensen, S. M. "Zur Darstellung der Kobaltammoniaksalze" — *Zeitschrift für Anorganische Chemie* 17: 455—479, 1898.
18. Schlessinger, G. "Trinitrotiamminecobalt (III)" — *Inorganic Syntheses* 6: 189—191, 1960.
19. Basolo, F. and R. K. Murmann. "Acidopentamminecobalt (III) Salts" — *ibid.* 4: 171—176, 1953.
20. Bjerrum, J. and J. P. McReynolds. "Hexamminecobalt (III) Salts" — *ibid.* 2: 216—221, 1946.

GLASNIK HEMIJSKOG DRUŠTVA, Vol. 32, No. 8-9-10, 1967, pp. 429—436

SPECTROPHOTOMETRIC DETERMINATION OF THE TWO-COMPONENT SYSTEM *Fe (III) — Ni (II)*

by

JELICA D. MIŠOVIĆ and MILENA M. JOVANOVIĆ

Simultaneous spectrophotometric determination of *Fe*(III) and *Ni*(II) is described. *Fe*(III) with EDTA and H_2O_2 gives a violet complex which has been studied by Cheng and Lott, and other authors[1, 2]. *Ni*(II) with EDTA gives a blue-green complex[3]. In the simultaneous determination the absorptions at 520 *nm* and 380 *nm* were measured. These wavelengths satisfy conditions given by Mellon[4], representing wavelengths at which the ratio of the absorptivities of the two components has a maximum and a minimum value, i.e. the absorbance of the two components is additive[5]. From absorptions measured at the given wavelengths the concentrations were calculated by solving two equations for the additive absorptions. The results are given in the experimental part. All measurements were carried out at *pH* 10 and the concentrations studied ranged from 0.48 to 3.84 *mg* of *Fe* /100 *ml* and from 15 to 90 *mg* of *Ni*/100 *ml*. The color of the *Ni*(II)-EDTA-H_2O_2 complex appeared at once, that of *Fe*(III)-EDTA-H_2O_2 only after adjustment of the *pH* to a value higher than 9. H_2O_2 had no effect on the color of the *Ni*(II)-EDTA complex. The colors were stable for 90 minutes. The complexes obeyed Beer's law for the given range of concentrations.

EXPERIMENTAL PART

Apparatus. All measurements were made on a Unicam SP 600 spectrophotometer in cells of 2 *cm*. *pH* was measured with a Radiometer-Copenhagen Type PHM 22 *r* *pH*-meter.

Reagents

Standard iron(III) *solution.* A solution of $FeCl_3$ containing 1.9220 mg *Fe/ml* was prepared. The solution was standardized gravimetrically by precipitating iron in the form of $Fe(OH)_3$.

Standard nickel(II) *solution.* A solution of $NiCl_2$ corresponding to 3.7145 *mg Ni/ml* was prepared. The solution was standardized gravimetrically by precipitating nickel in the form of *Ni*-dimethyl-glyoxime.

Standard aluminum solution. A solution containing 20.0250 *mg Al/ml* was prepared. The solution was standardized gravimetrically by precipitating aluminum in the form of $Al(OH)_3$.

Solution of H_2O_2. 30% H_2O_2 solution.

Ammonia solution. Concentrated 25% ammonia solution.

Procedure. In a 100 *ml* volumetric flask the corresponding concentrations of *Fe* and *Ni*, 20 *ml* of 0.1 *M* EDTA, and 10 *ml* of 30% H_2O_2 were placed, and the pH was adjusted to 10.0 with conc. ammonia. The mixture was then diluted up to the mark with distilled water. Distilled water was used in blank experiments since solutions of *Fe* and *Ni* in the concentration range studied were slightly colored. The solutions were left to stand for 10 min and then their transmittances were measured at 520 *nm* and 380 *nm*.

ABSORPTION SPECTRA OF Fe(III) - EDTA - H_2O_2 AND Ni(II) - EDTA COMPLEXES

Iron can be determined spectrophotometrically as *Fe*(III)-EDTA-H_2O_2 complex in the presence of small amounts of nickel (up to a concentration of 7.4 *mg Ni*/100 ml). According to our hypothesis if higher nickel concentrations are present, both elements could be determined spectrophotometrically as a two-component system.

In order to determine the wavelengths to be used and to examine the additivity of the components, the following were determined:

— the absorption spectrum of *Fe*(III)-EDTA-H_2O_2 complex
— the absorption spectrum of *Ni*(II)-EDTA complex
— the absorption spectrum of a mixture of *Fe*(III)-EDTA-H_2O_2 and *Ni*(II)-EDTA complexes, measured experimentally
— the theoretically predicted absorption spectrum of the same mixture.

The absorption spectrum of *Fe*(III)-EDTA-H_2O_2 complex was obtained by taking approximately the mean iron concentration (1.922 *mg Fe*/100 ml) of the range of concentrations studied, the solution being prepared as described above. The absorption curve from 365 *nm* to 800 *nm* is shown in Fig. 1, curve *A*, from which it is seen that the absorption maximum is at 520 *nm*.

For the determination of the absorption spectrum of *Ni*(II)-EDTA complex, 18.5572 mg *Ni*/100 *ml* was taken and the solution was prepared as described above. The results are shown in Fig. 1, curve *B*; they show that *Ni*(II)-EDTA complex has two absorption maxima, at 380 *nm* and 600 *nm*. The wavelength of 380 *nm* was selected for further work since, as shown by the curve, here the system exhibits a greater absorbance and the wavelength is very much different from the wavelength of the *Fe*(III)-EDTA-H_2O_2 system.

The theoretical absorption spectrum of two-component system was obtained by summing the ordinates of the curves of *Fe*(III)-EDTA-H_2O_2 and *Ni*(II)-EDTA (Fig. 1, curve *C*).

Its experimental absorption spectrum was obtained by measuring the absorption of a solution containing the same amounts of iron and nickel as in the determination of the individual components. The color of the

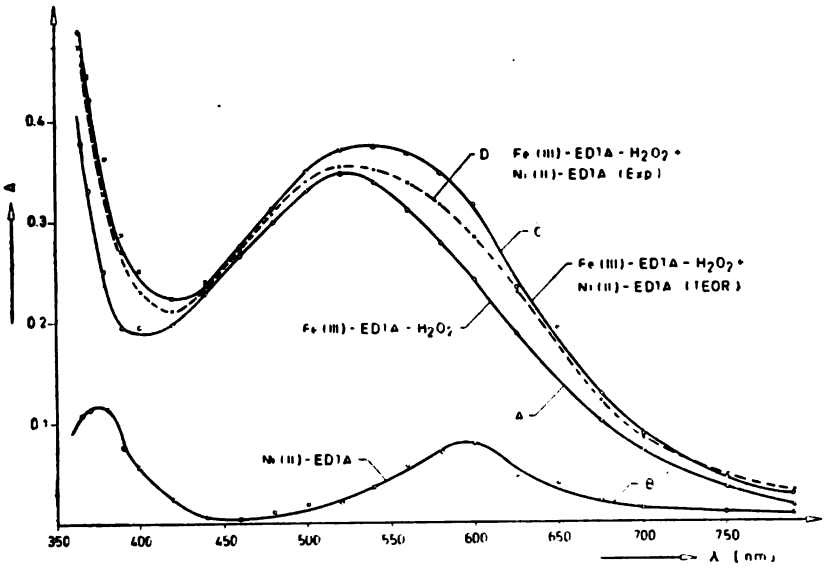

Figure 1

Absorption spectra of *Fe* (III) and *Ni* (II) complexes and of their mixtures

solution was violet. Absorption at different wavelengths are given in Fig. 1, curve *D*. The curve is very similar in shape to the theoretical one, Fig. 1, curve *C*. From these results it may be concluded that the absorptions of the two components are additive, i.e. that the absorption of the mixture is equal to the sum of the absorptions of the individual components measured in separate solutions.

THE EFFECT OF *pH* ON THE ABSORBANCE OF THE *Fe* (III) - EDTA - H_2O_2 AND *Ni* (II) - EDTA COMPLEXES

The color intensity of these complexes depends considerably on the *pH* of the solution. Therefore, before studying the determination of the two-component system, we examined the effect of *pH* on the absorbance of the individual complexes. Absorbances were measured at the wavelengths of the absorption maximums of the solutions.

The results for the *Fe*(III)-EDTA-H_2O_2 complex are given in Fig. 2, curve *A*; they show that in the *pH* region from 9.5 to 10.5 the absorbance is almost constant. The red-violet color of this complex was found to be unstable at *pH* 8—9; at *pH* lower than 8, no formation of a colored complex was observed. *Ni* with EDTA gives a colored complex at all *pH*-values but the absorbance changes considerably with *pH*. However, curve B in Fig. 2 shows that at *pH* from 9.5 to 11.0 it is constant. Since the iron complex exhibited a stable color in this region, further measurements were carried out at $pH = 10.0$.

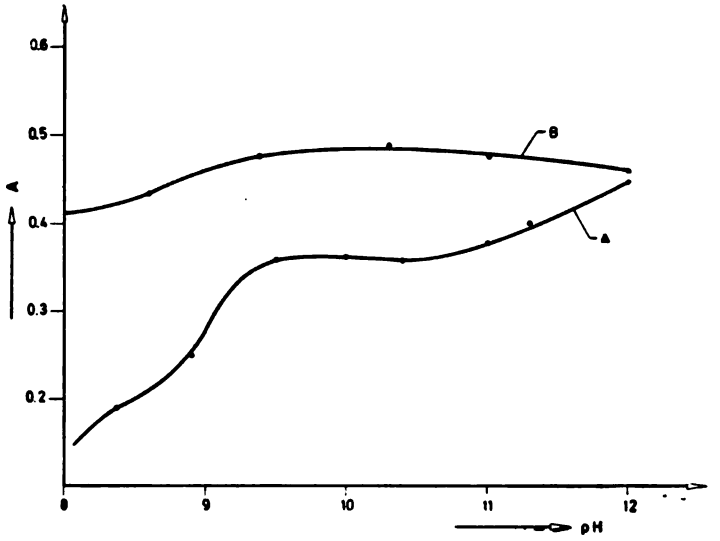

Figure 2
The influence of pH on the absorption of complexes *Fe*(III)-EDTA-H_2O_2 (curve A) and *Ni*(II)-EDTA (curve B)

COLOR STABILITY OF THE COMPLEXES IN SOLUTION

The color of *Fe*(III)-EDTA-H_2O_2 complex appears after adjustment of the *pH* to higher than 8, and at *pH* higher that 9.5 it is very stable. The color of *Ni*(II)-EDTA complex appears immediately after the addition of EDTA solution and it is also stable. By measuring the absorbance of a solution containing a mixture of these complexes at pH 10 at intervals of 10 minutes it was found that they were stable for 90 minutes, which was sufficient for the measurement of a series of 20 samples. Further measurements were carried out 10 to 15 minutes after color development.

SIMULTANEOUS DETERMINATION OF IRON AND NICKEL

To determine the *f*-values necessary for the calculation of the unknown concentrations of iron and nickel, we needed Beer's diagrams for the components of the system. The slope of the straight line obtained by plotting absorbance *A* against known concentrations *c* gives *f* at the selected wavelengths. Diagrams were plotted for concentrations ranging from 0.48 to 3.84 *mg* of *Fe*/100 *ml* and from 15 to 90 *mf* of *Ni*/100 *ml*, at wavelengths of 380 *nm* and 520 *nm*, since these concentrations were found to obey Beer's law. The solutions were prepared as already described.

Results for *Fe*(III)-EDTA-H_2O_2 are given in Fig. 3 and for *Ni*(II)-EDTA in Fig. 4. From these diagrams the following *f*-values were obtained:

$$f_{520,\,Fe} = 0.1875;\ f_{380,\,Fe} = 1300;\ f_{520,\,Ni} = 0.0007;\ \text{и}\ f_{380,\,Ni} = 0.0063.$$

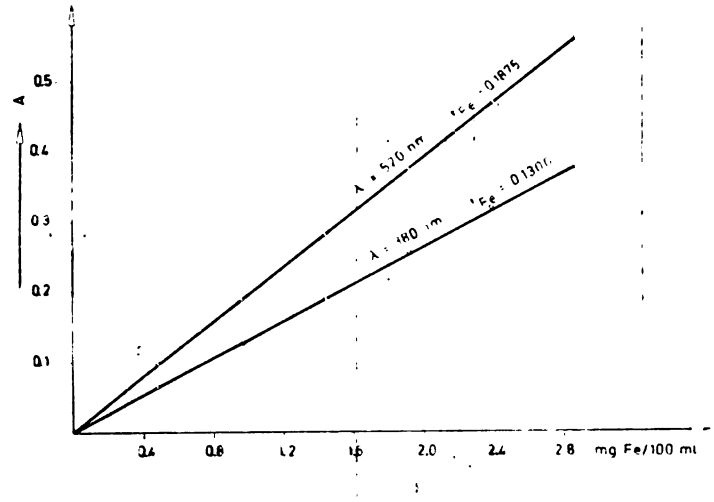

Figure 3

Beer's diagram for *Fe* (III)-EDTA-H_2O_2 complex

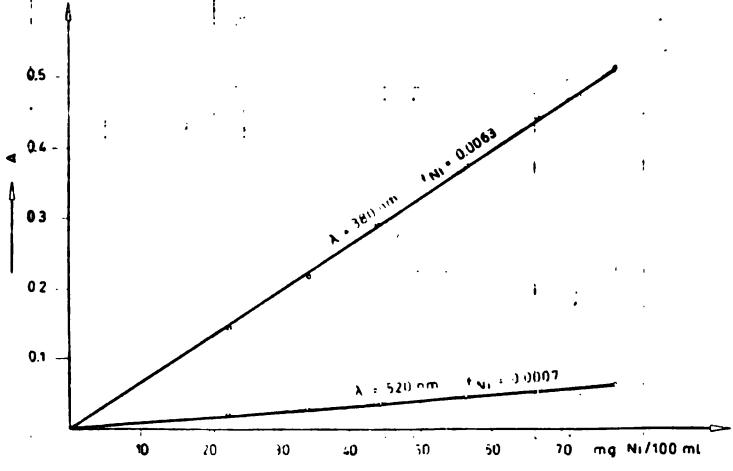

Figure 4

Beer's diagram for *Ni* (II)-EDTA complex

TABLE 1

Simultaneous spectrophotometric determination of Fe and Ni

Exp. No.	Taken *mg Fe*/100 *ml*	Taken *mg Ni*/100 *ml*	*A* λ = 520 nm	*A* λ = 380 nm	Found *mg Fe*/100 *ml*	Found *mg Ni*/100 *ml*	Relative error *Fe* %	*Ni* %
1	1.9220	33.4305	0.385	0.463	1.9274	33.7193	+0.28	+0.80
2	1.3454	26.0015	0.271	0.337	1.3496	25.6432	+0.31	—1.37
3	0.7688	40.8595	0.172	0.354	0.7666	40.3715	—0.30	—1.20
4	1.5376	44.5740	0.319	0.478	1.5364	44.1687	—0.08	—0.91
5	1.9220	29.7160	0.380	0.435	1.9165	29.5001	—0.28	—0.72

TABLE 2

Simultaneous Spectrophototometric Determination of Fe and Ni in the Presence of Aluminum

Exp. No.	Taken *mg Fe*/100 *ml*	Taken *mg Ni*/100 *ml*	Taken *mg Al*/100 *ml*	*A* λ = 520 nm	*A* λ = 380 nm	Found *mg Fe*/100 *ml*	Found *mg Ni*/100 *ml*	Relative error *Fe* %	*Ni* %
1	1.5376	24.1442	100.225	0.305	0.352	1.5364	24.1686	—0.08	+1.00
2	0.9610	37.1450	100.225	0.206	0.360	0.9592	37.3492	—0.02	+0.54

By measuring the absorbances of mixed iron and nickel solutions of various known concentrations at the two selected wavelengths, and solving the equations of additive absorbance

$$A_{520} = f_{520,Fe} \cdot c_{Fe} + f_{520,Ni} \cdot c_{Ni}$$
$$A_{380} = f_{520,Fe} \cdot c_{Fe} + f_{380,Ni} \cdot c_{Ni}$$

using the calculated f-values and the measured absorbances, we obtained the results given in Table 1. They lie within the limits of permissible error.

DETERMINATION OF IRON AND NICKEL IN THE PRESENCE OF ALUMINUM

We attempted to determine iron and nickel as the two-component system *Fe*(III)-EDTA-H_2O_2 and *Ni*(II)-EDTA in the presence of aluminum. We considered it would be possible since aluminum reacts with EDTA giving a colorless complex. However, it was found that higher concentrations of aluminum interfered with the determination of iron and nickel, probably on account of absorptive properties of aluminum. Measured values for iron and nickel were lower than those actually present by 3—6%. If instead of distilled water a solution of $AlCl_3$ to which EDTA and H_2O_2 had been added was taken as the reference solution, the error was less.

Determinations of *Fe*(III) and *Ni*(II) as a two-component system in the presence of aluminum at the given wavelengths are shown in Table 2. It may be seen that they lie within the limits of permissible error (± 1%).

DISCUSSION

Iron can be determined spectrophotometrically in the presence of nickel up to a concentration of 7.4 *mg*/100 *ml* with EDTA and H_2O_2, as a one-component system. With higher nickel concentrations the error increases with increasing concentration. However, at higher nickel concentrations, iron and nickel can be determined as a two-component system.

From the measurements given in Tables 1 and 2 it may be concluded that the spectrophotometric determination of iron and nickel as a two-component system is possible in the concentration range from 0.48 to 3.84 *mg Fe*/100 *ml* and from 15 to 90 *mg Ni*/100 *ml*. The results lie within the limits of permissible error. The method is fairly quick and the standard curves of the *Fe*(III)-EDTA-H_2O_2 and *Ni*(II)-EDTA complexes once determined can be used for subsequent determinations of unknown iron and nickel concentrations provided the measurements are made on the same apparatus.

Iron and nickel can also be determined in the presence of considerable concentrations of aluminum, but in this case a solution of *Al*(III), EDTA and H_2O_2 should be taken as the reference solution and the standard curves should be determined under the same conditions.

The presence of *Cu*(II) interferes with these determinations.

School of Technology
Beograd University

Received 22 June, 1967

REFERENCES

1. Cheng, L. K., and F. P. Lott "Reaction of Hydrogen Peroxide with Complexes of (Ethylenedianitrilo)-Tetraacetic Acid and Nitrilotriacetic Acid" — *Analytical Chemistry* (Easton-Washington) 28 (4): 462—465, 1956.
2. Ringbom A., S. Siitonen, and B. Saxen. "The Fe (III)-EDTA-H_2O_2 Complex and Its Analytical Use" — *Analytica Chimica Acta* (Amsterdam) 16: 541—545, 1957.
3. Nielsch W. and G. Böltz. "Eine neue Photometrische Bestimmung für Nickel mit Aethylendiaminetetraessigsäure" — *Analytica Chimica Acta* (Amsterdam) 11: 367—375, 1954.
4. Mellon, M. G. *Analytical Absorption Spectroscopy* — New York: Wiley and Sons, 1950, pp. 369—373.
5. Rrilley, H. C., and T. G. Sawyer. *Experiments for Instrumental Methods*, New York: McGraw Hill and Co., 1961, pp. 122—126.

GLASNIK HEMIJSKOG DRUŠTVA, Vol. 32, No. 8-9-10, 1967, pp. 437—443

APPLICATION OF SOME AMALGAMS IN CORROSIMETRIC TITRATION WITH DROPPING AMALGAM INDICATOR ELECTRODE*

by

ALEKSANDAR R. DESPIĆ and OLGA S. VITOROVIĆ

INTRODUCTION

In a previous paper[1] it was shown that under certain conditions the titration end point could be potentiometrically determined using a nonequilibrated indicator electrode. The following have to be satisfied: (a) the oxidation reaction of the material of the indicator electrode must be sufficiently fast and its standard potential considerably more negative than the standard potential of the species to be titrated; (b) the concentration of the titrated species should be sufficiently low for the limiting diffusion current of the reduction to be established immediately; (c) the diffusion conditions should be constant and reproducible in order to obtain a definite relationship between the limiting current and the concentration. Then, a definite concentration of indicator electrode oxidation products in the reaction layer surrounding the electrode is established, and thus also a definite reversible potential which indirectly keeps the concentration of the titrated species constant. It was shown that dropping amalgam electrodes can satisfy all these conditions, since the exchange currents of amalgam components are usually rather high[2], and the dropping mercury electrode is known from polarography to have a highly reproducible and theoretically predictable diffusion behavior[3].

In the present work we studied the possibility of applying different amalgams in the above titrimetric determinations. Titration of silver nitrate solution with potassium chloride was selected as a typical titration reaction on account of the known high precision of the end-point determination, due to the low solubility of silver chloride in water[4].

The dependence of the potentials of dropping amalgam electrodes on the silver ion concentration was examined first, and then a standard investigation of the validity of the method was made by carrying out a great number of titrations with different amounts and concentrations of silver ion.

* Communicated at the IInd Yugoslav Congress on Pure and Applied Chemistry held in Beograd, June 1965.

EXPERIMENTAL

Investigations were carried out with amalgams of bismuth, lead, cadmium and zinc, whose standard potentials with respect to hydrogen electrode potential are $+0.230\ V$, $-0.126\ V$, $-0.402\ V$ and $-0.763\ V$, respectively[5]. Amalgams were prepared by dissolving turnings of the corresponding metals in mercury to a concentration of about 0.5 weight percent, with heating on a water bath[6]. All metals were of p.a. purity, and the mercury was triple distilled. Silver wire of p.a. purity was used as the electrode in blank runs.

Silver nitrate and potassium chloride solutions of a concentration of $10^{-1}\ N$ were prepared from p. a. reagents in the usual way.

The dependence of the dropping amalgam electrode potential on the concentration of silver iron was studied with solutions of different concentrations made by diluting the standard solution with distilled water. Potentials were measured with respect to calomel electrode.

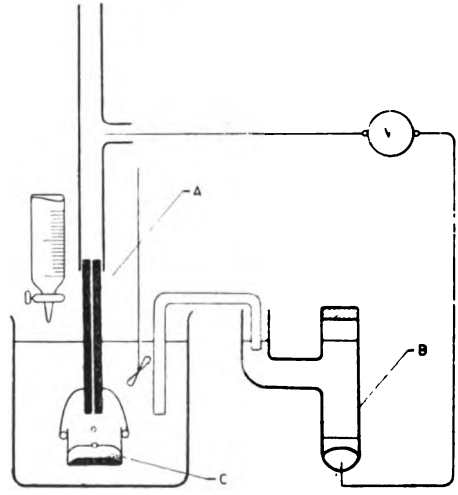

Figure 1

Apparatus for corrosimetric titrations: *(A)* dropping amalgam electrode; *(B)* reference electrode; *(C)* vessel with carbon tetrachloride.

Titrations were performed in the apparatus shown in Fig. 1. Below the dropping amalgam electrode there was a glass vessel containing carbon tetrachloride. When the amalgam entered the carbon tetrachloride the contact between the amalgam and the solution was broken, thus preventing the reduction of ions from the sample on the amalgam on the bottom of the vessel, which can cause significant negative systematic errors.

In blank runs the dropping electrode was replaced by silver wire. Samples of 25 *ml* were taken with a standard pipette and were diluted to 250 *ml* in a titration beaker. The titrant was added from a 50 *ml* standard burette. Oxygen was not expelled from the solution, either before or during titration.

The potential difference between the indicator and the reference electrode was read on a Radiometer 22 *pH*-meter to an accuracy of $\pm 2\ mV$. Since drops gradually swelled and then fell, the instrument needle showed a tendency to fluctuate with an amplitude which depended on the solution concentration, but never exceeded 40 *mV*. These fluctuations were considerably reduced by connecting a 200 μF capacitor in parallel with the cell; the potential was measured just before the drop fall, by reading the extreme position of the needle in the course of drop formation.

RESULTS AND DISCUSSION

Figure 2 shows the dependence of the potential of silver and of different amalgam electrodes on the concentration of silver nitrate in the solution. All the electrodes obeyed the Nernst equation in the concentration range from $10^{-3}\ N$ to $10^{-1}\ N$. At concentrations lower than $10^{-3}\ N$ the law was no longer obeyed on account of the effect of the reduction of contaminants, mainly oxygen, dissolved in the solution.

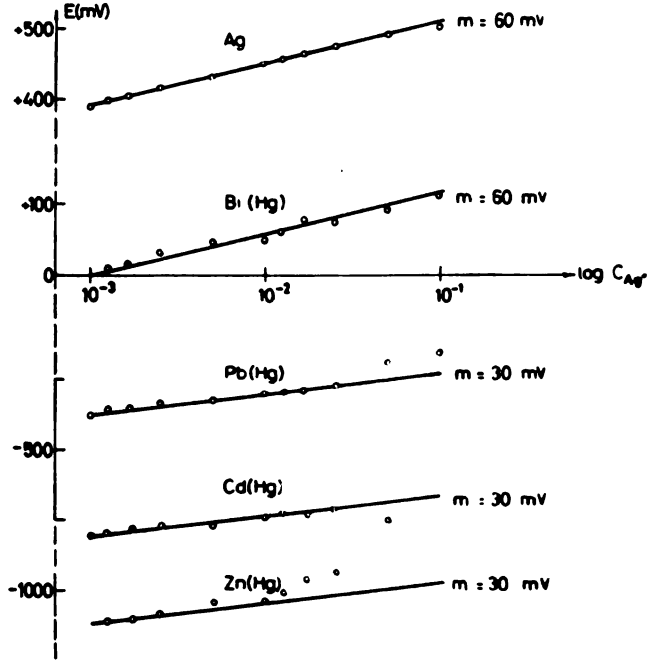

Figure 2

Potentials of different indicator electrodes as functions of silver ion concentration.

The slopes of the straight lines correspond to a reversible one-electron exchange reaction in the case of silver and two-electron exchange in the case of zinc, cadmium and lead amalgam. These reversible processes take place between the metal and the corresponding ions produced by the corrosion current.

Bismuth amalgam however, behaved differently with a slope of 60 mV plotted against log concentration. This slope could be ascribed to a relatively rapid oxidation of the metal to the univalent ion and inhibition to further oxidation to a polyvalent state, but a reliable explanation requires additional research. From the point of view of analytical application such a behaviour may be very useful since it promisses a greater potential jump at the titration end-point.

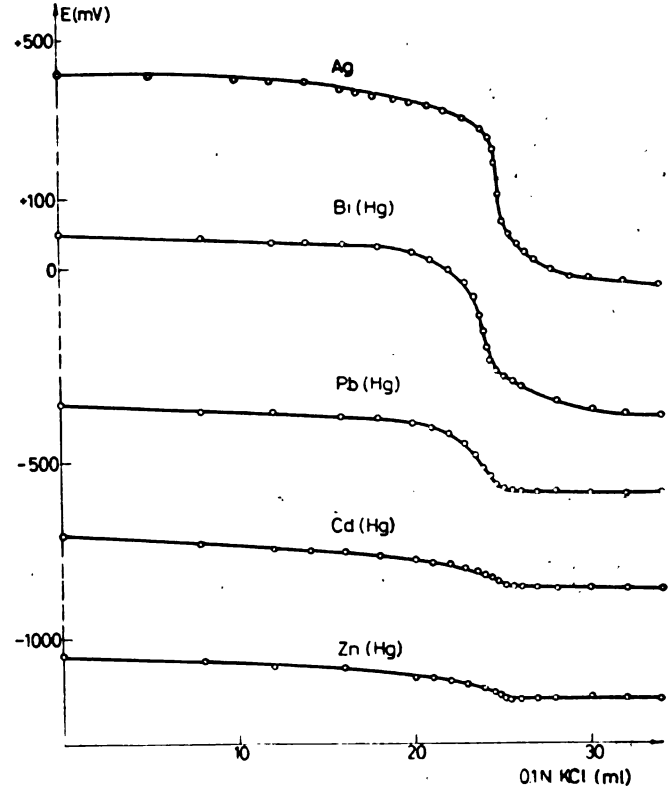

Figure 3

Typical titration curves obtained with different indicator electrodes.

From Fig. 3, which shows typical titration curves obtained with silver electrode and different amalgam eletrodes, it may be seen that by far the greatest jump was obtained with bismuth amalgam. Zinc amalgam gives a relatively small jump; this is due to its high negativity and the conse-

quently relatively high corrosion currents of impurities (comparable with the main corrosion current) which mask the drop in silver ion corrosion current.

TABLE 1

Titration of Silver Nitrate with 0.1 N Potassium Chloride Using Metallic Silver or Amalgam of Bismuth, Lead, Cadmium or Zinc

Corroding phase	Concentration of the sample	No. of titrations	Mean error	Maximum error
Ag	10^{-2}	10	0.02 %	−0.2 %
Bi	10^{-3}	2	−0.32%	−0.48%
	1.25×10^{-3}	2	−0.08%	−0.10%
	1.66×10^{-3}	2	−0.20%	−0.26%
	2.50×10^{-3}	2	+0.30%	+0.40%
	5.00×10^{-3}	2	+0.32%	+0.48%
	10^{-2}	9	−0.18%	−0.61%
	1.25×10^{-2}	2	+0.90%	+1.20%
	1.66×10^{-2}	2	+0.80%	+1.00%
	2.50×10^{-2}	2	−0.60%	−0.68%
	5.00×10^{-2}	2	−0.48%	−0.56%
	10^{-1}	2	−0.75%	−0.80%
Pb	10^{-3}	2	−0.30%	−0.40%
	1.25×10^{-3}	2	−0.30%	−0.40%
	1.66×10^{-3}	2	−0.32%	−0.40%
	2.50×10^{-3}	2	−0.05%	−0.10%
	5.00×10^{-3}	2	−0.08%	−0.10%
	10^{-2}	10	−0.28%	−0.80%
	1.25×10^{-2}	2	−0.26%	−0.32%
	1.66×10^{-2}	2	−0.40%	−0.48%
	2.50×10^{-2}	2	−0.08%	−0.10%
	5.00×10^{-2}	2	+0.40%	+0.50%
Cd	10^{-3}	2	−1.10%	−2.00%
	1.25×10^{-3}	2	−0.16%	−0.16%
	1.66×10^{-3}	2	−0.24%	−0.24%
	2.50×10^{-3}	2	−0.05%	−0.10%
	5.00×10^{-3}	2	−0.48%	−0.64%
	10^{-2}	10	−0.22%	+0.80%
	1.25×10^{-2}	2	−0.40%	−0.48%
	1.66×10^{-2}	2	−0.05%	−0.10%
	2.50×10^{-2}	2	−0.90%	−1.20%
	5.00×10^{-2}	2	−1.20%	−1.47%
Zn	1.66×10^{-3}	2	−2.75%	−4.00%
	2.50×10^{-3}	2	−0.16%	−0.30%
	5.00×10^{-3}	2	−0.60%	−0.60%
	10^{-2}	10	−0.33%	−0.80%
	1.25×10^{-2}	2	−0.36%	−0.40%
	1.66×10^{-2}	2	−0.48%	−0.52%
	2.50×10^{-2}	2	−0.90%	−0.96%

However, on account of the accuracy of the measurement and reproducibility of the potential values, even this jump is sufficient for a relatively precise determination of the end-point.

Table 1 gives the results of a series of titrations with different amalgam electrodes. They show that all the amalgams can be used as indicator electrodes in concentrations ranging from 10^{-1} N to 10^{-3} M with an accuracy usual in volumetry. The mean error with zinc amalgam was not much different from that with bismuth amalgam.

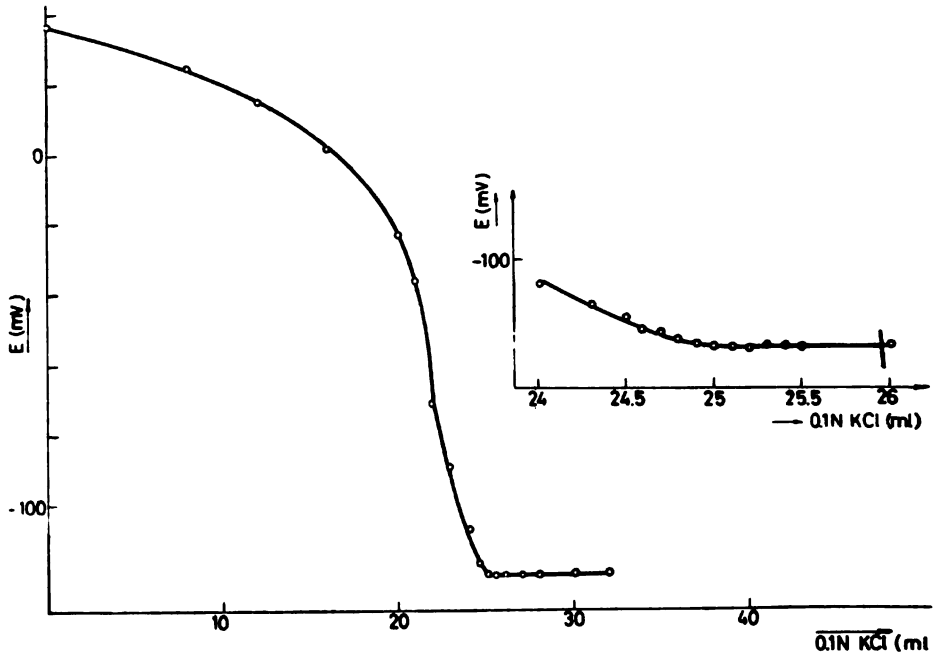

Figure 4

Curve of the titration of silver ion in the presence of zinc, cadmium, nickel and iron with dropping bismuth amalgam as indicator electrode

It should be noted that some phenomena associated with the coagulation of silver nitrate take place in the vicinity of the end-point, thus decreasing the accuracy of the determination. It should not be forgotten that the corrosion potential is less stable and more sensitive to exterior disturbances than the true reversible potential, so that sticking of the precipitate to the capillary may cause deviations of the potential curve.

Figure 4 shows the titration curve for the same system but in the presence of ions of iron, zinc, cadmium and nickel. It confirms the opinion that electronegative species have no direct effect on the electrode potential.

School of Technology
Beograd

Received 28 May, 1967

REFERENCES

1. Despić, A., and K. Popov-Sinđelić. "Corrosion Potentiometry and Potentiometric Titration with Dropping Amalgam Electrode" — *Journal of Electroanalytical Chemistry* 12: 347—353, 1966.
2. Vetter, K. J. *Elektrochemische Kinetic* — Berlin: Springer Verlag, 1961.
3. Kolthoff, M. J., and J. J. Lingane. *Polarography* — New York—London: Interscience Publishers, 1952.
4. Charlot, G., J. Badoz—Lambling, and B. Trémillon. *Electrochemical Reactions. Electrochemical Methods of Analysis* — Amsterdam—New York: Elsevier Publishing Company, 1962.
5. Latimer, M. M. *Oxidation Potentials of Elements* — New York: Prentice Hall Inc., 1952.
6. Pushin, N. A. "Über die Schmelzbarkeit der Legierung des Quecksilber mit *Zn, Cd, Bi, Pb* and *Sn*" — *Zeitschrift für anorganische Chemie* 36: 201—254, 1903.

GLASNIK HEMIJSKOG DRUŠTVA, Vol. 32, No. 8-9-10, 1967, pp. 445—453

CHROMATOGRAPHY ON ALUMINA AND RADIOMETRIC DETERMINATION OF MICRO AMOUNTS OF CHROMIC AND CHROMATE IONS

by

TOMISLAV J. JANJIĆ and SMILJA G. KOZOMARA

In the Hot Chemistry Laboratory of the Boris Kidrič Institute, Vinča, developed a method for the production of carrier-free ^{51}Cr in the form of $Na_2{}^{51}CrO_4$ in an isotonic sodium chloride solution has been developed. The chromate always contained some percentage of unoxidized chromic ion. Since $Na_2{}^{51}CrO_4$ is applied in human medecine, it should not contain more than 5% of Cr^{+3} and should be analized before delivery.

There are not many methods dealing with the separation and determination of trivalent and hexavalent chromium in mixtures. Apart from colorimetric methods for the determination of micro amounts of chromic[1] and chromate[2] ion, various chromatographic procedures have been developed: paper chromatography[3, 4, 5, 6], ion-exchange chromatography[7], and thin-layer chromatography[8].

Colorimetric methods are not suitable for the analysis because in cases where the amounts of chromic and chromate ion considerably differ, the ions have to be separated.

In paper-chromatographic separation of chromic and chromate ions it is usually found that hexavalent chromium is partly reduced to the trivalent state in the course of the separation: therefore this method is not satisfactory for quantitative determination[9]. Partial reduction was also observed by Galanteanu[8] when he attempted to reproduce the method given by Bighi[3] and Sastri[6]. Dizdar and Draganić[10] found that reduction took place even in the application of some organic resins, although Beliavskai and Shkrobot[7] described the separation of trivalent from hexavalent chromium by means of MMG-1 organic ion-exchanger, without mentioning any reduction.

In the present work we attempted separation by means of column adsorption chromatography on aluminum oxide, considering that this substance possesses no reducing properties. Mixtures of aluminum oxide and calcium sulphate were used by Galanteanu[8] in thin-layer chromatographic determination; he used a saturated sodium sulphate solution as the chromatographic developer and good separation of both valency states was obtained (R_f-values: $Cr^{3+} = 0.0$; $CrO_4^{2-} = 0.60$). The application of this method in our case would be complicated and would take rather long, since

^{51}Cr emits soft gamma rays (about 325 *keV*) so that direct measurement of the radioactivity would be very inaccurate because of absorption of the radiation by aluminum-oxide. For more accurate measurement the aluminum oxide layer containing the spots of one valency state would have to be taken off the plate and the chromium eluted and determined by means of a scintillation counter, which would be rather complicated.

EXPERIMENTAL

The columns were prepared by filling a 10 *cm* glass tube of diameter 5 *cm* with 0.5 *g* of acids, basic or neutral Merck chromatographic aluminum oxide. Solutions of sodium chromate and chromic chloride containing 200 μg of *Cr/ml* labelled with ^{51}Cr were passed through the column at a flow rate of 4 to 5 drops per minute. Fractions of 1 *ml* of effluent were collected in cells for radiometric measurements and their radioactivity was measured on a Nuclear Chicago Model DS-5-4 scintillation detector.

The capacity of aluminum oxide with respect to chromate was determined by running a solution of radioactive chromate in excess. The excess was then rinsed off with water and the adsorbed chromate eluted with 1 *N* sodium chloride solution.

To determine the capacity for chromic ions an excess of radioactive chromic ion solution was run. The column was then rinsed with 1 *N* sodium chloride solution, and the adsorbed chromic ion was eluted with 1 *N* hydrochloric acid solution.

From the effluent radioactivity the adsorbed chromium was calculated. The results are shown in Table 1.

TABLE 1

Capacity of 1 g of Aluminum Oxide in mg (meq)

	Basic Al_2O_3	Acid Al_2O_3	Neutral Al_2O_3
Cr^{3+}	4.9 (0.28)	1.1 (0.06)	3.0 (0.17)
CrO_4^{2-}	6.9 (0.12)	12.5 (0.21)	5.6 (0.10)

Since all our experiments were carried out with 200 μg of *Cr*(III) or *Cr*(IV) it may be concluded that only 7—36% of the capacity of the aluminum oxide was utilized.

RESULTS AND DISCUSSION

As described in the experimental part we used columns of basic, acid or neutral aluminum oxide. In all three cases we found that chromic and chromate ions were adsorbed by the column. Chromate was eluted either with hydrochloric acid solution, sodium chloride solution or sodium hydro-

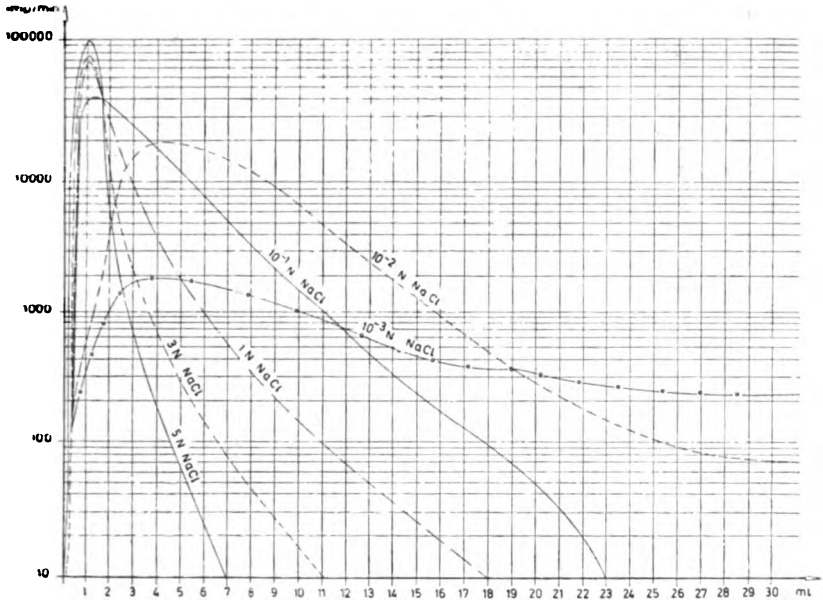

Figure 1

Elution curves of chromate ion from basic alumina. Eluent: sodium chloride. 1 *ml* of a $^{51}CrO_4^{2-}$ solution (200 μg *Cr/ml*) of 132340 count/min. activity was brought into the column

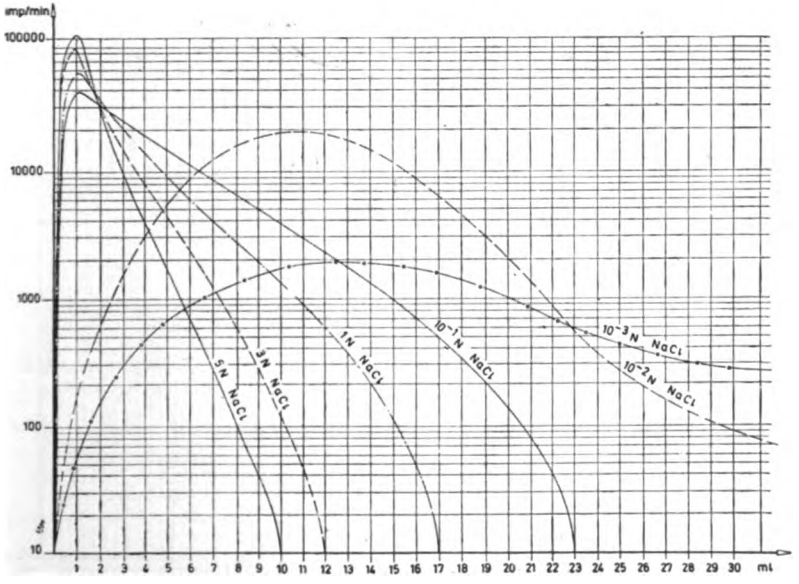

Figure 2

Elution curves of chromate ion from neutral alumina. Eluent: sodium chloride. 1 *ml* of a $^{51}CrO_4^{2-}$ solution (200 μg *Cr/ml*) of 132340 count/min. activity was brought into the column

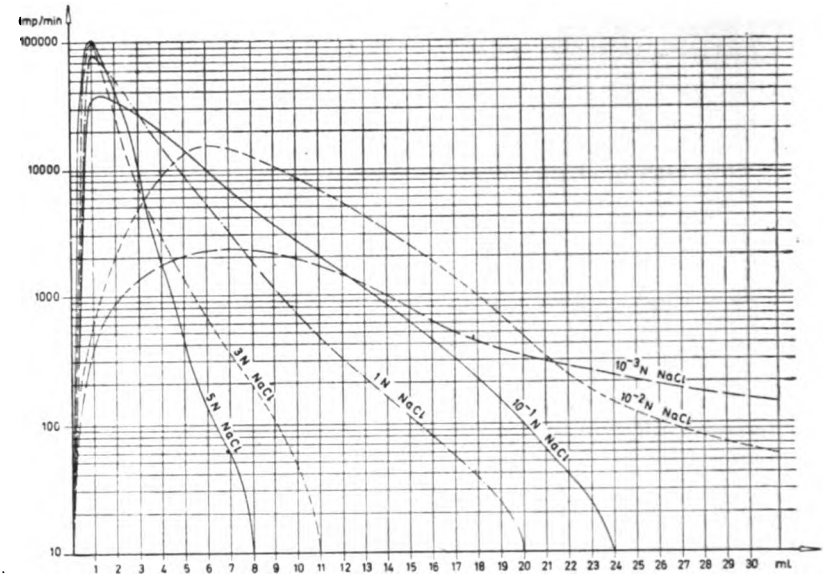

Figure 3

Elution curves of chromate ion from acid alumina. Eluent: sodium chloride. 1 *ml* of a $^{51}CrO_4^{2-}$ solution (200 μg *Cr/ml*) of 132340 count/min. activity was brought into the column

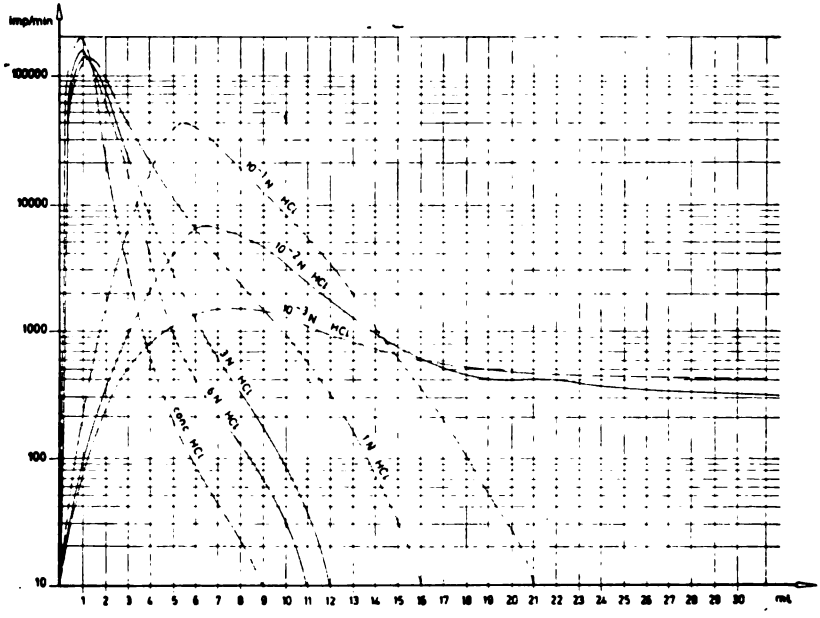

Слика 4 Figure

Elution curves of chromic ion from basic alumina. Eluent: hydrochloric acid. 1 *ml* of a $^{51}Cr^{3+}$ solution (200 μg *Cr/ml*) of 211038 count/min. activity was brought into the column.

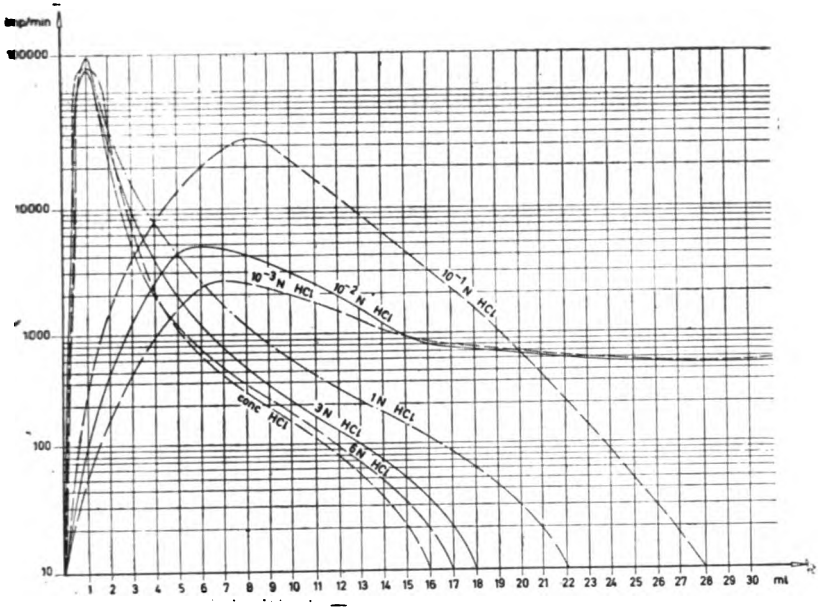

Figure 5

Elution curves of chromic ion from neutral alumina. Eluent: hydrochloric acid. 1 *ml* of a $^{51}Cr^{3+}$ solution (200 μg *Cr/ml*) of 211038 count/min. activity was brought into the column.

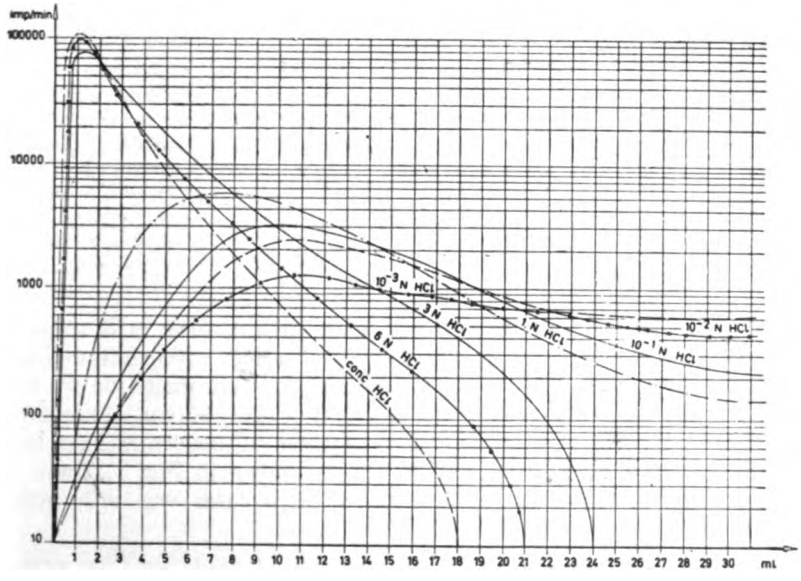

Figure 6

Elution curves of chromic ion from acid alumina. Eluent: hydrochloric acid. 1 *ml* of a $^{51}Cr^{3+}$ solution (200 μg Cr/*ml*) activity 211038 count/min. was brought into the column.

TABLE 2

Determination of Chromic and Chromate Ions in Mixtures

Cr(III)			*Cr*(VI)		
Taken μg	Found μg	Error %	Taken μg	Found μg	Error %
2	1.984	—0.80	198	198.4	+0.70
	1.990	—0.50		198.19	+0.09
10	9.97	—0.30	190	190.5	+0.26
	9.93	—0.70		190.21	+0.11
50	49.82	—0.36	150	149.0	—0.66
	50.05	+0.10		150.0	—
100	100.0	—	100	99.80	—0.20
	100.21	+0.21		99.98	—0.02
150	150.11	+0.06	50	49.80	—0.40
	149.95	—0.03		49.89	+0.22
190	190.3	+0.15	10	9.91	—0.90
	189.7	—0.68		9.95	—0.50
198	198.4	+0.20	2	1.99	—0.50
	199.0	+0.50		1.99	—0.50

xide solution. Chromic ion was eluted with hydrochloric acid solution or sodium hydroxide solution but could not be eluted with sodium chloride solution. Since sodium chloride solution eluted only chromate ion we wanted to establish the most suitable concentration of this eluent. Therefore we eluted chromate with sodium chloride solution of concentrations ranging from 1.10^{-3} *N* to 5 *N*. The elution curves are shown in Fig. 1, 2 and 3. As seen from figures, complete elution in all three cases was only achieved with solutions of $\geqslant 1.10^{-1}$ *M*.

To establish the most suitable eluent for chromic ion, we examined the elution properties of hydrochloric acid and sodium hydroxide solutions of different concentrations. The elution curves for hydrochloric acid are given in Figs. 4, 5 and 6. The curves show that *HCl* only elutes from basic

and neutral aluminum oxide at $\geqslant 1.10^{-1}$ *N*, and elution is only complete at a concentration of $\geqslant 3$ *N*. The curves show that chromic ion is most readily eluted from basic and least from acid alumina.

In the elution of chromic ions with sodium hydroxide solution the effluent was turbid which caused difficulties in radiometric determination of chromium.

In all cases described the effluents contained more than 99.5% of the starting amount of chromium.

On the basis of the experiments described above, in which the behavior of chromic and chromate ions was examined separately, it could be assumed that the best separation would be achieved with basic aluminum oxide. The procedure would involve first the elution of chromate ion with 1 *N* sodium chloride solution, and then chromatic ion with 1 *N* hydrochloric acid solution.

To check this method mixtures with both components radioactive were analyzed. Mixtures containing *Cr*(III) and *Cr*(IV) in ratios ranging from 99 : 1 to 1 : 99 were examined. In all cases the total amount of chromium was 200 μg. The results are given in Table 2. They show that *Cr*(III) and *Cr*(IV) can be determined in mixtures whose composition ranges from 1 : 99 to 99 : 1. The error of the method is $\pm 1\%$, which lies within the limits of statistical error of the counter equipment.

We also studied the mechanism of the separation. Schwab and Jockers[11] showed that in addition to adsorptive properties, aluminum oxide also possesses ion-exchange properties. Basic aluminum oxide exchanges cations and acid aluminum oxide anions. If the process of ionic exchange were predominant in our case, chromic ion would not be retained by a column of acid aluminum oxide, nor would chromate ion be retained by a basic column. However, we found that both ions were retained by basic, acid and neutral aluminum oxide in considerable amounts, as seen from the capacities (Table 1). Hence it may be concluded that the mechanism of separation involves mainly adsorption and only to a small extent ion exchange.

Institute of Chemistry
School of Sceince
Beograd University
Boris Kidrič Institute
of Nuclear Science,
Vinča

Received 19, June 1967

REFERENCES

1. Verma, M. R., V. M. Brucher., K. C. Agrawal., and R. K. Shrama. "Colorimetric Method for the Estimation of Trivalent Chromium" — *Microchimica Acta* 1959: 766—769.
2. Cline, R. W., R. E. Simmons and W. R. Rossmassler. "Determination of Trivalent Chromium in the Presence of Chromate" — *Analytical Chemistry* 30: 1117—1118, 1958.
3. Bighi, C. "Separation by Paper Chromatography of Ions $Cr^{\cdot\cdot}$, $Cr^{\cdot\cdot\cdot}$ and $CrO_4^{\cdot}$" — *Annales de Chimie* (Roma) 45: 1087—1090, 1955.
4. Pollard, F. H., J. F. W. McOmie., and A. J. Banister. "The Chromatographic Separation of Different Elements in Different Valency States" — *Chemistry and Industry* (London) 49: 1598, 1955.
5. Cohen, I. V., and I. Ingrand. *Etudes Recents sur le controle pharmaceutique des radioelements* (Rapport CEA-L803) — Centre d'Etudes Nucleaires de Saclay, 1960.
6. Sastri, M. N., and A. P. Rao. "Separation of the Valency States of Some Elements on Paper Impregnated with Zirconium Phosphate" — *Journal of Chromatography* 9 (2): 250—251, 1962.
7. Beliavskai, T. A. and Z. P. Shkrobot. "*Metody analiza redkikh i tsvetnykh metallov*" (Methods of Analysis for Rare and Non-Ferrous Metals) — Moskva: Izdatel'stvo Moskovskogo Universiteta, 1956, pp. 59—62.
8. Galanteanu, I. "Paper and Thin-Layer Chromatography Applied to the Separation of Chromium (III) from Chromium (VI)" — *Journal of Chromatography* 19 (1): 208—213, 1965.
9. Lederer, E., and M. Lederer. "*Chromatography*" — London: Elsevier Publ. Company, 1955, p. 339.
10. Dizdar, Z. I., and Z. D. Draganić. "Adsorption of Chromate Ions on Some Anion Exchangers" — *Bulletin of the Boris Kidrič Institute of Nuclera Sciences* 5: 79—87, 1955.
11. Schwab. G. M., and K. Jockers. "Anorganische Chromatographie" — *Zeitschrift für angewandte Chemie* 50: 546—553, 1937.

GLASNIK HEMIJSKOG DRUŠTVA, Vol. 32, No. 8-9-10, 1967, pp. 455—467

DETERMINATION OF NOVALGIN. II.

VOLUMETRIC METHODS

by

VILIM J. VAJGAND and VERA LJ. NIKOLIĆ

In a previous paper[1] we described disadvantages of existing gravimetric methods, which we modified, developing a new, very precise and quick gravimetric method involving the determination of sodium ion in the form of $NaZn(UO_2)_3(CH_3COO)\cdot 6H_2O$.

Volumetric methods for the determination of novalgin described so far in the literature can be divided into direct and indirect. Indirect methods involve the volumetric determination of sulphate after oxidation of novalgin[2, 3]; they were not studied. Direct methods are iodometric titration[4, 5, 6, 7, 8], and permanganometric oxidation in combination with iodometry[9, 10, 11].

Iodometric titration is the most rapid but very unreliable and has been often investigated. Budimlić and Dumanović[12] noticed that two different equations have been given for the reaction between novalgin and iodine. One originates from Wirth[5] and by analogy to the reaction with antipyrine it represents the addition of iodine to the double bond of the pyrazole nucleus in position 3,4. The other, given by Rapaport and Shvartsburd,[6] represents hydrolytic decomposition of novalgin with simultaneous oxidation of bisulphite by iodine:

$$Py^*{-}\overset{\displaystyle CH_3}{\underset{|}{N}}{-}CH_2SO_3Na + I_2 + 2H_2O = \left[Py{-}\overset{\displaystyle CH_3}{\underset{\vdots}{\underset{|}{N}}}{-}H \right] I + HCHO + NaHSO_4 + HI$$

This equation is confirmed by Budimlić and Dumanović[12], Wagner[13], and Kigasawa *et al.*[14]. However, knowledge of this reaction did not improve

* Py =

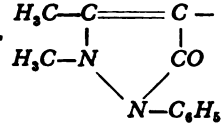

the accuracy of the iodometric determination of novalgin. Numerous papers have treated the problems of end-point determination, acidity and dilution of the reaction mixture and titration rate. All this indicates the empirical character of the method.

Schuleck and Maros[15] got low results in acid solutions (*pH* 1—2), but high results in the presence of acetic acid. The latter were ascribed to the oxidation of novalgin with four equivalents of iodine, analogous to the behavior of melubrine in the presence of sodium acetate[16], and the low results were explained by assuming hydrolytic decomposition of novalgin in dilute solutions yielding formaldehyde-bisulphite, which does not react with iodine. Therefore the iodometric determination was modified so that sulphite was first quantitatively liberated from both sulphonate groups by means of potassium cyanide in an alkaline medium and then, in acid solution, titrated with iodine.

The permanganometric determination of novalgin [9, 10, 11] involves the oxidative cleavage of the double bond of the pyrazole ring by means of potassium permanganate in alkaline solution. The determination is combined with an iodometric method since the excess of permanganate is reduced by the addition of potassium iodide, and the liberated iodine is titrated with sodium thiosulphate in acid solution. This determination originates from an analogous method for the determination of dimethylaminoantipyrine (pyramidone), which contains no $-SO_3Na$ group.

Since the iodometric method gave low and non-reproducible results we considered it necessary to study the mechanism of novalgin hydrolysis in acid solution, which we followed polarographically, determining the liberated formaldehyde gravimetrically.

Hydrolysis of novalgin has been studied by Wagner[13] and Pechtold[17]. Wagner identified hydrolysis products by means of paper chromatography and ionophoresis. Pechtold studied the rate of conversion of novalgin to methylaminoantipyrine as a function of time, concentration and *pH*, by means of column chromatography and spectrophotometry.

In an investigation of the adsorption properties of various salts of organic acids, Björling[18] noticed that the sodium ion of novalgin can be exchanged with hydrogen, by passing a novalgin solution through an ionic exchanger. On this principle we have developed a volumetric method for direct determination of novalgin. The sulphonic acid obtained can be titrated with a 0.1 *N* solution of a base, in the presence of phenolphthalein as indicator. Solutions of the sulphonic acid left to stand for one day show two jumps in the potentiometric titration, although the consumption of base is the same; this may be ascribed to a hydrolytic change of novalgin in acid solution. The method allows the quantitative study of novalgin hydrolysis and is the only reliable volumetric method for the determination of novalgin.

EXPERIMENTAL

We used "Hoest" novalgin, whose composition and purity was previously[1] determined. All other reagents were p. a., and water was double-distilled.

Iodometric method

The iodometric titration in aqueous solutions has not been described in detail in the literature, although the accuracy of the results depends on the technique. The first drop of 0.1 *N* iodine solution added to the colorless, neutral, about 0.1 *N* novalgin solution produces a yellow-brown precipitate, then the solution goes a transitient blue color which changes into green. If the next iodine drops are added rapidly, the green color changes into violet which disappears before the end-point. However if after the second drop a delay of a second is made, the green color turn into a light yellow which remains till the end of the titration. In the former case no indicator is required for the determination of the end-point, since the solution becomes permanently yellow on addition of the first drop of the solution, whereas in the latter case starch must be used. Since a pink coloration was observed in the titration of methylamino- and aminoantipyrine with iodine in the presence of sulphate ion, we believe that these colorations originate from the pyrazolone part of the novalgin molecule.

The yellow precipitate formed upon the addition of each iodine drop, dissolves upon stirring, with discoloring. If iodine is added rapidly, the accumulated precipitate in contact with air is converted into a resin which incorporates iodine. This process determines the rate of iodine addition, which should be about 1 drop per second, as was described by Wojahn[8]. If rate is slower the results are always low. Considerably low results are obtained when the aqueous solution of novalgin is left to stand for some time before titration. Because of autooxidation the solution goes yellow. Therefore the novalgin should be weighed and dissolved just before titration. We also attempted to determine the composition of the precipitate in order to verify the given chemical equation. By adding an excess of iodine to a titrated novalgin solution we obtained a lot of precipitate consisting of yellow monoclinic crystals which in contact with air turned into a resinous product. The precipitate was soluble in alcohol but it could not be purified and its elemental analysis gave no correct composition. The infrared spectrum was featureless. By the addition of sodium thiosulphate solution the precipitate was dissolved and discolored, showing that bound iodine was present in its molecular form, i.e. that the precipitate is a molecular compound of pyrazolone and iodine[19]. Of the related pyrazolones only methalamino- and dimethylaminoantipyrine yield crystalline precipitates with iodine in the presence of sulphate ion, whereas aminoantipyrine immediately gives a resinous prodcut.

The rate of iodine reaction is slow at the beginning of the titration, then getting faster and again falling very low at the end.

The change of pH in the course of titration is shown in Fig. 1, from which it may be seen that the reaction for the most part takes place in the *pH*-range from 3 to 1.5.

In a reproduction of the iodometric method given by Shub and Kobzareva[7], who recommend the dissolution of novalgin in only 5 *ml* of water, the results were 2.5—6% lower than the actual novalgin content (Table 1, a). When the titration was carried out in a solution which was acidified before titration, for example by the addition of acetic or hydrochloric acid,

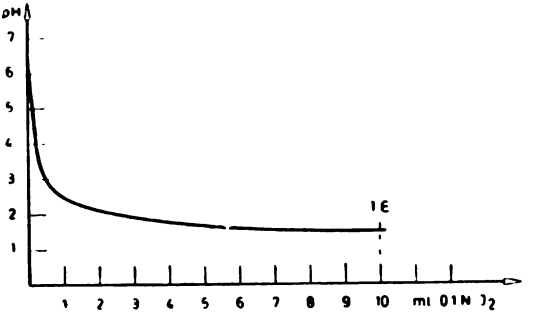

Figure 1

Change of *pH* in the course of the titration of 0.1 *N* aqueous novalgin solution with 0.1 *N* iodine solution.

TABLE 1

	Method	Number of determinations	% of novalgin
a	Titration in aqueous solution (5 *ml*)	37	95.5±1.9
b	Titration in aqueous solution of different *pH*		
	CH_3COOH buffer *pH* 2.6	11	95.9±1.8
	" " 2.2	1	97.2
	" " 1.8	4	97.0±0.2
	" " 7	1	119
c	Titration at a lower temperature (about 10°C)	2	98.9±0.5
d	Back titration in aqueous solution	17	98.1±1.8
e	Titration in alcoholic solution:		
	methanol CH_3OH	4	98.6±2.0
	ethanol C_2H_5OH	3	96.8±1.8
	Back titration in alcoholic solution:		
	methanol CH_3OH	3	102.1±0.1
f	ethanol C_2H_5OH	7	102.0±4.0
	with H_2SO_4 after 3 min	7	100.8±0.5
	" " " 10 "	2	102.5±5.0
g	Titration of iodine with novalgin	2	117 and 119
h	Iodometric determination after treatment with *KCN*	7	92.9±0.4
i	Permanganometric determination $E=M/4$	3	123±1.5
	$E=M/6$		82.5
	Titration in the presence of *HCHO* in excess:		
	immediately	2	97.8
j	after 15 min	1	93.9
	" 30 "	1	92.4
	" 60 "	2	91.9

or when the substance was dissolved directly in a buffer solution whose *pH* was 2.2 or 1.8 *(KCl+HCl)*, the results were also low and similar to those obtained in aqueous solution (Table 1, b). In more acid solutions a loss of gaseous SO_2 was observed. In solutions of *pH* above 4 (acetate or phosphate buffer) the consumption of iodine was much greater than required by the equation given by Rapaport and Shwartsburd[6]. Therefore the results obtained by Wirth's method in acetate buffer were considerably above 100%. At *pH* 7 the consumption of iodine was even greater. We are of the opinion that in buffered solution with *pH* above 4 the addition of iodine to the double bond occurs.

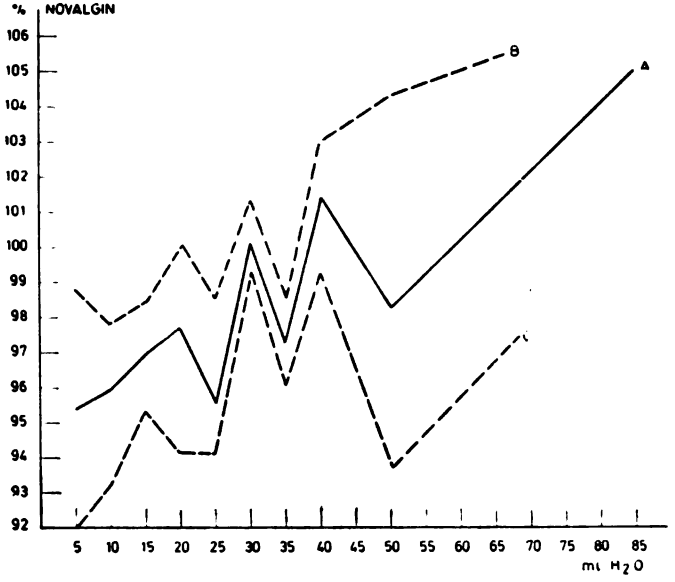

Figure 2

The effect of dilution on the results of iodometric determination of novalgin (0.2 *g*). *A* — mean value from five successive determinations, *B* — maximum, *C* — minimum.

The dilution has a great influence on the results of the titration. Figure 2 shows the mean values from five successive determinations at different dilutions (full line), and the maximum and the minimum values (dotted lines). It may be observed that the results go above 100% too, the more so the greater the initial dilution. At a dilution of 100—150 *ml* even a large excess of iodine disappears after some time together with the precipitate. The best results were obtained by dissolving about 0.2 *g* of novalgin in 30 *ml* of water, but on account of unsatisfactory reproducibility of the results we consider such a determination as unreliable. No volumetric method should depend so much upon the dilution.

The temperature of the solution in the range from 16 to 22°C had no effect on the reaction with iodine. At lower temperatures the results

were better (Table 1, *c*) but discoloring of the iodine at the beginning of the titration was very slow.

Back titration in aqueous solution involves dissolution of the precipitate. If no resin is formed and the precipitate dissolves easily upon the addition of sodium thiosulphate, the results are higher than in direct titration (Table 1, *d*). In this case a small excess of iodine (up to 5 *ml*) was added, and the period till the beginning of the back titration was 10 minutes.

Since the precipitate was soluble in alcohol, we also carried titrations in mixtures of alcohol methanol or ethanol and water; a 1 : 1 ratio yielded the best results, but they were not satisfactory (Table 1, *e*). Results obtained by back titration in such solutions were above 100%, and in case of methanol the equivalence-point was reached very slowly. Back titration of iodine in a mixture of ethanol, water and sulphuric acid after to Denoël[20] gave fairly satisfactory results. Hower, the accuracy of this method depends very much upon the time between the addition of iodine and the beginning of the back titration (Table 1, f). In addition, the back tritration of iodine with sodium thiosulphate in the presence of formaldehyde liberated in the course of the titration is unreliable[21].

The titration of an excess of iodine with novalgin solution gave extremely high results, indicating a reaction of the pyrazolone ring of novalgin with the excess of the oxidizing agent (Table, 1 *g*).

The possible catalytic effect of metal traces was eliminated by the addition of small amounts of EDTA; the results obtained in aqueous solutions were 0.5% higher than in the absence of EDTA.

An excess of potassium iodide reduces the redox potential of the system and slows down the initial reduction of iodine. Moreover, no colored products of oxidation of the pyrazolone ring were observed.

The effct of autoxidation of novalgin, accompanied by the appearance of a yellow color, is negligible since titrations in nitrogen atmosphere also gave very low results.

In the verification of the iodometric method given by Schulek and Maros[15] we confirmed the reproducibility in the analysis of aliquots of novalgin solution, but the results were very low (Table 1, *h*).

The permanganometric method[9] gave wrong results when the calculations were carried out using an $M/4$ equivalent (Table 1, *i*) as recommended by both pharmacopoeiae[10, 11]. It is incomprehensible that the authors[9] used the same equivalent as in the case of dimethylaminoantipyrine, since with novalgin the sulphite is oxidized as well, and that requires an equivalent of $M/6$. When the results were recalculated using this equivalent, they were low.

Low results in both the last two methods can be ascribed to a rapid oxidation of sulphite by air in alkaline solution.

DETERMINATION OF FORMALDEHYDE FROM NOVALGIN

Since it was assumed that the low results in iodometric determination of novalgin were due to formaldehyde, we studied its formation in novalgin hydrolysis under different conditions. Formaldehyde was determined gra-

vimetrically by precipitating it with dimedone[22]. The latter reagent is very suitable since it reacts with formaldehyde giving a condensation product insoluble in water and acetic acid, but does not react with formaldehyde bisulphite. Quantitative precipitation was achieved after 12 hours at room temperature or 10 minutes at the boiling temperature. Since the hydrolysis of novalgin was studied only at room temperature, the analyses were carried out at this temperature too.

To solutions of novalgin acidified with hydrochloric acid, acetate buffer was added after different time-periods since the optimum *pH* for the precipitation of the condensation product is 4.6. Alcoholic solution of the reagent was added to the alcoholic solution of novalgin. Methanol was chosen as the solvent since it dissolves both novalgin and formaldehyde bisulphite. The precipitation was induced by the addition of water. Samples of about 0.15 *g* of novalgin were taken. The results are shown in Table 2.

TABLE 2

Novalgin Solution	Number of determinations	% *HCHO* after 5 min.	after 1 hr	after 24 hrs
Aqueous, neutral	4	86	81	60—72
„ *pH* „ 0	4	81—87		
„ „ 1	4	78	83—85	74—78
„ „ 2	3	81		
„ „ 4.6	2	64	67	49
neutral, at 6°	2	56		
„ *tH* 1.5 (oxidized with equivalent amount of I_2)	10	99.8		
CH_3OH absol. neutral	2	77		
„ 83% „	2	76		
„ „ *pH* 0	2	65—67		
„ „ „ 1	2	66		
„ „ „ 2	2	74		

The values obtained are proportional to the degree of novalgin hydrolysis and depend upon the equilibrium constants of formaldehyde bisulphite and the condensation product of formaldehyde with dimedone, the hydrolysis constant of novalgin, the *pH* of the solution and the rates of the individual processes. Hence the percentages of formaldehyde obtained from novalgin under different hydrolysis conditions can be compared. From Table II it follows that: 1) all the formaldehyde can only be obtained after the oxidation of sulphite; 2) at lower temperatures and in very acid alcoholic solution considerably less formaldehyde is obtained; 3) on protracted standing in neutral solution the formaldehyde content decreases, whereas

in acid solutions (*pH* 1 and 2) an increase and then a decrease of formaldehyde content was observed. Since all the formaldehyde is obtained after oxidation, a gravimetric method for the determination of novalgin can be developed[20].

Neutralization method

Difficulties arising from the hydrolysis of novalgin which have prevented the development of reliable methods for its determination can be avoided by determining the novalgin as sodium ion or any other proportional species. By passing a novalgin solution through a strongly acid ion exchanger the corresponding sulphonic acid is obtained quantitatively; the latter can be determined either titrametrically with 0.1 *N* sodium hydroxide in the presence of phenolphtalein as indicator, or potentiometrically. In our experiments Merck I ion-exchanger was used. The column was 12 *mm* diameter and contained 6 *g* of the resin of a total capacity of 27 *meq*. 1—1.5 *g* of novalgin dissolved in 100 *ml* of water was passed through the column at a rate of 3.5 *ml*/min. The total volume of the solution after washing the column was 250 *ml*; aliquots of 50 *ml* were titrated. The time required for the analysis was an hour and a half. The results are shown in Table 3. The reproducibility was within the limits of volumetric methods, and the accuracy was satisfactory.

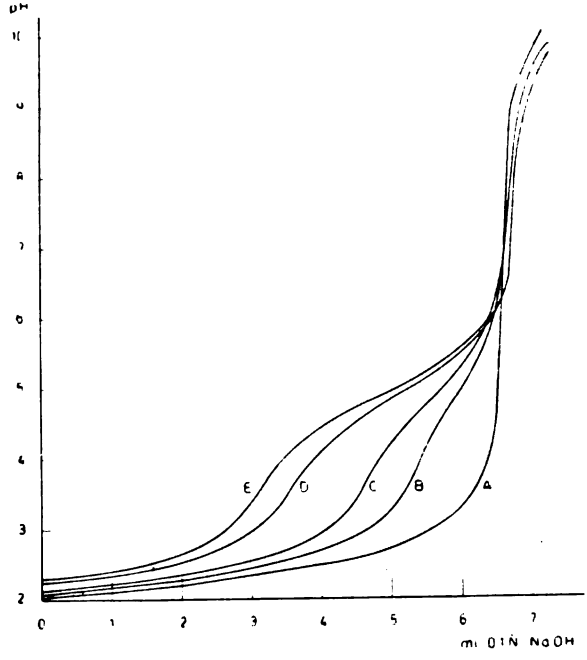

Figure 3

Neutralization curves of sulphonic acid from novalgin *A* — fresh solution, *B* — after standing for 1 day, *C* — after standing for 2 days, *D* — after standing for 5 days, *E* — after standing for 8 days.

TABLE 3

	% of novalgin
1	99.35
2	99.38
3	100.00
4	100.19
5	100.28
6	100.34
7	100.36
8	100.53
9	100.55
10	101.20
11	101.29
	100.31 ± 0.44
	$S = 0.61$

In the potentiometric titration of a fresh solution of novalgin only one jump was observed, and a pK value of 2.40 was obtained. Solutions which were left to stand for several days consumed the same amount of the base, but showed two jumps. The graph in Fig. 3 shows the titration curves of aliquots of the same solution analyzed in the course of eight days. In this case two acids were determined: sulphonic acid of novalgin with $pK_I = 2.40 \pm 0.06$, and its hydrolysis product protonized methylamino-antipyrine with $pK_{II} = 4.91 \pm 0.05$. The pH increased slightly with time, the amount of the former acid decreasing and of the latter increasing. Figure 4. shows novalgin hydrolysis as a function of time at pH 2.

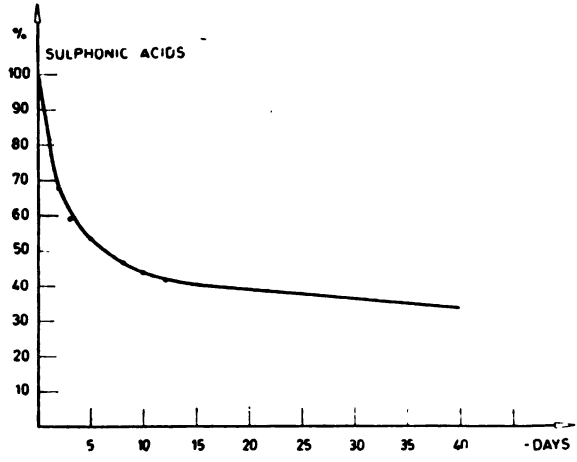

Figure 4

Hydrolysis of novalgin as a function of time

DISCUSSION OF METHODS DESCRIBED

We consider that the low results of iodometric methods may be ascribed to the reaction of formaldehyde and sodium bisulphite, which giving the stable addition product formaldehyde bisulphite (oxymethanesulphonate) which does not react with iodine. This is supported by the following observations:

1) A quantitative yield of sulphate ion from novalgin oxidation at room temperature by means of iodine in acid media is only obtained after some time, but by means of hydrogen peroxide in alkaline media it is obtained quickly.[1] This corresponds to the decomposition of formaldehyde bisulphite which takes place very slowly in acid (decomposition rate slowest at pH 1.26) and very rapidly in alkaline media[23].

2) If the liberated formaldehyde is determined in an alcoholic medium, less of it is formed, indicating a slower hydrolysis of novalgin. Under these

conditions the amount of novalgin determined iodometrically is high, which can be explained by a decreased formation of bisulphite in alcoholic solution.

3) At low temperature the rate of formation of the addition compound is slow[21, 24] and the results of iodometry are only 1% lower than theoretical.

4) The slower the titration, the lower are the results.

5) The titration of novalgin with iodine in the presence of a ten-fold excess of formaldehyde only gave lower results after 15 minutes, indicating a slow reaction of bisulphite with formaldehyde.

From the aforesaid it may be concluded that the reaction of novalgin with iodine cannot be taken as a basis for a good volumetric method, since it does not fulfill the requirement of a stoichiometric ratio between the titrated substance and the titrant. The determination involves the oxidation of bisulphite ion with iodine, but the direct titration of even pure bisulphite solution is known to be unreliable. In the course of the determination of novalgin, novalgin hydrolysis yields first bisulphite ion and then formaldehyde; these two hydrolysis products react and give formaldehyde bisulphite, which does not reacts with iodine. In addition, the pyrazolone part of the novalgin molecule reacts with iodine giving a precipitate, and only after the dissolution of the latter is the iodine reduced. All these reactions, with the exception of bisulphite oxidation, are slow and incomplete. Therefore, all the methods described so far are only empirical.

The results obtained by oxidation or neutralization of the acid obtained by passing novalgin solution through an ion exchanger column, or by gravimetric analysis of liberated formaldehyde, can be explained by means of the following scheme:

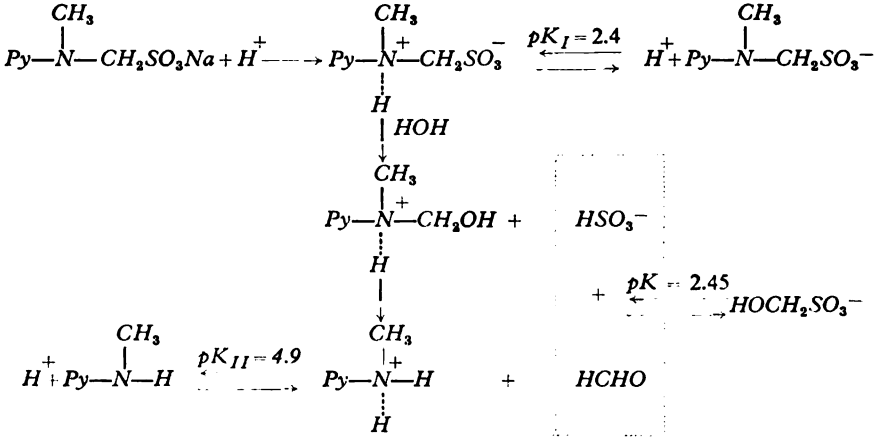

When an equivalent amount of hydrochloric acid is added to a novalgin solution, or when a novalgin solution is passed through a column of strongly acid ion-exchanger, the corresponding sulphonic acid is obtained immediately; its dissociation constant lies within the limits of sulphonic acid constants (pK 1—3). In acid solution it undergoes hydrolysis: the rate of hydrolsis was followed polarographically via the rate of bisulphite ion liberation. This process is relatively rapid. According to our investigations the

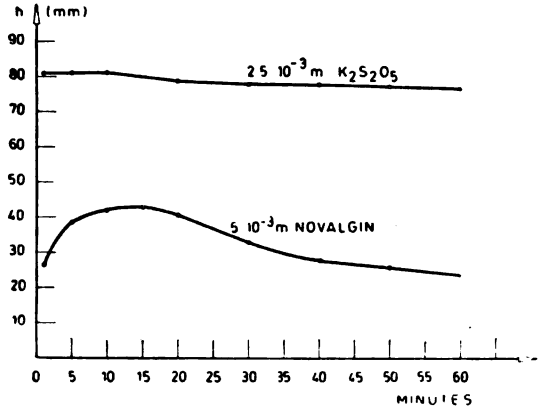

Figure 5

Change of HSO_3^- concentration with time, recorded polarographically
A — 5×10^{-3} M $C_{13}H_{16}O_4N_3SNa$,
B — 2.5×10^{-3} M $K_2S_2O_5$

liberation of sulphur dioxide is gradual, reaching a maximum value in 10—15 minutes in 10^{-2} — 10^{-3} M solutions at pH 0—2; later, its concentration decreases (Fig. 5). It should be noted that the fall of the curve cannot be ascribed to mechanical losses of SO_2 or to oxidation by atmospheric oxygen, since such losses were not observed in the polarography of potassium metabisulphite solution.

Polarographic determinations were carried out at a potential of — 0.6 V in the region of the limiting diffusion current of HSO_3^- or SO_2[25]. The height of the polarographic wave at the maximum of the novalgin curve for pH 0 is about 50% and pH 2 about 25% of the wave height of the equimolecular amount of potassium bisulphite determined under the same experimental conditions.

The fall of the polarographic curve due to bisulphite ion corresponds to the reaction of hydroxymethanesulphonic acid formation. This acid gives no polarographic wave under the given conditions. Hence it follows that in acid media novalgin is not decomposed into hydroxymethanesulphonate and methylaminoantipyrine, which would be the reverse of the last phase of novalgin synthesis[26].

The formation of hydroxymethanesulphonic acid proceeds slowly and depends upon the liberation of formaldehyde and the formation of pyrazolone. By comparing the rate of hydroxymethanesulphonic acid formation shown in Fig. 5 and the rate of pyrazolone base formation given in Fig. 4, it may be seen that this phase is the slowest in acid media, and is therfore rate-determining in hydrolysis.

Institute of Chemistry
School of Sciences
Beograd University

Received 25 May, 1967

REFERENCES

1. Vajgand, V., V. Nikolić, and D. Krstić. "Određivanje novalgina. I. Gravimetrijske metode" (Determination of Novalgin. I. Gravimetric Methods) — *Glasnik Hemijskog društva* (Beograd), in press.
2. Kaleis, O. Iü., and M. E. Volkova. "Kompleksometricheskoe opredelenie sulfatov i anal'gina" (Complexometric Determination of Sulphates and Novalgin) — *Aptechnoe Delo* (Moskva) 9 (2): 45—49, 1960.
3. Fecko, J. "Volumetric Determination of Sodium Noramidopyrine Methanosulphonate by Means of Barium Chloride" — *Acta Poloniae Pharmaceutica* (Warszaw) 20 (3): 225—228, 1963.
4. Munos Armestar, A., and A. Schultz. "The Iodometry of Novalgin", in: *Congr peruano quim. 3 rd. Congr., Lima, Peru,* 2, 1949 p. 458; *Chemical Abstracts* 35: 9786, 1952.
5. With, C. M. P. "Uber die Bestimmung von Novalgin" — *Pharmaceutica Acta Helvetiae* (Zurich) 6: 199—203, 1954.
6. Rapaport, L. I., and M. M. Schwartsburd. "Kvalitativno i kvantitativno opredelenie anal'gina" (Qualitative and Quantitative Determination of Novalgin) — *Aptechnoe Delo* (Moskva) 3 (5): 47—53, 1954.
7. Shub, M. E. and N. A. Kobzareva. "Volumetricheskoe opredelenie anal'gina" (Volumetric Determination of Novalgin) — *Aptechnoe Delo* (Moskva) 5 (4): 48—49, 1956.
8. Wojahn. H. *Deutsches Arnzbuch* — Bonn: 1959, pp. 276—280.
9. Schulek, E., and P. Meryhart. "Neues Verfahren zur titrimetrische Bestimmung des Pyramidons auch in Gegenwart von Antipyrin, Acetanilid, Phenacetin, Coffein usw". — *Zeitschrift für analitische Chemie* (München) 89: 426—439, 1932.
10. *Pharmacopoea Hungarica* Ed V. Tomus II — Budapest: Egészégügyi Kiado, 1954, pp. 79, 389.
11. *Östereichische Arzneibuch* 9. Ausgabe, Band II — Wien: 1960, p. 1043.
12. Budimlić, B., and D. Dumanović. "Prilog jodometrijskom određivanju novalgina" (Iodometric Determination of Novalgin) — *Glasnik Hemijskog društva* (Beograd) 27*: 293—298, 1962.
13. Wagner, C. "The Hydrolytic Decomposition of Novalgin" — *Archiv der Pharmazie und Berichte der deutschen pharmazeutischen Geselschaft* (Weinheim) 289: 121—124, 1956.
14. Kigasawa, K., H. Schimicu, S. Watari, N. Ikari, and H. Mikubo. "Studies on Iodometric Determination of Sulpirine" — *Yakugaku Zasshi* (Tokyo) 84 (7): 638—641, 1964.
15. Schulek, E., and L. Maros. "Beitrage zur Analitik einiger Mathansulfonsäurederivate. I. Jodometrische Bestimmung von Novalgin und Melubrin auch in Gegenwart von Antipyrin und Pyramidon" — *Analitica Chimica Acta* (Amsterdam) 19: 4—9, 1958.
16. Evers, M. M. H. "Die Jodometrische Titration von Natriumphenyldimethypyrazolonaminomethansulfonat (Melubrin)" — *Pharmaceutisch Weekblaly* (Hilversum) 77: 1081—1086, 1940; *Chemical Abstracts* 36: 6112, 1942.
17. Pechtold, F. "Quantitative Bestimmung des Hydrolysegrades von Pyrazolonen vom Metamizo-Typ" — *Arzneimittel Forschung* (Aulendorf, Würtemberg) 14 (12): 1328—1332, 1964.

18. Björling, C. O. "Adsorption Analysis of Salts of Organic Acids" — *Pharmacological Reviews* 48: 281—285, 1949; *Chemical Abstracts* 43: 5703, 1949.
19. Ketelaar, J. A. A. *Chemical Constitution* — Amsterdam: Elsevier Publishing Company, 1953, p. 333.
20. Denoël, M. "Dimethyl phenylpyrazolone méthylaminométhane sulfonate sodique" — *Journal de Pharmacie Belgique* (Brussel) (11—12): 544—552, 1952.
21. Kurtenacker, A. "Uber Anwendung der Aldehyd-Bisulfitreaktion in der Massanalyse" — *Zeitschrift für analytische Chemie* (München) 64: 56—61, 1924.
22. Yoe, J., and L. Reid. "Determination of Formaldehyde with 5,5-Dimetylcyclohexanedione-1,3" — *Industrial and Engineering Chemistry, Analytical Edition* (Washington) 13: 238—243, 1941.
23. Skrabal, A. and R. Skrabal. "Die Dynamik der Formaldehyd-Bisulfit Reaktion" — *Monatshefte für Chemie* (Leipzig, Wien) 69: 11—41, 1936.
24. Parkinson, A. E., and E. C. Wagner; "Estimation of Aldehyde by the Disulfite Methods" — *Industrial and Engineering Chemistry, Analytical Edition* (Washington) 6: 433—436, 1934.
25. Proszt, J., V. Cielszky, and K. Györbiró. *Polarográfia* — Budapest: Akadémiai Kiadó 1964, p. 331.
26. Khros, W., and O. Hensel. *Pyrazolone und Dioxopyrazolodine* — Aulendorf, Würtemberg: Editio Cantor, 1961, p. 91.

* Available in English translation from Clearinghouse for Federal Scientific and Technical Information, Springfield, Virginia, 22151.

GLASNIK HEMIJSKOG DRUŠTVA, Vol. 32, No. 8-9-10, 1067, pp. 460—480

SYNTHESIS OF SOME N-HETEROCYCLIC ALIPHATIC KETONES AND KETO ACIDS FROM TETRAHYDROPYRANYL ESTERS OF ALKYLMALONIC AND CARBOXYALKYLMALONIC ACIDS*

by

SLAVKA M. PAVLOV and VLADIMIR Č. ARSENIJEVIĆ

Although there are several methods for the preparation of *N*-heterocyclic aliphatic ketones and for the synthesis of *N*-hetocyclis aliphatic γ and δ keto acids, most of these compounds are considerably less well known than their aliphatic and aromatic-aliphatic analogues. Exceptions are the methyl pyridyl ketones, which are commercially produced and which are obtained in good yields from the corresponding β-keto esters.

N-heterocyclic aliphatic ketones are most often prepared by the action of Grignard's reagent on nitriles; this method is usually applied for the preparation of alkyl pyridyl ketones and alkyl quinolyl ketones. The yields vary depending on the position of the cyano group in the starting heterocyclic nitrile. The main disadvantage of this method is the alkylation of the heterocyclic ring in positions 2 and 4 by the action of Grignard's reagent. However, if the cyano group occupies one of these two positions, the corresponding ketones are obtained in good yields. By this method the following ketones have been prepared: 2-pyridyl alkyl ketones[1] in yields of 40—75%; 3-pyridyl alkyl ketones[2] in yields of about 40%; 2,6-diacetylpyridine[3] in a yield of 11%. 4-Propionylquinoline[4] was obtained in a yield of only 6%, whereas in the preparation of 2-propionylquinoline[5] a yield of 68% was reported. The reaction of dialkylcadmium compounds with acid chlorides has also been used for the synthesis of some pyridyl ketones; the yields were 20—30%[2].

The preparation of only some of the *N*-heterocyclic aliphatic γ and δ-keto acids and keto esters is described in the literature; the method used was Claisen's ester condensation. Thus γ-(2-pyridyl)-γ-oxo-butyrate[6] was prepared by the ketonic decomposition of the keto diester obtained by Claisen condensation of ethyl picolinate with ethyl succinate. The yield was only 30%. Ethyl δ-(3-pyridyl)-δ-oxo-valerate[7] was obtained by the alkylation of ethyl niconinoylacetate with ethyl β-bromopronionate followed by ketonic decomposition. The authors give no data about the yield; when we repeated this synthesis we got a yield of 12—15% (relative to starting ethyl picolinate).

* This paper is an excerpt from the doctoral thesis of Slavka Pavlov (University of Beograd, 1965); it was communicated at the 2nd Yugoslav Congress for Pure and Applied Chemistry, June, 1966.

Low yields and limitations encountered in syntheses of *N*-heterocyclic ketones and keto acids prompted us to investigate other methods for their preparation. These compounds were required as the starting material for the synthesis of azasteroids. Since recently tetrahydropyranyl esters of substituted malonic acids were successfully used for the synthesis of aliphatic and aliphatic-aromatic ketones and keto acids we considered that they might be convenient for the preparation of heterocyclic ketones and keto acids.

Bowman and Fordham[8] were the first to use tetrahydropyranyl esters of malonic acids for the preparation of ketones, making use of the observation of Jones and Taylor [9] that these esters can be hydrolyzed under mild conditions. The method is simple: by the action of dihydropyran in excess on a suspension of the corresponding alkylmalonic acid in benzene, in the presence of catalytic amounts of sulphuric acid, taking care that the temperature of the reaction mixture does not rise above 35°C, the corresponding bis-tetrahydropyranyl ester is obtained in quantitative yield. The ester is then converted into the sodium derivative which is acylated with an equivalent amount of the corresponding acid chloride. The β-keto ester obtained is unstable when heated, especially in the presence of acetic acid. Ketonic decomposition is carried out in boiling benzene to which a small amount of glacial acetic acid has been added, and ketone, dihydropyran and carbon dioxide are formed. This method was extended by Horeau[10] and one of the authors of this paper to the preparation of γ, δ and ε-keto acids. The starting material is 1, 1, 2-ethanetricarboxylic, 1, 1, 3-propanetricarboxylic or 1, 1, 4-butanetricarboxylic acid, which are easily converted into the corresponding tetrahydropyranyl esters by the action of dihydropyran at room temperature, in the presence of one drop of sulphuric aicd. The sodium derivatives of these esters (as in Bowman's method) are first acylated by means of the acid chloride, and then a few *ml* of glacial acetic acid is added and the benzene solution boiled for 3 to 4 hours. Both β-keto ester groups get decomposed and decarboxylated, whereas the third ester group, having no β-keto group, is left unchanged. In order to convert the tetrahydropyranyl ester of the keto acid into the free keto acid, the benzene solution was either heated for a few minutes with 2—3 *ml* of hydrochloric acid, or the ester was heated for a longer time with a base in excess. In this way the aromatic keto acids were obtained in a yield ranging from 70 to 95% whereas Bowman and Fordham synthesized a number of aliphatic ketones in yields of 45—92%.

Our attempts to apply these procedures directly for the preparation of some heterocyclic ketones and keto acids did not give satisfactory results. For example, in the preparation of 2- or 3-propionylpyridine, 2-propionylthiophene, 2-propionylfuran and other ketones whose boiling point is 80—110°C/12—16 *mm*, we found that the isolation of these compounds was very difficult and that fractional distillation or some other method was required for the separation of ketones from tetrahydropyranyl acetate, which boils at 82—83°C/13 *mm*. The latter ester was formed from glacial acetic acid (added to accelerate the ketonic decomposition) and dihydropyran liberated in the course of the decomposition. To avoid this disadvantage we omitted the addition of glacial acetic acid and carried out the ketonic decomposition in the following way: after acylation the solvent was removed, toluene

was added to the residue and the solution obtained was heated at 115—120°C for 1—2 hours. Under these conditions the β-keto ester decomposed rapidly. After distillation of toluene the pressure was reduced to 12—15 *mm* and the pure ketone was distilled. In this way the formation of tetrahydropyranyl acetate which would contaminate the ketone was avoided, and the time required for the ketonic decomposition was not greatly prolonged.

The results were also unsatisfactory in attempts to apply the method given by Arsenijević and Horeau[10] for the preparation of pyridyl and quinolyl keto acids. Difficulties were encountered in the isolation of these amphoteric compounds which, on acetolysis or alkaline hydrolysis of the third ester group, were obtained either in the form of alkaline salts or in the form of the corresponding hydrochlorides: it was very difficult to obtain free keto acids from these water-soluble salts. Precipitation or extraction at *pH* 3—3.5 (where the isoelectric point was expected to be) gave almost no results. It was evident that the decomposition of the third tetrahydropyranyl ester group by means of alkalis or mineral acids should be avoided. More detailed investigations led us to a more convenient procedure for the decomposition of this ester group: after acylation benzene was removed and a solvent with a higher boiling point, for example toluene, was added together with a few *ml* of glacial acetic acid. The solvent was then distilled whereby the liberated dihydropyran passed over, shifting the equilibrium in the direction of keto acid formation. In the course of distillation fresh toluene containing some acetic acid was added slowly. Complete decomposition was achieved after heating for several hours. The keto acid formed usually crystallized out on cooling of the toluene solution, evaporated to a s small volume.

In the course of this work, and in our previous investigations[10] on aromatic keto acids too, we established that tetrahydropyranyl esters of γ and δ-keto acids are stable when heated in benzene solution, even in the presence of small amounts of acetic acid. We also studied the stability of tetrahydropyranyl esters of alkylmalonic and carbetoxyalkylmalonic acids by boiling them in benzene solution for 1—2 hours, and established that under these conditions no pyrolytic decomposition occured. This fact proved to be of importance when sodium derivatives had to be acylated at temperatures above 35°C, i.e. when acylation was carried out with acid chlorides of low reactivity. We prepared some of these acid chlorides which reacted with sodium derivatives only at higher temperatures (chlorides of *N*-tosylpyrrolidine-2-carboxylic acid, *N*-trifluoroacetylpyrrolidine-2-carboxylic acid and *N*-carbobezoxypyrrolidine-2-carboxylic acid, *N*-tosylpyrroglutamyl chloride and *N*-methylpyrroglutamyl chloride). In this case too ketones and keto acids were obtained in good yields. These findings indicated that the heating in benzene solution in the absence of mineral acids had no effect on the tetrahydropyranyl esters of substituted malonic acids (except acylmalonic esters).

On the basis of these observations it was possible to modify Bowman's procedure and to prepare, starting from tetrahydropyranyl esters of alkylmalonic and carboxyalkylmalonic acids, a great number of ketones and keto acids containing a thiophene, furan, pyridine, quinoline or some other heterocyclic ring. The course of the reaction is as follows:

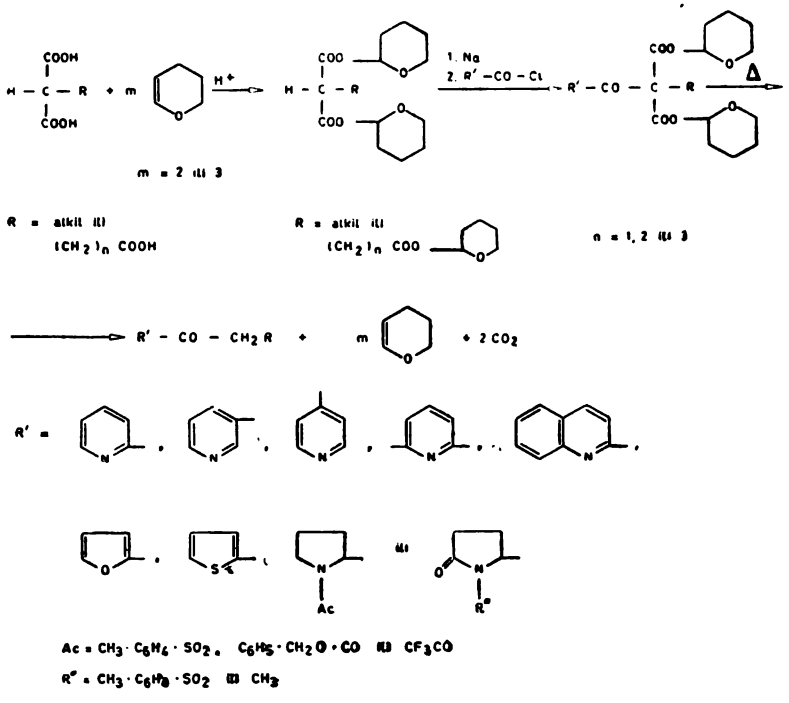

Some of these compounds were not previously known so far and cannot be obtained by other methods. In most cases the yields exceeded those of earlier methods.

EXPERIMENTAL*

General Procedure for the Preparation of Ketones and γ, δ and ε-Keto Acid

In a 1/2 *l* round-bottomed flask immersed in a water bath at room temperature 150 *ml* of anhydrous benzene, one drop of conc. sulphuric acid and 24 *ml* or 36 *ml* of 2, 3-dihydropyran (the amount of dihydropyran depends on whether dicarboxylic or tricarboxylic acid is esterified) are mixed. To the stirred reaction mixture** 0.1 mole of finely powdered and dry alkylmalonic or carboxyalkylmalonic acid*** is added gradually. The acid soon esterifies but mixing is continued for a further 2 hrs (in case of alkylmalonic acid) or 10 hrs (in case of carboxyalkylmalonic acid). To the solution obtained 0.5 *ml* of pyridine is added (to neutralize the catalyst) and benzene together with the excess of dihydropyran is evaporated in vacuum.

* Melting points were determined with a Kofler microscope.

** The use of a magnetic stirrer is recommended.

*** 1,1,2-ethanetricarboxylic acid, 1,1,3-propanetricarboxylic acid, and 1,1,4-butanetricarboxylic acid were used. The preparation of these acids was reported earlier [10]. A better yield of the triester of propanetricarboxylic acid was achieved by Nazarov (*Chemical Abstracts* 47: 5364d, 1953).

To the syrupy residue 30—40 *ml* of anhydrous benzene is added and the solvent evaporated in vacuum again. The residue is dissolved in 150 *ml* of anhydrous benzene and 0.1 gram atom of powdered sodium suspended in 50 *ml* of benzene is added (the flask is equipped with a calcium chloride tube). After mixing for 1 to 3 hrs (depending on the quality of the powdered sodium) all the sodium has usually reacted. Then 0.1 mole of the acid chloride dissolved in 100 *ml* of anhydrous benzene is added at once, and the reaction mixture stirred for a further 1—2 hrs. If the acid chloride is only slightly reactive, which can be recognized by the absence of spontaneous warming, the reaction mixture is refluxed for half an hour at 70—80°C. The flask is then cooled, the contents washed with water* and dried with magnesium sulphate. Further treatment of the benzene solution depends on whether ketones or keto acids are to be obtained. In the preparation of ketones which boil at up to 115°C/12—16 *mm*, the solvent is removed under atmospheric pressure, 100 *ml* of toluene is added and the solution boiled for 1—2 hrs. The cessation of the evolution of carbon dioxide was monitored by means of eudiometer. Toluene is then removed and the crude ketone purified by distillation in vacuum. If ketones of higher melting points are being synthesized, the ketonic decomposition is carried out according to the procedure given by Bowman and Fordham, i.e. by refluxing the benzene solution for 1.5—2 hrs after the addition of 5—10 *ml* of glacial acetic acid. Benzene is then evaporated, tetrahydropyranyl acetate (b. p. 82—83°C/13—14 *mm*) removed by distillation and the ketone purified either by distillation or crystallization.

To prepare the keto acids, 10 *ml* of glacial acetic acid is added to the benzene solution and the benzene then slowly distilled over with simultaneous addition of toluene (500 *ml*) and glacial acetic acid (10 *ml*). The distillation rate should be regulated so that the solvent mixture distills over in 4—5 hrs. On cooling the keto acids usually crystallize out and may be purified by recrystallization. The yield of the crude product is in most cases quantitative, but on recrystallization it falls by 10—30%.

Propyl 2-Pyridyl Ketone

Propyl 2-pyridyl ketone was obtained from ethylmalonic acid and picolinoyl chloride[11]. The yield was 81%; b.p. 100—103°C/14 *mm* (Lit. 217—218°C/750 *mm*)[12].

Picrate resrystallized from water, m. p. 74—75°C (Lit. 75°)[12].

Phenylhydrazone recrystallized from methanol, m. p. 82—83°C (Lit. 82°C)[12].

Ethyl 3-Pyridyl Ketone

Ethyl 3-pyridyl ketone was obtained from methylmalonic acid and nicotinoyl chloride[11]. The yield was 90%, b.p. 116—119°C/14 *mm* (Lit. b.p. 96—99°C/5 *mm*)[13].

Phenylhydrazone recrystallized from ethanol, m. p. 145°C (Lit. 145°C)[13].

* Washings should be neutral, but if acid, the benzene solution should be washed with 5% sodium bicarbonate solution and water, and then dried with magnesium sulphate.

Butyl 3-Pyridyl Ketone

Butyl 3-pyridyl ketone was prepared from propylmalonic acid and nicotinoyl chloride. The yield was 85%, b.p. 105—108°C/0.8 *mm*

Analysis:

Calculated for $C_{10}H_{13}ON$(163.21): *C* 73.59 *H* 8.03 *N* 8.58
Found: *C* 73.43 *H* 8.15 *N* 8.45

Iodomethylate, m.p. 93—94°C

Analysis:

Calculated for $C_{11}H_{16}ONI$(305): *N* 4.59
Found *N* 4.29

Butyl 4-Pyridyl Ketone

Butyl 4-pyridyl ketone was prepared from propylmalonic acid and izonicotinyl chloride[11]. The yield was 90%, b.p. 130—132°C/22 *mm* (Lit. 239—240°C)[12].

Picrate recrystallized from water, m.p. 106°C (Lit. 101°C).[12]

Semicarbazone recrystallized from ethanol, m.p. 180°C.

Analysis:

Calculated for $C_{11}H_{16}ON_4$(220.27): N 25.44
Found *N* 25.60

Ethyl 2-Quinolyl Ketone

Ethyl 2-quinolyl ketone was prepared from methylmalonic acid and quinaldinoyl chloride[14]. The sodium derivative was acylated by heating the benzene solution for half an hour at 70—80°. After evaporation of the solvent the remaining viscous oil crystallized on distillation in vacuum with a yiled of 80%. Crystals obtained by recrystallization from 50% ethanol melted at 60°C (Lit. 59—60°).[5]

Phenylhydrazone recrystallized from methanol, m.p. 105°C (Lit. 106°C) [15].

Butyl 2-Quinolyl Ketone

Butyl 2-quinolyl ketone was prepared from propylmalonic acid and the chloride of quinaldinic acid. Acylation was carried out by heating the sodium derivative with the acid chloride for half an hour at 70—80°C. Evaporation of the solvent gave a yellow viscous oil which crystallized after distillation in vacuum (b.p. 129—130°C/0.02 *mm*). The yield was 81%. After recrystallization from 50% ethanol the m.p. was 40°C.

Analysis:

Calculated for $C_{14}H_{15}ON$ (213.27) *C* 78.84 *H* 7.08 *N* 6.57
Found *C* 78.69 *H* 7.20 *N* 6.42

Picrate recrystallized from methanol, m.p. 109°C.

Analysis:

Calculated for $C_{20}H_{18}O_8N_4$ (442.38): *N* 12.67
Found *N* 12.52

Phenylhydrazone recrystallized from ethanol, m.p. 94—95°C.

Analysis:

Calculated for $C_{20}H_{21}N_3$ (303.38): *N* 13.85
Found *N* 13.70

Butyl N-Carbobenzoxy-2-Pyrrolidinyl Ketone

This ketone was obtained from propylmalonic acid (0.02 mole) and the chloride of *N*-carbobenzoxyproline (0.02 mole). The acid chloride was prepared from 4.9 *g* (0.02 mole) of *N*-carbobenzoxyproline and 6 *g* of oxalyl chloride. Acylation was carried out with the crude acid chloride, by heating the reaction mixture for one hour at 70—80°C. The ketone was obtained in the form of a viscous oil which was purified by column chromatography on aluminum oxide. Elution was performed with a benzene-ether (1 : 1) mixture. The evaporation of the solvent yielded an oil whose elemental analysis corresponded to that of the ketone.

Analysis:

Calculated for $C_{17}H_{23}O_3N$ (289.36): *C* 70.56 *H* 8.01 *N* 4.84
Found *C* 70.22 *H* 8.12 *N* 4.79

Phenylhydrazone (washed with methanol), m.p. 86°C.

Analysis:

Calculated for $C_{23}H_{29}O_2N_3$ (379.49): *C* 72.79 *H* 7.70 *N* 11.07
Found *C* 72.59 *H* 7.81 *N* 11.16

4-Picolinoylbutyric Acid

This acid was obtained from 0.02 mole of propanetricarboxylic acid[10] and crude picolinoyl chloride prepared from 3.5 *g* (0.022 mole) of potassium picolinate and 2.8 *g* (0.022 mole) of oxalyl chloride[11]. The crude acid melted at 81—83°C; recrystallized from water, m.p. 85—87°C. The yield was 72%.

Analysis:

Calculated for $C_{10}H_{11}O_3N$ (193.20): *C* 62.16 *H* 5.74 *N* 7.25
Found *C* 61.94 *H* 5.84 *N* 7.16

5-Picolinoylvaleric Acid

It was obtained from butanetricarboxylic acid[10] (0.01 mole) and crude picolinoyl chloride prepared from 1.77 *g* (0.011 mole) of potassium picolinate and 1.4 *g* (0.011 mole) of oxalyl chloride. Evaporation of the solvent yielded a dark brown oil which crystallized out on standing in a refrigerator for several hours. Recrystallization from water gave slightly colored crystals which melted at 70—71°C. The yield was 77%.

Analysis:

Calculated for $C_{11}H_{13}O_3N$ (207.22): C 63.75 *H* 6.32 *N* 6.76
Found *C* 63.59 *H* 6.10 *N* 6.91

Ethyl 5-picolinoylvalerate. 5-Picolinoylvaleric acid (1 *g*) was dissolved in absolute ethanol (15 *ml*) and esterified by introducing 1—2 *g* of dry hydrogen chloride. The solution was left to stand overnight and was then poured over 20 *g* of ice. After addition of potassium carbonate till saturation the aqueous layer was extracted with ether (3 × 10 *ml*). Evaporation of the solvent gave 1 *g* of an oily product which was distilled in high vacuum by means of Kober's apparatus.

Analysis:

Calculated for $C_{13}H_{17}O_3N$ (235.27):	*C* 66.36	*H* 7.27	*N* 5.95
Found	*C* 66.20	*H* 7.15	*N* 5.79

Picrate recrystallized from methanol, m.p. 59°C.

Analysis:

Calculated for $C_{19}H_{20}O_{10}N_4$ (464.38)	*C* 49.14	*H* 4.34	*N* 12.07
Found	*C* 49.21	*H* 4.18	*N* 12.22

3-Nicotinoylpropionic Acid

It was obtained from 8.2 *g* (0.05 mole) of ethanetricarboxylic acid[10] and 7 *g* of (0.05 mole) of nicotinoyl chloride[11]. On evaporation to a small volume and cooling crystallization took place but it was only completed after several days standing in a refrigerator. The crude product was washed with benzene and then recrystallized from water with the addition of active charcoal; m.p. 163—164°C (Lit. 163—164°C)[15]. The yield was 80%.

4-Nicotinoylbutyric Acid

It was obtained from propanetricarboxylic acid (0.05 mole) and nicotinoyl chloride (0.05 mole). Evaporation of the solvent gave a yellow oil which crystallized readily. The crystals were washed with an *n*-hexane-benzene mixture. After recrystallization from water the acid melted at 127—128°C. The yield was 85%.

Analysis:

Calculated for $C_{10}H_{11}O_3N$ (193.20):	*C* 62.16	*H* 5.74	*N* 7.25
Found	*C* 61.98	*H* 5.77	*N* 7.11

When instead of nicotinoyl chloride its hydrochloride[16] was used for acylation, the keto acid was obtained in a slightly smaller yield (79%).

Ethyl 4-nicotinoylbutyrate. This ester was obtained in the same way as ethyl 5-picolinoylvalerate. The yield was 71%, b.p. 147—153°C/0.6 *mm*.

Analysis:

Calculated for $C_{12}H_{15}O_3N$ (221.25):	*C* 65.14	*H* 6.83	*N* 6.33
Found:	*C* 64.82	*H* 6.93	*N* 5.99

5-Nicotinoylvaleric Acid

The acid was obtained from butanetricarboxylic acid and nicotinoyl chloride; after evaporation of toluene crystallization took place. The crystals were washed with cold benzene and recrystallized from water, m.p. 139—140°C. The yield was 82%.

Analysis:

Calculated for $C_{11}H_{13}O_3N$ (207.22):	*C* 63.75	*H* 6.32	*N* 6.76
Found	*C* 63.50	*H* 6.36	*N* 6.87

3-Izonicotinoylpropionic Acid

The acid was obtained from ethanetricarboxylic acid and izonicotinoyl chloride. The oil left after evaporation of the solvent crystallized on cooling. The crystals were filtered off and washed with cold benzene. The yield was 87%. After recrystallization from water, the m.p. was 185°C.

Analysis:

Calculated for $C_9H_9O_3N$ (179.17): *C* 60.33 *H* 5.06 *N* 7.82
Found *C* 60.50 *H* 4.90 *N* 7.75

4-Izonicotinoylbutyric Acid

It was obtained from propanetricarboxylic acid and izonicotinoyl chloride. The oily product obtained after evaporation of the solvent crystallized out on standing in the cold. The crystals were washed with a benzene-petroleum ether (3 : 1) mixture. The yield was 91%. Recrystallized from water the keto acid melted at 197—199°C. The yield after the recrystallization was 75%.

Analysis:

Calculated for $C_{10}H_{11}O_3N$ (193.20): *C* 62.16 *H* 5.74 *N* 7.25
Found *C* 62.01 *H* 5.63 *N* 7.09

5-Izonicotinoylvaleric Acid

It was obtained from butanetricarboxylic acid and izonicotinoyl chloride[11]. Evaporation of the solvent gave a mixture of crystals and oil. The crystals were washed with cold ether and recrystallized from water. The yield was 70%, m.p. 157—158°C.

Analysis:

Calculated for $C_{11}H_{13}O_3N$ (207.22): *C* 63.75 *H* 6.32 *N* 6.76
Found *C* 63.61 *H* 6.52 *N* 6.61

Ethyl 5-isonicotinoylvalerate: 5-Isonicotinoylvaleric acid (2 *g*), 20 *ml* of ethanol and 2 *ml* of conc. sulphuric acid were refluxed for 3 hrs. The cooled solution was poured into 30 *ml* of icy water, saturated with potassium carbonate, stirred for half an hour and extracted with ether. The ethereal solution was washed with water saturated with sodium chloride, dried, and the ether removed. The oily residue was purified by distillation from Kober's apparatus at 0.1—0.2 *mm*. A light yellow oil was obtained in a yield of 80%.

Analysis:

Calculated for $C_{13}H_{17}O_3N$ (235.27): *C* 66.36 *H* 7.28 *N* 5.95
Found *C* 66.21 *H* 7.14 *N* 5.82

Picrate recrystallized from ethanol, m.p. 99.5°C.

Analysis:

Calculated for $C_{19}H_{20}O_{10}N_4$ (464.3): *C* 49.14 *H* 4.34 *N* 12.07
Found *C* 49.02 *H* 4.21 *N* 12.27

4-(2-Quinolyl)-4-Ketobutyric Acid

It was obtained from ethanetricarboxylic acid and the chloride of quinaldinic acid. Acylation was carried out by refluxing the reaction mixture for half an hour at 80°C. Evaporation of the solvent yielded a viscous oil which crystallized out after standing for several days. The crude keto acid was recrystallized from ethanol, m.p. 145°C. The yield was 72%.

Analysis:

Calculated for $C_{13}H_{11}O_3N$ (229.23):	*C* 68.11	*H* 4.84	*N* 6.11
Found	*C* 67.86	*H* 4.96	*N* 6.19

Methyl 4(2-quinolyl)-4-ketobutyrate. The keto acid (1 g) was dissolved in ether and a slight excess of ethereal solution of diazomethane was added. Removal of the solvent yielded a viscous oil which crystallized on distillation in high vacuum (Kober's apparatus). m.p. 68—69°C.

Analysis:

Calculated for $C_{14}H_{13}O_3N$ (243.25):	*C* 69.12	*H* 5.39	*N* 5.76
Found	*C* 68.94	*H* 5.46	*N* 5.85

5-(2-Quinolyl)-5-Ketovaleric Acid

It was obtained from propane tricarboxylic acid and the chloride of quinaldinic acid. The sodium derivative was acylated by refluxing the reaction mixture for half an hour at 70—80°C. On evaporation of the solvent a viscous oil was obtained which crystallized after standing for 2 to 3 days. The unpurified product melted at 129—130°C. The yield was 80%.

After recrystallization from ethanol, m.p. 135°C.

Analysis:

Calculated for $C_{14}H_{13}O_3N$ (243.25):	*C* 69.12	*H* 5.39	*N* 5.76
Found	*C* 68.84	*H* 5.46	*N* 5.86

6-(2-Quinolyl)-6-Ketocaproic Acid

It was obtained from butanetricarboxylic acid and the chloride of quinaldinic acid. Acylation was carried out by heating the reaction mixture for half an hour at 70—80°C. The crude keto acid separated in the form of an oil which crystallized on standing. The crystals were washed with cold benzene and recrystallized from ethanol, m.p. 109°C. The yield was 74%.

Analysis:

Calculated for $C_{15}H_{15}O_3N$ (257.28):	*C* 70.02	*H* 5.88	*N* 5.44
Found	*C* 69.78	*H* 5.81	*N* 5.52

2,6-Pyridine-Bis (5-Ketovaleric Acid)

It was obtained from propanetricarboxylic acid and the dichloride of 2,6-pyridinecarboxylic acid (dipicolinic acid). Evaporation of toluene gave an oily residue which crystallized on standing. The crystals were washed with benzene and filtered off. The yield was 94%. Recrystallization from water gave needle like crystals, m.p. 121—123°C.

Analysis:

Calculated for $C_{15}H_{17}O_6N$ (307.29):	*C* 58.63	*H* 5.58	*N* 4.56
Found	*C* 58.26	*H* 5.42	*N* 4.64

3-(2-Furoyl)-Propionic Acid

It was obtained from ethanedicarboxylic acid and 2-furoyl chloride. On evaporation of the solvent and cooling a slightly yellow crystalline product was obtained. Recrystallization from water gave a colorless product of m.p. 118—119°C. The yield was 80.5%.

Analysis:

Calculated for $C_8H_8O_4$ (168.14): *C* 57.14 *H* 4.80
Found *C* 56.84 *H* 4.67

4-(2-Furoyl)-Butyric Acid

It was obtained from propanetricarboxylic acid and furoyl chloride; it crystallized readily from water, m.p. 130°C. The yield was 69%. Evaporation of the aqueous solution after recrystallization to one third of its initial volume gave some more crystals of m.p. 128—129°C so that the total yield was 82%.

Analysis:

Calculated for $C_9H_{10}O_4$ (182.17): *C* 59.33 *H* 5.53
Found *C* 59.12 *H* 5.39

3-(2-Thenoyl)-Propionic Acid

It was obtained from ethanetricarboxylic acid and 2-thenoyl chloride. Evaporation of the solvent yielded crystals and some oil. To remove the oil the crystals were dissolved in dilute sodium hydroxide, the solution extracted with ether and the aqueous layer, after being made colorless with active charcoal, was acidified with hydrochloric acid. Pure keto acid was obtained, m.p. 120°C (Lit. 120°C)[17]. The yield was 91%.

4-(2-Thenoyl-) Butyric Acid

It was obtained from propanetricarboxylic acid and 2-thenoyl chloride. It separated in the form of an oil but on cooling it crystallized. Purification was carried out by converting the acid into the sodium salt followed by treatment with active charcoal and precipitation with hydrochloric acid. Rectrystallization from water gave pure crystals, m.p. 95°C (Lit. 91°C)[18]. The yield was 82%.

4-(N-Tosylpyrroglutamyl)-Butyric Acid

It was obtained from propanetricarboxylic acid and *N*-tosylpyrroglutamyl chloride[19]. Acylation was carried out by boiling a benzene solution of the reactants for one hour. After evaporation of benzene a dark brown oil was obtained; it crystallized on standing in a refrigerator. The crude product was washed with benzene and recrystallized from water giving colorless needles, m.p. 186—187°C. The yield was 71%.

Analysis:

Calculated for $C_{16}H_{19}O_6NS$ (353.37): *C* 54.38 *H* 5.44 *N* 3.98
Found *C* 54.62 *H* 5.31 *N* 3.93

5-(N-Tosyl-2-Pyrrolidine)-5-Ketovaleric Acid

It was obtained from propanetricarboxylic acid and *N*-tosyl-*L*-proline chloride[20]. Acylation was carried out by boiling a benzene solution for one hour. Evaporation of the solvent yielded a viscous oil which was dissolved in sodium bicarbonate solution, bioled with active charcoal, filtered off and acidified with hydrochloric acid. The oily precipitate was dissolved in 10 *ml* of ethyl acetate to which a few *ml* of ether had been added. On cooling below 0°C the keto acid crystallized out. The crystals were washed in ether. M.p. 96—97°C. The yield was 66%.

Analysis:

Calculated for $C_{16}H_{21}O_5NS$ (339.39):	*C* 56.64	*H* 6.23	*N* 4.13
Found	*C* 56.75	*H* 6.12	*N* 4.02

5-(N-Trifluoroacetyl-2-Pyrrolidine)-5-Ketovaleric Acid

It was obtained from propanetricarboxylic acid and trifluoroacetyl--*L*-proline chloride. The acid chloride was prepared by acylation of *L*-proline (0.05 mole) with a small excess of trifluoroacetic anhydride[21], and then the acyl derivative was left to stand with an excess of oxalyl chloride at 60°C in benzene solution. Evaporation of the solvent yielded the crude acid chloride which acylated the sodium derivative of tetrahydropyranyl ester of propanetricarboxylic acid on heating the reactants for half an hour. After acylation and evaporation of the solvent the dark brown oil obtained was dissolved in sodium bicarbonate, the solution was extracted with ether, treated with active charcoal, filtered off and acidified. The resinous precipitate was dissolved in ethyl acetate and the solution was dried with magnesium sulphate. Evaporation of the solvent gave a viscous product which crystallized on standing for several days on a porous plate. The needle-like crystals melted at 71—73°.C.

Analysis:

Calculated for $C_{11}H_{14}O_4NF_3$ (281.23):	*C* 46.97	*H* 5.01	*N* 4.98
Found	*C* 46.94	*H* 5.11	*N* 5.60

Institute of Organic Chemistry, Beograd
School of Pharmacy, Beograd

Received 19. July, 1967

REFERENCES

1. Teague, P. S., A. R. Ballentine, and G. J. Rushton. "Some Pyridylhydantoins" — *Journal of the American Chemical Society* (Easton, Pa) 75: 3429—3430, 1953.
2. Frank, R. L., and C. Weatherbee. "3-*n*-Butylpyridine and an Unusual Alkylation in Its Synthesis" — *Journal of the American Chemical Society* (Easton, Pa) 70: 3482—3483, 1948.
3. Lukeš, J., and M. Pergal. "Homologues of the Pyridine. II. Synthesis and Reactions of Some α,α'-Disubstituted Pyridines" — *Collection of Czechoslovak Chemical Communications* (Praha) 24: 36—45, 1959.

4. Rabe, P., and R. Pasternack. "Uber γ-Chinolylketone. I." — *Berichte der deutschen chemischen Gesellschaft* (Berlin) 46: 1026—1032, 1913.
5. Kaufman, A., P. Dandliker, and H. Burkhardt. "Über Chinolylketone. III." — *Berichte der deutchen chemischen Gesellschaft* (Berlin) 46: 2929—2935, 1913.
6. Clemo, G. R., G. R. Ramage, and R. Raper. "Lupine Alkaloids" — *Journal of the Chemical Society* (London): 2959—2969, 1932.
7. Ferles, M. and J. Jizba *Chemie Pyridiny* (Pyridine Chemistry) — Praha: Československa akademie vied, 1957, p. 440.
8. Bowman, R. E., and W. D. Fordham. "Experiments on the Synthesis of Carbonyl Compounds. Part VI. A New General Synthesis of Ketones and β-Keto-Esters" — *Journal of the Chemical Society* (London) 758 (sic.): 3945—3949, 1952.
9. Jones, D. G., and A. W. Taylor. — *Quarterly Reviews* (London): 159—210, 1950.
10. Arsenijević, V. and A. Horeau. "Nouvelle préparation des acides γ,δ et ε-cétoniques" — *Bulletin de la Société chimique de France* (Paris) 311: 1943—1946, 1959.
11. Wingfield, H. H., W. R. Harlan, and H. R. Hanmer. "The Preparation of Nicotinoyl Chloride" — *Journal of the American Chemical Society* (Easton, Pa) 75: 4364, 1953.
12. Pinner, A. "Ueber Pyridoylessigester" — *Berichte der deutchen chemischen Gesellschaft* (Berlin) 34: 4234—4253, 1901.
13. Shivers, J. C., M. L. Dillon, and C. R. Hauser. "Acylations of Esters with Esters to Form β-Keto-Esters Using Sodium Amide" — *Journal of the American Chemical Society* (Easton, Pa) 69: 119—123, 1947.
14. Davis, J. W. "Studies with Quinolines. I. Synthesis of Quinaldic Acid and Some of Its Amide Derivatives" — *Journal of Organic Chemistry* (Easton, Pa) 24: 1691—1694, 1959.
15. Wada, E., and K. Yamasaki. "Degradation of Nicotine by Soil Bacteria" — *Journal of the American Chemical Society* (Easton, Pa.) 76: 155—157, 1954.
16. *Organic Syntheses* — New York: Jonn Wiley and Sons, 1963, p. 88.
17. Cagniant, D., and P. Cagniant. "Contribution a l'étude des hétérocycles soufrés condensés. V. Substitution dans le noyau du tétrahydro-4-5-6-7-thionaphtene au moyen de la réaction de Friedel-Crafts" — *Bulletin de la Société chimique de France* (Paris): 62—69, 1953.
18. Cagniant P., and A. Deluzarche. "Condensation du thiophéne avec l'anhydride glutarique" — *Comptes rendus des séances de l'académie des sciences* (Paris) 222: 1301—1302, 1946.
19. Swan, J. M., and V. du Vigneau. "Synthesis of *L*-Glutaminyl-*L*-Asparagine, *L*-Glutamine and *L*-Isoglutamine from *p*-Toluenesulfonyl-*L*-Glutamic Acid" — *Journal of the American Chemical Society* (Easton, Pa) 76: 3110—3113, 1954.
20. Beecham, A. F. "Tosyl-α-Amino Acids. I. Degradation of the Acid Chlorides and Azides by Aqueous Alkali" — *Journal of the American Chemical Society* (Easton, Pa) 79: 3257—3261, 1957.
21. Weygand, F., P. Klinke, and J. Eigen. "*N*-Trifluoracetyl-aminosäuren, *N*-trifluoracetyl-*L*-asparaginsäure-anhydrid und Trifluoracetyl-*L*-prolin-anhydrid" — *Chemische Berichte* (Berlin) 90: 1896—1905, 1957.

GLASNIK HEMIJSKOG DRUŠTVA, Vol. 32, No. 8-9-10, 1967, pp. 481—490

ORGANIC ACIDS, SACCHARIDES AND AMINO ACIDS OF POTATO IN THE COURSE OF GERMINATION

by

MILOVAN M. MILOVANČEV, SAVA G. STANIMIROVIĆ
and DARINKA L. STANIMIROVIĆ

On account of its high starch content, the potato takes a special place among vegetables. Since it contains little protein and fat, it is suitable for the study of starch metabolism and its intermediates in the course of storage. Most investigations reported so far refer to quantitative changes in starch and vitamin C in dependence on various factors. However, only a few papers deal with changes of intermediate products of starch during storage[1,2,3].

We have studied changes taking place in the course of germination. In the storage of potato special attention is paid to preventing germination, since the content of some nutrients, especially starch, then falls rapidly. Since the amount of starch in the potato is very large, considerable quantities of intermediate products of starch metabolism appear in the course of germination: monosaccharides, oligosaccharides and organic acids[4]. Along with these changes, qualitative and quantitative changes of amino acids, i.e. including proteins take place as well[5, 6].

EXPERIMENTAL

Our investigations involved identification of soluble saccharides, amino acids and organic acids. In addition, starch, soluble saccharides, free and total acidity were determined.

Investigations were carried out with tubers of Bintje potato from Opovo; tubers of approximately the same size, 5—7 *cm* long, were examined. Samples were stored in dim light at a temperature of 4—8°C, and then at 8—15°C, this inducing gradual germination lasting sixty days.

The following samples were examined:

I nongerminating tubers taken for analysis on 3 Dec, 1964

II germinating tubers with 1 *cm* long shoot, taken for analysis on 6 Jan. 1965

III germinating tubers with 2 *cm* long shoot, taken for analysis on 25 Jan., 1965

IV germinating tubers with 1 *cm* long shoot, taken for the analysis on 11 Feb., 1965.

After peeling a 1 *mm* thick skin, the tubers were cut into small pieces which then were well mixed. Some of this material was used for extraction, and the rest was dried in a vacuum oven at 50°C to constant weight.

The extraction (about 100 *g* of material) was carried out with hot 25% ethanol[7] and simultaneous treatment of the material with ultra Turax Type 18/2, whereby it was converted into a fine mash. Ethanol was removed by distillation under reduced pressure at 40°C. Part of the extract was used

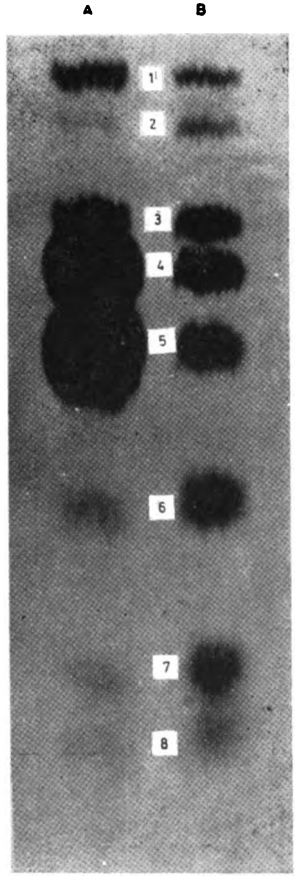

Figure 1

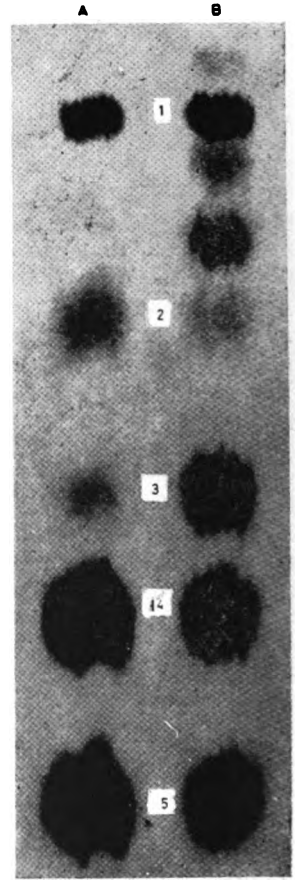

Figure 2

A. Potato saccharides
B. Standard test substances

1. — inositol
2. — sucrose
3. — galactose
4. — glucose
5. — fructose
6. — xylose
7. — ribose
8. — rhamnose

1. — inositol
2. — sucrose
3. — galactose
4. — glucose
5. — fructose

for the determination of the free acidity, the rest was passed through an Amberlite IR 120 (H^+) cation exchanger column and an Amberlite IRA 400 ($CO_3^=$) anion exchanger column in order to purify and separate the saccharides, amino acids and organic acids. The solutions obtained were then further analysed.

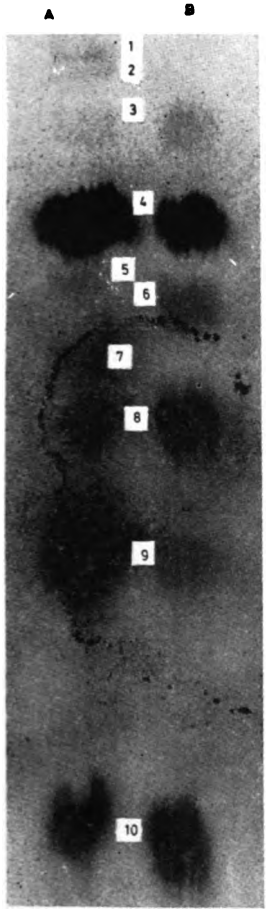

Figure 3

A. Potato saccharides
B. Standard test substances
1. — unidentified
2. — unidentified
3. — raffinose
4. — inositol
5. — nonidentified
6. — trehalose
7. — nonidentified
8. — maltose
9. — sucrose
10. — galactose

Figure 4

A. Organic acids from potato
B. Standard test substances
1. — glucose-*l*-phosphate
2. — phosphoric acid
3. — quinic acid
4. — citric acid
5. — malic acid

Organic acids, saccharides and amino acids were identified by chromatography on Whatmann No. 1 paper; for amino acids SS 2040 bM paper was used as well. The saccharides chromatograms were developed with a pyridine-ethyl acetate-water (11 : 40 : 6)[9] solvent mixture, chromatograms of organic acids with butanol-formic acid-water (40 : 2 : 15)[10] and those of amino acids with *n*-butanol-formic acid-water (600 : 50 : 50)[11, 12]. To

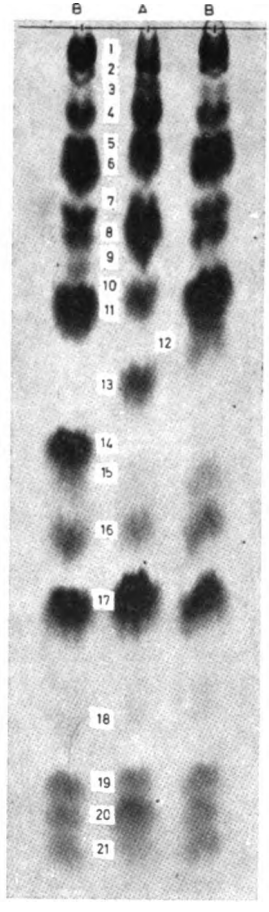

Figure 5

A. Amino acids and amides from potato
B. Standard test substances

1. Cys-S-S-Cys-Lys-His
2. Arg
3. Asp-NH_2
4. Glu-NH_2
5. Ser
6. Gly
7. Asp
8. Thr
9. Glu
10. Ala
11. Pro
12. γ-aminobutyric acid
13. nonidentified
14. α-aminobutyric acid
15. Tyr
16. Met
17. Val
18. Tri
19. Phe
20. Leu
21. Ileu

improve the resolution of components at the upper end of the chromatogram the developing time was prolonged to 65 h in case of saccharides (the temperature was about 20°C). Simultaneously, the corresponding standard substances (p. a.) were chromatographed. Detection was carried out with the corresponding reagents[12, 14]. Some specific reagents were also used[15, 16, 17, 18, 19].

Figures 1, 2 and 3 show saccharides chromatograms, Fig. 4 chromatograms of organic acids and Figs. 5 and 6 those of amino acids.

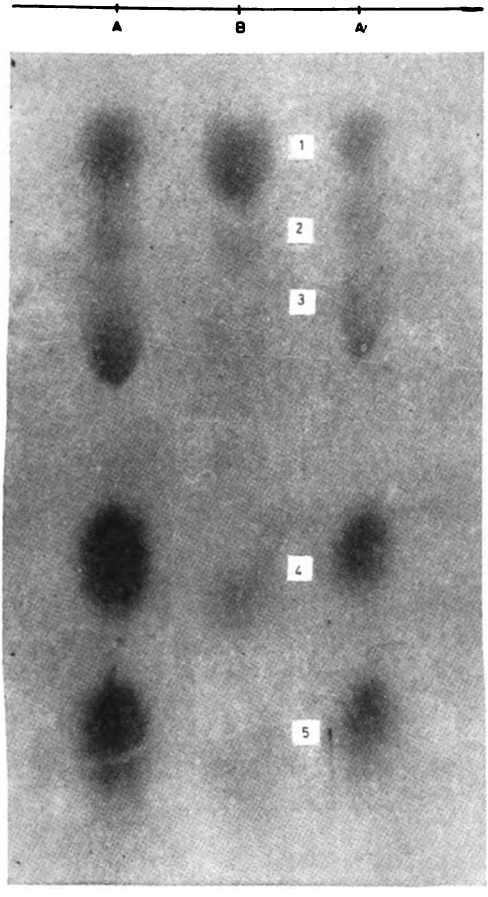

Figure 6

A. Amino acids from potato
B. Standard test substances

1. Cys-S-S-Csy-Lys
2. His
3. Arg
4. Asp-NH_2
5. Glu-NH_2

TABLE 1

Date of analysis	Sample	Acidity in *mE*								
		Free acidity			Total acidity			Bound acidity		
		per 100 *g* of dry potato	per 100 *g* of fresh potato	per tuber	per 100 *g* of dry potato	per 100 *g* of fresh potato	per tuber	per 100 *g* of dry potato	per 100 *g* of fresh potato	per tuber
3 Dec., 1964	without shoot	6.07	1.27	—	39.58	7.53	—	29.91	6.26	—
6 Jan., 1965	shoot of 1 *cm*	8.13	1.58	0.97	39.95	7.77	4.38	31.82	6.19	3.81
25 Jan., 1965	shoot of 2 *cm*	5.18	0.95	0.46	44.79	8.25	4.01	39.61	7.30	3.55
10 Feb., 1965	shoot of 5 *cm*	2.49	0.51	0.26	29.95	6.16	3.15	27.46	5.65	2.89

TABLE 2

Date of analysis	Sample		Reducing saccharides in *g*			Glucose in *g*			Fructose in *g*			Galactose in *g*			Sucrose in *g*		
			per 100 *g* of dry potato	per 100 *g* of fresh potato	per tuber	per 100 *g* of dry potato	per 100 *g* of fresh potato	per tuber	per 100 *g* of dry potato	per 100 *g* of fresh potato	per tuber	per 100 *g* of dry potato	per 100 *g* of fresh potato	per tuber	per 100 *g* of dry potato	per 100 *g* of fresh potato	per tuber
3 Dec., 1964	I	without shoot	1.17	0.36	—	0.43	0.09	—	0.43	0.09	—	0.023	0.005	—	0.51	0.11	—
6 Jan., 1965	II	shoot of 1 *cm*	1.97	0.38	0.236	0.79	0.15	0.095	0.98	0.19	0.118	0.021	0.004	0.0024	1.43	0.28	0.17
25 Jan., 1965	III	shoot of 2 *cm*	3.16	0.58	0.283	1.15	0.21	0.102	1.74	0.32	0.156	0.034	0.006	0.0025	—	—	—
10 Feb., 1965	IV	shoot of 5 *cm*	3.34	0.68	0.349	1.32	0.27	0.139	1.75	0.36	0.184	0.053	0.011	0.0056	2.36	0.48	0.25

Glucose, fructose, galactose and sucrose were determined from eluates obtained after their separation by paper chromatography[20]. Other saccharides were present in minimal amounts and could not be determined individually; therefore total reducing sugars was determined[21].

Starch was determined from the tubers dried in a vacuum oven[22].

Free acidity was determined by directly titrating the extract with 0.01 *N* sodium hydroxide solution; total acidity was determined in the same way but after passing the extract through a column of cation-exchanger. The difference between total and free acidity represents the bound acidity[23].

Determinations of saccharides are given in Table 1 and of starch in Table 2. Table 3 shows the results of acidity determinations.

TABLE 3

Date of analysis	Sample		Amid in *g*		
			per 100 *g* of dry potato	per 100 *g* of fresh potato	per tuber
3 Dec., 1964	I	without shoot	73.45	15.36	—
6 Jan., 1965	II	shoot of 1 *cm*	71.89	13.99	8.60
25 Jan., 1965	III	shoot of 2 *cm*	69.77	12.85	6.24
10 Feb., 1965	IV	shoot of 5 *cm*	68.65	14.12	7.21

CONCLUSION

The following substances were identified: rhamnose, ribose, xylose, fructose, glucose, galactose, sucrose, maltose, raffinose, malic acid, citric acid, malonic acid, succinic acid, fumaric acid, cystine, lysine, histidine, arginine, aspartamine, glutamine, serine, glycine, aspartic acid, threonine, glutamic acid, alanine, proline, tyrosine, methionine, valine, triptophan, phenylalanine, leucine and isoleucine.

The saccharide fraction was found to include inositol and glucose-1--phosphate was found among the organic acids.

In the course of germination no qualitative change in the components was detected.

With the growth of the shoot the content of reducing sugars and sucrose increased.

Equal amounts of glucose and fructose were found before germination, but during germination the content of fructose increased more rapidly. Galactose also increased during the course of germination.

The sucrose/monosaccharides ratio increased from 0.3 before germination to 0.7 in the germinating potato and remained constant through germination; this is the couvers of behavior during growth and maturation of the potato.

The content of starch decreased constantly.

The content of organic acids was initially high and then decreased. The amount of free acids was 4—5 times larger than that of acids present in the form of salts.

School of Pharmacy
Beograd University

Received 31 May, 1967

REFERENCES

1. Jelivet, E. "Variation des acides organiques dans le tubercule de semence de pomme de terre au cours de sa conservation hiverale et apres plantation" — *Comptes rendus hebdomadaires de* l'Academie des Sciences (Paris) 248 (22): 3208—3210, 1959.
2. Hansen, R. K., and M. Zucker. "The Biosynthesis of Chlorogenic Acid and Related Conjugates of Hydrocinnamic Acids. Chromatographic Separation and Characterization" — *The Journal of Biological Chemistry* (USA) 238: 1105—1115, 1963.
3. Samatus, B. and S. Schwimmer. "Specific Rotation of Potato Starches of Different Origin. B. Stamatus" — *Roczniki Technologii Chemii Zywnosci* 7: 109—125, 1961 (Cited in: Abstracts Journal of the Scientific Food Agriculture, 1963, pp. 147).
4. Minina, A. K. "Izmenchivost' soderzhaniia organicheskkikh kislot v listiakh i klubniakh kartofel'" (Variation in the Organic Acid Content of Potato Leaf and Tuber) — *Biokhimia* (Moskva) 18: 718—724, 1953.
5. Steward, F. C., W. E. Berry, C. Preston and T. K. Ramamurti. "The Absorption and Accumulation of Solutes by Living Plant Cells" — *Annals of Botany* (London) 7: 221—260, 1943.
6. Street, H. E., A. E. Kenyon and G. M. Watson. "Distribution of Various Forms of Nitrogen in the Potato" — *Annals of Applied Botany* (London) 33 (1): 1—12, 1946.
7. Wylam, C. R. "Analytical Study on the Carbohydrates of Grosses and Clovers. III. Carbohydrate Breakdown During Witlting and Ensilage" — *Journal of the Scientific Food Agriculture* (London) 4: 527—531, 1953.
8. Hulme, A. C. "An Action of Strongly Basic Anion-Exchange Resins and Solutions Containing Sugars" — *Nature* (London) 171 (11): 610—611, 1953.
9. Fischer, F. G. and D. Helmut. "Die quantitative Bestimmung reduzierender Zucker and Papierchromatogrammen" — *Hopper-Seyler's Zeitschrift für Physiologische Chemie* (Berlin) 296 (3—6), 164—178, 1954.
10. Kalyankar, G. D. "*Current Science* (India) 21: 220, 1953/ Cited in: Block, R., E. Durrum and G. Zwieg. *A Manual of Paper Chromatography and Paper Electrophoresis.* — New York: Academic Press Inc., 1955, p. 168.
11. Wiggins, L. F. and J. H. Williams, "Use of Butanol-Formic Acid-Water Mixture in the Paper Chromatography of Amino Acids Sugars" — *Nature* (London) 170: 279—280, 1952.
12. Slotta, K. H., and J. Primosigh. "Amino-Acid Composition of Crotoxin" — *Nature* (London) 168: 696—697, 1951.
13. Trevelyan, W. E., and D. P. Procter. "Detection of Sugars on Paper Chromatograms" — *Nature* (London) 166: 444, 1950.
14. Toenis, G., and J. J. Kelb. "Techniques and Reagents for Paper Chromatography" — *Analytical chemistry* (Washington) 93: 823—826, 1951.
15. Baar, S. "Estimation of Glucose by Paper Chromatography" — *Biochemical Journal* (Cambridge) 58: 175—176, 1954.
16. Dedonder, R. "Polysaccharides d'artichant de Jerusalèm. I. Demonstration des séries de glucofructosides dans les tubercules. L'isolation, l'analyse et la structure des membres moins polymerisés de la série — *Bulletin de la Société de chimie biologique* (Paris) 34: 144—156, 1952.

17. Moffat, E. D., J. Ralph, and R. J. Lytle. "Polychromatic Technique for the Identification of Amino Acids on Paper Chromatograms" — *Analytical Chemistry* (Washington) 31 (5): 926—928, 1959.

18. Fleury, P., and J. E. Courtois. "Sur l'emploi de la chromatographie sur papier pour la séparation du mésoinositol d'avec le scyllitol et leur caracterisation" — *Bulletin de la Société de Chimie biologique* (Paris) 35 (5—6): 537—540, 1953.

19. Hanes, C. S., and F. A. Isherwood. "Separation of Phosphoric Esters on the Filter Paper Chromatogram" — *Nature* (London) 164 (4): 1107—1112, 1949.

20. Nelson, N. J. "Photometric Adaptation of the Somogy Method for the Determination of Glucose." — Journal *of Biological Chemistry* (Baltimore) 153: 375—376, 1944.

21. Somogyi, M. "New Reagent for the Determination of Sugars", — *The Journal Biological Chemistry* (Baltimore) 160: 61—62, 1945.

22. Pasch, K. and M. V. Tracey. *Moderne Methoden der Pflanzenanalyse*, zweiter band — Berlin: Springer-verlag, 1955, pp. 156.

23. Jolchines, G. "Les acides organiques des feuilles de Bryophyllum daigremontianum berger, — *Bulletin de la Société de chimie biologique* (Paris) 38: 481—493, 1956.

GLASNIK HEMIJSKOG DRUŠTVA, Vol. 32, No. 8-9-10, 1967, pp. 491—504

SACCHARIDES, ORGANIC ACIDS AND AMINO ACIDS IN GRAPES FROM THE VRŠAC VINEYARDS

by

DANICA R. NASTIĆ, DARINKA L. STANIMIROVIĆ, VELJA M. VUČKOVIĆ and SAVA G. STANIMIROVIĆ

Many data are reported in the literature on the chemical composition and nutritive value of the grape, from which it may be concluded that regardless of climatic and soil conditions and the method of cultivation, the qualitative composition of grapes is almost the same, but the amounts of the different components vary greatly with these factors.

In Yugoslavia, which is an important grape producer, no systematic investigation of the components in different grape varieties has yet been performed. We have therefore carried out a detailed study on the chemical composition of different grape varieties from the S.R. of Serbia which may be of practical value for the improvement of viticulture in Yugoslavia. Better knowledge of the composition of grapes and grape products will undoubtedly have an influence on legal measures determining the limiting values for the individual components in different grape varieties.

EXPERIMENTAL

Material

Grape samples were taken in 1963 and 1964 from Vršac vineyards. In addition, a sample was taken from Venčac and one from Radmilovac. Analyses were carried out on grapes which had been selected for wine-making.

Must from the following varieties was examined:

1963

Dinka White	Italian Riesling
Dinka Rose	Prokupac — Venčac
Slankamenka	Smederevka — Radmilovac

1964

Chasselas Rose	Sauvignon Blanc
Gamay	Chasselas Dore
Semillon	Kreaca
Prokupac	Silvaner
Muscat Ottonel	Pinot Noir
Traminer	Muscat Hamburg

Dattier

Preparation of Samples for Analysis

About 1 *kg* of berries was carefully crushed in a porcelain dish in order not to wound the seed or skin. The juice was pressed through a double gauze filter and then centrifuged and separated by decantation. The juice thus obtained (must) was analyzed.

The free, bound and total acidity and *pH* were measured directly in the must. Identification and determination of saccharides, organic acids and amino acids were performed after purification of the must (50 *ml*) on Amberlite IR-120 (H^+) (1.8 × 10 *cm*) and Amberlite IRA-400 ($\overline{\overline{CO_3}}$) (1.8 × 21 *cm*) ion-exchange columns[1, 2].

The solution obtained after passing the must through both columns was used for identifying and determining saccharides.

Organic acids were eluted from the anion-exchange column with 1 *N* ammonium carbonate[3]. The ammonium carbonate was removed and the eluate concentrated by distillation under reduced pressure (60°C). A solution of free acids was obtained by passing the concentrated eluate through a column of cation exchanger; it was then used for the identification and determination of organic acids.

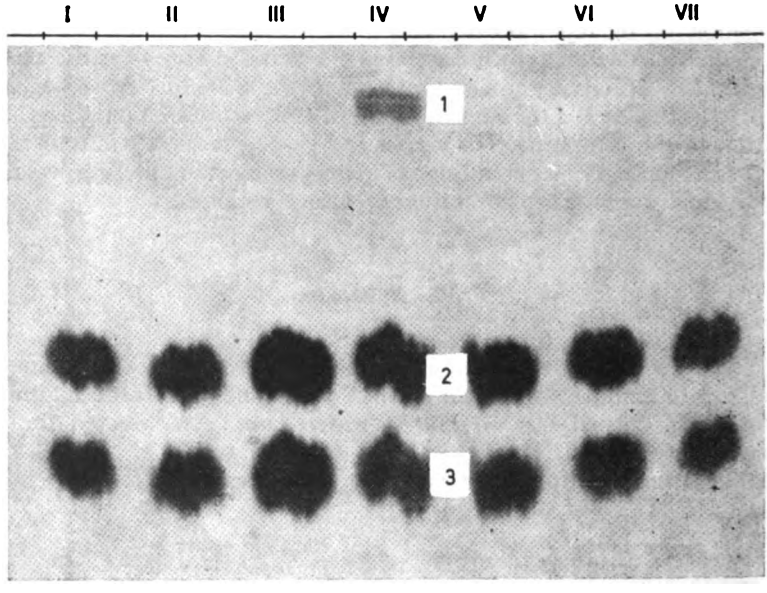

Figure 1

I — Traminer
II — Muscat Ottonel
III — Prokupac
IV — Sugar mixture
1) Inositol
2) Glucose
3) Fructose
V — Semillon
VI — Gamay
VII — Chasselas Rose

TABLE I

VARIETY	Total reducing sugars	Glucose	Fructose	G/F
	g/100 ml of must			
Dinka White	16.85	6.89	9.20	0.74
Slankamenka	16.81	7.22	9.75	0.74
Italian Riesling	27.78	12.85	14.54	0.88
Dinka Rose	16.80	6.83	9.20	0.74
Prokupac from Venčac	17.40	6.25	11.10	0.56
Smederevka from Radmilovac	21.00	10.00	11.10	0.95

Amino acids were eluted from the cation-exchange column 2 *N* ammonium hydroxide[4]. The excess of ammonium hydroxide was removed by evaporating the eluate to dryness under reduced pressure (40°C), and by repeated treatment of this residue with distilled water followed be evaporation.

Saccharides were identified by comparative paper chromatography of purified must solution and standard test substances.[5] For the detection of chromatograms and for the differentiation of aldoses from ketoses and other constituents the corresponding reagents[6, 7, 8, 9] were used.

Saccharide chromatograms are shown in Fig. 1.

Estimation of each sugar separatly was carried out after the chromatographic separation on paper from the corresponding water eluates[10]. As a check of the chromatography total reducing sugars was determined directly from must solutions[11].

* Figures 1, 2, 3 and 4 show chromatograms of sugars, amino acids and organic acids for some of the varieties. Chromatograms were however run for all varieties.

TABLE II

VARIETY	Total reducing sugars	Glucose	Fructose	G/F
	g/100 ml of must			
Chasselas Rose	16.90	6.70	9.85	0.68
Gamay	17.57	7.97	9.60	0.83
Semillon	24.60	11.18	11.91	0.94
Prokupac	17.50	8.41	9.60	0.87
Muscat Ottonel	20.40	9.31	11.61	0.80
Traminer	20.20	9.20	10.30	0.89
Sauvignon Blanc	21.90	10.00	11.00	0.90
Chasselas Dore	15.40	6.92	8.01	0.86
Kreaca	17.57	8.27	9.10	0.90
Silvaner	18.30	8.17	8.50	0.96
Pinot Noir	17.04	7.93	9.10	0.87
Muscat Hamburg	17.20	7.09	8.40	0.84
Dattier	13.80	6.67	7.00	0.95

TABLE III

VARIETY	Nitrogen of free amino-acids	Arg	Asp-NH_2	Glu-NH_2	Ser	Gly	Thre	Glu	Ala	Pro	γ-amino-n-butyric acid	Tyr	Meth	Val	Phe	Leu + Ileu
	mg/100 ml of must															
Dinka White	13.68	27.37	traces	1.37	0.52	1.15	2.30	3.71	0.75	7.82	2.31	0.34	1.62	0.34	0.75	1.62
Slankamenka	25.28	60.98	„	1.27	7.97	0.91	2.99	4.80	9.62	6.97	6.13	0.84	0.84	1.73	1.07	2.14
Italian Riesling	35.33	68.26	„	5.43	10.93	2.15	11.26	7.95	17.56	25.84	7.95	1.49	traces	3.97	2.98	7.62
Dinka Rose	9.75	24.50	„	0.54	0.22	0.23	1.32	0.57	0.60	1.52	0.19	7.36	0.09	1.06	—	0.66
Prokupac from Venčac	46.87	118.06	„	1.95	2.44	1.16	3.38	5.92	7.73	15.90	3.99	4.76	traces	5.41	10.37	14.76
Smederevka from Radmilovac	41.68	105.17	„	1.72	3.09	2.32	5.15	8.75	6.19	1.54	4.76	2.06	1.28	5.16	7.86	18.30

The results for saccharides are given in Table 1 and 2.

Amino acids were identified and determined by paper chromatography on SS 2046 *bM*[12]. The chromatograms were developed for 40 hrs at 20°C, but the resolution of amino acids with close R_f-values required a development of 60 hrs. For the separation of alanine from proline, another solvent system was used[13]. Chromatogram spots were detected with ninhydrin[14] and cupric sulphate[15].

Amino acid chromatograms are shown in Figs. 2 and 3.

After their chromatographic separation and detection, amino acids were determined spectrophotometrically[16] using the corresponding paper eluates.

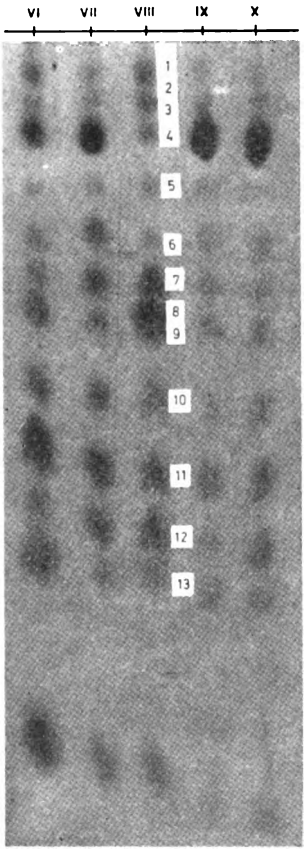

Figure 2
(developed for 60 hrs)
VI — Semillon

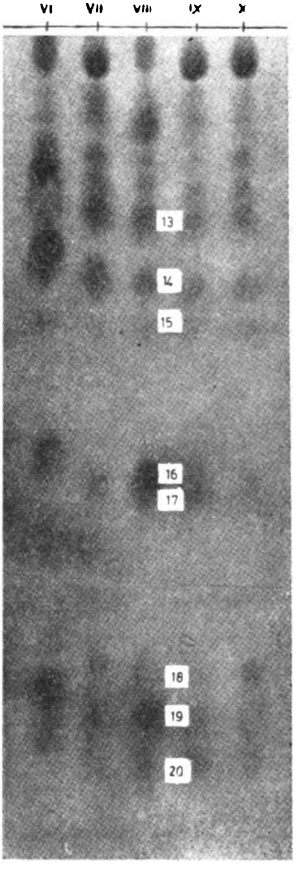

Figure 3
(developed for 40 hrs)
VII — Gamy
VIII — Amino acid mixture

1) Cys-S-S-Cys, 2) Lys, 3) His, 4) Arg, 5) Asp-NH_2, 6) Glu-NH_2, 7) Ser, 8) Gly, 9) Asp, 10) Thre, 11) Glu, 12) Ala, 13) Pro, 14) Tyr, 15) γ-aminobutyric acid, 16) Meth, 17) Val, 18) Phe, 19) Ileu, 20) Ieu

IX — Kreaca
X — Pinot Noir

The results for cysteine and lysine, and for leucine and isoleucine are sums for these pairs since they were not resolved by chromatography. The differences in extinctions for leucine and isoleucine, and for cystine and lysine, if the latter two amino acids are determined under the same conditions, are negligible, so the sum values were determined from the curve constructed from their mean extinctions.

Nitrogen of free amino acids was determined by a modified Kjeldahl method[17], as a check on the chromatographic results.

The results for amino acids and nitrogen of free amino aicds are shown in Tabels 3 and 4.

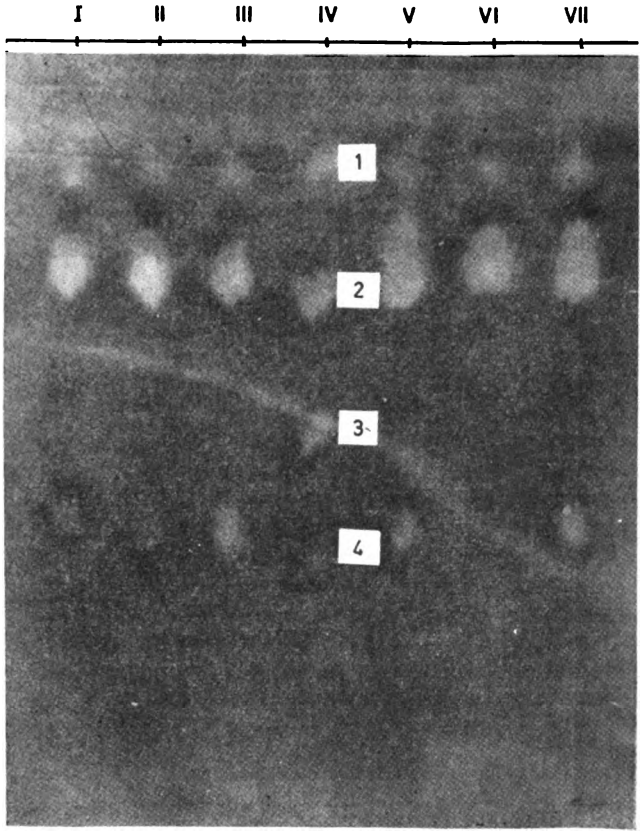

Figure 4

I — Chasselas Dore
II — Kreaca
III — Silvaner
IV — Organic acid mixture
1) Glucuronic acid
2) Tartaric acid
3) Citric acid
4) Malic acid
V — Pinot Noir
VI — Muscat Hamburg
VII — Dattier

TABLE V

VARIETY	*pH*	Free acids	Total acids	Bound acids*	Malic acid		Tartaric acid	
		mE/100 ml of the must			mE/100 ml of the must	%	mE/100 ml of the must	%
Dinka White	3.60	5.21	6.57	1.32	1.26	19.10	5.32	80.90
Slankamenka	3.50	5.72	10.32	4.60	1.42	13.20	8.90	86.80
Italian Riesling	3.52	7.27	13.37	6.10	3.56	26.60	9.81	73.40
Dinka Rose	3.41	4.17	8.67	4.50	0.77	8.90	7.89	91.10
Prokupac from Venčac	3.20	8.54	13.60	5.06	4.66	34.50	8.94	65.50
Smederevka from Radmilovac	3.60	6.85	11.12	4.27	1.41	12.60	9.71	87.40

* Bound acids = Total acids — Free acids

Organic acids were identified by paper chromatography of purified extracts[18]. Organic and uronic acids were detected with general and spespecific reagents[6, 7, 8]. An organic acid chromatogram is shown in Fig. 4.

Free acidity was determined by direct titration of the must with 0.1 *N* sodium hydroxide solution in the presence of methylred as indicator[19], and the total acidity by the same procedure but from the solution obtained after cation exchange. The content of bound acids was obtained as the difference between the total and the free acidity.

Organic acids were determined by chromatography of purified extracts on a silica gel column by the gradient elution procedure[2, 20]. The resolution of acids was checked by paper chromatography of fractions[18]. The results for tartaric acid, which is not easily eluted from a silica gel column, were calculated as the difference between total acids run and total acids eluted.

The results for free, bound and total acidity, and organic acids are given in Tables 5 and 6.

pH was measured on a Radiometer PH M type 22p. The results are given in Tabels 5 and 6.

DISCUSSION

Saccharides

The only sugars identified were glucose and fructose (Fig. 1); their presence in the grape has been known for many years[21, 22, 23, 24, 25, 26, 27]. However, in these varieties no traces of rhamnose, xylose, arabinose or saccharose were detected, although their presence in grapes is reported by some authors[24, 28, 29].

The total sugars varied from 17 to 20 *g*/100 *ml*, except in Italian Riesling (27.78 *g*/100 *ml*) and Semillon (24.60 *g*/100 *ml*) where it was considerably greater. Table varieties such as Dattier and Chasselas Dore contained much less total sugars (13.80 *g*/100 *ml* and 15.40 *g*/100 *ml*) (Tables 1 and 2). From these data it may be concluded that Dattier and Chasselas Dore are not suitable for the production of wine but may be used as table grapes, whereas, the other varieties may be used for the production of table and vintage wines.

In all samples the ratio G/F (glucose/fructose) was less than 1 (between 0.68 and 0.95). A specially high fructose content (twice that of glucose) was found in Prokupac from Venčac: the ratio G/F was only 0.56 (Tables 1 and 2).

Inositol was the only polyhydroxylic alcohol detected.

Amino Acids

The following amino acids were found: cystine, lysine, histidine, arginine, asparagine, glutamine, serine, glycine, aspartic acid, threonine, glutamic acid, alanine, proline, γ-aminobutyric acid, tyrosine, methionine, valine, phenylalanine, leucine and isoleucine (Fig. 2 and Fig. 3).

Nitrogen of free amino acids varied widely. It was lowest in Sauvignon (8.72 *mg*/100 *ml*) and Dinka Rose (9.75 *mg*/100 *ml*), and highest in Traminer (58.67 *mg*/100 *ml*), Silvaner (54.89 *mg*/100 *ml*) and Prokupac from Venčac (46.87 *mg*/100 *ml*). In other samples it ranged from 13 to 40 *mg*/100 *ml* of must (Tables 3 and 4). It is of interest to note that Zinchenko[30] found the highest content of nitrogen in Traminer cultivated in the Transcarpathian area.

If the free amino acid nitrogen is compared with the acidity, it may be seen that the highest nitrogen content was found in musts of the highest *pH*, i. e. least active acidity (Traminer and Silvaner). The nitrogen was very low in Sauvignon whose active acidity was the highest (Tables 3, 4, 5 and 6). It is probable that *pH* and the ability of the variety to absorb nitrogen from the soil have an influence on the free amino acid nitrogen level, since all other conditions which could affect it (climate, soil, etc.) were the same for all the varieties. Similar deductions in connection with acidity and free amino acid nitrogen were made by Peynaud and Maurié[31].

Arginine and proline were present in all samples, in amounts considerably greater than those of other amono acids. Arginine ranged from 121.00 (Silvanar) to 9.57 *mg*/100 *ml* (Sauvignon). The highest content of proline was found in Traminer (130 *mg*/100 *ml*) and the lowest in Dinka Rose (1.52 *mg*/100 *ml*). Of all the amino acids asparagine was found in the smallest amounts, only traces in all samples. Glycine was also only present in traces in most samples, but in an amount of 3.40 *mg*/100 *ml* in Pinot Noir. The amounts of cystine and lysine ranged from traces in Traminer to 2.38 *mg*/100 *ml* in Silvaner. The other amino acids also varied widely between varieties (Tables 3 and 4). A similar behavior of amino acids in different varieties were established by Eafon-Lafurcade and Peynaud[19].

The differences between varieties were least for cystine and lysine, glycine, glutamic acid, γ-aminobutyric acid, tyrosine and methionine; other amino acids showed considerable differences. These results are in good agreement with those reported by Castor[32] who found great differences in arginine and small differences in lysine and methionine. Contrary to our results however, Castor found great differences in glutamic acid and tyrosine and very small differences in leucine.

It should be noted that aspartic acid was only found in Sauvignon, in an amount of 5.00 *mg*/100 *ml* (Table 4).

Organic Acids

Tartaric, citric and malic acid and traces of glucuronic acid (Fig. 4) were detected. These results are consistent with those reported by most authors[33, 34, 35]. However, succinic, oxalic and glycolic acid were not detected, although these acids have been reported to cocur in grape[33, 34].

The lowest free acidity was found in Dinka Rose (4.17 *mE*/100 *ml*) and Chasselas Rose (4.60 *mE*/100 *ml*), and the highest in Gamay (10.68 *mE*/100 *ml*). In other varieties it ranged from 5 to 9 *mE*/100 *ml* (Tables 5 and 6)*. According to our investigations and to some earlier publications[36], low acidity seems to be associated with those varieties which are characteristic of the given vineyards.

* The free acidity should be slightly higher (6—16 mE 100 ml of must).

The total acidity was lowest in Dinka White (6.57 *mE*/100 *ml*) and slightly higher in Dinka Rose (8.67 *mE*/100 *ml*). In Chasselas Dore and Kreaca it was 9.5 *mE*/100 *ml*. It was highest in Gamay (16.44 *mE*/100 *ml*). In other varieties it ranged from 10.00 to 13.60 *mE*/100 *ml* (Tables 5 and 6). Varieties exhibiting a low total acidity also had a low free acidity.

The bound acidity varies with the variety (Tables 5 and 6). Expressed as a percentage of total acidity it was highest in Chasselas Dore (54%). In other varieties it was from 30 to 50% of the total acidity.

It should be noted that there is no definite relationship between the *pH* and the free acidity; must of Gamay grapes had the highest free acidity but its *pH* was not the lowest. The lowest *pH* found for Sauvignon although its acidity was not high. It is obvious that other factors as well affect the *pH*. Most probably, the *pH* depends mainly upon the ratio of free tartaric and malic acid, but it is also influenced by the content of free amino acids.

The *pH* of the must ranged from 2.9 to 3.5 (Tables 5 and 6). According to existing data it can vary from 2.7 to 3.8[37]. Since must acidity inhibits the growth of harmful lactic acid bacteria, the *pH* is of a special interest for the estimation of the resistance of the must to these bacteria: varieties with a *pH* above 3.4 have a low resistance[18].

Malic and tartaric acid are the most abundant acids in the must (Tables 5 and 6). Most of samples examined contained more tartaric than malic acid. Tartaric acid constituted 65—90% of the total acidity. However, in Kreaca and Muscat Hamburg grape tartaric acid content was slightly lower than that of malic acid. In Prokupac and Pinot Noir the two were about equal.

Citric acid was only found in traces. It was highest in Pinot Noir, amounting to 0.42 *mE*/100 *ml* (Table 6).

From the results obtained it may be concluded that the qualitative composition of the musts did not essentially differ from the must composition of the corresponding varieties examined by foreign authors[22, 34, 37, 38]. There were considerable differences in the contents of some components, not only between the varieties from Vršac vineyard and the same varieties cultivated abroad, but also between the varieties themselves.

School of Pharmacy
Beograd University

Received 13 June, 1967

REFERENCES

1. Bryant, F., and B. Overel "Displacement Chromatography on Ion — Exchange Columns of Carboxylic Acids in Plant Tissue Extracts" — *Nature* (London) 167: 361—363, 1951.
2. Jolchine, G. "Les acides organiques des feuilles de Bryophyllum daigremontianum berger" — *Bulletin de la Société de Chimie biologique* (Paris) 38: 481—493, 1956.
3. Kinzel, H. "Zur Metodik der analyse von Pflanzlichen Zellsaft- stoffen, mit besonderer Berucksichtigung der organischen Sauren" — *Journal of Chromatography* (Amsterdam) 7 (4): 493—506, 1962.
4. Redifield, R. "Two-Dimensional Paper Chromatographic System with High Resolving Power for Amino Acids" — *Biochimica et Biophysica Acta* (London) 10: 344—453, 1953.
5. Fischer, G. F., and D. Helmut. "Die quantitative Bestimmung reduzierender Zucker auf Papierchromatogrammen" — *Hoppe Seyler's Zeitschrift für Physiologische Chemie* (Berlin) 297 3—6: 164—178, 1954.
6. Trevelyan, W. E., D. P. Procter, and J. S. Harrison. "Detection of Sugars on Paper Chromatograms" — *Nature* (London) 166: 444—445, 1950.
7. Block, R., E. Durrum, and G. Zweig. *A Manual of Paper Chromatography and Paper Electrophoresis*" — New York: Academic Press Inc, 1955, p. 132.
8. Baar, S. "Estimation of Glucose by Paper Chromatography" — *The Biochemical Journal* (Cambridge) 58: 175—176, 1954.
9. Dedoner, R. "Polysaccharides d'artichant de Jérusalem. I. Demonstration des séries de glucofructosides dans les tubercules. L'isolation, l'annalyse et la structure des membres moins polymerisées de la série" — *Bulletin de la Société de Chimie Biologique* (Paris) 34: 144—156, 1952.
10. Nelson, N. "Photometric Adaptation of the Somogy Method for the Determination of Glucose" — *The Journal of Biological Chemistry* (Baltimore) 153: 375—376, 1944.
11. Somogy, M. "New Reagents for the Determination of Sugars" — *The Journal of Biological Chemistry* (Baltimore) 160: 61—62, 1945.
12. Wiggins, L. F. and H. Williams — "Use of Butanol-Formic Acid-Water Mixture in the Paper Chromatography of Amino Acids and Sugars" — *Nature* (London) 170: 279—280, 1952.
13. Slotta, K. H. and J. Primosigh "Amino Acid Composition of Crotoxin" — *Nature* (London) 168: 696—697, 1951.
14. Consden, R., A. H. Gordon, and A. J. P. Martin. "Qualitative Analysis of Proteins. A Partition Chromatographic Method Using Paper" — *The Biochemical Journal* (Cambridge) 38: 224—232, 1944.
15. Moffat, E. D., J. Ralph, and R. J. Lytle. "Polychromatic Technique for the Identification of Amino Acids on Paper Chromatograms" — *Analytical Chemistry* (Washington) 31: 926—928, 1959.
16. Biserte, G., T. Plaquet-Schoonaęrt, P. Boulanger, and P. Paysant. "Separation des acides aminés des milieux biologique complexes" — *Journal of Chromatography* (Amsterdam) 3 (1): 25—28, 1960.
17. a) Jacobs, B. M. "Micro Kjeldahl Methods for Biologicals" — *Journal of the American Pharmaceutical Association* (Scientific Edition) 40 (3): 151—153, 1951.
    b) Sheppard, L. D., and B. M. Jacobs. "Modified Micro-Kjeldahl Apparatus" — *Journal of the American Pharmaceutical Association* (Scientific Addition) (Washington) 40 (3): 154—155, 1951.

18. Kalyankar, G. D. *et al. Current Science* (India) 21: 220, 1952 (Cited in Block, R., E. Durrum, and G. Zweig. *A Manual of Paper Chromatography and Paper Electrophoresis* — New York: Academic Press Inc., 1955, p. 168.
19. Lafon-Lafurcade, S., and E. Peynaud — Dosage Microbiologique des acides aminés des mouts de raisin et des vins" *Vitis* (Gironde-France) 2: 45—56, 1959.
20. Bullen, W. A., J. E. Varner, and R. C. Burrell. "Separation of Organic Acids from Plant Tissues". Chromatographic Technique" — *Analytical Chemistry* (Washington) 24: 187—190, 1952.
21. Berg, H. W., F. Filipello, E. Hinreiner and A. D. Webb. "Evaluation of Thresholds and Minimum Difference Concentrations for Various Constituents of Wines. I. Water Solutions of Pure Substances" — *Food Technology* (Chicago, Illinois) 9 (1): 23—36, 1955.
22. Nechaev, L. N. "Rol' intensivnosti sakharonakopleniia i sostava organicheskiikh kislot vinograda v formirovanii organolepticheskikh kachestv soka i vin" (The Influence of Sugar Accumulation and Organic Acid Composition of Grape on the Organoleptic Properties of the Juice and Wine) — *Biokhimiia vinodeliia* (Moskva) 7: 25—42, 1963.
23. Stanimirović, S., D. Stanimirović and A. Damanski. "Prilog poznavanju dinamike glukoze, fruktoze, jabučne i vinske kiseline u plodu grožđa u toku vegetacione periode" (Contribution to the Knowledge of Glucose, Fructose, Malic Acid and Tartaric Acid Dinamics in Grape in the Course of a Vegetation Period) — *Acta Pharmaceutica Yugoslavica* (Zagreb) 12 (1): 11—16, 1962.
24. Amerine, M. A. and G. Toukis. "Glucose-Fructose Ratio of California Grapes" — *Vitis* (Gironde-France) 1: 224—229, 1958.
25. Gaivoronskaia, Z. I. "Ekstrakt kak pokazatel' kachestva dezertnyk vin i izmenenia ego v khode sozrevania vinograda" (Extract as an Indicator of Desert Wine Quality, and its Variation with the Maturation of Grape) — *Biokhimiia Vinodeliia* (Moskva) 7: 43—57, 1963.
26. Hilger, A. "Neues Vorkommen des Inozits im Pflanzenreiche und Überführung desselben in Paramilchsäure" — *Annalen der Chemie und Pharmacie* (Leipzig) 160: 333—337, 1871.
27. Mathews, J. "The Vitamin B Complex Content of Bottles Swiss Grape Juices" — *Vitis* (Gironde-France) 2: 57—64, 1958.
28. Tarantola, C. "Pentosi e pentosani e bilancio dei carbohidratix fermentescibili ed infermentiscibili" — *Rivista di viticoltora e di enologia* (Conegliano - Treviso) : 287—292, 1950.
29. Barbagallo, L; "Studio sulla composizione chimica dei vini dell'etna" — *Rivista di viticoltura a di enologia* (Conegliano-Treviso) 7: 227—236, 1954.
30. Zinchenko, V. I. "Dinamika azotist ykh veshchestv pri brozhenii vinogradnogo susla i vyderzhke molodogo vina" (Variations in Nitrogenous Substances during Fermentation of Grape Must and Maturation of Young Wine) — *Biokhimiia vinodeliia* (Moskva) 7: 58—73, 1963.
31. Peynaud, E. and A. Maurié. "Sur l'évolution de azote dans les differentes parties du raisin au cours de la maturation" — *Annales de l' institut national de la recherche agronomique* (Annales de Technologie agricole) (Paris) 2: 15—25, 83—94, 1953.
32. Castor, J. G. B. "Free Amino Acids of Musts and Wines. I. Microbiological Estimation of Fourteen Amino Acides in California Grape Musts" — *Food Research* (Chicago) 18: 135—145, 1953.
33. Gerasimov, M. A. "*Tekhnologiia vina*" (Wine Technology) — Moskva: Pishchevaia promyshlennost', 1940, p. 60.
34. Amerine, M. A., and W. V. Cruess. *The Technology of Wine Making* — Westport Conecticut: The AVI Publishing Company INC., 1960, pp. 92—108.
35. Serviere, P. R. "Valeur biologique de l'acide malique, nouvelle notion en oenologie" — *L'alimentation et la vie* (Paris) 50 (7, 8, 9): 191—195, 1962.
36. Toskić, V. *Prerada grožđa (enohemija)* (Grape Processing (Enochemistry)) — Beograd: Naučna knjiga 1950, p. 39.
37. Ribereau-Gayon, J. and E. Peynaud. *Analise et controle des vins* Paris et Liege: Liberaire Polytechnique Ch. Béranger, 1958, p. 151.
38. Preobrazenskii, A. A. "Biokhimicheskie osobennosti i tekhnologicheskie svoistva sortov vinograda, kultiviruemykh v uslovaniakh srednei Azii" (Biochemical and Technological Properties of Grape Varieties Cultivated in Central Asia) — *Biokhimiia vinodeliia* (Moskva) 5: 213—236, 1957.

GLASNIK HEMIJSKOG DRUŠTVA, Vol. 32, No. 8-9-10, 1967, pp. 505—514

EFFECT OF COOLING RATE FROM GAMMA AND BETA REGIONS ON THE SIZE AND DISTRIBUTION OF SECOND PHASES IN DILUTE URANIUM

by

MILAN T. JOVANOVIĆ

INTRODUCTION

Under irradiation different changes take place in uranium based fuel: anisotropic growth, radiation and thermal creep and swelling.

Research on binary and multi-component alloys of uranium containing small amounts of alloying elements has been going on for several years. One such alloy is the so-called adjusted uranium, a uranium alloy containing a small amount of iron and aluminum. The proportion of iron ranges from 200 to 500 ppm, and that of aluminum from 500 to 1200 ppm. By suitable thermal treatment it is possible to produce a finely dispersed second-phase precipitate which plays a double role:

1. It stabilized the fine-grain structure up to 550°C, the precipitate at grain boundaries making the greatest contribution[1];

2. Finely dispersed particles of the precipitate, whose density is reported by some authots[2] to be 3×10^{16} : cm^3, representing centers for the evolution of gaseous bubbles, preventing them coalescing into larger bubbles. This way reduces radiation swelling and improves dimension stability of the fuel[3].

The aim of this investigation was to study the effect of the rate of cooling from the gamma and beta regions on the size and distribution of precipitated dispersed phases in unalloyed uranium of domestic origin, and uranium alloyed with 1000 ppm of aluminum.

PREVIOUS PUBLICATIONS

Several authors have studied precipitated second phases in adjusted uranium by means of electron microscopy. Ryder and Nutting[4] studied them after annealing in the gamma region and air-cooling, and after quenching from the gamma region and ageing in the alpha region. In samples which were air-cooled three types of precipitate were differentiated: a) a rod-shaped precipitate at beta grain boundaries, most of the rods becoming

spheroidal in the course of cooling; b) a globular precipitate at alpha grain and subgrain boundaries; c) a finely dispersed precipitate inside the alpha grains. In samples which had been aged in the alpha region particles precipitated at alpha grain and subgrain boundaries. Finer particles precipitated at random inside the alpha grains and there were fewer of them than in air-cooled samples.

Marsh *et al.*[2] got similar results but they considered that the density of the precipitate produced in the course of ageing in the alpha region was considerably grater than of air-cooled samples.

Ostberg *et al.*[5] studied 2nd phase precipitation during isothermal decomposition of the beta phase. They found that before the precipitation of a network of rad-like particles, fine particles of globular shape appeared at random inside the beta grains. There were relatively few of these particles and they were observed only for very short isothermal decomposition times. Spheroidization of the rod-like precipitate was not observed.

1. EXPERIMENTAL

1.1. Material

The compositions are given in Table 1.

TABLE I

Alloy	Chemical Analysis					
	C	*Al*	*Fe*	*Cr*	*Ni*	*Si*
UB-Al 1000	700	1000	429	58	167	126
UB-2	700	—	429	58	167	126

Only a few experiments were performed with UB-2 alloy, mainly for comparison.

The dispersed phases were studied by optical and electron microscope. Samples for optical microscopy were in the form of disks of diameter 8 *mm* and thickness 2 *mm*. Samples for electron microscopy were cut from a 0.1 *mm* foil obtained by rolling. The area of the sample was 10×10 *mm*. After rolling the samples were annealed 1 hour at 850°C and then air-cooled.

1.2. Cooling from the Gamma Region

Samples were cooled at different rates, as follows:

a. UB-Al 1000

1. Annealed in the gamma region (24 hrs at 850°C) and air-cooled (mean cooling rate about 3°C/min);

2. Annealed in the gamma region and cooled in vacuum (mean cooling rate about 27°C/min);

3. Annealed in the gamma region and quenched in oil, water or a mixture of 10% *NaOH* and ice;

4. Annealed in the gamma region, quenched in a mixture of 10% *NaOH* and ice, aged for 1 hour or 24 hours at 550°C and quenched in water.

b. *UB-2 Alloy*

1. Annealed in the gamma region (24 hours at 850°C) and air-cooled.

1.3. Cooling from the Beta Region

a. UB-A1 1000

1. Rapid heating of quenched samples to predetermined temperatures in the beta region and immediate quenching in water.

1.4. *Preparation of Samples for Electron Microscopy and Metallography*

Samples for electron microscopy were thinned down by electropolishing after Azam[6], i.e. by spraying with an electrolyte jet. The electrolyte used was orthophosphoric acid. Eelctropolishing was carried out in a closed box at a temperature of — 5°C, a voltage of 40 *V* and a current of 0.2 *A*. The oxide layer formed on the sample in the course of electropolishing was removed electrolytically in a mixture of 75% sulphuric acid, 18% glycerol and 7% water, at a voltage of 10 *V*.

Samples for optical microscopy were prepared in the usual way: etching and electropolishing were done in a mixture of acetic acid, chromium trioxide and distilled water.

Thin foils were observed under a JEM-7 type electron microscope, at a voltage of 100 *KV*.

2. RESULTS

2.1. UB-A1 1000

Cast alloy. Samples of cast alloy were observed by optical microsope. On the micrograph (Fig. 1) a characteristic network of alpha boundary allotriomorphs is seen. Its formation may be ascribed to precipitation of the

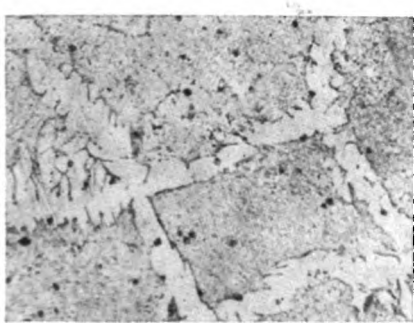

Figure 1

Crude cast. × 540

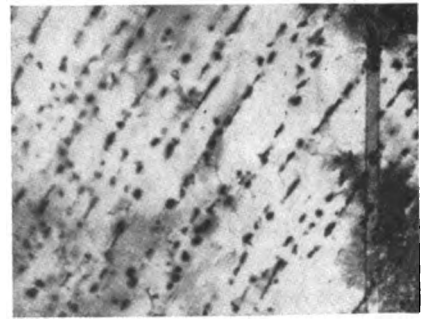

Figure 2

Crude cast. × 15.000

beta phase at gamma grain boundaries during cooling, whereas the rest of the gamma phase was converted into the eutectoid beta + UAl_2 at the eutectic temperature (757°C). At a lower temperatures (675°C) beta > alpha transformation accurs, and down to room temperature a new precipitate appears[1].

In samples observed by electron microscopy precipitate particles of a diametar of about 0.1 micron* were observed, always in parallel rows, some of the particles precipitating at dislocations (Figs. 2 and 3). In addition to this globular precipitate, occasionally a rod-like precipitate was also observed (Fig. 4).

Air-cooling from the gamma region. Samples were annealed in the gamma region and air-cooled to room temperature. Under the optical microscope a network of precipitate was observed (Fig. 5). The electron microscope revealed that the particles of the precipitate differed in size, shape and ordering, viz:

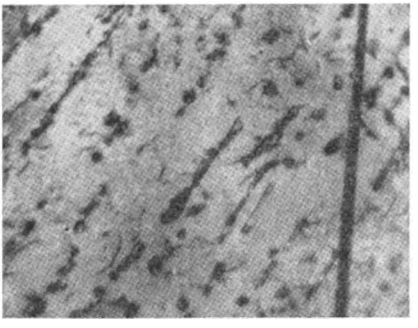

Figure 3

Crude cast. × 25.000

Figure 4

Crude cast. × 30.000

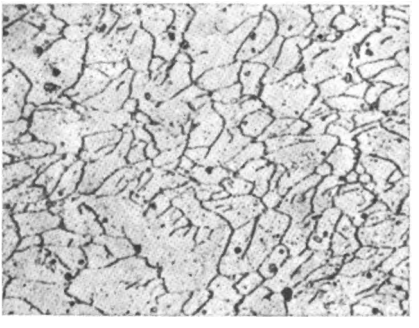

Figure 5

Furnace-cooled from the gamma region × 540

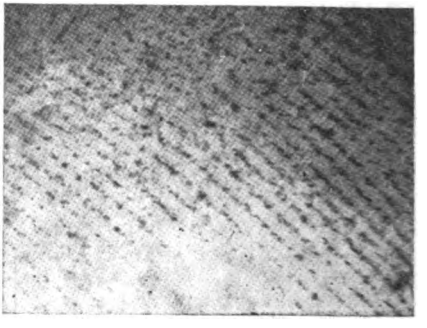

Figure 6

Furnace-cooled from the gamma region × 14.600

* These are mean values for measurements on several micrographs.

a. A finely dispersed precipitate inside the alpha grains (intragranular precipitate). The particle size from 0.02 to 0.04 microns in diameter. The particle were precipitate in parallel rows like in cast alloy, but the particles were smaller (Fig. 6).

b. A precipitate at alpha grain and subgrain boundaries (about 0.2 microns in diameter) (Fig. 7).

c. A coarse precipitate (about 0.3 microns diameter) appeared, usually in the form of a network which seemed to have no connection with the alpha phase. The particles were globular or rod-shaped (Fig. 8). According to some authors[2, 4] the rod-shaped particles precipitate on the boundaries of the beta phase during slow cooling from the gamma region, and on further cooling some of them became spheroidal.

Figure 7

Furnace-cooled from the gamma region
× 14.600

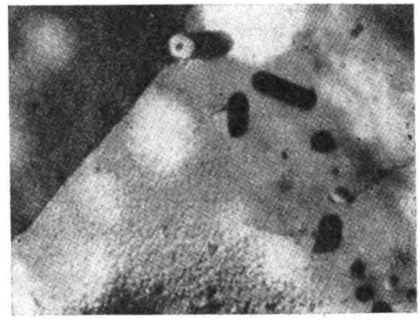

Figure 8

Furnace-cooled from the gamma region
× 21.400

Cooling in vacuum from the gamma region. Inside some alpha grains a very finely dispersed precipitate appeared whose particles (diameter about 0.01 microns) were arranged in parallel rows (Fig. 9). However, in most grains no precipitate was observed, which indicates that the precipitation is ionhomogenous. No precipitate was observed on alpha grain and subgrain boundaries either.

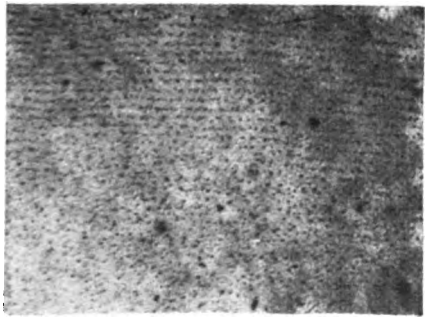

Figure 9

Vacuum-cooled from the gamme region
× 31.000

Quenching from the gamma region. The aim of these experiments was to establish whether quenching can give rise to a supersaturated solid solution, i.e. a metastable state without a precipitate. The quenched samples were aged in the alpha region. Quenching in a mixture of 10% *NaOH* and ice or in water yielded a structure in which no precipitate was observed. Therefore it can be assumed that during heating in the gamma region for 24 hrs all alloying elements are converted into a solid solution, and that the cooling rate during quenching (in 10%*NaOH* and ice or in water) is sufficiently rapid to prevent precipitation. In samples which were quenched in oil slight precipitation took place. Precipitation during quenching in oil was also observed by some other authors[4, 5]; moreover, according to some authors a precipitate appeared even during quenching in water[7].

Ageing in the alpha region. In samples which were aged for 1 hour precipitate particles with a diametar of about 0.2 microns occasionally appeared at alpha subgrain boundaries. No precipitate was observed inside the subgrains (Fig. 10). In samples which were aged for 24 hours a coarse precipitate was also observed at subgrain boundaries (Fig. 11), whereas inside the subgrains a very fine precipitate with particles of about 0.05 microns diameter was observed (Fig. 12). The former precipitate was random, not arranged in parallel rows as in air-cooled samples. The fine precipitate was not homogenous, i.e. in some subgrains it appeared in great amounts, in some in less, and in some it could not be observed.

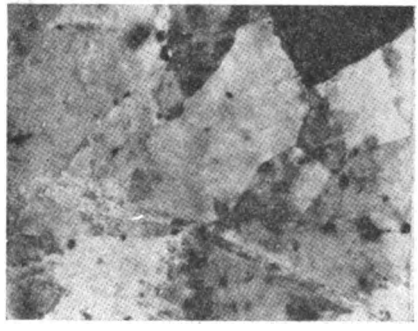

Figure 10

Ageing in alpha-region (550° for 1 h) × 15.000

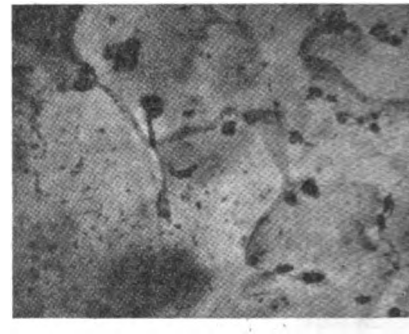

Figure 11

Ageing in alpha-region (550°C for 24 h) × 15.000

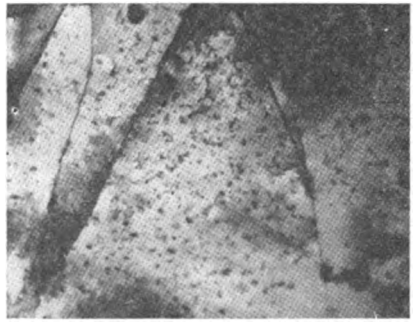

Figure 12

Ageing in alpha-region (550°C for 24 h) × 15.000

Quenching from the beta region. Samples were first quenched from the gamma region, rapidly heated to 670, 690 or 715°C and immediately on reaching the predetermined temperature (registered by means of a thermocouple), quenched in water. The precipitate which appeared at 715°C was globular and occurred inside the beta grains. The particle diameter was about 0.02 microns. (Fig. 13). A small amount of precipitate was observed at 690°C, while at 670°C none could be detected.

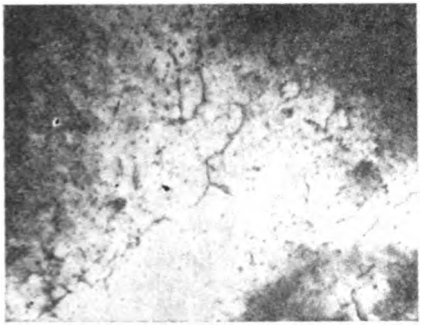

Figure 13
Rapidly heated to 715°C and water-quenched. × 15.000

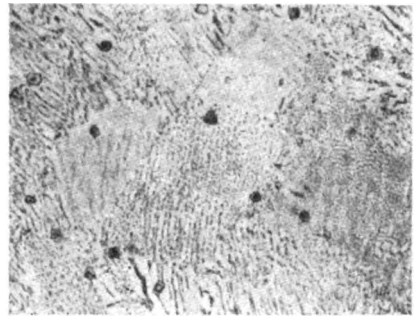

Figure 14
Crude cast. × 540

2.2. UB-2

Alloy in cast state. The cast structure observed by optical microscope showed a precipitate inside and at the boundaries of the alpha grains (Fig. 14). However, electron microphotographs of the samples showed that this alloy was poorer in precipitate than *UB-A1* 1000. A rod-shaped precipitate was arranged in parallel row inside the alpha grains (Fig. 15). Moreover, a very fine random precipitate was also observed inside the alpha grains but it was not easily detected since it appeared only in traces. The rod-shaped precipitate was similar to that observed by Marsh *et al.*[2] in *U-Fe* alloy which they identified as U_6Fe. When our results are compared with those of other authors, one should take into account the fact that nickel and silicon are only slightly soluble in the alpha phase and that they probably affect the composition and shape of the precipitate.

Figure 15
Crude cast. × 15.000

Air-cooling from the gamma region. Inside the alpha grains very fine particles (about 0.01 micron in diameter) arranged in parallel rows precipitated. The amount of precipitate was less than in the corresponding sample of *UB-A1* 1000. The formation of a rod-shaped precipitate was not observed (Fig. 16).

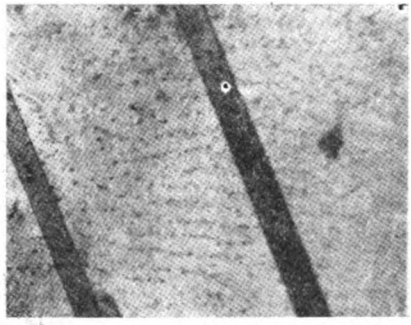

Figure 16
Furnace-cooled from the gamma region
× 15.000

DISCUSSION AND CONCLUSIONS

Our results show an obvious difference in the size and distribution of the precipitate in cast and air-colled samples of *UB-A1* 1000 alloy. It can be assumed that the thermal history of the sample has an influence on the precipitation.

The air-cooled alloy behaves in the same way as adjusted uranium[2, 4, 5], i.e. there appear

1. a precipitate in the form of big rods,
2. a slightly finer precipitate of globular shape at alpha grain and subgrain boundaries,
3. a very fine precipitate with particles in parallel rows inside the alpha grains.

In the Introduction it was stated that the rod-shaped precipitate separates in the beta phase region[2, 4]. By istothermal decomposition of the beta phase it was established that the precipitation of a network of rod-shaped particles is preceded by a globular precipitate[5]. Our experiments involving rapid heating of a supersaturated solid solution to different temperatures of the beta phase region and quenching in water (whereby it was assumed that the rate of heating through the alpha phase region was sufficiently high to prevent precipitation) do not enable use to draw definite conclusions on the precipitation of the rod-shaped particles on beta grain boundaries. However, the fact that only a fine precipitate appears indicates that this represents the first stage of the precipitation of second phases from the beta solid solution.

On comparing the structure of *UB-A1* 1000 with that of *UB-2* it may be seen that air-cooled samples of both alloys contained a precipitate of similar shape and distribution, with the exception that no rod-shaped precipitate was observed in *UB-2*. Taking into account the amount and

solubility of the alloying components in the beta phase, it may be concluded that all the alloying components of *UB-2* are present in the beta solid solution, and that precipitation in the beta phase temperature interval is not to be expected. This also provides confirmation of the hypothesis that the rod-shaped particles found in *UB-A1* 1000 samples precipitate from the beta phase, since the amount of aluminum in the alloy exceeds its maximum solubility in the beta phase (about 800 ppm)[1].

According to Ryder and Nutting[4] most of the finely dispersed precipitate appears at dislocations. In fact, when the sample is cooled slowly through the region of the beta → alpha transformation, the change over takes place predominantly by diffusion. The volume change (about 1%) in the transformation causes plastic deformation of the alpha phase which is softer than the beta phase at this temperature. In this way favorable conditions are created for the formation of dislocation which represent suitable sites for precipitation.

Upon cooling from the gamma region in vacuum, i.e. at a cooling rate between that of quenching in oil and air-cooling rate, a finely dispersed precipitate was observed with finer particles than those which precipitated upon air-cooling or ageing. It is possible that there exists an optimum cooling rate which would give an finer precipitate.

In samples which were quenched from the gamma region and then aged in the alpha region the amount of finely dispersed precipitate was less than in air-cooled samples. These findings are in agreement with the results of other authors[4]. The precipitate was randomly distributed, not in parallel rows, and the amount of it increased with increasing ageing time.

Boris Kidrič Institute of Nuclear Science, Beograd

Received 24 March, 1967

REFERENCES

1. Jepson, M. D., R. B. Kehoe, R. W. Nichols, and G. F. Slattery. "Transformation Behaviour of Some Dilute Uranium Alloy", in: *Proceedings of the 2nd International Conference on Peaceful Uses of Atomic Energy, Vol. 6* — Geneva: United Nations, pp. 42—54.
2. Marsh, D. J., G. F. Slattery, M. A. Dewey, and I. S. Brammer. "The Electron Metallography of Dilute Alloys of Uranium with Iron and Aluminium" — *The Journal of the Institute of Metals* (London) 93 (13): 471—475, 1958.
3. Bellamy, R. G. "The Swelling of Alfa-Uranium under Neutron Irradiation to 0.7% Burn-Up", in: *Uranium and Graphite, Proceedings of a Symposium held in London* — (London): The Institute of Metals, 1962.
4. Ryder, P. L., and J. Nutting. "The Precipitation of Intermetallic Compounds in Adjusted Uranium" — *The Journal of the Institute of Metals* (London) 93 (6): 178—181, 1965.
5. Ostberg, B., B. O. Haglund, B. Lehtinen, and L. Storm. "Isothermal Transformation of Gamma Phase Adjusted Uranium in the Beta Range" — *Arbetsrapport* (Stokholm), 1965.
6. Azam, N., and J. Bouleau. "Dispositif de polissage et d'amincissement electrolytiques" — *Journal de Microscopie* (Paris) 1 (2): 121—126, 1962.
7. Dixon, P. H., F. H. Fern, and B. R. Butcher. "The Solution of Precipitates in Very Dilute Uranium-Iron-Aluminium Alloys" — *The Journal of the Institute of Metals* (London) 93 (12): 423—428, 1965.